

THE CHEMISTRY OF BIOFILMS AND THEIR INHIBITORS

EDITED BY: Sergio F. Sousa, Manuel Simões and Nenad Filipović
PUBLISHED IN: Frontiers in Chemistry





frontiers

Frontiers eBook Copyright Statement

The copyright in the text of individual articles in this eBook is the property of their respective authors or their respective institutions or funders. The copyright in graphics and images within each article may be subject to copyright of other parties. In both cases this is subject to a license granted to Frontiers.

The compilation of articles constituting this eBook is the property of Frontiers.

Each article within this eBook, and the eBook itself, are published under the most recent version of the Creative Commons CC-BY licence.

The version current at the date of publication of this eBook is CC-BY 4.0. If the CC-BY licence is updated, the licence granted by Frontiers is automatically updated to the new version.

When exercising any right under the CC-BY licence, Frontiers must be attributed as the original publisher of the article or eBook, as applicable.

Authors have the responsibility of ensuring that any graphics or other materials which are the property of others may be included in the CC-BY licence, but this should be checked before relying on the CC-BY licence to reproduce those materials. Any copyright notices relating to those materials must be complied with.

Copyright and source acknowledgement notices may not be removed and must be displayed in any copy, derivative work or partial copy which includes the elements in question.

All copyright, and all rights therein, are protected by national and international copyright laws. The above represents a summary only. For further information please read Frontiers' Conditions for Website Use and Copyright Statement, and the applicable CC-BY licence.

ISSN 1664-8714

ISBN 978-2-88966-078-0

DOI 10.3389/978-2-88966-078-0

About Frontiers

Frontiers is more than just an open-access publisher of scholarly articles: it is a pioneering approach to the world of academia, radically improving the way scholarly research is managed. The grand vision of Frontiers is a world where all people have an equal opportunity to seek, share and generate knowledge. Frontiers provides immediate and permanent online open access to all its publications, but this alone is not enough to realize our grand goals.

Frontiers Journal Series

The Frontiers Journal Series is a multi-tier and interdisciplinary set of open-access, online journals, promising a paradigm shift from the current review, selection and dissemination processes in academic publishing. All Frontiers journals are driven by researchers for researchers; therefore, they constitute a service to the scholarly community. At the same time, the Frontiers Journal Series operates on a revolutionary invention, the tiered publishing system, initially addressing specific communities of scholars, and gradually climbing up to broader public understanding, thus serving the interests of the lay society, too.

Dedication to Quality

Each Frontiers article is a landmark of the highest quality, thanks to genuinely collaborative interactions between authors and review editors, who include some of the world's best academicians. Research must be certified by peers before entering a stream of knowledge that may eventually reach the public - and shape society; therefore, Frontiers only applies the most rigorous and unbiased reviews.

Frontiers revolutionizes research publishing by freely delivering the most outstanding research, evaluated with no bias from both the academic and social point of view. By applying the most advanced information technologies, Frontiers is catapulting scholarly publishing into a new generation.

What are Frontiers Research Topics?

Frontiers Research Topics are very popular trademarks of the Frontiers Journals Series: they are collections of at least ten articles, all centered on a particular subject. With their unique mix of varied contributions from Original Research to Review Articles, Frontiers Research Topics unify the most influential researchers, the latest key findings and historical advances in a hot research area! Find out more on how to host your own Frontiers Research Topic or contribute to one as an author by contacting the Frontiers Editorial Office: researchtopics@frontiersin.org

THE CHEMISTRY OF BIOFILMS AND THEIR INHIBITORS

Topic Editors:

Sergio F. Sousa, University of Porto, Portugal

Manuel Simões, University of Porto, Portugal

Nenad Filipović, University of Belgrade, Serbia

Citation: Sousa, S. F., Simões, M., Filipović, N., eds. (2020). The Chemistry of Biofilms and Their Inhibitors. Lausanne: Frontiers Media SA. doi: 10.3389/978-2-88966-078-0

Table of Contents

- 04 Editorial: The Chemistry of Biofilms and Their Inhibitors**
Sérgio F. Sousa, Manuel Simões and Nenad Filipović
- 06 Antimicrobial Activity of Naturally Occurring Phenols and Derivatives Against Biofilm and Planktonic Bacteria**
Danica J. Walsh, Tom Livinghouse, Darla M. Goeres, Madelyn Mettler and Philip S. Stewart
- 19 Small Molecule Anti-biofilm Agents Developed on the Basis of Mechanistic Understanding of Biofilm Formation**
Katrine Qvortrup, Louise Dahl Hultqvist, Martin Nilsson, Tim Holm Jakobsen, Charlotte Uldahl Jansen, Jesper Uhd, Jens Bo Andersen, Thomas E. Nielsen, Michael Givskov and Tim Tolker-Nielsen
- 46 Bacterial Biofilm Eradication Agents: A Current Review**
Anthony D. Verderosa, Makrina Totsika and Kathryn E. Fairfull-Smith
- 63 Applications and Perspectives of Cascade Reactions in Bacterial Infection Control**
Yuanfeng Li, Guang Yang, Yijin Ren, Linqi Shi, Rujiang Ma, Henny C. van der Mei and Henk J. Busscher
- 76 Lipid-Based Antimicrobial Delivery-Systems for the Treatment of Bacterial Infections**
Da-Yuan Wang, Henny C. van der Mei, Yijin Ren, Henk J. Busscher and Linqi Shi
- 91 Rapid Release Polymeric Fibers for Inhibition of *Porphyromonas gingivalis* Adherence to *Streptococcus gordonii***
Mohamed Y. Mahmoud, Sonali Sapare, Keegan C. Curry, Donald R. Demuth and Jill M. Steinbach-Rankins
- 107 Immobilized Acylase PvdQ Reduces *Pseudomonas aeruginosa* Biofilm Formation on PDMS Silicone**
Jan Vogel, Marijke Wakker-Havinga, Rita Setroikromo and Wim J. Quax
- 116 Screening for Diguanylate Cyclase (DGC) Inhibitors Mitigating Bacterial Biofilm Formation**
Kyu Hong Cho, R. Grant Tryon and Jeong-Ho Kim
- 126 Hit Identification of New Potent PqsR Antagonists as Inhibitors of Quorum Sensing in Planktonic and Biofilm Grown *Pseudomonas aeruginosa***
Fadi Soukarieh, Ruiling Liu, Manuel Romero, Shaun N. Roberston, William Richardson, Simone Lucanto, Eduard Vico Oton, Naim Ruhul Qudus, Alaa Mashabi, Scott Grossman, Sadiqur Ali, Tomás Sou, Irena Kukavica-Ibrulj, Roger C. Levesque, Christel A. S. Bergström, Nigel Halliday, Shailesh N. Mistry, Jonas Emsley, Stephan Heeb, Paul Williams, Miguel Cámara and Michael J. Stocks



Editorial: The Chemistry of Biofilms and Their Inhibitors

Sérgio F. Sousa^{1*†}, Manuel Simões^{2*†} and Nenad Filipović^{3*†}

¹ UCIBIO@REQUIMTE, BioSIM, Departamento de Biomedicina, Faculdade de Medicina, Universidade do Porto, Porto, Portugal, ² LEPABE, Department of Chemical Engineering, Faculty of Engineering, University of Porto, Porto, Portugal, ³ Department of Chemistry and Biochemistry, Faculty of Agriculture, University of Belgrade, Belgrade, Serbia

Keywords: biofilms, virtual screening, antibiotics, antimicrobials, bacterial infections

Editorial on the Research Topic

The Chemistry of Biofilms and Their Inhibitors

OPEN ACCESS

Edited and reviewed by:

Simone Brogi,
Department of Pharmacy, University of
Pisa, Italy

*Correspondence:

Sérgio F. Sousa
sergiofsousa@med.up.pt
Manuel Simões
mvs@fe.up.pt
Nenad Filipović
nenadf@agrif.bg.ac.rs

†ORCID:

Sérgio F. Sousa
orcid.org/0000-0002-6560-5284
Manuel Simões
orcid.org/0000-0002-3355-4398
Nenad Filipović
orcid.org/0000-0003-2982-5324

Specialty section:

This article was submitted to
Medicinal and Pharmaceutical
Chemistry,
a section of the journal
Frontiers in Chemistry

Received: 10 July 2020

Accepted: 17 July 2020

Published: 20 August 2020

Citation:

Sousa SF, Simões M and Filipović N
(2020) Editorial: The Chemistry of
Biofilms and Their Inhibitors.
Front. Chem. 8:746.
doi: 10.3389/fchem.2020.00746

Over the past few years, biofilm research has moved to the spotlight, resulting in a strong increase in the researchers studying such highly structured microbial community and in the number of articles published per year. The large body of work made available enabled the broadening of research in this field to new disciplines and methods, moving from the cellular level to new complementary perspectives that tackle the problem from a molecular and atomic level—the chemical perspective—focusing on how the molecules involved interact, the bonds formed and their stability, the specific conformations adopted, etc. At the moment, a number of molecular targets to counteract biofilm formation and development as well as synthetic and natural inhibitors are known. For some known antibiofilm agents, the mechanisms of action are still unknown. The future development in the field of antibiofilm agents needs to be shifted to computational design and synthesis of novel multi-targeting compounds as a more effective strategy for the treatment of multi-factorial diseases.

This special issue “The Chemistry of Biofilms and Their Inhibitors” compiles four original articles and five reviews outlining the most innovative researches regarding the chemistry of biofilms and chemical innovations to understand biofilm formation and promote its inhibition.

Soukariéh et al. reported the synthesis and biological evaluation of a new series of potent *Pseudomonas* quinolone signal regulator (PqsR) antagonists able to inhibit planktonic and biofilm grown of different strains of *Pseudomonas aeruginosa*. The work involved the hit-to-lead optimization, following an initial virtual screening of the University of Nottingham Managed Chemical Compound Collection (85,061 compounds), using OpenEye docking and *in vitro* screening of the top 500 results. The optimized compound showed very high inhibition activity against *P. aeruginosa* pyocyanin production and *Pseudomonas* quinolone signal (Pqs) system signaling, in both planktonic cultures and biofilms.

The contribution by Vogel et al. shows that the immobilization of acylase PvdQ (an N-terminal nucleophile hydrolase that is a part of the pyoverdine gene cluster, *pvd*) on polydimethylsiloxane silicone (PDMS) creates a surface with quorum quenching properties that significantly reduces biofilm formation by *P. aeruginosa*. These results suggest this as promising strategy to control infections by minimizing the colonization of indwelling medical devices such as urinary or intravascular catheters.

The contribution by Walsh et al. reports the antimicrobial activity of a variety of naturally occurring phenols and their derivatives, against *Staphylococcus epidermidis* and *P. aeruginosa* present in biofilm and in the planktonic state. In particular, the authors have evaluated thymol, carvacrol and eugenol, and their allyl, 2-methylallyl and propyl derivatives. The results demonstrated that for the bacteria in the planktonic state, the presence of an allyl group leads to an increase in

potency for both thymol and carvacrol. However, the parent compounds exhibited higher activity than their derivatives against bacteria in biofilms. A similar effect was observed for guaiacol/eugenol molecules, with the larger molecule (eugenol) exhibiting higher activity toward the bacteria in the planktonic state while the smaller one (guaiacol), displays higher activity in biofilms. The results stress the importance of performing biofilm assays to develop structure-activity relationships when the objective is to target biofilms.

The contribution of Mahmoud et al. reports the development and characterization of a rapid-release platform, composed of polymeric electrospun fibers (EF) that encapsulate a peptide (BAR, SspB Adherence Region), previously developed by the authors and with confirmed antibiofilm activity *in vivo* and *in vitro*. The study reports also the evaluation of fiber safety and functionality against *Porphyromonas gingivalis*/*Streptococcus gordonii* biofilms *in vitro*, suggesting that BAR-incorporated EFs may provide a safe and specifically-targeted rapid-release platform to inhibit and disrupt dual-species biofilms in the oral cavity.

Li et al. presented a contribution on the application of cascade reactions involving reactive oxygen species in the control of bacterial infections. In this perspective, the authors reported the potential usefulness of cascade reactions as a new infection control strategy, while stressing the vast amount of work that still remains to be done in this field. In particular, the authors highlighted the need to increase the bacterial killing efficacy to clinically effective levels, preferentially by using endogenously available substrates.

Verderosa et al. contribution reviews the current status of bacterial biofilm eradication agents. In particular, the authors focus on the current understanding of biofilm antibiotic tolerance mechanisms, providing also an overview of biofilm remediation strategies and concentrating on the most promising biofilm eradication agents and approaches.

Wang et al. contribution focus on the current status on lipid-based antimicrobial delivery-systems for the treatment of bacterial infections. In this review, the authors focus on antimicrobial nanocarriers, including micelles and liposomes, at different levels of complexity and sophistication, describing the different types, preparation strategies, and their application in the treatment of infectious biofilms. Special emphasis is dedicated to the traditional problems faced in the antimicrobial treatment of infectious biofilms and the advantages offered by liposomal antimicrobial nanocarriers.

The contribution by Cho et al. reviews the currently identified inhibitors of diguanylate cyclase that interfere with bacterial biofilm inhibition, including natural molecules, c-di-GMP

analogs, GTP analogs and small synthetic molecules. Particular attention is dedicated to their mode of action, the methods of high-throughput screening and assay involved in their discovery and the chemical libraries used in screening.

Qvortrup et al. contributed with a review dedicated to small molecules with anti-biofilm activity developed on the basis of a molecular understanding of the mechanisms involved in the formation and dispersion of biofilms. Special emphasis is given to pilicides and curlicides, inhibiting the initial steps of biofilm formation by *Escherichia coli*; compounds interfering with c-di-GMP signaling in *P. aeruginosa* and *E. coli*; as well as compounds that inhibit quorum-sensing in *P. aeruginosa* and *Acinetobacter baumannii*.

It has been a pleasure to participate in the edition of this exciting topic of Frontiers in Chemistry. The issue brings together a wide variety of articles and reviews focusing on biofilms, from a chemical perspective. The editors hope that the articles will be of interest to researchers in the field of medicinal and pharmaceutical chemistry, particularly those working with biofilms.

AUTHOR CONTRIBUTIONS

All authors listed have made a substantial, direct and intellectual contribution to the work, and approved it for publication.

FUNDING

This work was supported by national funds from Fundação para a Ciência e a Tecnologia (grant numbers: IF/00052/2014 and UIDB/04378/2020; projects UIDB/EQU/00511/2020 and PTDC/BII-BTI/30219/2017—POCI-01-0145-FEDER-030219).

This work was prepared as a result of work based on the agreement between Faculty of Agriculture—University of Belgrade and Ministry of Education, Science and Technological Development of Republic of Serbia, contract number 451-03-68/2020-14/200116.

Conflict of Interest: The authors declare that the research was conducted in the absence of any commercial or financial relationships that could be construed as a potential conflict of interest.

Copyright © 2020 Sousa, Simões and Filipović. This is an open-access article distributed under the terms of the Creative Commons Attribution License (CC BY). The use, distribution or reproduction in other forums is permitted, provided the original author(s) and the copyright owner(s) are credited and that the original publication in this journal is cited, in accordance with accepted academic practice. No use, distribution or reproduction is permitted which does not comply with these terms.



Antimicrobial Activity of Naturally Occurring Phenols and Derivatives Against Biofilm and Planktonic Bacteria

Danica J. Walsh^{1,2}, Tom Livinghouse^{1*}, Darla M. Goeres², Madelyn Mettler² and Philip S. Stewart^{2*}

¹ Chemistry and Biochemistry, Montana State University, Bozeman, MT, United States, ² Center for Biofilm Engineering, Montana State University, Bozeman, MT, United States

OPEN ACCESS

Edited by:

Manuel Simões,
University of Porto, Portugal

Reviewed by:

Umer Rashid,
COMSATS University Islamabad,
Abbottabad Campus, Pakistan
Rosanna Papa,
Sapienza University of Rome, Italy

*Correspondence:

Tom Livinghouse
thomas.livinghouse@montana.edu
Philip S. Stewart
phil_s@montana.edu

Specialty section:

This article was submitted to
Medicinal and Pharmaceutical
Chemistry,
a section of the journal
Frontiers in Chemistry

Received: 11 June 2019

Accepted: 11 September 2019

Published: 01 October 2019

Citation:

Walsh DJ, Livinghouse T, Goeres DM,
Mettler M and Stewart PS (2019)
Antimicrobial Activity of Naturally
Occurring Phenols and Derivatives
Against Biofilm and Planktonic
Bacteria. *Front. Chem.* 7:653.
doi: 10.3389/fchem.2019.00653

Biofilm-forming bacteria present formidable challenges across diverse settings, and there is a need for new antimicrobial agents that are both environmentally acceptable and relatively potent against microorganisms in the biofilm state. The antimicrobial activity of three naturally occurring, low molecular weight, phenols, and their derivatives were evaluated against planktonic and biofilm *Staphylococcus epidermidis* and *Pseudomonas aeruginosa*. The structure activity relationships of eugenol, thymol, carvacrol, and their corresponding 2- and 4-allyl, 2-methallyl, and 2- and 4-*n*-propyl derivatives were evaluated. Allyl derivatives showed a consistent increased potency with both killing and inhibiting planktonic cells but they exhibited a decrease in potency against biofilms. This result underscores the importance of using biofilm assays to develop structure-activity relationships when the end target is biofilm.

Keywords: biofilm, antimicrobial, anti-biofilm, biofilm inhibition, essential oil

INTRODUCTION

Pseudomonas aeruginosa is a Gram-negative, rod shaped bacterium with a pronounced tendency to form biofilms. It is also an opportunistic pathogen that exhibits multidrug resistance (Hubble et al., 2018). Its ubiquity in hospital-acquired infection has provided impetus for advancements in treating infections and diminishing the number of associated illnesses. *Staphylococcus epidermidis* is a Gram-positive bacterium typically found on human skin and mucosa. This pathogen is known for causing infections in prosthetic joints and valves as well as in postoperative wounds and the urinary tract, due to catheter use. *S. epidermidis* is also among the five most common organisms found to cause hospital acquired infections (Sakimura et al., 2015). Unlike *P. aeruginosa*, *S. epidermidis* is typically a harmless commensal bacteria, although its ability to form biofilms increases its persistence on medical devices. With recent advances in understanding biofilm development, including molecular mechanisms and cell surface proteins of *S. epidermidis*, this opportunistic pathogen is gaining increased interest within the medical field (Büttner et al., 2015).

The majority of microorganisms in nature, including those responsible for hospital-acquired infections, live in association with surfaces as biofilms (Persat et al., 2015). Due to the secretion of proteins, extracellular DNA and polysaccharides, biofilm communities are encased in a robust matrix which reduces their susceptibility to antimicrobial agents as well as the immune system (Costerton et al., 1999; Donlan, 2001; Nadell et al., 2015; Otto, 2018). This poses a health concern

due to the potential for these organisms to cause serious infections in patients with indwelling medical devices and those who are undergoing surgical procedures, stressing the need for novel methods in treating biofilm mediated infections (Richards and Melander, 2009; Xu et al., 2017). According to the Agency for Health care Research and Quality, hospital-acquired infections are in the top 10 leading causes of death in the United States, and are consequently responsible for nearly 100 thousand deaths per year (Collins, 2008). Several methods to prevent and inhibit biofilm formation have been proposed or implemented to varying degrees of success including chemical and physical modification of surfaces and application of antimicrobial compounds (Chmielewski and Frank, 2003; Cortés et al., 2011; Artini et al., 2017).

Phenols constitute an extensive class of compounds that have been shown to present antimicrobial properties against a wide range of bacteria (Lucchini et al., 1990; Cronin and Schultz, 1996; Puupponen-Pimia et al., 2001; Maddox et al., 2010; Alves et al., 2013; Shahzad et al., 2015; Villalobos Mdel et al., 2016; Pinheiro et al., 2018). Maddox et al. (2010) demonstrated that low-molecular weight phenolic compounds inhibit the growth of *X. fastidiosa*, a Gram-negative bacterium and plant pathogen, *in vitro*. Alves et al. (2013) studied phenolic compounds and their activity against *S. epidermidis*, *E. coli*, *Past. Multocida*, *N. gonorrhoeae*, MRSA, and several other Gram-negative and Gram-positive bacteria. Several essential oils have also been shown to present antimicrobial properties against taxonomically diverse bacteria both in planktonic and biofilm assays (Filoche et al., 2005; Ceylan and Ugur, 2015; Snoussi et al., 2015; Yang et al., 2015). This includes a variety of phenolic essential oils that have been studied as therapeutic and antimicrobial agents, such as thymol (**1a**), carvacrol (**2a**), and eugenol (**3a**) (Figure 1) which are plant metabolites (Juven et al., 1994; Shetty et al., 1996; Rasooli and Mirmostafa, 2003; Friedman, 2014; Marchese et al., 2017; Memar et al., 2017; Pinheiro et al., 2018). In a 2018 study, Pinheiro et al. (2018) studied thymol (**1a**), carvacrol (**2a**), eugenol (**3a**), “ortho-eugenol” (**3b**) and guaiacol (**3c**) as well as several chlorinated and allyl phenyl ether derivatives; these compounds were shown to be active toward several bacteria including *S. aureus* and *P. aeruginosa*. Eugenol has also been successfully evaluated for its antibacterial, antifungal, antiviral, anti-parasitic, and anti-cancer activity (Knobloch et al., 1989; Raja, 2015). In another study by Friedman (2014) several bioactivities of carvacrol (**2a**), including cell membrane disruptive properties, are extensively evaluated. This article also concludes that carvacrol has great potential to be used as a therapeutic for human infection and disease.

A number of structurally diverse essential oils, including thymol (**1b**), carvacrol (**2a**), and eugenol (**3a**) have been evaluated for their antimicrobial and anti-biofilm properties. Essential oils have been shown to act as biofilm inhibitors against *Staphylococci* (Al-Shuneigat et al., 2005; Noumi et al., 2018; Patsilnakos et al., 2019) as well as *Pseudomonas* (Carezzano et al., 2017; Farisa Banu et al., 2017; Artini et al., 2018). Thymol (**1a**) and carvacrol (**2a**) have demonstrated anti-biofilm properties, both alone and as a mixture, against diverse bacteria including *Cryptococcus* (Kumari et al., 2017), *Salmonella*

(Cabarkapa et al., 2019), *Staphylococci* (Neyret et al., 2014), *Enterococcus* (Pazarci et al., 2019), and *Escherichia* (Perez-Conesa et al., 2006). Eugenol (**3a**) has also been shown to exhibit anti-biofilm properties against a variety of Gram-negative and Gram-positive bacteria including *Porphyromonas* (Zhang et al., 2017), *Salmonella* (Miladi et al., 2017), *Escherichia* (Perez-Conesa et al., 2006), and *Listeria* (Liu et al., 2015).

The mechanism of action of several structurally varied naturally occurring phenols has been studied against a variety of microorganisms. The antimicrobial activity of essential oils has generally been attributed to a cascade of reactions involving the bacterial cell, as opposed to a single mode of action, which lead to degradation of the cytoplasmic membrane, damage of membrane proteins, reduced ATP synthesis, and increased membrane permeability (Knobloch et al., 1989; Lucchini et al., 1990; Lambert et al., 2001; Nazzaro et al., 2013). It has also been well-documented that the hydrophobicity of essential oils contributes to their antimicrobial activity by enabling them to disrupt the lipid bilayer in bacterial cells (Sikkema et al., 1994; Carson et al., 2002).

Carvacrol has been shown to destabilize the cytoplasmic membrane, increasing membrane fluidity causing leakage of ions, a decrease in the pH gradient across the cytoplasmic membrane and inhibition of ATP synthesis in *Bacillus cereus* (Ultee et al., 2002). The importance of the hydroxyl group on the aromatic ring in carvacrol has also been demonstrated by comparing carvacrol with similar compounds such as carvacrol methyl ester, methanol, and cymene; which lack the hydroxyl group that carvacrol possesses (Dorman and Deans, 2000; Ultee et al., 2002). Ultee et al. observed that carvacrol is able to diffuse through the cytoplasmic membrane, becoming deprotonated and then binding to a monovalent cation such as potassium it is able to diffuse out of the cytoplasm where it again takes up a proton from the external environment, there for acting as a transmembrane carrier of monovalent cations (Ultee et al., 2002). Another study by Knobloch et al. (1989) discusses the antimicrobial activity of essential oils as causing damage to the biological membrane. Knobloch et al. also speculated that the acidity of the hydroxyl group on thymol and carvacrol may attribute to their antimicrobial activity as well.

The effect of eugenol on the cell membrane has also been examined using *C. albicans* (Latifah-Munirah et al., 2015), showing that eugenol, like carvacrol, also targets the cytoplasmic membrane. Another study by Xu et al. (2016), demonstrated that eugenol disrupts the cell wall of *S. aureus*, increasing permeability, causing leakage of cellular constituents and permanent damage to the cell membrane. Eugenol has also been shown to bind to proteins in *E. aerogenes* and inhibit the production of enzymes in *B. cereus*, causing degradation of the cell membrane (Thoroski et al., 1989; Wendakoon and Sakaguchi, 1995).

A variety of phenolic essential oils and other aromatic alcohols that are not evaluated in this study, have also been studied for their mode of action. Wu et al. (2016) reported the antimicrobial activity and mechanism of action of the natural occurring phenol, 3-p-trans-coumaroyl-2-hydroxyquinic acid. In this study it was shown that this phenol caused the loss of cytoplasmic

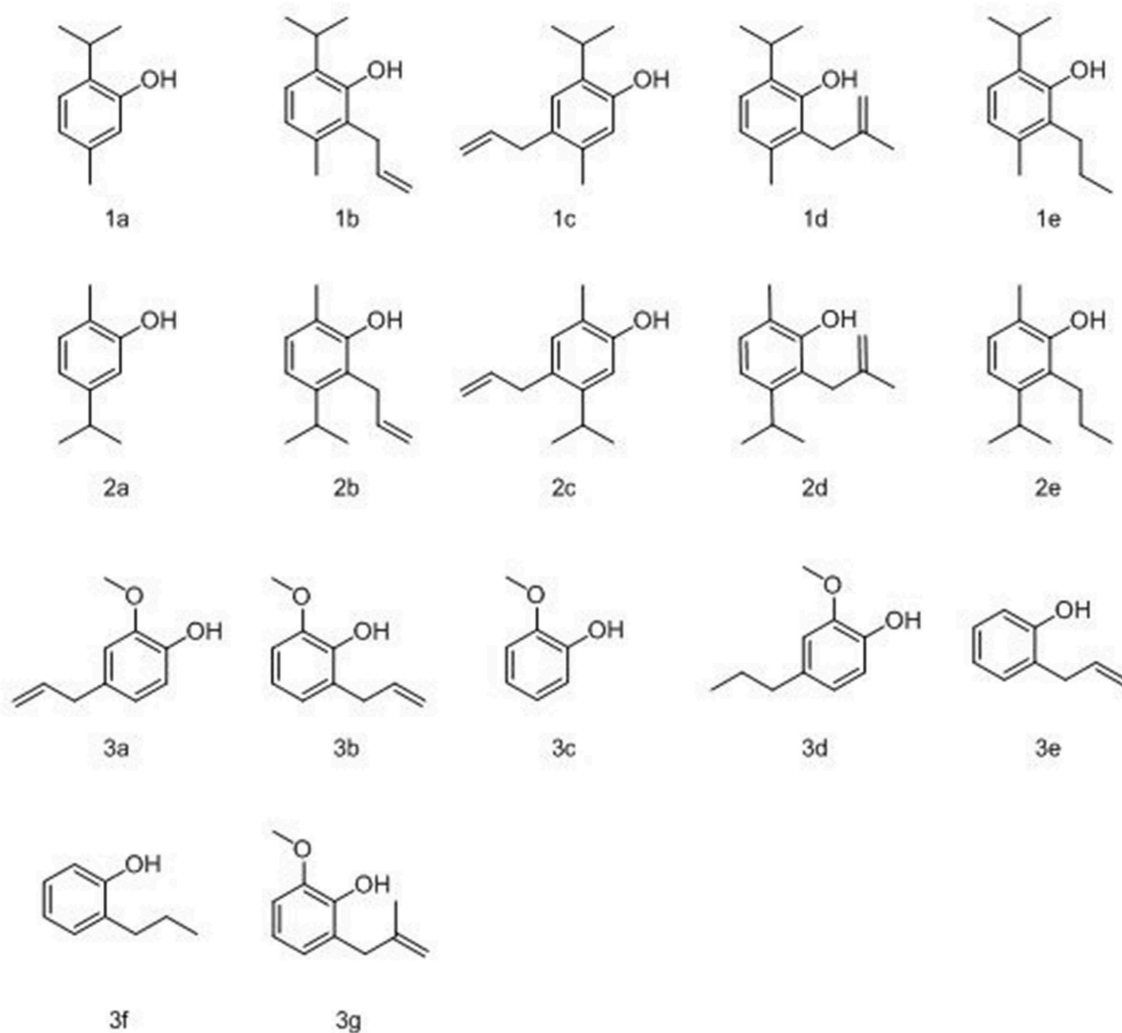


FIGURE 1 | Structures of parent compounds, thymol (**1a**), carvacrol (**2a**), and eugenol (**3a**) as well as allyl (**1b/c**, **2b/c**, and **3b/e**), 2-methylallyl (**1d**, **2d**, and **3g**), and propyl (**1e**, **2e**, and **3d/f**) derivatives.

membrane integrity, increased membrane fluidity and caused conformational changes in membrane proteins of *S. aureus*. Aromatic alcohols such as phenoxyethanol have also shown to increase permeability of the cytoplasmic membrane in *E. coli* (Gilbert et al., 1977; Fitzgerald et al., 1992).

In this communication, thymol (**1a**), carvacrol (**2a**), and eugenol (**3a**) as well as guaiacol are evaluated along with several 2- and 4- allyl, 2-methylallyl and 2-*n*-propyl derivatives (**Figure 1**). Thymol (**1a**), carvacrol (**2a**), and eugenol (**3a**) have also been evaluated for their ability to inhibit adherence and biofilm formation as well as biofilm eradication (Nostro et al., 2007; El Abed et al., 2011; Adil et al., 2014; Burt et al., 2014; Moran et al., 2014; Ceylan and Ugur, 2015; Kifer et al., 2016; Kim et al., 2016; Gaio et al., 2017; Lee et al., 2017; Miladi et al., 2017; Oh et al., 2017; Raei et al., 2017; Mohamed et al., 2018; Vazquez-Sanchez et al., 2018). Oh et al. (2017) has shown that thymol (**1a**) and carvacrol (**2a**) have anti-biofilm effects on the formation of *E.*

coli and *Salmonella*. Unlike previous studies, the parent phenolic compounds are being compared to their allyl, methylallyl, and propyl derivatives, which have not been extensively evaluated against either planktonic cells or biofilms.

Thymol (**1a**) and carvacrol (**2a**) are both monoterpenes and are constitutional isomers found in thyme, oregano, bergamot, and other culinary herbs (**Figure 1**). Both are used as a flavoring agents as well as in tinctures for their antifungal, antibacterial, and antiprotozoal properties (Escobar et al., 2010; Marchese et al., 2016). Eugenol (**3a**) is an essential oil found in plants such as vanilla, clove, nutmeg, and cinnamon. It is a flavoring agent utilized as well as for its antibacterial and anti-inflammatory properties (Marchese et al., 2017; Tsai et al., 2017). Guaiacol (**3c**) was also evaluated and is a naturally occurring phenol found in guaiacum, a shrub in the Zygophyllaceae family, and in creosote wood. It is structurally similar to eugenol, although it lacks the 4-allyl appendage. Guaiacol's ability to inhibit planktonic cell

growth as well as biofilm formation in a mixture has also been evaluated (Cooper, 2013; Pinheiro et al., 2018). In this study, these four compounds and several of their derivatives have been assessed for potency toward inhibiting planktonic cell growth as well as their ability to eradicate biofilms.

The 2- and 4-allyl (**1b**, **2b**, **1c**, and **2c**), *n*-propyl (**1e** and **2e**) and 2-methallyl (**1d** and **2d**) derivatives of thymol and carvacrol as well as the 4-*n*-propyl derivative of eugenol (**3d**) and 2-allyl and 2-methallyl derivative of guaiacol (**3b** and **3g**) were evaluated, all of which are previously synthesized derivatives of these essential oils (Bartz et al., 1935; Lupo et al., 2000; Tsang and Brimble, 2007; Horáček et al., 2013) (Figure 1). None of these derivatives have previously been evaluated for their antimicrobial activity against biofilms. The corresponding allyl ether derivatives of thymol (**1a**) and carvacrol (**1b**) have been studied, Pinheiro et al. (2018) although to our knowledge the 2- and 4- allyl derivatives as well as 2-methallyl and 2-propyl derivatives have yet to be evaluated against both planktonic cells and biofilms in the same study. This study not only evaluates the potency of the derivatives stated above against planktonic cells but against biofilms as well, illustrating the difference in potency and trends in potency between these two modes of microbial growth. The structures that are being evaluated here are allyl, methallyl, or propyl groups and whether these groups increase potency of the selected essential oils. The addition of an allyl group was selected in effort to increase lipophilicity, and thus to increase permeability toward the cell membrane. Lacey and Binder (2016) also demonstrated that ethylene binds to an ethylene binding protein in *Synechocystis* affecting pili, which are binding proteins. The 2-methallyl group was also selected to increase lipophilicity.

The simple analogs 2-allylphenol (**3e**) and 2-*n*-propylphenol (**3f**) were also evaluated for comparative purposes to the aforementioned 2-allyl derivatives of the selected essential oils. The purpose of this investigation was to develop structure activity relationships for naturally occurring phenol derivatives and to compare these relationships between planktonic and biofilm modes of bacterial growth.

MATERIALS AND METHODS

Experimental General Information

Thymol (**1a**) (99% pure), carvacrol (**2a**) (95% pure), guaiacol (99% pure), 2-allyl phenol (95% pure), and eugenol (**3a**) (99% pure) were purchased from Tokyo Chemical Industry Co. (TCI). All other reagents for chemical synthesis were purchased from commercial sources and used as received without further purification. Solvents for filtrations, transfers, and chromatography were certified ACS grade. Thin layer chromatography was performed on Silicycle Glass Backed TLC plates, and visualization was accomplished with UV light (254 nm), and/or potassium permanganate. All ¹H NMR spectra were recorded on a Bruker DRX300. All ¹³C NMR spectra were recorded on a Bruker DRX500, all NMR data was reported in ppm, employing the solvent resonance as the internal standard.

Pseudomonas aeruginosa (PA01 and PA015442) and *S. epidermidis* (35984) were obtained from American Type Culture

Collection (ATCC). All bacteria were sub-cultured onto tryptic soy agar (TSA) plates and incubated at 37°C for 24 h. Single colonies were transferred from the plates and inoculated into 25 mL tryptic soy broth (TSB) in Erlenmeyer flasks. Culture were incubated 37°C for 24 h and 10 µL of culture was transferred into 25 mL of TSB and the absorbance was read at 600 nm using a spectrophotometer and standardized to 10⁶-10⁷ CFU/mL.

Efficacy of Naturally Occurring Phenols and Derivatives on Inhibiting Planktonic Cells

The minimum inhibitory concentrations (MICs) of all compounds against *S. epidermidis* and *P. aeruginosa* were determined using a 96-well plate assay previously described by Xie et al. (2012). The data from at least three replicates were evaluated for each compound tested. Samples were diluted in dimethyl sulfoxide (DMSO) and DMSO controls were conducted as the negative control. Experiments were done in biological triplicate and technical duplicates were done. Tests for statistical significance were calculated with a two-tailed *t*-test assuming unequal variances.

Efficacy of Naturally Occurring Phenols and Derivatives on Killing Planktonic Cells

Parent compounds (**1a**, **2a**, and **3a**) were used as reference standards for each synthesized derivative. Both strains were cultured as described above. Compounds were diluted in 9.9 mL Phosphate-buffered saline (PBS) and 0.1 mL DMSO. Each tube was inoculated and allowed to sit at room temperature for 5 h, with sampling every hour. For sampling, three 10-fold dilutions were made in PBS. Each dilution was drop plated using 50 µL. Plates were incubated for 24 h and colony forming units (CFU) were counted. The concentration which showed no CFUs after 5 h was established as the lowest concentration which allowed for no bacterial growth. Negative controls with 9.9 mL PBS and 0.1 mL DMSO were done as well. Experiments were done in biological triplicate and technical duplicates were done. Standard deviations were determined by calculating the standard deviation for data from triplicate experiments. The mean log reduction was also determined for each compound evaluated using the following equation:

$$\text{Log reduction} = \log_{10} \left(\frac{A}{B} \right)$$

where, *A* is the average number of CFU before treatment and *B* is the average number of CFU after treatment.

Efficacy of Naturally Occurring Phenols and Derivatives on Biofilms

Biofilm Eradication Concentration Assays

Parent compounds (**1a**, **2a**, and **3a**) were used as reference standards for each synthesized derivative. Both strains were cultured as described above and biofilms were grown in Costar polystyrene 96-well plates at 37°C. After 24 h of incubation, the planktonic-phase cells were gently removed and the wells washed three times with PBS. Wells were filled with 150 µL

dilutions of the compound being evaluated. The 96-well plates were incubated for an additional 24 h at 37°C. The media was gently removed and each well filled with 150 μ L PBS and the biofilm broken up through stirring with sterile, wooden rods. Three 10-fold dilutions of each sample were taken and drop plated on TSA plates and incubated for 24 h. The biofilm eradication concentration (BEC) was determined to be the lowest concentration at which no bacterial growth occurred. This procedure was modeled based on previously reported procedures according to Pitts et al. (2003). Negative controls were also conducted with 150 μ L PBS in the absence of antimicrobial agent. Experiments were done in biological triplicate and technical duplicates were done. Tests for statistical significance were calculated with a two-tailed *t*-test assuming unequal variances.

Center for Disease Control (CDC) Biofilm Reactor Evaluation

The parent compound eugenol (**3a**) was used as a reference standards for the synthesized derivatives. A CDC biofilm reactor was also used to assess potency of compounds toward biofilms. American Society for Testing and Materials (ASTM) method E2562–17 which describes how to grow a biofilm in the CDC biofilm reactor under high shear and continuous flow, and ASTM method E2871–13, a biofilm efficacy test generally known as the single tube method were used for this procedure. Formation of 48 h biofilms in a CDC reactor was formed on glass coupons (4.02 cm²). A CDC reactor containing 340 mL of TSB (300 mg/L) was inoculated with 1 mL of a 3.21×10^8 CFU/mL overnight culture of *P. aeruginosa* (PA015442), which was grown in TSB (300 mg/L) overnight. The biofilm was grown in batch condition at room temperature at 125 rpm for 24 h, and then for 24 h at room temperature under continuous flow with a feed rate of 11.25 mL/min at 125 rpm. The continuous feed TSB was 100 mg/L. Coupons were then sampled from the reactor in triplicate. The mean log reduction in viable biofilms cells exposed to each compound for 1 h was quantitatively measured according to ASTM method E2871–13. After coupons were removed from the CDC reactor they were rinsed and transferred to separate, 50 mL conical tubes and 4 mL of a 100 mM solution of the antimicrobial compound being tested in sterile PBS buffer was added. The tubes were incubated at room temperature under static conditions or 1 h. After 1 h 36 mL DE broth was added and the biofilm was disaggregated by a series of vortexing and sonicating for 30 s each in the order of v/s/v/s/v. Each sample was diluted 10-fold six times and the diluted samples were drop plated on (Reasoner's 2A agar) R2A agar plates, incubated overnight at 37°C and enumerated. Experiments were done in biological duplicate and technical duplicates were done. The mean log reduction was also determined for each compound evaluated using the following equation:

$$\text{Log reduction} = \log_{10} \left(\frac{A}{B} \right)$$

where, *A* is the average number of CFU before treatment and *B* is the average number of CFU after treatment.

Chemical Synthesis Procedures

Preparation of

2-(2-propen-1-yl)-6-(1-methylethyl)-3-methylphenol (**1b**). Representative Procedure

A 25 mL round-bottom flask equipped with a magnetic stirring bar was charged with thymol **1a** (751 mg, 5 mmol, 1 equiv) and anhydrous acetone (5 mL) was added. Finely pulverized potassium carbonate (1.4 g, 10 mmol, 2 equiv) was then added at room temperature with stirring. The reactant mixture was heated to reflux and allyl bromide (0.5 mL, 6 mmol, 1.2 equiv) was added. The reactant mixture was heated to reflux for 5 h. The resulting mixture was cooled and filtered through celite, washed with brine and concentrated in vacuo to remove solvent and the by-product of diallyl ether. The crude phenyl ether was dissolved in *N,N*-diethylaniline (2 mL) and heated to 200°C with stirring for 12 h. *N,N*-diethylaniline was subsequently removed by washing the mixture with 10% sulfuric acid and extracting with ethyl acetate. The residue was purified via column chromatography (25% EtOAc/Hexane for elution) to afford 742 mg (78%) of **1b** as a yellow oil. ¹H NMR data taken in CDCl₃ and analytical data included the following. ¹H NMR (300 MHz, CDCl₃) **1b**: δ 6.98 (d, *J* = 7.82 Hz, 1H), 6.77 (d, *J* = 7.82 Hz, 1H), 5.95 (m, 1H), 5.12 (m, 2H), 4.93 (s, 1H), 3.44 (d, *J* = 5.88 Hz, 2H), 3.16 (sept, *J* = 6.87 Hz, 1H), 2.26 (s, 3H), 1.24 (d, *J* = 6.87 Hz, 6H). ¹³C NMR (500 MHz, CDCl₃) **1b**: δ 19.2 (CH₂), 22.9 (CH₃), 26.8 (CH₂), 29.3 (CH), 115.6 (CH₂), 124.3 (C), 128.8 (CH), 132.1 (C), 134.7 (CH), 137.3 (CH), 139.4 (C), 150.7 (C). ¹H NMR (300 MHz, CDCl₃) Spectral data and general procedures for compounds **1c**, **1d**, **2b**, **2c**, **2d**, and **3b** can be found in the **Supplementary Data**.

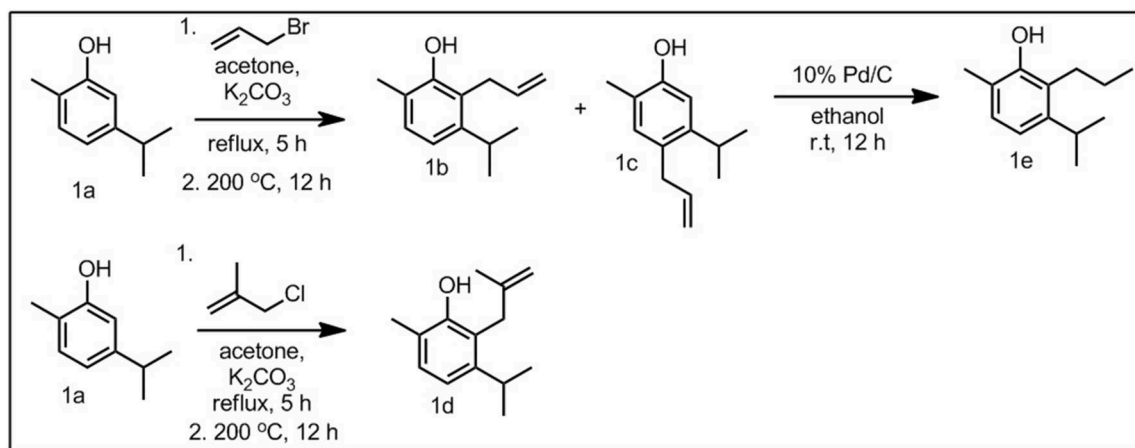
Preparation of

2-(2-*n*-propyl)-6-(1-methylethyl)-3-methylphenol (**1c**). Representative Procedure

A 10 mL round-bottom flask was charged with 10% Pd/C (30 mg, 0.28 mmol, 0.1 equiv). The round-bottom flask was put under an atmosphere of hydrogen and 100% ethanol (2 mL) was added. 2-allylthymol (**1b**) (300 mg, 1.5 mmol, 1 equiv) was added at room temperature and the reaction was allowed to stir for 12 h. The resulting mixture was filtered through silica and concentrated in vacuo to afford 260 mg (87%) of **1c** as a light, yellow oil. ¹H NMR data taken in CDCl₃ and analytical data included the following. ¹H NMR (300 MHz, CDCl₃) **1c**: δ 6.95 (d, *J* = 7.88 Hz, 1H), 6.81 (d, *J* = 7.88 Hz, 1H), 2.98 (sept, *J* = 6.81 Hz, 1H), 2.56 (t, *J* = 7.89 Hz, 2H), 2.25 (s, 3H), 1.59 (q, *J* = 7.89, 7.32 Hz, 2H), 1.36 (d, *J* = 6.81 Hz, 6H), 0.96 (t, *J* = 7.32 Hz, 3H). ¹³C NMR (500 MHz, CDCl₃) **1c**: δ 14.5 (CH₃), 19.4 (CH₃), 22.3 (CH₃), 22.7 (CH₂), 27.1 (CH₂), 28.8 (CH₂), 122.3 (CH), 123.1 (C), 126.5 (CH), 131.3 (CH), 134.7 (C), 150.8 (C). Spectral data and general procedures for compounds **2e**, **3d**, and **3f** can be found in the **Supplementary Data**.

RESULTS AND DISCUSSION

In this study, four 2-allyl derivatives were synthesized, with the corresponding 4-allyl derivative as a secondary product (**Scheme 1**). This was accomplished through the synthesis of



SCHEME 1 | Representative synthesis, using carvacrol (**1a**) and derivatives (**1b–1d**).

the corresponding allyl ether, followed by a thermal Claisen rearrangement. The allylated compounds **1b–3b**, **3a**, and **3e** were then hydrogenated to give the propyl derivatives (**1e**, **2e**, **3d**, and **3f**, **Figure 1**). Compounds **1a**, **2a**, and **3c** were also converted to the corresponding methallyl derivatives in an analogous manner.

In an initial study we assessed each naturally occurring phenol and its derivatives against planktonic cells. Studies have shown that thymol (**1a**) and carvacrol (**2a**) compromise the outer membrane of Gram-negative bacteria increasing the permeability of the cytoplasm (El Abed et al., 2011). The 2- and 4-allyl compounds for thymol (**1a**) and carvacrol (**2a**) all showed an increase in potency toward planktonic cells when compared to the parent compounds, as seen in **Table 1**. Interestingly, the 2-allyl derivatives (**1b** and **2b**) were more potent than the corresponding 4-allyl isomers (**1c** and **2c**) toward *P. aeruginosa*, whereas both isomers had identical MICs against *S. epidermidis* (**Table 1**). The transposed isomer “ortho-eugenol” (**3b**) was more potent toward both *S. epidermidis* and *P. aeruginosa* than the parent eugenol (**3a**). 4-*n*-propyl-2-methoxyphenol (**3d**) was more potent than eugenol (**3a**). Guaiacol (**3c**), which does not possess an allyl appendage was less potent toward *S. epidermidis* when compared to eugenol (**3a**) (**Table 1**). The methallyl derivative of carvacrol (**2d**) was more potent than the *n*-propyl derivative (**2e**) against *S. epidermidis*, though in the cases of methallyl thymol (**1d**) and methallyl eugenol (**3g**), the *n*-propyl derivatives (**1e** and **3f**) were more potent in comparison (**Table 1**).

Planktonic MICs of allyl derivatives were generally statistically significantly lower than the MIC of the parent compound. For example, the *p*-values for parent compounds and their allyl derivatives were also calculated. The *p*-value of **1a/b** against *S. epidermidis* is 0.041 and against *P. aeruginosa* is 0.025. The *p*-value of **2a/b** against *S. epidermidis* is 0.0003 and against *P. aeruginosa* is 0.0005. Likewise, the *p*-value of **3a/c** against *S. epidermidis* is 0.016 although against *P. aeruginosa* was calculated to be 0.42 due to the similarities in potency.

Time dependent killing data against planktonic bacteria were measured for all 2-allyl and parent compounds (**Figure 2**). It was shown that over the time period of 5 h, 2-allyl carvacrol

TABLE 1 | Minimum inhibitory concentrations in mM of parent compounds and derivatives against planktonic cells of *S. epidermidis* and *P. aeruginosa*.

Compound	MIC (mM)	
	<i>S. epidermidis</i> (35984)	<i>P. aeruginosa</i> (PA01)
Thymol (1a)	2.5	3.9
2-allylthymol (1b)	0.12	0.25
4-allylthymol (1c)	0.12	0.97
2-methylallylthymol (1d)	15	31.2
2- <i>n</i> -propylthymol (1e)	7.8	15.62
Carvacrol (2a)	2.5	3.9
2-allylcarvacrol (2b)	0.12	0.25
4-allylcarvacrol (2c)	0.12	0.97
2-methylallylcarvacrol (2d)	3.9	31.2
2- <i>n</i> -propylcarvacrol (2e)	7.8	15.62
Eugenol (3a)	15	31.2
ortho-eugenol (3b)	7.8	7.8
Guaiacol (3c)	31.2	31.2
2-methoxy-4- <i>n</i> -propylphenol (3d)	7.8	15.62
2-allylphenol (3e)	7.8	7.8
2- <i>n</i> -propylphenol (3f)	15.62	15.62
2-methylallyl-4-methoxyphenol (3g)	62.5	125

(**2b**) reduced bacterial growth by 79.80% against *S. epidermidis* and 79.63% against *P. aeruginosa*. The parent compound, carvacrol (**2a**), only reduced bacterial growth by 15.55% against *S. epidermidis* and 2.35% against *P. aeruginosa*. Similarly, 2-allyl thymol (**1b**) reduced the average bacterial growth by 79.00% for *S. epidermidis* and 77.93% for *P. aeruginosa*, while the average reduction of growth for thymol (**1a**) was 25.67% for *S. epidermidis* and 19.18% for *P. aeruginosa*. In the eugenol series, against *S. epidermidis*, eugenol (**3a**) and ortho eugenol (**3b**) had similar potency after 5 h with a decrease in bacterial growth of 79.76 and 79.34%, respectively. Although, at 4 h, eugenol (**3a**) was able to decrease growth by 79.76% while ortho eugenol (**3b**) decrease growth by 53.89%. Against *P. aeruginosa*, eugenol (**1a**) reduced

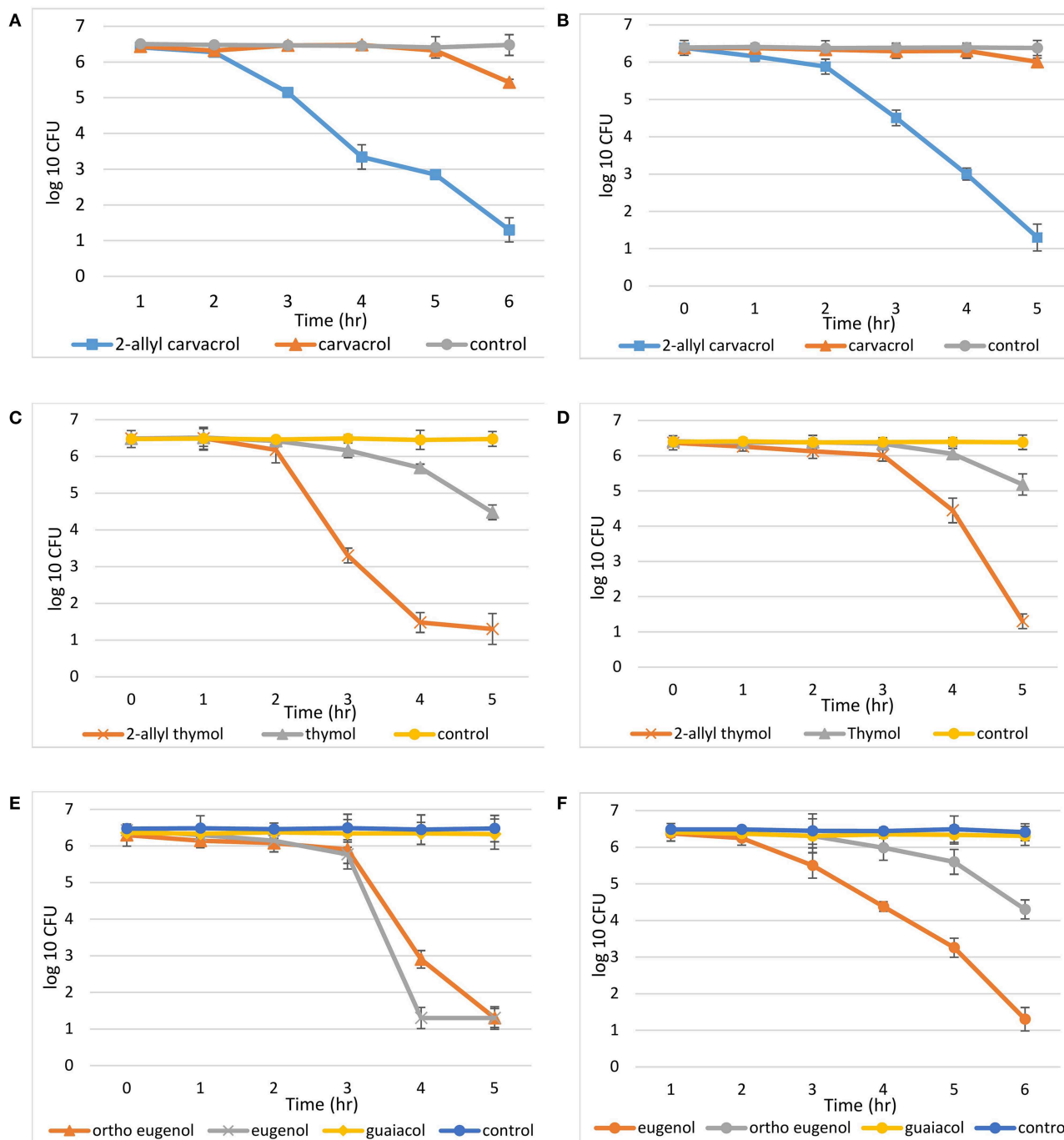


FIGURE 2 | Time kill assays. Compounds were diluted in PBS and DMSO, (9.9:0.1), all controls were PBS and DMSO: **(A)** carvacrol, 2-allyl carvacrol, and a control with *S. epidermidis*, while the concentration of both carvacrol and 2-allyl carvacrol was 1.7 mM; **(B)** carvacrol, 2-allyl carvacrol, and a control with *P. aeruginosa*. While the concentration of both carvacrol and 2-allyl carvacrol was 15.6 mM; **(C)** thymol, 2-allyl thymol, and a control with *S. epidermidis*, at a concentration of 7.8 mM; **(D)** thymol, 2-allyl thymol, and a control with *P. aeruginosa*, at a concentration of 30 mM; **(E)** eugenol, "ortho eugenol," guaiacol, and a control with *S. epidermidis*, at a concentration of 1.7 mM; **(F)** eugenol, "ortho eugenol," guaiacol, and a control with *P. aeruginosa*, at a concentration of 15.6 mM.

growth by 79.60%, while ortho eugenol (**3b**) reduced growth by 32.88%. Against both bacteria, guaiacol (**3c**) reduced growth by <2%. On average, the controls for each study showed a 0.079% decrease in growth for *S. epidermidis* and a 0.45% decrease in *P. aeruginosa*.

The mean log reduction after 5 h was recorded for all evaluated compounds as well (**Table 2**). In this assay the 2-allyl derivatives of thymol and carvacrol (**1b** and **2b**) exhibited greater potency than the parent compound. Like 2-allylthymol and 2-allyl carvacrol, eugenol (**3a**) also exhibited a 5 log reduction

TABLE 2 | Mean log reduction after 5 h against of exposure.

Compound	<i>S. epidermidis</i>		<i>P. aeruginosa</i>	
	Mean log reduction	Concentration (mM)	Mean log reduction	Concentrations (mM)
Thymol (1a)	1.9	7.8	1.2	30
2-allylthymol (1b)	5.1	7.8	5	30
Carvacrol (2a)	0.09	1.7	0.37	15.6
2-allylcarvacrol (2b)	5.1	1.7	5	15.6
Eugenol (3a)	5.2	1.7	5.1	15.6
Ortho-eugenol (3b)	2.6	1.7	2.1	15.6
Guaiacol (3c)	0.13	1.7	0.1	15.6

Concentrations of thymol and allyl thymol against *S. epidermis* was 7.8 and 30 mM against *P. aeruginosa*, while carvacrol, 2-allylcarvacrol, eugenol, ortho-eugenol, and guaiacol was exposed at 1.7 mM against *S. epidermidis* and 15.6 mM against *P. aeruginosa*.

after only 5 h, demonstrating that these allylate derivatives have bactericidal activity toward planktonic cells. Ortho-eugenol (**3b**) also exhibited a 5 log reduction against *S. epidermidis* after 5 h.

The lower mean log reduction further conveys the inferiority of thymol (**1a**) and carvacrol (**2a**) to their 2-allyl derivatives in killing bacteria (Table 2). This observation is consistent with the MIC data presented in Table 1. In the dynamic killing assay, eugenol (**3a**) was more potent than both guaiacol (**3c**) and “ortho-eugenol” (**3b**) with a mean log reduction of 5.2 against *S. epidermidis* and 5.1 against *P. aeruginosa* (Table 2). This corresponds to a differing trend in activity when compared to the MICs in Table 1, where “ortho-eugenol” (**3b**) demonstrated a stronger growth inhibition than eugenol (**3a**).

Efficacious concentrations varied greatly between MICs and BECs. BECs were consistently higher than MICs, conforming to the expected lower susceptibility of bacteria in the biofilm mode of growth. In addition, biofilm assays exhibited significant differences in the structure-activity relationship in comparison to planktonic results. Thymol (**1a**) and carvacrol (**2a**) continued to show a higher potency than their 2-*n*-propyl derivatives **1e** and **2e** (Table 1), although they were more potent than their 2-allyl derivatives **1b** and **2b** against biofilms (Table 3). The 4-allyl derivatives **1c** and **2c** however, did have an identical or a slightly lower BEC, against *P. aeruginosa* and thus were still more potent than their 2-allyl counterparts.

“Ortho-eugenol” (**3b**) continued to be more potent than eugenol (**3a**) against *P. aeruginosa* although the BECs for both compounds against *S. epidermidis* were identical. Guaiacol (**3c**) was the most potent against both bacteria in a biofilm when compared to other eugenol derivatives, which was dissimilar to the trend in potency against both killing and inhibiting planktonic cells (Table 1). The 4-*n*-propyl derivative of eugenol (**3d**) exhibited the same potency as “ortho-eugenol” (**3b**) against both bacteria (Table 3). It was interesting here that the MICs for the 4-*n*-propyl derivative **3d** were lower than eugenol (**3a**) against both bacteria tested, but the BEC against *S. epidermidis* was the same for both compounds (Table 3). This information illustrates that it is not reliable to predict structure activity relationships against biofilms based on planktonic cell data.

TABLE 3 | Biofilm eradication concentrations in mM of parent compounds and derivatives against *S. epidermidis* and *P. aeruginosa*.

Compound	BEC (mM)	
	<i>S. epidermidis</i>	<i>P. aeruginosa</i>
thymol (1a)	3.9	15.6
2-allylthymol (1b)	9.25	31.25
4-allylthymol (1c)	6.5	13
2- <i>n</i> -propylthymol (1e)	31.25	62.5
carvacrol (2a)	1.95	7.5
2-allylcarvacrol (2b)	9.25	31.25
4-allylcarvacrol (2c)	3.25	7.5
2- <i>n</i> -propylcarvacrol (2e)	31.25	62.5
eugenol (3a)	31.25	62.5
ortho-eugenol (3b)	31.25	31.25
guaiacol (3c)	7.8	15.6
2-methoxy-4- <i>n</i> -propylphenol (3d)	31.25	31.25

TABLE 4 | Mean log reductions of thymol, 2-allylthymol, and 2-*n*-propylthymol against *P. aeruginosa* (PA015442).

Compound	Mean log reduction	Concentration (mM)
Thymol (1a)	4.48	100
2-allylthymol (1b)	0.13	100
2- <i>n</i> -propylthymol (1e)	0.21	100

Unlike what was seen with MICs, the BECs of allyl derivatives were generally statistically significantly higher than the BECs of the corresponding parent compound. For example, the *p*-values for parent compounds and their allyl derivatives against biofilms were also calculated. The *p*-value of **1a/b** were calculated to 0.022 be against *S. epidermidis* and 0.019 against *P. aeruginosa*. The *p*-value of **2a/b** were calculated to be 0.009 against *S. epidermidis* and 0.023 against *P. aeruginosa*. The *p*-value of **3a/c** is 0.003 against *S. epidermidis* and 0.015 against *P. aeruginosa*.

A CDC Biofilm reactor assay was also used to substantiate the comparative efficacy of thymol and its allyl and *n*-propyl derivatives against *P. aeruginosa* (PA015442) (Table 4). Here biofilms were grown in a high shear environment as opposed to a static environment in 96-well plates as was done with BEC evaluations. This increases the biofilms adherence to the surface which it is grown. The CDC biofilm assay was chosen for this purpose. Methods were performed in accordance with ASTM; Designations: E 1054–08, E2562–17, and E2871–13. The *P. aeruginosa* strain (PA015442) used in this experiment was used because it was the strain named in the ASTM procedures. Results with the CDC biofilm reactor was consistent with the relative efficacies determined in the BEC assay (Tables 3, 4). Thymol (**1a**) had the highest mean log reduction, correlating with the highest potency (Table 4). The 2-allylthymol (**1b**) was less potent than the parent and the *n*-propyl derivative (**1e**).

MIC and BECs were also measured for strain PA015442 to compare with strain PA01 that was used with all other assays apart from the CDC biofilm reactor. As with strain PA01,

TABLE 5 | Biofilm eradication concentrations and minimum inhibitor concentrations of thymol, 2-allylthymol, and 2-*n*-propylthymol against *P. aeruginosa* PA015442, as well as mean log reduction at 100 mM.

	Mean log reduction	MIC (mM)	BEC (mM)
Compound	PA015442		
Thymol (1a)	4.48	0.68	1.37
2-allylthymol (1b)	0.13	0.08	6.5
2- <i>n</i> -propylthymol (1e)	0.21	3.125	25

2-allylthymol (**1b**) exhibited the highest degree of potency against planktonic cells of PA015442 with an MIC of 0.08 mM, whereas thymol (**1a**) had an MIC of 0.68 (Table 5). It was interesting that thymol (**1a**), 2-allylthymol (**1b**) and 2-*n*-propylthymol (**1e**) were more effective against PA015442 (Table 5) than against PA01 in biofilm assays; whereas thymol (**1a**) had a BEC of 15 mM, 2-allylthymol (**1b**) had a BEC of 31.25 mM and 2-*n*-propylthymol (**1e**) a BEC of 62.5 mM against the PA01 strain (Table 3). In planktonic cell assays, the three compounds evaluated against PA015442 were also more potent toward PA01 (Tables 3, 5). Again, in accordance with previously observed BEC trends, thymol (**1a**) exhibited a lower BEC than both 2-allylthymol (**1b**) and 2-*n*-propylthymol (**1e**) as seen in Table 5.

The addition of an allyl group to the naturally occurring phenols thymol (**1a**) and carvacrol (**2a**) increased the compounds potency toward both inhibiting and killing planktonic cells; although decreased their ability to eradicate biofilms. Similarly, the elimination of an allyl group from the essential oil eugenol (**3a**) decreased potency toward planktonic cells and increased potency toward biofilms.

Naturally occurring phenols such as thymol (**1a**), carvacrol (**2a**), and eugenol (**3a**) have been shown to present antimicrobial properties against both planktonic cells and biofilms (Nostro et al., 2007; El Abed et al., 2011; Adil et al., 2014; Burt et al., 2014; Ceylan and Ugur, 2015; Kifer et al., 2016; Lee et al., 2017; Miladi et al., 2017; Raei et al., 2017; Mohamed et al., 2018). Here we demonstrated that 2-allyl (**1b** and **2b**) and 4-allyl derivatives (**1c** and **2c**) of thymol (**1a**) and carvacrol (**2a**) showed an increase in potency in comparison to the parent compounds against planktonic cells in both growth inhibition and killing assays. In biofilm assays the opposite trend was always observed: the non-allylated, parent compounds exhibited a higher potency than the allyl derivatives. Similarly, the non-allylated guaiacol (**3c**) was less potent against planktonic bacteria but more potent than eugenol (**3a**) or ortho-eugenol (**3b**) against biofilm bacteria. These observations underscore that structure-activity relationships determined for planktonic bacteria can be completely different than those for biofilms formed by the same species.

The fact that structure-activity relationships diverge between planktonic and biofilm assays may indicate that these compounds experience different limitations to their efficacy against planktonic and biofilm forms of the bacteria. It can be for example, that the penetrations of the agents into the biofilm is rate-limiting. Alternatively it could be that the permeability

of the compounds into the cytoplasm of the cell becomes rate-limiting in the biofilm mode of growth. A third possibility is that the expression of molecular targets differs between planktonic and biofilm cells. If these mechanisms were better understood, it might be possible to rationally design superior anti-biofilm antimicrobial agents.

The 2-*n*-propyl derivatives (**1e** and **2e**) consistently were least potent compared to parent compounds and corresponding allyl derivatives. Here an allyl group will increase potency in comparison with a propyl group against both planktonic cells and biofilms. Both thymol (**1a**) and carvacrol (**2a**) have two alkyl groups, which are weakly electron donating. Eugenol (**3a**) in comparison has a methoxy group which is strongly electron donating as well as an allyl group; studies showed that eugenol (**3a**) was less potent than thymol (**1a**) and carvacrol (**2a**) in assays evaluating potency toward killing biofilms and inhibiting planktonic cell growth. Although was more efficacious toward killing planktonic cells, this is likely due to the presence of an allyl group.

Thymol (**1a**) and carvacrol (**2a**) are constitution isomers and had identical MICs against both *S. epidermidis* and *P. aeruginosa* (Table 1). The same was observed with their 2-allyl derivatives (**1b** and **2b**), as well as both 4-allyl derivatives (**1c** and **2c**) (Table 1). The 2-allyl derivative of thymol (**1b**) though, was less efficient in killing, as shown in Table 2, where the mean log reduction of thymol is 5.1 at 7.8 mM but the mean log reduction for carvacrol is 5.1 at 1.7 mM, although carvacrol (**2a**) was less potent than thymol (**1a**) (Table 2).

In biofilm eradication assays, carvacrol (**2a**) was more potent than thymol (**1a**) against both bacteria (Table 3). 4-allylcarvacrol (**2c**) was also more potent than 4-allylthymol (**1c**), although the 2-allyl derivatives exhibited the same BEC. Over all, there was very little difference in changing the allyl group from the 2 to the 4 position. The decreased potency of thymol against biofilms may result from the isopropyl group in the 2 position (Figure 1), creating more steric hindrance around the phenol, this would suggest that steric hindrance around the phenol has more of an affect with assays involving biofilms. Steric hindrance may play two different roles here; inhibiting permeation through the biofilm extracellular matrix, and obstruction of the alcohol group. These also may contribute to the observed decrease in potency with 2-allyl and 4-allyl derivatives against biofilms when compared to their parent compounds. The addition of an allyl group does slightly increase polarity, which may also inhibit the compounds ability to permeate through the biofilm matrix.

In the case of eugenol (**1b**), the 2-allyl derivative, “ortho-eugenol” (**3b**) was more potent in inhibiting planktonic cells of *S. epidermidis* although they shared the same BEC against *S. epidermidis*. **3b** also had lower BEC with *P. aeruginosa* with both planktonic cells and biofilms. This observation was in accordance with the trend found in thymol (**1a**) and carvacrol (**2a**) in which allyl derivatives were less affective against biofilms.

In this study, mammalian cells were not evaluated. Although oral LD₅₀ (median lethal dose) for carvacrol and thymol has been calculated in rats to be 810 mg/kg body weight and 980 mg/kg body weight, respectively (Jenner et al., 1964). Cytotoxicity of carvacrol and thymol was also evaluated against intestinal

cells (Caco-2), finding no cytotoxic effects of thymol although carvacrol was found to cause cell death (Llana-Ruiz-Cabello et al., 2014). In a study by Machado et al. (2011) concluded that eugenol did not exhibit cytotoxicity *in vitro* toward mammalian cells at the IC₅₀ determined for growth inhibition for *G. lamblia*.

Various structure activity relationships of antimicrobial compounds, including natural products and plant metabolites, and their potency toward planktonic cells and biofilms have been evaluated (Huigens et al., 2007; Richards et al., 2008, 2009; Catto et al., 2015; Garrison et al., 2015; Peeters et al., 2016; Yang et al., 2016; Choi et al., 2017; Gill et al., 2017). Richards et al. (2008) synthesized and assayed a 50-compound library of oroidin-based natural products for their anti-biofilm activity against two strains of *P. aeruginosa*, classifying several compounds as inhibitors of biofilm formation.

Structural factors such as stereochemistry, alkyl chain length, and substitution patterns have also been examined in the context of biofilms (Huigens et al., 2007; Choi et al., 2017; Gill et al., 2017). No uniform correlation of biofilm potency with planktonic potency is evident. Some studies show equipotent activity of compounds against planktonic cells and biofilms (Spoering and Lewis, 2001; Garrison et al., 2015), while other reports provide support that biofilms are more resistant to antimicrobials than planktonic cells (Costerton et al., 1999; Anderl et al., 2000; Donlan, 2001; Parsek and Singh, 2003) and still others have found that compounds exhibiting an increase in activity against planktonic cells also show increased potency against biofilms (Gill et al., 2017). The present study demonstrates that essential oil derivatives exhibiting greater activity against planktonic cells were often less effective when tested against biofilms.

CONCLUSION

The presence of an allyl group in either the 2 or 4 position relative to the hydroxy phenol increases the potency of the small, phenolic essential oils thymol (**1a**) and carvacrol (**2a**) when

evaluated against planktonic cells of both the Gram-positive *S. epidermidis* and the Gram-negative *P. aeruginosa*. In contrast, when the same compounds were evaluated against biofilms, the parent compounds were more potent. Similarly, eugenol (**3a**) which has an allyl group in the 4 position, was more potent than guaiacol (**3c**) against *S. epidermidis* in planktonic cell inhibition assays although less effective in killing planktonic cells and biofilms. The 2-methallyl derivatives (**1d**, **2d**, and **3g**) evaluated against planktonic cells were in all cases less potent than allyl; and when compared to propyl derivatives, were less potent the majority of the time. This study illustrates the importance of using biofilm assays to determine structure-activity relationships of antimicrobials when the end target is a biofilm.

DATA AVAILABILITY STATEMENT

All datasets generated for this study are included in the manuscript/**Supplementary Files**.

AUTHOR CONTRIBUTIONS

DW performed chemical synthesis and biological evaluation against biofilm and planktonic cells with support and project supervision from TL and PS. MM performed CDC biofilm reactor assays with support from DG. The manuscript was written by DW with input from all authors.

FUNDING

Generous funding for this research was provided by the National Institute for General Medical Science.

SUPPLEMENTARY MATERIAL

The Supplementary Material for this article can be found online at: <https://www.frontiersin.org/articles/10.3389/fchem.2019.00653/full#supplementary-material>

REFERENCES

- Adil, M., Singh, K., Verma, P. K., and Khan, A. U. (2014). Eugenol-induced suppression of biofilm-forming genes in *Streptococcus mutans*: an approach to inhibit biofilms. *J. Glob. Antimicrob. Resist.* 2, 286–292. doi: 10.1016/j.jgar.2014.05.006
- Al-Shuneigat, J., Cox, S. D., and Markham, J. L. (2005). Effects of a topical essential oil-containing formulation on biofilm-forming coagulase-negative staphylococci. *Lett. Appl. Microbiol.* 41, 52–55. doi: 10.1111/j.1472-765X.2005.01699.x
- Alves, M. J., Ferreira, I. C., Froufe, H. J., Abreu, R. M., Martins, A., and Pintado, M. (2013). Antimicrobial activity of phenolic compounds identified in wild mushrooms, SAR analysis and docking studies. *J. Appl. Microbiol.* 115, 346–357. doi: 10.1111/jam.12196
- Anderl, J. N., Franklin, M. J., and Stewart, P. S. (2000). role of antibiotic penetration limitation in klebsiella pneumoniae biofilm resistance to ampicillin and ciprofloxacin. *Antimicrob. Agents Chemother.* 44, 1818–1824. doi: 10.1128/AAC.44.7.1818-1824.2000
- Artini, M., Cicatiello, P., Ricciardelli, A., Papa, R., Selan, L., Dardano, P., et al. (2017). Hydrophobin coating prevents *Staphylococcus epidermidis* biofilm formation on different surfaces. *Biofouling* 33, 601–611. doi: 10.1080/08927014.2017.1338690
- Artini, M., Patsilnakos, A., Papa, R., Bozovic, M., Sabatino, M., Garzoli, S., et al. (2018). Antimicrobial and antibiofilm activity and machine learning classification analysis of essential oils from different Mediterranean plants against *Pseudomonas aeruginosa*. *Molecules* 23:482. doi: 10.3390/molecules23020482
- Bartz, Q. R., Miller, R. F., and Adams, R. (1935). The introduction of isobutyl groups into phenols, cresols and homologous compounds. *J. Am. Chem. Soc.* 57, 371–376. doi: 10.1021/ja01305a044
- Burt, S. A., Ojo-Fakunle, V. T. A., Woertman, J., and Veldhuizen, E. J. A. (2014). The natural antimicrobial carvacrol inhibits quorum sensing in *Chromobacterium violaceum* and reduces bacterial biofilm formation at sub-lethal concentrations. *PLoS ONE* 9:e93414. doi: 10.1371/journal.pone.0093414
- Büttner, H., Mack, D., and Rohde, H. (2015). Structural basis of *Staphylococcus epidermidis* biofilm formation: mechanisms and molecular interactions. *Front. Cell. Infect. Microbiol.* 5:14. doi: 10.3389/fcimb.2015.00014
- Cabarkapa, I., Colovic, R., Duragic, O., Popovic, S., Kokic, B., Milanov, D., et al. (2019). Anti-biofilm activities of essential oils rich in carvacrol

- and thymol against *Salmonella enteritidis*. *Biofouling* 35, 361–375. doi: 10.1080/08927014.2019.1610169
- Carezzano, M. E., Sotelo, J. P., Primo, E., Reinoso, E. B., Paletti Rovey, M. F., Demo, M. S., et al. (2017). Inhibitory effect of *Thymus vulgaris* and *Origanum vulgare* essential oils on virulence factors of phytopathogenic *Pseudomonas syringae* strains. *Plant Biol.* 19, 599–607. doi: 10.1111/plb.12572
- Carson, C. F., Mee, B. J., and Riley, T. V. (2002). Mechanism of action of *Melaleuca alternifolia* (tea tree) oil on *Staphylococcus aureus* determined by time-kill, lysis, leakage, and salt tolerance assays and electron microscopy. *Antimicrob. Agents Chemother.* 46:1914. doi: 10.1128/AAC.46.6.1914-1920.2002
- Catto, C., Dell'Orto, S., Villa, F., Villa, S., Gelain, A., Vitali, A., et al. (2015). Unravelling the structural and molecular basis responsible for the anti-biofilm activity of zosteric acid. *PLoS ONE* 10:e0131519. doi: 10.1371/journal.pone.0131519
- Ceylan, O., and Ugur, A. (2015). Chemical composition and anti-biofilm activity of *Thymus sipyleus* BOISS. subsp. *sipyleus* BOISS. var. *davisanus* RONNIGER essential oil. *Arch. Pharm. Res.* 38, 957–965. doi: 10.1007/s12272-014-0516-0
- Chmielewski, R. A. N., and Frank, J. F. (2003). Biofilm formation and control in food processing facilities. *Compr. Rev. Food Sci. Food Saf.* 2, 22–32. doi: 10.1111/j.1541-4337.2003.tb00012.x
- Choi, H., Ham, S.-Y., Cha, E., Shin, Y., Kim, H.-S., Bang, J. K., et al. (2017). Structure–activity relationships of 6- and 8-geraniol analogs as anti-biofilm agents. *J. Med. Chem.* 60, 9821–9837. doi: 10.1021/acs.jmedchem.7b01426
- Collins, A. S. (2008). “Advances in patient safety preventing health care-associated infections,” in *Patient Safety and Quality: An Evidence-Based Handbook for Nurses*, ed R. G. Hughes (Rockville, MD: Agency for Healthcare Research and Quality).
- Cooper, R. A. (2013). Inhibition of biofilms by glucose oxidase, lactoperoxidase and guaicol: the active antibacterial component in an enzyme alginate. *Int. Wound J.* 10, 630–637. doi: 10.1111/iwj.12083
- Cortés, M. E., Consuegra, J., and Ruben, D. S. (2011). Biofilm formation, control and novel strategies for eradication. *Sci. Against Microbial. Pathog. Commun. Curr. Res. Technol. Adv.* 2, 896–905.
- Costerton, J. W., Stewart, P. S., and Greenberg, E. P. (1999). Bacterial biofilms: a common cause of persistent infections. *Science* 284, 1318–1322. doi: 10.1126/science.284.5418.1318
- Cronin, M. T. D., and Schultz, T. W. (1996). Structure-toxicity relationships for phenols to *Tetrahymena pyriformis*. *Chemosphere* 32, 1453–1468. doi: 10.1016/0045-6535(96)00054-9
- Donlan, R. M. (2001). Biofilm formation: a clinically relevant microbiological process. *Clin. Infect. Dis.* 33, 1387–1392. doi: 10.1086/322972
- Dorman, H. J. D., and Deans, S. G. (2000). Antimicrobial agents from plants: antibacterial activity of plant volatile oils. *J. Appl. Microbiol.* 88, 308–316. doi: 10.1046/j.1365-2672.2000.00969.x
- El Abed, S., Saad, I., Latrache, H., Ghizlane, Z., Hind, M., and Remmal, A. (2011). Carvacrol and thymol components inhibiting *Pseudomonas aeruginosa* adherence and biofilm formation. *Afr. J. Microbiol. Res.* 5, 3229–3232. doi: 10.5897/AJMR11.275
- Escobar, P., Milena Leal, S., Herrera, L. V., Martinez, J. R., and Stashenko, E. (2010). Chemical composition and antiprotazoal activities of *Colombian Lippia* spp. essential oils and their major components. *Memórias Instituto Oswaldo Cruz* 105, 184–190. doi: 10.1590/S0074-02762010000200013
- Farisa Banu, S., Rubini, D., Rakshitaa, S., Chandrasekar, K., Murugan, R., Wilson, A., et al. (2017). Antiviral properties of underexplored cinnamomum tamala essential oil and its synergistic effects with DNase against *Pseudomonas aeruginosa* biofilms - an *in vitro* study. *Front. Microbiol.* 8:1144. doi: 10.3389/fmicb.2017.01144
- Filoche, S. K., Soma, K., and Sissons, C. H. (2005). Antimicrobial effects of essential oils in combination with chlorhexidine digluconate. *Oral Microbiol. Immunol.* 20, 221–225. doi: 10.1111/j.1399-302X.2005.00216.x
- Fitzgerald, K. A., Davies, A., and Russell, A. D. (1992). Mechanism of action of chlorhexidine diacetate and phenoxethanol singly and in combination against gram-negative bacteria. *Microbios* 70, 215–230.
- Friedman, M. (2014). Chemistry and multibeneficial bioactivities of carvacrol (4-isopropyl-2-methylphenol), a component of essential oils produced by aromatic plants and spices. *J. Agric. Food Chem.* 62, 7652–7670. doi: 10.1021/jf5023862
- Gaio, V., Lima, C. A., Oliveira, F., Franca, A., and Cerca, N. (2017). Carvacrol is highly disruptive against coagulase-negative staphylococci in *in vitro* biofilms. *Future Microbiol.* 12, 1487–1496. doi: 10.2217/fmb-2017-0122
- Garrison, A. T., Abouelhassan, Y., Kallifidas, D., Bai, F., Ukhanova, M., Mai, V., et al. (2015). Halogenated phenazines that potentially eradicate biofilms, MRSA persister cells in non-biofilm cultures, and *Mycobacterium tuberculosis*. *Angew. Chem.* 54, 14819–14823. doi: 10.1002/anie.201508155
- Gilbert, P., Beveridge, E. G., and Crone, P. B. (1977). Effect of phenoxyethanol on the permeability of *Escherichia coli* NCTC 5933 to inorganic ions. *Microbios* 19, 17–26.
- Gill, R. K., Kumar, V., Robijns, S. C. A., Steenackers, H. P. L., Van der Eycken, E. V., and Bariwal, J. (2017). Polysubstituted 2-aminoimidazoles as anti-biofilm and antiproliferative agents: discovery of potent lead. *Eur. J. Med. Chem.* 138, 152–169. doi: 10.1016/j.ejmech.2017.06.043
- Horáček, J., Štávková, G., Kelbichová, V., and Kubička, D. (2013). Zeolite-beta-supported platinum catalysts for hydrogenation/hydrodeoxygenation of pyrolysis oil model compounds. *Catal. Today* 204, 38–45. doi: 10.1016/j.cattod.2012.08.015
- Hubble, V. B., Hubbard, B. A., Minrovic, B. M., Melander, R. J., and Melander, C. (2018). Using small-molecule adjuvants to repurpose azithromycin for use against *Pseudomonas aeruginosa*. *ACS Infect. Dis.* 5, 141–151. doi: 10.1021/acsinfecdis.8b00288
- Huigns, R. W., Richards, J. J., Parise, G., Ballard, T. E., Zeng, W., Deora, R., et al. (2007). Inhibition of *Pseudomonas aeruginosa* biofilm formation with bromoageliferin analogues. *J. Am. Chem. Soc.* 129, 6966–6967. doi: 10.1021/ja069017t
- Jenner, P. M., Hagan, E. C., Taylor, J. M., Cook, E. L., and Fitzhugh, O. G. (1964). Food flavourings and compounds of related structure I. Acute oral toxicity. *Food Cosmet. Toxicol.* 2, 327–343. doi: 10.1016/S0015-6264(64)80192-9
- Juven, B. J., Kanner, J., Schved, F., and Weisslowicz, H. (1994). Factors that interact with the antibacterial action of thyme essential oil and its active constituents. *J. Appl. Bacteriol.* 76, 626–631. doi: 10.1111/j.1365-2672.1994.tb01661.x
- Kifer, D., Muzinic, V., and Klaric, M. S. (2016). Antimicrobial potency of single and combined mupirocin and monoterpenes, thymol, menthol and 1,8-cineole against *Staphylococcus aureus* planktonic and biofilm growth. *J. Antibiot.* 69, 689–696. doi: 10.1038/ja.2016.10
- Kim, Y. G., Lee, J. H., Gwon, G., Kim, S. I., Park, J. G., and Lee, J. (2016). Essential oils and eugenols inhibit biofilm formation and the virulence of *Escherichia coli* O157:H7. *Sci. Rep.* 6:36377. doi: 10.1038/srep36377
- Knobloch, K., Pauli, A., Iberl, B., Weigand, H., and Weis, N. (1989). Antibacterial and antifungal properties of essential oil components. *J. Essent. Oil Res.* 1, 119–128. doi: 10.1080/10412905.1989.9697767
- Kumari, P., Mishra, R., Arora, N., Chatrath, A., Gangwar, R., Roy, P., et al. (2017). Antifungal and anti-biofilm activity of essential oil active components against *Cryptococcus neoformans* and *Cryptococcus laurentii*. *Front. Microbiol.* 8:2161. doi: 10.3389/fmicb.2017.02161
- Lacey, R. F., and Binder, B. M. (2016). Ethylene regulates the physiology of the *Cyanobacterium synechocystis* sp. PCC 6803 via an ethylene receptor. *Plant Physiol.* 171, 2798–809. doi: 10.1104/pp.16.00602
- Lambert, R. J. W., Skandamis, P. N., Coote, P. J., and Nychas, G.-J. E. (2001). A study of the minimum inhibitory concentration and mode of action of oregano essential oil, thymol and carvacrol. *J. Appl. Microbiol.* 91, 453–462. doi: 10.1046/j.1365-2672.2001.01428.x
- Latifah-Munirah, B., Himratul-Aznita, W. H., and Mohd Zain, N. (2015). Eugenol, an essential oil of clove, causes disruption to the cell wall of *Candida albicans* (ATCC3 1405). *Front. Life Sci.* 8, 231–240. doi: 10.1080/21553769.2015.1045628
- Lee, J. H., Kim, Y. G., and Lee, J. (2017). Carvacrol-rich oregano oil and thymol-rich thyme red oil inhibit biofilm formation and the virulence of uropathogenic *Escherichia coli*. *J. Appl. Microbiol.* 123, 1420–1428. doi: 10.1111/jam.13602
- Liu, Q., Niu, H., Zhang, W., Mu, H., Sun, C., and Duan, J. (2015). Synergy among thymol, eugenol, berberine, cinnamaldehyde and streptomycin against planktonic and biofilm-associated food-borne pathogens. *Lett. Appl. Microbiol.* 60, 421–430. doi: 10.1111/lam.12401
- Llana-Ruiz-Cabello, M., Gutierrez-Praena, D., Pichardo, S., Moreno, F. J., Bermudez, J. M., Aucejo, S., et al. (2014). Cytotoxicity and morphological effects induced by carvacrol and thymol on the human cell line Caco-2. *Food Chem. Toxicol.* 64, 281–290. doi: 10.1016/j.fct.2013.12.005

- Lucchini, J. J., Corre, J., and Cremieux, A. (1990). Antibacterial activity of phenolic compounds and aromatic alcohols. *Res. Microbiol.* 141, 499–510. doi: 10.1016/0923-2508(90)90075-2
- Lupo, A. T., Nakatsu, T., Caldwell, J., Kang Raphael, K. L., Cilia Alba, T., Van Loveren Augustinus, G., et al. (2000). *Substituted Phenols as Fragrance, Flavor and Antimicrobial Compounds*. U.S. Patent No. 6,110,888.
- Machado, M., Dinis, A. M., Salgueiro, L., Custódio, J. B. A., Cavaleiro, C., and Sousa, M. C. (2011). Anti-Giardia activity of *Syzygium aromaticum* essential oil and eugenol: effects on growth, viability, adherence and ultrastructure. *Exp. Parasitol.* 127, 732–739. doi: 10.1016/j.exppara.2011.01.011
- Maddox, C. E., Laur, L. M., and Tian, L. (2010). Antibacterial activity of phenolic compounds against the phytopathogen *Xylella fastidiosa*. *Curr. Microbiol.* 60, 53–58. doi: 10.1007/s00284-009-9501-0
- Marchese, A., Barbieri, R., Coppo, E., Orhan, I. E., Daglia, M., Nabavi, S. F., et al. (2017). Antimicrobial activity of eugenol and essential oils containing eugenol: a mechanistic viewpoint. *Crit. Rev. Microbiol.* 43, 668–689. doi: 10.1080/1040841X.2017.1295225
- Marchese, A., Orhan, I. E., Daglia, M., Barbieri, R., Di Lorenzo, A., Nabavi, S. F., et al. (2016). Antibacterial and antifungal activities of thymol: a brief review of the literature. *Food Chem.* 210, 402–414. doi: 10.1016/j.foodchem.2016.04.111
- Memar, M. Y., Raei, P., Alizadeh, N., Akbari Aghdam, M., and Kafil, H. S. (2017). Carvacrol and thymol: strong antimicrobial agents against resistant isolates. *Rev. Med. Microbiol.* 28, 63–68. doi: 10.1097/MRM.0000000000000100
- Miladi, H., Zmantar, T., Kouidhi, B., Chaabouni, Y., Mahdouani, K., Bakhrouf, A., et al. (2017). Use of carvacrol, thymol, and eugenol for biofilm eradication and resistance modifying susceptibility of *Salmonella enterica* serovar Typhimurium strains to nalidixic acid. *Microb. Pathog.* 104, 56–63. doi: 10.1016/j.micpath.2017.01.012
- Mohamed, S. H., Mohamed, M. S. M., Khalil, M. S., Azmy, M., and Mabrouk, M. I. (2018). Combination of essential oil and ciprofloxacin to inhibit/eradicate biofilms in multidrug-resistant *Klebsiella pneumoniae*. *J. Appl. Microbiol.* 125, 84–95. doi: 10.1111/jam.13755
- Moran, A., Gutierrez, S., Martinez-Blanco, H., Ferrero, M. A., Monteagudo-Mera, A., and Rodriguez-Aparicio, L. B. (2014). Non-toxic plant metabolites regulate *Staphylococcus* viability and biofilm formation: a natural therapeutic strategy useful in the treatment and prevention of skin infections. *Biofouling* 30, 1175–1182. doi: 10.1080/08927014.2014.976207
- Nadell, C. D., Drescher, K., Wingreen, N. S., and Bassler, B. L. (2015). Extracellular matrix structure governs invasion resistance in bacterial biofilms. *ISME J.* 9, 1700–1709. doi: 10.1038/ismej.2014.246
- Nazzaro, F., Fratianni, F., De Martino, L., Coppola, R., and De Feo, V. (2013). Effect of essential oils on pathogenic bacteria. *Pharmaceuticals* 6, 1451–1474. doi: 10.3390/ph6121451
- Neyret, C., Herry, J. M., Meylheuc, T., and Dubois-Brissonnet, F. (2014). Plant-derived compounds as natural antimicrobials to control paper mill biofilms. *J. Ind. Microbiol. Biotechnol.* 41, 87–96. doi: 10.1007/s10295-013-1365-4
- Nostro, A., Sudano Roccato, A., Bisignano, G., Marino, A., Cannatelli, M. A., Pizzimenti, F. C., et al. (2007). Effects of oregano, carvacrol and thymol on *Staphylococcus aureus* and *Staphylococcus epidermidis* biofilms. *J. Med. Microbiol.* 56(Pt 4), 519–523. doi: 10.1099/jmm.0.46804-0
- Noumi, E., Merghni, A., M., M. A., Haddad, O., Akmadar, G., De Martino, L., et al. (2018). Chromobacterium violaceum and *Pseudomonas aeruginosa* PAO1: models for evaluating anti-quorum sensing activity of melaleuca alternifolia essential oil and its main component terpinen-4-ol. *Molecules* 23:2672. doi: 10.3390/molecules23102672
- Oh, S. Y., Yun, W., Lee, J. H., Lee, C. H., Kwak, W. K., and Cho, J. H. (2017). Effects of essential oil (blended and single essential oils) on anti-biofilm formation of *Salmonella* and *Escherichia coli*. *J. Anim. Sci. Technol.* 59, 4–4. doi: 10.1186/s40781-017-0127-7
- Otto, M. (2018). Staphylococcal biofilms. *Microbiol. Spect.* 6:GPP3-0023-2018. doi: 10.1128/microbiolspec.GPP3-0023-2018
- Parsek, M. R., and Singh, P. K. (2003). bacterial biofilms: an emerging link to disease pathogenesis. *Annu. Rev. Microbiol.* 57, 677–701. doi: 10.1146/annurev.micro.57.030502.090720
- Patsilinas, A., Artini, M., Papa, R., Sabatino, M., Bozovic, M., Garzoli, S., et al. (2019). Machine learning analyses on data including essential oil chemical composition and *in vitro* experimental antibiofilm activities against staphylococcus species. *Molecules* 24:890. doi: 10.3390/molecules24050890
- Pazarci, O., Tutar, U., and Kilinc, S. (2019). Investigation of the antibiofilm effects of mentha longifolia essential oil on titanium and stainless steel orthopedic implant surfaces. *Eurasian J. Med.* 51, 128–132. doi: 10.5152/eurasianjmed.2019.18432
- Peeters, E., Hooyberghs, G., Robijns, S., Waldrant, K., De Weerd, A., Delattin, N., et al. (2016). Modulation of the substitution pattern of 5-aryl-2-aminoimidazoles allows fine-tuning of their antibiofilm activity spectrum and toxicity. *Antimicrob. Agents Chemother.* 60, 6483–6497. doi: 10.1128/AAC.00035-16
- Perez-Conesa, D., McLandsborough, L., and Weiss, J. (2006). Inhibition and inactivation of *Listeria monocytogenes* and *Escherichia coli* O157:H7 colony biofilms by micellar-encapsulated eugenol and carvacrol. *J. Food Prot.* 69, 2947–2954. doi: 10.4315/0362-028X-69.12.2947
- Persat, A., Nadell, C. D., Kim, M. K., Ingremeau, F., Sityaporn, A., Drescher, K., et al. (2015). The mechanical world of bacteria. *Cell* 161, 988–997. doi: 10.1016/j.cell.2015.05.005
- Pinheiro, P. F., Menini, L. A. P., Bernardes, P. C., Saraiva, S. H., Carneiro, J. W. M., Costa, A. V., et al. (2018). Semisynthetic phenol derivatives obtained from natural phenols: antimicrobial activity and molecular properties. *J. Agric. Food Chem.* 66, 323–330. doi: 10.1021/acs.jafc.7b04418
- Pitts, B., Hamilton, M. A., Zilver, N., and Stewart, P. S. (2003). A microtiter-plate screening method for biofilm disinfection and removal. *J. Microbiol. Methods* 54, 269–276. doi: 10.1016/S0167-7012(03)00034-4
- Puupponen-Pimia, R., Nohynek, L., Meier, C., Kahkonen, M., Heinonen, M., Hopia, A., et al. (2001). Antimicrobial properties of phenolic compounds from berries. *J. Appl. Microbiol.* 90, 494–507. doi: 10.1046/j.1365-2672.2001.01271.x
- Raei, P., Pourlak, T., Memar, M. Y., Alizadeh, N., Aghamali, M., Zeinalzadeh, E., et al. (2017). Thymol and carvacrol strongly inhibit biofilm formation and growth of carbapenemase-producing Gram negative bacilli. *Cell. Mol. Biol.* 63, 108–112. doi: 10.14715/cmb/2017.63.5.20
- Raja, M. R. C. (2015). Versatile and synergistic potential of eugenol: a review. *Pharm. Anal. Acta* 6:1000367. doi: 10.4172/2153-2435.1000367
- Rasooli, I., and Mirmostafa, S. A. (2003). Bacterial susceptibility to and chemical composition of essential oils from *Thymus kotschyianus* and *Thymus persicus*. *J. Agric. Food Chem.* 51, 2200–2205. doi: 10.1021/jf0261755
- Richards, J. J., Ballard, T. E., Huigens, R. W. III, and Melander, C. (2008). Synthesis and screening of an oroidin library against *Pseudomonas aeruginosa* biofilms. *Chembiochem* 9, 1267–1279. doi: 10.1002/cbic.200700774
- Richards, J. J., and Melander, C. (2009). Controlling bacterial biofilms. *Chembiochem* 10, 2287–2294. doi: 10.1002/cbic.200900317
- Richards, J. J., Reyes, S., Stowe, S. D., Tucker, A. T., Ballard, T. E., Mathies, L. D., et al. (2009). Amide isosteres of oroidin: assessment of antibiofilm activity and *C. elegans* toxicity. *J. Med. Chem.* 52, 4582–4585. doi: 10.1021/jm900378s
- Sakimura, T., Kajiyama, S., Adachi, S., Chiba, K., Yonekura, A., Tomita, M., et al. (2015). Biofilm-forming *Staphylococcus epidermidis* expressing vancomycin resistance early after adhesion to a metal surface. *Biomed Res. Int.* 2015:943056. doi: 10.1155/2015/943056
- Shahzad, M., Millhouse, E., Culshaw, S., Edwards, C. A., Ramage, G., and Combet, E. (2015). Selected dietary (poly)phenols inhibit periodontal pathogen growth and biofilm formation. *Food Funct.* 6, 719–729. doi: 10.1039/C4FO01087F
- Shetty, K., Cassagnol, G., and Peleg, M. (1996). Comparison of the inhibitory and lethal effects of synthetic versions of plant metabolites (anethole, carvacrol, eugenol, and thymol) on a food spoilage yeast (*Debaryomyces hansenii*) AU - Curtis, O. F. *Food Biotechnol.* 10, 55–73. doi: 10.1080/08905439609549901
- Sikkema, J., de Bont, J. A., and Poolman, B. (1994). Interactions of cyclic hydrocarbons with biological membranes. *J. Biol. Chem.* 269, 8022–8028.
- Snoussi, M., Noumi, E., Trabelsi, N., Flamini, G., Papetti, A., and De Feo, V. (2015). Mentha spicata essential oil: chemical composition, antioxidant and antibacterial activities against planktonic and biofilm cultures of *Vibrio* spp. strains. *Molecules* 20, 14402–14424. doi: 10.3390/molecules200814402
- Spoering, A. L., and Lewis, K. (2001). Biofilms and planktonic cells of *Pseudomonas aeruginosa* have similar resistance to killing by antimicrobials. *J. Bacteriol.* 183, 6746–6751. doi: 10.1128/JB.183.23.6746-6751.2001
- Thorski, J., Blank, G., and Biliaderis, C. (1989). Eugenol induced inhibition of extracellular enzyme production by *Bacillus subtilis*. *J. Food Prot.* 52, 399–403. doi: 10.4315/0362-028X-52.6.399

- Tsai, T.-H., Huang, W.-C., Lien, T.-J., Huang, Y.-H., Chang, H., Yu, C.-H., et al. (2017). Clove extract and eugenol suppress inflammatory responses elicited by *Propionibacterium acnes* *in vitro* and *in vivo*. *Food Agric. Immunol.* 28, 916–931. doi: 10.1080/09540105.2017.1320357
- Tsang, K. Y., and Brimble, M. A. (2007). Synthesis of aromatic spiroacetals related to γ -rubromycin based on a 3H-spiro[1-benzofuran-2,2'-chromane] skeleton. *Tetrahedron* 63, 6015–6034. doi: 10.1016/j.tet.2007.02.033
- Ultee, A., Bennik, M. H. J., and Moezelaar, R. (2002). The phenolic hydroxyl group of carvacrol is essential for action against the food-borne pathogen *Bacillus cereus*. *Appl. Environ. Microbiol.* 68, 1561–1568. doi: 10.1128/AEM.68.4.1561-1568.2002
- Vazquez-Sanchez, D., Galvao, J. A., Mazine, M. R., Gloria, E. M., and Oetterer, M. (2018). Control of *Staphylococcus aureus* biofilms by the application of single and combined treatments based in plant essential oils. *Int. J. Food Microbiol.* 286, 128–138. doi: 10.1016/j.ijfoodmicro.2018.08.007
- Villalobos Mdel, C., Serradilla, M. J., Martin, A., Ordiales, E., Ruiz-Moyano, S., and Cordoba Mde, G. (2016). Antioxidant and antimicrobial activity of natural phenolic extract from defatted soybean flour by-product for stone fruit postharvest application. *J. Sci. Food Agric.* 96, 2116–2124. doi: 10.1002/jsf.a.7327
- Wendakoon, C., and Sakaguchi, M. (1995). Inhibition of amino acid decarboxylase activity of enterobacter aerogenes by active components in spices. *J. Food Prot.* 58, 280–283. doi: 10.4315/0362-028X-58.3.280
- Wu, Y., Bai, J., Zhong, K., Huang, Y., Qi, H., Jiang, Y., et al. (2016). Antibacterial activity and membrane-disruptive mechanism of 3-p-trans-coumaroyl-2-hydroxyquinic acid, a novel phenolic compound from pine needles of *Cedrus deodara*, against *Staphylococcus aureus*. *Molecules* 21:1084. doi: 10.3390/molecules21081084
- Xie, J. L., Singh-Babak, S. D., and Cowen, L. E. (2012). Minimum inhibitory concentration (MIC) assay for antifungal drugs. *Bio-Protocol* 2:e252. doi: 10.21769/BioProtoc.252
- Xu, J. G., Liu, T., Hu, Q. P., and Cao, X. M. (2016). Chemical composition, antibacterial properties and mechanism of action of essential oil from clove buds against *Staphylococcus aureus*. *Molecules* 21:1194. doi: 10.3390/molecules21091194
- Xu, Y., Larsen, L. H., Lorenzen, J., Hall-Stoodley, L., Kikhney, J., Moter, A., et al. (2017). Microbiological diagnosis of device-related biofilm infections. *APMIS* 125, 289–303. doi: 10.1111/apm.12676
- Yang, C., Hu, D. H., and Feng, Y. (2015). Essential oil of *Artemisia vestita* exhibits potent *in vitro* and *in vivo* antibacterial activity: investigation of the effect of oil on biofilm formation, leakage of potassium ions and survival curve measurement. *Mol. Med. Rep.* 12, 5762–5770. doi: 10.3892/mmr.2015.4210
- Yang, Z., Liu, Y., Ahn, J., Qiao, Z., Endres, J. L., Gautam, N., et al. (2016). Novel fluorinated pyrrolomycins as potent anti-staphylococcal biofilm agents: design, synthesis, pharmacokinetics and antibacterial activities. *Eur. J. Med. Chem.* 124, 129–137. doi: 10.1016/j.ejmech.2016.08.017
- Zhang, Y., Wang, Y., Zhu, X., Cao, P., Wei, S., and Lu, Y. (2017). Antibacterial and antibiofilm activities of eugenol from essential oil of *Syzygium aromaticum* (L.) Merr. & L. M. Perry (clove) leaf against periodontal pathogen *Porphyromonas gingivalis*. *Microb. Pathog.* 113, 396–402. doi: 10.1016/j.micpath.2017.10.054

Conflict of Interest: The authors declare that the research was conducted in the absence of any commercial or financial relationships that could be construed as a potential conflict of interest.

Copyright © 2019 Walsh, Livinghouse, Goeres, Mettler and Stewart. This is an open-access article distributed under the terms of the Creative Commons Attribution License (CC BY). The use, distribution or reproduction in other forums is permitted, provided the original author(s) and the copyright owner(s) are credited and that the original publication in this journal is cited, in accordance with accepted academic practice. No use, distribution or reproduction is permitted which does not comply with these terms.



Small Molecule Anti-biofilm Agents Developed on the Basis of Mechanistic Understanding of Biofilm Formation

Katrine Qvortrup¹, Louise Dahl Hultqvist², Martin Nilsson², Tim Holm Jakobsen², Charlotte Uldahl Jansen¹, Jesper Uhd¹, Jens Bo Andersen², Thomas E. Nielsen^{2,3}, Michael Givskov^{2,3} and Tim Tolker-Nielsen^{2*}

¹ Department of Chemistry, Technical University of Denmark, Lyngby, Denmark, ² Department of Immunology and Microbiology, Costerton Biofilm Center, Faculty of Health and Medical Sciences, University of Copenhagen, Copenhagen, Denmark, ³ Singapore Centre for Environmental Life Sciences Engineering, Nanyang Technological University, Singapore, Singapore

OPEN ACCESS

Edited by:

Manuel Simões,
University of Porto, Portugal

Reviewed by:

Bin Yu,
Zhengzhou University, China
Letizia Crocetti,
University of Florence, Italy

*Correspondence:

Tim Tolker-Nielsen
ttn@sund.ku.dk

Specialty section:

This article was submitted to
Medicinal and Pharmaceutical
Chemistry,
a section of the journal
Frontiers in Chemistry

Received: 23 August 2019

Accepted: 17 October 2019

Published: 01 November 2019

Citation:

Qvortrup K, Hultqvist LD, Nilsson M, Jakobsen TH, Jansen CU, Uhd J, Andersen JB, Nielsen TE, Givskov M and Tolker-Nielsen T (2019) Small Molecule Anti-biofilm Agents Developed on the Basis of Mechanistic Understanding of Biofilm Formation. *Front. Chem.* 7:742. doi: 10.3389/fchem.2019.00742

Microbial biofilms are the cause of persistent infections associated with various medical implants and distinct body sites such as the urinary tract, lungs, and wounds. Compared with their free living counterparts, bacteria in biofilms display a highly increased resistance to immune system activities and antibiotic treatment. Therefore, biofilm infections are difficult or impossible to treat with our current armory of antibiotics. The challenges associated with biofilm infections have urged researchers to pursue a better understanding of the molecular mechanisms that are involved in the formation and dispersal of biofilms, and this has led to the identification of several steps that could be targeted in order to eradicate these challenging infections. Here we describe mechanisms that are involved in the regulation of biofilm development in *Pseudomonas aeruginosa*, *Escherichia coli*, and *Acinetobacter baumannii*, and provide examples of chemical compounds that have been developed to specifically inhibit these processes. These compounds include (i) pilicides and curlicides which inhibit the initial steps of biofilm formation by *E. coli*; (ii) compounds that interfere with c-di-GMP signaling in *P. aeruginosa* and *E. coli*; and (iii) compounds that inhibit quorum-sensing in *P. aeruginosa* and *A. baumannii*. In cases where compound series have a defined molecular target, we focus on elucidating structure activity relationship (SAR) trends within the particular compound series.

Keywords: *Pseudomonas aeruginosa*, *Escherichia coli*, *Acinetobacter baumannii*, c-di-GMP, pilicides and curlicides, quorum sensing, anti-biofilm compounds

INTRODUCTION

During the last two decades it has been realized that the biofilm mode of growth is the predominant life-mode of most bacterial species (Flemming and Wuerzt, 2019). In biofilms bacteria are located in densely packed microcolonies concealed in a protective matrix of biopolymers (Tolker-Nielsen, 2015). The ability of bacteria to form biofilms is an ancient trait that during evolution has offered protection from grazing amoebae and antimicrobials. When higher organisms evolved, bacteria

adapted to form biofilms at various body sites, and today the extensive use of medical devices in modern health care has provided numerous new niches for bacterial biofilm formation. In the biofilm life-mode the bacteria are tolerant to our present assortment of antibiotics as well as immune system activities (Rybtke et al., 2015; Ciofu and Tolker-Nielsen, 2019). Accordingly, biofilms are the cause of persistent infections associated with various medical implants, and distinct disease states such as urinary tract infection, cystic fibrosis, chronic obstructive pulmonary disease and chronic wounds. The US National Institutes of Health has estimated that more than 80% of all microbial infections in the developed countries involve biofilms.

The problematic infections caused by biofilms have urged researchers to study the molecular mechanisms underlying biofilm formation and biofilm dispersal. This has led to the identification of distinct molecules and mechanisms that could serve as target for novel anti-biofilm drugs. Based on this knowledge, development of several potential anti-biofilm drug candidates is underway. Here we describe our current knowledge of the molecular mechanisms involved in biofilm development for the Gram negative opportunistic pathogens *Pseudomonas aeruginosa*, *Escherichia coli*, and *Acinetobacter baumannii*, which are all causing problematic biofilm infections. Subsequently, we provide examples of chemical compounds that have been developed to inhibit specific biofilm formation processes. These compounds include i) pilicides and curlicides which inhibit the initial steps of biofilm formation by *E. coli*; ii) compounds that interfere with c-di-GMP signaling in *P. aeruginosa* and *E. coli*; and iii) compounds that inhibit quorum sensing in *P. aeruginosa* and *A. baumannii*.

MOLECULAR MECHANISMS INVOLVED IN BIOFILM FORMATION

In this section we review biofilm formation processes of *P. aeruginosa*, *E. coli*, and *A. baumannii* with an emphasis on the molecular mechanisms which are used as targets for the development of anti-biofilm chemicals.

Biofilm formation requires an extracellular matrix that under most conditions is produced by the biofilm forming organism. Compelling evidence suggests that various bacterial species employ so-called c-di-GMP signaling to regulate whether they produce an extracellular matrix and form biofilm, or assume a planktonic lifestyle (Fazli et al., 2014; Jenal et al., 2017). Diguanylate cyclase enzymes (DGCs) catalyze formation of the molecule c-di-GMP, whereas specific phosphodiesterase enzymes (PDEs) catalyze degradation of c-di-GMP in the bacteria. Bacteria typically produce several different DGCs and PDEs, and the available evidence suggests that specificity of c-di-GMP signaling is warranted through physical interactions of specific DGC, PDE, and c-di-GMP effectors (Sarenko et al., 2017). In addition to their catalytic domains these enzymes often contain regulatory domains, and are thought to regulate the life-style (planktonic vs. biofilm) of bacteria in response to environmental cues. An elevated cellular level of c-di-GMP induces the

production of biofilm matrix components and drives bacteria to form biofilms, whereas a reduction in the c-di-GMP level down regulates the production of biofilm matrix components and causes dispersal of biofilm bacteria into the planktonic mode of life (Gjermansen et al., 2006, 2010; Christensen et al., 2013). The DGCs and PDEs that make and break c-di-GMP have conserved catalytic GGDEF (Gly-Gly-Asp-Glu-Phe) and EAL (Glu-Ala-Leu)/HD-GYP (His-Asp-Gly-Tyr-Pro) domains, respectively. Genomic analyses have shown that the GGDEF and EAL domains are the most abundant motives among *Bacteria*. Accordingly, c-di-GMP has been found to be the central biofilm regulator in all Gram negative bacteria investigated to date, and in a number of Gram positive bacteria (Jenal et al., 2017). On the contrary, c-di-GMP is not produced by humans or other mammals.

Quorum sensing (QS) is another regulatory process that plays a role in biofilm formation of a variety of bacterial species, and also functions as an overall regulator of the expression of virulence factors (Juhas et al., 2005). QS is a bacterial cell-to-cell communication process that relies on the production, sensing and response to extracellular signaling molecules. QS allows groups of bacteria to synchronously alter the expression of specific genes, mainly in response to changes in their population density. In Gram negative bacteria the majority of QS systems employ acyl homoserine lactone (AHL) signal molecules. The systems function by means of one or more AHL synthases that produce AHL molecules which can pass the bacterial membranes and upon reaching a threshold concentration binds to and activates one or more transcriptional activators which in turn activate transcription of specific target genes. The concentrations of signal molecules correlate to the density of the bacterial population, enabling density dependent control of gene expression.

Pseudomonas aeruginosa

P. aeruginosa biofilms are causing a number of persistent infections, including cystic fibrosis pneumonia, chronic obstructive pulmonary disease related infections, chronic wound infections, chronic otitis media, chronic bacterial prostatitis, and medical device-related infections especially associated with urinary tract catheters and endotracheal tubes (Tolker-Nielsen, 2014).

Biofilm formation by *P. aeruginosa* can initiate through the adhesive action of several components, including flagella (O'Toole and Kolter, 1998), type IV pili (O'Toole and Kolter, 1998; Deziel et al., 2001; Chiang and Burrows, 2003), Cup fimbria (Vallet et al., 2001), extracellular DNA (Whitchurch et al., 2002), and Psl polysaccharide (Ma et al., 2006). Many of these components are also important constituents of the extracellular matrix at later stages of biofilm formation. The exopolysaccharide Psl is cell-surface associated and functions as an adhesin in the initial phase of biofilm formation, but relocates as a peripheral exopolysaccharide at later stages of biofilm formation (Ma et al., 2009). The surface adhesin CdrA binds to Psl, and it is required for Psl-mediated aggregation of *P. aeruginosa* cells (Borlee et al., 2010). Pel is a cationic exopolysaccharide produced by *P. aeruginosa*, and it has been shown to cross-link

extracellular DNA in the biofilm matrix (Jennings et al., 2015). Overproduction of alginate exopolysaccharide enables mucoid *P. aeruginosa* strains to form biofilm persistent infections in the lungs of cystic fibrosis patients (Hoiby, 1977). Moreover, *P. aeruginosa* rugose small colony variants that overproduce Psl and Pel exopolysaccharide show enhanced persistence in cystic fibrosis lungs (Starkey et al., 2009). In addition, the lectins LecA/LecB and the functional amyloid protein Fap can play a role as matrix components in *P. aeruginosa* biofilms (Tielker et al., 2005; Diggle et al., 2006b; Dueholm et al., 2013).

Synthesis in *P. aeruginosa* of the biofilm matrix components Psl, Pel, alginate, CdrA, type IV pili, and Cup fimbriae is positively regulated by c-di-GMP (Fazli et al., 2014). Conversely, c-di-GMP is a negative regulator of motility of *P. aeruginosa* (Simm et al., 2004). The c-di-GMP content in *P. aeruginosa* is adjusted via the activity of 17 proteins with a GGDEF domain, 9 proteins with an EAL/HD-GYP domain, and 16 proteins with both a GGDEF and an EAL domain. Christensen et al. (2013) constructed a recombinant bacterial *P. aeruginosa* strain, where the cellular level of c-di-GMP can be reduced by addition of an inducer that activates transcription of a PDE gene, and demonstrated that *in vitro* *P. aeruginosa* biofilms disperse in response to a reduction in the cellular c-di-GMP content (Christensen et al., 2013). In addition, evidence was provided that murine implant-associated *P. aeruginosa* biofilm infections can be cured through a reduction of the bacterial c-di-GMP content (Christensen et al., 2013).

QS in *P. aeruginosa* is mediated through the LasI/LasR and RhlI/RhlR proteins that produces and senses the signal molecules 3-oxo-C12-homoserine lactone (HSL) and C4-homoserine lactone (C4-HSL) (Schuster and Greenberg, 2006). Moreover, *P. aeruginosa* employs a Pqs system that produces and senses 2-heptyl-3-hydroxy-4-quinolone (termed PQS) (Diggle et al., 2006a). The systems are hierarchically arranged with LasR regulating the Rhl and Pqs systems (Diggle et al., 2006a). QS regulates the production of a number of compounds that play a role in the formation and persistence of *P. aeruginosa* biofilms. Among these QS-regulated factors is extracellular DNA that contributes to the stability of *P. aeruginosa* biofilms and plays a role in the antimicrobial tolerance displayed by the biofilms (Allesen-Holm et al., 2006; Chiang et al., 2013). Moreover, the production of rhamnolipid is QS regulated, and this amphipathic molecule plays a role in biofilm development and resistance of *P. aeruginosa* biofilms to phagocytizing immune cells (Pamp and Tolker-Nielsen, 2007; Alhede et al., 2009). Thus, inhibition of QS decreases the antibiotic tolerance of *P. aeruginosa* biofilms and reduces resistance to host immune responses (Jakobsen et al., 2017a).

Escherichia coli

E. coli is the primary infectious agent in urinary tract infections, including cystitis (infection of the bladder or lower part of the urinary tract) and pyelonephritis (infection of the kidneys or infections associated with the upper urinary tract). The bacterium is able to form biofilms on catheter material, on the bladder wall, and within bladder epithelial cells, and biofilm formation is often related to infection relapses (Anderson et al., 2003; Justice et al., 2004; Soto et al., 2006; Rosen et al., 2007, 2008).

Biofilm formation by *E. coli* can be governed by a number of different adhesins and extracellular matrix components. Flagella may play a role in transport of the bacteria to a surface, and in adhesion to the surface (Pratt and Kolter, 1998). The proteinaceous curli fibers are a major component of the *E. coli* biofilm matrix, and they are required in the initial stages of *E. coli* attachment to proteins on the host cells (Olsen et al., 1989; Ben Nasr et al., 1996; Prigent-Combaret et al., 2000; Chapman et al., 2002; Serra et al., 2013). Curli fibers are comprised of the two proteins, CsgA and CsgB, where CsgB primes the polymerization of CsgA (Hammar et al., 1995). Type 1 and P pili are adhesive surface structures which are important in *E. coli* infections (Pratt and Kolter, 1998; Schembri and Klemm, 2001; Niba et al., 2007). Type 1 pili are central for the irreversible attachment of the cells to a surface, and type 1 pili deficient strains shows significant impairment in biofilm formation (Pratt and Kolter, 1998; Niba et al., 2007). Using a mouse model, it has been shown that uropathogenic *E. coli* (UPEC) strains, that expresses type 1 pili, have a survival advantage in the bladder (Mulvey et al., 1998), and that *E. coli* lacking type 1 or P pili is greatly attenuated in causing urinary tract infections (Sivick and Mobley, 2010). Type 1 pili contain repeating FimA subunits which assemble to a coli-rod structure that is tipped with FimH adhesin molecules (Brinton, 1965; Barnhart et al., 2003; Korea et al., 2011). Absence of FimH reduces adhesion both *in vitro* and in the bladders of mice (Langermann et al., 1997; Mulvey et al., 1998). FimH is responsible for a specific adhesion to mannose residues on epithelial cells, thereby facilitating infection (Pratt and Kolter, 1998; Hertig and Vogel, 2012; Rakshit and Sivasankar, 2014). P pili contain PapA subunits assembled to a helical structure, which at the tip anchors the adhesin PapG (Gong and Makowski, 1992; Bullitt and Makowski, 1995). PapG enables *E. coli* cells to bind to epithelial kidney cells in the host (Busch et al., 2015). Antigen43 is an autotransporter protein, which has been linked with higher intracellular persistence in urinary tract infections (Anderson et al., 2003; Klemm and Schembri, 2004; Van Der Woude and Henderson, 2008; Luthje and Brauner, 2010). In addition to the protein components, the exopolysaccharides cellulose, poly-GlcNAc (PGA), and colanic acid are important structural components of the matrix of *E. coli* biofilms (Danese et al., 2000; Wang et al., 2004; Serra et al., 2013; Subashchandrabose et al., 2013; Besharova et al., 2016). Moreover, extracellular DNA can function as an important matrix component in *E. coli* biofilms (Devaraj et al., 2015).

Synthesis in *E. coli* of the biofilm matrix components cellulose, PGA and curli fimbria is positively regulated by c-di-GMP (Brown et al., 2001; Brombacher et al., 2003, 2006; Weber et al., 2006; Jonas et al., 2008; Pesavento et al., 2008; Boehm et al., 2009). Conversely, c-di-GMP is a negative regulator of motility of *E. coli* (Simm et al., 2004). The c-di-GMP content in *E. coli* is determined by the activity of several GGDEF/EAL/HD-GYP domain proteins; e.g., the lab strain *E. coli* K12 possess 12 DGCs and 13 PDEs (Hengge et al., 2016; Povolotsky and Hengge, 2016). Evidence has been provided that there is a hierarchical arrangement of DGCs and PDEs, with a few master controllers (Sarenko et al., 2017). The PDE, PdeH (formerly YhjH) was shown to eradicate global effects of several DGCs, thereby limiting them to act on local systems. The major DGC

was found to be DgcE, which is a primary controller of the c-di-GMP level in *E. coli* (Sarenko et al., 2017).

E. coli does not encode an AHL based QS system. However, it evidently employs a furanosyl borate diester (AI-2) based QS system, and evidence has been presented that this system is involved in regulation of the synthesis of some of the biofilm matrix components (Beloin et al., 2008).

Acinetobacter baumannii

The most common infections caused by *A. baumannii* are pneumonia, meningitis, urinary tract infection, skin and soft tissue infection, wound infections and bacteremia (Visca et al., 2011). The increased use of mechanical ventilation and central venous and urinary catheterization has greatly increased the incidence of *A. baumannii* infections (Wong et al., 2017). The ability of *A. baumannii* to form biofilm is contributing significantly to the recalcitrance of these infections to antibiotic treatment.

The mechanisms involved in biofilm formation for *A. baumannii* are less studied than for *P. aeruginosa* and *E. coli*. However, a number of adhesins and extracellular components have been identified as playing a role in biofilm formation of *A. baumannii*. The bacteria lack flagella, but surface adhesion is facilitated by Csu pili and the OmpA outer membrane protein (Dorsey et al., 2002; Tomaras et al., 2003; Gaddy et al., 2009). Besides adhesion to abiotic surfaces, OmpA binds to epithelial cells and thus mediate biofilm formation on biotic surfaces (Gaddy et al., 2009). In addition, a biofilm associated protein (Bap) has been reported to play a role in *A. baumannii* biofilm formation (Loehfelm et al., 2008). Evidence was provided that Bap is important in cell-cell adhesion and in keeping the structure of mature biofilms (Loehfelm et al., 2008). Moreover, *A. baumannii* can synthesize the exopolysaccharides alginate and poly- β -1,6-N-acetylglucosamine (PNAG) which can function as important constituents of the biofilm matrix (Lee et al., 2008; Choi et al., 2009). Extracellular DNA is also a matrix component in *A. baumannii* biofilms (Sahu et al., 2012).

There is a lack of knowledge regarding a role of c-di-GMP signaling in the regulation of biofilm formation by *A. baumannii*. However, a study employing an *in silico* pharmacophore-based screen to identify small-molecule inhibitors of DGC enzymes, found that the hit compounds could inhibit biofilm formation of *A. baumannii* (Sambanthamoorthy et al., 2014). Synthesis of Csu pili is known to be regulated by the BfmSR two-component system in *A. baumannii* (Tomaras et al., 2008; Liou et al., 2014).

QS has been shown to play a role in regulation of biofilm formation by *Acinetobacter* species (Anbazhagan et al., 2012). *A. baumannii* possess an AHL-based QS system with AbaI functioning as the AHL synthase and AbaR functioning as the AHL receptor. An *abaI* mutant, not able to produce AHL, was shown to have defects in the later stages of biofilm formation (Niu et al., 2008). In addition, it was shown that addition of AHL to *A. baumannii* cells resulted in an increased expression of Csu pili, and a stimulation of biofilm formation (Luo et al., 2015). Moreover, a low concentration of Fe^{3+} was found to induce AHL-based QS in *A. baumannii*, and to promote the formation of robust biofilms (Modarresi et al., 2015). *A. baumannii* is capable

of producing a quorum quenching enzyme designated AidA, and Lopes et al. found that activation of AidA in *A. baumannii* resulted in inhibition of biofilm formation (Lopez et al., 2017).

COMPOUNDS THAT INTERFERE WITH BIOFILM FORMATION

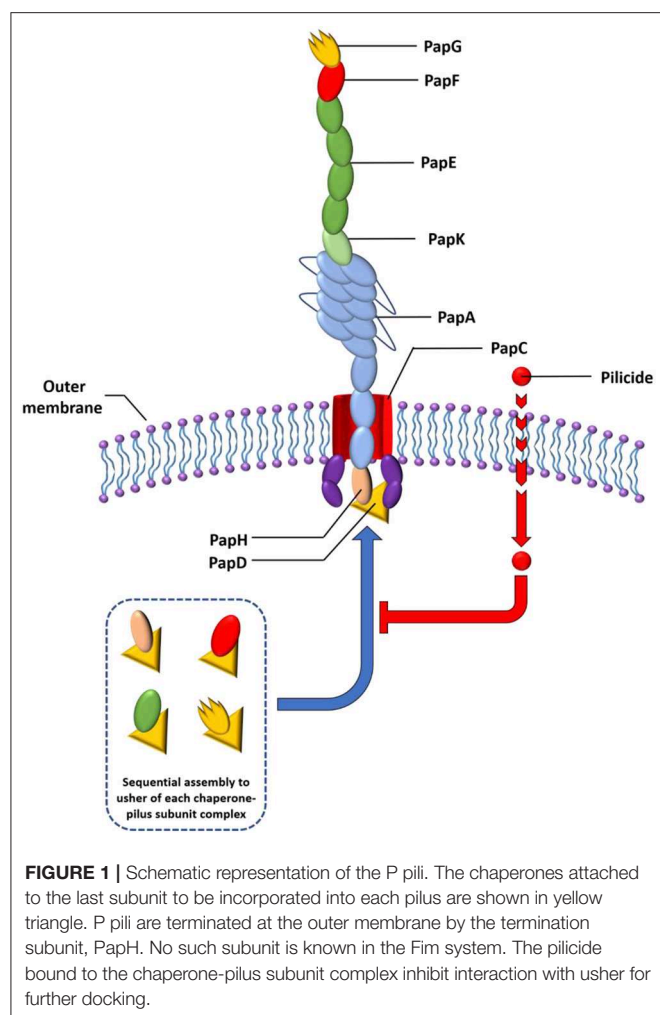
In this section we describe pilicides and curlicides which inhibit the initial steps of biofilm formation by *E. coli*, and compounds that interfere with c-di-GMP signaling in *P. aeruginosa* and *E. coli*, as well as compounds that inhibit QS in *P. aeruginosa* and *A. baumannii*. A direct comparison of compound efficiencies is difficult due to the lack of standardization between assays used in the different studies. Even in studies investigating modulation of the same protein, there is often a variation in the used bacterial strains, growth media and assay. This makes a quantitative comparison of activities (e.g., IC₅₀ values) from various studies problematic and in some cases even misleading. Therefore, this review is focused on reviewing activity trends observed within each assay as well as giving a more qualitative comparison of structures and relative biological effects across different studies.

Compounds That Modulate the Function of Pili and Curli in *Escherichia coli*

Bacterial attachment is an essential step in most bacterial infections, and failure to attach leads to eradication of the pathogenic organism. Accordingly, bacteria have evolved sophisticated pili and fimbriae systems for epithelial surface attachment (Mulvey, 2002; Fronzes et al., 2008; Cusumano and Hultgren, 2009), hereby facilitating invasion and colonization of the underlying tissue. Type 1 and p pili are two of such pili systems involved in attachment and invasion of UPEC strains in the host, leading to urinary tract infections. Specifically, Type 1 pili have been implicated in infections of the lower urinary tract, which results in cystitis (infection of the bladder), while p pili are associated with pyelonephritis (infection of the kidney). The p pili and type 1 pili are both consisting of a pilus rod connected to a flexible end tip (fibrillum) that enable interactions with the target.

Pili are often assembled via a highly conserved mechanism called the chaperone–usher pathway (CUP) utilized by numerous adhesive organelles in Gram negative bacteria, including *E. coli* and *P. aeruginosa* (Figure 1) (Jacob-Dubuisson et al., 1994; Nuccio and Baumler, 2007). The construction of pili by the CUP proceeds from the top to bottom, meaning that the first subunit to be introduced is the adhesin (PapG or FimH), which is followed by introduction of the rest of the tip fibrillum and adaptor subunits (PapF, E, and K or FimG and F), the pilus base (PapA or FimA) and lastly, in the case of the Pap system, the termination and anchor subunit (PapH) (Busch et al., 2015). The CUP pili construction system contains several feasible targets for the development of compounds that block this assembly and thus pili formation.

Among this kind of compounds are mannocides that compete for binding in the mannose binding pocket present in the FimH pilus lectin of type I pili, blocking its binding with their mannose



rich receptors in eukaryotic cells. To date, compounds like biphenylmannosides have proved effective *in vitro* to prevent biofilm formation of the UPEC and also to disrupt preformed biofilm (Han et al., 2010). Their oral administration was effective in clearing chronic urinary tract infections in mice and in potentiating the activity of the antibiotic trimethoprim sulfamethoxazole (Cusumano et al., 2011). Bacterial pilus assembly requires the presence of periplasmic chaperones. Thus, development of compounds that bind to chaperones have been of high interest. By inhibiting pilus assembly, such compounds would interfere with bacterial attachment to the host, and therefore they constitute potential novel antibiofilm agents. This type of compounds is referred to as pilicides (Aberg and Almqvist, 2007).

P pili are assembled by the chaperone PapD that binds to and caps interactive surfaces on each pilus subunit thus preventing premature aggregation during their secretion into the periplasmic space. The high degree of structural homology and conserved mechanism of action between the CUP proteins in various pathogens (Rose et al., 2008), make compounds that target this system attractive as potential broad-spectrum anti-virulence compounds.

C-Terminal peptides of both PapG (1, **Figure 2**) and PapH have been shown to bind to the chaperone, leading to effective inhibition of further binding of pilus subunits (Karlsson et al., 1998). This has provided efficient probe molecules useful for studying the intricate processes in the CUPs. However, the use of peptides as drugs has several drawbacks, including poor absorption after oral administration, rapid degradation and/or excretion. Therefore, focus has been given to development of small-molecule peptidomimetics as potential anti-virulence compounds.

The high amount of information available regarding PapG C-terminus interactions with the chaperone (Svensson et al., 2001; Emtenas et al., 2003a) has been used for a structure-based design of small-molecule structures that mimic the PapG C-terminal. The dihydrothiazolo ring-fused 2-pyridone scaffold (2, **Figure 2**) is the most widely studied pilicide structures, targeting the Arg8/Lys112 cleft region of the chaperone. This scaffold has the terminal carboxylic acid moiety, important for interaction with the Arg8 and Lys112 residues in the chaperone cleft (**Figure 2**). Furthermore, the scaffold can be further decorated by the installation of substituents at various positions to introduce important hydrophobic motifs (e.g., Leu311 residue) and/or exploit other potentially useful interactions.

The importance of the bicyclic 2-pyridone system was clearly indicated, as the monocyclic 2-pyridone (3, **Figure 2**) showed a considerable lower biological activity as compared to the corresponding bicyclic compound (Pemberton et al., 2008).

The first generation bicyclic 2-pyridone pilicides (4, 5, **Figure 3**) (Svensson et al., 2001; Lee, 2003), suffered from poor water solubility, which limited their utility. However, introducing an aminomethylene substituent in the open C6 position in the 2-pyridone scaffold (R3, **Figure 2**) solved this problem, resulting in 2-pyridone (6, **Figure 3**) binding chaperones in the low millimolar range (**Figure 3**) (Hedenstrom et al., 2005).

The carboxylic acid group on the pilicide scaffold is vital for the activity of the pilicides, and exchanging the carboxylic acid for other functionalities, including $-\text{CO}_2\text{Me}$, $-\text{CH}_2\text{OH}$, $-\text{CH}_2\text{OMe}$, $-\text{CHO}$, or $-\text{CH}_3$ substantially reduced the pilicide activity (Aberg et al., 2005a). However, carboxylic acid isosteres comprising tetrazoles (8, **Figure 3**), acyl sulfonamides (9, **Figure 3**) and hydroxamic acids (10, **Figure 3**) are tolerated and can in some cases lead to improved pilicide's potency (Åberg et al., 2008).

The carboxylic acid functionality was originally designed to interact with Arg8 and Lys112 in the chaperone cleft (**Figure 2**). However, a later NMR-based study elucidating the pilicides' binding site revealed that the cleft of the chaperone is not the only possible binding site (Hedenstrom et al., 2005). Instead, the study suggested that pilicides affect *E. coli* pilus formation either by binding in the chaperone cleft, or by affecting the orientation of the flexible F1-G1 loop of the chaperone, both of which are part of the surface that is involved in interactions with pilus subunits. This latter binding site was later verified by X-ray crystallography of a pilicide-PapD complex (Pinkner et al., 2006).

The effect of varying the C-7 and C-8 (Emtenas et al., 2002; Aberg et al., 2005b; Aberg and Almqvist, 2007; Cegelski et al., 2009; Chorell et al., 2012) position of the 2-pyridone scaffold (**Figure 2**) have been intensively examined, based on two main

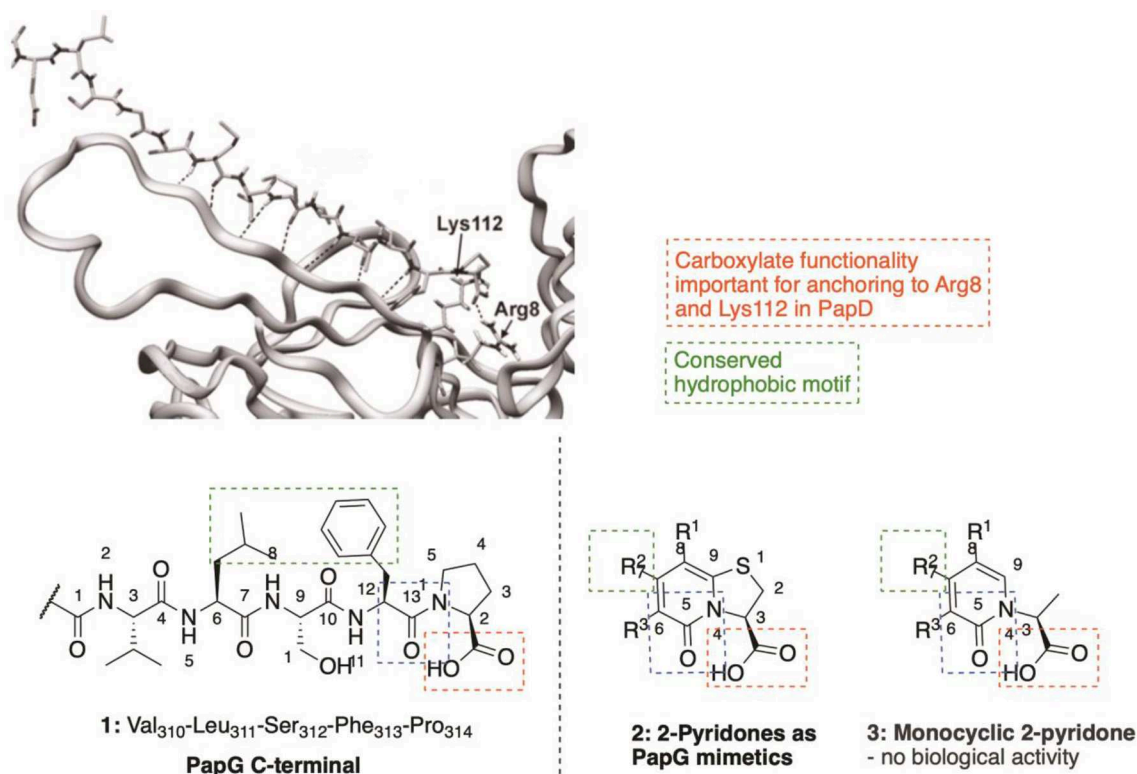


FIGURE 2 | The two final amino acids (Phe₃₁₃-Pro₃₁₄) in the C-terminal of PapG bound to PapD served as template for design of the pilicide scaffold that inhibit pilus assembly.

objectives. First, to improve the peptide mimicking properties of the identified hits, and secondly to establish structure-activity relationships (SARs) regarding pilicide activity. In general, the nature of the substituent at both the C-7 and C-8 position was found to strongly affect the biological response (Emtenas et al., 2002; Chorell et al., 2012).

In 2011, Chorell et al. conducted a detailed SAR study of the effect of C7 substitution (Chorell et al., 2011). Based on their studies, Almquist et al. delineated two broad activity trends: (1) Hydrophobic, sterically demanding C-7 substituents are beneficial. (2) Extended ether linkers are allowed and can in some cases improve activity whereas linkers incorporating basic amines, amides and sulphonamides, as well as heteroaryls diminish biofilm inhibition capacity. Overall, the most promising C-7 substituents were found to be 1-naphthylmethyl, naphthoxymethyl, 3-tolylethyl, and 2,3-dimethylphenoxyethyl groups.

Similarly, large and hydrophobic aromatic substituents are important in the R1 position of the 2-pyridinone to get good binding to the chaperone. Compounds containing a phenyl, indole, thiophene or 3,4-methylenedioxyphenyl group at C-8 were effective, while incorporation of pyridine and the smaller methoxy, cyclopropyl, and isopropyl substituents resulted in compounds with reduced potency (Chorell et al., 2012). Furthermore, the R1 substituent has been shown to have

an impact on the C2-position in the 2-pyridone (Emtenäs et al., 2003b). For example, 2-pyridone with cyclopropyl at the R1 position was more prone to racemization than 2-pyridone with phenyl at the R1 position.

In 2010 Chorell et al. published a study investigating substitution of the C-2 position in the pilicide scaffold, including both saturated and unsaturated analogs (12, 13, Figure 3) (Chorell et al., 2010). As a result of their analysis, Almquist and co-workers could draw some general conclusions regarding the structural features of the C-2 position in dihydrothiazolo ring-fused 2-pyridone molecules that are necessary for blocking pilus formation. Their results disclosed that the addition of substituents in the C-2 position of the pilicide scaffold significantly enhanced the potency of the pilicides, leading to increased inhibition of pili dependent biofilm formation. However, the effect of the spatial arrangement on activity was different between the analogs. For example, with phenyl substitution in the C-2 position, the unsaturated analog had higher potency than the saturated counterpart, whereas with methyl in the C-2 position, the situation was the opposite; the saturated analog had higher potency than the unsaturated.

On the basis of the results with the unsaturated phenyl analog, a more comprehensive SAR study with unsaturated C-2 aryl and heteroaryl substituents (13, Figure 3) was performed. Many of the compounds containing aryl and heteroaryl-substituents

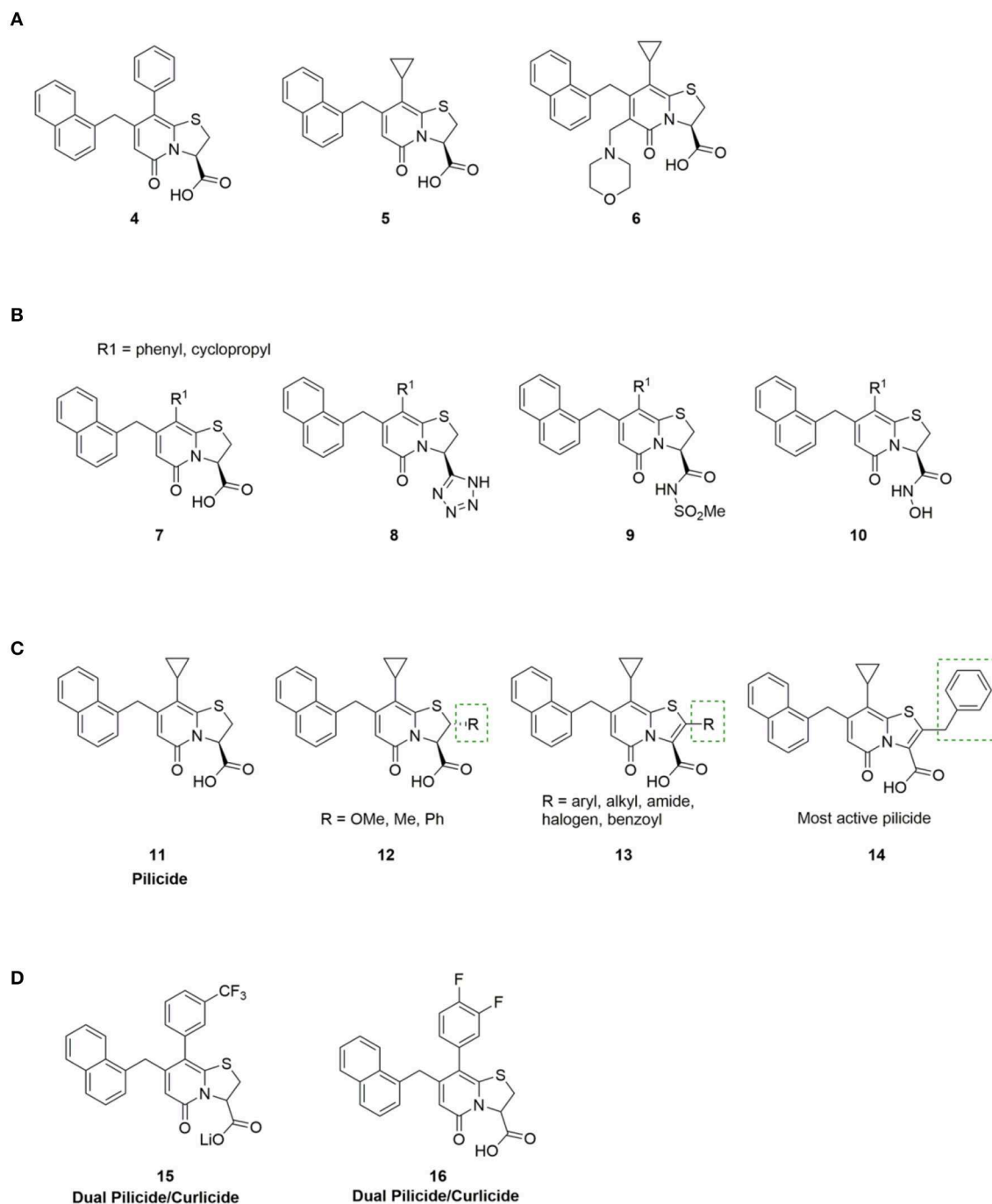


FIGURE 3 | (A) First generation pilicides, compound **4** and **5** (Svensson et al., 2001; Lee, 2003) suffered from low solubility. Aminomethylene substitution of pilicide **5** resulted in compound **6** with improved solubility properties (Hedenstrom et al., 2005). **(B)** Pilicides containing carboxylic acid isosteres, including tetrazoles (**8**), acyl sulfonamides (**9**) and hydroxamic acids (**10**) are tolerated (Åberg et al., 2008). **(C)** SAR study to investigate substitution of position C-2 in the pilicide scaffold, including both saturated (**12**) and unsaturated (**13**) analogs (Chorell et al., 2010). **(D)** Small modifications in the phenyl ring allowed identification of ring-fused 2-pyridones that exhibit dual pilicide-curlicide activity (Cegelski et al., 2009).

efficiently inhibited the formation of pili dependent biofilm. Especially, the benzyl substituted compound **14** (Figure 3) showed promising properties with an estimated EC₅₀ of 7 μM. Interestingly, compounds containing more sterically demanding

substituents, including indole and bensodioxane were not tolerated and resulted in no activity.

Almqvist et al. also investigated the importance of the heteroatom in the fused 2-pyridone scaffold, drawing attention

to imidazolines and oxazolines. While exchanging the sulfur for a secondary amine resulted in a distinct drop in activity, activities of the oxazolo fused 2-pyridones were comparable to the parent sulfur containing pilicides (Pemberton et al., 2008).

Besides the pili described in the preceding section, *E. coli* and other Enterobacteriaceae produce and display adhesive amyloid fibers termed curli at the bacterial cell surface (Olsen et al., 1989; Kikuchi et al., 2005). Curli are critical for biofilm development in *E. coli*, making this extracellular macromolecule a highly relevant anti-biofilm target. Assembly of curli depends upon at least six proteins known as CsgA, CsgB, CsgD, CsgE, CsgF, and CsgG. CsgA and CsgB are the major and minor curli subunits, respectively, while CsgE, CsgF, and CsgG are accessory proteins that direct the extracellular localization and facilitate assembly of curli subunits into fibers.

Curlicides designate compounds that inhibit uropathogenic *E. coli* curli biogenesis and prevent the polymerization of CsgA; being important for anchoring the curli amyloid fiber to the bacterial outer membrane (Hammar et al., 1996). Thiazolo ring-fused 2-pyridones are peptidomimetics that target important protein-protein interactions in macromolecular assembly (Svensson et al., 2001; Emtenäs et al., 2003a), which, as discussed above, provides an excellent scaffold for development of pilicides (for example **11**, **Figure 3**). However, their ability to disrupt protein-protein interactions has also been investigated to identify scaffolds that show inhibitory effects on curli biogenesis (Aberg et al., 2005b). While the cyclopropyl-substituted pyridone **11** (**Figure 3**) with strong pilicide activity, exerted no anti-curli activity (Cegelski et al., 2009), exchange of the cyclopropyl group of **11** with larger aryl substituents generated compound **15** and **16** (**Figure 3**) that gained curlicide activity and blocked curli-dependent biofilms. Interestingly, **15** and **16** both retained their ability to prevent pili formation, thus exhibiting dual pilicide-curlicide activity (Cegelski et al., 2009). Compounds that can act as both pilicides and curlicides could have increased therapeutic value as they could inhibit the formation of several adhesion fibers that are important in biofilm formation (Cegelski et al., 2009).

Modulators of c-di-GMP Signaling in *Pseudomonas aeruginosa* and *Escherichia coli*

Cyclic di-GMP has emerged as an almost universal positive regulator of biofilm formation in Gram negative bacteria (**Figure 4**) (Jenal et al., 2017). There are two basic concepts for external intervention that reduces the c-di-GMP level in bacteria: decreasing c-di-GMP formation by inhibition of DGCs or increasing c-di-GMP degradation by activation of PDEs.

DGCs contain GGDEF catalytic domains and function as homodimers. The GGDEF domains are placed at the interface of the dimer and are important for the binding of two molecules of GTP as well as their conversion into c-di-GMP with Mg^{2+} functioning as cofactor (Valentini and Filloux, 2016). Some DGC proteins, such as PelD from *C. crescentus*, WspR from *P. aeruginosa*, and YdaM from *E. coli* as well as DgcK and DgcL

from *Vibrio cholera*, possess an inhibitory site (I-site), placed only five amino acids away from the active site (Valentini and Filloux, 2016). A characteristic motif of the I-site is an RxxD sequence (x is any amino acid), where the c-di-GMP product can bind to, thereby allosterically inhibiting its own synthesis (Chan et al., 2004; Kalia et al., 2013).

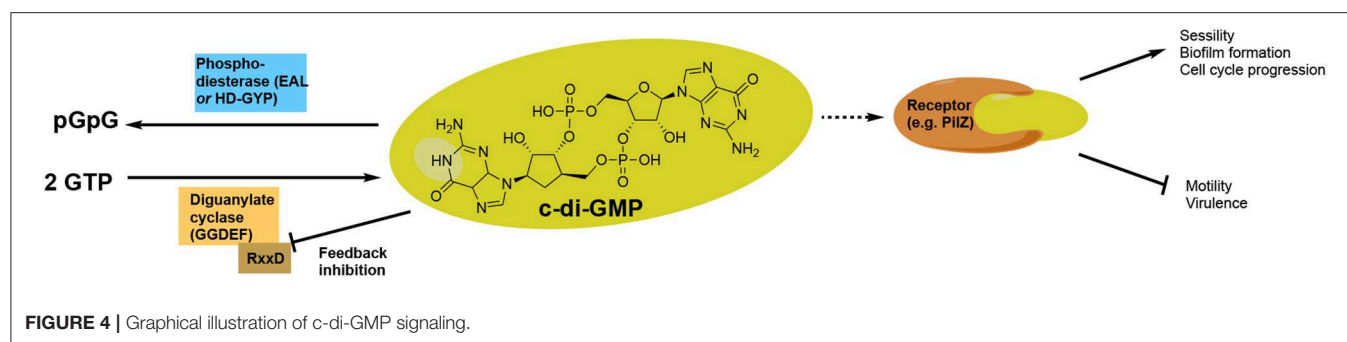
So far, two main types of c-di-GMP PDEs have been characterized, containing either the EAL or HD-GYP domain (Schirmer and Jenal, 2009; Romling et al., 2013). The primary role of EAL domain PDEs is to linearize c-di-GMP into 5'-phosphoguanlyl-guanosine (5'-pGpG) and only slowly hydrolyze 5'-pGpG to GMP. EAL-domain-containing proteins require Mg^{2+} or Mn^{2+} ions for catalysis, while inhibited by Ca^{2+} (Schmidt et al., 2005). The HD-GYP domain-containing PDEs are the second group of c-di-GMP specific PDEs, functioning by hydrolyzing c-di-GMP directly into two GMP molecules. Like the EAL domain proteins, the HD-GYP domain proteins have a binuclear Fe^{2+} or Mn^{2+} center (Romling et al., 2013).

Due to the highly conserved nature of c-di-GMP signaling systems in bacteria, and the strong evidence for their role in regulating biofilm formation, targeting c-di-GMP signaling systems is a promising approach for development of broad-spectrum small molecules for treatment of biofilm-associated infections.

Both PDEs and DGCs interact extensively with c-di-GMP, making it challenging to design c-di-GMP analogs that selectively target PDEs and not DGCs, and vice versa. In addition, most bacteria synthesize multiple DGCs and PDEs, each of which affect distinct phenotypes (Opoku-Temeng and Sintim, 2017). For example, Lory et al. observed that *P. aeruginosa* overexpressing the DGC PA2870, and other GGDEF domain proteins such as SiaD and PA0575, showed no change in ability to form biofilm, while *P. aeruginosa* overexpressing the DGCs WspR, RoeA, and PA3702 showed increased biofilm formation (Kulasakara et al., 2006). Just like DGCs, not all PDEs affect the global concentrations of c-di-GMP but regulate other processes, e.g., the synthesis of virulence factors (Opoku-Temeng and Sintim, 2017). Therefore, targeting inhibition of some of these virulence-associated PDEs (as long as they do not regulate biofilm dispersal) with small molecules could be pursued for blockage of virulence. However, the complexity of the c-di-GMP signaling pathway is challenging when developing small molecule modulators. Nonetheless, some progress has been made and several inhibitors of c-di-GMP metabolizing enzymes that affect biofilm formation and motility have been described. Here we discuss various reported inhibitors of c-di-GMP signaling.

Small Molecule Inhibitors

The history of small molecule DGC-inhibitors started in 2006 with work by Webb and colleagues, who discovered that the molecule nitric oxide (NO) can induce dispersal of *P. aeruginosa* biofilms (Barraud et al., 2006). The authors suggested a combined treatment approach with a NO donor and an antimicrobial agent to eradicate biofilm infections. They examined various NO donors, specifically sodium nitroprusside (SNP) **17**, S-nitroso-L-glutathione (GSNO) **18** and S-nitroso-N-acetylpenicillamine (SNAP) **19** (**Figure 5**) in combination with the antimicrobial



agents tobramycin, hydrogen peroxide, and sodium dodecyl sulfate. Of the investigated NO donors, SNP was shown to be the most potent inhibitor of biofilm formation in *P. aeruginosa* (Barraud et al., 2006).

Although NO-donors were shown to exert biofilm inhibitory effects, it was not until 2009 that the biochemical understanding of this effect was revealed (Barraud et al., 2009). Kjelleberg et al. showed that low nontoxic levels of NO stimulated PDE activity in *P. aeruginosa*, causing an overall decrease in intracellular c-di-GMP, leading to biofilm-dispersal. Besides the reduction of the intracellular c-di-GMP level, NO-donors cause a downregulation of the synthesis of pyoverdine (Kang et al., 2017), which is a siderophore responsible for recruitment of essential iron for biofilm formation (Kang and Kirienko, 2017).

In 2010, Antoniani et al. developed an assay for high throughput screening of DGC-inhibitors. They screened a library of 1120 compounds, which allowed them to identify the antimicrobial sulfathiazole **20** (Figure 5), as an efficient inhibitor of the *E. coli* DGC-protein AdrA (Antoniani et al., 2010). Sulfathiazole consists of a free aniline, an aromatic sulfonamide and a thiazole ring, all polar and rather electron rich components. This results in a molecular structure with two planar sides that is bended around the sulfonamide moiety (Figure 5). Subsequently, Landini et al. provided evidence that azathioprine **21** (Figure 5), an anti-inflammatory drug used in treatment of several autoimmune conditions, can impede c-di-GMP biosynthesis in *E. coli* (Antoniani et al., 2013).

Comparing azathioprine **21** to sulfathiazole **20** (Figure 5), they share structural similarities with to (hetero) aromatic parts bended around a polar moiety (sulfide and sulfonamide, respectively). Sulfathiazole **20** and azathioprine **21** (Figure 5) do not interfere with the c-di-GMP biosynthesis through inhibition of DGC activity. Instead, sulfathiazole **20** and azathioprine **21** was shown to affect nucleotide metabolism, leading to an alteration of nucleotide pools, hereby affecting c-di-GMP substrate availability.

In 2012, Sambanthamoorthy et al. published the screening of approx. 66.000 compounds for inhibition of DGC activity in *Vibrio cholerae* (Sambanthamoorthy et al., 2012). After several rounds of screening and optimization, 8 compounds were identified with good antagonistic effect toward multiple DGC enzymes, with N-(4-anilinophenyl)benzamide **22** (Figure 5)

showing significant reduction of biofilm formation also in *P. aeruginosa*.

In 2014, Palys et al. reported an *in silico* pharmacophore-based screening of ~15.000 small molecules for their ability to inhibit DGC and control biofilm development (Sambanthamoorthy et al., 2014). Four compounds, LP 3134 **23**, LP 3145 **24**, LP 4010 **25**, and LP 1062 **26** (Figure 5), were identified that significantly reduced WspR activity in *P. aeruginosa*. Further studies revealed that the compounds significantly prevented biofilm formation by *P. aeruginosa* and *A. baumannii* in a continuous-flow system (Sambanthamoorthy et al., 2014). All four molecules were found to disperse biofilm in *P. aeruginosa* and inhibited biofilm development on urinary catheters, whereas only one of the molecules (**23**) dispersed *A. baumannii* biofilms.

A virtual screening approach was also undertaken by Rinaldo and coworkers, who reported the *in silico* screening of ~2.3·10⁷ compounds from the ZINC database, with the aim to identify potent DGC inhibitors targeting the active site (Fericola et al., 2016). The active site of the DGC PleD from *C. crescentus* was used as structural template. Seven of the tested compounds showed significant reduction in PleD DGC activity, with Amb2250085 **27a** and Amb379455 **27b** (Figure 6) both containing the sulfonylhydrazide, the nitro-group and the catechol moiety, being the most efficient PleD inhibitors. Further studies revealed that **27a** was very sensitive to metals, such as Mg²⁺, which completely abolished the inhibitory activity of both PleD, WspR and YfiN. However, **27b** proved not to be interfered by the presence of the divalent metal ion. **27b** showed strong inhibition of DGCs, including WspR and YfiN from *P. aeruginosa*, through binding to the active site of the DGCs.

It is relevant to notice the structural similarity when comparing Amb379455 **27b** and the previously mentioned LP 3134 **23**, as illustrated in Figure 6. Both DGC inhibitors share the *N*-benzylidenebenzohydrazide moiety that is predicted to interact with an amino group in the active site (the Asn335 residue). Furthermore, they both contain the pyrogallol unit, a moiety with high polarity and strong coordination properties. Polyphenols characteristically possess a significant binding affinity for proteins (Papadopoulou and Frazier, 2004). Furthermore, pyrogallol can undergo reversible oxidation, to generate reactive oxygen species (ROS), resulting in DNA damage (Beaber et al., 2004; Kohanski et al., 2007). Worth mentioning, evidence suggests that polyphenolic

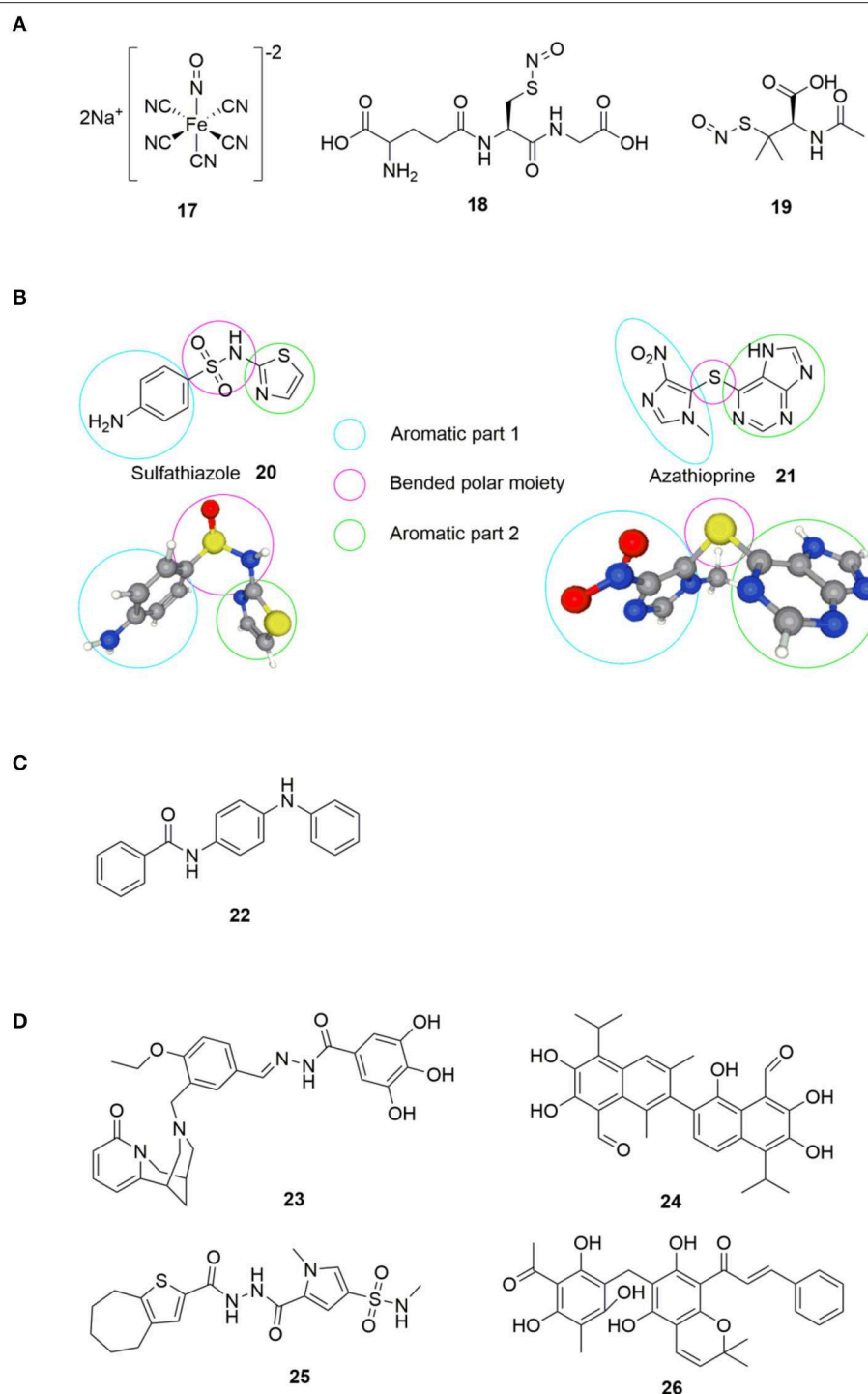


FIGURE 5 | (A) NO donors exerting biofilm-inhibitory effect (Barraud et al., 2006). **(B)** Sulfathiazole **20** and azathioprine **21**; small molecules found to interfere with c-di-GMP biosynthesis by the group of Antoniani et al. (2010, 2013). **(C)** Compound identified as DGC inhibitor (DI) by Sambanthamoorthy et al. (2014). **(D)** Inhibitors of DGC discovered by Sambanthamoorthy et al. (2014).

compounds can interfere with bacterial QS by blocking AHL-mediated signaling between bacteria (Huber et al., 2003).

In 2014, Lieberman et al. identified the small molecule, ebselen (Eb) **28a** (Figure 6), as an inhibitor of allosteric binding of c-di-GMP to receptors containing an RxxD domain, including

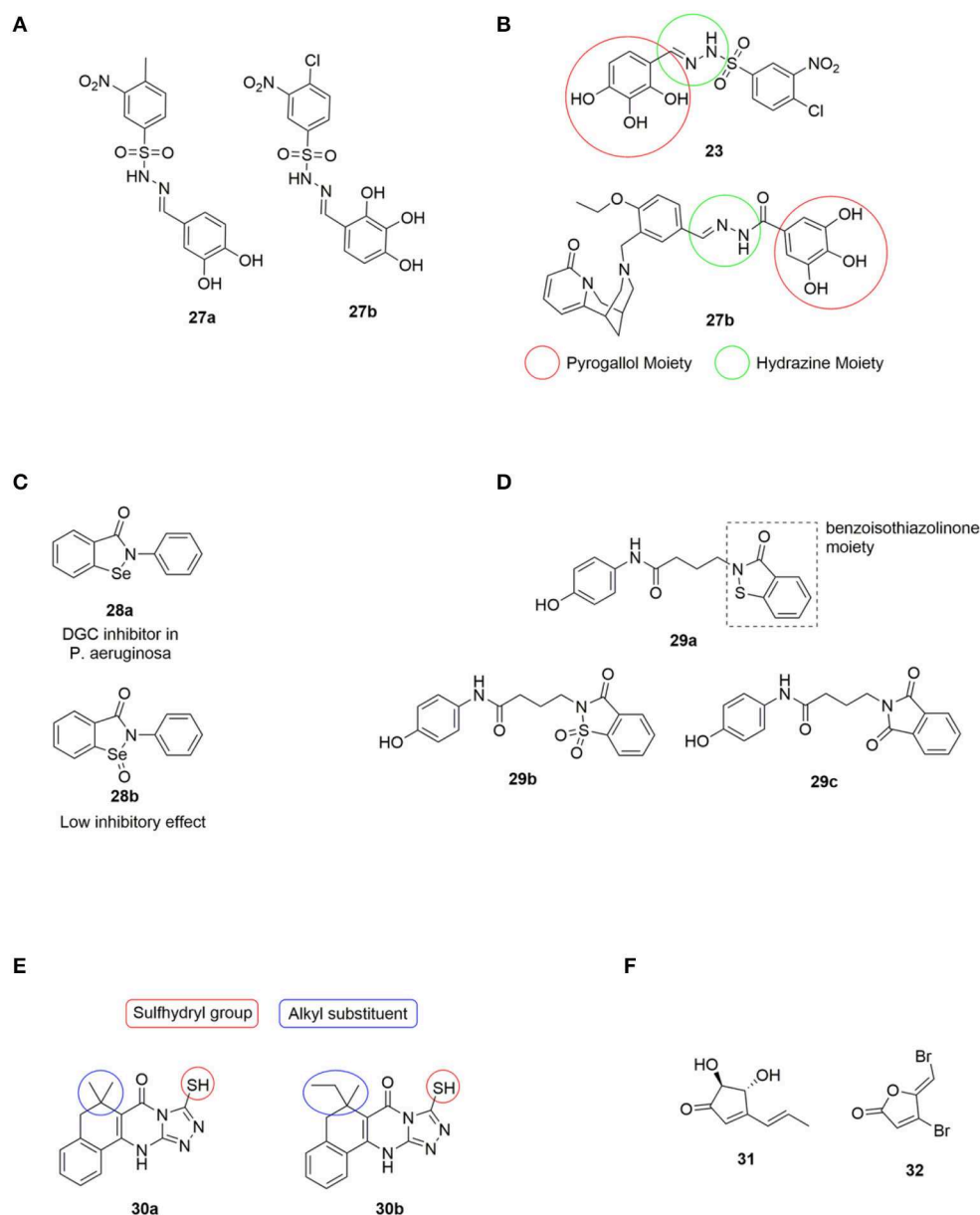
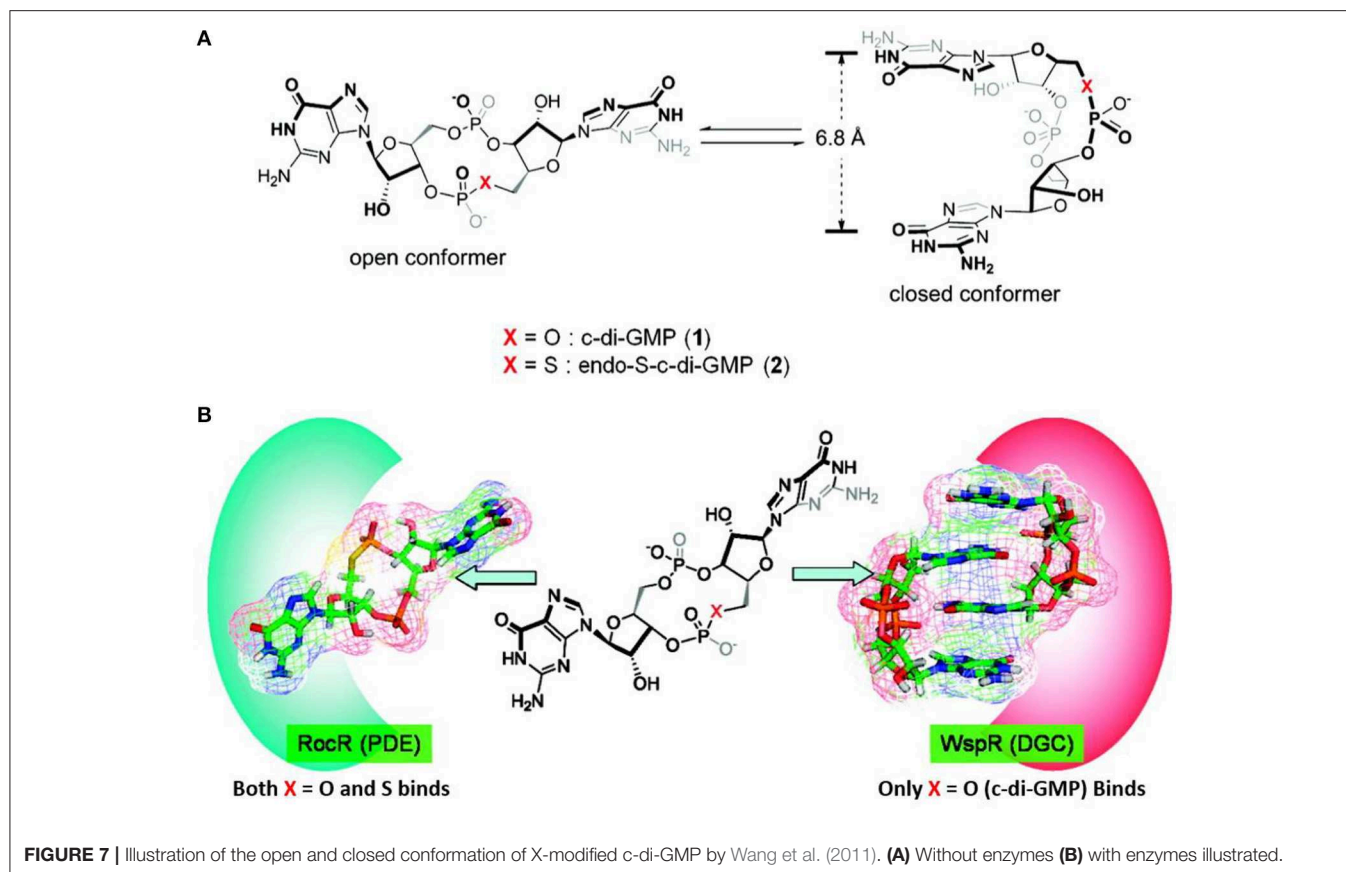


FIGURE 6 | (A) DGC inhibitors investigated by Rinaldo et al., all significantly reduced PleD activity. Amb379455 **27b** being the most promising (Fornicola et al., 2016). **(B)** Structural comparison of LP3134 **23** and Amb379455 **27b**. **(C)** The small molecule ebselen (Eb) **28a** identified as an DGC inhibitor by Lee and coworkers, and its oxidized form ebselen oxide (EbO) **28b** (Lieberman et al., 2014). **(D)** **29a** discovered by the Sintim group, and further investigated the importance of the benzisothiazolinone moiety by testing **29b** and **29c** (Zheng et al., 2016). **(E)** H19 **30a** and 925 **30b**; two Alg44 (pilZ domain) inhibitors identified by Wang et al., and structural features further investigated by Zhou et al. (2017). **(F)** The small molecules terrein **31** and **32** used by Kim et al. in studying the correlation between regulation of c-di-GMP levels and QS.

WspR and PelD of *P. aeruginosa* (Lieberman et al., 2014). It was found that Eb **28a** covalently modified DGCs by forming a bond between the selenium in Eb **28a** and a thiol in a cysteine residue in the allosteric inhibitory site. It was further demonstrated that the allosteric inhibition of DGCs also inhibited the activity of the DGCs. The oxidation state of selenium was important for activity, as the corresponding ebselen oxide (EbO) **28b** (Figure 6) showed reduced inhibition.

In 2016, Sintim et al., screened 250.000 compounds in order to find a small molecule PDE inhibitor that bind to the EAL domain of YahA in *E. coli* (Zheng et al., 2016). A handful of such PDE binders were identified and tested for their inhibitory effect of RocR (from *P. aeruginosa*) with only the benzisothiazolinone derivative **29a** (Figure 6) successfully inhibiting the hydrolysis of c-di-GMP. **29a** was tested against a series of PDEs from different bacteria and shown to be highly selective toward



inhibition of RocR. The importance of the benzoisothiazolinone moiety was clearly indicated as **29b** and **29c** (Figure 6) showed a dramatic decrease in inhibitory effect. RocR is an example of a virulence-associated PDE that does not affect the global c-di-GMP level in *P. aeruginosa* and therefore, inhibition of RocR may hold potential for inhibiting virulence. **29a** was the first example of cell-permeable PDE inhibitors that selectively inhibits one type of PDE without affecting other PDEs. The tested PDEs were YahA (*E. coli*), DipA (*P. aeruginosa*), PvrR (*P. aeruginosa*), PA4108 (*P. aeruginosa*), and RocR (*P. aeruginosa*). Furthermore, they showed no effect on the DGCs WspR and D70E from *P. aeruginosa*.

In 2017, Wang et al. identified two compounds, H19 **30a** and 925 **30b** (Figure 6) that interrupted c-di-GMP binding to Alg44 (PilZ domain) in *P. aeruginosa*, thereby inhibiting its ability to produce alginate, an exopolysaccharide polymer which is part of the biofilm matrix (Zhou et al., 2017). The sulfhydryl group, forming a covalent disulfide bond with Cys-98 in Alg44 (Figure 6), was found to be of high importance for activity. Furthermore, a broad range of alkyl substituents was tested without any improvement of inhibitory activity (Zhou et al., 2017).

In 2018, Kim et al. published a study that suggested a connection between c-di-GMP signaling and QS in *P. aeruginosa* (Kim et al., 2018). Terrein **31** (Figure 6) was found to inhibit biofilm formation by blocking QS receptors, similar to the effect

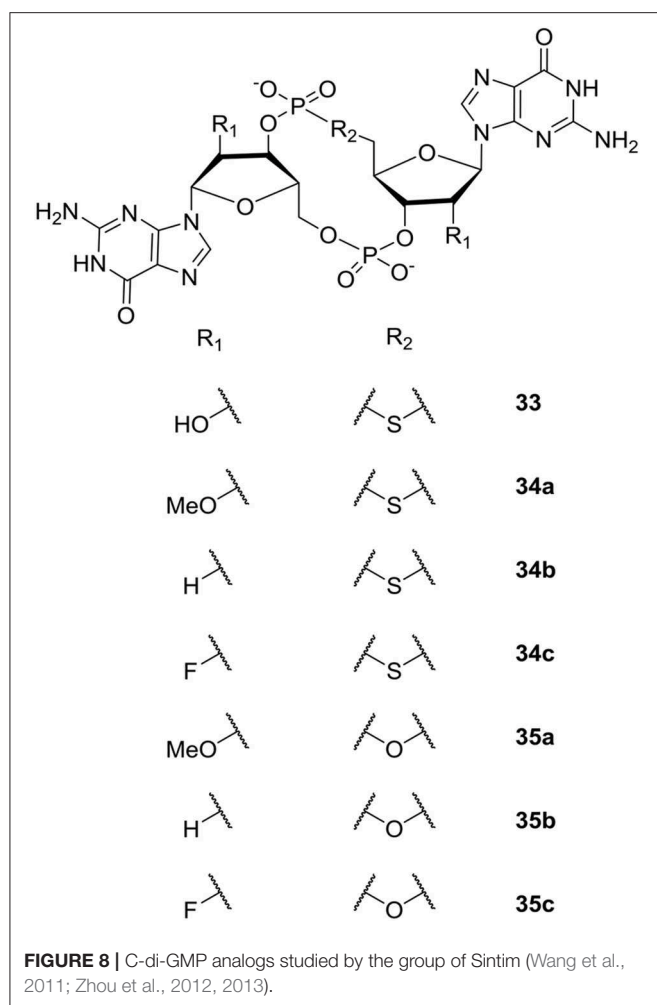
observed for furanone C-30 **32** (Costas et al., 2015). However, terrein **31** was found to decrease c-di-GMP levels; while furanone C-30 **32** increased it. The study of Kim et al. suggested that the QS system controls the c-di-GMP levels by regulating the activity of DGCs and PDEs. DGC activity seemed to be regulated by Las-QS via LasR and PDE by Rhl-QS (Costas et al., 2015).

Substrate and/or Product Analogs

Another approach for development of enzyme inhibitors is based on compounds that mimic the electronic and/or geometric characteristics of the substrate(s) or product(s), inducing enzyme inhibition due to competitive binding or a negative feedback loop, respectively.

In 2011 Sintim et al. performed the first of many studies on analogs of c-di-GMP (Wang et al., 2011). They studied the two conformations (open and closed) of c-di-GMP (Figure 7) and investigated how changing the bridging heteroatom X could shift the equilibrium between the conformations. C-di-GMP binds to PDEs in an open conformation, while it binds to DGCs in a closed conformation as a dimer (Figure 7) (Wang et al., 2011). Therefore, developing c-di-GMP analogs that prefers an “open” vs. “closed” conformer could allow for a control of the binding affinity toward PDEs vs. DGCs.

The study by Sintim et al. revealed that the sulfur-substituted analog endo-S-c-di-GMP **33** (Figure 8) that predominantly stay in an open form, selectively inhibited PDEs without affecting the



potent *P. aeruginosa* DGC WspR. Although not directly relevant for inhibition of biofilm, the work nicely demonstrated that selective binding to specific classes of c-di-GMP binding proteins can be accomplished by altering conformer populations of the analog (so-called conformational steering). This could be utilized as design principle when developing selective PDE-activators or DGC-inhibitors that interfere with biofilm formation and/or persistence. Furthermore, as discussed previously, selective inhibition of some of the virulence-associated PDEs that do not regulate biofilm dispersal could be relevant for treatment of biofilm-associated infections.

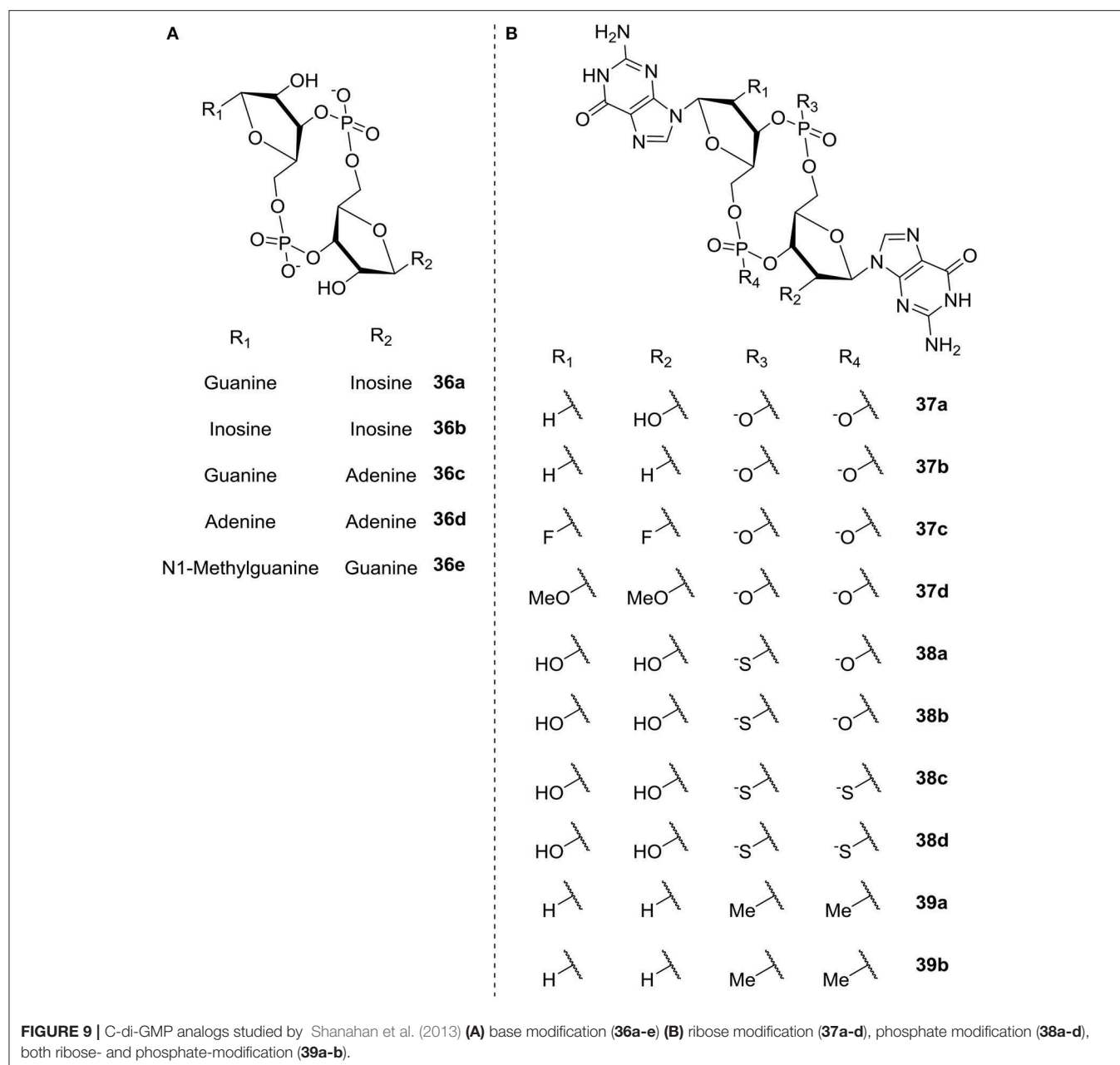
Subsequently, the Sintim group expanded their studies of c-di-GMP analogs to include modification of the 2'-position of the ribose moiety (Zhou et al., 2012, 2013). Both analogs bridged with sulfur (Zhou et al., 2012) and oxygen (Zhou et al., 2013) were studied (see **Figure 8**). Biophysical characterization and comparison of relative energies showed that endo-S-c-di-GMP **33** and the fluor-substituted endo-S-c-di-GMP analog (2'-F-endo-S-c-di-GMP **34c**, **Figure 8**) preferred the closed form, whereas the methoxy-substituted 2'-OMe-endo-S-c-di-GMP **34a** (**Figure 8**) preferred the open form. In comparison, the 2'-H-endo-S-c-di-GMP **34b** (**Figure 8**) showed similar energies for

both conformations. Sintim et al. then investigated the binding of the c-di-GMP analogs to a Vc2 RNA riboswitch. So far, two classes of riboswitches that binds c-di-GMP have been identified; the c-di-GMP-I riboswitch (class I) and c-di-GMP-II riboswitch (class II). The Vc2 RNA is a class I riboswitch, and crystal structure studies have shown that class I riboswitches bind c-di-GMP in the closed conformation. Of the new analogs, the fluor-substituted 2'-F-endo-S-c-di-GMP **34c** had the highest relative binding to the class I riboswitch. Although more enzyme-selective, the binding affinity was similar to the binding affinity of native c-di-GMP and endo-S-c-di-GMP **33** (**Figure 8**). The investigations showed that the 2'-position is essential for binding to the class I riboswitch, Vc2 RNA, which can be used to design analogs that only target specific c-di-GMP proteins.

Studying the ribose-modified analogs bridged with oxygen (Zhou et al., 2013) (**Figure 8**), Sintim et al. found that the 2'-F-substituted ribose analogs (c-di-2'-F-GMP **35c**) bind to the I-site of DGC four times better than c-di-GMP, while c-di-GMP bound 10 times better to PDEs than c-di-2'-F-GMP **35c**. Although, the c-di-2'-F-GMP **35c** was seen to still inhibit PDEs, their results showed the potential of designing selective DGC-inhibitors through investigation of I-site binders. The bulky 2'-OMe-substituted **35a** analog was found to be a poor DGC-inhibitor, which they explained with lack of space in the binding pocket of the enzymes tested. The polarity reduced 2'-H-substituted analog **35b** was shown to have similar binding-affinity as c-di-GMP.

Shanahan et al. (2013) also studied c-di-GMP analogs; here with the aim of identifying analogs that were resistant to hydrolysis by PDE, in order to apply them for riboswitch control. The different analogs studied are illustrated in **Figure 9** and divided into two groups according to the modification; base modification (A, **36a-e**) and ribose- and phosphate modification (B, ribose **37a-d**, phosphate **38a-d**, both **39a-b**), respectively. The authors evaluated the rate of hydrolysis by PDE as compared to c-di-GMP. In the three categories base, ribose and phosphate, the latter gave the best overall results. They found that substitution of the phosphates with phosphorothioate (e.g., c-(R_pR_p)-di-G_{ps} **38c** and c-(R_pS_p)-di-G_{ps}, **38d**, **Figure 9**) yielded analogs with good binding affinity toward both classes of riboswitches (Shanahan et al., 2011). Additionally the thio-substituted analogs showed good binding affinity toward the EAL domain without being degraded; indicating their potential as PDE-inhibitors.

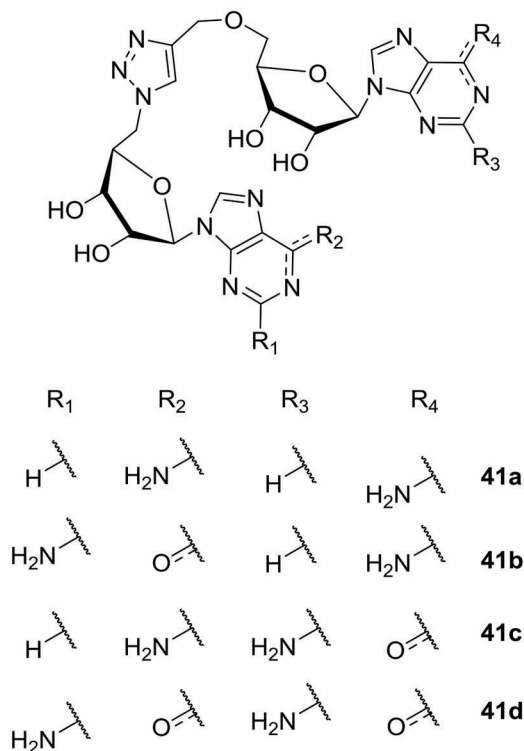
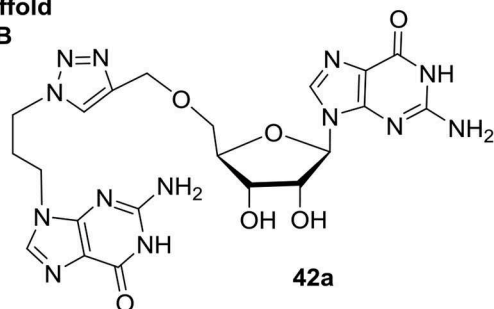
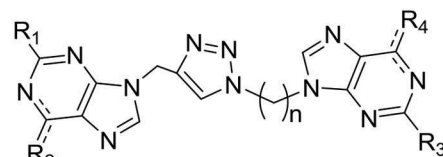
In 2015 Cutruzzolá et al. investigated c-di-GMP analogs to identify allosteric inhibitors of DGCs that does not affect PDEs (Fericola et al., 2015). They synthesized and screened a series of 16 analogs where the phosphate/ribose moiety was replaced with a non-hydrolyzable 1,2,3-triazole. Different analogs were investigated with variation of the guanine base moiety (Scaffold A, **Figure 10**), as well as analogs where one (Scaffold B, **Figure 10**) or both (Scaffold C, **Figure 10**) of the two ribose-moieties was omitted. Of the tested analogs, the simple analog DCI061 **43b** (Scaffold C, **Figure 10**) showed good inhibition of the *P. aeruginosa* PDE; RocR. When further investigating the DCI061(**43b**)-scaffold, Fericola et al. were able to draw some general conclusions: (1) Introducing bulky substituents in the guanine base, resulted in a dramatic loss of inhibitory



activity toward RocR. (2) The electrophilic character of the substituent in the C-6 position proved to be crucial for binding to the inhibitory site of DGCs and anti-binding to the EAL active site (PDEs). (3) The 2-amino group in guanine is important for binding of DGC, while not crucial for binding to EAL. (4) The distance between the two purines was crucial, with a 3-carbon spacer resulting in optimal interaction, while both a 2- and 4-carbon spacer resulted in complete loss of inhibitory activity.

Guanosin-tetraphosphate (ppGpp), i.e., phosphorylated analogs of GTP and GDP, is produced by the Rel proteins and accumulates in a variety of bacterial species as a stress response to amino acid starvation. Under these conditions

amino acids are maintained and RNA synthesis is inhibited; causing, among other effects, low ability to sustain biofilm formation (Wexselblatt et al., 2010). Therefore, inhibition of the synthetic activity of Rel proteins may prevent bacteria from sensing conditions where amino-acids are absent in their environment, which, in turn, may ultimately lead to bacterial self-starvation and death. In 2010 Wexselblatt et al. studied ppGpp analogs (see **Figure 11**) (Wexselblatt et al., 2010), and tested them as competitive inhibitors of Rel proteins. Vidavski et al. observed that 2'-deoxyguanosine-3'-5'-di(methylene bisphosphonate) (**40i**, **Figure 11**) is a competitive binder for GTP in the Rel protein; causing inhibition of the protein and lowering of ppGpp production.

Scaffold A**Scaffold B****Scaffold C**

R ₁	R ₂	R ₃	R ₄	n	
H ₂ N	Cl	H ₂ N	Cl	3	43a
H ₂ N	O	H ₂ N	O	3	43b
H	Cl	H	Cl	3	43c
H	H ₂ N	H	H ₂ N	2	43d
H ₂ N	Cl	H ₂ N	Cl	4	43e
H ₂ N	O	H ₂ N	O	4	43f
H ₂ N	Cl	H ₂ N	Cl	2	43g
H ₂ N	Me-NH	H ₂ N	Me-NH	3	43h
H ₂ N	O	H ₂ N	O	2	43i
H ₂ N	Bn-NH	H ₂ N	Bn-NH	3	43j

FIGURE 10 | C-di-GMP analogs, with a 1,2,3-triazole moiety incorporated, investigated for their allosteric inhibitory effect on DGC by Cutruzzolá et al. The analogs are grouped into three Scaffold types (A–C; Fericola et al., 2015).

Inhibitors of QS in *Pseudomonas aeruginosa* and *Acinetobacter baumannii*

This section presents an overview of small molecules identified as QS inhibitors (QSIs) targeting *P. aeruginosa* and *A. baumannii*. QS inhibition is a way to attenuate pathogenicity without obstructing processes that are essential for bacterial growth. In this section we will focus on compounds targeting the AI-1 system used by both *P. aeruginosa* and *A. baumannii* and not

cover molecules targeting the PQS system only used by *P. aeruginosa*. Several comprehensive reviews about QS inhibitors have been published, some of which focus on the biological activity of the compounds (Jakobsen et al., 2013, 2017a; Kalia, 2013) and others on the structures providing knowledge as to the molecular characteristics important for inhibition (Geske et al., 2008b; Galloway et al., 2011). *P. aeruginosa* is by far the most studied organism in relation to inhibition of AHL-mediated QS,

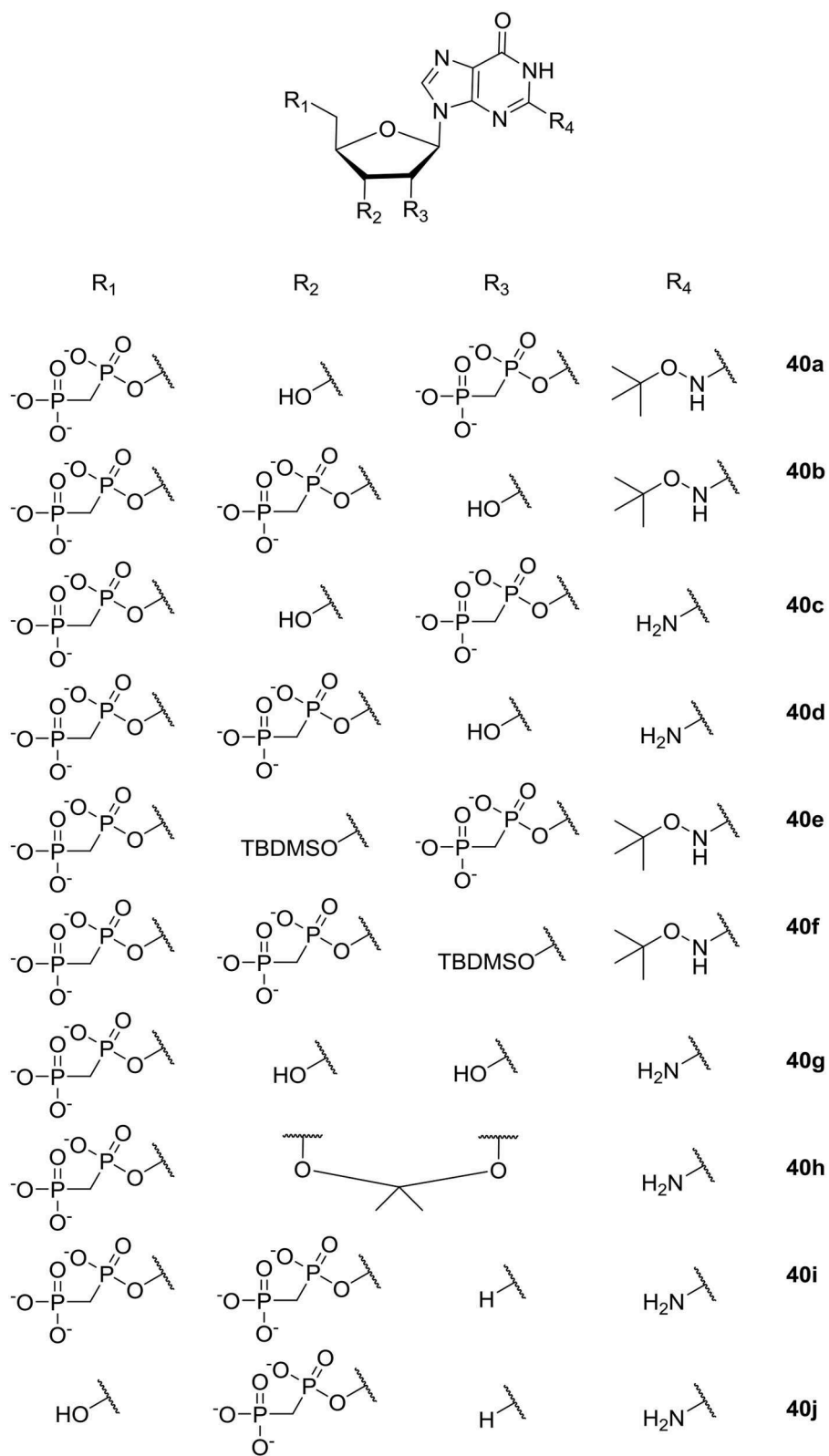
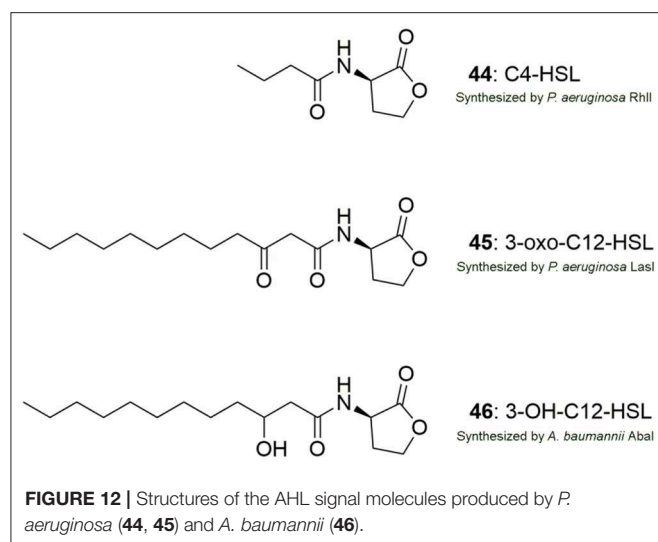


FIGURE 11 | ppGpp analogs studied by Wexselblatt et al. (2010).



whereas the number of studies investigating QS inhibition of *A. baumannii* is more limited.

The quest for small molecules capable of lowering the efficacies of QS systems has gained considerable attention for more than two decades, and it has resulted in the identification of a large variety of QS inhibitors. It has been shown that a QS-deficient *P. aeruginosa* biofilm established either by the use of QS deficient mutants or treatment with QS inhibitors shows a decrease in survival in a mouse lung infection model compared to a *P. aeruginosa* infection with a functional QS system (Wu et al., 2004; Bjarnsholt et al., 2005; Jakobsen et al., 2012b). Three factors that are most likely involved in this change in *P. aeruginosa* are rhamnolipids, extracellular DNA and pyocyanin. They are all partially or completely QS regulated and are shown to provide protection from host immunity as well as antibiotic therapy (Davey et al., 2003; Allesen-Holm et al., 2006; Jensen et al., 2007; Chiang et al., 2013; Das et al., 2015).

Modulators of AHL-Based QS Systems

A general perspective is that there are three targets to chemically affect AHL mediated QS systems by small molecules: (I) the signal production (LuxI-type synthase), (II) the signal molecule (AHL-ligand) and (III) the signal receptor (LuxR-type receptor) (Rasmussen and Givskov, 2006). However, this is a perspective with modifications and differences between the AHL QS systems in bacterial organisms exist. For instance, the AHL QS system in *P. aeruginosa* consists of two LuxIR-type systems, LasIR and RhlIR, which are interlinked, contrary to the QS system in *A. baumannii* which is based on only a single LuxIR system, AbaIR. The structure of the signal molecules employed by these QS systems is shown in Figure 12. In addition, the *P. aeruginosa* QS system is comprised of additional systems such as IQS and PQS connected to the Las and the Rhl system making the inhibition of the system more complex.

Inhibition of the AHL synthase can be an effective strategy to disconnect cell to cell signaling, however at present there are very few studies with a thorough investigation of small molecules

targeting the signal production. Studies have investigated the potential of using analogs of S-adenosylmethionine (SAM), which is the amino donor for the formation of the homoserine lactone ring moiety. Three analogs, S-adenosyl-homocysteine 47a, sinefungin 47b (Figure 13) and butyryl SAM have been shown to inhibit *P. aeruginosa* RhlI synthase and block AHL production *in vitro* (Parsek et al., 1999).

Targeting QS signaling directly by enzymatic degradation of the signal molecule can be achieved by an AHL-lactonase, AHL-acylase or a paraoxonase that break the AHL molecule or by oxidoreductases that reduce the carbonyl to a hydroxyl group (Chen et al., 2013). Several AHL-lactonases have been discovered to date including the enzyme MomL that was identified from *Muricauda olearia* Th120. MomL was shown to efficiently degrade a number of different AHLs (Tang et al., 2015). Recently, MomL was shown to reduce biofilm formation of *P. aeruginosa* and *A. baumannii* as well as to increase biofilm susceptibility to different antibiotics. However, no activity was detectable in a wound biofilm model or in a *C. elegans* model questioning the *in vivo* anti-QS effect of MomL (Zhang et al., 2017). AiiA lactonase isolated from the soil bacterium *Bacillus* sp. 240B1 was the first lactonase to be described (Dong et al., 2000). Later the AiiM lactonase was shown to be an effective inhibitor of *P. aeruginosa* QS and to reduce a *P. aeruginosa* infection in a mouse model of acute pneumonia (Migiyama et al., 2013). Paraoxonases (PON) has been identified in several different mammals. They have strong degradation activity toward the acylated chain of AHLs especially if the chain is long. The *P. aeruginosa* signal molecule 3-oxo-C12-HSL is effectively hydrolyzed by PON resulting in attenuation of the QS system (Chun et al., 2004; Yang et al., 2005; Teiber et al., 2008).

Most studies investigating QS inhibition by small molecules have been focused upon identification of compounds that interact and paralyze the LuxR-homolog receptor. By using AHL analogs that match the LuxR-homolog, a signal-receptor complex is generated that is competitive to the native active complex leading to disruption of signaling. Several studies have successfully identified a range of both QS activators and inhibitors by introducing changes to the lactone moiety or the acyl chain of the native signal molecules. The generated X-ray crystal structure of some LuxR-type receptors in a complex with their natural AHL ligands has given the opportunity to use this information in the design of synthetic AHL ligands. The crystal structure of the ligand-binding domain of LasR has been solved (Bottomley et al., 2007), whereas no structure of AbaR has been reported to date. In addition, to the search for AHL analogs there has been a significant effort to identify small molecules that are distinct from the native AHL molecules. The commonly used methods have been screening of random chemical libraries consisting of either natural products isolates or synthetic made compounds together with bioassay-guided fractionation of natural products.

Studies on AHL-Derived QS Modulators

Several comprehensive SAR analyses of synthetic non-natural AHL analogs targeting *P. aeruginosa* have been reported. In 2008 Geske et al. published a review that summarizes SARs for non-natural AHL analogs in a range of bacterial species (Geske

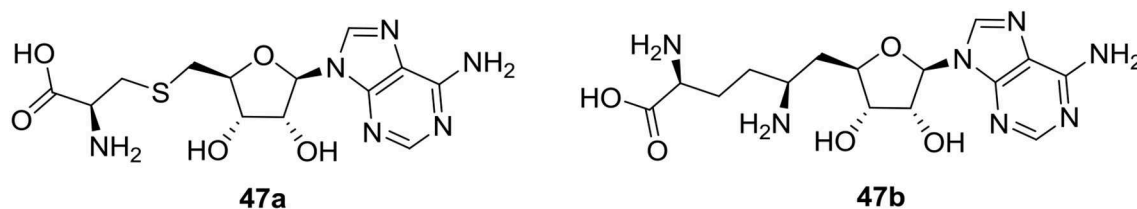


FIGURE 13 | Structures of S-adenosyl-homocysteine (47a) and sinefungin (47b).

et al., 2008b), while Spring et al. (Galloway et al., 2011) in 2011 published a SAR analysis on AHL QS modulators. Below is a short summary of the SAR trends highlighted in these reviews, and **Figure 14** outlines the most potent inhibitors. Geske et al. delineated some broad activity trends for the AHL mimics (see below). These trends are highlighted with colored spheres in **Figure 14** for AHL analogs found to inhibit QS in *P. aeruginosa*. **Trend 1** concerns the length of the acyl chain, which in general have to be close to the length of the natural AHL to have high activity. **Trend 2** and **Trend 3** relate to the third carbon on the acyl chain, and in **Trend 2** it is seen that a carbonyl group in this position is important for activity. However, the carbonyl is not essential, and **Trend 3** summarizes AHL inhibitors that do not contain this carbonyl. **Trend 4** highlights the importance of stereochemistry where the L-stereoisomer of the natural AHL lactone ring is important. However, studies investigating racemic mixtures has also resulted in identification of good inhibitors. Therefore, it is uncertain whether the L-isomer is the only active species. **Trend 5** concerns modifications of the lactone ring, which has been shown to be tolerated in some systems but most often has led to a decrease in activity. Lastly, **Trend 6** shows AHL inhibitors that incorporate aromatic functionalities either by replacing the lactone ring or as substituent on the acyl chain.

In 2012 Stacy et al. published a SAR study of non-natural AHL analogues' ability to activate and inhibit *A. baumannii* QS by agonizing or antagonizing the AbaR receptor (Stacy et al., 2012). In general, the strongest AbaR antagonist contained aromatic acyl groups. Phenylacetanoyls homoserine lactones (PHLs) (55a) with substituents on the phenyl ring showed good antagonistic activity. Among the halogenated PHLs, antagonistic activity was found to increase with increasing size and decreasing electronegativity of the halogen. For example, the iodo PHLs (55b) was strongly inhibitory as the most active group followed by bromo and chloro being good to moderate inhibitors and fluoro PHLs being weakly inhibitory (**Figure 15**). Compounds containing substitutions in the 3-position of the PHL aromatic ring were found to generally show stronger inhibition, whereas inhibitor activity was lowered when substitutions were introduced in the 2- and 4-positions. A previous study reported a similar trend with non-native AHLs containing a PHL group showing antagonistic activity of the *P. aeruginosa* LasR protein (Geske et al., 2008c). Stacy et al. suggested that the mode of action of the investigated class of PHLs in LasR and AbaR could be similar (Stacy et al., 2012).

Based on the activity of PHL described above, a recent study investigated two carbon extended N-(phenylbutanoyl)

L-homoserine lactone (PBHL) ligands for inhibition of AbaR and LasR activity. The examined PBHL either contained unsubstituted or chlorine- or iodine-substituted phenyl groups and varied in the oxidation states of the 3-position (56a, **Figure 15**). It was reported that inhibition of LasR moderately depended on oxidation state, whereas AbaR inhibition was not significantly affected by the oxidation state of the PBHL ligand.

Studies on Non-AHL-Based QS Modulators

The mode of actions of non-AHL like QS inhibitory compounds have in many cases not been specified questioning which part of the QS system is targeted. Therefore, is it possible that some of the compounds presented in the following section do not target the QS system through modulation of the LuxR-type receptor specifically. In addition, there is often a considerable difference between the molecular structures of the identified QS inhibitors from various studies of non-AHL based QS modulators which limit the number of compounds to build adequate SAR studies. Nevertheless, the structures of the different identified QS inhibitors are relevant for further discussion of what might be potentially active compounds.

Some of the first identified and intensively studied QS inhibitors originating from natural sources were the brominated furanones. Since the bioactivity of furanones, extracted from the marine algae *Delisea pulchra*, was hypothesized to exert its activity by paralyzing the AHL regulated QS system (Givskov et al., 1996), several studies have investigated QS modulation activity of a great number of furanone derivatives. In 2003, the Givskov group delivered proof of concept regarding QS inhibition as an antimicrobial principle (Hentzer et al., 2003). With chemically modified halogenated furanones they showed a significant impact on QS controlled gene expression (first transcriptomic analyses to be undertaken), as well as decreases in QS regulated virulence factors, and accelerated clearance of *P. aeruginosa* in a lung infection mouse model (Hentzer et al., 2003; Wu et al., 2004). For a more detailed description of investigated furanones together with related structural analogs the reader is referred to Galloway et al. (2011).

Phytochemicals such as flavonoids, flavanones, polyphenols, furacoumarins, and hydrolysable tannins has been shown to disrupt the QS system in a number of different bacteria (Kalia et al., 2013). By bioassay guided fractionation of *Glycyrrhiza glabra*, commonly known as liquorice, a methanol extract was shown to inhibit motility and biofilm formation of *A. baumannii*. In addition, the production of 3-OH-C12-HSL was significantly reduced indicating disruption of the QS system. Q-TOF MS and

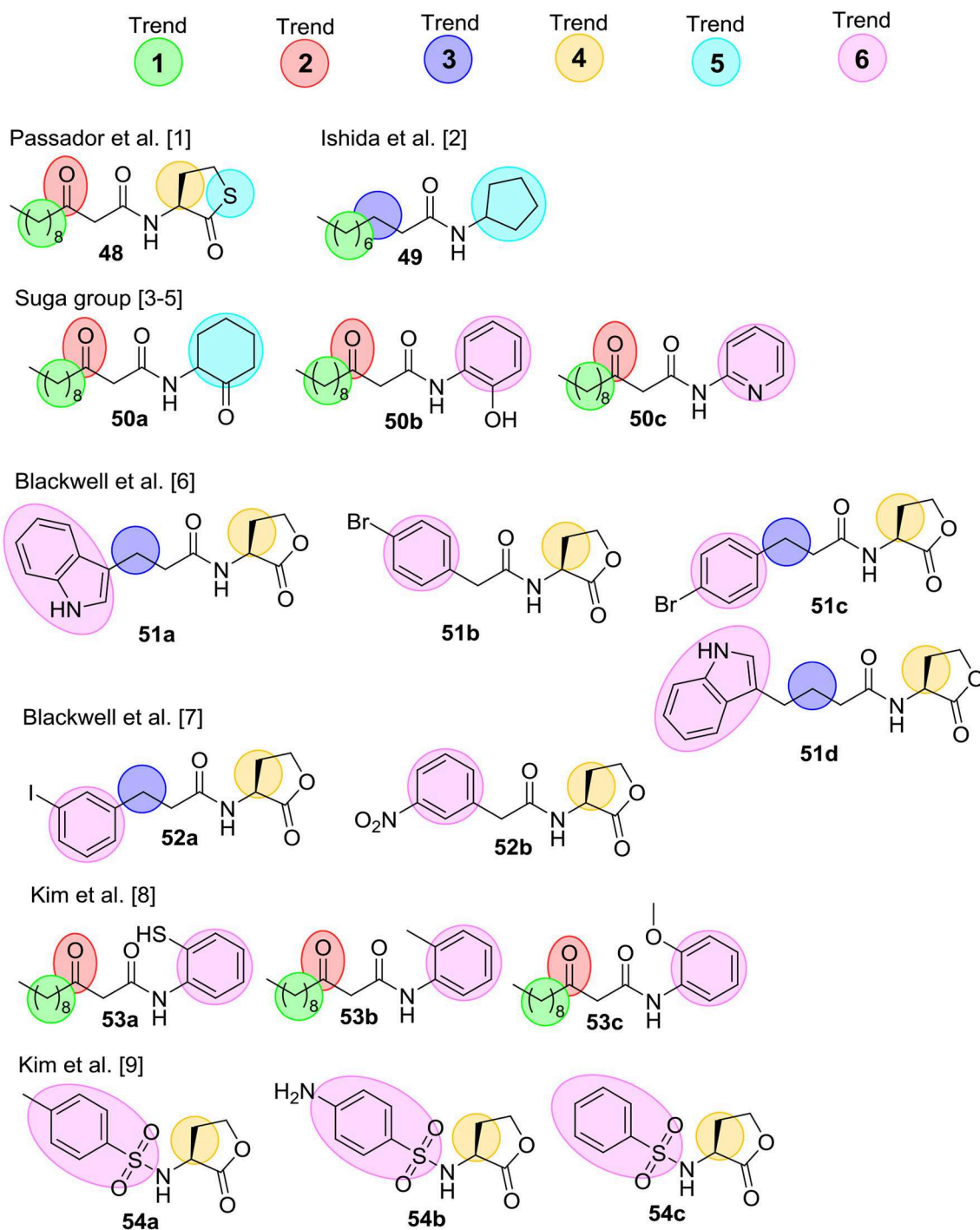
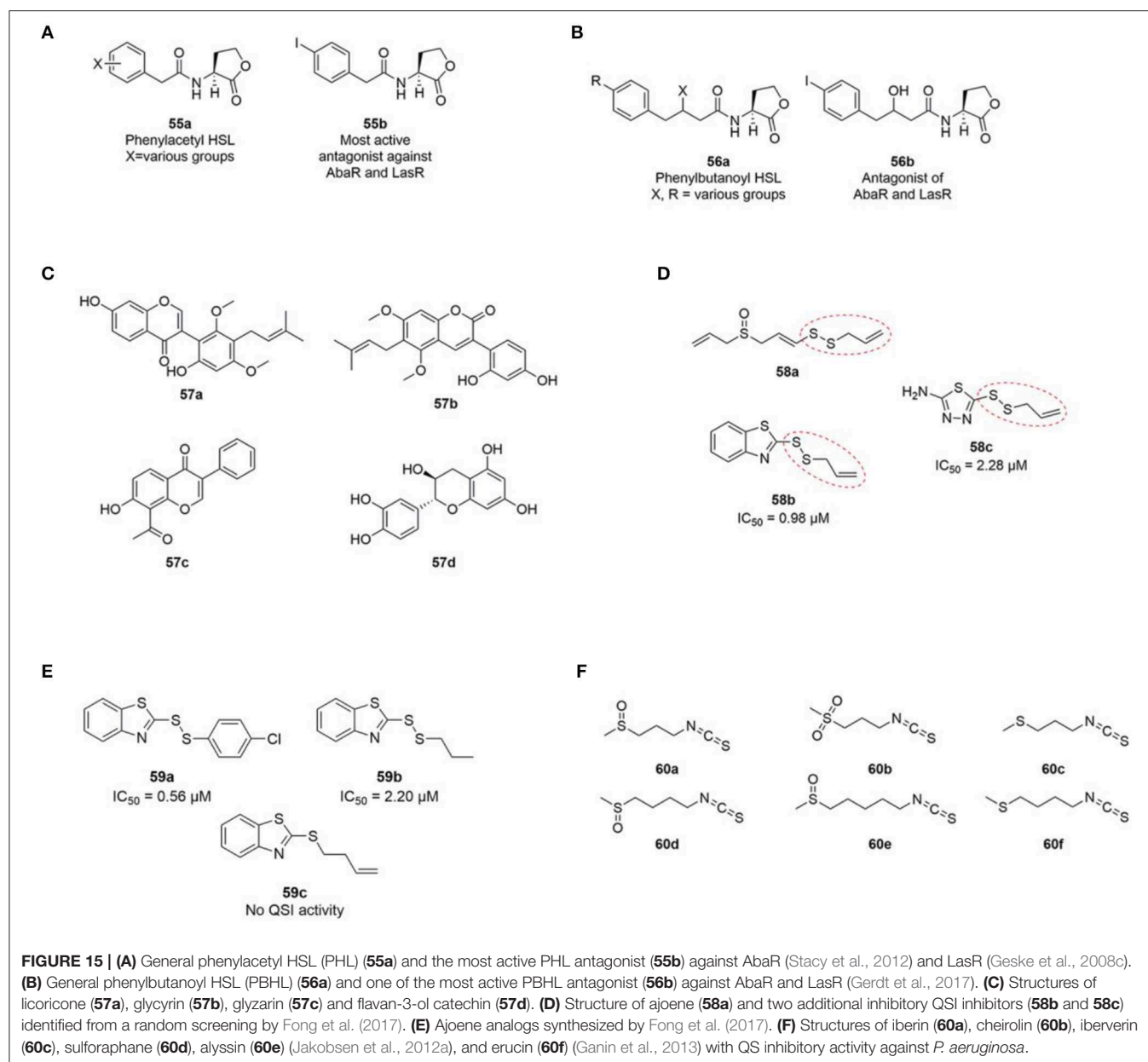


FIGURE 14 | Collection of the most potential QS inhibitors mentioned in Geske et al. (2008b) and Galloway et al. (2011). [1] (Passador et al., 1996) [2] (Ishida et al., 2007) [3] (Smith et al., 2003a) [4] (Smith et al., 2003b) [5] (Jog et al., 2006) [6] (Geske et al., 2005) [7] (Geske et al., 2008a) [8] (Kim et al., 2009a), and [9] (Kim et al., 2009b).

Q-TRAP MS/MS analysis of the extract suggested the presence of the following three flavonoids; licoricone (57a), and glycyrin (57b) and glyzarine (57c) (Figure 15) (Bhargava et al., 2015). The flavonoid flavan-3-ol catechin (57d) extracted from the

bark of *Combrenum albiflorum* has been reported to decrease the expression of *P. aeruginosa* QS regulated genes as well as to inhibit the production of QS regulated virulence factors (Vandeputte et al., 2010).



A number of sulfur containing compounds has been reported as QS inhibitors of *P. aeruginosa*. Ajoene **58a** (Figure 15) from crushed garlic was reported to inhibit a subset of QS controlled genes including rhamnolipid production, and to increase the susceptibility of *P. aeruginosa* biofilms to tobramycin and significantly decrease *P. aeruginosa* infection in the lungs of mice (Jakobsen et al., 2012b). Ajoene displays its activity by lowering the expression of the two small RNAs RsmY and RsmZ located upstream of the central QS system in *P. aeruginosa* (Jakobsen et al., 2017b). From a random screening of a chemical compound library two sulfur containing compounds **58b** and **58c** (Figure 15) with structural similarities to ajoene were reported as QS inhibitors of *P. aeruginosa* (Fong et al., 2017). Both compounds share the same allylic

disulphide bond with ajoene marked with a red dotted line in Figure 15.

Subsequently, syntheses of 25 disulphide bond-containing analogs were carried out to investigate the importance of the allyl disulphide group for bioactivity (Fong et al., 2017). The authors reported that the allyl group was not strictly important for QS activity, which was shown with the saturated analog **58b** that displayed excellent QS inhibitory activity (Figure 15). A *p*-chlorophenyl derivative (**59a**) showed the highest QSI activity among the tested compounds, whereas the absence of disulphide bond diminished the QS inhibitory activity completely as shown with **59c** in Figure 15. In addition, two compounds devoid of the benzothiazole functional group did not display any QS inhibitory activity. The two compounds

59b and **59a** were reported to decrease production of the three important QS regulated virulence factors; elastase, pyocyanine, and rhamnolipid. In addition, both compounds significantly decreased *P. aeruginosa* bacterial counts in a foreign-body implant mouse model compared to an untreated control group. This relative small SAR analysis of ajoene analogs indicates that the presence of a disulphide bond is important for bioactivity. In addition, the presence of a benzothiazole moiety increases the QS inhibitory activity substantially compared with ajoene.

Additional sulfur containing compounds have been identified as QS inhibitors of *P. aeruginosa*. By means of bioassay-guided fractionation of horseradish, 1-isothiocyanato-3-(methylsulfinyl) propane, commonly known as iberin (**60a**, **Figure 15**) was identified as an efficient QS inhibitor of *P. aeruginosa* (Jakobsen et al., 2012a). Iberin **60a** is a natural isothiocyanate with a sulfinyl group found in many members of the Brassicaceae family. Together with iberin **60a**, the following four related structural isothiocyanate analogs was reported as inhibitors: cheirolin (**60b**), iberiverin (**60c**), sulforaphane (**60d**) and alyssin (**60e**) (**Figure 15**), however, they all showed lower QS inhibitory activities than iberin **60a** (IC₅₀ values of ~2, 6, 10, and 30 times higher, respectively). Another study also reported sulforaphane to inhibit the QS system of *P. aeruginosa* together with the isothiocyanate erucin (**60f**, **Figure 15**) extracted from broccoli (Ganin et al., 2013).

Taken together, the number of different sulfur containing compounds that have been reported with excellent QS inhibitory activities makes it an interesting class of molecules to be studied further. The identified compounds have little structural similarity to native AHLs. This can be an advantage compared to AHL like compounds when considering that the homoserine lactone moiety is unstable at alkaline pH and potentially can be degraded by mammalian lactonases.

CONCLUSIONS AND PERSPECTIVES

According to WHO and UN, antimicrobial resistance is rising to unmanageable levels in all parts of the world and has become a top global threat. This grim perspective is paralleled by the fact that only two new classes of antibiotics have been clinically approved over the past 30 years. So far, the majority of clinically approved antibiotics have been designed to efficiently kill free-living (planktonic), growing bacteria. In the environment however, the preferred life-mode of bacteria is as densely packed microcolonies concealed in a protective matrix of biopolymers that offer protection against the otherwise lethal action of a wide variety of environmental stressors including antimicrobials. In this biofilm life-mode, bacteria are also believed to cause a significant number of human microbial infections. Nosocomial infections are estimated to be the fourth leading cause of death in the U.S. with 2 million cases annually, and about 60–70% of these nosocomial infections are caused by bacterial biofilms (Bryers, 2008). Because of the general neglect of the biofilm-mode in past antibiotic development, the central problem with biofilm infections is that the involved bacteria are generally not susceptible to our present assortment of antibiotics. Adding to

this the resistance to the antimicrobial activities of the immune system in general, the biofilm mode offers an almost unlimited capacity to survive in the infected host (Costerton et al., 1999; Rybtke et al., 2015).

With the increase in infectious diseases showing multiple resistances and the paralleled downsizing in antibiotic development there is, more than ever, an urgent need for development of antimicrobials with new and different modes of action. Such antimicrobials may be designed to include non-lethal targets associated with the biofilm life-mode, where the chemistry and mode of actions of some of those compounds have been reviewed in the present paper. Conceptually such drugs function to attenuate biofilm formation and/or pathogenicity without obstructing processes that are essential for bacterial growth and reproduction. Among the few identified targets are two key biofilm gateways; the one that controls the switch between the biofilm-planktonic life modes in responses to the internal levels of c-di-GMP, and QS which governs the production of virulence factors and some of the protective mechanisms operating in the biofilm mode. Proof of concept driven research initiated more than 20 years ago by us have shown the signaling gateways to be viable drug targets for a new class of what can generally be referred to as non-lethal antibiotics (Hentzer et al., 2003). It has been postulated, but not directly demonstrated, that such modes of drug action would reduce the selection pressure for resistant bacterial variants. While this may to a certain extent be correct for QS, we have unpublished experimental data showing that in an environment where biofilm formation promotes growth and provides a hold-fast of bacteria, chemical obstruction of biofilm formation raises a significant selection pressure for insensitive mutants and resistance seems to arise as frequently as it does to the action of conventional antibiotics.

We and others are currently in pursuit of the development of chemical compounds capable of preventing formation of biofilms. Most of the work done so far aims at targeting (inhibiting) c-di-GMP synthesis. One of the rationales for this is the highly conserved composition of the GGDEF domains in multiple Gram negative species. Aiming for this target would then be expected to result in development of broad spectrum anti-biofilm drugs. We have been following this strategy too, but with disappointing results. We are currently pursuing stimulation of PDE activities to accomplice a reduction in the cellular c-di-GMP content. This strategy comes from our findings that overexpression of an *E. coli* PDE (PdeH) in *P. aeruginosa* plummets the c-di-GMP level and results in massive biofilm dispersal (Christensen et al., 2013). This concept is functional *in vivo* as judged from our mouse implant model of infection (Christensen et al., 2013). However, success of this strategy depends on selection of the right PDE, since overexpression of some of the PDEs in *P. aeruginosa* evidently do not lead to biofilm dispersal (Chambers et al., 2017), which is in agreement with the emerging theme that DGCs, PDEs and c-di-GMP effectors often work via protein-protein interactions. Treatment of biofilm infections by means of large scale dispersal of bacteria from the biofilms, would require combinatorial treatments with conventional antibiotics that eradicate the dispersed bacteria.

Whereas, the success criteria for lethal antibiotics have largely been based on low MIC values, the process of designing non-lethal antibiotics that would in turn work in concert with their lethal counter parts is significantly more elaborative and challenging. As emphasized in this review, small molecules continue to emerge as efficient modulators of bacterial biofilm formation. An increasing number of new molecular scaffolds and chemotypes, derived from both natural products and of entirely synthetic origin, have been developed. The reported compounds are currently useful as tools to study the molecular mechanisms involved in biofilm formation, growth and dispersal, but may also serve as hits to guide early discovery efforts. There is academic and industrial consensus on the unique promise for translational applications, such as new antimicrobial medicines, anti-biofouling and crop protection agents, but the path forward for small-molecule biofilm modulation remains long. Driven by academic research efforts, it is only natural that most SAR studies have been balancing synthetic feasibility and *in vitro* studies as a prequel to devoted medicinal chemistry campaigns. For example, virtually no knowledge is available on the performance of biofilm

modulating scaffolds in integrated ADME/TOX evaluation studies, pointing to all the usual challenges of small molecule drug discovery. As a further complication, a combination of poor assay standardization and studies on clinically irrelevant bacterial strains has significantly hampered target evaluation and drugability assessment. The biofilm scientific community must address the myriad of hard-to-reproduce biological data to leverage the value of the many novel compounds emerging from academic laboratories, and ultimately secure the fundamental basis of clinical translation.

AUTHOR CONTRIBUTIONS

All authors listed have made a substantial, direct and intellectual contribution to the work, and approved it for publication.

FUNDING

This work was supported by grants from the Danish Council for Independent Research, the Lundbeck Foundation, the Novo Nordisk Foundation, and the Carlsberg Foundation.

REFERENCES

- Åberg, V., Das, P., Chorell, E., Hedenstrom, M., Pinkner, J. S., Hultgren, S. J., et al. (2008). Carboxylic acid isosteres improve the activity of ring-fused 2-pyridones that inhibit pilus biogenesis in *E. coli*. *Bioorg. Med. Chem. Lett.* 18, 3536–3540. doi: 10.1016/j.bmcl.2008.05.020
- Åberg, V., and Almqvist, F. (2007). Pilicides-small molecules targeting bacterial virulence. *Org. Biomol. Chem.* 5, 1827–1834. doi: 10.1039/B702397A
- Åberg, V., Hedenstrom, M., Pinkner, J. S., Hultgren, S. J., and Almqvist, F. (2005a). C-Terminal properties are important for ring-fused 2-pyridones that interfere with the chaperone function in uropathogenic *E. coli*. *Org. Biomol. Chem.* 3, 3886–3892. doi: 10.1039/b509376g
- Åberg, V., Norman, F., Chorell, E., Westermarck, A., Olofsson, A., Sauer-Eriksson, A. E., et al. (2005b). Microwave-assisted decarboxylation of bicyclic 2-pyridone scaffolds and identification of Abeta-peptide aggregation inhibitors. *Org. Biomol. Chem.* 3, 2817–2823. doi: 10.1039/b503294f
- Alhede, M., Bjarnsholt, T., Jensen, P. O., Phipps, R. K., Moser, C., Christophersen, L., et al. (2009). *Pseudomonas aeruginosa* recognizes and responds aggressively to the presence of polymorphonuclear leukocytes. *Microbiology* 155, 3500–3508. doi: 10.1099/mic.0.031443-0
- Allesen-Holm, M., Barken, K. B., Yang, L., Klausen, M., Webb, J. S., Kjelleberg, S., et al. (2006). A characterization of DNA release in *Pseudomonas aeruginosa* cultures and biofilms. *Mol. Microbiol.* 59, 1114–1128. doi: 10.1111/j.1365-2958.2005.05008.x
- Anbazhagan, D., Mansor, M., Yan, G. O., Md Yusof, M. Y., Hassan, H., and Sekaran, S. D. (2012). Detection of quorum sensing signal molecules and identification of an autoinducer synthase gene among biofilm forming clinical isolates of *Acinetobacter* spp. *PLoS ONE* 7:e36696. doi: 10.1371/journal.pone.0036696
- Anderson, G. G., Palermo, J. J., Schilling, J. D., Roth, R., Heuser, J., and Hultgren, S. J. (2003). Intracellular bacterial biofilm-like pods in urinary tract infections. *Science* 301, 105–107. doi: 10.1126/science.1084550
- Antoniani, D., Bocci, P., Maciag, A., Raffaelli, N., and Landini, P. (2010). Monitoring of diguanylate cyclase activity and of cyclic-di-GMP biosynthesis by whole-cell assays suitable for high-throughput screening of biofilm inhibitors. *Appl. Microbiol. Biotechnol.* 85, 1095–1104. doi: 10.1007/s00253-009-2199-x
- Antoniani, D., Rossi, E., Rinaldo, S., Bocci, P., Lolicato, M., Paiardini, A., et al. (2013). The immunosuppressive drug azathioprine inhibits biosynthesis of the bacterial signal molecule cyclic-di-GMP by interfering with intracellular nucleotide pool availability. *Appl. Microbiol. Biotechnol.* 97, 7325–7336. doi: 10.1007/s00253-013-4875-0
- Barnhart, M. M., Sauer, F. G., Pinkner, J. S., and Hultgren, S. J. (2003). Chaperone-subunit-usher interactions required for donor strand exchange during bacterial pilus assembly. *J. Bacteriol.* 185, 2723–2730. doi: 10.1128/JB.185.9.2723-2730.2003
- Barraud, N., Hassett, D. J., Hwang, S. H., Rice, S. A., Kjelleberg, S., and Webb, J. S. (2006). Involvement of nitric oxide in biofilm dispersal of *Pseudomonas aeruginosa*. *J. Bacteriol.* 188, 7344–7353. doi: 10.1128/JB.00779-06
- Barraud, N., Schleheck, D., Klebensberger, J., Webb, J. S., Hassett, D. J., Rice, S. A., et al. (2009). Nitric oxide signaling in *Pseudomonas aeruginosa* biofilms mediates phosphodiesterase activity, decreased cyclic di-GMP levels, and enhanced dispersal. *J. Bacteriol.* 191, 7333–7342. doi: 10.1128/JB.00975-09
- Beaber, J. W., Hochhut, B., and Waldor, M. K. (2004). SOS response promotes horizontal dissemination of antibiotic resistance genes. *Nature* 427, 72–74. doi: 10.1038/nature02241
- Beloin, C., Roux, A., and Ghigo, J. M. (2008). *Escherichia coli* biofilms. *Curr. Top. Microbiol. Immunol.* 322, 249–289. doi: 10.1007/978-3-540-75418-3_12
- Ben Nasr, A., Olsen, A., Sjöbring, U., Müller-Esterl, W., and Björck, L. (1996). Assembly of human contact phase proteins and release of bradykinin at the surface of curli-expressing *Escherichia coli*. *Mol. Microbiol.* 20, 927–935. doi: 10.1111/j.1365-2958.1996.tb02534.x
- Besharova, O., Suchanek, V. M., Hartmann, R., Drescher, K., and Sourjik, V. (2016). Diversification of gene expression during formation of static submerged biofilms by *Escherichia coli*. *Front. Microbiol.* 7:1568. doi: 10.3389/fmicb.2016.01568
- Bhargava, N., Singh, S. P., Sharma, A., Sharma, P., and Capalash, N. (2015). Attenuation of quorum sensing-mediated virulence of *Acinetobacter baumannii* by Glycyrrhiza glabra flavonoids. *Future Microbiol.* 10, 1953–1968. doi: 10.2217/fmb.15.107
- Bjarnsholt, T., Jensen, P. O., Burmolle, M., Hentzer, M., Haagensen, J. A., Høugen, H. P., et al. (2005). *Pseudomonas aeruginosa* tolerance to tobramycin, hydrogen peroxide and polymorphonuclear leukocytes is quorum-sensing dependent. *Microbiology* 151, 373–383. doi: 10.1099/mic.0.27463-0
- Boehm, A., Steiner, S., Zaehring, F., Casanova, A., Hamburger, F., Ritz, D., et al. (2009). Second messenger signalling governs *Escherichia coli* biofilm induction upon ribosomal stress. *Mol. Microbiol.* 72, 1500–1516. doi: 10.1111/j.1365-2958.2009.06739.x
- Borlee, B. R., Goldman, A. D., Murakami, K., Samudrala, R., Wozniak, D. J., and Parsek, M. R. (2010). *Pseudomonas aeruginosa* uses a cyclic-di-GMP-regulated

- adhesin to reinforce the biofilm extracellular matrix. *Mol. Microbiol.* 75, 827–842. doi: 10.1111/j.1365-2958.2009.06991.x
- Bottomley, M. J., Muraglia, E., Bazzo, R., and Carfi, A. (2007). Molecular insights into quorum sensing in the human pathogen *Pseudomonas aeruginosa* from the structure of the virulence regulator LasR bound to its autoinducer. *J. Biol. Chem.* 282, 13592–13600. doi: 10.1074/jbc.M700556200
- Brinton, C. C. Jr. (1965). The structure, function, synthesis and genetic control of bacterial pili and a molecular model for DNA and RNA transport in gram negative bacteria. *Trans. N. Y. Acad. Sci.* 27, 1003–1054. doi: 10.1111/j.2164-0947.1965.tb02342.x
- Brombacher, E., Baratto, A., Dorel, C., and Landini, P. (2006). Gene expression regulation by the Curli activator CsgD protein: modulation of cellulose biosynthesis and control of negative determinants for microbial adhesion. *J. Bacteriol.* 188, 2027–2037. doi: 10.1128/JB.188.6.2027-2037.2006
- Brombacher, E., Dorel, C., Zehnder, A. J., and Landini, P. (2003). The curli biosynthesis regulator CsgD co-ordinates the expression of both positive and negative determinants for biofilm formation in *Escherichia coli*. *Microbiology* 149, 2847–2857. doi: 10.1099/mic.0.26306-0
- Brown, P. K., Dozois, C. M., Nickerson, C. A., Zuppardo, A., Terlonge, J., and Curtiss, R. III. (2001). MlrA, a novel regulator of curli (Agf) and extracellular matrix synthesis by *Escherichia coli* and *Salmonella enterica* serovar Typhimurium. *Mol. Microbiol.* 41, 349–363. doi: 10.1046/j.1365-2958.2001.02529.x
- Bryers, J. D. (2008). Medical biofilms. *Biotechnol. Bioeng.* 100, 1–18. doi: 10.1002/bit.21838
- Bullitt, E., and Makowski, L. (1995). Structural polymorphism of bacterial adhesion pili. *Nature* 373, 164–167. doi: 10.1038/373164a0
- Busch, A., Phan, G., and Waksman, G. (2015). Molecular mechanism of bacterial type 1 and P pili assembly. *Philos. Trans. A Math. Phys. Eng. Sci.* 373:20130153. doi: 10.1098/rsta.2013.0153
- Cegelski, L., Pinkner, J. S., Hammer, N. D., Cusumano, C. K., Hung, C. S., Chorell, E., et al. (2009). Small-molecule inhibitors target *Escherichia coli* amyloid biogenesis and biofilm formation. *Nat. Chem. Biol.* 5, 913–919. doi: 10.1038/nchembio.242
- Chambers, J. R., Cherny, K. E., and Sauer, K. (2017). Susceptibility of *Pseudomonas aeruginosa* dispersed cells to antimicrobial agents is dependent on the dispersion cue and class of the antimicrobial agent used. *Antimicrob. Agents Chemother.* 61:e00846–17. doi: 10.1128/AAC.00846-17
- Chan, C., Paul, R., Samoray, D., Amiot, N. C., Giese, B., Jenal, U., et al. (2004). Structural basis of activity and allosteric control of diguanylate cyclase. *Proc. Natl. Acad. Sci. U.S.A.* 101, 17084–17089. doi: 10.1073/pnas.0406134101
- Chapman, M. R., Robinson, L. S., Pinkner, J. S., Roth, R., Heuser, J., Hammar, M., et al. (2002). Role of *Escherichia coli* curli operons in directing amyloid fiber formation. *Science* 295, 851–855. doi: 10.1126/science.1067484
- Chen, F., Gao, Y., Chen, X., Yu, Z., and Li, X. (2013). Quorum quenching enzymes and their application in degrading signal molecules to block quorum sensing-dependent infection. *Int. J. Mol. Sci.* 14, 17477–17500. doi: 10.3390/ijms140917477
- Chiang, P., and Burrows, L. L. (2003). Biofilm formation by hyperpiliated mutants of *Pseudomonas aeruginosa*. *J. Bacteriol.* 185, 2374–2378. doi: 10.1128/JB.185.7.2374-2378.2003
- Chiang, W. C., Nilsson, M., Jensen, P. O., Hoiby, N., Nielsen, T. E., Givskov, M., et al. (2013). Extracellular DNA shields against aminoglycosides in *Pseudomonas aeruginosa* biofilms. *Antimicrob. Agents Chemother.* 57, 2352–2361. doi: 10.1128/AAC.00001-13
- Choi, A., Slamti, L., Avci, F. Y., Pier, G. B., and Maira-Litran, T. (2009). The pgaABCD locus of *Acinetobacter baumannii* encodes the production of poly-beta-1-6-N-acetylglucosamine, which is critical for biofilm formation. *J. Bacteriol.* 191, 5953–5963. doi: 10.1128/JB.00647-09
- Chorell, E., Bengtsson, C., Sainte-Luce Banchelin, T., Das, P., Uvell, H., Sinha, A. K., et al. (2011). Synthesis and application of a bromomethyl substituted scaffold to be used for efficient optimization of anti-virulence activity. *Eur. J. Med. Chem.* 46, 1103–1116. doi: 10.1016/j.ejmech.2011.01.025
- Chorell, E., Pinkner, J. S., Bengtsson, C., Banchelin, T. S., Edvinsson, S., Linusson, A., et al. (2012). Mapping pilicide anti-virulence effect in *Escherichia coli*, a comprehensive structure-activity study. *Bioorg. Med. Chem.* 20, 3128–3142. doi: 10.1016/j.bmc.2012.01.048
- Chorell, E., Pinkner, J. S., Phan, G., Edvinsson, S., Buelens, F., Remaut, H., et al. (2010). Design and synthesis of C-2 substituted thiazolo and dihydrothiazolo ring-fused 2-pyridones: pilicides with increased antivirulence activity. *J. Med. Chem.* 53, 5690–5695. doi: 10.1021/jm100470t
- Christensen, L. D., Van Gennip, M., Rybtke, M. T., Wu, H., Chiang, W. C., Alhede, M., et al. (2013). Clearance of *Pseudomonas aeruginosa* foreign-body biofilm infections through reduction of the cyclic Di-GMP level in the bacteria. *Infect. Immun.* 81, 2705–2713. doi: 10.1128/IAI.00332-13
- Chun, C. K., Ozer, E. A., Welsh, M. J., Zabner, J., and Greenberg, E. P. (2004). Inactivation of a *Pseudomonas aeruginosa* quorum-sensing signal by human airway epithelia. *Proc. Natl. Acad. Sci. U.S.A.* 101, 3587–3590. doi: 10.1073/pnas.0308750101
- Ciofu, O., and Tolker-Nielsen, T. (2019). Tolerance and Resistance of *Pseudomonas aeruginosa* Biofilms to Antimicrobial Agents-How *P. aeruginosa* can escape antibiotics. *Front. Microbiol.* 10:913. doi: 10.3389/fmicb.2019.00913
- Costas, C., López-Puente, V., Bodelón, G., González-Bello, C., Pérez-Juste, J., Pastoriza-Santos, I., et al. (2015). Using surface enhanced raman scattering to analyze the interactions of protein receptors with bacterial quorum sensing modulators. *ACS Nano* 9, 5567–5576. doi: 10.1021/acsnano.5b01800
- Costerton, J. W., Stewart, P. S., and Greenberg, E. P. (1999). Bacterial biofilms: a common cause of persistent infections. *Science* 284, 1318–1322. doi: 10.1126/science.284.5418.1318
- Cusumano, C. K., and Hultgren, S. J. (2009). Bacterial adhesion - a source of alternate antibiotic targets. *IDrugs* 12, 699–705.
- Cusumano, C. K., Pinkner, J. S., Han, Z., Greene, S. E., Ford, B. A., Crowley, J. R., et al. (2011). Treatment and prevention of urinary tract infection with orally active FimH inhibitors. *Sci. Transl. Med.* 3:109ra115. doi: 10.1126/scitranslmed.3003021
- Danese, P. N., Pratt, L. A., Dove, S. L., and Kolter, R. (2000). The outer membrane protein, antigen 43, mediates cell-to-cell interactions within *Escherichia coli* biofilms. *Mol. Microbiol.* 37, 424–432. doi: 10.1046/j.1365-2958.2000.02008.x
- Das, T., Kutty, S. K., Tavallaie, R., Ibugo, A. I., Panchompoo, J., Sehar, S., et al. (2015). Phenazine virulence factor binding to extracellular DNA is important for *Pseudomonas aeruginosa* biofilm formation. *Sci. Rep.* 5:8398. doi: 10.1038/srep08398
- Davey, M. E., Caiazza, N. C., and O'toole, G. A. (2003). Rhamnolipid surfactant production affects biofilm architecture in *Pseudomonas aeruginosa* PAO1. *J. Bacteriol.* 185, 1027–1036. doi: 10.1128/JB.185.3.1027-1036.2003
- Devaraj, A., Justice, S. S., Bakaletz, L. O., and Goodman, S. D. (2015). DNABII proteins play a central role in UPEC biofilm structure. *Mol. Microbiol.* 96, 1119–1135. doi: 10.1111/mmi.12994
- Deziel, E., Comeau, Y., and Villemur, R. (2001). Initiation of biofilm formation by *Pseudomonas aeruginosa* 57RP correlates with emergence of hyperpiliated and highly adherent phenotypic variants deficient in swimming, swarming, and twitching motilities. *J. Bacteriol.* 183, 1195–1204. doi: 10.1128/JB.183.4.1195-1204.2001
- Diggle, S. P., Cornelis, P., Williams, P., and Camara, M. (2006a). 4-quinolone signalling in *Pseudomonas aeruginosa*: old molecules, new perspectives. *Int. J. Med. Microbiol.* 296, 83–91. doi: 10.1016/j.ijmm.2006.01.038
- Diggle, S. P., Stacey, R. E., Dodd, C., Camara, M., Williams, P., and Winzer, K. (2006b). The galactophilic lectin, LecA, contributes to biofilm development in *Pseudomonas aeruginosa*. *Environ. Microbiol.* 8, 1095–1104. doi: 10.1111/j.1462-2920.2006.001001.x
- Dong, Y. H., Xu, J. L., Li, X. Z., and Zhang, L. H. (2000). AiiA, an enzyme that inactivates the acylhomoserine lactone quorum-sensing signal and attenuates the virulence of *Erwinia carotovora*. *Proc. Natl. Acad. Sci. U.S.A.* 97, 3526–3531. doi: 10.1073/pnas.97.7.3526
- Dorsey, C. W., Tomaras, A. P., and Actis, L. A. (2002). Genetic and phenotypic analysis of *Acinetobacter baumannii* insertion derivatives generated with a transposome system. *Appl. Environ. Microbiol.* 68, 6353–6360. doi: 10.1128/AEM.68.12.6353-6360.2002
- Dueholm, M. S., Sondergaard, M. T., Nilsson, M., Christiansen, G., Stensballe, A., Overgaard, M. T., et al. (2013). Expression of Fap amyloids in *Pseudomonas aeruginosa*, *P. fluorescens*, and *P. putida* results in aggregation and increased biofilm formation. *Microbiologyopen* 2, 365–382. doi: 10.1002/mbo3.81
- Emtenas, H., Åhlin, K., Pinkner, J. S., Hultgren, S. J., and Almqvist, F. (2002). Design and parallel solid-phase synthesis of ring-fused 2-pyridinones that

- target pilus biogenesis in pathogenic bacteria. *J. Comb. Chem.* 4, 630–639. doi: 10.1021/cc020032d
- Emtenäs, H., Carlsson, M., Pinkner, J. S., Hultgren, S. J., and Almqvist, F. (2003a). Stereoselective synthesis of optically active bicyclic β -lactam carboxylic acids that target pilus biogenesis in pathogenic bacteria. Electronic supplementary information (ESI) available: ¹³C NMR spectra of 7(a–g), 10–14, 16(a and d) and 17(a–b). See <http://www.rsc.org/suppdata/ob/b2/b210551a>. *Organ. Biomol. Chem.* 1, 1308–1314. doi: 10.1039/b210551a
- Emtenäs, H., Taflin, C., and Almqvist, F. (2003b). Efficient microwave assisted synthesis of optically active bicyclic 2-pyridinones via Δ 2-thiazolines. *Mol. Divers.* 7, 165–169. doi: 10.1023/B:MODI.0000006800.46154.99
- Fazli, M., Almlblad, H., Rytke, M. L., Givskov, M., Eberl, L., and Tolker-Nielsen, T. (2014). Regulation of biofilm formation in *Pseudomonas* and *Burkholderia* species. *Environ. Microbiol.* 16, 1961–1981. doi: 10.1111/1462-2920.12448
- Fernicola, S., Paiardini, A., Giardina, G., Rampioni, G., Leoni, L., Cutruzzola, F., et al. (2016). *in silico* discovery and *in vitro* validation of catechol-containing sulfonohydrazide compounds as potent inhibitors of the diguanylate cyclase PleD. *J. Bacteriol.* 198, 147–156. doi: 10.1128/JB.00742-15
- Fernicola, S., Torquati, I., Paiardini, A., Giardina, G., Rampioni, G., Messina, M., et al. (2015). Synthesis of triazole-linked analogues of c-di-GMP and their interactions with diguanylate cyclase. *J. Med. Chem.* 58, 8269–8284. doi: 10.1021/acs.jmedchem.5b01184
- Flemming, H. C., and Wuerzt, S. (2019). Bacteria and archaea on Earth and their abundance in biofilms. *Nat. Rev. Microbiol.* 17, 247–260. doi: 10.1038/s41579-019-0158-9
- Fong, J., Yuan, M., Jakobsen, T. H., Mortensen, K. T., Delos Santos, M. M., Chua, S. L., et al. (2017). Disulfide bond-containing ajoene analogues as novel quorum sensing inhibitors of *Pseudomonas aeruginosa*. *J. Med. Chem.* 60, 215–227. doi: 10.1021/acs.jmedchem.6b01025
- Fronzes, R., Remaut, H., and Waksman, G. (2008). Architectures and biogenesis of non-flagellar protein appendages in Gram-negative bacteria. *EMBO J.* 27, 2271–2280. doi: 10.1038/emboj.2008.155
- Gaddy, J. A., Tomaras, A. P., and Actis, L. A. (2009). The *Acinetobacter baumannii* 19606 OmpA protein plays a role in biofilm formation on abiotic surfaces and in the interaction of this pathogen with eukaryotic cells. *Infect. Immun.* 77, 3150–3160. doi: 10.1128/IAI.00096-09
- Galloway, W. R., Hodgkinson, J. T., Bowden, S. D., Welch, M., and Spring, D. R. (2011). Quorum sensing in Gram-negative bacteria: small-molecule modulation of AHL and AI-2 quorum sensing pathways. *Chem. Rev.* 111, 28–67. doi: 10.1021/cr100109t
- Ganin, H., Rayo, J., Amara, N., Levy, N., Krief, P., and Meijler, M. M. (2013). Sulforaphane and erucin, natural isothiocyanates from broccoli, inhibit bacterial quorum sensing. *Medchemcomm* 4, 175–179. doi: 10.1039/C2MD20196H
- Gerd, J. P., Wittenwyler, D. M., Combs, J. B., Boursier, M. E., Brummond, J. W., Xu, H., et al. (2017). Chemical interrogation of LuxR-type quorum sensing receptors reveals new insights into receptor selectivity and the potential for interspecies bacterial signaling. *ACS Chem. Biol.* 12, 2457–2464. doi: 10.1021/acschembio.7b00458
- Geske, G. D., Mattmann, M. E., and Blackwell, H. E. (2008a). Evaluation of a focused library of N-aryl L-homoserine lactones reveals a new set of potent quorum sensing modulators. *Bioorg. Med. Chem. Lett.* 18, 5978–5981. doi: 10.1016/j.bmcl.2008.07.089
- Geske, G. D., O'Neill, J. C., and Blackwell, H. E. (2008b). Expanding dialogues: from natural autoinducers to non-natural analogues that modulate quorum sensing in Gram-negative bacteria. *Chem. Soc. Rev.* 37, 1432–1447. doi: 10.1039/b703021p
- Geske, G. D., O'Neill, J. C., Miller, D. M., Wezeman, R. J., Mattmann, M. E., Lin, Q., et al. (2008c). Comparative analyses of N-acylated homoserine lactones reveal unique structural features that dictate their ability to activate or inhibit quorum sensing. *Chembiochem* 9, 389–400. doi: 10.1002/cbic.200700551
- Geske, G. D., Wezeman, R. J., Siegel, A. P., and Blackwell, H. E. (2005). Small molecule inhibitors of bacterial quorum sensing and biofilm formation. *J. Am. Chem. Soc.* 127, 12762–12763. doi: 10.1021/ja0530321
- Givskov, M., De Nys, R., Manefield, M., Gram, L., Maximilien, R., Eberl, L., et al. (1996). Eukaryotic interference with homoserine lactone-mediated prokaryotic signalling. *J. Bacteriol.* 178, 6618–6622. doi: 10.1128/jb.178.22.6618-6622.1996
- Gjermansen, M., Nilsson, M., Yang, L., and Tolker-Nielsen, T. (2010). Characterization of starvation-induced dispersion in *Pseudomonas putida* biofilms: genetic elements and molecular mechanisms. *Mol. Microbiol.* 75, 815–826. doi: 10.1111/j.1365-2958.2009.06793.x
- Gjermansen, M., Ragas, P., and Tolker-Nielsen, T. (2006). Proteins with GGDEF and EAL domains regulate *Pseudomonas putida* biofilm formation and dispersal. *FEMS Microbiol. Lett.* 265, 215–224. doi: 10.1111/j.1574-6968.2006.00493.x
- Gong, M., and Makowski, L. (1992). Helical structure of P pili from *Escherichia coli*. Evidence from X-ray fiber diffraction and scanning transmission electron microscopy. *J. Mol. Biol.* 228, 735–742. doi: 10.1016/0022-2836(92)90860-M
- Hammar, M., Bian, Z., and Normark, S. (1996). Nucleator-dependent intercellular assembly of adhesive curli organelles in *Escherichia coli*. *Proc. Natl. Acad. Sci. U.S.A.* 93, 6562–6566. doi: 10.1073/pnas.93.13.6562
- Hammar, M. R., Arnqvist, A., Bian, Z., Olsen, A., and Normark, S. (1995). Expression of two csg operons is required for production of fibronectin- and Congo red-binding curli polymers in *Escherichia coli* K-12. *Mol. Microbiol.* 18, 661–670. doi: 10.1111/j.1365-2958.1995.mmi_18040661.x
- Han, Z., Pinkner, J. S., Ford, B., Obermann, R., Nolan, W., Wildman, S. A., et al. (2010). Structure-based drug design and optimization of mannoside bacterial FimH antagonists. *J. Med. Chem.* 53, 4779–4792. doi: 10.1021/jm100438s
- Hedenstrom, M., Emtenas, H., Pemberton, N., Aberg, V., Hultgren, S. J., Pinkner, J. S., et al. (2005). NMR studies of interactions between periplasmic chaperones from uropathogenic *E. coli* and pilicides that interfere with chaperone function and pilus assembly. *Org. Biomol. Chem.* 3, 4193–4200. doi: 10.1039/b511857c
- Hengge, R., Galperin, M. Y., Ghigo, J. M., Gomelsky, M., Green, J., Hughes, K. T., et al. (2016). Systematic nomenclature for GGDEF and EAL domain-containing Cyclic Di-GMP turnover proteins of *Escherichia coli*. *J. Bacteriol.* 198, 7–11. doi: 10.1128/JB.00424-15
- Hentzer, M., Wu, H., Andersen, J. B., Riedel, K., Rasmussen, T. B., Bagge, N., et al. (2003). Attenuation of *Pseudomonas aeruginosa* virulence by quorum sensing inhibitors. *EMBO J.* 22, 3803–3815. doi: 10.1093/emboj/cdg366
- Hertig, S., and Vogel, V. (2012). Catch bonds. *Curr. Biol.* 22, R823–825. doi: 10.1016/j.cub.2012.08.035
- Hoiby, N. (1977). *Pseudomonas aeruginosa* infection in cystic fibrosis. *Acta Pathol. Microbiol. Scand. Suppl.* 262, 1–96.
- Huber, B., Eberl, L., Feucht, W., and Polster, J. (2003). Influence of polyphenols on bacterial biofilm formation and quorum-sensing. *Z. Naturforsch. C* 58, 879–884. doi: 10.1515/znc-2003-11-1224
- Ishida, T., Ikeda, T., Takiguchi, N., Kuroda, A., Ohtake, H., and Kato, J. (2007). Inhibition of quorum sensing in *Pseudomonas aeruginosa* by N-acyl cyclopentylamides. *Appl. Environ. Microbiol.* 73, 3183–3188. doi: 10.1128/AEM.02233-06
- Jacob-Dubuisson, F., Striker, R., and Hultgren, S. J. (1994). Chaperone-assisted self-assembly of pili independent of cellular energy. *J. Biol. Chem.* 269, 12447–12455.
- Jakobsen, T. H., Bjarnsholt, T., Jensen, P. O., Givskov, M., and Hoiby, N. (2013). Targeting quorum sensing in *Pseudomonas aeruginosa* biofilms: current and emerging inhibitors. *Future Microbiol.* 8, 901–921. doi: 10.2217/fmb.13.57
- Jakobsen, T. H., Bragason, S. K., Phipps, R. K., Christensen, L. D., Van Gennip, M., Alhede, M., et al. (2012a). Food as a source for quorum sensing inhibitors: iberin from horseradish revealed as a quorum sensing inhibitor of *Pseudomonas aeruginosa*. *Appl. Environ. Microbiol.* 78, 2410–2421. doi: 10.1128/AEM.05992-11
- Jakobsen, T. H., Tolker-Nielsen, T., and Givskov, M. (2017a). Bacterial biofilm control by perturbation of bacterial signaling processes. *Int. J. Mol. Sci.* 18:E1970. doi: 10.3390/ijms18091970
- Jakobsen, T. H., Van Gennip, M., Phipps, R. K., Shanmugham, M. S., Christensen, L. D., Alhede, M., et al. (2012b). Ajoene, a sulfur-rich molecule from garlic, inhibits genes controlled by quorum sensing. *Antimicrob. Agents Chemother.* 56, 2314–2325. doi: 10.1128/AAC.05919-11
- Jakobsen, T. H., Warming, A. N., Vejborg, R. M., Moscoso, J. A., Stegger, M., Lorenzen, F., et al. (2017b). A broad range quorum sensing inhibitor working through sRNA inhibition. *Sci. Rep.* 7:9857. doi: 10.1038/s41598-017-09886-8
- Jenal, U., Reinders, A., and Lori, C. (2017). Cyclic di-GMP: second messenger extraordinaire. *Nat. Rev. Microbiol.* 15, 271–284. doi: 10.1038/nrmicro.2016.190

- Jennings, L. K., Storek, K. M., Ledvina, H. E., Coulon, C., Marmont, L. S., Sadvinskaya, I., et al. (2015). Pel is a cationic exopolysaccharide that cross-links extracellular DNA in the *Pseudomonas aeruginosa* biofilm matrix. *Proc. Natl. Acad. Sci. U.S.A.* 112, 11353–11358. doi: 10.1073/pnas.1503058112
- Jensen, P. O., Bjarnsholt, T., Phipps, R., Rasmussen, T. B., Calum, H., Christoffersen, L., et al. (2007). Rapid necrotic killing of polymorphonuclear leukocytes is caused by quorum-sensing-controlled production of rhamnolipid by *Pseudomonas aeruginosa*. *Microbiology* 153, 1329–1338. doi: 10.1099/mic.0.2006/003863-0
- Jog, G. J., Igarashi, J., and Suga, H. (2006). Stereoisomers of *P. aeruginosa* autoinducer analog to probe the regulator binding site. *Chem. Biol.* 13, 123–128. doi: 10.1016/j.chembiol.2005.12.013
- Jonas, K., Edwards, A. N., Simm, R., Romeo, T., Romling, U., and Meleforts, O. (2008). The RNA binding protein CsrA controls cyclic di-GMP metabolism by directly regulating the expression of GGDEF proteins. *Mol. Microbiol.* 70, 236–257. doi: 10.1111/j.1365-2958.2008.06411.x
- Juhas, M., Eberl, L., and Tummeler, B. (2005). Quorum sensing: the power of cooperation in the world of *Pseudomonas*. *Environ. Microbiol.* 7, 459–471. doi: 10.1111/j.1462-2920.2005.00769.x
- Justice, S. S., Hung, C., Theriot, J. A., Fletcher, D. A., Anderson, G. G., Footer, M. J., et al. (2004). Differentiation and developmental pathways of uropathogenic *Escherichia coli* in urinary tract pathogenesis. *Proc. Natl. Acad. Sci. U.S.A.* 101, 1333–1338. doi: 10.1073/pnas.0308125100
- Kalia, D., Merey, G., Nakayama, S., Zheng, Y., Zhou, J., Luo, Y., et al. (2013). Nucleotide, c-di-GMP, c-di-AMP, cGMP, cAMP, (p)ppGpp signaling in bacteria and implications in pathogenesis. *Chem. Soc. Rev.* 42, 305–341. doi: 10.1039/C2CS35206K
- Kalia, V. C. (2013). Quorum sensing inhibitors: an overview. *Biotechnol. Adv.* 31, 224–245. doi: 10.1016/j.biotechadv.2012.10.004
- Kang, D., and Kirienko, N. V. (2017). High-throughput genetic screen reveals that early attachment and biofilm formation are necessary for full pyoverdine production by *Pseudomonas aeruginosa*. *Front. Microbiol.* 8:1707. doi: 10.3389/fmicb.2017.01707
- Kang, D., Turner, K. E., and Kirienko, N. V. (2017). PqsA Promotes Pyoverdine Production via Biofilm Formation. *Pathogens* 7:E3. doi: 10.3390/pathogens7010003
- Karlsson, K. F., Walse, B., Drakenberg, T., Roy, S., Bergquist, K., Pinkner, J. S., et al. (1998). Binding of peptides in solution by the *Escherichia coli* Chaperone PapD as revealed using an inhibition ELISA and NMR spectroscopy. *Bioorgan. Med. Chem.* 6, 2085–2101. doi: 10.1016/S0968-0896(98)00162-X
- Kikuchi, T., Mizunoe, Y., Takade, A., Naito, S., and Yoshida, S. (2005). Curli fibers are required for development of biofilm architecture in *Escherichia coli* K-12 and enhance bacterial adherence to human uroepithelial cells. *Microbiol. Immunol.* 49, 875–884. doi: 10.1111/j.1348-0421.2005.tb03678.x
- Kim, B., Park, J. S., Choi, H. Y., Yoon, S. S., and Kim, W. G. (2018). Terrein is an inhibitor of quorum sensing and c-di-GMP in *Pseudomonas aeruginosa*: a connection between quorum sensing and c-di-GMP. *Sci. Rep.* 8:8617. doi: 10.1038/s41598-018-26974-5
- Kim, C., Kim, J., Park, H. Y., Lee, J. H., Park, H. J., Kim, C. K., et al. (2009a). Structural understanding of quorum-sensing inhibitors by molecular modeling study in *Pseudomonas aeruginosa*. *Appl. Microbiol. Biotechnol.* 83, 1095–1103. doi: 10.1007/s00253-009-1954-3
- Kim, C., Kim, J., Park, H. Y., Park, H. J., Kim, C. K., Yoon, J., et al. (2009b). Development of inhibitors against TraR quorum-sensing system in *Agrobacterium tumefaciens* by molecular modeling of the ligand-receptor interaction. *Mol. Cells* 28, 447–453. doi: 10.1007/s10059-009-0144-6
- Klemm, P., and Schembri, M. (2004). Type 1 Fimbriae, Curli, and Antigen 43: adhesion, colonization, and biofilm formation. *EcoSal Plus*. doi: 10.1128/ecosal.8.3.2.6
- Kohanski, M. A., Dwyer, D. J., Hayete, B., Lawrence, C. A., and Collins, J. J. (2007). A common mechanism of cellular death induced by bactericidal antibiotics. *Cell* 130, 797–810. doi: 10.1016/j.cell.2007.06.049
- Korea, C. G., Ghigo, J. M., and Beloin, C. (2011). The sweet connection: Solving the riddle of multiple sugar-binding fimbrial adhesins in *Escherichia coli*: multiple *E. coli* fimbriae form a versatile arsenal of sugar-binding lectins potentially involved in surface-colonisation and tissue tropism. *Bioessays* 33, 300–311. doi: 10.1002/bies.201000121
- Kulasakara, H., Lee, V., Brencic, A., Liberati, N., Urbach, J., Miyata, S., et al. (2006). Analysis of *Pseudomonas aeruginosa* diguanylate cyclases and phosphodiesterases reveals a role for bis-(3'-5')-cyclic-GMP in virulence. *Proc. Natl. Acad. Sci. U.S.A.* 103, 2839–2844. doi: 10.1073/pnas.0511090103
- Langermann, S., Palaszynski, S., Barnhart, M., Auguste, G., Pinkner, J. S., Burlein, J., et al. (1997). Prevention of mucosal *Escherichia coli* infection by FimH-adhesin-based systemic vaccination. *Science* 276, 607–611. doi: 10.1126/science.276.5312.607
- Lee, H. W., Koh, Y. M., Kim, J., Lee, J. C., Lee, Y. C., Seol, S. Y., et al. (2008). Capacity of multidrug-resistant clinical isolates of *Acinetobacter baumannii* to form biofilm and adhere to epithelial cell surfaces. *Clin. Microbiol. Infect.* 14, 49–54. doi: 10.1111/j.1469-0691.2007.01842.x
- Lee, Y. (2003). Targeting virulence for antimicrobial chemotherapy. *Curr. Opin. Pharmacol.* 3, 513–519. doi: 10.1016/j.coph.2003.04.001
- Lieberman, O. J., Orr, M. W., Wang, Y., and Lee, V. T. (2014). High-throughput screening using the differential radial capillary action of ligand assay identifies ebbsen as an inhibitor of diguanylate cyclases. *ACS Chem. Biol.* 9, 183–192. doi: 10.1021/cb400485k
- Liou, M. L., Soo, P. C., Ling, S. R., Kuo, H. Y., Tang, C. Y., and Chang, K. C. (2014). The sensor kinase BfmS mediates virulence in *Acinetobacter baumannii*. *J. Microbiol. Immunol. Infect.* 47, 275–281. doi: 10.1016/j.jmii.2012.12.004
- Loehfelm, T. W., Luke, N. R., and Campagnari, A. A. (2008). Identification and characterization of an *Acinetobacter baumannii* biofilm-associated protein. *J. Bacteriol.* 190, 1036–1044. doi: 10.1128/JB.01416-07
- Lopez, M., Mayer, C., Fernandez-Garcia, L., Blasco, L., Muras, A., Ruiz, F. M., et al. (2017). Quorum sensing network in clinical strains of *A. baumannii*: AidA is a new quorum quenching enzyme. *PLoS ONE* 12:e0174454. doi: 10.1371/journal.pone.0174454
- Luo, L. M., Wu, L. J., Xiao, Y. L., Zhao, D., Chen, Z. X., Kang, M., et al. (2015). Enhancing pili assembly and biofilm formation in *Acinetobacter baumannii* ATCC19606 using non-native acyl-homoserine lactones. *BMC Microbiol.* 15:62. doi: 10.1186/s12866-015-0397-5
- Luthje, P., and Brauner, A. (2010). Ag43 promotes persistence of uropathogenic *Escherichia coli* isolates in the urinary tract. *J. Clin. Microbiol.* 48, 2316–2317. doi: 10.1128/JCM.00611-10
- Ma, L., Conover, M., Lu, H., Parsek, M. R., Bayles, K., and Wozniak, D. J. (2009). Assembly and development of the *Pseudomonas aeruginosa* biofilm matrix. *PLoS Pathog.* 5:e1000354. doi: 10.1371/journal.ppat.1000354
- Ma, L., Jackson, K. D., Landry, R. M., Parsek, M. R., and Wozniak, D. J. (2006). Analysis of *Pseudomonas aeruginosa* conditional psl variants reveals roles for the psl polysaccharide in adhesion and maintaining biofilm structure postattachment. *J. Bacteriol.* 188, 8213–8221. doi: 10.1128/JB.01202-06
- Migiyama, Y., Kaneko, Y., Yanagihara, K., Morohoshi, T., Morinaga, Y., Nakamura, S., et al. (2013). Efficacy of AiiM, an N-acylhomoserine lactonase, against *Pseudomonas aeruginosa* in a mouse model of acute pneumonia. *Antimicrob. Agents Chemother.* 57, 3653–3658. doi: 10.1128/AAC.00456-13
- Modarresi, F., Azizi, O., Shakibaie, M. R., Motamedifar, M., Mosadegh, E., and Mansouri, S. (2015). Iron limitation enhances acyl homoserine lactone (AHL) production and biofilm formation in clinical isolates of *Acinetobacter baumannii*. *Virulence* 6, 152–161. doi: 10.1080/21505594.2014.1003001
- Mulvey, M. A. (2002). Adhesion and entry of uropathogenic *Escherichia coli*. *Cell. Microbiol.* 4, 257–271. doi: 10.1046/j.1462-5822.2002.00193.x
- Mulvey, M. A., Lopez-Boado, Y. S., Wilson, C. L., Roth, R., Parks, W. C., Heuser, J., et al. (1998). Induction and evasion of host defenses by type 1-piliated uropathogenic *Escherichia coli*. *Science* 282, 1494–1497. doi: 10.1126/science.282.5393.1494
- Niba, E. T., Naka, Y., Nagase, M., Mori, H., and Kitakawa, M. (2007). A genome-wide approach to identify the genes involved in biofilm formation in *E. coli*. *DNA Res.* 14, 237–246. doi: 10.1093/dnares/dsm024
- Niu, C., Clemmer, K. M., Bonomo, R. A., and Rather, P. N. (2008). Isolation and characterization of an autoinducer synthase from *Acinetobacter baumannii*. *J. Bacteriol.* 190, 3386–3392. doi: 10.1128/JB.01929-07
- Nuccio, S. P., and Baumber, A. J. (2007). Evolution of the chaperone/usher assembly pathway: fimbrial classification goes Greek. *Microbiol. Mol. Biol. Rev.* 71, 551–575. doi: 10.1128/MMBR.00014-07
- Olsen, A., Jonsson, A., and Normark, S. (1989). Fibronectin binding mediated by a novel class of surface organelles on *Escherichia coli*. *Nature* 338, 652–655. doi: 10.1038/338652a0

- Opoku-Temeng, C., and Sintim, H. O. (2017). "Targeting c-di-GMP signaling, biofilm formation, and bacterial motility with small molecules," in *c-di-GMP Signaling, Methods and Protocols*, ed K. Sauer (New York, NY: Humana Press), 419–430. doi: 10.1007/978-1-4939-7240-1_31
- O'Toole, G. A., and Kolter, R. (1998). Flagellar and twitching motility are necessary for *Pseudomonas aeruginosa* biofilm development. *Mol. Microbiol.* 30, 295–304. doi: 10.1046/j.1365-2958.1998.01062.x
- Pamp, S. J., and Tolker-Nielsen, T. (2007). Multiple roles of biosurfactants in structural biofilm development by *Pseudomonas aeruginosa*. *J. Bacteriol.* 189, 2531–2539. doi: 10.1128/JB.01515-06
- Papadopoulos, A., and Frazier, R. A. (2004). Characterization of protein–polyphenol interactions. *Trends Food Sci. Technol.* 15, 186–190. doi: 10.1016/j.tifs.2003.09.017
- Parsek, M. R., Val, D. L., Hanzelka, B. L., Cronan, J. E. Jr., and Greenberg, E. P. (1999). Acyl homoserine-lactone quorum-sensing signal generation. *Proc. Natl. Acad. Sci. U.S.A.* 96, 4360–4365. doi: 10.1073/pnas.96.8.4360
- Passador, L., Tucker, K. D., Guertin, K. R., Journet, M. P., Kende, A. S., and Iglewski, B. H. (1996). Functional analysis of the *Pseudomonas aeruginosa* Autoinducer PAI. *J. Bacteriol.* 178, 5995–6000. doi: 10.1128/jb.178.20.5995-6000.1996
- Pemberton, N., Pinkner, J. S., Edvinsson, S., Hultgren, S. J., and Almqvist, F. (2008). Synthesis and evaluation of dihydroimidazolo and dihydrooxazolo ring-fused 2-pyridones—targeting pilus biogenesis in uropathogenic bacteria. *Tetrahedron* 64, 9368–9376. doi: 10.1016/j.tet.2008.07.015
- Pesavento, C., Becker, G., Sommerfeldt, N., Possling, A., Tschowri, N., Mehli, A., et al. (2008). Inverse regulatory coordination of motility and curli-mediated adhesion in *Escherichia coli*. *Genes Dev.* 22, 2434–2446. doi: 10.1101/gad.475808
- Pinkner, J. S., Remaut, H., Buelens, F., Miller, E., Åberg, V., Pemberton, N., et al. (2006). Rationally designed small compounds inhibit pilus biogenesis in uropathogenic bacteria. *Proc. Natl. Acad. Sci. U.S.A.* 103, 17897–17902. doi: 10.1073/pnas.0606795103
- Povolotsky, T. L., and Hengge, R. (2016). Genome-based comparison of cyclic di-GMP signaling in pathogenic and commensal *Escherichia coli* strains. *J. Bacteriol.* 198, 111–126. doi: 10.1128/JB.00520-15
- Pratt, L. A., and Kolter, R. (1998). Genetic analysis of *Escherichia coli* biofilm formation: roles of flagella, motility, chemotaxis and type I pili. *Mol. Microbiol.* 30, 285–293. doi: 10.1046/j.1365-2958.1998.01061.x
- Prigent-Combaret, C., Prensier, G., Le Thi, T. T., Vidal, O., Lejeune, P., and Dorel, C. (2000). Developmental pathway for biofilm formation in curli-producing *Escherichia coli* strains: role of flagella, curli and colanic acid. *Environ. Microbiol.* 2, 450–464. doi: 10.1046/j.1462-2920.2000.00128.x
- Rakshit, S., and Sivasankar, S. (2014). Biomechanics of cell adhesion: how force regulates the lifetime of adhesive bonds at the single molecule level. *Phys. Chem. Chem. Phys.* 16, 2211–2223. doi: 10.1039/c3cp53963f
- Rasmussen, T. B., and Givskov, M. (2006). Quorum-sensing inhibitors as anti-pathogenic drugs. *Int. J. Med. Microbiol.* 296, 149–161. doi: 10.1016/j.ijmm.2006.02.005
- Romling, U., Galperin, M. Y., and Gomelsky, M. (2013). Cyclic di-GMP: the first 25 years of a universal bacterial second messenger. *Microbiol. Mol. Biol. Rev.* 77, 1–52. doi: 10.1128/MMBR.00043-12
- Rose, R. J., Verger, D., Daviter, T., Remaut, H., Paci, E., Waksman, G., et al. (2008). Unraveling the molecular basis of subunit specificity in P pilus assembly by mass spectrometry. *Proc. Natl. Acad. Sci. U.S.A.* 105, 12873–12878. doi: 10.1073/pnas.0802177105
- Rosen, D. A., Hooton, T. M., Stamm, W. E., Humphrey, P. A., and Hultgren, S. J. (2007). Detection of intracellular bacterial communities in human urinary tract infection. *PLoS Med.* 4:e329. doi: 10.1371/journal.pmed.0040329
- Rosen, D. A., Pinkner, J. S., Walker, J. N., Elam, J. S., Jones, J. M., and Hultgren, S. J. (2008). Molecular variations in *Klebsiella pneumoniae* and *Escherichia coli* FimH affect function and pathogenesis in the urinary tract. *Infect. Immun.* 76, 3346–3356. doi: 10.1128/IAI.00340-08
- Rybtke, M., Hultqvist, L. D., Givskov, M., and Tolker-Nielsen, T. (2015). *Pseudomonas aeruginosa* biofilm infections: community structure, antimicrobial tolerance and immune response. *J. Mol. Biol.* 427, 3628–3645. doi: 10.1016/j.jmb.2015.08.016
- Sahu, P. K., Iyer, P. S., Oak, A. M., Pardesi, K. R., and Chopade, B. A. (2012). Characterization of eDNA from the clinical strain *Acinetobacter baumannii* AIIMS 7 and its role in biofilm formation. *ScientificWorldJournal*. 2012:973436. doi: 10.1100/2012/973436
- Sambanthamoorthy, K., Luo, C., Pattabiraman, N., Feng, X., Koestler, B., Waters, C. M., et al. (2014). Identification of small molecules inhibiting diguanylate cyclases to control bacterial biofilm development. *Biofouling* 30, 17–28. doi: 10.1080/08927014.2013.832224
- Sambanthamoorthy, K., Sloup, R. E., Parashar, V., Smith, J. M., Kim, E. E., Semmelhack, M. F., et al. (2012). Identification of small molecules that antagonize diguanylate cyclase enzymes to inhibit biofilm formation. *Antimicrob. Agents Chemother.* 56, 5202–5211. doi: 10.1128/AAC.01396-12
- Sarenko, O., Klauck, G., Wilke, F. M., Pfiffer, V., Richter, A. M., Herbst, S., et al. (2017). More than enzymes that make or break cyclic Di-GMP-local signaling in the interactome of GGDEF/EAL domain proteins of *Escherichia coli*. *MBio* 8:e01639–17. doi: 10.1128/mBio.01639-17
- Schembri, M. A., and Klemm, P. (2001). Coordinate gene regulation by fimbriae-induced signal transduction. *EMBO J.* 20, 3074–3081. doi: 10.1093/emboj/20.12.3074
- Schirmer, T., and Jenal, U. (2009). Structural and mechanistic determinants of c-di-GMP signalling. *Nat. Rev. Microbiol.* 7, 724–735. doi: 10.1038/nrmicro2203
- Schmidt, A. J., Ryjenkov, D. A., and Gomelsky, M. (2005). The ubiquitous protein domain EAL is a cyclic diguanylate-specific phosphodiesterase: enzymatically active and inactive EAL domains. *J. Bacteriol.* 187, 4774–4781. doi: 10.1128/JB.187.14.4774-4781.2005
- Schuster, M., and Greenberg, E. P. (2006). A network of networks: quorum-sensing gene regulation in *Pseudomonas aeruginosa*. *Int. J. Med. Microbiol.* 296, 73–81. doi: 10.1016/j.ijmm.2006.01.036
- Serra, D. O., Richter, A. M., and Hengge, R. (2013). Cellulose as an architectural element in spatially structured *Escherichia coli* biofilms. *J. Bacteriol.* 195, 5540–5554. doi: 10.1128/JB.00946-13
- Shanahan, C. A., Gaffney, B. L., Jones, R. A., and Strobel, S. A. (2011). Differential analogue binding by two classes of c-di-GMP riboswitches. *J. Am. Chem. Soc.* 133, 15578–15592. doi: 10.1021/ja204650q
- Shanahan, C. A., Gaffney, B. L., Jones, R. A., and Strobel, S. A. (2013). Identification of c-di-GMP derivatives resistant to an EAL domain phosphodiesterase. *Biochemistry* 52, 365–377. doi: 10.1021/bi301510v
- Simm, R., Morr, M., Kader, A., Nimtz, M., and Romling, U. (2004). GGDEF and EAL domains inversely regulate cyclic di-GMP levels and transition from sessility to motility. *Mol. Microbiol.* 53, 1123–1134. doi: 10.1111/j.1365-2958.2004.04206.x
- Sivick, K. E., and Mobley, H. L. (2010). Waging war against uropathogenic *Escherichia coli*: winning back the urinary tract. *Infect. Immun.* 78, 568–585. doi: 10.1128/IAI.01000-09
- Smith, K. M., Bu, Y., and Suga, H. (2003a). Induction and inhibition of *Pseudomonas aeruginosa* quorum sensing by synthetic autoinducer analogs. *Chem. Biol.* 10, 81–89. doi: 10.1016/S1074-5521(03)00002-4
- Smith, K. M., Bu, Y., and Suga, H. (2003b). Library screening for synthetic agonists and antagonists of a *Pseudomonas aeruginosa* autoinducer. *Chem. Biol.* 10, 563–571. doi: 10.1016/S1074-5521(03)00107-8
- Soto, S. M., Smithson, A., Horcajada, J. P., Martinez, J. A., Mensa, J. P., and Vila, J. (2006). Implication of biofilm formation in the persistence of urinary tract infection caused by uropathogenic *Escherichia coli*. *Clin. Microbiol. Infect.* 12, 1034–1036. doi: 10.1111/j.1469-0691.2006.01543.x
- Stacy, D. M., Welsh, M. A., Rather, P. N., and Blackwell, H. E. (2012). Attenuation of quorum sensing in the pathogen *Acinetobacter baumannii* using non-native N-Acyl homoserine lactones. *ACS Chem. Biol.* 7, 1719–1728. doi: 10.1021/cb300351x
- Starkey, M., Hickman, J. H., Ma, L., Zhang, N., De Long, S., Hinz, A., et al. (2009). *Pseudomonas aeruginosa* rugose small-colony variants have adaptations that likely promote persistence in the cystic fibrosis lung. *J. Bacteriol.* 191, 3492–3503. doi: 10.1128/JB.00119-09
- Subashchandrabose, S., Smith, S. N., Spurbeck, R. R., Kole, M. M., and Mobley, H. L. (2013). Genome-wide detection of fitness genes in uropathogenic *Escherichia coli* during systemic infection. *PLoS Pathog.* 9:e1003788. doi: 10.1371/journal.ppat.1003788
- Svensson, A., Larsson, L., Emtenas, H., Hedenström, M., Fex, T., Hultgren, S. J., et al. (2001). Design and evaluation of pilicides: potential novel antibacterial agents directed against uropathogenic *Escherichia coli*. *Chembiochem* 12,

- 915–918. doi: 10.1002/1439-7633(20011203)2:12<915::AID-CBIC915>3.0.CO;2-M
- Tang, K., Su, Y., Brackman, G., Cui, F., Zhang, Y., Shi, X., et al. (2015). MomL, a novel marine-derived N-acyl homoserine lactonase from *Muricauda olearia*. *Appl. Environ. Microbiol.* 81, 774–782. doi: 10.1128/AEM.02805-14
- Teiber, J. F., Horke, S., Haines, D. C., Chowdhary, P. K., Xiao, J., Kramer, G. L., et al. (2008). Dominant role of paraoxonases in inactivation of the *Pseudomonas aeruginosa* quorum-sensing signal N-(3-oxododecanoyl)-L-homoserine lactone. *Infect. Immun.* 76, 2512–2519. doi: 10.1128/IAI.01606-07
- Tielker, D., Hacker, S., Loris, R., Strathmann, M., Wingender, J., Wilhelm, S., et al. (2005). *Pseudomonas aeruginosa* lectin LecB is located in the outer membrane and is involved in biofilm formation. *Microbiology* 151, 1313–1323. doi: 10.1099/mic.0.27701-0
- Tolker-Nielsen, T. (2014). *Pseudomonas aeruginosa* biofilm infections: from molecular biofilm biology to new treatment possibilities. *APMIS Suppl.* 122 (Suppl. 138):1–51. doi: 10.1111/apm.12335
- Tolker-Nielsen, T. (2015). Biofilm development. *Microbiol. Spectr.* 3:MB-0001–2014. doi: 10.1128/microbiolspec.MB-0001-2014
- Tomaras, A. P., Dorsey, C. W., Edelmann, R. E., and Actis, L. A. (2003). Attachment to and biofilm formation on abiotic surfaces by *Acinetobacter baumannii*: involvement of a novel chaperone-usher pili assembly system. *Microbiology* 149, 3473–3484. doi: 10.1099/mic.0.26541-0
- Tomaras, A. P., Flagler, M. J., Dorsey, C. W., Gaddy, J. A., and Actis, L. A. (2008). Characterization of a two-component regulatory system from *Acinetobacter baumannii* that controls biofilm formation and cellular morphology. *Microbiology* 154, 3398–3409. doi: 10.1099/mic.0.2008/019471-0
- Valentini, M., and Filloux, A. (2016). Biofilms and Cyclic di-GMP (c-di-GMP) Signaling: lessons from *Pseudomonas aeruginosa* and other bacteria. *J. Biol. Chem.* 291, 12547–12555. doi: 10.1074/jbc.R115.711507
- Vallet, I., Olson, J. W., Lory, S., Lazdunski, A., and Filloux, A. (2001). The chaperone/usher pathways of *Pseudomonas aeruginosa*: identification of fimbrial gene clusters (cup) and their involvement in biofilm formation. *Proc. Natl. Acad. Sci. U.S.A.* 98, 6911–6916. doi: 10.1073/pnas.111551898
- Van Der Woude, M. W., and Henderson, I. R. (2008). Regulation and function of Ag43 (flu). *Annu. Rev. Microbiol.* 62, 153–169. doi: 10.1146/annurev.micro.62.081307.162938
- Vandeputte, O. M., Kiendrebego, M., Rajaonson, S., Diallo, B., Mol, A., El Jaziri, M., et al. (2010). Identification of catechin as one of the flavonoids from *Combretum albiflorum* bark extract that reduces the production of quorum-sensing-controlled virulence factors in *Pseudomonas aeruginosa* PAO1. *Appl. Environ. Microbiol.* 76, 243–253. doi: 10.1128/AEM.01059-09
- Visca, P., Seifert, H., and Towner, K. J. (2011). *Acinetobacter* infection—an emerging threat to human health. *IUBMB Life* 63, 1048–1054. doi: 10.1002/iub.534
- Wang, J., Zhou, J., Donaldson, G. P., Nakayama, S., Yan, L., Lam, Y. F., et al. (2011). Conservative change to the phosphate moiety of cyclic diguanylic monophosphate remarkably affects its polymorphism and ability to bind DGC, PDE, and PilZ proteins. *J. Am. Chem. Soc.* 133, 9320–9330. doi: 10.1021/ja1112029
- Wang, X., Preston, J. F. III, and Romeo, T. (2004). The pgaABCD locus of *Escherichia coli* promotes the synthesis of a polysaccharide adhesin required for biofilm formation. *J. Bacteriol.* 186, 2724–2734. doi: 10.1128/JB.186.9.2724-2734.2004
- Weber, H., Pesavento, C., Possling, A., Tischendorf, G., and Hengge, R. (2006). Cyclic-di-GMP-mediated signalling within the sigma network of *Escherichia coli*. *Mol. Microbiol.* 62, 1014–1034. doi: 10.1111/j.1365-2958.2006.05440.x
- Wexselblatt, E., Katzhendler, J., Saleem-Batcha, R., Hansen, G., Hilgenfeld, R., Glaser, G., et al. (2010). ppGpp analogues inhibit synthetase activity of Rel proteins from Gram-negative and Gram-positive bacteria. *Bioorg. Med. Chem.* 18, 4485–4497. doi: 10.1016/j.bmc.2010.04.064
- Whitchurch, C. B., Tolker-Nielsen, T., Ragas, P. C., and Mattick, J. S. (2002). Extracellular DNA required for bacterial biofilm formation. *Science* 295:1487. doi: 10.1126/science.295.5559.1487
- Wong, D., Nielsen, T. B., Bonomo, R. A., Pantapalangkoor, P., Luna, B., and Spellberg, B. (2017). Clinical and pathophysiological overview of acinetobacter infections: a century of challenges. *Clin. Microbiol. Rev.* 30, 409–447. doi: 10.1128/CMR.00058-16
- Wu, H., Song, Z., Hentzer, M., Andersen, J. B., Molin, S., Givskov, M., et al. (2004). Synthetic furanones inhibit quorum-sensing and enhance bacterial clearance in *Pseudomonas aeruginosa* lung infection in mice. *J. Antimicrob. Chemother.* 53, 1054–1061. doi: 10.1093/jac/dkh223
- Yang, F., Wang, L. H., Wang, J., Dong, Y. H., Hu, J. Y., and Zhang, L. H. (2005). Quorum quenching enzyme activity is widely conserved in the sera of mammalian species. *FEBS Lett.* 579, 3713–3717. doi: 10.1016/j.febslet.2005.05.060
- Zhang, Y., Brackman, G., and Coenye, T. (2017). Pitfalls associated with evaluating enzymatic quorum quenching activity: the case of MomL and its effect on *Pseudomonas aeruginosa* and *Acinetobacter baumannii* biofilms. *PeerJ* 5:e3251. doi: 10.7717/peerj.3251
- Zheng, Y., Tsuji, G., Opoku-Temeng, C., and Sintim, H. O. (2016). Inhibition of *P. aeruginosa* c-di-GMP phosphodiesterase RocR and swarming motility by a benzoisothiazolinone derivative. *Chem. Sci.* 7, 6238–6244. doi: 10.1039/C6SC02103D
- Zhou, E., Seminara, A. B., Kim, S. K., Hall, C. L., Wang, Y., and Lee, V. T. (2017). Thiol-benzo-triazolo-quinazolinone Inhibits Alg44 Binding to c-di-GMP and reduces alginate production by *Pseudomonas aeruginosa*. *ACS Chem. Biol.* 12, 3076–3085. doi: 10.1021/acscchembio.7b00826
- Zhou, J., Sayre, D. A., Wang, J., Pahadi, N., and Sintim, H. O. (2012). Endo-S-c-di-GMP analogues-polymorphism and binding studies with class I riboswitch. *Molecules* 17, 13376–13389. doi: 10.3390/molecules171113376
- Zhou, J., Watt, S., Wang, J., Nakayama, S., Sayre, D. A., Lam, Y. F., et al. (2013). Potent suppression of c-di-GMP synthesis via I-site allosteric inhibition of diguanylate cyclases with 2'-F-c-di-GMP. *Bioorg. Med. Chem.* 21, 4396–4404. doi: 10.1016/j.bmc.2013.04.050

Conflict of Interest: The authors declare that the research was conducted in the absence of any commercial or financial relationships that could be construed as a potential conflict of interest.

Copyright © 2019 Qvortrup, Hultqvist, Nilsson, Jakobsen, Jansen, Uhd, Andersen, Nielsen, Givskov and Tolker-Nielsen. This is an open-access article distributed under the terms of the Creative Commons Attribution License (CC BY). The use, distribution or reproduction in other forums is permitted, provided the original author(s) and the copyright owner(s) are credited and that the original publication in this journal is cited, in accordance with accepted academic practice. No use, distribution or reproduction is permitted which does not comply with these terms.



Bacterial Biofilm Eradication Agents: A Current Review

Anthony D. Verderosa^{1,2,3*}, Makrina Totsika^{1,2} and Kathryn E. Fairfull-Smith³

¹ Institute of Health and Biomedical Innovation, Queensland University of Technology, Brisbane, QLD, Australia, ² School of Biomedical Sciences, Queensland University of Technology, Brisbane, QLD, Australia, ³ School of Chemistry, Physics, and Mechanical Engineering, Queensland University of Technology, Brisbane, QLD, Australia

OPEN ACCESS

Edited by:

Nenad Filipović,
Faculty of Agriculture, University of
Belgrade, Serbia

Reviewed by:

Fany Reffuveille,
Université de Reims
Champagne-Ardenne, France
Jelena Lozo,
Faculty of Biology, University of
Belgrade, Serbia

*Correspondence:

Anthony D. Verderosa
anthony.verderosa@qut.edu.au

Specialty section:

This article was submitted to
Medicinal and Pharmaceutical
Chemistry,
a section of the journal
Frontiers in Chemistry

Received: 02 September 2019

Accepted: 12 November 2019

Published: 28 November 2019

Citation:

Verderosa AD, Totsika M and
Fairfull-Smith KE (2019) Bacterial
Biofilm Eradication Agents: A Current
Review. *Front. Chem.* 7:824.
doi: 10.3389/fchem.2019.00824

Most free-living bacteria can attach to surfaces and aggregate to grow into multicellular communities encased in extracellular polymeric substances called biofilms. Biofilms are recalcitrant to antibiotic therapy and a major cause of persistent and recurrent infections by clinically important pathogens worldwide (e.g., *Pseudomonas aeruginosa*, *Escherichia coli*, and *Staphylococcus aureus*). Currently, most biofilm remediation strategies involve the development of biofilm-inhibition agents, aimed at preventing the early stages of biofilm formation, or biofilm-dispersal agents, aimed at disrupting the biofilm cell community. While both strategies offer some clinical promise, neither represents a direct treatment and eradication strategy for established biofilms. Consequently, the discovery and development of biofilm eradication agents as comprehensive, stand-alone biofilm treatment options has become a fundamental area of research. Here we review our current understanding of biofilm antibiotic tolerance mechanisms and provide an overview of biofilm remediation strategies, focusing primarily on the most promising biofilm eradication agents and approaches. Many of these offer exciting prospects for the future of biofilm therapeutics for a large number of infections that are currently refractory to conventional antibiotics.

Keywords: antibiotics, bacteria, biofilm, biofilm antibiotic tolerance, biofilm eradication agent, infection, resistance

INTRODUCTION

Biofilm formation is a significant virulence mechanism in the pathogenesis of many medically important bacterial pathogens, such as *Pseudomonas aeruginosa* (Gellatly and Hancock, 2013), *Staphylococcus aureus* (Gordon and Lowy, 2008), and *Escherichia coli* (Beloin et al., 2008). The number of diseases being attributed or associated with biofilm infections is large, with some common examples including vaginitis (Machado et al., 2016), colitis (von Rosenvinge et al., 2013), conjunctivitis (Behlau and Gilmore, 2008), gingivitis (Vieira Colombo et al., 2016), urethritis (Delcaru et al., 2016), and otitis (Post, 2001). In fact, it is estimated that ~80% of all microbial infections in humans are a direct result of biofilms (Davies, 2003). One biofilm-related infection of particular medical concern is *P. aeruginosa* biofilms in the lungs of cystic fibrosis patients. This opportunistic pathogen has been known to cause acute and chronic lung infections that can result in significant morbidity and mortality (Wagner and Iglewski, 2008). A second area of considerable concern is that of chronic wound infections. Highly persistent biofilm-related wound infections, which commonly involve the pathogens *P. aeruginosa* and *S. aureus* (Omar et al., 2017), are suggested to be responsible for over 80% of the 100,000 limb amputations carried out on diabetic patients in each year (James et al., 2008). An additional area of importance when

considering biofilm-related infection is implanted medical devices. Microbial adhesion resulting in biofilm formation on implanted medical devices is a common occurrence and can lead to serious illness and death (Habash and Reid, 1999). These implanted medical devices, which can include intravascular catheters, urinary catheters, pacemakers, heart valves, stents, and orthopedic implants, are commonly used to save lives but can present a significant health risk when colonized by bacterial biofilms (Francolini and Donelli, 2010).

Most antimicrobial treatments available are generally developed and evaluated against microorganisms in the planktonic (free-living) mode of life. Consequently, these treatments are often ineffective against pathogenic biofilms (Costerton et al., 1987; Lebeaux et al., 2014), which can be up to one thousand times more tolerant to antimicrobial treatments (Stewart and William Costerton, 2001; Luppens et al., 2002; Davies, 2003). The phenomenon of biofilm recalcitrance makes them extremely difficult to treat and eradicate effectively. Thus, new strategies for the prevention, dispersal and treatment of bacterial biofilms are urgently required. This review presents an overview of bacterial biofilm development and the current methods used to prevent, disperse, and treat bacterial biofilms, with a particular focus on the development of novel biofilm eradication strategies.

BIOFILM FORMATION

Biofilms are complex three-dimensional communities of microorganisms adhering to a surface and encased in a protective exopolymeric substance. Biofilm formation progresses over five main stages (Figure 1). In stage one, individual planktonic cells migrate and adhere to a surface. Providing the correct conditions are present, these adherent cells then initiate biofilm production on the surface and become encased in small quantities of exopolymeric material. In stage two, adherent cells exude an extracellular polymeric substance (EPS) and become irreversibly attached to the surface, which results in cell aggregation and matrix formation. In stage three, the biofilm begins to mature by developing microcolonies and water channel architecture, while also becoming significantly more layered. In stage four, the fully mature biofilm reaches its maximum cell density and is now considered a three-dimensional community. In stage five, the mature biofilm releases microcolonies of cells from the main community, which are free to migrate to new surfaces spreading the infection to other locations (Stoodley et al., 2002; Schachter, 2003).

THE EXTRACELLULAR POLYMERIC SUBSTANCE (EPS)

The extracellular matrix encasing the cells in a biofilm, also referred to as the EPS, is composed of a complex mixture of proteins, lipids, nucleic acids (extracellular-DNA), and polysaccharides (Annous et al., 2009). These constituents not only assist in securing the biofilm to the surface, but also trap nutrients, provide structural support, and shield against

host immune responses and antimicrobial treatments (Flemming et al., 2007). In addition to the above functions, the EPS is also responsible for holding the community of biofilm cells in close proximity, thereby enabling cell-to-cell communication (quorum sensing), and facilitating the exchange of genetic material through horizontal gene transfer (Hausner and Wuerz, 1999).

CELL-TO-CELL COMMUNICATION (QUORUM SENSING)

Biofilms are known to control their population density through a cell-to-cell signaling mechanism known as quorum sensing (Schachter, 2003). Cell-to-cell communication is a complex regulatory process which prevents biofilm cell density from reaching an unsustainable level (Nadell et al., 2008). Quorum sensing is reliant on signaling molecules known as autoinducers (Figure 2). These autoinducers are constantly being produced by the bacterial cells, and thus, as cell density increases, so does the level of autoinducers (Figure 3). At a specific cell density, a critical threshold concentration of autoinducers is reached, which is known as the quorum level (Annous et al., 2009). During this time, autoinducer receptor binding leads to the repression or activation of several target genes. This modulation of the quorum sensing process allows bacteria to display a unified response that benefits the entire bacterial community by maintaining the optimal biofilm size and co-ordinating virulence phenotypes (Nadell et al., 2008; Annous et al., 2009; Dickschat, 2010). This unified response allows the biofilm to behave more like a multicellular organism, which enables the bacterial community to adapt to changing environmental conditions. The benefit of quorum sensing is not limited to controlling population density. In fact, quorum sensing has also been shown to aid the spread of beneficial mutations throughout the biofilm colony, enhance access to nutrients, and contribute to antibiotic tolerance (Hannan et al., 2010).

BIOFILM ANTIBIOTIC TOLERANCE (BAT)

Bacteria in biofilms are inherently more tolerant to antimicrobial treatment when compared directly to planktonic cells of the same strain. In fact, studies have shown that bacteria growing in biofilms are often thousands of times more tolerant to antimicrobial treatment than their planktonic counterparts (Stewart and William Costerton, 2001; Luppens et al., 2002; Davies, 2003). While, the mechanisms of antibiotic resistance in planktonic bacteria are generally well-understood (Munita and Arias, 2016), those same mechanisms (mutations, efflux pumps, and antibiotic modifying enzymes) do not appear to be the main cause of biofilm-mediated antibiotic tolerance. For example, inherently drug-susceptible bacterial strains often exhibit significant antibiotic tolerance when in the biofilm mode of life, however, when biofilm-residing cells are dispersed (released) from the main community, antimicrobial susceptibility is quickly restored for these cells (Anderl et al., 2000). Thus, biofilm antibiotic tolerance (BAT) is thought to involve alternative mechanisms to bacterial antimicrobial resistance.

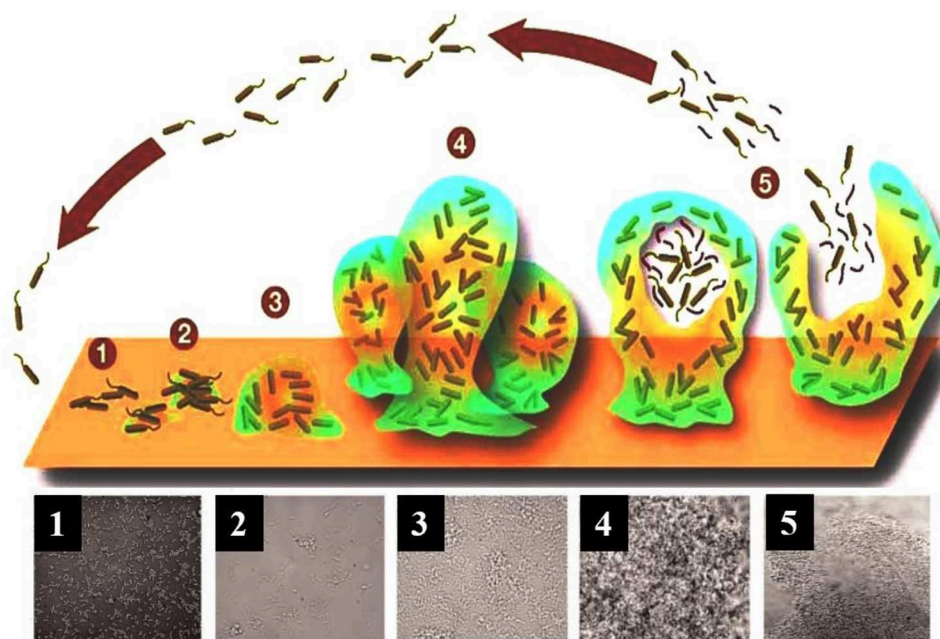
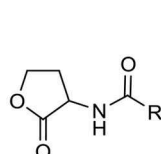
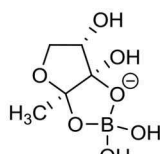


FIGURE 1 | A model showing the typical stage-wise development of a bacterial biofilm accompanied by transmitted light microscopy images showing these different stages for a *P. aeruginosa* biofilm. Republished with permission of Annual Reviews, Inc. (Stoodley et al., 2002); permission conveyed through Copyright Clearance Center, Inc.



***N*-acyl-homoserine lactones**



furanosyl borate diester

FIGURE 2 | Chemical structure of two predominant types of small molecule autoinducers involved in quorum sensing.

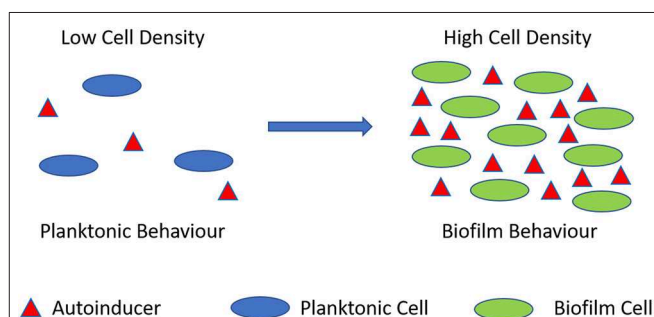


FIGURE 3 | Quorum sensing illustration. During planktonic cell growth (blue ovals), the relative amount of autoinducers (red triangles) is proportionally low. As cells enter a densely populated mode of growth (green ovals) the relative proportion of autoinducers increases.

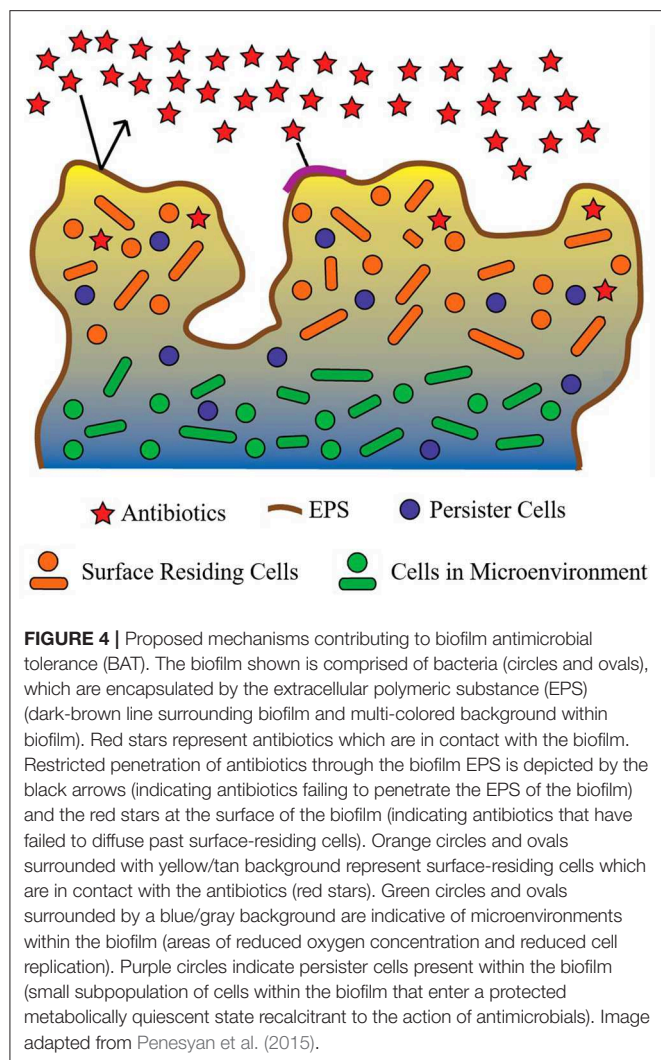
BAT has been defined as the ability of biofilm-residing bacteria to survive antimicrobial treatment by utilizing their existing complement of genes (Anderson and O'Toole, 2008). BAT can be grouped into two categories: innate (resulting from growth in a biofilm) and induced (resulting as a response to antimicrobial treatment). Several major innate factors have been identified which directly influence BAT (Costerton et al., 1999; Lewis, 2001; Donlan and Costerton, 2002; Dunne, 2002; Stewart, 2002; Hoiby et al., 2010) and are briefly discussed below (Figure 4).

INNATE FACTORS MEDIATING BAT

Restricted Penetration

The EPS of a biofilm has long been considered the major contributor to BAT (Donlan and Costerton, 2002). However, the supporting evidence for this is conflicting. The EPS of several biofilm-forming species have demonstrated an innate

ability to prevent antibiotic penetration (Campanac et al., 2002; Davenport et al., 2014). However, this phenomenon is not conserved between the EPS of all biofilm-forming species and also appears to be antibiotic specific. For example, ciprofloxacin and ampicillin were found to effectively penetrate and diffuse through *Klebsiella pneumoniae* biofilms, ultimately reaching distal cells (Anderl et al., 2000). Furthermore, ciprofloxacin also exhibited similar penetration and diffusion activity in *P. aeruginosa* biofilms (Walters et al., 2003). Likewise, tetracycline was able to effectively reach all cells within *E. coli* biofilms (Stone et al., 2002). Interestingly, many of these antibiotics are still ineffective at eradicating



the biofilm. While restricted penetration may be a major contributing factor of BAT for some antibiotics in some biofilms, its effects are certainly not universal. Thus, additional or complementary mechanisms that facilitate BAT also exist.

Reduced Growth Rate

While restricted penetration does not always explain BAT, reduced growth rate appears to play a far more evident role in BAT. The complex internal structure of a biofilm is known to produce microenvironments, which are deprived of oxygen and nutrients (Brown et al., 1988). Deprivation of oxygen and nutrients are well-established cues for slowed bacterial growth and antimicrobial resistance in many species (Brown et al., 1988; Field et al., 2005). Considering most antibiotics target rapidly replicating bacterial cells, it is of little surprise that areas of slow-growing or dormant cells within a biofilm would be unaffected by antibiotics and thus exhibit high levels of antibiotic tolerance. Several studies have demonstrated a direct link between biofilm microenvironments, which produce slow-growing cells and BAT

(Anderl et al., 2003; Walters et al., 2003; Borriello et al., 2004). However, not all antimicrobial agents require rapidly replicating cells to facilitate their mode of action, and many of these agents are still highly tolerated by biofilms, for example, chlorine in the treatment of multi-species biofilms (Barraud et al., 2009). Thus, slow bacterial growth alone is not sufficient to confer BAT either.

Persister Cells

Persister cells represent a minute subpopulation of bacterial cells, which exist in a dormant state and exhibit extreme antimicrobial tolerance (Wood et al., 2013). The presence of persister cells within a bacterial population is not a recent discovery; in fact, their existence was first described as early as 1942 (Hobby et al., 1942). Early studies discovered that when a planktonic population of *S. aureus* cells was treated with penicillin, ~1% of the cells were not killed. Two years later, Bigger supported this finding and documented that one out of a million *S. aureus* cells was not killed by treatment with penicillin (Bigger, 1944). Furthermore, Bigger also determined that these surviving cells, which he termed persisters to differentiate them from resistant mutants, had not undergone a genetic alteration, but instead were simply a phenotypic variant that was tolerant to antibiotics. Despite their early discovery, the role of persister cells in bacterial pathogenesis remained largely unexplored until the study of bacterial biofilms uncovered the significant role of persister cells in BAT (Lewis, 2010).

Unlike planktonic bacterial populations the presence of persister cells within a biofilm community affords them protection from elimination by the immune system, and despite their small numbers, their contribution to pathogenesis becomes more significant in biofilm infections (Lewis, 2005, 2010). Several studies have now demonstrated that after treating a biofilm with antibiotics, a small population of persister cells will remain regardless of the concentration of antibiotic utilized (Spoering and Lewis, 2001; Harrison et al., 2005a,b). Once the treatment ceases and the antibiotic concentration decreases, these remaining persister cells can act as a nucleation point to repopulate the biofilm, ultimately producing a relapsing biofilm infection (Lewis, 2001). Interestingly, the majority of these repopulated biofilm residing cells exhibit no additional antimicrobial tolerance or resistance compared to the original cells that were eradicated, strongly supporting that the persister state is a phenotypic variant rather than a mutation.

The universal presence of persister cells within biofilms is perhaps the most plausible innate mechanism of BAT described so far, and while persisters do not harbor antimicrobial resistance genes directly, they certainly provide a perfect platform for the development of resistant mutants. Consequently, many research groups have focused their efforts on investigating the mechanisms of persister cell formation (Keren et al., 2004a,b; Spoering et al., 2006), with the hope that their findings will enable the development of antibacterial agents which can target and eradicate these fascinating cells.

INDUCED BAT MECHANISMS

The mechanisms of induced BAT appear to be more complicated than the innate factors contributing to this phenomenon and are less well-understood with only a few studies on the topic (Bagge et al., 2004a,b; Szomolay et al., 2005; Redelman et al., 2014; Zhao et al., 2015). Antimicrobial treatment represents a significant stress signal for biofilm-residing cells, and consequently, it is reasonable to assume that antimicrobial treatment could select biofilm-specific antimicrobial resistance genes, and these genes would contribute to BAT. An interesting example of how antibiotics can induce such a response in biofilms is the effect that some antibiotics have on EPS production. Ziebuhr et al. documented how administering sub-inhibitory concentrations of several common antibiotics to *Staphylococcus epidermidis* biofilms activated the expression of the *ica* gene cluster, which mediates the production of polysaccharide intercellular adhesin (PIA), a vital factor for *S. epidermidis* biofilm formation (Rachid et al., 2000). Young et al. and Hoiby et al. found similar effects, albeit with different genes in *E. coli* and *P. aeruginosa*, respectively (Sailer et al., 2003; Bagge et al., 2004b). While these examples have not specifically been linked to BAT the idea that biofilm residing bacteria may regulate the expression of specific genes in response to antimicrobials to facilitate BAT certainly appears plausible.

BIOFILM INHIBITION STRATEGIES

The material matrix of implanted medical devices and biomaterials provide an ideal site for bacterial adhesion promoting mature biofilm formation (Arciola et al., 2012). Thus, methods which prevent bacterial attachment to these materials represent an obvious preventative strategy. The most common method for preventing bacterial adhesion is surface modification. Here, the exterior surface of the implanted medical device or biomaterial is altered, either directly or with the aid of a coating, to produce a barrier which is inhospitable to bacteria (Bazaka et al., 2012). This strategy has shown significant promise for preventing biofilm-related infections resulting from orthopedic implants (Arciola et al., 2012). Thus, the area of surface modification to prevent biofilm formation is a large field, and many comprehensive reviews on this topic already exist (Katsikogianni and Missirlis, 2004; Arciola et al., 2012; Bazaka et al., 2012; Campoccia et al., 2013).

The use of small molecule biofilm inhibitors is another approach used to prevent biofilm formation. In fact, the anti-biofilm properties of a biofilm inhibitor are often employed to passivate the surface of an implanted medical device or biomaterial (Nablo et al., 2005; Boase et al., 2018). The use of biofilm inhibitors is one of the largest areas in biofilm remediation research with a plethora of unique biofilm inhibitors currently described (e.g., phenols, imidazoles, furanone, indole, bromopyrrole, etc.) (Rabin et al., 2015). As such, there are many comprehensive reviews on the topic of biofilm inhibition agents (Simões et al., 2010; Worthington et al., 2012; Rabin et al., 2015).

BIOFILM DISPERSAL AS A TREATMENT STRATEGY

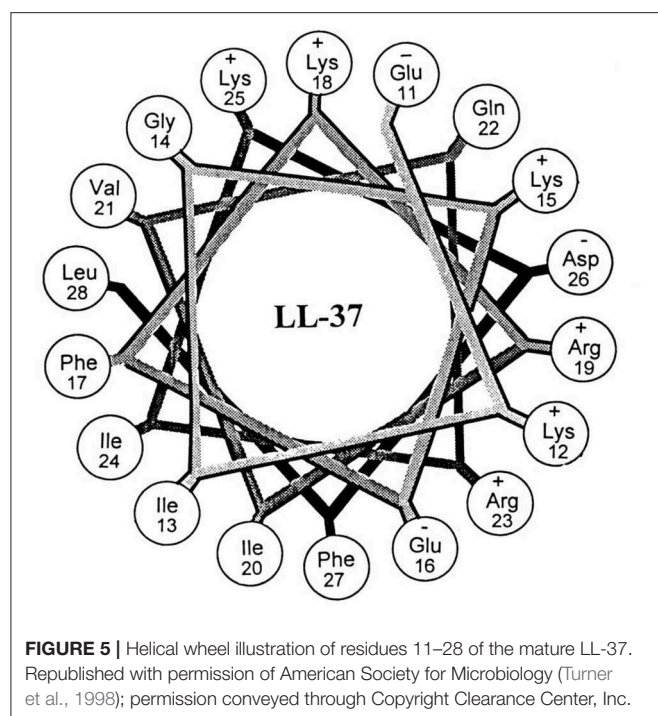
Biofilm dispersal agents generally interfere with chemical pathways or processes, such as quorum sensing, which are required for bacteria to maintain the biofilm mode of existence (McDougald et al., 2012). As disperser cells are generally more susceptible to antimicrobial treatment than biofilm-residing cells, this strategy has recently become an intense area of study. Consequently, a variety of new and promising biofilm dispersal agents have been discovered and reviewed by others (Fleming and Rumbaugh, 2017; Guilhen et al., 2017; Roy et al., 2018). While promising, the use of biofilm-dispersal agents as a treatment strategy can be problematic, as disperser cells, if left untreated, are likely to translocate and seed infection in new areas, ultimately spreading the initial infection. Hence, most dispersal agents are utilized as a combined treatment where the dispersal agent is co-administered with an antimicrobial agent (Marvasi et al., 2014; Reffuveille et al., 2015). Co-treatment generally involves administering a combination of drugs concurrently, in this case, a biofilm dispersal agent and an antibiotic, to exert a synergistic effect. While co-administering a dispersal agent with an antibiotic has yielded some promising results *in vitro* (Barraud et al., 2006; Reffuveille et al., 2015; Roizman et al., 2017), this treatment strategy can be challenging to translate in the clinic, as ensuring that both agents are present at the target site in the correct concentration is often difficult (Fleming and Rumbaugh, 2018). Furthermore, drug co-administration treatments are often associated with several challenges, including complex treatment schedules, increased risk of adverse effects, increased treatment costs, and antagonism (Rybak and McGrath, 1996; Tamma et al., 2012). Consequently, standalone treatments, such as the development of biofilm eradication agents (BEAs) have become an attractive option.

BIOFILM ERADICATION AGENTS

BEAs are antibiotics which can target and eradicate biofilm-residing cells as a standalone treatment. The design and discovery of BEAs constitute an emerging area in biofilm remediation research. A variety of promising BEAs have already been developed, and their activity, design, and potential uses are reviewed below.

ANTIMICROBIAL PEPTIDES

Antimicrobial peptides (AMPs) are one of the most well-studied classes of BEAs and are often considered an attractive alternative to antibiotics (Baltzer and Brown, 2011). They are ubiquitous compounds, produced in a variety of plant, invertebrate, and animal species. AMPs can vary greatly in size (between five to over ninety amino acids) and molecular mass (between 1 and 5 kDa). They are most commonly cationic in nature (overall positive charge), which has led to them being referred to as cationic antimicrobial peptides (Brown and Hancock, 2006); however, anionic forms have also been reported (Harris et al.,



2009). Their antimicrobial mechanism of action is still not fully understood, but their activity is often linked to cytoplasmic membrane disruption and inhibition of protein folding or enzyme activity (Shai, 1999; Bechinger and Gorr, 2017). While the potential use of AMPs as an alternative to antibiotics has received a great deal of attention over the past several decades, their use against microbial biofilms is far most recent.

LL-37 (**Figure 5**) was one of the first AMPs reported as possessing the potential for biofilm eradication (Overhage et al., 2008). LL-37 is a human cathelicidin-derived broad spectrum AMP, which is amphipathic and found in most bodily fluids (Burton and Steel, 2009; Nijnik and Hancock, 2009). Hancock first reported that low concentrations (0.11 μM) of LL-37 were able to decrease *P. aeruginosa* cell attachment to plastic surfaces, while higher concentrations (0.9 μM) reduced the overall thickness of established biofilms (40% reduction in thickness) (Overhage et al., 2008). In a subsequent study by Cohen, LL-37 was found to eradicate *P. aeruginosa* biofilms in an *in vivo* animal model at a concentration of 556 μM (Chennupati et al., 2009). Interestingly, in a separate study by Marchini, LL-37 was also shown to exhibit anti-biofilm activity against the Gram-positive pathogen *Staphylococcus epidermidis* with low concentrations (0.22 μM) preventing cell attachment and higher concentrations (0.22–7.12 μM) preventing mature biofilm establishment (Hell et al., 2010). While the study did not directly examine *S. epidermidis* biofilm eradication by LL-37, similarities in its biofilm inhibition concentrations with *P. aeruginosa* would suggest that its eradication activity is likely to be broad-spectrum. In a more recent study by Li and co-works, LL-37 was found to exhibit potent *S. aureus* biofilm eradication activity (Kang et al., 2019). LL-37 was able to significantly eradicate *S. aureus* biofilm

residing cells (>4-log reduction in CFU) (Kang et al., 2019). LL-37 certainly appears to exhibit many of the characteristics of a promising BEA, it has both Gram-negative and Gram-positive efficacy, and low human cell toxicity (Gordon et al., 2005), however, its use as a BEA remains limited. Instead, LL-37 seems to function better as a biofilm inhibitor (Overhage et al., 2008) rather than a true BEA. Nevertheless, the potential of this AMP has undoubtedly been demonstrated, and hopefully investigations into its use as a BEA will continue.

Another AMP with promising biofilm eradication activity is oritavancin (**Figure 6**). Oritavancin is a semi-synthetic lipoglycopeptide, which has been developed for the treatment of medically problematic Gram-positive infections, such as methicillin-susceptible *S. aureus* (MSSA), methicillin-resistant *S. aureus* (MRSA), and vancomycin-resistant *S. aureus* (VRSA) (Allen, 2010). Moeck and coworkers demonstrated that oritavancin possessed both impressive planktonic and biofilm eradication activity (Belley et al., 2009). Oritavancin was able to completely eradicate (99.9%) MSSA, MRSA, and VRSA biofilms at concentrations between 0.3 and 4.5 μM . Most importantly, the concentration required to completely eradicate established biofilms were within one doubling dilution of the respective concentration required to kill planktonic cells of the same strain. Thus, it appears that the activity of oritavancin is not significantly diminished by the formation of a biofilm. Interestingly, oritavancin, which is a structurally related analog of vancomycin, is significantly less toxic to humans than other lipoglycopeptides, such as vancomycin and telavancin (Darpo et al., 2010). This property along with the high potency of this AMP certainly suggests that oritavancin is a promising BEA, at least against Gram-positive pathogens.

While several other AMPs have exhibited some level of biofilm eradication activity (Wei et al., 2006; Beckloff et al., 2007; Hou et al., 2010), most AMPs appear to exhibit more potent anti-biofilm action (inhibition or dispersal) than biofilm eradication activity (Overhage et al., 2008; Flemming et al., 2009; Hou et al., 2009). Consequently, many AMPs are often utilized in combination with antimicrobial treatment (Dashper et al., 2005; Eckert et al., 2006). For example, G10KHc, a novispirin G10 derived AMP, acted synergistically with tobramycin when administered as a co-treatment against *P. aeruginosa* biofilms (Eckert et al., 2006). Considering the promising anti-biofilm properties of these compounds and their demonstrated synergistic effect with antimicrobials, AMPs represent one promising avenue for the development of treatments for biofilm-related infections. However, as their inherent structures are often quite large and complicated, compared to other antibiotic classes, such as fluoroquinolones and beta-lactams, their modification, development and utilization as BEAs may ultimately be limited.

QUATERNARY AMMONIUM COMPOUNDS

Quaternary ammonium compounds (QACs) are a large class of broad-spectrum bactericidal agents. Their core structure is amphiphilic comprising a hydrophobic alkyl chain and a hydrophilic quaternary ammonium group, and they are often

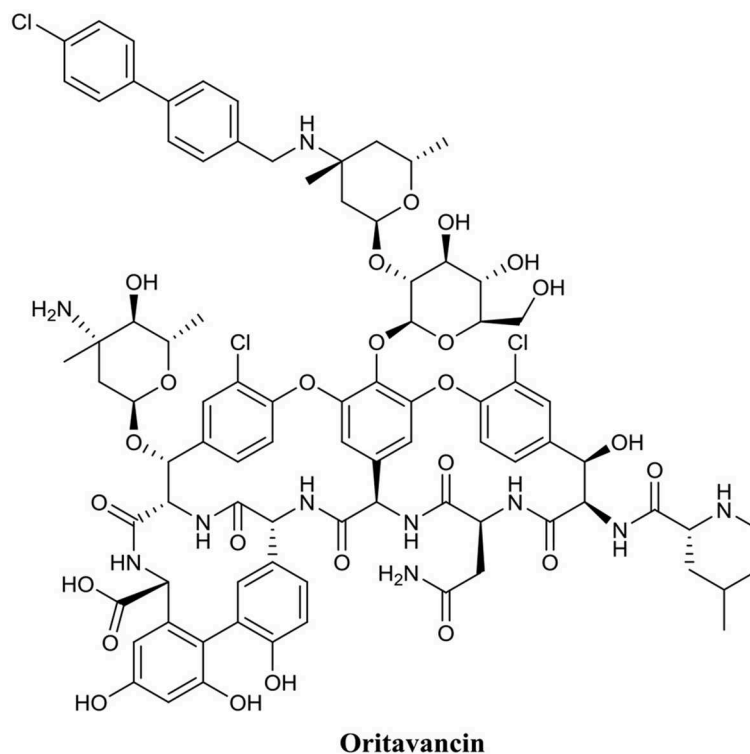


FIGURE 6 | Chemical structure of Oritavancin.

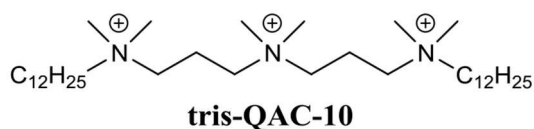


FIGURE 7 | Chemical structure of tris-QAC-10.

referred to as AMP mimics, however, their structures are far simpler. Their activity is associated with disruption of the bacterial plasma membrane, which leads to metabolite leakage, and eventual cell lysis (Ioannou et al., 2007). The antibacterial activity of this class of compounds is well-documented, and consequently, many of these types of compounds are already in common commercial use as antiseptics, disinfectants, and preservatives (Russell, 2003). However, their use as BEAs has only recently been explored.

Wuest et al. developed a variety of mono-, bis-, and tris-QACs and demonstrated biofilm eradication activity against pre-formed *S. aureus* and *E. faecalis* biofilms (Jennings et al., 2014). In particular, tris-QAC-10 (**Figure 7**) was able to completely eradicate established biofilms of *S. aureus* at 50 μ M, and *E. faecalis* at 25 μ M (Jennings et al., 2014). While tris-QAC-10 also exhibiting potent planktonic activity against *E. coli* and *P. aeruginosa* (MIC 0.5 and 1 μ M, respectively), its biofilm eradication activity against these Gram-negative species was not investigated (Jennings et al., 2014). The reported QACs exhibited

significant eukaryotic cell toxicity, with authors noting that the development of less toxic analogs was currently underway (Jennings et al., 2014). In a follow-up publication by the same group, a set of multiQACs was reported that not only exhibited impressive biofilm eradication activity (complete eradication of *S. aureus* biofilms at 25 μ M) but were also considerably less toxic compared to earlier QACs (Forman et al., 2016). Considering the development of these compounds as BEAs is relatively recent, their potency and spectrum of activity are highly impressive. Providing that human cell toxicity can be reduced further in subsequent derivatives, these compounds are certainly one of the more promising approaches for the development of BEAs.

Another recent study reported on two unique dicationic porphyrin QACs XF-70 and XF-73 (**Figure 8**) with demonstrated potent planktonic antibacterial activity (Farrell et al., 2010). Chopra et al. evaluated these two QACs for biofilm eradication activity against *S. aureus* biofilms (Ooi et al., 2010). Both XF-70 and XF-73 completely eradicated pre-formed *S. aureus* biofilms at a concentration of only 2.6 μ M. In addition, XF-70 and XF-73 were also compared to a diverse panel of commonly administered antimicrobial agents and were found to be >128-fold more potent than all other tested agents under the same assay conditions against the same *S. aureus* strain. Furthermore, in a subsequent study by Love et al., XF-73 demonstrated a remarkably low propensity for inducing bacterial resistance (Farrell et al., 2011). With the impressive properties of these QACs there is little surprise that at the time of writing Destiny

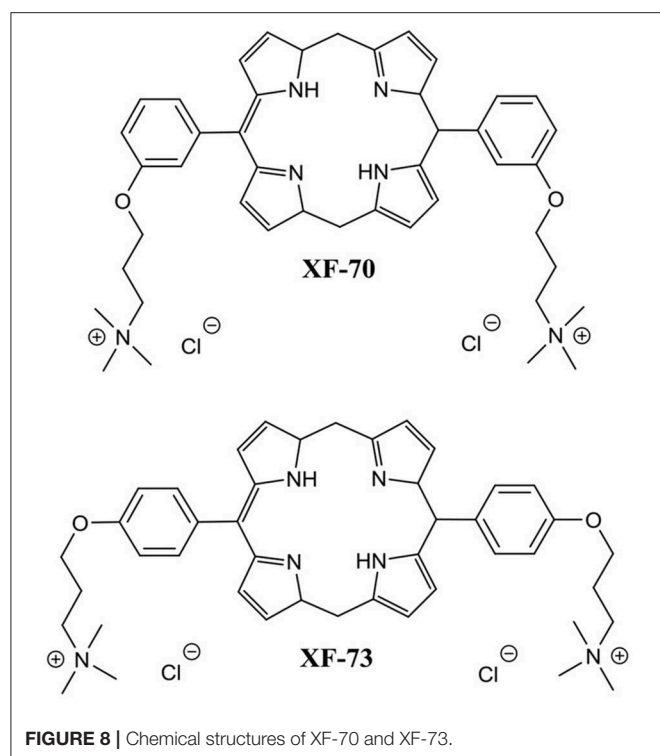


FIGURE 8 | Chemical structures of XF-70 and XF-73.

Pharma has already completed and passed phase 1 clinical trials with XF-73 (Yendewa et al., 2019).

The biofilm eradication properties of QACs position them as a promising strategy for the treatment of biofilm-related infections, however, their inherent toxicity is still a hurdle which will need to be overcome or may limit their clinical use to mostly topical treatments. Furthermore, much like AMPs, the BEA activity of QACs appears to be far more conducive to the treatment of Gram-positive pathogens as opposed to Gram-negative ones. However, as their structures are considerably less complicated and smaller than AMPs, the potential to synthetically modify their core structures to enhance Gram-negative activity is certainly a more plausible task.

ANTIMICROBIAL LIPIDS

Antimicrobial lipids, which include fatty acids and monoglycerides, are defined as single-chain lipid amphiphiles (Yoon et al., 2018). The antimicrobial properties of these compounds have been known since the 1800s after Koch et al. first documented the antibacterial effects of soap, and later observed that fatty acids could inhibit the growth of *Bacillus anthracis* the causative pathogen of anthrax (Thormar, 2010). Since then the antimicrobial properties of fatty acids and monoglycerides have been extensively explored (Kabara and Vrabie, 1977; Desbois and Smith, 2010; Desbois, 2012). Antimicrobial lipids are known to act through a variety of mechanisms, such as increased membrane permeability, cell lysis, disruption of electron transport chain, and inhibition of bacterial enzymes (Yoon et al., 2018). While the antimicrobial

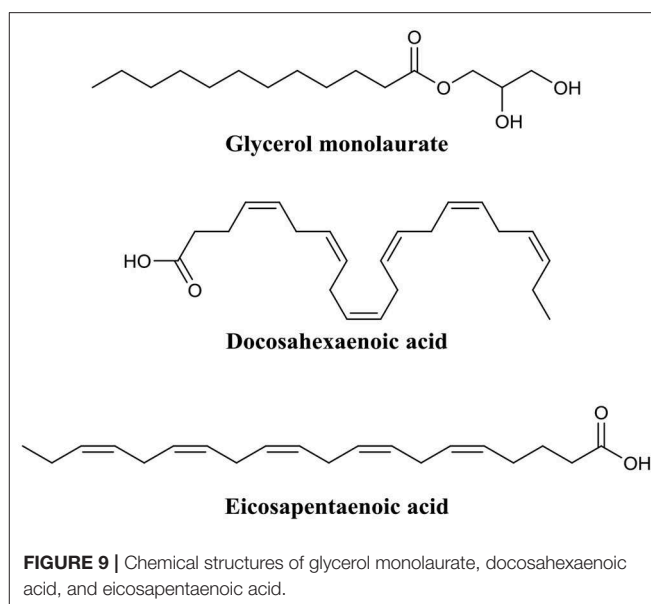


FIGURE 9 | Chemical structures of glycerol monolaurate, docosahexaenoic acid, and eicosapentaenoic acid.

properties of these compounds have been known for some time their use as anti-biofilm agents or BEAs is far more recent.

Marshall and Oh were among the first to investigate the use of the monoglyceride, glycerol monolaurate (**Figure 9**) for the treatment of biofilms (Oh and Marshall, 1995). They examined the biofilm eradication potential of glycerol monolaurate and heat on the foodborne pathogen *Listeria monocytogenes*. Glycerol monolaurate (182 μ M) combined with heat (65°C) were found to completely eradicate 7-days-old adherent cells (biofilms) with only 5 min of contact time (Oh and Marshall, 1995). In a subsequent publication by Peterson and Schlievert, glycerol monolaurate alone was found to completely eradicate *S. aureus* and *Haemophilus influenzae* biofilms at a concentration of 1,822 μ M (Schlievert and Peterson, 2012). Recently, Santos et al. developed a glycerol monolaurate nanocapsule that was reduced *P. aeruginosa* biofilm biomass by up to 78% when administered at a concentration of 228 μ M. These studies clearly evidence that glycerol monolaurate has some level of biofilm eradication potential. However, the active concentration required for biofilm eradication is still quite high compared to other BEAs, particularly for some pathogens. Nevertheless, results using glycerol monolaurate certainly suggest that monoglycerides may someday find use as BEAs.

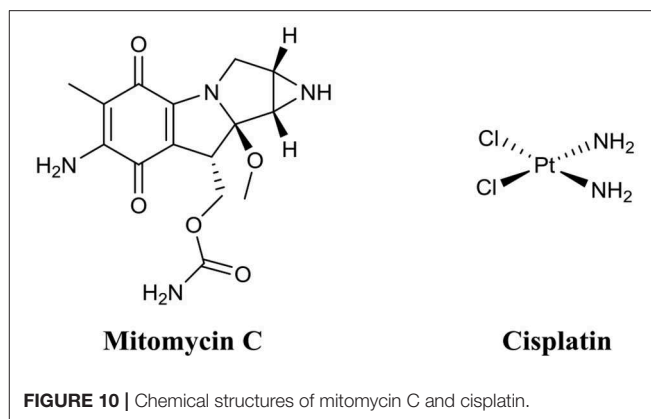
Shu et al. recently explored the biofilm eradication capabilities of the two fatty acids, docosahexaenoic acid and eicosapentaenoic acid (**Figure 9**) against *Porphyromonas gingivalis* and *Fusobacterium nucleatum* biofilms (Sun et al., 2016). Administration of docosahexaenoic acid or eicosapentaenoic acid (100 μ M) to mature *P. gingivalis* biofilms eradicated a significant proportion of the live cell population (61 and 47%, respectively). The same effect was also evident, albeit to a lower degree, for *F. nucleatum* biofilms (19 and 32%, respectively) (Sun et al., 2016). In a follow-up publication by the same group, these same two fatty acids were assessed for activity

against *Streptococcus mutans* biofilms (Sun et al., 2017). Both docosaheptaenoic acid and eicosapentaenoic acid were found to significantly damaged the outer membrane of biofilm residing cells (58.8 and 62.5%, respectively), and consequently reduced biofilm thickness by 19 and 42%, respectively, in *S. mutans* (Sun et al., 2017). Importantly, several studies have demonstrated that both docosaheptaenoic acid and eicosapentaenoic acid are relatively non-toxic to human cells at concentrations up to 100 μ M (docosaheptaenoic acid) and 200 μ M (eicosapentaenoic acid) (Peng et al., 2012; Yang et al., 2013; Sun et al., 2016).

Considering the low toxicity and promising anti-biofilm and biofilm eradication activity of antimicrobial lipids, there is little question that their use as BEAs merits further investigation. However, as both monoglycerides and fatty acids are present in typical human diets the potential for frequent exposure to these compounds and the subsequent development of resistance is something that must be considered and investigated.

ANTICANCER DRUGS MITOMYCIN C AND CISPLATIN

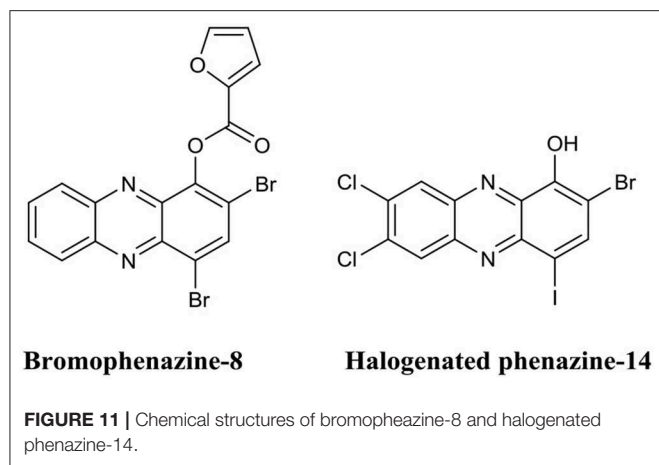
Mitomycin C (Figure 10) is an FDA approved chemotherapy agent with antitumor activity (Doll et al., 1985). It is currently administered for the treatment of a variety of cancers, including cervical, lung, gastric, breast, bladder, head and neck, and pancreatic (Bradner, 2001). Mitomycin C is an amphipathic compound, which enters the cell membrane through passive diffusion (Byfield and Calabro-Jones, 1981) and subsequently initiates DNA crosslinking between adjacent guanine nucleotides (Tomasz, 1995). While the anti-tumor properties of mitomycin C are well-established, its potential as a BEA is only a fairly recent discovery (Kwan et al., 2015). Kwan et al. initially demonstrate that mitomycin C possessed potent planktonic antimicrobial activity against both actively replicating and quiescent (persister) cells against a range of pathogenic bacterial species including *E. coli*, *S. aureus*, and *P. aeruginosa* (Wood et al., 2013). However, the MICs of mitomycin C against the above species were often higher than that of ciprofloxacin (Wood et al., 2013). Interestingly, when mitomycin C was administered to established biofilms of either *E. coli* O157:H7 or *S. aureus* ATCC 25219 almost complete eradication resulted ($<1 \times 10^1$ CFU remaining after treatment, >7 -log reduction) (Wood et al., 2013). Conversely, under the same conditions ciprofloxacin was significantly less active than mitomycin C against biofilms of *E. coli* O157:H7 ($>1 \times 10^7$ CFU remaining after treatment) or *S. aureus* ATCC 25219 ($>1 \times 10^6$ CFU remaining after treatment) (Wood et al., 2013). The biofilm eradication activity of mitomycin C has been attributed to its ability to target and eradicate both actively replicating and persister cells and while encouraging, the concentrations utilized in these experiments (30–40 μ M) was significantly higher than the therapeutic concentrations approved for cancer treatment (1.5–6 μ M) (Bradner, 2001; Kwan et al., 2015). Thus, the toxicity of these higher concentrations on human health would need to be considered. In an additional study by Wood et al., mitomycin C was also demonstrated to possess potent eradication activity



against established *Acinetobacter baumannii* biofilms; however, the concentrations required in this case were even higher ($\sim 750 \mu$ M) (Cruz-Muniz et al., 2017).

A second anticancer drug with demonstrated biofilm eradication activity is cisplatin (Figure 10) (Chowdhury et al., 2016; Yuan et al., 2018). Cisplatin is also an FDA approved treatment for head and neck, bladder, ovarian, and testicular cancers (Eastman, 1987). Like mitomycin C, cisplatin is also a DNA crosslinker; however, crosslinks occur mostly on the same strand rather than opposing strands like mitomycin C (Eastman, 1987). Wood and coworkers were the first to document the potent eradication activity of cisplatin against established *P. aeruginosa* biofilms ($<1 \times 10^1$ CFU remaining after treatment, >7 -log reduction), however, the dose required for this activity was quite high (833 μ M) (Chowdhury et al., 2016). In a subsequent study by Nielsen and colleagues, cisplatin was also shown to have potent *P. aeruginosa* biofilm eradication activity (>1 -log reduction) (Yuan et al., 2018). However, complete eradication of biofilms was not observed at the maximum concentration tested (42 μ M).

While the biofilm eradication activity of anticancer drugs, such as mitomycin C and cisplatin, might be encouraging, strong consideration must be given to their clinical toxicity. Mitomycin C is known to cause bone marrow damage, lung fibrosis, renal failure, and haemolytic anemia (Doll et al., 1985). Cisplatin can cause bone marrow suppression, kidney damage, hearing impairment, and heart disease (Oun et al., 2018). Interestingly, mitomycin C has also been investigated as a topical treatment for extensive, recurrent conjunctival-corneal squamous cell carcinoma (Shields et al., 2002). In this study, Shields et al. found that mitomycin C was not only highly effective as a topical treatment, but also safe at concentrations up to 2.6 mM (Shields et al., 2002). Thus, while anticancer drugs, such as mitomycin C may be too toxic for the treatment of internal biofilm-related infections, they may find use in the treatment of external biofilm-related infections, such as those seen in chronic wounds, diabetic foot ulcers or in skin burns. Furthermore, as both drugs are already FDA-approved and have been in clinical use, they are certainly worth considering as last-resort treatment options for biofilm infections highly recalcitrant to antibiotic therapy.



PHENAZINES AND QUINOLINES

Phenazines are redox-active secondary metabolites, which are produced naturally by many Gram-negative and Gram-positive bacterial species for example, *P. aeruginosa* (Cezairliyan et al., 2013), *Streptomyces* spp. (Karnetova et al., 1983), and *Pantoea agglomerans* (Ali et al., 2016). They consist of a dibenzo annulated pyrazine, and the most well-known example (pyocyanin) originates from *P. aeruginosa* (Lau et al., 2004). Phenazines and their derivatives exhibit activity against both Gram-negative and Gram-positive species; however, Gram-positive species appear to be more susceptible (Baron and Rowe, 1981). Interest in the potential use of phenazines as BEAs arose from the finding that pyocyanin allowed *P. aeruginosa* biofilm infections to outcompete *S. aureus* biofilm infections in the lungs of cystic fibrosis patients (Saiman, 2004; Dietrich et al., 2013).

Huigens et al. were the first to investigate the biofilm eradication activity of phenazine based compounds and demonstrate their impressive biofilm eradication activity against *S. aureus* biofilms (Garrison et al., 2015b). The most potent of these derivatives was bromophenazine-8 (**Figure 11**) which completely eradicated biofilms at concentrations between 62.5 and 100 μM . In a subsequent publication by the same group, they prepared an additional library of halogenated phenazines, which this time exhibited biofilm eradication activity against several Gram-positive species (*S. aureus*, *Staphylococcus epidermidis* and *Enterococcus faecium*) (Garrison et al., 2015a). Halogenated phenazine-14 (**Figure 11**) exhibited the most potent biofilm eradication activity against all three pathogens with complete eradication occurring at concentrations between 0.2 and 12 μM (Garrison et al., 2015a). Furthermore, the authors also demonstrated that halogenated phenazines are non-toxic to mammalian cells indicating that these compounds or their derivatives represent promising therapeutic candidates for the treatment of Gram-positive biofilm-related infections (Garrison et al., 2015a). The biofilm eradication activity of halogenated quinolones is impressive, at least against Gram-positive pathogens. However, considering the origins of the core phenazine structure (Gram-negative bacterial species), it is doubtful that the activity of this class of BEA will ever

extent to Gram-negative pathogens, such as *P. aeruginosa*. Furthermore, bacterially derived phenazines, for example, pyocyanin from *P. aeruginosa*, are well-established virulence factors and key quorum sensing molecules (Lau et al., 2004; Karatuna and Yagci, 2010). Thus, it would also be important to investigate the response of Gram-negative species to these BEAs to ensure that halogenated phenazines do not trigger biofilm formation or increased virulence in bacterial species known to utilize these molecules for quorum sensing. This would be of particular clinical importance in cases where mixed biofilms are typically observed, such as oral and skin infections (Elias and Banin, 2012).

Quinolines are heterocyclic aromatic compounds which bear some structural resemblance to phenazines. However, unlike phenazines, quinolines are generally associated with antimalarial drugs (Foley and Tilley, 1998). Interestingly, the structural similarities between these two compounds have led to quinolines being investigated as BEAs. Huigens et al. utilized a scaffold hopping strategy (Sun et al., 2012) to develop quinolines based on the halogenated phenazine-14 core structure (Abouelhasan et al., 2014). They produced a variety of halogenated quinolines which exhibited biofilm inhibition activity against *S. aureus* and *S. epidermidis* but possessed little biofilm eradication activity. In subsequent studies by the same group, they improved the biofilm eradication activity of halogenated phenazines against *S. epidermidis* and *E. faecium* (Basak et al., 2015, 2016). Of those, halogenated quinoline-3 (**Figure 12**) completely eradicated *S. epidermidis* biofilms at only 3.0 μM , while halogenated quinoline-4 eradicated (**Figure 12**) *E. faecium* biofilm at just 1.0 μM (Basak et al., 2015, 2016). The potential of phenazines as biofilm eradication agents was comprehensively reviewed by the same authors recently (Huigens et al., 2019).

Both halogenated phenazines and quinolines have certainly demonstrated potent biofilm eradication activity. However, their activity appears to be limited to the Gram-positive pathogens *S. aureus*, *S. epidermidis*, and *E. faecium*. Despite the impressive activity and low cytotoxicity of these compounds, no *in vivo* analyses have been conducted to date. Nevertheless, these compounds are some of the most promising BEAs documented thus far.

NITRIC OXIDE-RELEASING ANTIBIOTICS

The use of nitric oxide in biofilm dispersal has been well-documented (Barraud et al., 2006, 2015), however, nitric oxide is a notoriously challenging molecule to handle, and thus its administration and delivery to a target site is often difficult. Furthermore, nitric oxide induces biofilm dispersal at specific concentrations that are sub-lethal to bacteria (below MIC), which means treatment with nitric oxide will require subsequent or combinational treatment with an antimicrobial agent to eradicate dispersed cells. To address the issues surrounding the use of nitric oxide, an innovative approach has been to develop antimicrobials which release nitric oxide or a nitric oxide donor upon interaction with the target

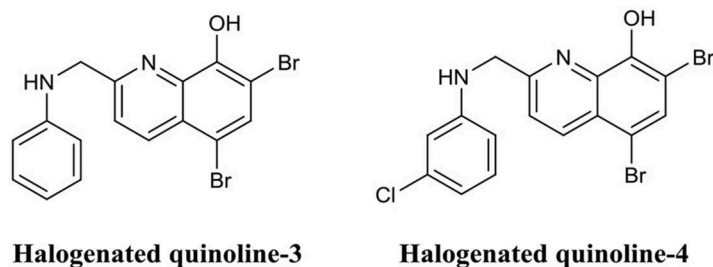
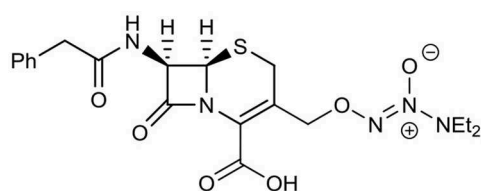


FIGURE 12 | Chemical structures of halogenated quinoline-3 and halogenated quinoline-4.



Cephalosporin-3'-diazoniumdiolate

FIGURE 13 | Chemical structure of cephalosporin-3'-diazoniumdiolate.

site. Kelso and team were able to produce a nitric oxide-releasing prodrug based on the cephalosporin core structure (Barraud et al., 2012). Here they covalently linked the nitric oxide donor diazeniumdiolate (NONOate) to the 3' position of Cefaloram to produce cephalosporin-3'-diazoniumdiolate (**Figure 13**), which upon interaction with the bacterial enzyme β -lactamase released the nitric oxide donor that subsequently decomposes to release nitric oxide. When cephalosporin-3'-diazoniumdiolate was administered to established *P. aeruginosa* biofilms, a significant reduction in biofilm-residing cells (70%) was achieved at a concentration of only 10 μ M (Barraud et al., 2012). It is not clear however, if these removed cells were killed or remained viable and thus the potential of cephalosporin-3'-diazoniumdiolate as a BEA remains to be demonstrated. Yet this study clearly demonstrated the use of cephalosporin-3'-diazoniumdiolate as a targeted nitric oxide-releasing agent, and more agents have now been reported by the same group that significantly reduce a biofilm population, however, these compounds remain to be tested for biofilm eradication (Yepuri et al., 2013).

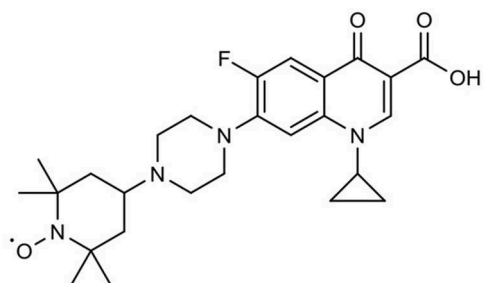
In a similar approach, Schoenfisch et al. functionalised an alkyl chain modified poly(amidoamine) (PAMAM) dendrimer with a nitric oxide donor to produce a nitric oxide-releasing antimicrobial agent (Worley et al., 2015). Their lead compounds exhibited a 6-log reduction against *P. aeruginosa* biofilms and a 4-log reduction against *S. aureus* biofilms (Worley et al., 2015). Furthermore, most nitric oxide functionalised conjugates were found to be significantly more potent (2-fold) than their non-nitric oxide containing parent molecules (Worley et al., 2015), a result which suggests that the ability to release nitric oxide greatly improved the biofilm eradication activity of these conjugates.

Interestingly, these compounds appear to exhibit a dual action which incorporates the anti-biofilm activity of nitric oxide with the antimicrobial activity of the alkyl chain modified PAMAM dendrimers. As such they represent an interesting new class of BEAs which are potentially dual-acting. Such dual-acting BEAs, combine the activity of two individual compounds to produce a single compound which is more effective than either of its comprising moieties.

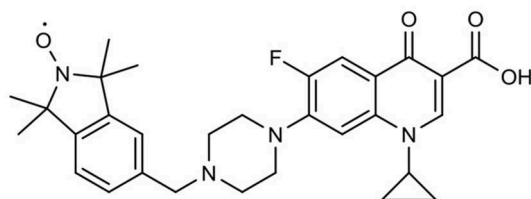
NITROXIDE FUNCTIONALISED ANTIBIOTICS

The use of nitric oxide in the BEAs discussed above is complicated by its requirement for release upon contact with the target site (nitric oxide donors must decompose to release nitric oxide). Thus, an another approach that does not require release from the antimicrobial agent would be to utilize a nitric oxide alternative. Recently Fairfull-Smith et al. have utilized this approach in the development of nitroxide functionalised antibiotics as BEAs (Verderosa et al., 2016, 2017, 2019a). Nitroxides are not bound by the same limitations as nitric oxide (such as low stability, high reactivity, and gaseous at room temperature). Thus, nitroxides, which have documented anti-biofilm properties (de la Fuente-Núñez et al., 2013; Boase et al., 2018; Woehlk et al., 2019), do not require a delivery or release system. Consequently, they can be synthetically incorporated or linked to other agents, such as antibiotics, without negatively impacting their anti-biofilm properties.

Fairfull-Smith et al. were the first to produce and demonstrate the biofilm eradication activity of nitroxide functionalised antibiotics (Verderosa et al., 2016). Here they synthesized two different ciprofloxacin-nitroxide hybrids (**Figure 14**) that showed biofilm eradication efficacy against *P. aeruginosa* biofilms (Verderosa et al., 2016). Ciprofloxacin-nitroxide-10 eradicated 95% of biofilm-residing cells at only 40 μ M. This represented a major improvement over the parent compound ciprofloxacin, which had little to no effect on biofilm-residing cells in the same assay system (Reffuveille et al., 2014). These studies also evidenced the fundamental role of the free radical nitroxide to the activity of the compound as removal of the free radical character from the hybrid compound significantly reduced its activity as a BEA. In a follow up publication by the same group, a second generation of



Ciprofloxacin-nitroxide-10

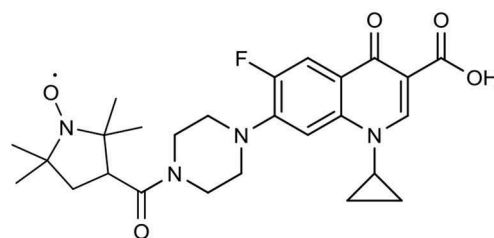


Ciprofloxacin-nitroxide-16

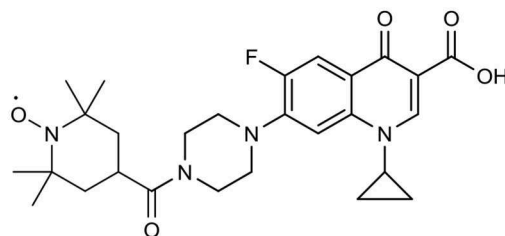
FIGURE 14 | Chemical structures of ciprofloxacin-nitroxide-10 and ciprofloxacin-nitroxide-16.

ciprofloxacin-nitroxide hybrids (**Figure 15**) were produced and shown to be almost twice as potent as the first-generation hybrids (94% eradication at 20 μ M) against *P. aeruginosa* biofilms and also had no mammalian cell toxicity (Verderosa et al., 2017). Recently, Fairfull-Smith et al. produced the third generation of ciprofloxacin-nitroxide hybrids with an optimized nitroxide to antibiotic ratio (Verderosa et al., 2019a). These new hybrids were shown to have improved potency against uropathogenic *E. coli* biofilms (99.7% eradication at 12.5 μ M) (Verderosa et al., 2019a). The mechanism of action of these promising BEAs was recently investigated through the development of profluorescent fluoroquinolone nitroxides (Verderosa et al., 2019c). This was the first demonstration that nitroxide-functionalised fluoroquinolones can enter and eradicate both Gram-negative (*P. aeruginosa* and *E. coli*) and Gram-positive pathogen cells (*S. aureus* and *Enterococcus faecalis*) (Verderosa et al., 2019c), demonstrating the broad-spectrum potential of this group of BEAs. In a subsequent publication by Totsika et al., the activity of ciprofloxacin-nitroxides-23, ciprofloxacin-nitroxides-25, and ciprofloxacin-nitroxides-27 (**Figure 15**) were investigated for efficacy against *S. aureus* biofilms (Verderosa et al., 2019b). Here they found that ciprofloxacin-nitroxide-27 was able to completely (99.9%) eradicate established *S. aureus* biofilm at a concentration of only 64 μ M (Verderosa et al., 2019b).

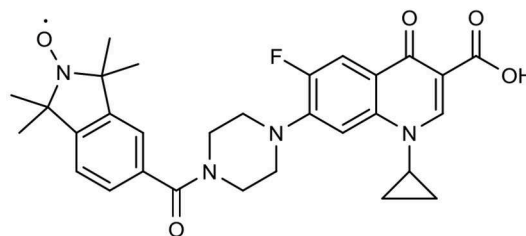
Overall, nitroxide functionalised antibiotics are highly potent (low μ M range), exhibit a broad spectrum of activity, have no or low mammalian cytotoxicity, and are based on the structure



Ciprofloxacin-nitroxide-23



Ciprofloxacin-nitroxide-25



Ciprofloxacin-nitroxide-27

FIGURE 15 | Chemical structures of ciprofloxacin-nitroxide-23, ciprofloxacin-nitroxide-25, and ciprofloxacin-nitroxide-27.

of a well-established class of antibiotics (fluoroquinolones), making them attractive BEA candidates. In the future, it would be important to examine if other classes of antibiotics can be successfully functionalised with nitroxides to expand this promising group of BEAs.

CONCLUSIONS

Most bacteria in nature exist in the form of biofilms. For the medical profession, biofilms present a considerable challenge, as not only are they associated with most infections in humans, but they are also extremely difficult to treat due to their inherent tolerance to immune responses and antimicrobials. Despite this, most antibiotics are developed and tested against free-living bacteria. Yet our understanding of biofilm formation by several clinically important bacteria and the mechanisms contributing to bacterial antibiotic tolerance has significantly advanced over the past 20 years. This new knowledge has led to the development of several biofilm remediation strategies and the discovery

of many promising agents. While the development of anti-biofilm agents that inhibit or disperse biofilms have received significant attention their inherent lack of antimicrobial activity necessitates their use in conjunction with antibiotics, which distances them from offering a clinically reliable standalone solution. The development of BEAs, even though still at early stages, appears capable to address many of these issues with several promising agents already described. The advantage of BEAs is that they do not require supplementation with other drugs and are designed to specifically target biofilm-residing cells. In addition, many BEAs exhibit both anti-biofilm and biofilm eradication activities, such as AMPs and nitroxide functionalised antibiotics. This feature, coupled with their low human cell toxicity, positions BEAs as a potentially complete strategy for the treatment of both planktonic and biofilm-related infections. The BEAs presented in this review exemplify how increasing understanding of biofilm antibiotic tolerance mechanisms can lead to the design and development of new antibiotics that could offer effective solutions against biofilms. As our understanding of these mechanisms continues to improve, so will our ability

to develop compounds which can circumvent them. In the near future, research will hopefully unravel the complete mechanisms of biofilm antimicrobial tolerance, and the questions of how to best design and develop new antibiotics will become apparent.

AUTHOR CONTRIBUTIONS

AV, MT, and KF-S conceived the concept of the review. AV drafted the manuscript, searched for updated bibliography, and prepared the figures. AV, KF-S, and MT revised, corrected, and edited the manuscript.

FUNDING

This work was supported by a Queensland University of Technology (QUT) grant (to MT and KF-S) and in part by a Clive and Vera Ramaciotti Health Investment Grant (2017HIG0119 to MT). KF-S was supported by an Australian Research Council Future Fellowship (FT140100746) and MT by a QUT Vice-Chancellor's Research Fellowship.

REFERENCES

- Abouelhassan, Y., Garrison, A. T., Burch, G. M., Wong, W., Norwood, V. M., and Huigens, R. W. III. (2014). Discovery of quinoline small molecules with potent dispersal activity against methicillin-resistant *Staphylococcus aureus* and *Staphylococcus epidermidis* biofilms using a scaffold hopping strategy. *Bioorg. Med. Chem. Lett.* 24, 5076–5080. doi: 10.1016/j.bmcl.2014.09.009
- Ali, H. M., El-Shikh, M. S., Salem, M. Z., and M, M. (2016). Isolation of bioactive phenazine-1-carboxamide from the soil bacterium *Pantoea agglomerans* and study of its anticancer potency on different cancer cell lines. *J. AOAC Int.* 99, 1233–1239. doi: 10.5740/jaoacint.16-0090
- Allen, N. E. (2010). From vancomycin to oritavancin: the discovery and development of a novel lipoglycopeptide antibiotic. *Antimicrob. Agents Chem.* 9, 23–47. doi: 10.2174/187152110790886745
- Anderl, J. N., Franklin, M. J., and Stewart, P. S. (2000). Role of antibiotic penetration limitation in *Klebsiella pneumoniae* biofilm resistance to ampicillin and ciprofloxacin. *Antimicrob. Agents Chemother.* 44, 1818–1824. doi: 10.1128/AAC.44.7.1818-1824.2000
- Anderl, J. N., Zahller, J., Roe, F., and Stewart, P. S. (2003). Role of nutrient limitation and stationary-phase existence in *Klebsiella pneumoniae* biofilm resistance to ampicillin and ciprofloxacin. *Antimicrob. Agents Chemother.* 47, 1251–1256. doi: 10.1128/AAC.47.4.1251-1256.2003
- Anderson, G. G., and O'Toole, G. A. (2008). Innate and induced resistance mechanisms of bacterial biofilms. *Curr. Top. Microbiol. Immunol.* 322, 85–105. doi: 10.1007/978-3-540-75418-3_5
- Annous, B. A., Frattamico, P. M., and Smith, J. L. (2009). Quorum sensing in biofilms: why bacteria behave the way they do. *J. Food Sci.* 74, R24–R37. doi: 10.1111/j.1750-3841.2008.01022.x
- Arciola, C. R., Campoccia, D., Speziale, P., Montanaro, L., and Costerton, J. W. (2012). Biofilm formation in *Staphylococcus* implant infections. A review of molecular mechanisms and implications for biofilm-resistant materials. *Biomaterials* 33, 5967–5982. doi: 10.1016/j.biomaterials.2012.05.031
- Bagge, N., Hentzer, M., Andersen, J. B., Ciofu, O., Givskov, M., and Hoiby, N. (2004a). Dynamics and spatial distribution of beta-lactamase expression in *Pseudomonas aeruginosa* biofilms. *Antimicrob. Agents Chemother.* 48, 1168–1174. doi: 10.1128/AAC.48.4.1168-1174.2004
- Bagge, N., Schuster, M., Hentzer, M., Ciofu, O., Givskov, M., Greenberg, E. P., et al. (2004b). *Pseudomonas aeruginosa* biofilms exposed to imipenem exhibit changes in global gene expression and beta-lactamase and alginate production. *Antimicrob. Agents Chemother.* 48, 1175–1187. doi: 10.1128/AAC.48.4.1175-1187.2004
- Baltzer, S. A., and Brown, M. H. (2011). Antimicrobial peptides: promising alternatives to conventional antibiotics. *J. Mol. Microbiol. Biotechnol.* 20, 228–235. doi: 10.1159/000331009
- Baron, S. S., and Rowe, J. J. (1981). Antibiotic action of pyocyanin. *Antimicrob. Agents Chemother.* 20, 814–820. doi: 10.1128/AAC.20.6.814
- Barraud, N., Hassett, D. J., Hwang, S.-H., Rice, S. A., Kjelleberg, S., and Webb, J. S. (2006). Involvement of nitric oxide in biofilm dispersal of *Pseudomonas aeruginosa*. *J. Bacteriol.* 188, 7344–7353. doi: 10.1128/JB.00779-06
- Barraud, N., Kardak, B. G., Yepuri, N. R., Howlin, R. P., Webb, J. S., Faust, S. N., et al. (2012). Cephalosporin-3'-diazoniumdiolates: targeted NO-donor prodrugs for dispersing bacterial biofilms. *Angew. Chem. Int. Ed. Engl.* 51, 9057–9060. doi: 10.1002/anie.201202414
- Barraud, N., Kelso, M. J., Rice, S. A., and Kjelleberg, S. (2015). Nitric oxide: a key mediator of biofilm dispersal with applications in infectious diseases. *Curr. Pharm. Des.* 21, 31–42. doi: 10.2174/1381612820666140905112822
- Barraud, N., Storey, M. V., Moore, Z. P., Webb, J. S., Rice, S. A., and Kjelleberg, S. (2009). Nitric oxide-mediated dispersal in single- and multi-species biofilms of clinically and industrially relevant microorganisms. *Microb. Biotechnol.* 2, 370–378. doi: 10.1111/j.1751-7915.2009.00098.x
- Basak, A., Abouelhassan, Y., and Huigens, R. W. III. (2015). Halogenated quinolines discovered through reductive amination with potent eradication activities against MRSA, MRSE and VRE biofilms. *Org. Biomol. Chem.* 13, 10290–10294. doi: 10.1039/C5OB01883H
- Basak, A., Abouelhassan, Y., Norwood IV, V. M., Bai, F., Nguyen, M. T., Jin, S., et al. (2016). Synthetically tuning the 2-position of halogenated quinolines: optimizing antibacterial and biofilm eradication activities via alkylation and reductive amination pathways. *Chem. Eur. J.* 22, 9181–9189. doi: 10.1002/chem.201600926
- Bazaka, K., Jacob, M. V., Crawford, R. J., and Ivanova, E. P. (2012). Efficient surface modification of biomaterial to prevent biofilm formation and the attachment of microorganisms. *Appl. Microbiol. Biotechnol.* 95, 299–311. doi: 10.1007/s00253-012-4144-7
- Bechinger, B., and Gorr, S. U. (2017). Antimicrobial peptides: mechanisms of action and resistance. *J. Dent. Res.* 96, 254–260. doi: 10.1177/0022034516679973
- Beckloff, N., Laube, D., Castro, T., Furgang, D., Park, S., Perlin, D., et al. (2007). Activity of an antimicrobial peptide mimetic against planktonic and biofilm cultures of oral pathogens. *Antimicrob. Agents Chemother.* 51:4125. doi: 10.1128/AAC.00208-07
- Behlau, I., and Gilmore, M. S. (2008). Microbial biofilms in ophthalmology and infectious disease. *Arch. Ophthalmol.* 126, 1572–1581. doi: 10.1001/archophth.126.11.1572

- Belley, A., Neesham-Grenon, E., McKay, G., Arhin, F. F., Harris, R., Beveridge, T., et al. (2009). Oritavancin kills stationary-phase and biofilm *Staphylococcus aureus* cells *in vitro*. *Antimicrob. Agents Chemother.* 53:918. doi: 10.1128/AAC.00766-08
- Beloin, C., Roux, A., and Ghigo, J. M. (2008). *Escherichia coli* biofilms. *Curr. Top. Microbiol.* 322, 249–289. doi: 10.1007/978-3-540-75418-3_12
- Bigger, J. (1944). Treatment of *Staphylococcal* infections with penicillin by intermittent sterilisation. *Lancet* 244, 497–500. doi: 10.1016/S0140-6736(00)74210-3
- Boase, N. R. B., Torres, M. D. T., Fletcher, N. L., de la Fuente-Nunez, C., and Fairfull-Smith, K. E. (2018). Polynitroxide copolymers to reduce biofilm fouling on surfaces. *Polym. Chem.* 9, 5308–5318. doi: 10.1039/C8PY01101J
- Borriello, G., Werner, E., Roe, F., Kim, A. M., Ehrlich, G. D., and Stewart, P. S. (2004). Oxygen limitation contributes to antibiotic tolerance of *Pseudomonas aeruginosa* in biofilms. *Antimicrob. Agents Chemother.* 48, 2659–2664. doi: 10.1128/AAC.48.7.2659-2664.2004
- Bradner, W. T. (2001). Mitomycin C: a clinical update. *Cancer Treat. Rev.* 27, 35–50. doi: 10.1053/ctrv.2000.0202
- Brown, K. L., and Hancock, R. E. (2006). Cationic host defense (antimicrobial) peptides. *Curr. Opin. Immunol.* 18, 24–30. doi: 10.1016/j.coi.2005.11.004
- Brown, M. R., Allison, D. G., and Gilbert, P. (1988). Resistance of bacterial biofilms to antibiotics a growth-rate related effect? *J. Antimicrob. Chemother.* 22, 777–780. doi: 10.1093/jac/22.6.777
- Burton, M. F., and Steel, P. G. (2009). The chemistry and biology of LL-37. *Nat. Prod. Rep.* 26, 1572–1584. doi: 10.1039/b912533g
- Byfield, J. E., and Calabro-Jones, P. M. (1981). Carrier-dependent and carrier-independent transport of anti-cancer alkylating agents. *Nature* 294, 281–283. doi: 10.1038/294281a0
- Campanac, C., Pineau, L., Payard, A., Baziard-Mouysset, G., and Roques, C. (2002). Interactions between biocide cationic agents and bacterial biofilms. *Antimicrob. Agents Chemother.* 46, 1469–1474. doi: 10.1128/AAC.46.5.1469-1474.2002
- Campoccia, D., Montanaro, L., and Arciola, C. R. (2013). A review of the biomaterials technologies for infection-resistant surfaces. *Biomaterials* 34, 8533–8554. doi: 10.1016/j.biomaterials.2013.07.089
- Cezairliyan, B., Vinayavekhin, N., Grenfell-Lee, D., Yuen, G. J., Saghatelian, A., and Ausubel, F. M. (2013). Identification of *Pseudomonas aeruginosa* phenazines that kill *Caenorhabditis elegans*. *PLoS Pathog.* 9:e1003101. doi: 10.1371/journal.ppat.1003101
- Chennupati, S. K., Chiu, A. G., Tamashiro, E., Banks, C. A., Cohen, M. B., Bleier, B. S., et al. (2009). Effects of an LL-37-derived antimicrobial peptide in an animal model of biofilm *Pseudomonas sinusitis*. *Am. J. Rhinol. Allergy* 23, 46–51. doi: 10.2500/ajra.2009.23.3261
- Chowdhury, N., Wood, T. L., Martinez-Vazquez, M., Garcia-Contreras, R., and Wood, T. K. (2016). DNA-crosslinker cisplatin eradicates bacterial persister cells. *Biotechnol. Bioeng.* 113, 1984–1992. doi: 10.1002/bit.25963
- Costerton, J. W., Cheng, K. J., Geesey, G. G., Ladd, T. I., Nickel, J. C., Dasgupta, M., et al. (1987). Bacterial biofilms in nature and disease. *Annu. Rev. Microbiol.* 41, 435–464. doi: 10.1146/annurev.mi.41.100187.002251
- Costerton, J. W., Stewart, P. S., and Greenberg, E. P. (1999). Bacterial biofilms: a common cause of persistent infections. *Science* 284, 1318–1322. doi: 10.1126/science.284.5418.1318
- Cruz-Muniz, M. Y., Lopez-Jacome, L. E., Hernandez-Duran, M., Franco-Cendejas, R., Licona-Limon, P., Ramos-Balderas, J. L., et al. (2017). Repurposing the anticancer drug mitomycin C for the treatment of persistent *Acinetobacter baumannii* infections. *Int. J. Antimicrob. Agents* 49, 88–92. doi: 10.1016/j.ijantimicag.2016.08.022
- Darpo, B., Lee, S. K., Moon, T. E., Sills, N., and Mason, J. W. (2010). Oritavancin, a new lipoglycopeptide antibiotic: results from a thorough QT study. *J. Clin. Pharmacol.* 50, 895–903. doi: 10.1177/0091270009355449
- Dashper, S. G., Brien-Simpson, N. M., Cross, K. J., Paolini, R. A., Hoffmann, B., Catmull, D. V., et al. (2005). Divalent metal cations increase the activity of the antimicrobial peptide kappacin. *Antimicrob. Agents Chemother.* 49:2322. doi: 10.1128/AAC.49.6.2322-2328.2005
- Davenport, E. K., Call, D. R., and Beyenal, H. (2014). Differential protection from tobramycin by extracellular polymeric substances from *Acinetobacter baumannii* and *Staphylococcus aureus* biofilms. *Antimicrob. Agents Chemother.* 58, 4755–4761. doi: 10.1128/AAC.03071-14
- Davies, D. (2003). Understanding biofilm resistance to antibacterial agents. *Nat. Rev. Drug Discov.* 2, 114–122. doi: 10.1038/nrd1008
- de la Fuente-Núñez, C., Reffuveille, F., Fairfull-Smith, K. E., and Hancock, R. E. W. (2013). Effect of nitroxides on swarming motility and biofilm formation, multicellular behaviors in *Pseudomonas aeruginosa*. *Antimicrob. Agents Chemother.* 57, 4877–4881. doi: 10.1128/AAC.01381-13
- Delcaru, C., Alexandru, I., Podgoreanu, P., Grosu, M., Stavropoulos, E., Chifiriuc, M. C., et al. (2016). Microbial biofilms in urinary tract infections and prostatitis: etiology, pathogenicity, and combating strategies. *Pathogens* 5:65. doi: 10.3390/pathogens5040065
- Desbois, A. P. (2012). Potential applications of antimicrobial fatty acids in medicine, agriculture and other industries. *Recent Pat. Antiinfect. Drug Discov.* 7, 111–122. doi: 10.2174/157489112801619728
- Desbois, A. P., and Smith, V. J. (2010). Antibacterial free fatty acids: activities, mechanisms of action and biotechnological potential. *Appl. Microbiol. Biotechnol.* 85, 1629–1642. doi: 10.1007/s00253-009-2355-3
- Dickschat, J. S. (2010). Quorum sensing and bacterial biofilms. *Nat. Prod. Rep.* 27, 343–369. doi: 10.1039/b804469b
- Dietrich, L. E. P., Okegbe, C., Price-Whelan, A., Sakhtah, H., Hunter, R. C., and Newman, D. K. (2013). Bacterial community morphogenesis is intimately linked to the intracellular redox state. *J. Bacteriol.* 195:1371. doi: 10.1128/JB.02273-12
- Doll, D. C., Weiss, R. B., and Issell, B. F. (1985). Mitomycin: ten years after approval for marketing. *J. Clin. Oncol.* 3, 276–286. doi: 10.1200/JCO.1985.3.2.276
- Donlan, R. M., and Costerton, J. W. (2002). Biofilms: survival mechanisms of clinically relevant microorganisms. *Clin. Microbiol. Rev.* 15, 167–193. doi: 10.1128/CMR.15.2.167-193.2002
- Dunne, W. M. Jr. (2002). Bacterial adhesion: seen any good biofilms lately? *Clin. Microbiol. Rev.* 15, 155–166. doi: 10.1128/CMR.15.2.155-166.2002
- Eastman, A. (1987). The formation, isolation and characterization of DNA adducts produced by anticancer platinum complexes. *Pharmacol. Ther.* 34, 155–166. doi: 10.1016/0163-7258(87)90009-X
- Eckert, R., Brady, K. M., Greenberg, E. P., Qi, F., Yarbrough, D. K., He, J., et al. (2006). Enhancement of antimicrobial activity against *Pseudomonas aeruginosa* by coadministration of G10KHc and tobramycin. *Antimicrob. Agents Chemother.* 50:3833. doi: 10.1128/AAC.00509-06
- Elias, S., and Banin, E. (2012). Multi-species biofilms: living with friendly neighbors. *FEMS Microbiol. Rev.* 36, 990–1004. doi: 10.1111/j.1574-6976.2012.00325.x
- Farrell, D. J., Robbins, M., Rhys-Williams, W., and Love, W. G. (2010). *In vitro* activity of XF-73, a novel antibacterial agent, against antibiotic-sensitive and -resistant Gram-positive and Gram-negative bacterial species. *Int. J. Antimicrob. Agents* 35, 531–536. doi: 10.1016/j.ijantimicag.2010.02.008
- Farrell, D. J., Robbins, M., Rhys-Williams, W., and Love, W. G. (2011). Investigation of the potential for mutational resistance to XF-73, retapamulin, mupirocin, fusidic acid, daptomycin, and vancomycin in methicillin-resistant *Staphylococcus aureus* isolates during a 55-passage study. *Antimicrob. Agents Chemother.* 55:1177. doi: 10.1128/AAC.01285-10
- Field, T. R., White, A., Elborn, J. S., and Tunney, M. M. (2005). Effect of oxygen limitation on the *in vitro* antimicrobial susceptibility of clinical isolates of *Pseudomonas aeruginosa* grown planktonically and as biofilms. *Eur. J. Clin. Microbiol. Infect. Dis.* 24, 677–687. doi: 10.1007/s10096-005-0031-9
- Fleming, D., and Rumbaugh, K. (2018). The consequences of biofilm dispersal on the host. *Sci. Rep.* 8:10738. doi: 10.1038/s41598-018-29121-2
- Fleming, D., and Rumbaugh, K. P. (2017). Approaches to dispersing medical biofilms. *Microorganisms* 5:15. doi: 10.3390/microorganisms5020015
- Flemming, H.-C., Neu, T. R., and Wozniak, D. J. (2007). The EPS matrix: the “house of biofilm cells”. *J. Bacteriol.* 189, 7945–7947. doi: 10.1128/JB.00858-07
- Flemming, K., Klingenberg, C., Cavanagh, J. P., Sletteng, M., Stensen, W., Svendsen, J. S., et al. (2009). High *in vitro* antimicrobial activity of synthetic antimicrobial peptidomimetics against *staphylococcal* biofilms. *J. Antimicrob. Chemother.* 63, 136–145. doi: 10.1093/jac/dkn464
- Foley, M., and Tilley, L. (1998). Quinoline antimalarials: mechanisms of action and resistance and prospects for new agents. *Pharmacol. Ther.* 79, 55–87. doi: 10.1016/S0163-7258(98)00012-6
- Forman, M. E., Jennings, M. C., Wuest, W. M., and Minbiole, K. P. (2016). Building a better quaternary ammonium compound (QAC): branched

- tetracationic antiseptic amphiphiles. *Chem. Med. Chem.* 11, 1401–1405. doi: 10.1002/cmdc.201600176
- Francolini, I., and Donelli, G. (2010). Prevention and control of biofilm-based medical-device-related infections. *FEMS Immunol. Med. Microbiol.* 59, 227–238. doi: 10.1111/j.1574-695X.2010.00665.x
- Garrison, A. T., Abouelhassan, Y., Kallifidas, D., Bai, F., Ukhanova, M., Mai, V., et al. (2015a). Halogenated phenazines that potently eradicate biofilms, MRSA persister cells in non-biofilm cultures, and *Mycobacterium tuberculosis*. *Angew. Chem. Int. Ed. Engl.* 54, 14819–14823. doi: 10.1002/anie.201508155
- Garrison, A. T., Bai, F., Abouelhassan, Y., Paciaroni, N. G., Jin, S., and Huigens III, R. W. (2015b). Bromophenazine derivatives with potent inhibition, dispersion and eradication activities against *Staphylococcus aureus* biofilms. *RSC Adv.* 5, 1120–1124. doi: 10.1039/C4RA08728C
- Gellatly, S. L., and Hancock, R. E. (2013). *Pseudomonas aeruginosa*: new insights into pathogenesis and host defenses. *Pathog. Dis.* 67, 159–173. doi: 10.1111/2049-632X.12033
- Gordon, R. J., and Lowy, F. D. (2008). Pathogenesis of methicillin-resistant *Staphylococcus aureus* infection. *Clin. Infect. Dis.* 46, S350–S359. doi: 10.1086/533591
- Gordon, Y. J., Huang, L. C., Romanowski, E. G., Yates, K. A., Proske, R. J., and McDermott, A. M. (2005). Human cathelicidin (LL-37), a multifunctional peptide, is expressed by ocular surface epithelia and has potent antibacterial and antiviral activity. *Curr. Eye Res.* 30, 385–394. doi: 10.1080/02713680590934111
- Guilhen, C., Forestier, C., and Balestrino, D. (2017). Biofilm dispersal: multiple elaborate strategies for dissemination of bacteria with unique properties. *Mol. Microbiol.* 105, 188–210. doi: 10.1111/mmi.13698
- Habash, M., and Reid, G. (1999). Microbial biofilms: their development and significance for medical device-related infections. *J. Clin. Pharmacol.* 39, 887–898. doi: 10.1177/00912709922008506
- Hannan, S., Ready, D., Jasni, A. S., Rogers, M., Pratten, J., and Roberts, A. P. (2010). Transfer of antibiotic resistance by transformation with eDNA within oral biofilms. *FEMS Immunol. Med. Microbiol.* 59, 345–349. doi: 10.1111/j.1574-695X.2010.00661.x
- Harris, F., Dennison, S. R., and Phoenix, D. A. (2009). Anionic antimicrobial peptides from eukaryotic organisms. *Curr. Protein Pept. Sci.* 10, 585–606. doi: 10.2174/138920309789630589
- Harrison, J. J., Ceri, H., Roper, N. J., Badry, E. A., Sproule, K. M., and Turner, R. J. (2005a). Persister cells mediate tolerance to metal oxyanions in *Escherichia coli*. *Microbiology* 151, 3181–3195. doi: 10.1099/mic.0.27794-0
- Harrison, J. J., Turner, R. J., and Ceri, H. (2005b). Persister cells, the biofilm matrix and tolerance to metal cations in biofilm and planktonic *Pseudomonas aeruginosa*. *Environ. Microbiol.* 7, 981–994. doi: 10.1111/j.1462-2920.2005.00777.x
- Hausner, M., and Wuertz, S. (1999). High rates of conjugation in bacterial biofilms as determined by quantitative *in situ* analysis. *Appl. Environ. Microbiol.* 65, 3710–3713.
- Hell, E., Giske, C. G., Nelson, A., Romling, U., and Marchini, G. (2010). Human cathelicidin peptide LL37 inhibits both attachment capability and biofilm formation of *Staphylococcus epidermidis*. *Lett. Appl. Microbiol.* 50, 211–215. doi: 10.1111/j.1472-765X.2009.02778.x
- Hobby, G. L., Meyer, K., and Chaffee, E. (1942). Observations on the mechanism of action of penicillin. *Proc. Soc. Exp. Biol. Med.* 50, 281–285. doi: 10.3181/00379727-50-13773
- Hoiby, N., Bjarnsholt, T., Givskov, M., Molin, S., and Ciofu, O. (2010). Antibiotic resistance of bacterial biofilms. *Int. J. Antimicrob. Agents* 35, 322–332. doi: 10.1016/j.ijantimicag.2009.12.011
- Hou, S., Liu, Z., Young, A. W., Mark, S. L., Kallenbach, N. R., and Ren, D. (2010). Effects of Trp- and Arg-containing antimicrobial-peptide structure on inhibition of *Escherichia coli* planktonic growth and biofilm formation. *Appl. Environ. Microbiol.* 76, 1967–1974. doi: 10.1128/AEM.02321-09
- Hou, S., Zhou, C., Liu, Z., Young, A. W., Shi, Z., Ren, D., et al. (2009). Antimicrobial dendrimer active against *Escherichia coli* biofilms. *Bioorg. Med. Chem. Lett.* 19, 5478–5481. doi: 10.1016/j.bmcl.2009.07.077
- Huigens, III, R. W., Abouelhassan, Y., and Yang, H. (2019). Phenazine antibiotic inspired discovery of bacterial biofilm-eradicating agents. *Chem. Med. Chem.* 20, 1–19. doi: 10.1002/cbic.201900116
- Ioannou, C. J., Hanlon, G. W., and Denyer, S. P. (2007). Action of disinfectant quaternary ammonium compounds against *Staphylococcus aureus*. *Antimicrob. Agents Chemother.* 51, 296–306. doi: 10.1128/AAC.00375-06
- James, G. A., Swogger, E., Wolcott, R., Pulcini, E. D., Secor, P., Sestrich, J., et al. (2008). Biofilms in chronic wounds. *Wound Repair Regen.* 16, 37–44. doi: 10.1111/j.1524-475X.2007.00321.x
- Jennings, M. C., Ator, L. E., Paniak, T. J., Minbiole, K. P., and Wuest, W. M. (2014). Biofilm-eradicating properties of quaternary ammonium amphiphiles: simple mimics of antimicrobial peptides. *Chem. Bio. Chem.* 15, 2211–2215. doi: 10.1002/cbic.201402254
- Kabara, J. J., and Vrable, R. (1977). Antimicrobial lipids: natural and synthetic fatty acids and monoglycerides. *Lipids* 12, 753–759. doi: 10.1007/BF02570908
- Kang, J., Dietz, M. J., and Li, B. (2019). Antimicrobial peptide LL-37 is bactericidal against *Staphylococcus aureus* biofilms. *PLoS ONE* 14:e0216676. doi: 10.1371/journal.pone.0216676
- Karatuna, O., and Yagci, A. (2010). Analysis of quorum sensing-dependent virulence factor production and its relationship with antimicrobial susceptibility in *Pseudomonas aeruginosa* respiratory isolates. *Clin. Microbiol. Infect.* 16, 1770–1775. doi: 10.1111/j.1469-0691.2010.03177.x
- Karnetova, J., Tax, J., Stajner, K., Vanek, Z., and Krumphanzl, V. (1983). Production of phenazines by *Streptomyces cinnamonensis*. *Folia Microbiol. (Praha)* 28, 51–53. doi: 10.1007/BF02877385
- Katsikogianni, M., and Missirlis, Y. F. (2004). Concise review of mechanisms of bacterial adhesion to biomaterials and of techniques used in estimating bacteria-material interactions. *Eur. Cell Mater.* 8, 37–57. doi: 10.22203/eCM.v008a05
- Keren, I., Kaldalu, N., Spoering, A., Wang, Y., and Lewis, K. (2004a). Persister cells and tolerance to antimicrobials. *FEMS Microbiol. Lett.* 230, 13–18. doi: 10.1016/S0378-1097(03)00856-5
- Keren, I., Shah, D., Spoering, A., Kaldalu, N., and Lewis, K. (2004b). Specialized persister cells and the mechanism of multidrug tolerance in *Escherichia coli*. *J. Bacteriol.* 186, 8172–8180. doi: 10.1128/JB.186.24.8172-8180.2004
- Kwan, B. W., Chowdhury, N., and Wood, T. K. (2015). Combatting bacterial infections by killing persister cells with mitomycin C. *Environ. Microbiol.* 17, 4406–4414. doi: 10.1111/1462-2920.12873
- Lau, G. W., Hassett, D. J., Ran, H., and Kong, F. (2004). The role of pyocyanin in *Pseudomonas aeruginosa* infection. *Trends Mol. Med.* 10, 599–606. doi: 10.1016/j.molmed.2004.10.002
- Lebeaux, D., Ghigo, J.-M., and Beloin, C. (2014). Biofilm-related infections: bridging the gap between clinical management and fundamental aspects of recalcitrance toward antibiotics. *Microbiol. Mol. Biol. Rev.* 78, 510–543. doi: 10.1128/MMBR.00013-14
- Lewis, K. (2001). Riddle of biofilm resistance. *Antimicrob. Agents Chemother.* 45, 999–1007. doi: 10.1128/AAC.45.4.999-1007.2001
- Lewis, K. (2005). Persister cells and the riddle of biofilm survival. *Biochemistry (Mosc.)* 70, 267–274. doi: 10.1007/s10541-005-0111-6
- Lewis, K. (2010). Persister cells. *Annu. Rev. Microbiol.* 64, 357–372. doi: 10.1146/annurev.micro.112408.134306
- Luppens, S. B. I., Reij, M. W., van der Heijden, R. W. L., Rombouts, F. M., and Abee, T. (2002). Development of a standard test to assess the resistance of *Staphylococcus aureus* biofilm cells to disinfectants. *Appl. Environ. Microbiol.* 68, 4194–4200. doi: 10.1128/AEM.68.9.4194-4200.2002
- Machado, D., Castro, J., Palmeira-de-Oliveira, A., Martinez-de-Oliveira, J., and Cerca, N. (2016). Bacterial vaginosis biofilms: challenges to current therapies and emerging solutions. *Front. Microbiol.* 6:1528. doi: 10.3389/fmicb.2015.01528
- Marvasi, M., Chen, C., Carrazana, M., Durie, I. A., and Teplitski, M. (2014). Systematic analysis of the ability of nitric oxide donors to dislodge biofilms formed by *Salmonella enterica* and *Escherichia coli* O157:H7. *AMB Express* 4, 1–11. doi: 10.1186/s13568-014-0042-y
- McDougald, D., Rice, S. A., Barraud, N., Steinberg, P. D., and Kjelleberg, S. (2012). Should we stay or should we go: mechanisms and ecological consequences for biofilm dispersal. *Nat. Rev. Microbiol.* 10, 39–50. doi: 10.1038/nrmicro2695
- Munita, J. M., and Arias, C. A. (2016). Mechanisms of antibiotic resistance. *Microbiol. Spectr.* 4:10.1128/microbiolspec.VMBF-0016-2015. doi: 10.1128/microbiolspec.VMBF-0016-2015

- Nablo, B. J., Rothrock, A. R., and Schoenfisch, M. H. (2005). Nitric oxide-releasing sol-gels as antibacterial coatings for orthopedic implants. *Biomaterials* 26, 917–924. doi: 10.1016/j.biomaterials.2004.03.031
- Nadell, C. D., Xavier, J. B., Levin, S. A., and Foster, K. R. (2008). The evolution of quorum sensing in bacterial biofilms. *PLoS Biol.* 6:e14. doi: 10.1371/journal.pbio.0060014
- Nijnik, A., and Hancock, R. E. (2009). The roles of cathelicidin LL-37 in immune defences and novel clinical applications. *Curr. Opin. Hematol.* 16, 41–47. doi: 10.1097/MOH.0b013e32831ac517
- Oh, D.-H., and Marshall, D. L. (1995). Destruction of *Listeria monocytogenes* biofilms on stainless steel using monolaurin and heat. *J. Food Prot.* 58, 251–255. doi: 10.4315/0362-028X-58.3.251
- Omar, A., Wright, J. B., Schultz, G., Burrell, R., and Nadworny, P. (2017). Microbial biofilms and chronic wounds. *Microorganisms* 5:9. doi: 10.3390/microorganisms5010009
- Ooi, N., Miller, K., Randall, C., Rhys-Williams, W., Love, W., and Chopra, I. (2010). XF-70 and XF-73, novel antibacterial agents active against slow-growing and non-dividing cultures of *Staphylococcus aureus* including biofilms. *J. Antimicrob. Chemother.* 65, 72–78. doi: 10.1093/jac/dkp409
- Oun, R., Moussa, Y. E., and Wheate, N. J. (2018). The side effects of platinum-based chemotherapy drugs: a review for chemists. *Dalton Trans.* 47, 6645–6653. doi: 10.1039/C8DT00838H
- Overhage, J., Campisano, A., Bains, M., Torfs, E. C., Rehm, B. H., and Hancock, R. E. (2008). Human host defense peptide LL-37 prevents bacterial biofilm formation. *Infect. Immun.* 76, 4176–4182. doi: 10.1128/IAI.00318-08
- Penesyan, A., Gillings, M., and Paulsen, I. T. (2015). Antibiotic discovery: combatting bacterial resistance in cells and in biofilm communities. *Molecules* 20, 5286–5298. doi: 10.3390/molecules20045286
- Peng, Y., Zheng, Y., Zhang, Y., Zhao, J., Chang, F., Lu, T., et al. (2012). Different effects of omega-3 fatty acids on the cell cycle in C2C12 myoblast proliferation. *Mol. Cell. Biochem.* 367, 165–173. doi: 10.1007/s11010-012-1329-4
- Post, J. C. (2001). Direct evidence of bacterial biofilms in otitis media. *Laryngoscope* 111, 2083–2094. doi: 10.1097/00005537-200112000-00001
- Rabin, N., Zheng, Y., Opoku-Temeng, C., Du, Y., Bonsu, E., and Sintim, H. O. (2015). Agents that inhibit bacterial biofilm formation. *Fut. Med. Chem.* 7, 647–671. doi: 10.4155/fmc.15.7
- Rachid, S., Ohlsen, K., Witte, W., Hacker, J., and Ziebuhr, W. (2000). Effect of subinhibitory antibiotic concentrations on polysaccharide intercellular adhesin expression in biofilm-forming *Staphylococcus epidermidis*. *Antimicrob. Agents Chemother.* 44, 3357–3363. doi: 10.1128/AAC.44.12.3357-3363.2000
- Redelman, C. V., Chakravarty, S., and Anderson, G. G. (2014). Antibiotic treatment of *Pseudomonas aeruginosa* biofilms stimulates expression of the magnesium transporter gene *mgE*. *Microbiology* 160, 165–178. doi: 10.1099/mic.0.070144-0
- Reffuveille, F., de la Fuente-Núñez, C., Hancock, R. E. W., and Fairfull-Smith, K. E. (2015). Potentiation of ciprofloxacin action against gram-negative bacterial biofilms by a nitroxide. *Pathog. Dis.* 73:ftv016. doi: 10.1093/femspd/ftv016
- Reffuveille, F., de la Fuente-Núñez, C., Mansour, S., and Hancock, R. E. (2014). A broad-spectrum antibiofilm peptide enhances antibiotic action against bacterial biofilms. *Antimicrob. Agents Chemother.* 58, 5363–5371. doi: 10.1128/AAC.03163-14
- Roizman, D., Vidaillac, C., Givskov, M., and Yang, L. (2017). *In vitro* evaluation of biofilm dispersal as a therapeutic strategy to restore antimicrobial efficacy. *Antimicrob. Agents Chemother.* 61, e01088–e01017. doi: 10.1128/AAC.01088-17
- Roy, R., Tiwari, M., Donelli, G., and Tiwari, V. (2018). Strategies for combating bacterial biofilms: a focus on anti-biofilm agents and their mechanisms of action. *Virulence* 9, 522–554. doi: 10.1080/21505594.2017.1313372
- Russell, A. D. (2003). Biocide use and antibiotic resistance: the relevance of laboratory findings to clinical and environmental situations. *Lancet Infect. Dis.* 3, 794–803. doi: 10.1016/S1473-3099(03)00833-8
- Rybak, M. J., and McGrath, B. J. (1996). Combination antimicrobial therapy for bacterial infections. Guidelines for the clinician. *Drugs* 52, 390–405. doi: 10.2165/00003495-199652030-00005
- Sailer, F. C., Meberg, B. M., and Young, K. D. (2003). beta-Lactam induction of colanic acid gene expression in *Escherichia coli*. *FEMS Microbiol. Lett.* 226, 245–249. doi: 10.1016/S0378-1097(03)00616-5
- Saiman, L. (2004). Microbiology of early CF lung disease. *Paediatr. Respir. Rev.* 5, S367–S369. doi: 10.1016/S1526-0542(04)90065-6
- Schachter, B. (2003). Slimy business—the biotechnology of biofilms. *Nat. Biotechnol.* 21, 361–365. doi: 10.1038/nbt0403-361
- Schlievert, P. M., and Peterson, M. L. (2012). Glycerol monolaurate antibacterial activity in broth and biofilm cultures. *PLoS ONE* 7:e40350. doi: 10.1371/journal.pone.0040350
- Shai, Y. (1999). Mechanism of the binding, insertion and destabilization of phospholipid bilayer membranes by alpha-helical antimicrobial and cell non-selective membrane-lytic peptides. *Biochim. Biophys. Acta* 1462, 55–70. doi: 10.1016/S0005-2736(99)00200-X
- Shields, C. L., Naseripour, M., and Shields, J. A. (2002). Topical mitomycin C for extensive, recurrent conjunctival-corneal squamous cell carcinoma. *Am. J. Ophthalmol.* 133, 601–606. doi: 10.1016/S0002-9394(02)01400-9
- Simões, M., Simões, L. C., and Vieira, M. J. (2010). A review of current and emergent biofilm control strategies. *LWT Food Sci. Technol.* 43, 573–583. doi: 10.1016/j.lwt.2009.12.008
- Spoering, A. L., and Lewis, K. (2001). Biofilms and planktonic cells of *Pseudomonas aeruginosa* have similar resistance to killing by antimicrobials. *J. Bacteriol.* 183, 6746–6751. doi: 10.1128/JB.183.23.6746-6751.2001
- Spoering, A. L., Vulić, M., and Lewis, K. (2006). GlpD and PlsB participate in persister cell formation in *Escherichia coli*. *J. Bacteriol.* 188:5136. doi: 10.1128/JB.00369-06
- Stewart, P. S. (2002). Mechanisms of antibiotic resistance in bacterial biofilms. *Int. J. Med. Microbiol.* 292, 107–113. doi: 10.1078/1438-4221-00196
- Stewart, P. S., and William Costerton, J. (2001). Antibiotic resistance of bacteria in biofilms. *Lancet* 358, 135–138. doi: 10.1016/S0140-6736(01)05321-1
- Stone, G., Wood, P., Dixon, L., Keyhan, M., and Matin, A. (2002). Tetracycline rapidly reaches all the constituent cells of uropathogenic *Escherichia coli* biofilms. *Antimicrob. Agents Chemother.* 46, 2458–2461. doi: 10.1128/AAC.46.8.2458-2461.2002
- Stoodley, P., Sauer, K., Davies, D. G., and Costerton, J. W. (2002). Biofilms as complex differentiated communities. *Annu. Rev. Microbiol.* 56, 187–209. doi: 10.1146/annurev.micro.56.012302.160705
- Sun, H., Tawa, G., and Wallqvist, A. (2012). Classification of scaffold-hopping approaches. *Drug Discov. Today* 17, 310–324. doi: 10.1016/j.drudis.2011.10.024
- Sun, M., Dong, J., Xia, Y., and Shu, R. (2017). Antibacterial activities of docosahexaenoic acid (DHA) and eicosapentaenoic acid (EPA) against planktonic and biofilm growing *Streptococcus mutans*. *Microb. Pathog.* 107, 212–218. doi: 10.1016/j.micpath.2017.03.040
- Sun, M., Zhou, Z., Dong, J., Zhang, J., Xia, Y., and Shu, R. (2016). Antibacterial and antibiofilm activities of docosahexaenoic acid (DHA) and eicosapentaenoic acid (EPA) against periodontopathic bacteria. *Microb. Pathog.* 99, 196–203. doi: 10.1016/j.micpath.2016.08.025
- Szomolay, B., Klapper, I., Dockery, J., and Stewart, P. S. (2005). Adaptive responses to antimicrobial agents in biofilms. *Environ. Microbiol.* 7, 1186–1191. doi: 10.1111/j.1462-2920.2005.00797.x
- Tamma, P. D., Cosgrove, S. E., and Maragakis, L. L. (2012). Combination therapy for treatment of infections with gram-negative bacteria. *Clin. Microbiol. Rev.* 25:450. doi: 10.1128/CMR.05041-11
- Thormar, H. (2010). “Antibacterial effects of lipids: historical review (1881 to 1960),” in *Lipids and Essential Oils as Antimicrobial Agents*, ed H. Thormar, (Hoboken, NJ: Wiley), 25–45. doi: 10.1002/9780470976623.ch2
- Tomasz, M. (1995). Mitomycin C: small, fast and deadly (but very selective). *Chem. Biol.* 2, 575–579. doi: 10.1016/1074-5521(95)90120-5
- Turner, J., Cho, Y., Dinh, N.-N., Waring, A. J., and Lehrer, R. I. (1998). Activities of LL-37, a cathelin-associated antimicrobial peptide of human neutrophils. *Antimicrob. Agents Chemother.* 42:2206. doi: 10.1128/AAC.42.9.2206
- Verderosa, A., Harris, J., Dhoubi, R., Totsika, M., and Fairfull-Smith, K. (2019a). Eradicating uropathogenic *Escherichia coli* biofilms with a ciprofloxacin-dinitroxide conjugate. *Med. Chem. Comm.* 10, 699–711. doi: 10.1039/C9MD00062C
- Verderosa, A. D., de la Fuente-Núñez, C., Mansour, S. C., Cao, J., Lu, T. K., Hancock, R. E. W., et al. (2017). Ciprofloxacin-nitroxide hybrids with potential for biofilm control. *Eur. J. Med. Chem.* 138, 590–601. doi: 10.1016/j.ejmech.2017.06.058
- Verderosa, A. D., Dhoubi, R., Fairfull-Smith, K. E., and Totsika, M. (2019b). Nitroxide functionalized antibiotics are promising eradication agents

- against *Staphylococcus aureus* biofilms. *Antimicrob. Agents Chemother.* doi: 10.1128/AAC.01685-19. [Epub ahead of print].
- Verderosa, A. D., Dhoub, R., Fairfull-Smith, K. E., and Totsika, M. (2019c). Profluorescent fluoroquinolone-nitroxides for investigating antibiotic-bacterial interactions. *Antibiotics* 8:E19. doi: 10.3390/antibiotics8010019
- Verderosa, A. D., Mansour, S. C., de la Fuente-Núñez, C., Hancock, R. E., and Fairfull-Smith, K. E. (2016). Synthesis and evaluation of ciprofloxacin-nitroxide conjugates as anti-biofilm agents. *Molecules* 21:841. doi: 10.3390/molecules21070841
- Vieira Colombo, A. P., Magalhães, C. B., Hartenbach, F. A., Martins do Souto, R., and Maciel da Silva-Boghossian, C. (2016). Periodontal-disease-associated biofilm: a reservoir for pathogens of medical importance. *Microbial. Pathog.* 94, 27–34. doi: 10.1016/j.micpath.2015.09.009
- von Rosenvinge, E. C., O'May, G. A., Macfarlane, S., Macfarlane, G. T., and Shirliff, M. E. (2013). Microbial biofilms and gastrointestinal diseases. *Pathog. Dis.* 67, 25–38. doi: 10.1111/2049-632X.12020
- Wagner, V. E., and Iglewski, B. H. (2008). *P. aeruginosa* biofilms in CF infection. *Clin. Rev. Allergy Immunol.* 35, 124–134. doi: 10.1007/s12016-008-8079-9
- Walters, M. C. III, Roe, F., Bugnicourt, A., Franklin, M. J., and Stewart, P. (2003). Contributions of antibiotic penetration, oxygen limitation, and low metabolic activity to tolerance of *Pseudomonas aeruginosa* biofilms to ciprofloxacin and tobramycin. *Antimicrob. Agents Chemother.* 47, 317–323. doi: 10.1128/AAC.47.1.317-323.2003
- Wei, G. X., Campagna, A. N., and Bobek, L. A. (2006). Effect of MUC7 peptides on the growth of bacteria and on *Streptococcus mutans* biofilm. *J. Antimicrob. Chemother.* 57, 1100–1109. doi: 10.1093/jac/dkl120
- Woehlk, H., Trimble, M. J., Mansour, S. C., Pletzer, D., Trouillet, V., Welle, A., et al. (2019). Controlling biofilm formation with nitroxide functional surfaces. *Polym. Chem.* 10, 4252–4258. doi: 10.1039/C9PY00690G
- Wood, T. K., Knabel, S. J., and Kwan, B. W. (2013). Bacterial persister cell formation and dormancy. *Appl. Environ. Microbiol.* 79, 7116–7121. doi: 10.1128/AEM.02636-13
- Worley, B. V., Schilly, K. M., and Schoenfisch, M. H. (2015). Anti-biofilm efficacy of dual-action nitric oxide-releasing alkyl chain modified poly(amidoamine) dendrimers. *Mol. Pharm.* 12, 1573–1583. doi: 10.1021/acs.molpharmaceut.5b00006
- Worthington, R. J., Richards, J. J., and Melander, C. (2012). Small molecule control of bacterial biofilms. *Org. Biomol. Chem.* 10, 7457–7474. doi: 10.1039/c2ob25835h
- Yang, Y. C., Lii, C. K., Wei, Y. L., Li, C. C., Lu, C. Y., Liu, K. L., et al. (2013). Docosahexaenoic acid inhibition of inflammation is partially via cross-talk between Nrf2/heme oxygenase 1 and IKK/NF-kappaB pathways. *J. Nutr. Biochem.* 24, 204–212. doi: 10.1016/j.jnutbio.2012.05.003
- Yendewa, G. A., Griffiss, J. M., Jacobs, M. R., Fulton, S. A., O'Riordan, M. A., Gray, W. A., et al. (2019). A two-part phase I study to establish and compare the safety and local tolerability of two nasal formulations of XF-73 for decolonization of *Staphylococcus aureus*: a previously investigated 0.5 mg/g viscosified gel formulation versus a modified formulation. *J. Glob. Antimicrob. Resist.* doi: 10.1016/j.jgar.2019.09.017. [Epub ahead of print].
- Yepuri, N. R., Barraud, N., Mohammadi, N. S., Kardak, B. G., Kjelleberg, S., Rice, S. A., et al. (2013). Synthesis of cephalosporin-3'-diazoniumdiolates: biofilm dispersing NO-donor prodrugs activated by beta-lactamase. *Chem. Commun. (Camb)*. 49, 4791–4793. doi: 10.1039/c3cc40869h
- Yoon, B. K., Jackman, J. A., Valle-González, E. R., and Cho, N.-J. (2018). Antibacterial free fatty acids and monoglycerides: biological activities, experimental testing, and therapeutic applications. *Int. J. Mol. Sci.* 19:1114. doi: 10.3390/ijms19041114
- Yuan, M., Chua, S. L., Liu, Y., Drautz-Moses, D. I., Yam, J. K. H., Aung, T. T., et al. (2018). Repurposing the anticancer drug cisplatin with the aim of developing novel *Pseudomonas aeruginosa* infection control agents. *Beilstein J. Org. Chem.* 14, 3059–3069. doi: 10.3762/bjoc.14.284
- Zhao, J., Jiang, H., Cheng, W., Wu, J., Zhao, J., Wang, J., et al. (2015). The role of quorum sensing system in antimicrobial induced ampC expression in *Pseudomonas aeruginosa* biofilm. *J. Basic Microbiol.* 55, 671–678. doi: 10.1002/jobm.201300987

Conflict of Interest: The authors declare that the research was conducted in the absence of any commercial or financial relationships that could be construed as a potential conflict of interest.

Copyright © 2019 Verderosa, Totsika and Fairfull-Smith. This is an open-access article distributed under the terms of the Creative Commons Attribution License (CC BY). The use, distribution or reproduction in other forums is permitted, provided the original author(s) and the copyright owner(s) are credited and that the original publication in this journal is cited, in accordance with accepted academic practice. No use, distribution or reproduction is permitted which does not comply with these terms.



Applications and Perspectives of Cascade Reactions in Bacterial Infection Control

Yuanfeng Li^{1,2†}, Guang Yang^{1,2†}, Yijin Ren³, Linqi Shi^{1*}, Rujiang Ma¹, Henny C. van der Mei^{2*} and Henk J. Busscher^{1,2*}

¹ State Key Laboratory of Medicinal Chemical Biology, Key Laboratory of Functional Polymer Materials, Ministry of Education, Institute of Polymer Chemistry, College of Chemistry, Nankai University, Tianjin, China, ² Department of Biomedical Engineering, University of Groningen and University Medical Center Groningen, Groningen, Netherlands, ³ Department of Orthodontics, University of Groningen and University Medical Center Groningen, Groningen, Netherlands

OPEN ACCESS

Edited by:

Sergio F. Sousa,
University of Porto, Portugal

Reviewed by:

Geelsu Hwang,
University of Pennsylvania,
United States
Hyun Lee,
University of Illinois at Chicago,
United States

*Correspondence:

Linqi Shi
shilingqi@nankai.edu.cn
Henny C. van der Mei
h.c.van.der.mei@umcg.nl
Henk J. Busscher
h.j.busscher@umcg.nl

[†]These authors have contributed
equally to this work

Specialty section:

This article was submitted to
Medicinal and Pharmaceutical
Chemistry,
a section of the journal
Frontiers in Chemistry

Received: 23 September 2019

Accepted: 26 November 2019

Published: 08 January 2020

Citation:

Li Y, Yang G, Ren Y, Shi L, Ma R, van der Mei HC and Busscher HJ (2020) Applications and Perspectives of Cascade Reactions in Bacterial Infection Control. *Front. Chem.* 7:861. doi: 10.3389/fchem.2019.00861

Cascade reactions integrate two or more reactions, of which each subsequent reaction can only start when the previous reaction step is completed. Employing natural substrates in the human body such as glucose and oxygen, cascade reactions can generate reactive oxygen species (ROS) to kill tumor cells, but cascade reactions may also have potential as a direly needed, novel bacterial infection-control strategy. ROS can disintegrate the EPS matrix of infectious biofilm, disrupt bacterial cell membranes, and damage intra-cellular DNA. Application of cascade reactions producing ROS as a new infection-control strategy is still in its infancy. The main advantages for infection-control cascade reactions include the fact that they are non-antibiotic based and induction of ROS resistance is unlikely. However, the amount of ROS generated is generally low and antimicrobial efficacies reported are still far <3–4 log units necessary for clinical efficacy. Increasing the amounts of ROS generated by adding more substrate bears the risk of collateral damage to tissue surrounding an infection site. Collateral tissue damage upon increasing substrate concentrations may be prevented by locally increasing substrate concentrations, for instance, using smart nanocarriers. Smart, pH-responsive nanocarriers can self-target and accumulate in infectious biofilms from the blood circulation to confine ROS production inside the biofilm to yield long-term presence of ROS, despite the short lifetime (nanoseconds) of individual ROS molecules. Increasing bacterial killing efficacies using cascade reaction components containing nanocarriers constitutes a first, major challenge in the development of infection-control cascade reactions. Nevertheless, their use in combination with clinical antibiotic treatment may already yield synergistic effects, but this remains to be established for cascade reactions. Furthermore, specific patient groups possessing elevated levels of endogenous substrate (for instance, diabetic or cancer patients) may benefit from the use of cascade reaction components containing nanocarriers.

Keywords: bacterial biofilm, cascade reaction, infection, glucose, hydrogen peroxide, ROS

INTRODUCTION

Bacterial infections have threatened mankind ever since its first existence. Infection control gained a major success with the discovery of antibiotics in 1923. However, this success lasted less than a century, and toward the turn of the century, the first reports of antibiotic-resistant bacterial pathogens appeared (Davies and Davies, 2010). The latest new antibiotic class was discovered in 1986, after which shortening of the effective lifetime of new antibiotics, and financial and regulatory hurdles cooled down the passion of pharmaceutical companies to develop new antibiotics. It is estimated that the number of deaths attributable to antimicrobial-resistant bacterial infections will rise to 10 million per year by 2050, at a cost of more than US\$100 trillion (O'Neill, 2014).

An additional problem in infection control, next to antibiotic resistance, is the presentation of infectious bacteria in a biofilm mode of growth. In a biofilm mode of growth, adhering bacteria produce a matrix of extracellular polymeric substances (EPS), in which they protect themselves against the host immune system and environmental attacks, such as posed by UV exposure, pH changes, and antibiotics (Hall-Stoodley et al., 2004). The EPS matrix impedes penetration of antibiotics, yielding survival of bacteria residing in the depth of a biofilm, which necessitates long-term and high-dose antimicrobial treatment to eradicate infectious biofilms, not seldom followed by recurrence of the infection after treatment (Fux et al., 2005).

To counter the increasing threat of bacterial infections, numerous nanotechnology-based antimicrobials and smart, antimicrobial-delivery nanocarriers are being designed (Liu et al., 2019a), such as carbon quantum dots, graphene, gold, silver, iron oxide, or polymeric nanoparticles, including micelles or antimicrobial dendrimers. However, the antimicrobial efficacy of many new nanoparticles are insignificant for clinical usage and only achieve about 90% reductions in bacterial viability (1 log unit), while a minimum of 99.9–99.99% (3–4 log units) is required to achieve any clinical efficacy (Liu X. et al., 2019). ROS are sometimes called “the sword of nanotechnology,” and taking lessons from cancer therapy, several methods have become available to generate ROS (Sun et al., 2014; Liu X. et al., 2019). ROS produced by different types of nanoparticles in combination with the addition of external H₂O₂ (Gao et al., 2016; Liu et al., 2018; Naha et al., 2019) has been shown to be effective in biofilm eradication. However, the use of cascade reactions to counter bacterial infections through ROS production using endogenously present substrate, i.e., without addition of external H₂O₂, has not yet been extensively considered.

A cascade reaction, also called tandem or domino reaction, is a chemical process that integrates at least two reactions, of which each subsequent reaction can only start when the previous reaction step is completed (Ricca et al., 2011). Enzymatic cascade reactions combine a series of enzymatic substrate transformations to produce a final product. In liner cascade reactions, the product of the first enzymatic reaction becomes the substrate of a second reaction (Ricca et al., 2011). Enzymatic cascade reactions widely occur in living organisms (Ricca et al., 2011). Photosynthesis and aerobic respiration, for instance,

are enzymatic cascade reactions producing carbohydrates and carbon dioxide, respectively. Industrially, enzymatic cascade reactions are used in the one-pot synthesis of chemicals. Liner cascade reactions are the most widely used type of cascade reaction in cancer and infection therapy. Using naturally occurring substrates in the human body such as endogenous glucose and oxygen, cascade reactions can be used to produce highly toxic ROS (**Figure 1A**) (Yan et al., 2018), as an anti-cancer drug (Li et al., 2017) or antimicrobial (André et al., 2011; Liu et al., 2017; Liu X. et al., 2019) (**Figure 1B**).

In this review, we will focus on recent progress in the design of cascade reactions as a new strategy in infection control, taking lessons from current developments aimed toward using cascade reactions in cancer therapy. Use of cascade reactions for infection control is slowly emerging, yet offering equal or more perspective than new antibiotics or non-ROS-based infection-control strategies, because hitherto bacterial resistance to ROS has not been reported and is generally considered highly unlikely to develop.

CHEMISTRY OF CASCADE REACTIONS

In this section, different kinds of cascade reactions are classified by substrate. The conditions and mechanisms to achieve these cascade reactions are summarized.

Glucose and Oxygen

Glucose is the most important carbohydrate in the human body and can yield gluconic acid and H₂O₂ upon reaction with oxygen (Itskov and Carlos, 2013; Fan et al., 2017), according to



The production of H₂O₂ according to reaction (1) can be catalyzed by glucose oxidase (GOx), as the first reaction in a liner cascade reaction (**Figure 1A**). This catalytic process can be divided into a reductive and oxidative half-reaction, as shown in **Figure 2A**. In the reductive half-reaction, β-D-glucose loses two electrons to form δ-gluconolactone, which is subsequently hydrolyzed to gluconic acid. After receiving two electrons from the reductive half-reaction, the flavin ring of GOx becomes reduced to FADH₂ after which, in the oxidative half-reaction, the same two electrons transferred from GOx-FADH₂ to oxygen yield H₂O₂ and GOx in an oxidized state (Witt et al., 2000). Reaction (1) can also be catalyzed by gold nanoparticles and modified graphitic carbon nitride, as shown schematically in **Figures 2B,C**, respectively.

In the second reaction of the cascade, different artificial, catalytic nanoparticles can be employed to transform H₂O₂ into ·OH, ¹O₂ (singlet oxygen), and ·O₂[−] (Cho et al., 2019). These catalytic nanoparticles include AuNPs (Zhang et al., 2019), iron oxide (Fan et al., 2012; Duan et al., 2015; Gao et al., 2016; Liu et al., 2018; Naha et al., 2019), silver halides (Wang et al., 2014), platinum (Liu X. et al., 2016; Wu et al., 2018), cerium oxide (Niu et al., 2007; Celardo et al., 2011), vanadium oxide (André et al., 2011), 2D metallo-porphyrinic metal-organic framework (MOF) nanosheets (Huang et al., 2017), and molybdenum

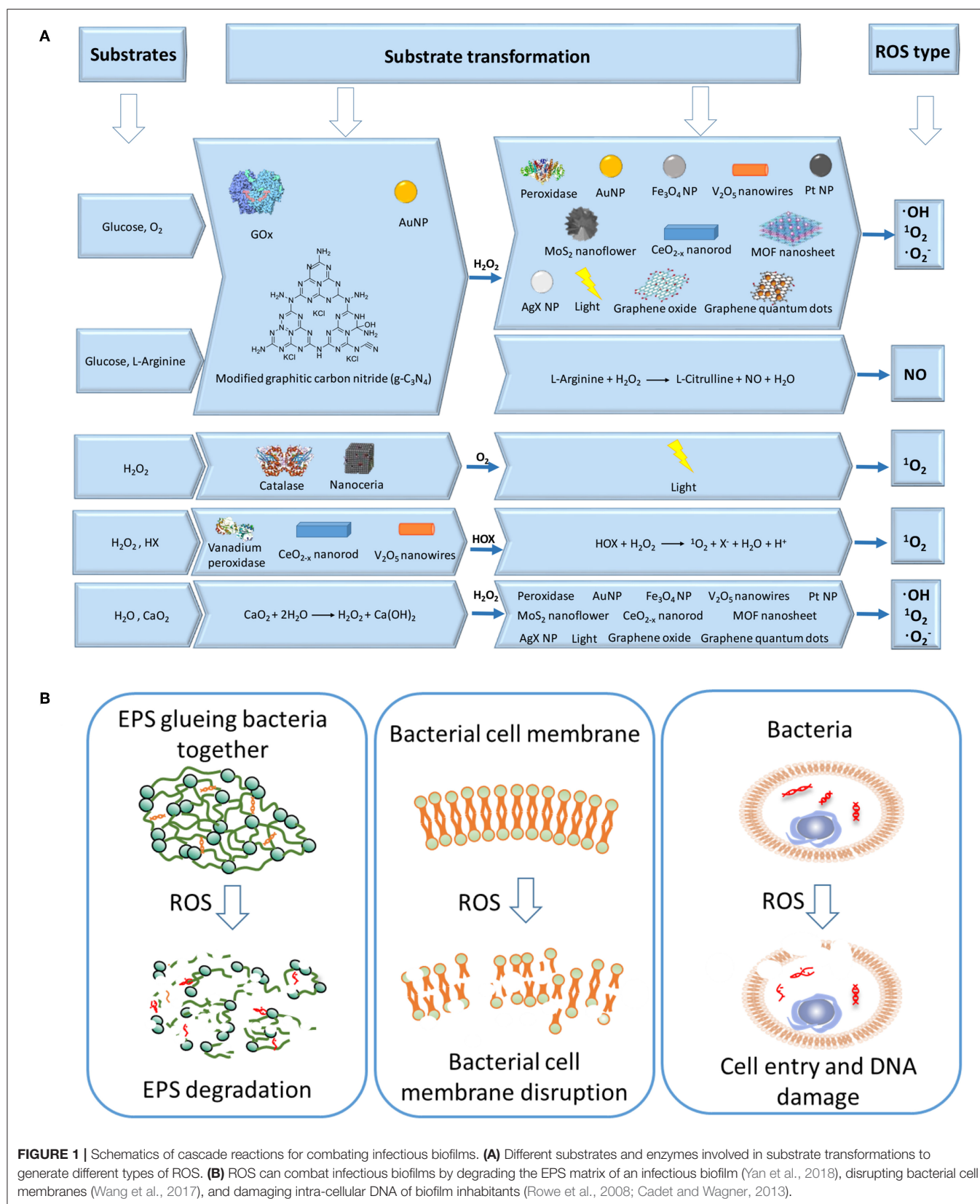
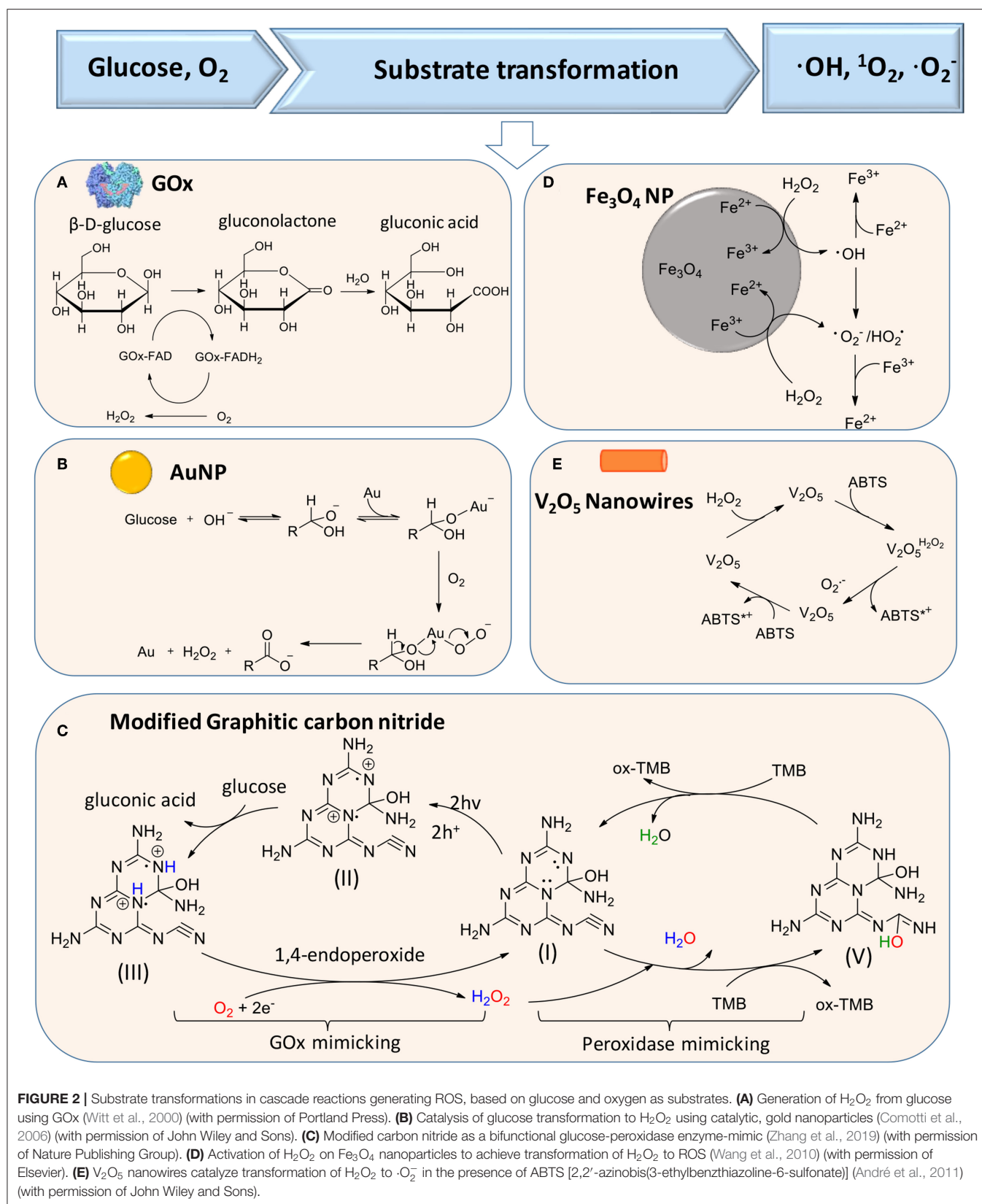


FIGURE 1 | Schematics of cascade reactions for combating infectious biofilms. **(A)** Different substrates and enzymes involved in substrate transformations to generate different types of ROS. **(B)** ROS can combat infectious biofilms by degrading the EPS matrix of an infectious biofilm (Yan et al., 2018), disrupting bacterial cell membranes (Wang et al., 2017), and damaging intra-cellular DNA of biofilm inhabitants (Rowe et al., 2008; Cadet and Wagner, 2013).



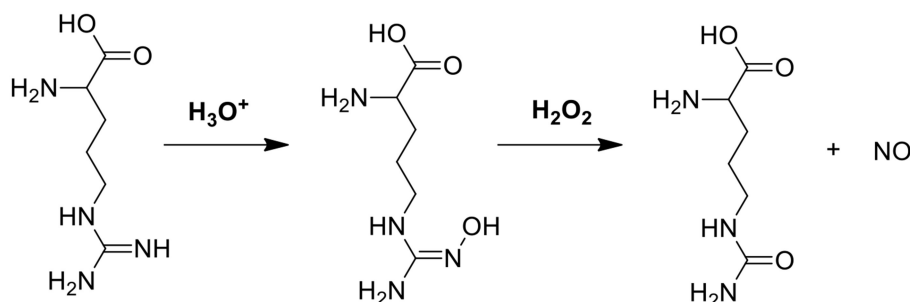


FIGURE 3 | The mechanism of NO generation through reaction between L-arginine and H₂O₂ (Fan et al., 2017).

disulfide (MoS₂) nanoflowers (Yin et al., 2016). Metal-free artificial catalysts include modified carbon nitride (Yin et al., 2016), graphene oxide (Song et al., 2010), and graphene quantum dots (Sun et al., 2014; Duan et al., 2015). Importantly, these catalytic nanoparticles can be functionally modified to enhance their catalytic activity. However, mechanisms to transform H₂O₂ into ·OH, ¹O₂, and ·O₂[−] are different for different artificial catalytic nanoparticles. Proposed catalytic mechanisms for iron oxide nanoparticles and V₂O₅ nanowires are summarized in **Figures 2D,E** (Natalio et al., 2012). Light irradiation can also be used as a catalytic mediator to split H₂O₂ into two ·OH (Chang et al., 2017).

Glucose and L-arginine

In another cascade reaction involving glucose (**Figure 1A**), L-arginine can be employed to produce highly toxic nitric oxide (NO) by oxidation of the guanidine function of L-arginine (see also **Figure 3**). Interestingly, gluconic acid, as a by-product in reaction (1), leads to a pH decrease, accelerating L-arginine catalytic transformation of H₂O₂ into NO (Fan et al., 2017).

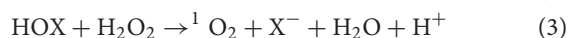
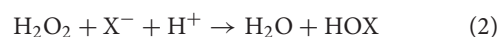
H₂O₂

H₂O₂ can also act as a substrate for generating ¹O₂ in cascade reactions, as catalyzed in the first cascade reaction by catalase, a tetrameric heme protein (**Figure 4A**) (Alfonso-Prieto et al., 2009) or artificial, catalytic nanoparticles, such as cerium oxide nanoparticles (**Figure 4B**) (Herget et al., 2017). In the second reaction, also light can be used to transform O₂ into singlet oxygen, which requires the presence of a suitable photosensitizer (Li et al., 2017), such as tetrapyrroles (absorption band around 400 nm), porphyrins (absorption band around 630 nm), chlorins (absorption band around 650–690 nm), or “bacteriochlorins” with an absorption band shifted further into the red (Castano et al., 2004).

H₂O₂ and halides

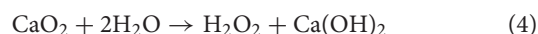
In the presence of H₂O₂ and halides X[−] [such as chloride (Cl[−]) or bromide (Br[−]) ions], vanadium peroxidase (see **Figure 5A**), V₂O₅ nanowires (Natalio et al., 2012) (**Figure 5B**), and CeO_{2−x} nanorods (Herget et al., 2017) (**Figure 5C**) can also be used in the first cascade reaction [see reaction (2)], followed by the second

reaction [reaction (3)]



H₂O and CaO₂

An H₂O₂-free cascade reaction is based on water (H₂O) and calcium peroxide (CaO₂), as substrates (**Figure 1A**) according to Yan et al. (2018)



CaO₂ reacts with H₂O through a redox reaction, in which CaO₂ as a reducing agent loses four electrons. After obtaining the corresponding electrons, H₂O is oxidized to H₂O₂ after which, in the second reaction of the cascade, H₂O₂ can be transformed into ·OH, ¹O₂ and ·O₂[−] by any of the reactions described in sections Glucose and Oxygen and Glucose and L-Arginine.

APPLICATION OF CASCADE REACTIONS IN CANCER THERAPY

The main substrates and enzymes in cascade reactions producing ROS that are currently considered for anti-tumor therapy involve glucose and oxygen, glucose and L-arginine, or H₂O₂/Cl[−] as substrates (**Figure 6**). GOx and Fe₃O₄ nanoparticles have been contained into dendritic silica nanocarriers to initiate a cascade reaction, using endogenous glucose present in tumor cells to generate H₂O₂ (Huo et al., 2017). As a second step, the Fe₃O₄ nanoparticles catalyze H₂O₂ into highly toxic ·OH. *In vivo*, this cascade reaction demonstrated suppression of mammary tumor growth. Instead of using GOx and Fe₃O₄ nanoparticles in dendritic silica to produce ROS (hydroxyl radicals), GOx and catalase have also been integrated in MOF nanocarriers (Li et al., 2017). Here, as the second step in the cascade reaction, H₂O₂ produced endogenously or from oxidation of glucose by GOx, is converted to oxygen by catalase. After that, singlet oxygen (¹O₂) is generated under 660-nm light irradiation (Li et al., 2017). Alternatively, another cascade reaction involving photodynamics based on one enzyme was described (Chang et al., 2017), in which GOx

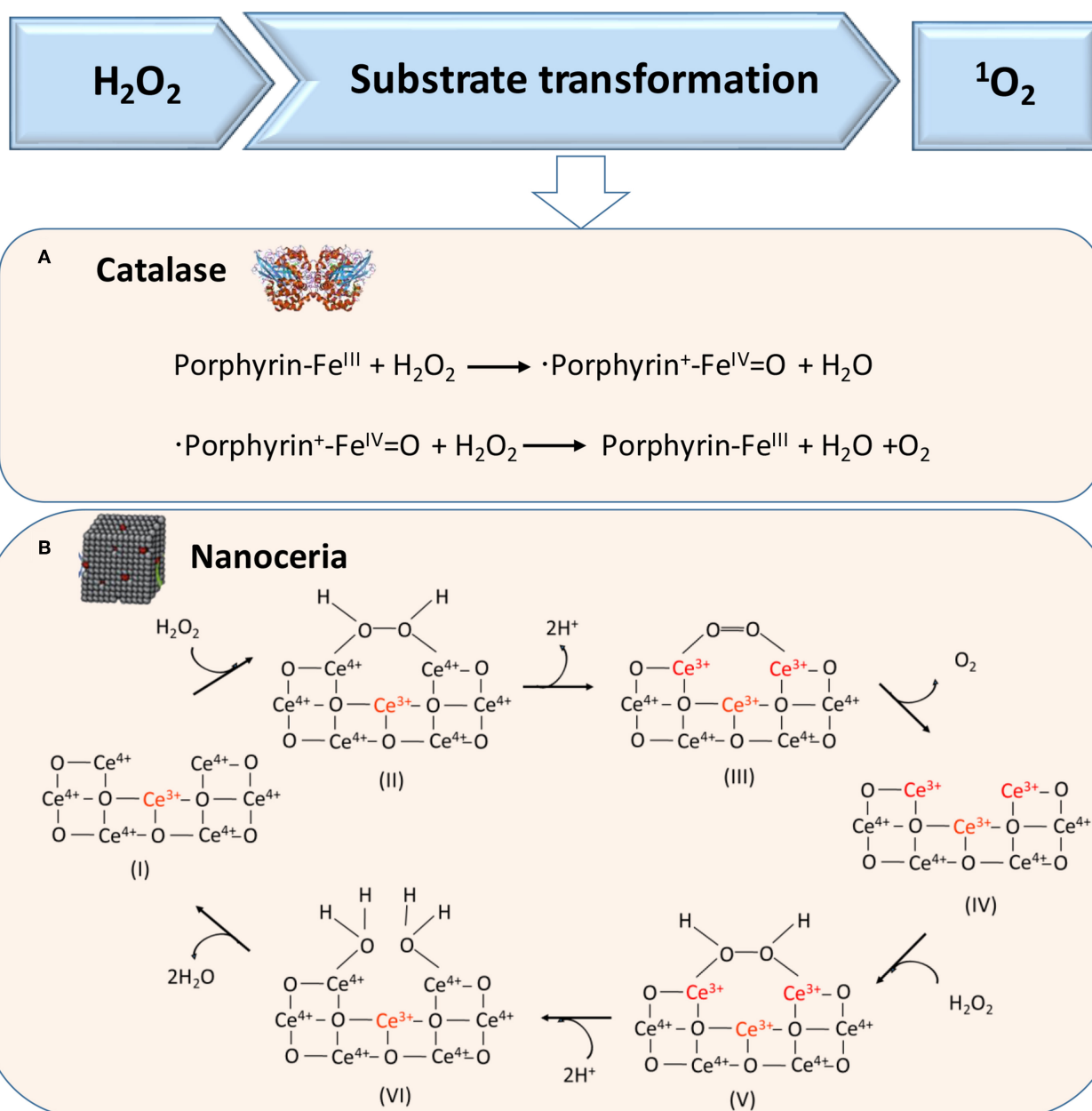


FIGURE 4 | Proposed mechanisms of enzymatic transformations using H_2O_2 as a substrate. **(A)** Transformation of H_2O_2 by catalase into O_2 (Alfonso-Prieto et al., 2009). **(B)** Transformation of H_2O_2 using catalytic cerium oxide nanoparticles ("nanoceria") into O_2 (Celardo et al., 2011) (with permission of the Royal Society of Chemistry).

was conjugated to polymer dots to convert glucose into H_2O_2 . Under light irradiation, the H_2O_2 generated was photolyzed to hydroxyl radicals.

Glucose and L-arginine have also been used as substrates in cascade reactions to produce NO (see also **Figure 6**) in order to kill tumor cells (Fan et al., 2017). To this end, GOx and L-arginine have been contained in hollow, mesoporous organosilica nanocarriers, and after generation of H_2O_2 from glucose present in tumor sites using GOx, reaction of H_2O_2 with

L-arginine generated NO, which was shown to prolong the life of tumor-bearing mice.

Finally, endogenous $\cdot\text{O}_2^-$ and Cl^- have been used as substrates in cascade reactions (Wang et al., 2014). Using superoxide dismutase (SOD) and chloroperoxidase (CPO), endogenous $\cdot\text{O}_2^-$ can be catalyzed by SOD to H_2O_2 , which is subsequently further oxidized with the aid of Cl^- and CPO to $^1\text{O}_2$. This cascade reaction showed negligible toxicity to healthy cells, but was highly toxic to tumor cells.

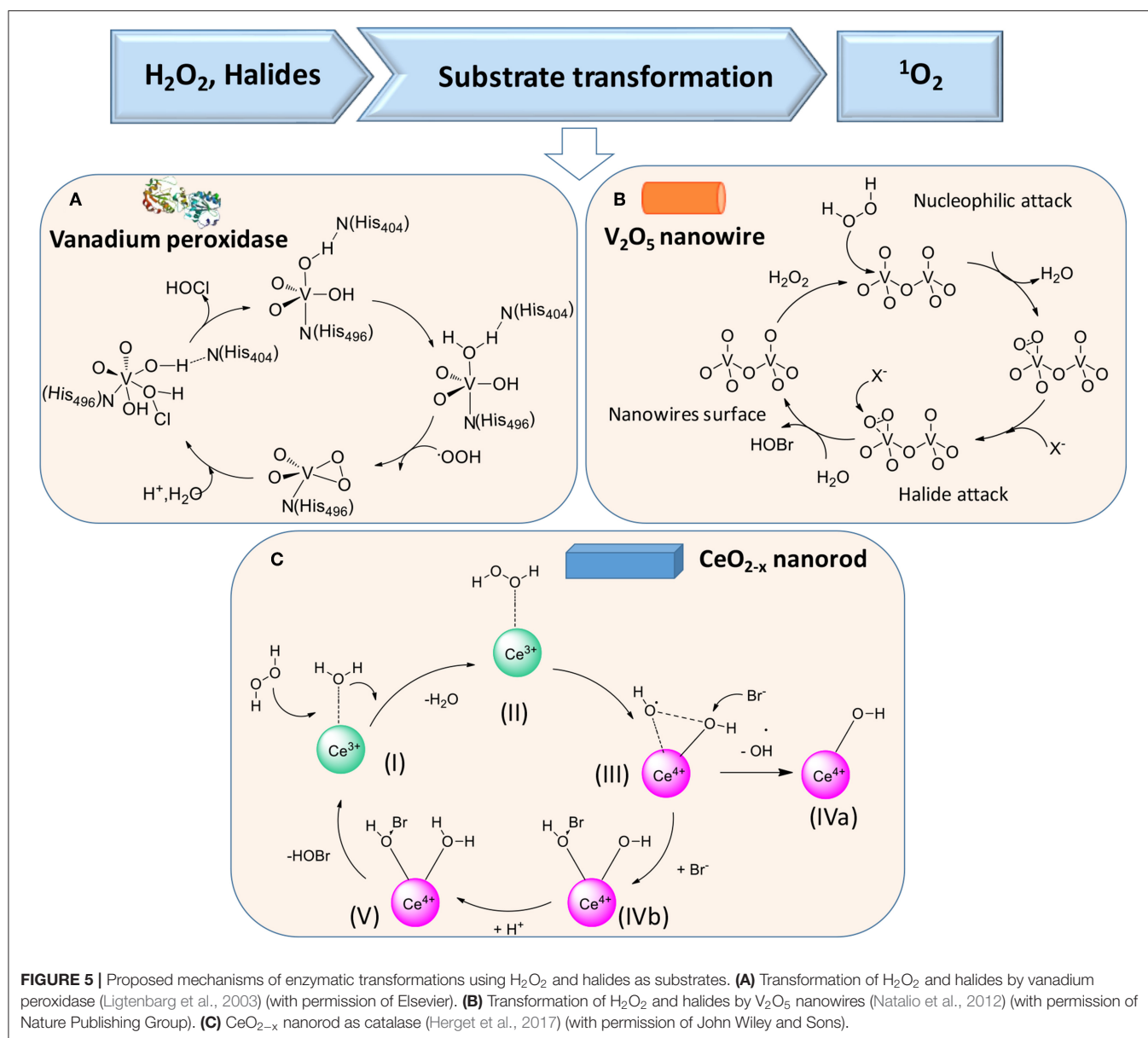


FIGURE 5 | Proposed mechanisms of enzymatic transformations using H₂O₂ and halides as substrates. **(A)** Transformation of H₂O₂ and halides by vanadium peroxidase (Ligtenbarg et al., 2003) (with permission of Elsevier). **(B)** Transformation of H₂O₂ and halides by V₂O₅ nanowires (Natalio et al., 2012) (with permission of Nature Publishing Group). **(C)** CeO_{2-x} nanorod as catalase (Herget et al., 2017) (with permission of John Wiley and Sons).

APPLICATION OF CASCADE REACTIONS FOR BACTERIAL INFECTION CONTROL: LESSONS FROM TUMOR TREATMENT

Based on the similarity between tumor sites and bacterial biofilms (Table 1), we can take lessons from the cascade reactions considered for tumor therapy, as shown in Figure 6. All endogenous substrates used for cancer therapy are available in bacterial infection sites, and ROS shows highly toxic toward all bacterial pathogens, regardless of their Gram character (Vatansever et al., 2013). Therefore, cascade reactions are nowadays started to be considered as an alternative strategy for the control of infectious biofilms. The number of studies applying cascade reaction for bacterial infection control is limited however (see overview in Table 2), but their results

warrant analysis and offer future perspective that are new for infection control.

Cascade Reactions Considered for Bacterial Infection Control

Application of cascade reactions as a new infection-control strategy is currently in its infancy, and to our knowledge, only four studies so far have considered the use of cascade reactions for infection control (see Table 2) that employ different nanocarriers for the cascade reaction components.

Two cascade reactions based on glucose and O₂ as substrate have been evaluated for their antimicrobial activity. GOx absorbed in ultrathin two-dimensional (2D) MOF nanosheet carriers (Liu X. et al., 2019), *in vitro* generated ROS that killed planktonic *Escherichia coli* and *Staphylococcus aureus*

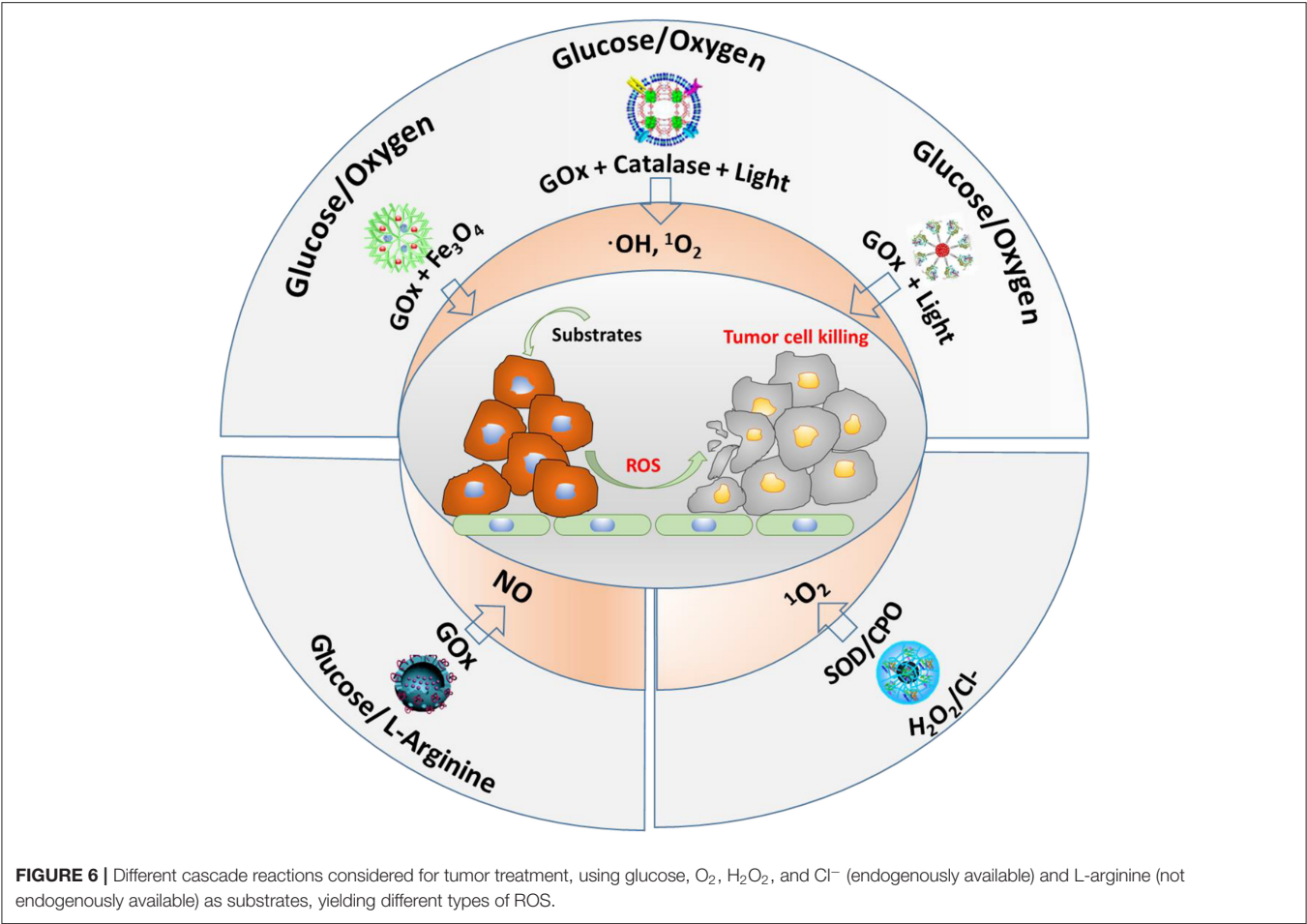


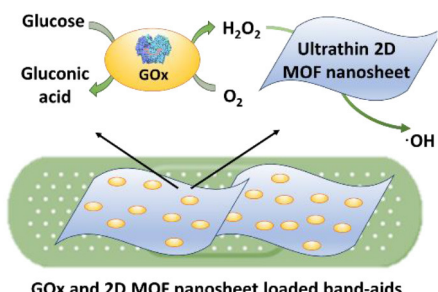
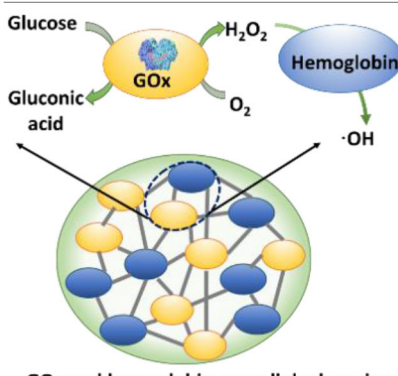
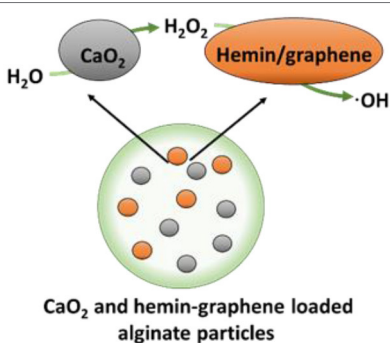
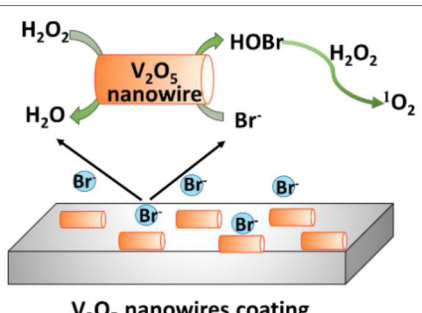
TABLE 1 | Similarities between tumor sites and infectious biofilms, stimulating the application of cascade reactions in infectious bacterial biofilms, taking lessons from their application in tumor treatment.

Similarity	Tumor site	Infectious biofilm
Hampered transport	Tumors larger than 2 mm ³ , limit oxygen diffusion (Trédan et al., 2007; Danhier et al., 2010).	The EPS matrix limits transport of nutrients to the depth of a biofilm (Flemming et al., 2007; Billings et al., 2015).
Acidic pH	Acidic pH between 6.0 and 7.0 (Justus et al., 2013).	Acidic pH < 6.0 (Koo et al., 2017; Liu et al., 2019a).
Endogenous substrate availability	High killing efficacy of ROS toward tumor cells (Postiglione et al., 2011).	ROS can destruct the EPS matrix and kill biofilm bacteria (Walch et al., 2015).
Clinical treatment	Occurrence of resistance against chemotherapeutics, recurrence of tumor growth (Mansoori et al., 2017).	Occurrence of resistance against antimicrobials, recurrence of infection (Aslam et al., 2018).

after 5 h incubation with 15 mM glucose in the growth medium. Bacterial killing was far lower (88 and 90% for *E. coli* and *S. aureus*, respectively) than the 99.9–99.99% efficacy limit considered to be required for clinical efficacy (Liu et al., 2019a). However, when locally applied as a 2D MOF/GOx band-aid on infected (3×10^7 CFU/site *S. aureus*) wounds in mice, mice treated with 2D MOF/GOx band-aids containing 50 μ l of a 10 mM glucose solution showed faster wound healing after 3 days of treatment, retrieving less (91% reduction) CFUs than when treated with blank band-aids.

Glucose and O₂ were also used as substrates in combination with another peroxidase, hemoglobin (Hb) to catalyze H₂O₂ into ·OH. Cascade reaction components were contained in MnCO₃ nanocarriers (Li et al., 2019). In growth medium supplemented with glucose to a concentration of 12.5 mM, i.e., substantially higher than endogenously occurring (before eating <6.1 mM; Stumvoll et al., 2005), GOx-Hb nanocarriers yielded 7 log unit inhibition in planktonic MRSA growth (Figure 7). In addition, biomass analysis based on Crystal Violet staining indicated the ability of GOx-Hb nanocarriers

TABLE 2 | Summary of cascade reactions considered for infection control, including substrates required, nanocarriers of cascade reaction components, types of ROS generated, and antimicrobial activities observed.

Substrate	Nanocarrier	ROS	Antimicrobial activity	References
	 <p>GOx and 2D MOF nanosheet loaded band-aids</p>	·OH	<ul style="list-style-type: none"> - Against planktonic <i>S. aureus</i> and <i>E. coli</i> - Improved infected wound healing in mice 	Liu X. et al., 2019
Glucose/Oxygen	 <p>GOx and hemoglobin cross-linked carriers</p>	·OH	<ul style="list-style-type: none"> - Against planktonic MRSA - Inhibiting MRSA biofilm formation 	Li et al., 2019
CaO ₂ /H ₂ O	 <p>CaO₂ and hemin-graphene loaded alginate particles</p>	·OH	<ul style="list-style-type: none"> - Against planktonic <i>S. aureus</i> and <i>E. coli</i> - Inhibiting <i>S. aureus</i> biofilm formation - Dispersing <i>S. aureus</i> biofilm - <i>In vivo</i> implant-related periprosthetic infection of mice 	Yan et al., 2018
H ₂ O ₂ /Br ⁻	 <p>V₂O₅ nanowires coating</p>	¹ O ₂	<ul style="list-style-type: none"> - Against planktonic <i>S. aureus</i> and <i>E. coli</i> - Inhibiting <i>S. aureus</i>, and <i>E. coli</i> biofilm formation 	Natalio et al., 2012

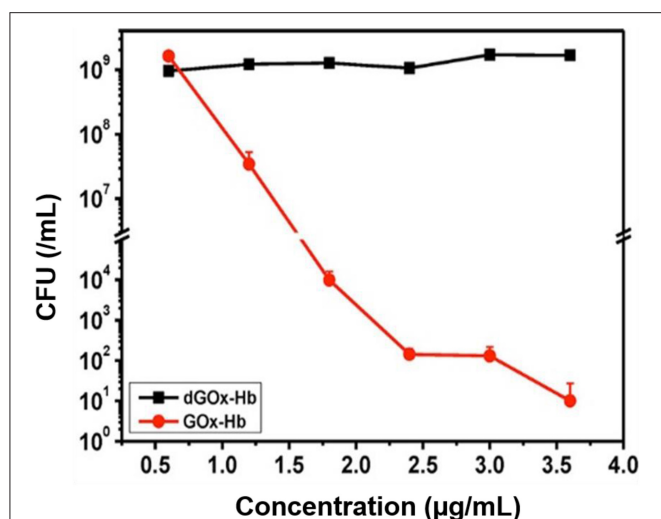


FIGURE 7 | CFUs (MRSA) in growth medium supplemented with glucose (12.5 mM) after 24 h of growth, as a function of GOx-Hb nanocarrier concentration. For control, nanocarriers with denatured GOx (dGOx-Hb) were included (Li et al., 2019) (with permission of ACS).

to inhibit MRSA biofilm formation during 48 h exposure to GOx-Hb and incubation in glucose supplemented growth medium. Nanocarriers containing denatured GOx did not inhibit biofilm formation.

A cascade reaction using CaO_2 and H_2O as substrates to generate hydroxyl radicals was fabricated by containing CaO_2 and hemin-carrying graphene into alginate (Yan et al., 2018). Importantly, these alginate nanocarriers did not contain any H_2O_2 as a substrate and CaO_2 and H_2O were locally converted into ROS. Planktonically, these nanocarriers yielded relatively low killing of *S. aureus* and *E. coli* (90 and 95%, respectively, after 6 h exposure). Also, 72-h *S. aureus* biofilm growth in the presence of the cascade reaction components containing nanocarriers was low, yielding <5-μm-thick biofilms vs. 25 μm in their absence. In addition, exposure of an existing *S. aureus* biofilm to the cascade reaction components containing nanocarriers eradicated 81% of its inhabitants. Interestingly, these cascade reaction components containing nanocarriers caused biofilm dispersal, degrading DNA and proteins, as major components of the EPS-matrix holding a biofilm together. Finally, *S. aureus*-infected wounds (1×10^5 CFU/site) in rats gradually healed after 7 days (>90% bacterial killing) when treated with these alginate nanocarriers, with obvious swelling and pus formation in control groups.

H_2O_2 has also been used in combination with Br^- as substrates in the presence of V_2O_5 nanowires, with an intended, initial use in the marine environment (Natalio et al., 2012). V_2O_5 nanowires can work as natural haloperoxidases to transform bromide ions to hypobromous acid (HOBr) in the presence of H_2O_2 (Natalio et al., 2012). The antimicrobial activity against human pathogens was low, however, decreasing planktonic growth of *E. coli* by only 78% and of *S. aureus* by only 96% in the presence of V_2O_5 nanowires (0.075 mg/ml), Br_2 (1 mM), and

H_2O_2 (10 μM), and as compared to bacteria grown in the absence of additives.

Advantages and Disadvantages of Cascade Reactions for Biofilm Control

The main advantages for infection-control cascade reactions include the fact that they are non-antibiotic based. Bacteria possess little or no resistance against ROS, although some bacterial species can develop resistance against specific ROS species, such as O_2^- and H_2O_2 , but not against OH^\bullet and $^1\text{O}_2$ (Vatansever et al., 2013). Often, however, different species of ROS are generated at the same time in catalytic reactions. ROS as generated in cascade reactions kills both Gram-positive and Gram-negative bacterial strains in a non-specific way. On the one hand, this may be considered an advantage, but on the other hand, the commensal microflora can also be affected, unless the cascade reaction can be localized in or near the infection site. Although nanocarriers and artificial enzymes used in cascade reactions are relatively easy to synthesize and modify, confining ROS generation to an infection site may be more troublesome.

As a drawback of the current status of cascade reactions, the amount of ROS generated is generally low and antimicrobial efficacies reported are below the limit of 3–4 log units considered necessary for clinical efficacy (Yan et al., 2018; Liu et al., 2019a). Although the amount of ROS generated can be enhanced by adding more substrate (Fan et al., 2017), this needs to be done carefully in order to prevent collateral damage to tissue surrounding an infection site. This, too, requires confining of ROS generation to an infection site.

PERSPECTIVES OF THE USE OF CASCADE REACTIONS FOR INFECTION CONTROL

The antimicrobial activity of ROS (Rowe et al., 2008; Cadet and Wagner, 2013; Vatansever et al., 2013; Gao et al., 2016; Wang et al., 2017; Liu et al., 2018; Yan et al., 2018) and the potential advantages of the use of cascade reaction as a new infection-control strategy warrant their further development for infection control, but several challenges have to be overcome before their clinical use becomes into sight. The biggest challenge in the further development of infection-control cascade reactions is to increase their bacterial killing efficacy to levels that can be expected to be clinically effective (i.e., minimally 3-log unit reductions in CFUs, equal to minimal percentage reductions of 99.9–99.99%). This should preferentially be done using endogenously available substrates, but this option should be carefully balanced against the potential damage that high concentrations of ROS can do to tissue cells surrounding an infection site (Li et al., 2019). Alternatively, additional substrate can be locally administered to increase local ROS generation, which may reduce collateral tissue damage. Collateral tissue cell damage might be fully prevented by using self-targeting, pH-responsive nanocarriers that penetrate and accumulate in infectious biofilms (Liu Y. et al., 2016), to confine the occurrence of the cascade reaction and generation of ROS to inside the

biofilm itself. A further advantage of such confinement would be that it will create long-term presence of ROS in a biofilm to enhance bacterial killing, despite the short lifetime (nanoseconds) of individual ROS molecules, arguably too short to yield effective bacterial killing.

Nevertheless, cascade reactions generating relatively low levels of ROS might still be clinically useful in combination with clinically applied antibiotics to enhance their fading efficacies (Nguyen et al., 2016). Synergistic action between different antimicrobials is a common phenomenon, and it is known to even yield killing of bacterial pathogens that are resistant to either of the antimicrobials when applied in monotherapy (Klahn and Brönstrup, 2017). This approach bears advantages for downward clinical translation of infection-control cascade reactions, because it builds on existing clinically applied antibiotics, from which further development of infection-control cascade reactions can be facilitated more easily. Moreover, it might increase the effective lifetime of current and new antibiotics to be developed (Liu et al., 2019b), with the potential to reduce the induction of antibiotic resistance (Mao et al., 2018).

As a final perspective of infection-control cascade reactions, specific patient groups with elevated endogenous substrate levels may benefit from cascade reactions. Diabetic patients, for instance, can suffer from difficult-to-heal infected wounds and have elevated glucose levels (ranging from ≥ 7.0 mM before to ≥ 11.1 mM after eating) compared with healthy glucose levels (ranging from < 5.6 mM before to 7.8 mM after eating) (Stumvoll et al., 2005). Local generation of ROS through suitable cascade reactions may be extremely suitable for treating diabetic

foot ulcers that have been demonstrated to be caused by hard-to-treat infectious biofilms (Neut et al., 2011). Cancer patients are another specific patient group for which infection-control cascade reactions could be useful. There is growing evidence that bacteria can metabolize chemotherapeutic drugs (Geller et al., 2017). Accordingly, intra-tumor bacteria may contribute to resistance against chemotherapeutic drugs among certain tumors. Since tumor sites possess elevated levels of H_2O_2 (50–100 μM around a tumor site vs. 20 nM elsewhere in the body) (De Garcia Lux et al., 2012), infection-control cascade reactions based on endogenous H_2O_2 substrate availability may play a role for this specific patient groups in treating tumor-associated infections.

In short, cascade reactions have potential as a new infection control strategy, but much work remains to be done to solve the challenges listed above in order to make cascade reactions into a real clinical addendum to the antimicrobial armamentarium of modern medicine.

AUTHOR CONTRIBUTIONS

All authors listed have made a substantial, direct and intellectual contribution to the work, and approved it for publication.

FUNDING

This work was financially supported by the National Natural Science Foundation of China (21620102005, 51933006, and 51773099).

REFERENCES

- Alfonso-Prieto, M., Biarnes, X., Vidossich, P., and Rovira, C. (2009). The molecular mechanism of the catalase reaction. *J. Am. Chem. Soc.* 131, 11751–11761. doi: 10.1021/ja9018572
- André, R., Natálio, F., Humanes, M., Leppin, J., Heinze, K., Wever, R., et al. (2011). V_2O_5 Nanowires with an intrinsic peroxidase-like activity. *Adv. Funct. Mater.* 21, 501–509. doi: 10.1002/adfm.201001302
- Aslam, B., Wang, W., Arshad, M. I., Khurshid, M., Muzammil, S., Rasool, M. H., et al. (2018). Antibiotic resistance: a rundown of a global crisis. *Infect. Drug. Resist.* 11, 1645–1658. doi: 10.2147/IDR.S173867
- Billings, N., Birjiniuk, A., Samad, T. S., Doyle, P. S., and Ribbeck, K. (2015). Material properties of biofilms—a review of methods for understanding permeability and mechanics. *Rep. Prog. Phys.* 78:036601. doi: 10.1088/0034-4885/78/3/036601
- Cadet, J., and Wagner, J. R. (2013). DNA base damage by reactive oxygen species, oxidizing agents, and UV radiation. *Cold Spring Harb. Perspect. Biol.* 5:a12559. doi: 10.1101/cshperspect.a012559
- Castano, A. P., Demidova, T. N., and Hamblin, M. R. (2004). Mechanisms in photodynamic therapy: part one—photosensitizers, photochemistry and cellular localization. *Photodiol. Photodyn.* 1, 279–293. doi: 10.1016/S1572-1000(05)00007-4
- Celardo, I., Pedersen, J. Z., Traversa, E., and Ghibelli, L. (2011). Pharmacological potential of cerium oxide nanoparticles. *Nanoscale* 3, 1411–1420. doi: 10.1039/c0nr00875c
- Chang, K., Liu, Z., Fang, X., Chen, H., Men, X., Yuan, Y., et al. (2017). Enhanced phototherapy by nanoparticle-enzyme via generation and photolysis of hydrogen peroxide. *Nano Lett.* 17, 4323–4329. doi: 10.1021/acs.nanolett.7b01382
- Cho, M., Blatchley, M., Duh, E. J., and Gerecht, S. (2019). Acellular and cellular approaches to improve diabetic wound healing. *Adv. Drug. Deliver. Rev.* 146, 267–288. doi: 10.1016/j.addr.2018.07.019
- Comotti, M., Della Pina, C., Falletta, E., and Rossi, M. (2006). Aerobic oxidation of glucose with gold catalyst: hydrogen peroxide as intermediate and reagent. *Adv. Synth. Catal.* 348, 313–316. doi: 10.1002/adsc.200505389
- Danhier, F., Feron, O., and Preat, V. (2010). To exploit the tumor microenvironment: passive and active tumor targeting of nanocarriers for anti-cancer drug delivery. *J. Control. Release* 148, 135–146. doi: 10.1016/j.jconrel.2010.08.027
- Davies, J., and Davies, D. (2010). Origins and evolution of antibiotic resistance. *Microbiol. Mol. Biol. Rev.* 74, 417–433. doi: 10.1128/MMBR.00016-10
- De Garcia Lux, C., Joshi-Barr, S., Nguyen, T., Mahmoud, E., Schopf, E., Fomina, N., et al. (2012). Biocompatible polymeric nanoparticles degrade and release cargo in response to biologically relevant levels of hydrogen peroxide. *JACS* 134, 15758–15764. doi: 10.1021/ja303372u
- Duan, D., Fan, K., Zhang, D., Tan, S., Liang, M., Liu, Y., et al. (2015). Nanozymestrip for rapid local diagnosis of Ebola. *Biosens. Bioelectron.* 74, 134–141. doi: 10.1016/j.bios.2015.05.025
- Fan, K., Cao, C., Pan, Y., Lu, D., Yang, D., Feng, J., et al. (2012). Magnetaferitin nanoparticles for targeting and visualizing tumour tissues. *Nat. Nanotechnol.* 7, 459–464. doi: 10.1038/nnano.2012.90
- Fan, W., Lu, N., Huang, P., Liu, Y., Yang, Z., Wang, S., et al. (2017). Glucose-responsive sequential generation of hydrogen peroxide and nitric oxide for synergistic cancer starving-like/gas therapy. *Angew. Chem. Int. Ed.* 56, 1229–1233. doi: 10.1002/anie.201610682
- Flemming, H.-C., Neu, T. R., and Wozniak, D. J. (2007). The EPS matrix: the “House of biofilm cells.” *J. Bacteriol.* 189, 7945–7947. doi: 10.1128/JB.00858-07

- Fux, C. A., Costerton, J. W., Stewart, P. S., and Stoodley, P. (2005). Survival strategies of infectious biofilms. *Trends Microbiol.* 13, 34–40. doi: 10.1016/j.tim.2004.11.010
- Gao, L., Liu, Y., Kim, D., Li, Y., Hwang, G., Naha, P. C., et al. (2016). Nanocatalysts promote *Streptococcus mutans* biofilm matrix degradation and enhance bacterial killing to suppress dental caries *in vivo*. *Biomaterials* 101, 272–284. doi: 10.1016/j.biomaterials.2016.05.051
- Geller, L. T., Barzily-Rokni, M., Danino, T., Jonas, O. H., Shental, N., Nejman, D., et al. (2017). Potential role of intratumor bacteria in mediating tumor resistance to the chemotherapeutic drug gemcitabine. *Science* 357, 1156–1160. doi: 10.1126/science.aah5043
- Hall-Stoodley, L., Costerton, J. W., and Stoodley, P. (2004). Bacterial biofilms: from the natural environment to infectious diseases. *Nat. Rev. Microbiol.* 2, 95–108. doi: 10.1038/nrmicro821
- Herget, K., Hubach, P., Pusch, S., Deglmann, P., Götz, H., Gorelik, T. E., et al. (2017). Haloperoxidase mimicry by CeO₂-x nanorods combats biofouling. *Adv. Mater.* 29:1603823. doi: 10.1002/adma.201603823
- Huang, Y., Zhao, M., Han, S., Lai, Z., Yang, J., Tan, C., et al. (2017). Growth of Au nanoparticles on 2D metalloporphyrinic metal-organic framework nanosheets used as biomimetic catalysts for cascade reactions. *Adv. Mater.* 29:1700102. doi: 10.1002/adma.201700102
- Huo, M., Wang, L., Chen, Y., and Shi, J. (2017). Tumor-selective catalytic nanomedicine by nanocatalyst delivery. *Nat. Commun.* 8:357. doi: 10.1038/s41467-017-00424-8
- Itskov, P. M., and Carlos, R. (2013). The dilemmas of the gourmet fly: the molecular and neuronal mechanisms of feeding and nutrient decision making in *Drosophila*. *Front. Neurosci.* 7:12. doi: 10.3389/fnins.2013.00012
- Justus, C. R., Dong, L., and Yang, L. V. (2013). Acidic tumor microenvironment and pH-sensing G protein-coupled receptors. *Front. Physiol.* 4:354. doi: 10.3389/fphys.2013.00354
- Klahn, P., and Brönstrup, M. (2017). Bifunctional antimicrobial conjugates and hybrid antimicrobials. *Nat. Prod. Rep.* 34, 832–885. doi: 10.1039/C7NP00006E
- Koo, H., Allan, R. N., Howlin, R. P., Stoodley, P., and Hall-Stoodley, L. (2017). Targeting microbial biofilms: current and prospective therapeutic strategies. *Nat. Rev. Microbiol.* 15, 740–755. doi: 10.1038/nrmicro.2017.99
- Li, S. Y., Cheng, H., Xie, B. R., Qiu, W. X., Zeng, J. Y., Li, C. X., et al. (2017). Cancer cell membrane camouflaged cascade bioreactor for cancer targeted starvation and photodynamic therapy. *ACS Nano* 11, 7006–7018. doi: 10.1021/acs.nano.7b02533
- Li, T., Li, J., Pang, Q., Ma, L., Tong, W., and Gao, C. (2019). Construction of microreactors for cascade reaction and their potential applications as antibacterial agents. *ACS Appl. Mater. Interf.* 11, 6789–6795. doi: 10.1021/acsami.8b20069
- Ligtenberg, A. G. J., Hage, R., and Feringa, B. L. (2003). Catalytic oxidations by vanadium complexes. *Coordin. Chem. Rev.* 237, 89–101. doi: 10.1016/S0010-8545(02)00308-9
- Liu, X., Yan, Z., Zhang, Y., Liu, Z., Sun, Y., Ren, J., et al. (2019). Two-dimensional metal-organic framework/enzyme hybrid nanocatalyst as a benign and self-activated cascade reagent for *in vivo* wound healing. *ACS Nano* 13, 5222–5230. doi: 10.1021/acs.nano.8b09501
- Liu, X., Zhang, Z., Zhang, Y., Guan, Y., Liu, Z., Ren, J., et al. (2016). Artificial metalloenzyme-based enzyme replacement therapy for the treatment of hyperuricemia. *Adv. Funct. Mater.* 26, 7921–7928. doi: 10.1002/adfm.201602932
- Liu, Y., Busscher, H. J., Zhao, B., Li, Y., Zhang, Z., Van der Mei, H. C., et al. (2016). Surface-adaptive, antimicrobially loaded, micellar nanocarriers with enhanced penetration and killing efficiency in staphylococcal biofilms. *ACS Nano* 10, 4779–4789. doi: 10.1021/acs.nano.6b01370
- Liu, Y., Naha, P. C., Hwang, G., Kim, D., Huang, Y., Simon-Soro, A., et al. (2018). Topical ferumoxylol nanoparticles disrupt biofilms and prevent tooth decay *in vivo* via intrinsic catalytic activity. *Nat. Commun.* 9:2920. doi: 10.1038/s41467-018-05342-x
- Liu, Y., Shi, L., Su, L., Van der Mei, H. C., Jutte, P. C., Ren, Y., et al. (2019a). Nanotechnology-based antimicrobials and delivery systems for biofilm-infection control. *Chem. Soc. Rev.* 48, 428–446. doi: 10.1039/C7CS00807D
- Liu, Y., Shi, L., Van der Mei, H. C., Ren, Y., and Busscher, H. J. (2019b). “Perspectives on and need to develop new infection control methods”, in *Racing for the Surface: Pathogenesis of Implant Infection and Advanced Antimicrobial Strategies*, eds B. Li, T. F. Moriarty, T. Webster, and M. Xing (Cham: Springer).
- Liu, Y., Van der Mei, H. C., Zhao, B., Zhai, Y., Cheng, T., Li, Y., et al. (2017). Eradication of multidrug-resistant staphylococcal infections by light-activatable micellar nanocarriers in a murine model. *Adv. Funct. Mater.* 27:1701974. doi: 10.1002/adfm.201701974
- Mansoori, B., Mohammadi, A., Davudian, S., Shirjang, S., and Baradaran, B. (2017). The different mechanisms of cancer drug resistance: a brief review. *Adv. Pharm. Bull.* 7, 339–348. doi: 10.15171/apb.2017.041
- Mao, D., Hu, F., Kenry, J., S., Wu, W., Ding, D., et al. (2018). Metal-organic-framework-assisted *in vivo* bacterial metabolic labeling and precise antibacterial therapy. *Adv. Mater.* 30:1706831. doi: 10.1002/adma.201706831
- Naha, P. C., Liu, Y., Hwang, G., Huang, Y., Gubara, S., Jonnakuti, V., et al. (2019). Dextran-coated iron oxide nanoparticles as biomimetic catalysts for localized and pH-activated biofilm disruption. *ACS Nano* 13, 4960–4971. doi: 10.1021/acs.nano.8b08702
- Natalio, F., André, R., Hartog, A. F., Stoll, B., Jochum, K. P., Wever, R., et al. (2012). Vanadium pentoxide nanoparticles mimic vanadium haloperoxidases and thwart biofilm formation. *Nat. Nanotechnol.* 7, 530–535. doi: 10.1038/nnano.2012.91
- Neut, D., Tijdens-Creusen, E. J. A., Bulstra, S. K., Van der Mei, H. C., and Busscher, H. J. (2011). Biofilms in chronic diabetic foot ulcers—a study of 2 cases. *Acta Orthop.* 82, 383–385. doi: 10.3109/17453674.2011.581265
- Nguyen, T. K., Selvanayagam, R., Ho, K. K. K., Chen, R., Kutty, S. K., Rice, S. A., et al. (2016). Co-delivery of nitric oxide and antibiotic using polymeric nanoparticles. *Chem. Sci.* 7:1016. doi: 10.1039/C5SC02769A
- Niu, J., Azfer, A., Rogers, L. M., Wang, X., and Kolattukudy, P. E. (2007). Cardioprotective effects of cerium oxide nanoparticles in a transgenic murine model of cardiomyopathy. *Cardiovasc. Res.* 73, 549–559. doi: 10.1016/j.cardiores.2006.11.031
- O'Neill, J. (2014). *Antimicrobial Resistance: Tackling a Crisis for the Health and Wealth of Nations. Review on Antimicrobial Resistance*. Creative Commons Attribution 4.0 International Public Licence.
- Postiglione, I., Chiaviello, A., and Palumbo, G. (2011). Enhancing photodynamic therapy efficacy by combination therapy: dated, current and oncoming strategies. *Cancers* 3, 2597–2629. doi: 10.3390/cancers3022597
- Ricca, E., Brucher, B., and Schrittwieser, J. H. (2011). Multi-enzymatic cascade reactions: overview and perspectives. *Adv. Synth. Catal.* 353, 2239–2262. doi: 10.1002/adsc.201100256
- Rowe, L. A., Degtyareva, N., and Doetsch, P. W. (2008). DNA damage-induced reactive oxygen species (ROS) stress response in *Saccharomyces cerevisiae*. *Free Radical Biol. Med.* 45, 1167–1177. doi: 10.1016/j.freeradbiomed.2008.07.018
- Song, Y., Qu, K., Zhao, C., Ren, J., and Qu, X. (2010). Graphene oxide: intrinsic peroxidase catalytic activity and its application to glucose detection. *Adv. Mater.* 22, 2206–2210. doi: 10.1002/adma.200903783
- Stumvoll, M., Goldstein, B. J., and Van Haeften, T. W. (2005). Type 2 diabetes: principles of pathogenesis and therapy. *Lancet* 365, 1333–1346. doi: 10.1016/S0140-6736(05)61032-X
- Sun, H., Gao, N., Dong, K., Ren, J., and Qu, X. (2014). Graphene quantum dots-band-aids used for wound disinfection. *ACS Nano* 8, 6202–6210. doi: 10.1021/nm501640q
- Trédan, O., Galmarini, C. M., Patel, K., and Tannock, I. F. (2007). Drug resistance and the solid tumor microenvironment. *J. Natl. Cancer. Inst.* 99, 1441–1454. doi: 10.1093/jnci/djm135
- Vatansever, F., De Melo, W. C. M. A., Avci, P., Vecchio, D., Sadasivam, M., Gupta, A., et al. (2013). Antimicrobial strategies centered around reactive oxygen species- bactericidal antibiotics, photodynamic therapy, and beyond. *FEMS Microbiol. Rev.* 37, 955–989. doi: 10.1111/1574-6976.12026
- Walch, M., Dotiwala, F., Mulik, S., Thiery, J., Kirchhausen, T., Clayberger, C., et al. (2015). Cytotoxic cells kill intracellular bacteria through granulysin-mediated delivery of granzymes. *Cell* 161, 1229–1229. doi: 10.1016/j.cell.2015.05.021
- Wang, G. L., Xu, X. F., Qiu, L., Dong, Y. M., Li, Z. J., and Zhang, C. (2014). Dual responsive enzyme mimicking activity of AgX (X=Cl, Br, I) nanoparticles and its application for cancer cell detection. *ACS Appl. Mater. Interf.* 6, 6434–6442. doi: 10.1021/am501830v

- Wang, N., Zhu, L., Wang, D., Wang, M., Lin, Z., and Tang, H. (2010). Sono-assisted preparation of highly-efficient peroxidase-like Fe₃O₄ magnetic nanoparticles for catalytic removal of organic pollutants with H₂O₂. *Ultrasonic Sonochem.* 17, 526–533. doi: 10.1016/j.ultsonch.2009.11.001
- Wang, T. Y., Libardo, M. D. J., Angeles-Boza, A. M., and Pellois, J. P. (2017). Membrane oxidation in cell delivery and cell killing applications. *ACS Chem. Biol.* 12, 1170–1182. doi: 10.1021/acscchembio.7b00237
- Witt, S., Wohlfahrt, G., Schomburg, D., Hecht, H. J., and Kalisz, H. M. (2000). Conserved arginine-516 of *Penicillium amagasakiense* glucose oxidase is essential for the efficient binding of beta-D-glucose. *Biochem. J.* 347, 553–559. doi: 10.1042/bj3470553
- Wu, R., Chong, Y., Fang, G., Jiang, X., Pan, Y., Chen, C., et al. (2018). Synthesis of Pt hollow nanodendrites with enhanced peroxidase-like activity against bacterial infections: implication for wound healing. *Adv. Funct. Mater.* 28:1801484. doi: 10.1002/adfm.201801484
- Yan, Z., Bing, W., Ding, C., Dong, K., Ren, J., and Qu, X. (2018). A H₂O₂-free depot for treating bacterial infection: localized cascade reactions to eradicate biofilms *in vivo*. *Nanoscale* 10, 17656–17662. doi: 10.1039/C8NR03963A
- Yin, W., Yu, J., Lv, F., Yan, L., Zheng, L. R., Gu, Z., et al. (2016). Functionalized nano-MoS₂ with peroxidase catalytic and near-infrared photothermal activities for safe and synergetic wound antibacterial applications. *ACS Nano* 10, 11000–11011. doi: 10.1021/acsnano.6b05810
- Zhang, P., Sun, D., Cho, A., Weon, S., Lee, S., Lee, J., et al. (2019). Modified carbon nitride nanozyme as bifunctional glucose oxidase-peroxidase for metal-free bioinspired cascade photocatalysis. *Nat. Commun.* 10:940. doi: 10.1038/s41467-019-08731-y

Conflict of Interest: HB is also director of a consulting company, SASA BV.

The remaining authors declare no conflicts of interest with respect to authorship and/or publication of this article. Opinions and assertions contained herein are those of the authors and are not construed as necessarily representing views of their respective employers.

Copyright © 2020 Li, Yang, Ren, Shi, Ma, van der Mei and Busscher. This is an open-access article distributed under the terms of the Creative Commons Attribution License (CC BY). The use, distribution or reproduction in other forums is permitted, provided the original author(s) and the copyright owner(s) are credited and that the original publication in this journal is cited, in accordance with accepted academic practice. No use, distribution or reproduction is permitted which does not comply with these terms.



Lipid-Based Antimicrobial Delivery-Systems for the Treatment of Bacterial Infections

Da-Yuan Wang^{1,2}, Henny C. van der Mei^{2*}, Yijin Ren³, Henk J. Busscher^{2*} and Linqi Shi^{1*}

¹ State Key Laboratory of Medicinal Chemical Biology, Key Laboratory of Functional Polymer Materials, Ministry of Education, Institute of Polymer Chemistry, College of Chemistry, Nankai University, Tianjin, China, ² Department of Biomedical Engineering, University of Groningen and University Medical Center Groningen, Groningen, Netherlands, ³ Department of Orthodontics, University of Groningen and University Medical Center Groningen, Groningen, Netherlands

OPEN ACCESS

Edited by:

Manuel Simões,
University of Porto, Portugal

Reviewed by:

Yohann Corvis,
Université de Paris, France
Edson Roberto Silva,
University of São Paulo, Brazil

*Correspondence:

Henny C. van der Mei
h.c.van.der.mei@umcg.nl
Henk J. Busscher
h.j.busscher@umcg.nl
Linqi Shi
shilingqi@nankai.edu.cn

Specialty section:

This article was submitted to
Medicinal and Pharmaceutical
Chemistry,
a section of the journal
Frontiers in Chemistry

Received: 10 October 2019

Accepted: 03 December 2019

Published: 10 January 2020

Citation:

Wang D-Y, van der Mei HC, Ren Y,
Busscher HJ and Shi L (2020)
Lipid-Based Antimicrobial
Delivery-Systems for the Treatment of
Bacterial Infections.
Front. Chem. 7:872.
doi: 10.3389/fchem.2019.00872

Many nanotechnology-based antimicrobials and antimicrobial-delivery-systems have been developed over the past decades with the aim to provide alternatives to antibiotic treatment of infectious-biofilms across the human body. Antimicrobials can be loaded into nanocarriers to protect them against de-activation, and to reduce their toxicity and potential, harmful side-effects. Moreover, antimicrobial nanocarriers such as micelles, can be equipped with stealth and pH-responsive features that allow self-targeting and accumulation in infectious-biofilms at high concentrations. Micellar and liposomal nanocarriers differ in hydrophilicity of their outer-surface and inner-core. Micelles are self-assembled, spherical core-shell structures composed of single layers of surfactants, with hydrophilic head-groups and hydrophobic tail-groups pointing to the micellar core. Liposomes are composed of lipids, self-assembled into bilayers. The hydrophilic head of the lipids determines the surface properties of liposomes, while the hydrophobic tail, internal to the bilayer, determines the fluidity of liposomal-membranes. Therefore, whereas micelles can only be loaded with hydrophobic antimicrobials, hydrophilic antimicrobials can be encapsulated in the hydrophilic, aqueous core of liposomes and hydrophobic or amphiphilic antimicrobials can be inserted in the phospholipid bilayer. Nanotechnology-derived liposomes can be prepared with diameters <100–200 nm, required to prevent reticulo-endothelial rejection and allow penetration into infectious-biofilms. However, surface-functionalization of liposomes is considerably more difficult than of micelles, which explains while self-targeting, pH-responsive liposomes that find their way through the blood circulation toward infectious-biofilms are still challenging to prepare. Equally, development of liposomes that penetrate over the entire thickness of biofilms to provide deep killing of biofilm inhabitants still provides a challenge. The liposomal phospholipid bilayer easily fuses with bacterial cell membranes to release high antimicrobial-doses directly inside bacteria. Arguably, protection against de-activation of antibiotics in liposomal nanocarriers and their fusogenicity constitute the biggest advantage of liposomal antimicrobial carriers over antimicrobials free in solution. Many Gram-negative and Gram-positive bacterial strains, resistant to specific antibiotics,

have been demonstrated to be susceptible to these antibiotics when encapsulated in liposomal nanocarriers. Recently, also progress has been made concerning large-scale production and long-term storage of liposomes. Therewith, the remaining challenges to develop self-targeting liposomes that penetrate, accumulate and kill deeply in infectious-biofilms remain worthwhile to pursue.

Keywords: bacterial biofilm, micelles, zeta potentials, hydrophobicity, lipids, liposomes, infection, fusogenicity

INTRODUCTION

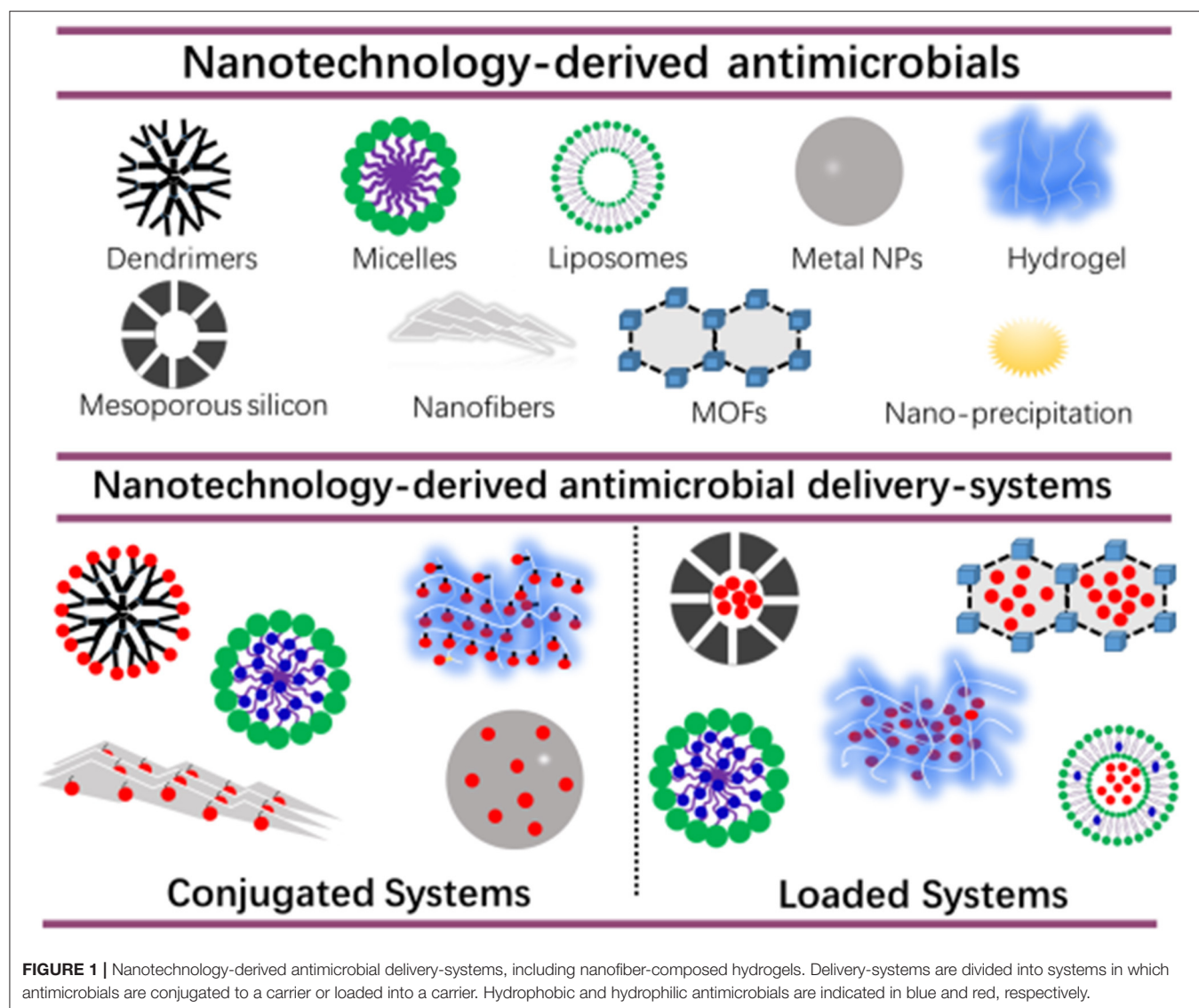
The threat posed to mankind of hard to treat, antibiotic-resistant infectious biofilms is better realized world-wide than ever. With cancer being considered more and more as a chronic disease, infection by antibiotic-resistant bacteria is expected to become the number one cause of death by the year 2050 (Humphreys and Fleck, 2016). This frightening scenario has many reasons. First of all, infectious biofilms are tenacious by nature and antimicrobials have difficulty penetrating the biofilm matrix embedding its bacterial inhabitants (Gupta et al., 2018). The biofilm matrix is composed of Extracellular Polymeric Substances (EPS) (Bjarnsholt et al., 2013) containing proteins, polysaccharides, humic acids, and eDNA (Flemming et al., 2016). The EPS-matrix acts as a glue holding biofilm-bacteria together and protecting them against the host immune system and environmental challenges, amongst which antimicrobials (Liu et al., 2019a). Secondly, rampant overuse of antibiotics has yielded, and still is yielding new antibiotic-resistant strains that cannot be killed by known antibiotics (Neville and Jia, 2019). Thirdly, development of new antibiotics is stalling (N'Guessan et al., 2018; Jangra et al., 2019), because their effective life-time before the first resistant strains arise, is becoming shorter and shorter, decreasing the incentive for commercialization and therewith clinical use of new antibiotics (Liu et al., 2019b).

A first challenge in the development of new infection-control strategies, is to develop an antimicrobial or antimicrobial delivery-system that allows the antimicrobial to penetrate deeply into a biofilm and kill biofilm-bacteria across the entire thickness of the biofilm (Drbohlavova et al., 2013; Liu et al., 2019a). Many nanotechnology-based drugs and drug-delivery-systems have been developed over the past decades with the aim of self-targeting, penetrating and eradicating tumors (Kong

et al., 2019; Majumder et al., 2019; Paunovska et al., 2019). Biofilms and tumors are on the one hand very different, yet are both characterized by a low pH environment, allowing self-targeting of pH adaptive, smart carriers (Liu et al., 2016). Also, their clinical treatment poses the same challenges, including prevention of resistance and recurrence. Not surprisingly, new strategies for infection-control are arising nowadays, that are derived from technologies initially designed for tumor treatment. **Figure 1** gives an overview of nanotechnology-derived antimicrobial delivery-systems currently considered for infection-control, many of which are derived from new tumor treatment strategies.

Nanotechnology-derived antimicrobial delivery systems have excellent biocompatibility, and can be designed to be environmentally-responsive and self-targeting (Lopes and Brandelli, 2018; Wolfmeier et al., 2018; Zhao et al., 2018), provided their diameter is below the limit for reticulo-endothelial rejection of around 100–200 nm (Wang et al., 2019). However, without suitable functionalization of their outermost surface or drug-loading (**Figure 1**), their antimicrobial efficacy is usually low. In conjugated systems, antibiotics, peptides or other antimicrobials are bound to dendrimers (Kumar et al., 2015; Xue et al., 2015), and hydrogels (Zendehdel et al., 2015) which should be done carefully in order not to sacrifice bio-active groups. To a certain extent, this restricts the application of antimicrobial-conjugated systems. Alternatively, antimicrobials can be loaded into nanotechnology-derived antimicrobial delivery-systems, to protect antimicrobials underway through the blood circulation from de-activation, reduce their toxicity and prevent potential, harmful side-effects of the antimicrobials. Moreover, antimicrobial nanocarriers can be equipped with stealth and pH-responsive features that allow self-targeting and accumulation in infectious biofilms at high concentrations. Micelles can be made for instance, consisting of a hydrophilic poly(ethylene glycol) (PEG)-shell and pH-responsive poly(β -amino ester) (PAE). This renders stealth properties to the micelles at physiological pH due to the exposure of the PEG-shell allowing their presence in the blood circulation without negative side-effects and penetration in a tumor or infectious biofilm. However, once in a more acidic, pathological site, such as in a tumor (Ray et al., 2019) or biofilm (Liu et al., 2016; Wu et al., 2019) (becoming even more acidic toward its bottom; Peeridogaheh et al., 2019), pH-responsive PAE groups become positively-charged causing self-targeting and accumulation (Liu et al., 2012, 2016). Micelles are more suitable for functionalizing of their surface without affecting their hydrophilicity ratio than liposomes,

Abbreviations: CF, carboxyfluoresceine; Chol, cholesterol; DGDG, digalactosyldiacylglycerol; DMPC, dimyristoyl phosphatidylcholine; DMPG, dimyristoyl phosphatidylglycerol; DOPA, 3,4-dihydroxyphenylalanine; DOPC, 1, 2-dioleoyl-sn-glycero-3-phosphocholine; DOPE, 1,2-dioleoyl-3-trimethylammonium-propane; DOPS, 1,2-dioleoyl-sn-glycero-3-phospho-L-serine; DOTAP, 1,2-dioleoyl-3-trimethylammonium-propane; DPPC, dipalmitoyl phosphatidylcholine; DPPG, dipalmitoylphosphatidylglycerol; DSPC, 1,2-distearoyl-sn-glycero-3-phosphocholine; DSPE, distearoyl phosphoethanolamine; EPC, egg phosphatidylcholine; EPS, extracellular polymeric substances; FDA, food and drug administration; HAD, hexadecylamine; IEP, iso-electric point; LP, lipid-PEG; MOFs, metal organic framework; MIC, minimal inhibitory concentration; MRSA, methicillin-resistant *Staphylococcus aureus*; NPs, nanoparticles; PAE, poly(β -amino ester); PEG, polyethylene glycol; PSD, poly(methacryloyl sulfadimethoxine).



because of the relatively low molecular weight of the lipids involved in liposomes (1,200–1,800 g/mol) compared with the surfactants used in micelles (>8,000 g/mol). Inadvertent leakage remains a concern in antimicrobial-loaded systems (Kim et al., 2019).

The two most common nanocarriers considered for drug loading are micelles and lipid-based liposomes. The structure and composition of liposomes, also known as vesicles, bear similarity to the one of cell membranes. The main difference between micelles and liposomes is the hydrophilicity of their outer surface and inner core (Table 1). Micelles are self-assembled, spherical core-shell structures composed of a single layer of surfactants, with a hydrophilic head-group and a hydrophobic tail-group pointing to the micellar core. Liposomes are composed of lipids and due to their amphiphilic nature can assemble into bilayers, similar to the structure and composition of cell membranes. The hydrophilic head

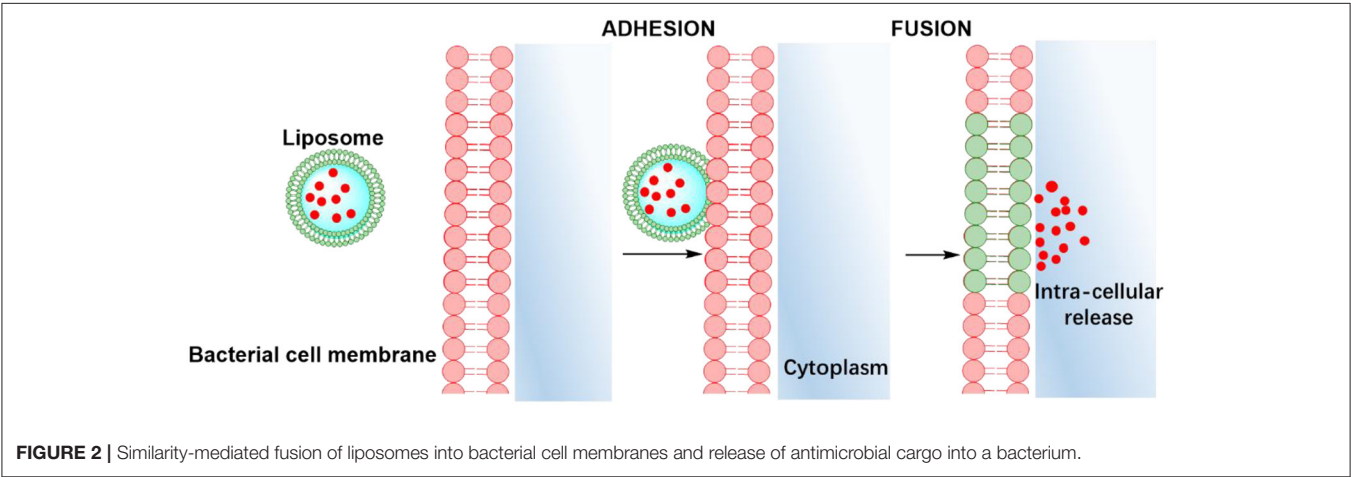
of the lipids determines the surface properties of liposomes, while the hydrophobic tail, internal to the bilayer, determines the fluidity of liposomal membranes. Therefore, whereas micelles can only be loaded with hydrophobic antimicrobials of which there are few candidates, hydrophilic antimicrobials can be encapsulated in the hydrophilic, aqueous core of liposomes and hydrophobic or amphiphilic antimicrobials can be inserted in the phospholipid bilayer. As a consequence, the number of candidate antimicrobials for liposome-loading, is relatively large, while the loading capacity of liposomes is relatively high (Ehsan and Clancy, 2015; Liu et al., 2019a; see also Table 1).

Apart from offering a wider choice of candidate antimicrobials for loading and higher loading, another advantage of lipid-based antimicrobial delivery-system is their fusogenicity, i.e., the ability of liposomes to fuse with the outer membrane of bacteria (see also Table 1), due to the fluidity of their

TABLE 1 | Main differences between liposomal and micellar drug carriers, candidate antimicrobials for loading into liposomes or micelles and the relative advantages of both types of nanocarriers.

Liposomes	Micelles
Candidate antimicrobials for loading Amikacin (Mugabe et al., 2006), Gentamicin (Mugabe et al., 2005, 2006), Tobramycin (Sachetelli et al., 2000; Marier et al., 2002; Mugabe et al., 2006; Messiaen et al., 2013), Triclosan (Sanderson et al., 1996), Vancomycin (Nicolosi et al., 2010; Chakraborty et al., 2012), Azithromycin (Solleti et al., 2015), Metronidazole (Vyas et al., 2001), Oxacillin (Meers et al., 2008), Daptomycin (Hu et al., 2019), Antimicrobial peptides (Dashper et al., 2005)	Candidate antimicrobials for loading Triclosan (Liu et al., 2016), Curcumin (Huang et al., 2017), Silver NPs (Lin et al., 2019), Rifampicin and isoniazid (Praphakar et al., 2019), Bedaquiline (Soria-Carrera et al., 2019)
Liposome advantages <ul style="list-style-type: none">- Hydrophilic and hydrophobic antimicrobial loading- High loading capacity- Intra-cellular release of cargo through fusion with bacterial cell membranes- Fusogenicity at the expense of cargo leakage- FDA approved dosage forms for clinical use	Micelle advantages <ul style="list-style-type: none">- Relatively little leakage of hydrophobic cargo- Relatively easy functionalization

Hydrophobic and hydrophilic antimicrobials are indicated in blue and red, respectively.



phospholipid bilayer structure. The liposomal phospholipid bilayer resembles the structure of bacterial cell membranes, which facilitates fusion based on similarity (Figure 2). Upon fusion, high antimicrobial-doses are directly available inside a bacterium (Akbarzadeh et al., 2013).

In this review, we summarize the different types of lipid-based antimicrobial delivery-systems according to their lipid bilayer composition, membrane fluidity, outer surface properties and ability to trigger the release of the

encapsulated antimicrobials upon fusion. Applications and perspectives of liposomal, antimicrobial delivery-systems for the treatment of bacterial infections will be discussed.

PREPARATION OF LIPOSOMES

Liposome preparation method is an important factor affecting the structure and size of liposomes. Although liposome

preparation methods have been well-established, a short but comprehensive summary of the most used methods will be given to allow better understanding by a multi-disciplinary readership (Figure 3; Pick et al., 2018). *In situ* lipid synthesis and formation of liposomes by self-assembly into bilayered lipid structures yields liposomes of widely varying size. Liposomes can also be prepared by rehydration of dried lipid films, which spontaneously yields liposomes, with an enhanced yield when performed on conducting electrodes in the presence of an applied electric field. Liposomes size can be well-controlled by filtering, while sonication can be applied to decrease liposome size. Proteolipids can be applied in identical ways to create liposomes. Finally, large liposomes can be used to contain lipids and proteins to form proteoliposomes *in situ*, i.e., inside the larger liposomes.

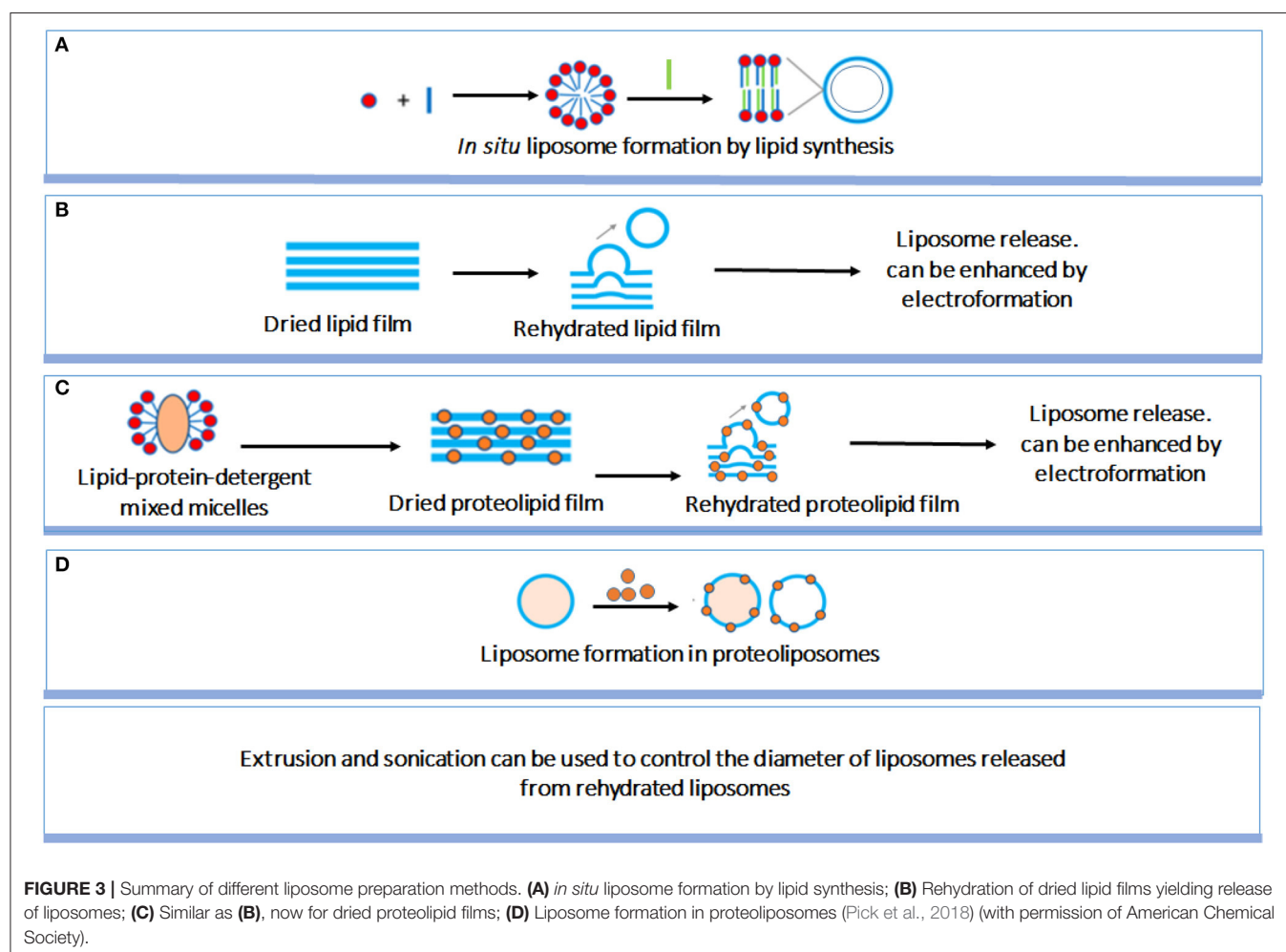
SUMMARY OF DIFFERENT TYPES OF LIPOSOMES

Liposomes can be classified according to different criteria. Based on diameter, small (<50 nm), large (50–500 nm) and giant (>500 nm) liposomes can be distinguished (Banerjee, 2001; Morton et al., 2012). Alternatively, a classification can be made on the basis of whether a liposome possesses

uni-, oligo-, or multi-lamellar bilayers (Morton et al., 2012; Manaia et al., 2017). Liposomes can consist of naturally-occurring lipids or synthetically-made lipids (sometimes called “artificial” liposomes). Accordingly, liposomes can have widely different properties and for the purpose of infection-control (i.e., interaction with negatively-charged bacterial cell surfaces; Nederberg et al., 2011; Ng et al., 2013), it is relevant to classify them into natural lipid-based, cationic, anionic, zwitterionic liposomes, and fusogenic liposomes. Diameter and diameter distribution are the most important factors for *in vivo* use of liposomes (Malekar et al., 2015) and in order to prevent rejection by the reticulo-endothelial system (Wang et al., 2019) and allow penetration through water channels (Greiner et al., 2005) in infectious biofilms, liposomes for infection-control should preferentially have diameters that maximally range up to 100–200 nm (Liu et al., 2019a). Therefore, we will now confine this review to smaller liposomes with diameters of maximally 200 nm and briefly summarize the physico-chemistry underlying these liposomes.

Natural Lipid-Based Liposomes

Natural liposomes are composed of naturally-occurring phospholipids, such as phosphatidylcholine, phosphatidylserine,



soybean lecithin, or egg yolk lecithin, sometimes complemented with other lipids. Natural lipids contain a polar, hydrophilic head, and several hydrophobic lipid chains. Since the hydrophilic head of natural phospholipids is electrically neutral (Smith et al., 2017), the surface potential of lipids is electrically neutral, corresponding in general with zeta potentials between -10 and $+10$ mV (Smith et al., 2017; **Figure 4**). Liposomes in suspension require zeta potentials more negative than -30 mV or more positive than $+30$ mV in order to experience sufficient electrostatic double-layer repulsion to create stable suspensions. Given the importance of zeta potentials for the stability of liposome suspensions and interaction with their environment, including proteins or bacteria, liposomes have been equipped with several cationic and anionic functionalities to adjust their surface charge (see also **Figure 5**; Kamaly et al., 2012). In addition to their stability in suspension, also the stability of the

lipid bilayer in a liposome sometimes needs enforcement, such as when highly charged lipids are used (Kaszuba et al., 2010) or due to oxidation of the membrane lipids. Oxidation induced instability of liposomes can be prevented by adding reductants to the membrane lipids (Khan et al., 1990).

Cationic Liposomes

Cationic liposomes can be made using natural or synthetic lipids with cationic functionalities, such as ammonium (Jacobs et al., 1916; Gottenbos et al., 2001; Lu et al., 2007), sulfonium (Ghattas and Leroux, 2009), or phosphonium ions (Popa et al., 2003; Chang et al., 2010; **Figure 5**). As an example, **Figure 6** presents the zeta potentials of cholesterol DSPC liposomes made positively-charged through DOPA, containing positively-charged ammonium groups. Within the range of DOPA concentrations applied, zeta potentials remained below the critical limit of

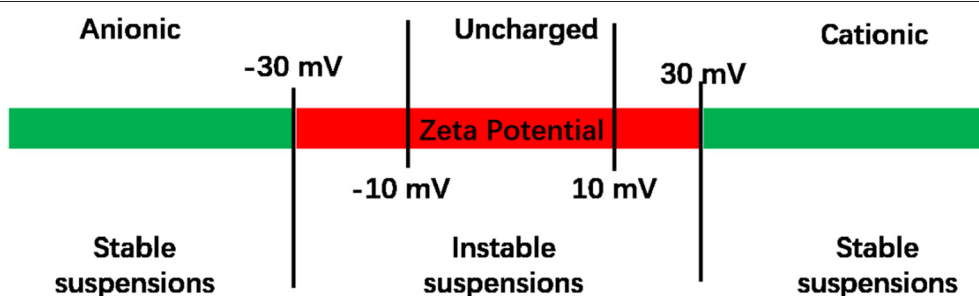


FIGURE 4 | Zeta potentials of liposomes. Liposome suspensions are considered to be unstable when their zeta potential is between -30 and $+30$ mV (Manaia et al., 2017). Zeta potentials between -10 and $+10$ mV are considered to represent uncharged liposomes.

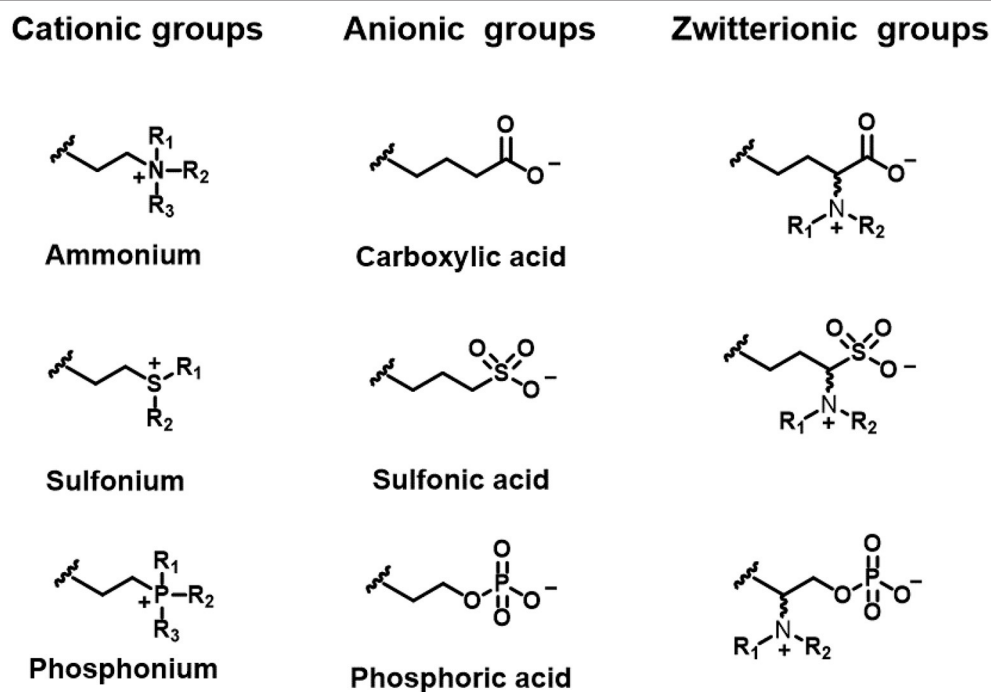


FIGURE 5 | Functional groups of lipids to create differently charged liposomes.

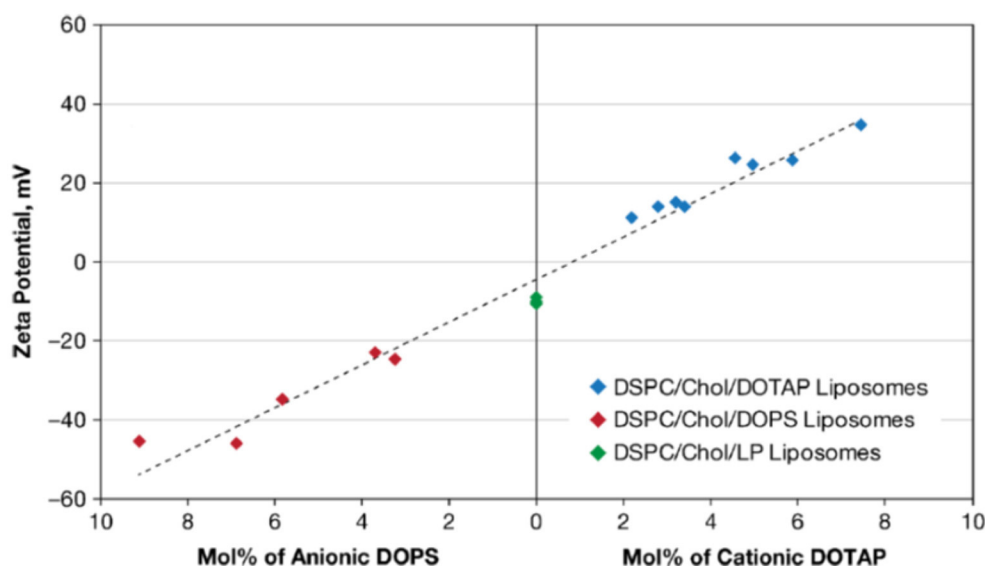


FIGURE 6 | Zeta potentials in 0.01 mol/L NaCl (pH 7.4–7.7) of cholesterol (Chol), 1,2-distearoyl-sn-glycero-3-phosphocholine (DSPC) liposomes. Liposomes were made positively-charged with varying mol% of DOTAP (1,2-dioleoyl-3-trimethylammonium-propane) or negatively-charged with DOPS (1,2-dioleoyl-sn-glycero-3-phospho-L-serine). Liposomes indicated as DSPC/Chol/LP liposomes were prepared with lipid-PEG (poly-ethylene glycol) added (Smith et al., 2017) (with permission of Springer).

+30 mV required for stable suspensions and accordingly these liposome suspensions were mentioned to aggregate within 24 h of processing. Interestingly, addition of 1.6 mol% lipid-PEG yielded a zeta potential of nearly zero. Yet, lipid-PEG containing liposome suspensions were described to be stable and stealth (Kataria et al., 2011), presumably due to steric stabilization and repulsion. Cationic liposomes have been suggested as a drug-releasing coating of natural surfaces, such as skin-associated bacteria (Sanderson and Jones, 1996) or teeth (Nguyen et al., 2013), both bearing a negative charge.

Instability of the liposomal bilayer structure in drug-loaded liposomes can result in inadvertent drug leakage (Drulis-Kawa and Dorotkiewicz-Jach, 2010). The stability of the lipid bilayer of cationic liposomes can be increased by coating with bacterial S-layer proteins. Zeta potentials of cationic liposomes composed of dipalmitoylphosphatidylcholine (DPPC), cholesterol and hexadecylamine [HDA: (+29.1 mV)] became negatively-charged (−27.1 mV) upon coating with S-layer proteins, which increased their stability against mechanical challenges (Figure 7; Mader et al., 1999).

Anionic Liposomes

Anionic liposomes bear negatively-charged functional groups (Figure 5), such as carboxylic (Cheow et al., 2011), phosphoric or sulfonic acid (Derbali et al., 2019; Zhang and Lemay, 2019). Cholesterol-DSPC liposomes could be made positively-charged using DOTAP, but using DOPS, negative charge could be conveyed to these liposomes in a concentration dependent fashion (Figure 6; Smith et al., 2017). As a main advantage of anionic liposomes, opposite to cationic liposomes, anionic

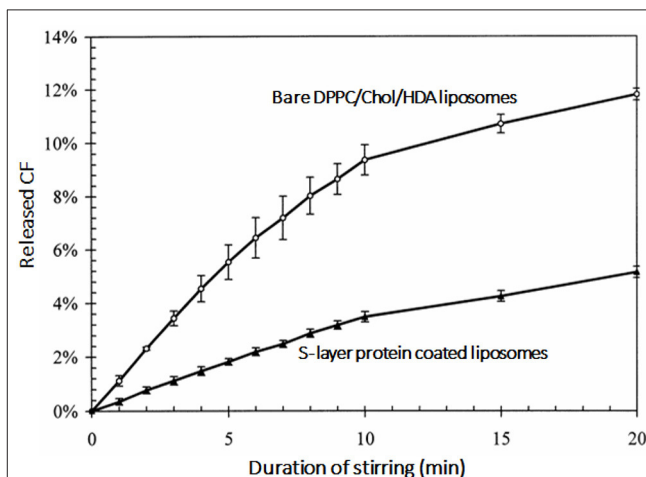


FIGURE 7 | Release of fluorescent carboxyfluorescein (CF) as an indication of the lipid bilayer stability of dipalmitoylphosphatidylcholine (DPPC), cholesterol and hexadecylamine (HDA) liposomes as a function of stirring time in the absence and presence of a bacterial S-layer coating on the liposomes (Mader et al., 1999) (with permission of Elsevier).

liposomes can more effectively encapsulate positively charged antimicrobials (Messiaen et al., 2013) and prolong their release time (Kaszuba et al., 1995; Robinson et al., 1998, 2000; Tang et al., 2009). Anionic liposomes composed of DPPG and DOPC could be loaded with eight-fold higher amounts of antibiotic than uncharged, natural-lipid based liposomes (Table 2; Messiaen et al., 2013).

Zwitterionic Liposomes

Whereas, cationic and anionic liposomes usually demonstrate pH-dependent zeta potentials, they do not show complete charge

TABLE 2 | Increased loading of an antibiotic in anionic liposomes.

Liposome type	Zeta potential (mV)	Tobramycin concentration (a.u.)
DPPC/Chol	−0.5	100
DOPC/DPPG	−22.3	800

Tobramycin-loading in anionic liposomes is eight times higher than in natural neutral liposomes due to the electrostatic interaction between negatively charged lipids and tobramycin. Data taken from Messiaen et al. (2013).

reversal from being positively to negatively charged. Zwitterionic lipids have both acidic and alkaline functional groups (**Figure 5**; Hu et al., 2019; Makhathini et al., 2019) that allow full charge reversal below and above their iso-electric point (**Figure 8A**; Vila-Caballer et al., 2016; Liu et al., 2018). This feature allows the fabrication of liposomes that are negatively-charged under physiological pH conditions and become positively-charged under more acidic conditions, such as poly(methacryloyl sulfadimethoxine) (PSD) liposomes (**Figure 8B**; Couffin-Hoarau and Leroux, 2004; Ghattas and Leroux, 2009; Lu et al., 2018). Negative charge at physiological pH values aids transport of liposomes through the blood circulation without major interaction with other negatively-charged blood components (Hamal et al., 2019), while adaptation of a positive charge

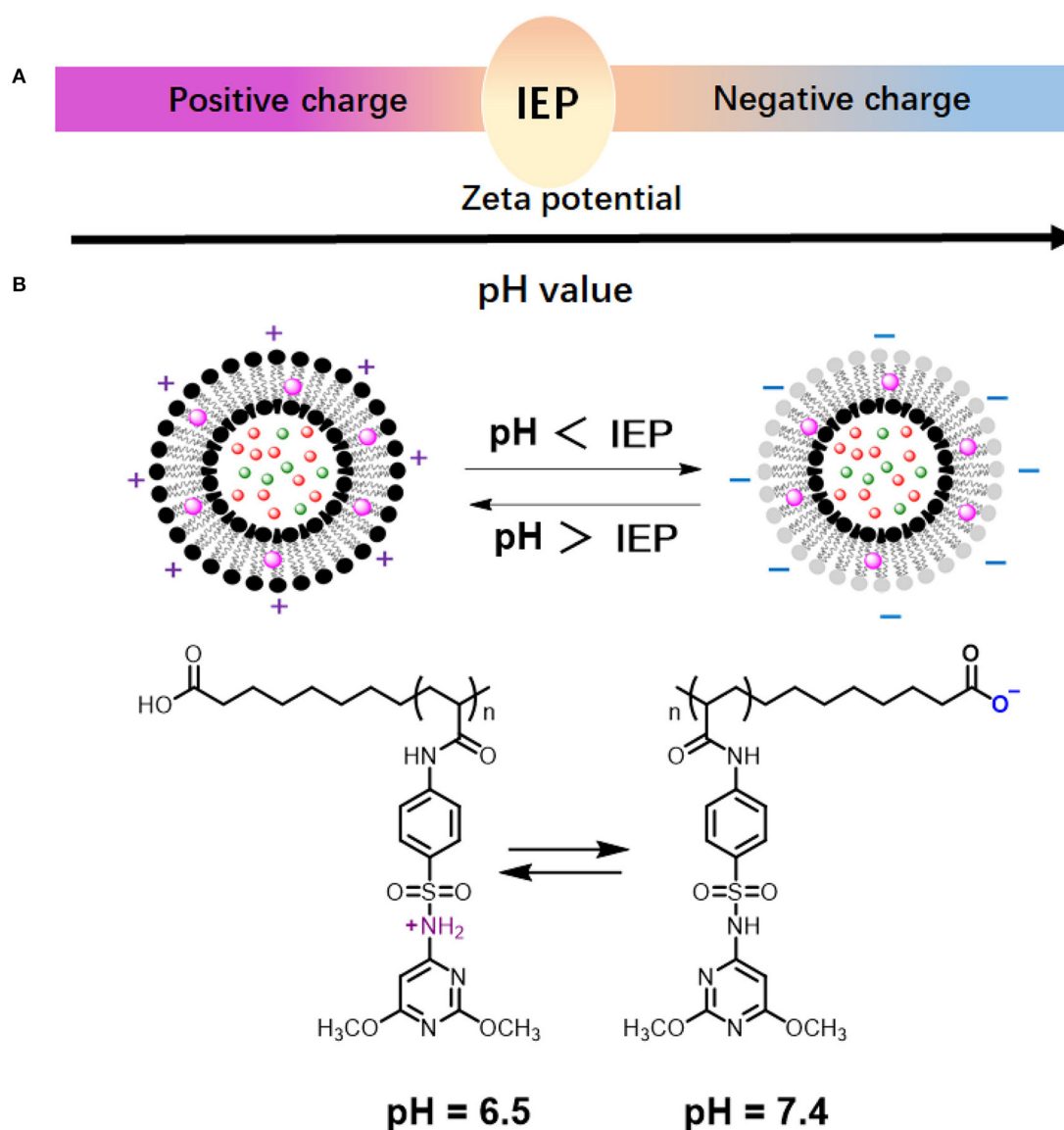


FIGURE 8 | pH-dependent behavior of zwitterionic lipids and liposomes. **(A)** Zwitterionic liposomes reverse their charge from cationic to anionic when suspension pH increases from below to above the Iso-Electric Point (IEP) of the constituting lipids or vice versa. **(B)** Charge reversal of poly(methacryloyl sulfadimethoxine) (PSD) liposomes (Chen et al., 2018) (with permission of Elsevier).

inside the acidic environment of a biofilm facilitates better interaction with negatively-charged bacteria (Robinson et al., 2001; Nederberg et al., 2011; Ng et al., 2013) in the biofilm.

Fusogenic Liposomes

The fusogenicity of liposomes with cellular membranes is a most distinguishing feature of liposomes and is related with the fluidity of the lipid bilayer. Generally, lower melting temperatures of the lipids imply higher fluidity of the liposome membrane and therewith a greater fusogenicity (Zora and Željka, 2016). **Figure 9** summarizes the relation between melting temperatures and structure/composition of lipids. Both location of unsaturated bonds (**Figure 9A**; Nagahama et al., 2007) and alkyl chain length (**Figure 9B**) influence lipid melting temperatures (Feitosa et al., 2006) and therewith the fusogenicity of liposomes. Cholesterol hemisuccinate for instance, combined with dioleoylphosphatidylethanolamine (DOPE) and dipalmitoylphosphatidylcholine (DPPC) in a 4:2:4

molar ratio yielded highly fusogenic liposomes (**Figure 9C**). Increasing fusogenicity however, may go at the expense of the stability of the lipid bilayer constituting the membrane and liposomes with increased fusogenicity are more prone to bilayer membrane instability, rupture, and inadvertent cargo release (Marier et al., 2002; Li et al., 2013; **Figure 9D**).

APPLICATION OF ANTIMICROBIAL-LOADED LIPOSOMES TOWARD INFECTIOUS BIOFILMS

The problems to be overcome for the successful treatment of infectious biofilms in the human body are many-fold and some of them have persisted for centuries. Rather than aiming for a comprehensive overview of all studies attempting to apply liposomal antimicrobial-loaded nanocarriers for infection-control, we first present a brief overview of

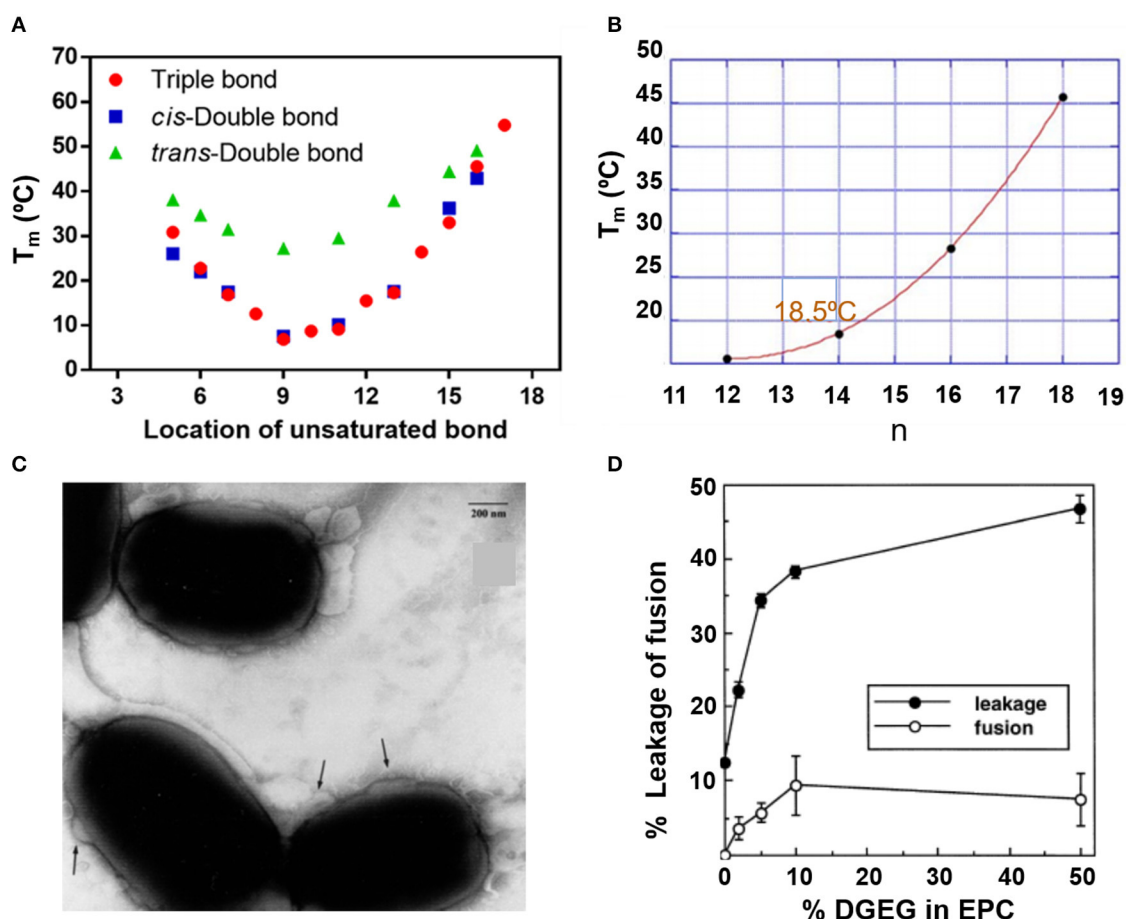


FIGURE 9 | Fluidity of liposomes in relation with their lipid structure. Melting temperature T_m of lipids as an indication of fluidity. **(A)** Melting temperature as a function of unsaturated bond location in (f sn-1 saturated/sn-2 monosaturated phosphatidylcholine) (Nagahama et al., 2007). **(B)** Melting temperature of 5.0 mM dialkyldimethylammonium bromide in water as a function of the number (n) of carbon atoms in the alkyl chains (Feitosa et al., 2006) (with permission of Elsevier). **(C)** Transmission electron micrographs of the fusion (indicated by the arrows) of fusogenic, DOPE-DPPC-cholesterol hemisuccinate liposomes with *E. coli*. Bar marker equals 200 nm (Nicolosi et al., 2010) (with permission of Elsevier). **(D)** The % fused liposomes and % release of fluorescent carboxyfluorescein as a function of the % digalactosyldiacylglycerol (DGDG) in egg phosphatidylcholine (EPC) liposomes (Hincha et al., 1998) (with permission of Elsevier).

the problems encountered in the treatment of infectious biofilms using antimicrobials. Next, it will be addressed which problems can probably be successfully addressed using liposomal antimicrobial-loaded nanocarriers, and the steps that need to be taken for successful downward clinical translation.

Traditional Problems in Antimicrobial Treatment of Infectious Biofilms

Eradication of infectious biofilms is a highly complicated process for which there is no adequate treatment available ever since Van Leeuwenhoek noticed that the vinegar which he used to clean his teeth from oral biofilm killed only bacteria residing at the outside of the biofilm, but left the ones in the depth of a biofilm alive (Van Leeuwenhoek, 1684). One of the current struggles indeed, still is the penetration, accumulation and killing of antimicrobials over the entire thickness of an infectious biofilm, as noticed by Van Leeuwenhoek over three centuries ago (Figure 10). This includes prevention of wash-out of an antimicrobial in the dynamic environment of the human body. In addition, antimicrobials may be enzymatically de-activated underway to a biofilm in the blood circulation or once inside a biofilm (Albayaty et al., 2018). Taken together, these factors make bacterial killing into the depth of a biofilm impossible (Sutherland, 2001), contributing to recurrence of infection after treatment (Wolfmeier et al., 2018).

Penetration and accumulation can only occur once the antimicrobial has “found its way,” often from within the blood circulation, to the infectious biofilm. Since it may be undesirable to have high concentrations of an antimicrobial circulating through the body due to potential collateral tissue damage, self-targeting carriers are under design that can find their way at low blood concentrations to accumulate in sufficiently high amounts in an infectious biofilm (Forier et al., 2014).

Once accumulated inside a biofilm, the antimicrobial should perform its antimicrobial action, which can either be based on generating cell wall damage, or entry into a bacterium to interfere with vital metabolic processes. Both can be difficult, especially since bacteria have developed a large array of protective mechanisms, that we summarize under the common denominator of antimicrobial resistance (Kumar et al., 2016). Adding to this, is the problem of bacteria seeking shelter against antimicrobials in mammalian cells (Mantovani et al., 2011), in which many antimicrobials cannot enter. Bacteria have even been found sheltering in macrophages intended by nature to kill them, de-activating macrophageal killing mechanisms (Knodler et al., 2001).

There are no antimicrobials or antimicrobial carriers that solve all the issues summarized above (see also Figure 10). Liposomal nanocarriers constitute no exception to this. Yet, liposomes possess a number of unique qualities, like stealth properties, protection of encapsulated antimicrobials against de-activation and entry in tissue cells and bacteria, as will be summarized below.

Solutions to Traditional Problems in Antimicrobial Treatment of Infectious Biofilms Offered by Liposomal Antimicrobial Nanocarriers

Blood circulation times of liposomes have become much longer since the inclusion of lipid-PEG in the bilayer membrane. Liposomes without lipid-PEG were rapidly removed from the circulation by macrophageal uptake (Hofmann et al., 2010) but stealth (Romberg et al., 2008) liposomes containing lipid-PEG demonstrated reduced reticulo-endothelial uptake.

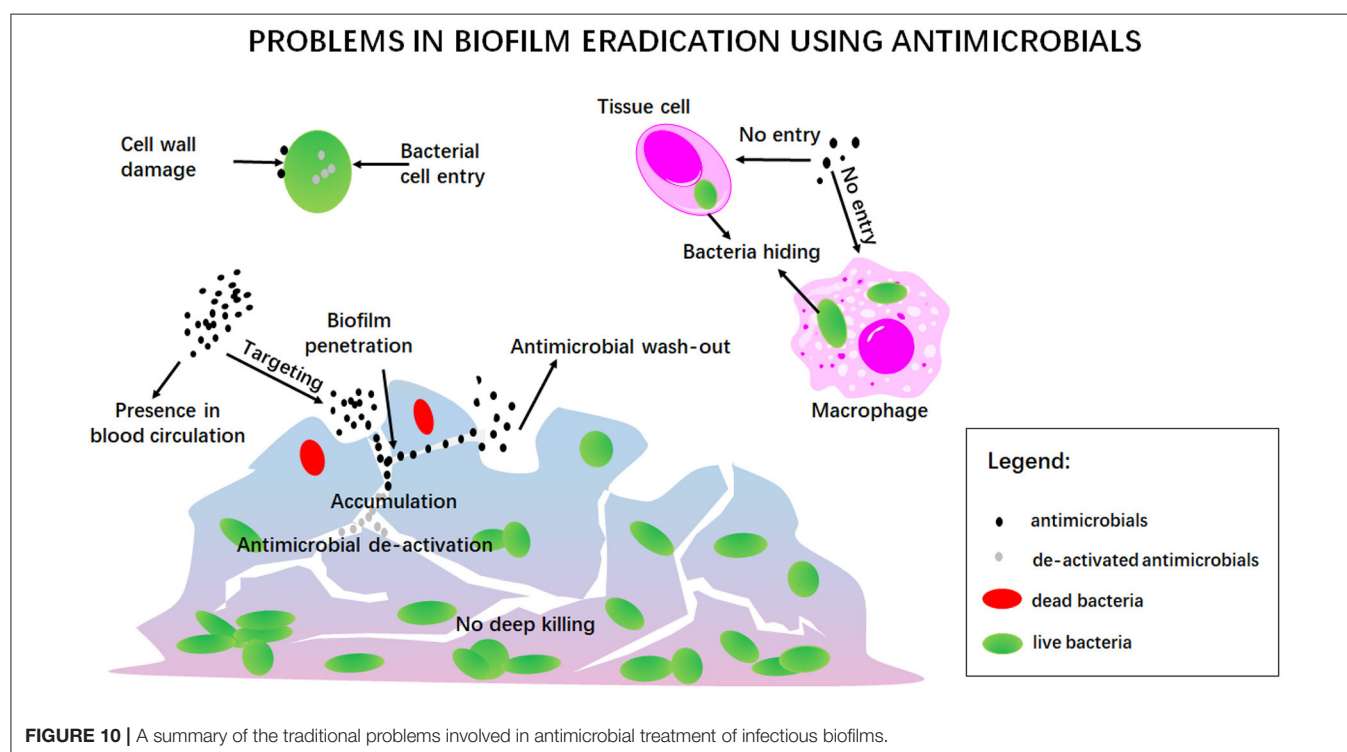


TABLE 3 | Minimal inhibitory concentrations of different bacterial strains against antibiotic-loaded liposomes.

Strain	MIC against free antibiotics (mg/L)	MIC against liposomal encapsulated antibiotics (mg/L)	References
Vancomycin			
<i>E. coli</i>	512	6–25	Nicolosi et al., 2010
	512	10.5	
<i>Klebsiella</i>	512	25–50	
<i>P. aeruginosa</i>	512	50	
	512	83.7	
	512	6–125	
<i>Acinetobacter baumannii</i>	512		
<i>S. aureus (MRSA)</i>	1	0.5	Bhise et al., 2018
Amikacin			
<i>P. aeruginosa</i>	8	4	Mugabe et al., 2006
	16	4	
	252	8	
	4	2	
	512	8	
<i>B. cenocepacia</i>	256	8	Halwani et al., 2007
	256	32	
	128	16	
	>512	8	
	4	1	
Gentamicin			
<i>P. aeruginosa</i>	4	2	Mugabe et al., 2006
	16	2	
	32	4	
	32	0.5	
	256	8	
<i>B. cenocepacia</i>	>512	32	Halwani et al., 2007
	256	64	
	256	16	
	>512	32	
	1	0.25	
Tobramycin			
<i>P. aeruginosa</i>	2	1	Mugabe et al., 2006
	4	4	
	64	2	
	1	0.5	
	1024	8	
<i>B. cenocepacia</i>	512	8	Halwani et al., 2007
	>512	64	
	128	16	
	>512	16	
	1	0.25	
Piperacillin			
<i>S. aureus</i>	64	32	Nacucchio et al., 1985
Cefepime			
<i>P. aeruginosa</i>	8	4	Torres et al., 2012

(Continued)

TABLE 3 | Continued

Strain	MIC against free antibiotics (mg/L)	MIC against liposomal encapsulated antibiotics (mg/L)	References
Ceftazidime			
<i>P. aeruginosa</i>	8	4	Torres et al., 2012
Levofloxacin			
<i>P. aeruginosa</i>	0.5	0.5	Derbali et al., 2019
Voriconazole			
<i>Aspergillus</i> sp.	0.5	0.5	Veloso et al., 2018
	0.25	0.25	
	0.5	0.25	
	1	0.5	
<i>Candida</i> sp.	0.03	0.03	
	0.06	0.06	
	0.03	0.03	
	0.03	0.03	
Meropenem			
<i>P. aeruginosa</i>	125	1.5	Zahra et al., 2017
	62.5	6.25	
	62.5	6.25	
	125	50	
	250	100	
	25	6.25	
	250	100	
	62.5	6.25	
	250	50	
Clarithromycin			
<i>S. aureus</i> ATCC29213	0.25	0.25	Meng et al., 2016
<i>S. aureus</i> MRSA	64	16	Alhajjan et al., 2013
<i>P. aeruginosa</i>	>256	8–64	
	256	8–64	
	256	8–64	
	256	8–6,432; 64; 8	
	>256	8–64	
	>256	8–64	
	>256	8–64	
	>256	8–64	
	256	8–64	
Azithromycin			
<i>P. aeruginosa</i>	128	16	Solleti et al., 2015
	64	8	
	512	32	
	128	16	
	256	32	
	512	32	
	512	128	
	256	32	
	512	64	
	256	16	

Multiple MIC values for the same strain, antibiotic and reference, refer to different isolates of the same strain or different liposomes in the same reference.

Generally, cationic liposomes demonstrate better interaction with negatively charged bacterial cell surfaces (Robinson et al., 2001; Nederberg et al., 2011; Ng et al., 2013). However, pH-responsive liposomes that self-target from the blood circulation toward bacteria in an infectious biofilm have not been extensively explored. Zwitterionic liposomes prepared from pH-responsive quaternary ammonium chitosan with charge reversal from -9.08 mV at pH 7.4 to $+8.92$ mV at pH 4.5 have been described for the treatment of periodontal infection (Zhou et al., 2018; Hu et al., 2019). However, according to **Figure 4** this change does not qualify as a charge reversal as these liposomes would have to be classified as uncharged at both pH values. Moreover, periodontal application does not imply self-targeting from the blood circulation, as required for the treatment of many other, internal infections. Interestingly, these zwitterionic liposomes were highly biocompatible and disruptive to periodontal biofilm.

Many Gram-negative and Gram-positive bacterial strains, resistant to a specific antibiotic free in solution, have been demonstrated to be susceptible to these antibiotics when encapsulated in a liposomal nanocarrier (**Table 3**). This may arguably be considered as the biggest advantage of liposomes over other nanocarriers. Although some have suggested that this must be attributed to the protection offered by liposomal encapsulation against enzymatic de-activation (Nacucchio et al., 1985), fusogenicity (Mugabe et al., 2006; Halwani et al., 2007) of liposomes can also significantly improve the antibacterial activity of antibiotics (Beaulac et al., 1996; Sachtelli et al., 1999; Li et al., 2013). Liposomes with enhanced fusogenicity possessing cholesterol hemisuccinate (Nicolosi et al., 2010) loaded with vancomycin for instance, had much lower minimal inhibitory concentrations (MIC) than vancomycin free in solution against a variety of Gram-negative bacterial strains, that would be considered vancomycin-resistant based on their MIC (see also **Table 3**). Also fusogenic liposomes composed of dipalmitoylphosphatidylcholine (DPPC) and dimiristoylphosphatidylglycerol (DMPG) in a ratio of 18:1 (w/w) loaded with tobramycin eradicated a mucoid chronic, pulmonary *Pseudomonas aeruginosa* infection, whereas tobramycin free in solution was not effective (Beaulac et al., 1996, 1998).

PERSPECTIVES OF LIPID-BASED ANTIMICROBIAL NANOCARRIERS FOR TREATING BACTERIAL BIOFILM INFECTION

Protection of antibiotics against enzymatic de-activation and fusogenicity to enhance antibiotic efficacy, constitute

unique advantages of liposomal antimicrobial nanocarriers that justify further research. Challenges in the ongoing development of liposomal antimicrobial nanocarriers include the realization of biofilm targeting from the blood circulation, penetration, and accumulation over the entire thickness of an infectious biofilm, associated with deep killing in the biofilm. Deep killing is necessary in order to prevent recurrence of infection, one of the troublesome features of clinical infection treatment. In this respect, it is also worthwhile to investigate whether liposomal antimicrobial nanocarriers can be designed that aid in the killing of bacteria seeking shelter in mammalian cells, impenetrable to many antimicrobials.

Downward clinical translation of liposomal drug nanocarriers has long been hampered for difficulties in large-scale production and storage. However, ethanol injection, membrane dispersion, and Shirasu porous glass membranes have enabled large-scale production of liposomes (Laouini et al., 2012). Equally, liposome storage problems are on their way to be solved. For commercial liposome products, storage in the fluid form is preferred since lyophilization and subsequent rehydration may lead to size changes and cargo leakage (Stark et al., 2010). Addition of stabilizers such as 2-morpholinoethansulfonic acid yielded low phospholipid degradation in liposomes after 12 months storage at $2-8^{\circ}\text{C}$ (Doi et al., 2019).

Owing to these developments, liposomes are nowadays an FDA approved form of drug delivery and liposome encapsulated tobramycin, marketed under the name FluidosomesTM is clinically applied for the treatment of chronic pulmonary infections in cystic fibrosis patients. A phase II clinical study is ongoing in Europe (Zora and Željka, 2016).

In conclusion, the challenges to further develop liposomes as a novel infection-control strategy supplementing antibiotic treatment are highly worthwhile to pursue.

AUTHOR CONTRIBUTIONS

All authors listed have made a substantial, direct and intellectual contribution to the work, and approved it for publication.

FUNDING

This work was financially supported by the National Natural Science Foundation of China (21620102005, 51933006, 51773099).

REFERENCES

- Akbarzadeh, A., Rezaei-Sadabady, R., Davaran, S., Joo, S. W., Zarghami, N., Hanifehpour, Y., et al. (2013). Liposome: classification, preparation, and applications. *Nanoscale Res. Lett.* 8:102. doi: 10.1186/1556-276X-8-102
- Albayaty, Y. N., Thomas, N., Hasan, S., and Prestidge, C. A. (2018). Penetration of topically used antimicrobials through *Staphylococcus aureus* biofilms: a comparative study using different models. *J. Drug Del. Sci. Technol.* 48, 429–436. doi: 10.1016/j.jddst.2018.10.015
- Alhajlan, M., Alhariri, M., and Omri, A. (2013). Efficacy and safety of liposomal clarithromycin and its effect on *Pseudomonas aeruginosa* virulence factors. *Antimicrob. Agents Chemother.* 57, 2694–2704. doi: 10.1128/AAC.00235-13
- Banerjee, R. (2001). Liposomes: applications in medicine. *J. Biomater. Appl.* 16, 3–21. doi: 10.1106/RA7U-1V9C-RV7C-8QXL

- Beaulac, C., Clément-Major, S., Hawari, J., and Lagacé, J. (1996). Eradication of mucoid *Pseudomonas aeruginosa* with fluid liposome-encapsulated tobramycin in an animal model of chronic pulmonary infection. *Antimicrob. Agents Chemother.* 40, 665–669. doi: 10.1128/AAC.40.3.665
- Beaulac, C., Sachetelli, S., and Lagace, J. (1998). *In-vitro* bactericidal efficacy of sub-MIC concentrations of liposome-encapsulated antibiotic against gram-negative and gram-positive bacteria. *J. Antimicrob. Chemother.* 41:35. doi: 10.1093/jac/41.1.35
- Bhise, K., Sau, S., Kebriaei, R., Rice, S. A., Stamper, K. C., Alsaab, H. O., et al. (2018). Combination of vancomycin and cefazolin lipid nanoparticles for overcoming antibiotic resistance of MRSA. *Materials* 11:1245. doi: 10.3390/ma11071245
- Bjarnsholt, T., Alhede, M., Alhede, M., Eickhardt-Soerensen, S. R., Moser, C., Kuhl, M., et al. (2013). The *in vivo* biofilm. *Trends Microbiol.* 21, 466–474. doi: 10.1016/j.tim.2013.06.002
- Chakraborty, S. P., Sahu, S. K., Pramanik, P., and Roy, S. (2012). *In vitro* antimicrobial activity of nanoconjugated vancomycin against drug resistant *Staphylococcus aureus*. *Int. J. Pharmaceut.* 436, 659–676. doi: 10.1016/j.ijpharm.2012.07.033
- Chang, H.-I., Yang, M.-S., and Liang, M. (2010). The synthesis, characterization and antibacterial activity of quaternized poly(2,6-dimethyl-1,4-phenylene oxide)s modified with ammonium and phosphonium salts. *React. Funct. Polym.* 70, 944–950. doi: 10.1016/j.reactfunctpolym.2010.09.005
- Chen, M.-M., Song, F.-F., Feng, M., Liu, Y., Liu, Y.-Y., Tian, J., et al. (2018). pH-sensitive charge-conversional and NIR responsive bubble-generating liposomal system for synergetic thermo-chemotherapy. *Coll. Surf. B Biointer.* 167, 104–114. doi: 10.1016/j.colsurfb.2018.04.001
- Cheow, W. S., Chang, M. W., and Hadinoto, K. (2011). The roles of lipid in anti-biofilm efficacy of lipid-polymer hybrid nanoparticles encapsulating antibiotics. *Coll. Surf. A Physicochem. Eng. Aspects* 389, 158–165. doi: 10.1016/j.colsurfa.2011.08.035
- Couffin-Hoarau, A.-C., and Leroux, J.-C. (2004). Report on the use of poly(organophosphazenes) for the design of stimuli-responsive vesicles. *Biomacromolecules* 5, 2082–2087. doi: 10.1021/bm0400527
- Dashper, S. G., O'Brien-Simpson, N. M., Cross, K. J., Paolini, R. A., Hoffmann, B., Catmull, D. V., et al. (2005). Divalent metal cations increase the activity of the antimicrobial peptide kappacin. *Antimicrob. Agents Chemother.* 49, 2322–2328. doi: 10.1128/AAC.49.6.2322-2328.2005
- Derbali, R. M., Aoun, V., Moussa, G., Frei, G., Tehrani, S. F., Del'Orto, J. C., et al. (2019). Tailored nanocarriers for the pulmonary delivery of levofloxacin against *Pseudomonas aeruginosa*: a comparative study. *Mol. Pharmaceut.* 16, 1906–1916. doi: 10.1021/acs.molpharmaceut.8b01256
- Doi, Y., Shimizu, T., Ishima, Y., and Ishida, T. (2019). Long-term storage of PEGylated liposomal oxaliplatin with improved stability and long circulation times *in vivo*. *Int. J. Pharm.* 564, 237–243. doi: 10.1016/j.ijpharm.2019.04.042
- Drbohlavova, J., Chomoucka, J., Adam, V., Ryvolova, M., Eckschlager, T., Hubalek, J., et al. (2013). Nanocarriers for anticancer drugs—new trends in nanomedicine. *Curr. Drug Metab.* 14, 547–564. doi: 10.2174/1389200211314050005
- Drulis-Kawa, A., and Dorotkiewicz-Jach, A. (2010). Liposomes as delivery systems for antibiotics. *Int. J. Pharm.* 387, 187–198. doi: 10.1016/j.ijpharm.2009.11.033
- Ehsan, Z. E., and Clancy, J. P. (2015). Management of *Pseudomonas aeruginosa* infection in cystic fibrosis patients using inhaled antibiotics with a focus on nebulized liposomal amikacin. *Fut. Microbiol.* 10, 1901–1912. doi: 10.2217/fmb.15.117
- Feitosa, E., Jansson, J., and Lindman, B. (2006). The effect of chain length on the melting temperature and size of dialkyltrimethylammonium bromide vesicles. *Chem. Phys. Lipids* 142, 128–132. doi: 10.1016/j.chemphyslip.2006.02.001
- Flemming, H. C., Wingender, J., Szewzyk, U., Steinberg, P., Rice, S. A., and Kjelleberg, S. (2016). Biofilms: an emergent form of bacterial life. *Nat. Rev. Microbiol.* 14, 563–575. doi: 10.1038/nrmicro.2016.94
- Forier, K., Raemdonck, K., De Smedt, S. C., Demeester, J., Coenye, T., and Braeckmans, K. (2014). Lipid and polymer nanoparticles for drug delivery to bacterial biofilms. *J. Control. Rel.* 190, 607–623. doi: 10.1016/j.jconrel.2014.03.055
- Ghaffas, D., and Leroux, J.-C. (2009). *Amphiphilic Ionizable Polyphosphazenes for The Preparation of pH-Responsive Liposomes*. Hoboken, NJ: John Wiley & Sons, Inc. 227–247.
- Gottenbos, B., Grijpma, D. W., Van der Mei, H. C., Feijen, J., and Busscher, H. J. (2001). Antimicrobial effects of positively charged surfaces on adhering gram-positive and gram-negative bacteria. *J. Antimicrob. Chemother.* 48, 7–13. doi: 10.1093/jac/48.1.7
- Greiner, L. L., Edwards, J. L., Shao, J., Rabinak, C., Entz, D., and Apicella, M. A. (2005). Biofilm formation by *Neisseria gonorrhoeae*. *Infect. Immun.* 73, 1964–1970. doi: 10.1128/IAI.73.4.1964-1970.2005
- Gupta, T. T., Karki, S. B., Fournier, R., and Ayan, H. (2018). Mathematical modelling of the effects of plasma treatment on the diffusivity of biofilm. *Appl. Sci.* 8:1729. doi: 10.3390/app8101729
- Halwani, M., Mugabe, C., Azghani, A. O., Lafrenie, R. M., Kumar, A., and Omri, A. (2007). Bactericidal efficacy of liposomal aminoglycosides against *Burkholderia cenocepacia*. *J. Antimicrob. Chemother.* 60, 760–769. doi: 10.1093/jac/dkm289
- Hamal, P., Nguyenhuu, H., Subasinghe, Don, V., Kumal, R. R., Kumar, R., McCarley, R. L., et al. (2019). Molecular adsorption and transport at liposome surfaces studied by molecular dynamics simulations and second harmonic generation spectroscopy. *J. Phys. Chem. B* 123, 7722–7730. doi: 10.1021/acs.jpcc.9b05954
- Hincha, D. K., Oliver, A. E., and Crowe, J. H. (1998). The effects of chloroplast lipids on the stability of liposomes during freezing and drying. *Biochim. Biophys. Acta Biomembr.* 1368, 150–156. doi: 10.1016/S0005-2736(97)00204-6
- Hofmann, A. M., Wurm, F., Hühn, E., Nawroth, T., Langguth, P., and Frey, H. (2010). Hyperbranched polyglycerol-based lipids via oxyanionic polymerization: toward multifunctional stealth liposomes. *Biomacromolecules* 11, 568–574. doi: 10.1021/bm901123j
- Hu, F., Zhou, Z., Xu, Q., Fan, C., Wang, L., Ren, H., et al. (2019). A novel pH-responsive quaternary ammonium chitosan-liposome nanoparticles for periodontal treatment. *Int. J. Biol. Macromol.* 129, 1113–1119. doi: 10.1016/j.ijbiomac.2018.09.057
- Huang, F., Gao, Y., Zhang, Y., Cheng, T., Ou, H., Yang, L., et al. (2017). Silver-decorated polymeric micelles combined with curcumin for enhanced antibacterial activity. *ACS Appl. Mater. Interfaces* 9, 16880–16889. doi: 10.1021/acsami.7b03347
- Humphreys, G., and Fleck, F. (2016). United nations meeting on antimicrobial resistance. *Bull. World Health Organ.* 94, 638–639. doi: 10.2471/BLT.16.020916
- Jacobs, W. A., Heidelberger, M., and Bull, C. G. (1916). Bactericidal properties of the quaternary salts of hexamethylenetetramine. III. Relation between constitution and bactericidal action in the quaternary salts obtained from haloacetyl compounds. *J. Exp. Med.* 23, 577–601. doi: 10.1084/jem.23.5.577
- Jangra, M., Kaur, M., Tambat, R., Rana, R., Maurya, S. K., Khatri, N., et al. (2019). Tridecaptin M, a new variant discovered in mud bacterium, shows activity against colistin- and extremely drug-resistant enterobacteriaceae. *Antimicrob. Agents Chemother.* 63, e00338–e00319. doi: 10.1128/AAC.00338-19
- Kamaly, N., Xiao, Z., Valencia, P. M., Radovic-Moreno, A. F., and Farokhzad, O. C. (2012). Targeted polymeric therapeutic nanoparticles: design, development and clinical translation. *Chem. Soc. Rev.* 41, 2971–3010. doi: 10.1039/c2cs15344k
- Kaszuba, M., Corbett, J., Watson, F. M., and Jones, A. (2010). High-concentration zeta potential measurements using light-scattering techniques. *Philos. Trans. R. Soc. A* 368, 4439–4451. doi: 10.1098/rsta.2010.0175
- Kaszuba, M., Lyle, I. G., and Jones, M. N. (1995). The targeting of lectin-bearing liposomes to skin-associated bacteria. *Colloids Surf. B* 4, 151–158. doi: 10.1016/0927-7765(95)01168-1
- Kataria, S., Sandhu, P., Bilandi, A., Middha, A., and Kapoor, B. (2011). Stealth liposomes: a review. *Int. J. Res. Ayurveda Pharm.* 2, 1534–1538.
- Khan, M. R., Gray, A. I., Waterman, P. G., and Sadler, I. H. (1990). Clerodane diterpenes from *Casearia corymbosa* stem bark. *Phytochemistry* 29, 3591–3595. doi: 10.1016/0031-9422(90)85282-K
- Kim, H. Y., Kang, M., Choo, Y. W., Go, S.-H., Kwon, S. P., Song, S. Y., et al. (2019). Immunomodulatory liposome complex functionalized with photosensitizer-embedded cancer cell membrane inhibits tumor growth and metastasis. *Nano Lett.* 19, 5185–5193. doi: 10.1021/acs.nanolett.9b01571
- Knodler, L. A., Celli, J., and Finlay, B. B. (2001). Pathogenic trickery: deception of host cell processes. *Nat. Rev. Mol. Cell Biol.* 2, 578–588. doi: 10.1038/35085062
- Kong, X., Liu, Y., Huang, X., Huang, S., Gao, F., Rong, P., et al. (2019). Cancer therapy based on smart drug delivery with advanced nanoparticles. *Anti-Cancer Agents Med. Chem.* 19, 720–730. doi: 10.2174/1871520619666190212124944
- Kumar, P., Shenoi, R. A., Lai, B. F. L., Nguyen, M., Kizhakkedathu, J. N., and Straus, S. K. (2015). Conjugation of aurein 2.2 to HPG yields an antimicrobial with better properties. *Biomacromolecules* 16, 913–923. doi: 10.1021/bm5018244

- Kumar, S., He, G., Kakarla, P., Shrestha, U., Ranjana, K. C., Ranaweera, I., et al. (2016). Bacterial multidrug efflux pumps of the major facilitator superfamily as targets for modulation. *Infect. Disord. Drug Targets* 16, 28–43. doi: 10.2174/1871526516666160407113848
- Laouini, A., Jaafar-Maalej, C., Gandoura-Sfar, S., Charcosset, C., and Fessi, H. (2012). Spironolactone-loaded liposomes produced using a membrane contactor method: an improvement of the ethanol injection technique. *Prog. Colloid Polym. Sci.* 139, 23–28. doi: 10.1007/978-3-642-28974-3_5
- Li, C., Zhang, X., Huang, X., Wang, X., Liao, G., and Chen, Z. (2013). Preparation and characterization of flexible nanoliposomes loaded with daptomycin, a novel antibiotic, for topical skin therapy. *Int. J. Nanomed.* 8, 1285–1292. doi: 10.2147/IJN.S41695
- Lin, W., Huang, K., Li, Y., Qin, Y., Xiong, D., Ling, J., et al. (2019). Facile *in situ* preparation and *in vitro* antibacterial activity of PDMAEMA-based silver-bearing copolymer micelles. *Nanoscale Res. Lett.* 14:256. doi: 10.1186/s11671-019-3074-z
- Liu, K., Li, H., Williams, G. R., Wu, J., and Zhu, L.-M. (2018). pH-responsive liposomes self-assembled from electrosprayed microparticles, and their drug release properties. *Colloids Surf. A* 537, 20–27. doi: 10.1016/j.colsurfa.2017.09.046
- Liu, X., Ma, R., Shen, J., Xu, Y., An, Y., and Shi, L. (2012). Controlled release of ionic drugs from complex micelles with charged channels. *Biomacromolecules* 13, 1307–1314. doi: 10.1021/bm2018382
- Liu, Y., Busscher, H. J., Zhao, B., Li, Y., Zhang, Z., Van der Mei, H. C., et al. (2016). Surface-adaptive, antimicrobially loaded, micellar nanocarriers with enhanced penetration and killing efficiency in *Staphylococcal* biofilms. *ACS Nano* 10, 4779–4789. doi: 10.1021/acsnano.6b01370
- Liu, Y., Shi, L., Su, L., Van der Mei, H. C., Jutte, P. C., Ren, Y., et al. (2019a). Nanotechnology-based antimicrobials and delivery systems for biofilm-infection control. *Chem. Soc. Rev.* 48, 428–446. doi: 10.1039/C7CS00807D
- Liu, Y., Shi, L., Van der Mei, H. C., Ren, Y., and Busscher, H. J. (2019b). “Perspectives on and need to develop new infection control methods,” in *Racing for the Surface: Advances in Antimicrobial and Osteoinductive Studies*, eds B. Li, T. F. Moriarty, T. Webster, and M. Xing (Cham: Springer In press).
- Lopes, N. A., and Brandelli, A. (2018). Nanostructures for delivery of natural antimicrobials in food. *Crit. Rev. Food Sci. Nutr.* 58, 2202–2212. doi: 10.1080/10408398.2017.1308915
- Lu, G., Wu, D., and Fu, R. (2007). Studies on the synthesis and antibacterial activities of polymeric quaternary ammonium salts from dimethylaminoethyl methacrylate. *React. Funct. Polym.* 67, 355–366. doi: 10.1016/j.reactfunctpolym.2007.01.008
- Lu, M.-M., Ge, Y., Qiu, J., Shao, D., Zhang, Y., Bai, J., et al. (2018). Redox/pH dual-controlled release of chlorhexidine and silver ions from biodegradable mesoporous silica nanoparticles against oral biofilms. *Int. J. Nanomed.* 13, 7697–7709. doi: 10.2147/IJN.S181168
- Mader, C., Küpcü, S., Sára, M., and Sleytr, U. B. (1999). Stabilizing effect of an S-layer on liposomes towards thermal and mechanical stress. *BBA-Biomembranes* 1418, 106–116. doi: 10.1016/S0005-2736(99)00030-9
- Majumder, J., Taratula, O., and Minko, T. (2019). Nanocarrier-based systems for targeted and site specific therapeutic delivery. *Adv. Drug Delivery Rev.* 144, 57–77. doi: 10.1016/j.addr.2019.07.010
- Makhathini, S. S., Kalhapure, R. S., Jadhav, M., Waddad, A. Y., Gannimani, R., Omolo, C. A., et al. (2019). Novel two-chain fatty acid-based lipids for development of vancomycin pH-responsive liposomes against *Staphylococcus aureus* and methicillin-resistant *Staphylococcus aureus* (MRSA). *J. Drug Target* 27, 1094–1107. doi: 10.1080/1061186X.2019.1599380
- Malekar, S. A., Sarode, A. L., Bach, A. C., Bose, A., Bothun, G., and Worthen, D. R. (2015). Radio frequency-activated nanoliposomes for controlled combination drug delivery. *AAPS PharmSciTech.* 16, 1335–1343. doi: 10.1208/s12249-015-0323-z
- Manaia, E. B., Abuçafy, M. P., Chiari-Andréo, B. G., Silva, B. L., Oshiro-Júnior, J. A., and Chivacchi, L. (2017). Physicochemical characterization of drug nanocarriers. *Int. J. Nanomed.* 12, 4991–5011. doi: 10.2147/IJN.S133832
- Mantovani, A., Cassatella, M. A., Costantini, C., and Jaillon, S. (2011). Neutrophils in the activation and regulation of innate and adaptive immunity. *Nat. Rev. Immunol.* 11, 519–531. doi: 10.1038/nri3024
- Marier, J. F., Lavigne, J., and Ducharme, M. P. (2002). Pharmacokinetics and efficacies of liposomal and conventional formulations of tobramycin after intratracheal administration in rats with pulmonary *Burkholderia cepacia* infection. *Antimicrob. Agents Chemother.* 46, 3776–3781. doi: 10.1128/AAC.46.12.3776-3781.2002
- Meers, P., Neville, M., Malinin, V., Scotto, A. W., Sardaryan, G., Kurumunda, R., et al. (2008). Biofilm penetration, triggered release and *in vivo* activity of inhaled liposomal amikacin in chronic *Pseudomonas aeruginosa* lung infections. *J. Antimicrob. Chemother.* 61, 859–868. doi: 10.1093/jac/dkn059
- Meng, Y., Hou, X., Lei, J., Chen, M., Cong, S., Zhang, Y., et al. (2016). Multi-functional liposomes enhancing target and antibacterial immunity for antimicrobial and anti-biofilm against methicillin-resistant *Staphylococcus aureus*. *Pharm. Res.* 33, 763–775. doi: 10.1007/s11095-015-1825-9
- Messiaen, A. S., Forier, K., Nelis, H., Braeckmans, K., and Coenye, T. (2013). Transport of nanoparticles and tobramycin-loaded liposomes in *Burkholderia cepacia* complex biofilms. *PLoS ONE* 8:e79220. doi: 10.1371/journal.pone.0079220
- Morton, L. A., Saludes, J. P., and Yin, H. (2012). Constant pressure-controlled extrusion method for the preparation of nano-sized lipid vesicles. *J. Vis. Exp.* 64:e4151. doi: 10.3791/4151
- Mugabe, C., Azghani, A. O., and Omri, A. (2005). Liposome-mediated gentamicin delivery: development and activity against resistant strains of *Pseudomonas aeruginosa* isolated from cystic fibrosis patients. *J. Antimicrob. Chemother.* 55, 269–271. doi: 10.1093/jac/dkh518
- Mugabe, C., Halwani, M., Azghani, A. O., Lafrenie, R. M., and Abdelwahab, O. (2006). Mechanism of enhanced activity of liposome-entrapped aminoglycosides against resistant strains of *Pseudomonas aeruginosa*. *Antimicrob. Agents Chemother.* 50, 2016–2022. doi: 10.1128/AAC.01547-05
- Nacucchio, M. C., Gatto Bellora, M. J., Sordelli, D. O., and D’Aquino, M. (1985). Enhanced liposome-mediated activity of piperacillin against *Staphylococci*. *Antimicrob. Agents Chemother.* 27, 137–139. doi: 10.1128/AAC.27.1.137
- Nagahama, M., Otsuka, A., Oda, M., Singh, R. K., Ziora, Z. M., Imagawa, H., et al. (2007). Effect of unsaturated bonds in the sn-2 acyl chain of phosphatidylcholine on the membrane-damaging action of *Clostridium perfringens* alpha-toxin toward liposomes. *Biochim. Biophys. Acta Biomembr.* 1768, 2940–2945. doi: 10.1016/j.bbamem.2007.08.016
- Nederberg, F., Zhang, Y., Tan, J. P., Xu, K., Wang, H., Yang, C., et al. (2011). Biodegradable nanostructures with selective lysis of microbial membranes. *Nat. Chem.* 3, 409–414. doi: 10.1038/nchem.1012
- Neville, N., and Jia, Z. (2019). Approaches to the structure-based design of antivirulence drugs: therapeutics for the post-antibiotic era. *Molecules* 24:378. doi: 10.3390/molecules24030378
- Ng, V. W. L., Ke, X., Lee, A. L. Z., Hedrick, J. L., and Yang, Y. Y. (2013). Synergistic co-delivery of membrane-disrupting polymers with commercial antibiotics against highly opportunistic bacteria. *Adv. Mater.* 25, 6730–6736. doi: 10.1002/adma.201302952
- N’Guessan, D. U. J.-P., Ouattara, M., Coulibaly, S., Kone, M. W., and Sissouma, D. (2018). Antibacterial activity of imidazo [1,2- α] pyridinylchalcones derivatives against *Enterococcus faecalis*. *World J. Pharm. Res.* 7, 21–33. doi: 10.20959/wjpr201818-13501
- Nguyen, S., Hiorth, M., Rykke, M., and Smistad, G. (2013). Polymer coated liposomes for dental drug delivery – Interactions with parotid saliva and dental enamel. *Eur. J. Pharm. Sci.* 50, 78–85. doi: 10.1016/j.ejps.2013.03.004
- Nicolosi, D., Scalia, M., Nicolosi, V. M., and Pignatello, R. (2010). Encapsulation in fusogenic liposomes broadens the spectrum of action of vancomycin against gram-negative bacteria. *Int. J. Antimicrob. Agents* 35, 553–558. doi: 10.1016/j.ijantimicag.2010.01.015
- Paunovska, K., Loughrey, D., Sago, C. D., Langer, R., and Dahlman, J. E. (2019). Using large datasets to understand nanotechnology. *Adv. Mater.* 31:1902798. doi: 10.1002/adma.201902798
- Peeridogaheh, H., Pourhajabagher, M., Barikani, H. R., and Bahador, A. (2019). The impact of *Aggregatibacter actinomycetemcomitans* biofilm-derived effectors following antimicrobial photodynamic therapy on cytokine production in human gingival fibroblasts. *Photodiagn. Photodyn. Ther.* 27, 1–6. doi: 10.1016/j.pdpdt.2019.05.025
- Pick, H., Alves, A. C., and Vogel, H. (2018). Single-vesicle assays using liposomes and cell-derived vesicles: from modeling complex membrane processes to synthetic biology and biomedical applications. *Chem. Rev.* 118, 8598–8654. doi: 10.1021/acs.chemrev.7b00777

- Popa, A., Davidescu, C. M., Trif, R., Ilia, G., Iliescu, S., and Dehelean, G. (2003). Study of quaternary onium salts grafted on polymers: antibacterial activity of quaternary phosphonium salts grafted on 'gel-type' styrene-divinylbenzene copolymers. *React. Funct. Polym.* 55, 151–158. doi: 10.1016/S1381-5148(02)00224-9
- Praphakar, R. A., Ebenezer, R. S., Vignesh, S., Shakila, H., and Rajan, M. (2019). Versatile pH-responsive chitosan-g-polycaprolactone/maleic anhydride-ioniazid polymer micelle to improve the bioavailability of tuberculosis multiazugs. *ACS Appl. Bio Mater.* 2, 1931–1943. doi: 10.1021/acsabm.9b00003
- Ray, K. J., Simard, M. A., Larkin, J. R., Coates, J., Kinches, P., Smart, S. C., et al. (2019). Tumor pH and protein concentration contribute to the signal of amide proton transfer magnetic resonance imaging. *Cancer Res.* 79, 1343–1352. doi: 10.1158/0008-5472.CAN-18-2168
- Robinson, A. M., Bannister, M., Creeth, J. E., and Jones, M. N. (2001). The interaction of phospholipid liposomes with mixed bacterial biofilms and their use in the delivery of bactericide. *Colloids Surf. A* 186, 43–53. doi: 10.1016/S0927-7757(01)00481-2
- Robinson, A. M., Creeth, J. E., and Jones, M. N. (1998). The specificity and affinity of immunoliposome targeting to oral bacteria. *BBA-Biomembranes* 1369, 278–286. doi: 10.1016/S0005-2736(97)00231-9
- Robinson, A. M., Creeth, J. E., and Jones, M. N. (2000). The use of immunoliposomes for specific delivery of antimicrobial agents to oral bacteria immobilized on polystyrene. *J. Biomater. Sci. Polym. Ed.* 11, 1381–1393. doi: 10.1163/156856200744408
- Romberg, B., Hennink, W. E., and Storm, G. (2008). Sheddable coatings for long-circulating nanoparticles. *Pharmaceut. Res.* 25, 55–71. doi: 10.1007/s11095-007-9348-7
- Sachetelli, S., Beaulac, C., Riffon, R., and Lagacé, J. (1999). Evaluation of the pulmonary and systemic immunogenicity of fluidosomes, a fluid liposomal-tobramycin formulation for the treatment of chronic infections in lungs. *Biochim. Biophys. Acta* 1428, 334–340. doi: 10.1016/S0304-4165(99)00078-1
- Sachetelli, S., Khalil, H., Chen, T., Beaulac, C., Senecal, S., and Lagace, J. (2000). Demonstration of a fusion mechanism between a fluid bactericidal liposomal formulation and bacterial cells. *BBA-Biomembranes* 1463, 254–266. doi: 10.1016/S0005-2736(99)00217-5
- Sanderson, N. M., Guo, B., Jacob, A. E., Handley, P. S., Cuniffe, J. G., and Jones, M. N. (1996). The interaction of cationic liposomes with the skin-associated bacterium *Staphylococcus epidermidis*: effects of ionic strength and temperature. *Biochim. Biophys. Acta* 1283, 207–214. doi: 10.1016/0005-2736(96)00099-5
- Sanderson, N. M., and Jones, M. N. (1996). Targeting of cationic liposomes to skin-associated bacteria. *J. Pesticide Sci.* 46, 255–261. doi: 10.1002/(SICI)1096-9063(199603)46:3<255::AID-PS345>3.0.CO;2-Y
- Smith, M. C., Crist, R. M., Clogston, J. D., and McNeil, S. E. (2017). Zeta potential: a case study of cationic, anionic, and neutral liposomes. *Anal. Bioanal. Chem.* 409, 5779–5787. doi: 10.1007/s00216-017-0527-z
- Solleti, V. S., Alhariri, M., Halwani, M., and Omri, A. (2015). Antimicrobial properties of liposomal azithromycin for *Pseudomonas* infections in cystic fibrosis patients. *J. Antimicrob. Chemother.* 70, 784–796. doi: 10.1093/jac/dku452
- Soria-Carrera, H., Lucia, A., De Matteis, L., Ainsa, J. A., de la Fuente, J. M., and Martin-Rapun, R. (2019). Polypeptidic micelles stabilized with sodium alginate enhance the activity of encapsulated bedaquiline. *Macromol. Biosci.* 19:1800397. doi: 10.1002/mabi.201800397
- Stark, B., Pabst, G., and Prassl, R. (2010). Long-term stability of sterically stabilized liposomes by freeze-drying: effects of cryoprotectants on structure. *Eur. J. Pharm. Sci.* 41, 546–555. doi: 10.1016/j.ejps.2010.08.010
- Sutherland, I. W. (2001). The biofilm matrix. an immobilized but dynamic microbial environment. *Trends Microbiol.* 9, 222–227. doi: 10.1016/S0966-842X(01)02012-1
- Tang, H., Xu, Y., Zheng, T., Li, G., You, Y., Jiang, M., et al. (2009). Treatment of osteomyelitis by liposomal gentamicin-impregnated calcium sulfate. *Arch. Orthop. Trauma Surg.* 129, 1301–1308. doi: 10.1007/s00402-008-0782-8
- Torres, I. M. S., Bento, E. B., da Cunha Almeida, L., de Sá, L. Z., and Lima, E. M. (2012). Preparation, characterization and *in vitro* antimicrobial activity of liposomal ceftazidime and cefepime against *Pseudomonas aeruginosa* strains. *Braz. J. Microbiol.* 43, 984–992. doi: 10.1590/S1517-83822012000300020
- Van Leewenhoek, A. (1684). An abstract of a letter from Mr. Anthony Leevvenhoeck at Delft, dated Sep. 17. 1683. containing some microscopical observations, about animals in the scurf of the teeth, the substance call'd worms in the nose, the cuticula consisting of scales. *Philos. Trans.* 14, 568–574. doi: 10.1098/rstl.1684.0030
- Veloso, D. F. M. C., Benedetti, N. I. G. M., Avila, R. I., Bastos, T. S. A., Silva, T. C., Silva, M. R. R., et al. (2018). Intravenous delivery of a liposomal formulation of voriconazole improves drug pharmacokinetics, tissue distribution, and enhances antifungal activity. *Drug Deliv.* 25, 1585–1594. doi: 10.1080/10717544.2018.1492046
- Vila-Caballer, M., Codolo, G., Munari, F., Malfanti, A., Fassan, M., Rugge, M., et al. (2016). A pH-sensitive stearyl-PEG-poly(methacryloyl sulfadimethoxine)-decorated liposome system for protein delivery: an application for bladder cancer treatment. *J. Control. Rel.* 238, 31–42. doi: 10.1016/j.jconrel.2016.07.024
- Vyas, S. P., Sihorkar, V., and Dubey, P. K. (2001). Preparation, characterization and *in vitro* antimicrobial activity of metronidazole bearing lectinized liposomes for intra-periodontal pocket delivery. *Pharmazie* 56, 554–560.
- Wang, Y., Wang, Z., Xu, C., Tian, H., and Chen, X. (2019). A disassembling strategy overcomes the EPR effect and renal clearance dilemma of the multifunctional theranostic nanoparticles for cancer therapy. *Biomaterials* 197, 284–293. doi: 10.1016/j.biomaterials.2019.01.025
- Wolfmeier, H., Pletzer, D., Mansour, S. C., and Hancock, R. E. W. (2018). New perspectives in biofilm eradication. *ACS Infect. Dis.* 4, 93–106. doi: 10.1021/acsinfecdis.7b00170
- Wu, J., Li, F., Hu, X., Lu, J., Sun, X., Gao, J., et al. (2019). Responsive assembly of silver nanoclusters with a biofilm locally amplified bactericidal effect to enhance treatments against multi-drug-resistant bacterial infections. *ACS Cent. Sci.* 5, 1366–1376. doi: 10.1021/acscentsci.9b00359
- Xue, X.-Y., Mao, X.-G., Li, Z., Chen, Z., Zhou, Y., Hou, Z., et al. (2015). A potent and selective antimicrobial poly(amidoamine) dendrimer conjugate with LED209 targeting QseC receptor to inhibit the virulence genes of gram negative bacteria. *Nanomedicine* 11, 329–339. doi: 10.1016/j.nano.2014.09.016
- Zahra, M.-J., Hamed, H., Mohammad, R.-Y., Nosratollah, Z., Akbarzadeh, A., and Morteza, M. (2017). Evaluation and study of antimicrobial activity of nanoliposomal meropenem against *Pseudomonas aeruginosa* isolates. *Artif. Cells Nanomed. Biotechnol.* 45, 975–980. doi: 10.1080/21691401.2016.1198362
- Zendehele, M., Zendehele, A., Hoseini, F., and Azarkish, M. (2015). Investigation of removal of chemical oxygen demand (COD) wastewater and antibacterial activity of nanosilver incorporated in poly (acrylamide-co-acrylic acid)/NaY zeolite nanocomposite. *Polym. Bull.* 72, 1281–1300. doi: 10.1007/s00289-015-1326-3
- Zhang, M., and Lemay, S. G. (2019). Interaction of anionic bulk nanobubbles with cationic liposomes: evidence for reentrant condensation. *Langmuir* 35, 4146–4151. doi: 10.1021/acs.langmuir.8b03927
- Zhao, D., Shuang, Y., Sun, B., Shuang, G., Guo, S., and Kai, Z. (2018). Biomedical applications of chitosan and its derivative nanoparticles. *Polymers* 10:462. doi: 10.3390/polym10040462
- Zhou, Z., Fang, H., Hu, S., Ming, K., Chao, F., Liu, Y., et al. (2018). pH-activated nanoparticles with targeting for the treatment of oral plaque biofilm. *J. Mater. Chem. B* 6, 586–592. doi: 10.1039/C7TB02682J
- Zora, R., and Željka, V. (2016). Current trends in development of liposomes for targeting bacterial biofilms. *Pharmaceutics* 8:18. doi: 10.3390/pharmaceutics8020018

Conflict of Interest: HB is also director of a consulting company, SASA BV.

The remaining authors declare no conflicts of interest with respect to authorship and/or publication of this article. Opinions and assertions contained herein are those of the authors and are not construed as necessarily representing views of their respective employers.

Copyright © 2020 Wang, van der Mei, Ren, Busscher and Shi. This is an open-access article distributed under the terms of the Creative Commons Attribution License (CC BY). The use, distribution or reproduction in other forums is permitted, provided the original author(s) and the copyright owner(s) are credited and that the original publication in this journal is cited, in accordance with accepted academic practice. No use, distribution or reproduction is permitted which does not comply with these terms.



Rapid Release Polymeric Fibers for Inhibition of *Porphyromonas gingivalis* Adherence to *Streptococcus gordonii*

Mohamed Y. Mahmoud^{1,2,3†}, Sonali Sapare^{4,5†}, Keegan C. Curry⁶, Donald R. Demuth^{4,5*†} and Jill M. Steinbach-Rankins^{1,2,5,7*†}

OPEN ACCESS

Edited by:

Manuel Simões,
University of Porto, Portugal

Reviewed by:

Ruibing Wang,
University of Macau, China
Rajeev K. Singla,
K.R. Mangalam University, India

*Correspondence:

Donald R. Demuth
drdemu01@louisville.edu
Jill M. Steinbach-Rankins
jmstei01@louisville.edu

[†]These authors share first authorship

[‡]These authors share
senior authorship

Specialty section:

This article was submitted to
Medicinal and Pharmaceutical
Chemistry,
a section of the journal
Frontiers in Chemistry

Received: 08 July 2019

Accepted: 18 December 2019

Published: 21 January 2020

Citation:

Mahmoud MY, Sapare S, Curry KC,
Demuth DR and
Steinbach-Rankins JM (2020) Rapid
Release Polymeric Fibers for Inhibition
of *Porphyromonas gingivalis*
Adherence to *Streptococcus gordonii*.
Front. Chem. 7:926.
doi: 10.3389/fchem.2019.00926

¹ Department of Pharmacology and Toxicology, University of Louisville School of Medicine, Louisville, KY, United States, ² Center for Predictive Medicine, University of Louisville, Louisville, KY, United States, ³ Department of Toxicology, Forensic Medicine and Veterinary Regulations, Faculty of Veterinary Medicine, Cairo University, Giza, Egypt, ⁴ Department of Oral Immunology and Infectious Diseases, University of Louisville School of Dentistry, Louisville, KY, United States, ⁵ Department of Microbiology and Immunology, University of Louisville School of Medicine, Louisville, KY, United States, ⁶ Department of Biology, University of Louisville, Louisville, KY, United States, ⁷ Department of Bioengineering, University of Louisville Speed School of Engineering, Louisville, KY, United States

Active agents targeting key bacterial interactions that initiate biofilm formation in the oral cavity, may alter periodontitis progression; however, to date, specifically-targeted prophylactic and treatment strategies have been limited. Previously we developed a peptide, BAR (SspB Adherence Region), that inhibits oral *P. gingivalis*/*S. gordonii* biofilm formation *in vitro* and *in vivo*, and BAR nanoparticles that increase BAR effectiveness via multivalency and prolonged delivery. However, limited BAR loading and nanoparticle retention in the oral cavity can result in inadequate release and efficaciousness. Given this, an effective delivery platform that can release concentrations of BAR suitable for twice-daily applications, may offer an alternative that enhances loading, ease of administration, and retention in the oral cavity. With this in mind, the study objectives were to develop and characterize a rapid-release platform, composed of polymeric electrospun fibers (EFs) that encapsulate BAR, and to evaluate fiber safety and functionality against *P. gingivalis*/*S. gordonii* biofilms *in vitro*. Poly(lactic-co-glycolic acid) (PLGA), poly(L-lactic acid) (PLLA), and polycaprolactone (PCL) were electrospun alone or blended with polyethylene oxide (PEO), to provide high BAR loading and rapid-release. The most promising formulation, 10:90 PLGA:PEO EFs, provided 95% BAR release after 4 h, dose-dependent inhibition of biofilm formation (IC₅₀ = 1.3 μM), disruption of established dual-species biofilms (IC₅₀ = 2 μM), and maintained high cell viability. These results suggest that BAR-incorporated EFs may provide a safe and specifically-targeted rapid-release platform to inhibit and disrupt dual-species biofilms, that we envision may be applied twice-daily to exert prophylactic effect in the oral cavity.

Keywords: periodontal disease, *Porphyromonas gingivalis*, *Streptococcus gordonii*, oral biofilm, electrospun fibers, peptide delivery

INTRODUCTION

Periodontal disease is a group of chronic inflammatory diseases that are globally prevalent, affecting over 65 million adults in the U.S., with increased incidence in developing countries. Moreover, the prevalence and severity of periodontal disease has been shown to increase from 47 to 64% in adults from age 30–65 (Eke et al., 2015). Advanced periodontal disease (subgingival pocket depths > 6 mm) occurs in up to 11% of adults worldwide (Kassebaum et al., 2014), and is a chronic, irreversible inflammatory disease that results in destruction of connective tissue, vascular proliferation, and alveolar bone resorption (Pihlstrom et al., 2005). *Porphyromonas gingivalis* is strongly associated with chronic adult periodontitis (Socransky et al., 1998; Darveau et al., 2012; Griffen et al., 2012) and has been considered to be a key pathogen that may promote disease by perturbing host-microbe homeostasis, leading to uncontrolled inflammation (Darveau et al., 2012). While the primary niche of *P. gingivalis* is the anaerobic environment of the subgingival pocket, *P. gingivalis* initially colonizes the oral cavity by interacting with Gram-positive commensal streptococci in the supragingival environment (Marsh, 1994). These initial adhesive interactions thus represent ideal points for intervention to prevent *P. gingivalis* colonization and can be targeted with specifically designed biologics that may effectively curtail the progression of periodontal disease (Daep et al., 2006).

Previous work in our groups has shown that the adherence of *P. gingivalis* with commensal oral streptococci such as *S. gordonii*, is mediated by the interaction of the minor fimbrial antigen, Mfa1, of *P. gingivalis* with the streptococcal antigen I/II protein (e.g., SspB). We also showed that a discrete region, designated BAR (SspB Adherence Region), is essential to adherence (Brooks et al., 1997). A synthetic peptide comprised of amino acids 1167–1193 from this region potently inhibited adherence of *P. gingivalis* with *S. gordonii* (IC₅₀ = 1.3 μM) (Daep et al., 2006), and significantly reduced *P. gingivalis* virulence in a mouse model of periodontitis (Daep et al., 2011). However, BAR peptide exhibited weaker and more transient effectiveness against pre-established dual-species biofilms and more complex biofilms. In addition, alternative non-targeted prophylactic therapies including scaling and root planning have only been temporarily effective in removing the subgingival biofilm and halting the corresponding inflammatory cascade (Herrera et al., 2012), since the biofilm begins to re-form shortly after prophylaxis is completed. Furthermore, while current medicinal therapies, consisting of systemic and local antibiotic administration, are initially effective, they can result in side effects due to an inadequate concentration of drug reaching the periodontal pockets, corresponding transient activity (Drisko, 1996; Walker, 1996; Allaker and Ian Douglas, 2015), and the development of antimicrobial resistance. Moreover, the non-specific nature of current antibiotic agents can adversely impact the commensal microbial community. Given these challenges, new prophylactic and therapeutic approaches that provide more specific targeting of periodontal pathogen interactions are urgently needed to address these shortcomings and to improve oral therapeutic outcomes.

Delivery vehicles that localize the delivery and maintain the stability of specifically-targeted biologics, such as BAR peptide, may offer improved functional activity, thereby enhancing the therapeutic efficacy (Garg et al., 2012). Delivery platforms such as electrospun fibers (EFs) have been used in a variety of applications like wound dressing (Liu et al., 2017), tissue regeneration (Inanç et al., 2009; Yang et al., 2009), and antimicrobial delivery (Reise et al., 2012; Chaturvedi et al., 2013) to incorporate water-soluble bioactive agents such as proteins, peptides, nucleic acids and hydrophilic/hydrophobic drugs. Polymeric fibers can protect encapsulated cargo from premature degradation, in addition to minimizing systemic absorption and associated side effects. Moreover, electrospinning offers a cost-effective, reproducible, and highly tunable method to provide efficient encapsulation and release based on the needs of rapid-onset or prolonged delivery applications. Many studies have shown that fibers composed of natural, synthetic, and semi-synthetic polymers and polymer blends can tune drug miscibility and that the resulting drug-polymer interactions may lead to different release profiles (Chou and Woodrow, 2017).

We previously showed that BAR-modified and BAR-encapsulated nanoparticles inhibit *P. gingivalis* biofilm formation (Kalia et al., 2017; Mahmoud et al., 2018, 2019). These vehicles were envisioned to serve in formulations such as an oral gel, varnish or mouthwash that require two to three daily applications. Here we sought to develop and characterize EFs that may be administered in future applications, as rapid-release dental strips in the oral cavity. We proposed that the development of an effective oral delivery system that can release BAR within a time frame desired for twice-daily applications, may offer an alternative platform that increases loading, facilitates ease of administration, and provides the potential of enhanced retention in the oral cavity. Since biocompatible, biodegradable, and Food and Drug Administration (FDA) approved polymers including poly(lactic-co-glycolic) acid (PLGA) (Li et al., 2002), poly(L-lactic acid) (PLLA) (Jun et al., 2003), polycaprolactone (PCL) (Chaturvedi et al., 2013), and polyethylene oxide (PEO) (Son et al., 2004) have been successfully electrospun and used in clinical applications, we hypothesized that EFs comprised of these polymers may offer advantages to BAR peptide administration in the oral cavity. To obtain maximal delivery within our time frame of interest (e.g., twice-daily), we hypothesized that BAR release may be modulated by changing the hydrophobic:hydrophilic polymer ratios of the blended fibers.

Given this, the goal of this work was to synthesize, characterize, and demonstrate the preliminary inhibitory and disruptive capabilities of non-blended and blended EF formulations to prevent and treat *P. gingivalis*/*S. gordonii* biofilm formation. We demonstrated that changing the hydrophobic:hydrophilic polymer ratios altered the release kinetics of BAR peptide for durations relevant to oral application. Moreover, we functionally characterized the effectiveness of EFs in preventing the formation of *P. gingivalis*/*S. gordonii* biofilms *in vitro*. These results suggest that BAR-incorporated EFs can be formulated to release peptide over a time frame of hours and may represent a new dosage form that can release targeting molecules

in the oral cavity. Long-term, we envision that BAR-EFs may provide a promising rapid-release platform to deliver BAR peptide to the oral cavity in the form of strips or gum that can be conveniently applied twice-daily to inhibit biofilm formation.

MATERIALS AND METHODS

Materials

Hydrophobic polymers including poly(lactic-co-glycolic acid) (PLGA, 50:50 lactic:glycolic acid, MW 30,000–60,000), poly(L-lactic acid) (PLLA, MW 50,000), and polycaprolactone (PCL, MW 80,000), and the hydrophilic polymer, polyethylene oxide (PEO, MW 100,000) were purchased from Sigma-Aldrich (St. Louis, MO, USA). Tris-EDTA (TE) buffer (pH 8.0), phosphate buffered saline (PBS), and the organic solvents chloroform, dimethyl sulfoxide (DMSO), and hexafluoroisopropanol (HFIP) were also purchased from Sigma-Aldrich (St. Louis, MO, USA). All chemicals were used directly without further purification. One milliliter plastic syringes, petri dishes, and 20 mL scintillation vials were obtained from VWR. One milliliter glass syringes were purchased from Fisher Scientific. The electrospinner was provided courtesy of Dr. Stuart Williams at the Cardiovascular Innovative Institute, University of Louisville.

Peptide Synthesis

The peptide used in this study (NH₂-LEAAPKKVQDLLKKANI TVKGAFQLFS-COOH) (Daep et al., 2008) was synthesized by BioSynthesis, Inc. (Lewisville, TX). It was obtained with purity <94% and comprised residues 1167–1193 of the SspB (Antigen I/II) protein sequence of *S. gordonii*. A fluorescent BAR peptide (F-BAR), synthesized by covalently attaching 6-carboxyfluorescein (F-BAR) to the epsilon amine of the lysine residue underlined in the sequence above, was used to more easily characterize BAR loading and release from the fibers via fluorescence detection (Kalia et al., 2017).

Preparation of Polymer Solutions

To prepare the hydrophobic-only (non-blended) polymer fiber batches, PLGA and PLLA were dissolved in HFIP at a concentration of 15% (w/w), while PCL was dissolved in HFIP at a concentration of 12% w/w due to increased viscosity. The polymer solutions were aspirated into a 7 mL glass scintillation vials, and sealed using aluminum foil and parafilm to prevent evaporation of the organic solvent. The vials were placed in a shaker at 150 rpm and incubated at 37°C overnight to solubilize the polymer. The final volume of each polymer solution was 1 mL. The following day, F-BAR peptide was dissolved in 200 μ L TE buffer and mixed with the polymer solvents at a concentration of 1% w/w (e.g., 2.4 mg F-BAR/240 mg polymer).

To prepare blended polymers, the hydrophobic polymers PLGA, PLLA, and PCL were mixed with PEO at different ratios (40:60, 20:80, 10:90 w/w) to form PLGA:PEO, PLLA:PEO, and PCL:PEO blends in chloroform at a concentration of 15% (w/v). The blended solutions were aspirated into 20 mL glass scintillation vials, and sealed using parafilm to prevent evaporation of the organic solvent. The vials were placed in a shaker at 150 rpm and incubated at 37°C overnight to solubilize

the polymer. The final volume of each polymer solution was 1 mL. The following day, F-BAR peptide was dissolved in 60 μ L DMSO. The F-BAR solutions were mixed with the polymer solvent at a concentration of 1% w/w (BAR/polymer content) (Kim et al., 2007).

Electrospinning

For the non-blended polymer solutions, 1 mL of the mixed polymer suspension was aspirated into a 1 mL plastic syringe with an 18-gauge blunt needle tip. The internal diameter of the BD plastic syringe (4.78 mm), was set in the syringe pump program. The collector was adjusted such that there was at least 10 cm distance maintained from the needle tip. The syringe pump motor controls were adjusted by setting the “slide” control to 4.5 and the “rotor” to 8. The voltage supply was set at 20 kV, and the syringe pump flow rate was set to 0.8 mL per hour. The polymer solution was electrospun at room temperature, under atmospheric conditions, for 1 h 15 min, and the resulting fine mist was collected on the mandrel and allowed to dry for 15 min. The mandrel was removed from the collector and the fiber was cut and gently peeled off the mandrel. The fiber was placed in a labeled petri dish and kept in a desiccator for 24 h before characterization. The desiccated fibers were stored in 4°C until use (Tyo et al., 2017).

For the blended polymer solutions, 1 mL of the mixed dual-polymer suspension was aspirated into a 1 mL glass syringe with a 22-gauge blunt needle tip. The internal diameter of the Hamilton gastight syringe (4.61 mm), was set in the syringe pump program. A distance of 15 cm was kept between the needle tip and the collector. The “slide” control was set to 4.5 and the “rotor” control was set to 8. A voltage of 20–25 kV was applied, at a flow rate of 0.3 mL per hour. The electrospinning processes were employed under ambient conditions for 3 h 20 min. The stretched and solidified polymeric fibers were collected on a 4 mm diameter stainless steel mandrel and allowed to dry for 15 min. Similar desiccation and storage conditions were followed, as noted for the non-blended fibers.

EF Characterization: EF Morphology, Diameter, BAR Loading, and Release

Fiber morphology and size were evaluated using scanning electron microscopy (SEM) (JSM-820, JEOL, Tokyo, Japan), and fiber diameters were obtained by analyzing SEM images with NIH ImageJ. The loading and encapsulation efficiency (EE) of F-BAR peptide in the non-blended and blended fibers were determined by dissolving F-BAR fibers in DMSO. The fiber solution was subsequently vortexed, sonicated for 5 min, and dissolved for 1 h in a dark room. The quantity of extracted F-BAR was determined by measuring the fluorescence using a spectrophotometer (488/518 nm excitation/emission), relative to an F-BAR standard (Kalia et al., 2017; Mahmoud et al., 2018, 2019). A standard curve of F-BAR was obtained by adding 0.1 mg F-BAR to 1 mL of 1:9 DMSO:TE, and serially diluting in 1:9 DMSO:TE. The diluted solutions (100 μ L/well) were transferred to a 96-well clear bottom microtiter plate in triplicate. For the dissolved fiber samples, after the incubation period, the fiber sample solutions were vortexed and sonicated again. The

solutions were diluted 1:2, 1:5, 1:10, and 1:100 in 1:9 DMSO:TE solution, and transferred to a microtiter plate.

The *in vitro* release of F-BAR from fibers was measured by gentle agitation of EFs in phosphate buffered saline (PBS, pH 7.4) at 37°C. At fixed time points (1, 2, 4, 8, 12, and 24 h), samples were collected and the amount of F-BAR released from the EFs was quantified via fluorescence spectroscopy, against an F-BAR standard in PBS (Kalia et al., 2017; Tyo et al., 2017; Mahmoud et al., 2018).

Growth of Bacterial Strains

P. gingivalis (ATCC 33277) was grown in Trypticase soy broth (Difco Laboratories Inc., Livonia, MI, USA) supplemented with 0.5% (w/v) yeast extract, 1 µg/mL menadione, and 5 µg/mL hemin. The medium was reduced for 24 h under anaerobic conditions (10% CO₂, 10% H₂, and 80% N₂) and *P. gingivalis* was subsequently inoculated and grown anaerobically for 48 h at 37°C. *S. gordonii* DL-1 was cultured aerobically without shaking in brain-heart infusion broth (Difco Laboratories Inc.) supplemented with 1% yeast extract for 16 h at 37°C (Daep et al., 2006).

Biofilm Inhibition Assay

To assess the effectiveness of BAR-incorporated EFs to prevent the interaction of *P. gingivalis* with *S. gordonii*, *S. gordonii* was harvested from culture and labeled with 20 µL of 5 mg/mL hexidium iodide for 15 min at room temperature. Following incubation, cells were centrifuged to remove unbound fluorescent dye. The bacterial concentration was subsequently measured by the O.D. (600 nm) from 20-fold diluted cultures of *S. gordonii*. The optical density of *S. gordonii* cells was adjusted to 0.8 O.D. (1×10^9 CFU/mL) to obtain uniformity between cell counts in each well. After adjusting the optical density, 1 mL of *S. gordonii* cells was added to each well of 12-well culture plates containing a sterilized micro-cover slip. The cell culture plates were wrapped in aluminum foil to protect the labeled cells from light and placed on a rocker platform in the anaerobic chamber for 24 h.

P. gingivalis cultures were optimized using a similar approach, utilizing a different fluorescent label (20 µL of 4 mg/mL carboxyfluorescein-succinylester). *P. gingivalis* was incubated with the fluorescent dye for 30 min on a rocker platform and protected from light. The same procedures were followed as performed with *S. gordonii* to determine cell concentration, with slight adaptations. The optical density of *P. gingivalis* was adjusted from 0.8–0.4 O.D. (5×10^7 CFU/mL) by diluting *P. gingivalis* cultures with an equal volume of 1X PBS containing BAR-EFs, free BAR, or blank EFs as a control, to a final volume 1 mL. The final concentration of BAR-EFs or free BAR ranged from 0.3–3 µM based on the previously determined IC₅₀ of free BAR (1.3 µM). *P. gingivalis* was incubated with BAR-EFs, free BAR, or blank EFs at 25°C for 30 min before transferring to wells containing *S. gordonii*.

Plates containing *P. gingivalis* and *S. gordonii* were subsequently incubated for 24 h at 37°C in anaerobic conditions. The following day, the supernatant was removed and cells were washed with PBS. Adherent cells were fixed

with 4% (w/v) paraformaldehyde and the cover glass was mounted on a glass slide. Biofilms were visualized using a Leica SP8 confocal microscope (Leica Microsystems Inc., Buffalo Grove, IL) under 60× magnification. Background noise was minimized using software provided with the Leica SP8 and three-dimensional z-stack biofilm images were obtained from 30 randomly chosen frames using a z-step size of 0.7 µm. Images were analyzed with Volocity image analysis software (version 6.3; Perkin Elmer, Waltham, MA, USA) to determine the ratio of green to red fluorescence (GR), representing *P. gingivalis* and *S. gordonii*, respectively. Control samples were used to subtract background levels of auto-fluorescence. Briefly, triplicate samples of *S. gordonii* alone were immobilized without *P. gingivalis* or BAR in 12-well culture plates and the same procedures for dual-species biofilm were followed. *S. gordonii*-only coverslips were visualized and images were analyzed as described above. The GR background was subtracted using the following formula: GR sample or control–GR *S. gordonii*-only. Each treatment group (BAR-EFs or free BAR) was analyzed in triplicate and three independent frames were measured for each well. GraphPad InStat (La Jolla, CA) was used for data analysis and differences were considered to be statistically significant when $P \leq 0.05$. The percent inhibition of *P. gingivalis* adherence was calculated with the following formula: GR sample/GR control (Kalia et al., 2017; Mahmoud et al., 2018).

Biofilm Disruption Assay

The same procedures utilized in the inhibition assay were followed, except *P. gingivalis* was allowed to adhere to streptococci in the absence of BAR peptide or BAR-EFs to demonstrate the ability of BAR-incorporated EFs to disrupt or “treat” pre-established biofilms. The resulting *P. gingivalis*/*S. gordonii* biofilms were then treated for the maximum duration observed for free BAR to disrupt existing biofilms (3 h) (Kalia et al., 2017). Established biofilms were administered BAR-EFs, free BAR or blank EFs at various concentrations in 1 mL PBS, and processed and analyzed as described above. The mean and standard deviation (SD) between samples were determined and the percent disruption of *P. gingivalis* adherence was calculated with the following formula: GR sample/GR control (Kalia et al., 2017; Mahmoud et al., 2018).

Tissue Culture

Telomerase immortalized gingival keratinocytes (TIGKs) were grown on 12-well collagen-coated plates (Becton Dickinson, Bedford, MA) and cultured using DermaLife K Calcium Free Medium (LifeFactors®) supplemented with penicillin/streptomycin (100 U/mL final concentration; St. Louis, MO), insulin (5 µg/mL), recombinant human (rh), L-glutamine (6 mM), apo-transferrin (5 µg/mL), epinephrine (1 µM), rh TGF-α (0.5 ng/mL), extract PTM, calcium chloride (0.06 mM) and hydrocortisone hemisuccinate (100 ng/mL). The cells were incubated at 37°C in the presence of 5% CO₂ for 6 days until they reached 95% confluence (Mahmoud et al., 2019).

Determination of BAR and BAR-EFs Safety *in vitro*

Hemolytic Assay

A sample of 250 μL of 1% sheep erythrocytes (Rockland Inc., Pennsylvania, USA) was suspended in sterile PBS. The IC₅₀ and maximum effective concentrations (1.3 and 3.4 μM , respectively) of free BAR peptide or BAR in 10:90 PLGA:PEO BAR-EFs used in *in vitro* and *in vivo* studies, were added to sheep erythrocytes. Water replaced PBS as a positive control for cell hemolysis. The suspension was incubated at 37°C for 3 h then centrifuged at $3,500 \times g$. Hemoglobin released due to cell lysis was analyzed by measuring the absorbance at 541 nm (Mahmoud et al., 2019).

MTT Assay

TIGK cells were seeded in 12-well plates at a density of 6×10^4 cells in 1 mL media per well and incubated for 24 h to allow for 60–70% confluency and sufficient adhesion. Cells were treated with 1.3 or 3.4 μM of BAR or 10:90 PLGA-PEO BAR-EFs. After 24 h, 100 μL of MTT solution was added to the media of all samples. After 4 h incubation at 37°C, 550 μL of lysis buffer was added to the media of each well and plates were incubated for overnight. The absorbance of each well was read at 570 nm, and the sample absorbance was normalized to the absorbance of medium-only treated cells. Cells were treated with 10% DMSO media (100 μL DMSO in 900 μL media) as a positive control for cell death (Tyo et al., 2017; Mahmoud et al., 2019).

ATP Assay

The metabolic activity of TIGK cells was assessed by measuring total ATP levels using the CellTiter-Glo reagent (Promega, Madison WI), as described by the manufacturer. TIGK cells were seeded at a density of 6×10^4 cells in 1 mL media per well and incubated at 37°C, 5% CO₂ for 24 h in a 12-well flat bottom plate. Cells were then incubated with BAR or 10:90 PLGA-PEO BAR-EFs (1.3 or 3.4 μM) for 24 h at 37°C in 5% CO₂. Cells were then lysed with 500 μL of 0.1% Triton X-100 for 30 min at 37°C. The lysates were collected and centrifuged at $1,000 \times g$ for 10 min at 4°C, and 50 μL of supernatant was mixed with 50 μL of CellTiter-Glo reagent. Samples were incubated at ambient temperature for 10 min in a black 96-well plate in the dark. Total luminescence was measured with a Victor 3 luminometer (Perkin-Elmer, Inc.). Cells incubated with 1 ng of staurosporine or with medium-only served as positive and negative controls for cell death, respectively (Mahmoud et al., 2019).

LDH Assay

Cell membrane leakage was measured by assessing the release of lactate dehydrogenase (LDH). Extracellular LDH was quantified using a CytoTox96[®] non-radioactive cytotoxicity assay (Promega, Madison WI) as described by the manufacturer. TIGK cells were plated at density of 6×10^4 cells in 1 mL media per well in a 12-well flat bottom plate, and incubated at 37°C, 5% CO₂ for 24 h. BAR or 10:90 PLGA-PEO BAR-EFs (1.3 or 3.4 μM) were added to cells in triplicate for 24 h at 37°C in 5% CO₂. Fifty microliters of supernatant from free BAR and BAR-EF-treated (1.3 and 3.4 μM) cells were added to the LDH substrate and incubated at room temperature for 30 min. Then

the reactions were terminated by adding 50 μL of stop solution. LDH activity was determined by measuring the optical density of the solution at 490 nm. Cells incubated with staurosporine or with medium-only served as positive and negative controls for toxicity, respectively (Mahmoud et al., 2019).

Oxidative DNA Damage

Free radicals and other reactive species are generated from cells under stress and cause oxidative damage to biomolecules. DNA is the most targeted site of oxidative attack. The apurinic/apyrimidine (AP or abasic) site is a prevalent oxidative DNA damage lesion. OxiSelect[™] Oxidative DNA Damage Quantitation Kit (Cell Biolabs, INC., San Diego, CA, USA) was used to quantify AP sites in cells treated with free BAR or 10:90 PLGA-PEO BAR-EFs (1.3 or 3.4 μM) as described by the manufacturer. TIGK cells were plated at density of 6×10^4 cells in 1 mL media per well in a 12-well flat bottom plate, and incubated at 37°C, 5% CO₂ for 24 h. BAR or BAR-EFs (1.3 or 3.4 μM) were added to cells in triplicate for 24 h at 37°C in 5% CO₂. Cells treated with 2 mM H₂O₂ or medium-only served as positive and negative controls for DNA damage, respectively. Genomic DNA was isolated from TIGK cells by QIAamp DNA Mini kit (Qiagen). AP sites were determined in genomic DNA by using a biotinylated aldehyde reactive probe (ARP) that reacts specifically with an aldehyde group of AP sites, followed by colorimetric detection using a streptavidin–enzyme conjugate (450 nm). The quantity of AP sites in DNA samples was determined by comparing the absorbance with standard curve of known amount of AP sites (Thakur et al., 2018).

Statistical Analysis

Data from each of the toxicity tests were analyzed using ANOVA after passing Bartlett's and Brown-Forsythe tests for homogeneity of variances using GraphPad InStat (La Jolla, CA). A pair-wise, parametric analysis of variance using a Bonferroni multiple comparison *post-hoc* test was used to determine the statistical difference among the individual groups. A $P \leq 0.05$ was considered to be statistically significant.

RESULTS

EF Characterization: EF Morphology, Diameter, BAR Loading, and Release

Fiber morphologies and diameters are shown in **Figures 1, 2**. The average diameters of EFs ranged from 0.7 to 1.3 μm with no statistical significance observed within or across different formulations, as a function of polymer type or blend ratio.

BAR Loading and Release

The overall polymer yield after electrospinning ranged from 40 to 60% for the non-blended fiber formulations, while the blended fibers achieved higher yields spanning 80–90%. The total F-BAR loading for non-blended and blended EFs ranged between 4.6 and 6.9 μg BAR/mg polymer and 6.0–9.2 μg BAR/mg polymer, respectively, indicating that high loading of F-BAR was achieved in all fiber formulations (**Table 1**). To determine the amount of F-BAR release from the different fiber formulations, F-BAR EFs

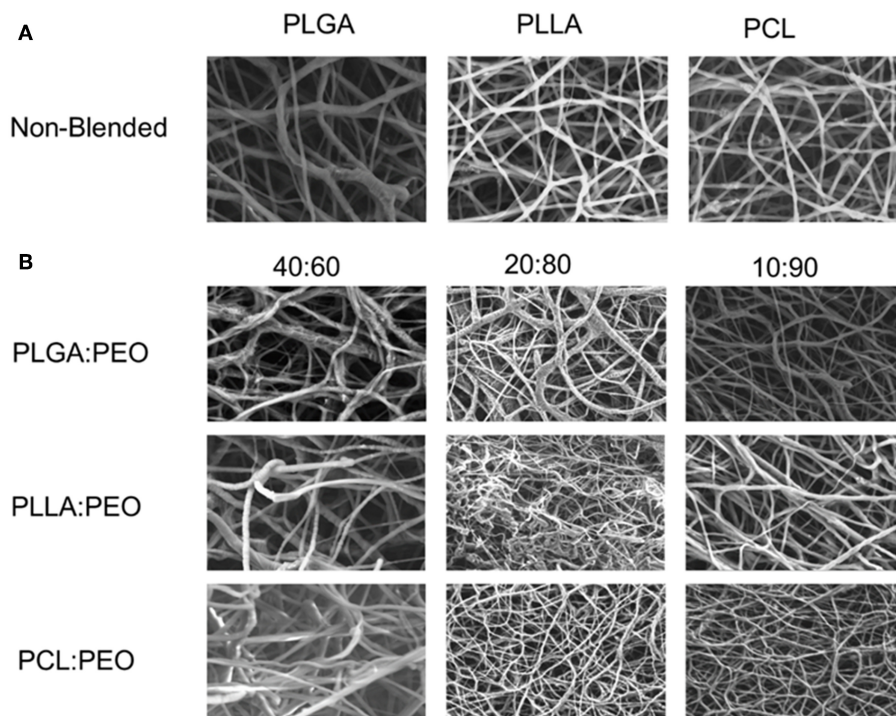


FIGURE 1 | (A) SEM images of 1% w/w BAR PLGA, PLLA, and PCL non-blended fibers. **(B)** SEM images of 40:60, 20:80, and 10:90 1% w/w BAR blended PLGA:PEO, PLLA:PEO, and PCL:PEO fibers.

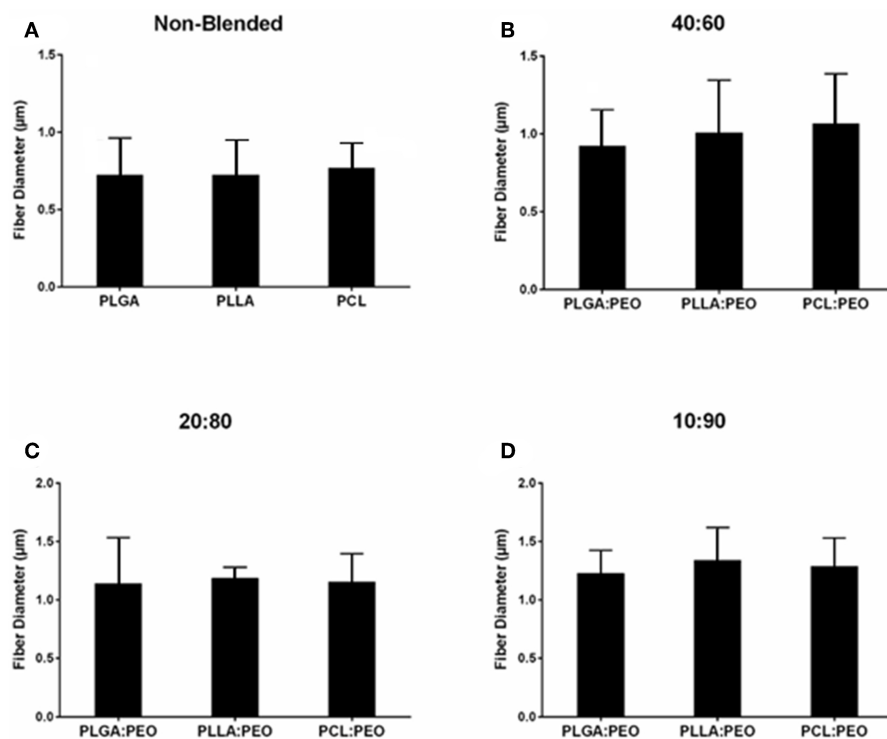


FIGURE 2 | Average diameters of electrospun fibers measured from SEM images, using ImageJ. **(A)** Non-blended and blended **(B)** 40:60, **(C)** 20:80, and **(D)** 10:90 PLGA:PEO, PLLA:PEO, and PCL:PEO 1% w/w BAR fibers. Error bars represent the mean ± the standard deviation (n = 3) of three independent experiments.

were incubated in PBS at 37°C. The fluorescence of the collected supernatant was measured at 1, 2, 4, 8, 12, and 24 h. **Figure 3** shows the cumulative release of F-BAR from non-blended EFs at each time point over a 24 h duration. PLGA EFs demonstrated minimal release of F-BAR (9.5% of total loading) after 24 h, while PLLA and PCL fibers showed even less release during the same duration. Overall, EFs consisting of only hydrophobic polymers (i.e., non-blended formulations) demonstrated minimal release relative to the PEO-blended EFs.

The release of F-BAR from blended PLGA:PEO, PLLA:PEO, and PCL:PEO fibers with different blend ratios (40:60, 20:80, 10:90) as a function of hydrophobic polymer type, is shown in

TABLE 1 | The amount of BAR loaded in non-blended and blended polymeric EF formulations ($\mu\text{g}/\text{mg}$) and percent of total BAR loaded in blended and blended EFs.

Fiber formulation	Blend ratio	Overall polymer yield (%)	Loading BAR/fiber ($\mu\text{g}/\text{mg}$)	Encapsulation efficiency (%)
PLGA	100:0	59.0	6.9 ± 0.1	69 ± 2.5
PCL		51.0	6.0 ± 0.4	60 ± 4.0
PLLA		42.3	4.6 ± 0.6	46 ± 5.2
PLGA:PEO	40:60	82.9	7.4 ± 0.5	74 ± 5.5
PCL:PEO		91.5	8.6 ± 0.2	86 ± 2.4
PLLA:PEO		82.0	9.1 ± 0.3	92 ± 3.1
PLGA:PEO	20:80	80.9	8.8 ± 0.2	88 ± 2.6
PCL:PEO		89.3	8.9 ± 0.4	89 ± 4.0
PLLA:PEO		85.2	8.3 ± 0.4	83 ± 4.2
PLGA:PEO	10:90	82.8	8.8 ± 0.5	88 ± 5.6
PCL:PEO		80.0	6.0 ± 0.4	60 ± 4.0
PLLA:PEO		80.9	8.5 ± 0.3	85 ± 3.5

High loading and encapsulation efficiency were achieved in all fiber formulations. However, non-blended EFs showed comparatively lower polymer yield and encapsulation efficiency, relative to the blended EFs. Data represent the mean \pm standard deviation ($n = 3$) of three independent samples.

Figure 4. The importance of the PEO ratio in each hydrophobic fiber type, is emphasized in **Figure 4**, with the 10:90 formulation providing maximum release of F-BAR for each hydrophobic blend. Fibers comprised of 10:90 PLGA:PEO released $8.39 \pm 0.06 \mu\text{g}$ BAR/mg EF, corresponding to $95 \pm 0.26\%$ of the incorporated F-BAR within the first 4 h, relative to PLLA:PEO and PCL:PEO 10:90 fibers with $76.8 \pm 0.8\%$ and $50.6 \pm 0.8\%$ of F-BAR release, respectively (**Figures 4, 5**). A significant reduction in the release of F-BAR was observed after 4 h for the 10:90 PLGA:PEO EFs and after 8 h for the other 10:90 PEO-blended formulations (**Figure 4**). For the 20:80 blended formulations, the PLGA:PEO fibers showed a maximum release of $88.7 \pm 0.3\%$, compared to PLLA:PEO and PCL:PEO with $62.4 \pm 2.1\%$ and $29.6 \pm 0.06\%$ release, respectively, after 4 h. Similar trends in F-BAR release were observed for the 40:60 formulations with PLGA:PEO exhibiting the maximum release of $81.2 \pm 0.1\%$, and PLLA:PEO and PCL:PEO releasing $50.6 \pm 3.1\%$ and $21.3 \pm 0.2\%$ after 4 h. Of the tested formulations, 40:60 PLGA:PEO, PLLA:PEO, and PCL:PEO released the least F-BAR within the first 4 h, and a significant reduction in release was observed after ~ 4 h for both the 20:80 and 40:60 formulations. Overall, the release trends for the different ratios of polymer blends were similar, with PLGA blends achieving the highest F-BAR release, followed by PLLA and PCL formulations.

P. gingivalis/S. gordonii Biofilm Inhibition

Given that the 10:90 PLGA:PEO blends achieved the highest release of F-BAR, the ability of the 10:90 PLGA:PEO BAR-EFs to inhibit or “prevent” *P. gingivalis* biofilm formation was assessed, relative to the administration of free BAR. To assess inhibition, 10:90 PLGA:PEO BAR-EFs or free BAR were administered to *P. gingivalis* for 24 h. Subsequently, BAR-EF or free BAR-treated *P. gingivalis* was incubated with immobilized *S. gordonii*. As shown in **Figures 6, 8A**, *P. gingivalis* adherence was significantly reduced in the presence of 10:90 PLGA:PEO BAR-EFs. Biofilm formation was inhibited by 31, 42, or 82% by 0.3, 0.7, and $3.0 \mu\text{M}$ BAR-EFs, respectively. The maximum

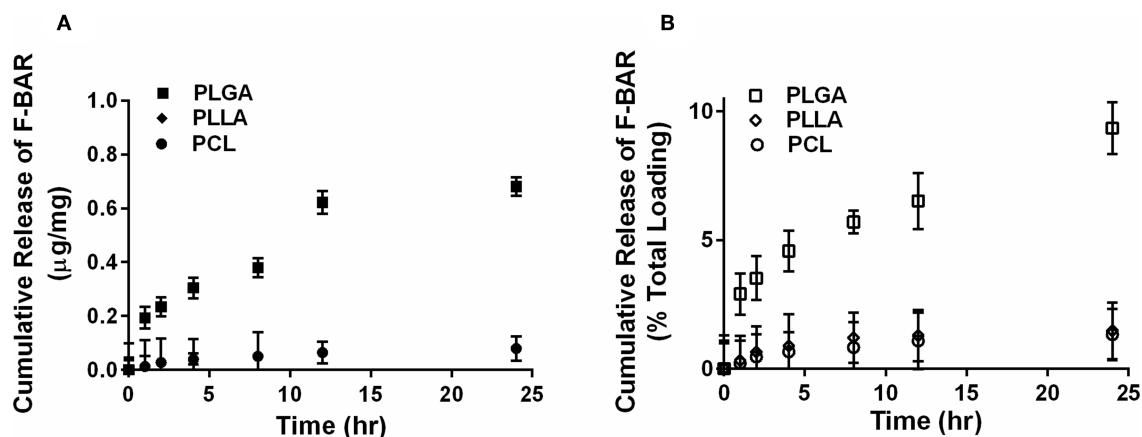


FIGURE 3 | The cumulative release of F-BAR from 1% w/w F-BAR non-blended (100:0) PLGA, PLLA, and PCL fibers. The cumulative release is reported as (A) μg F-BAR per mg of fiber, and (B) percent of total loaded F-BAR. PLGA showed the greatest release of incorporated BAR among the non-blended formulations at 24 h. Error bars represent the mean \pm the standard deviation ($n = 3$) of three independent experiments.

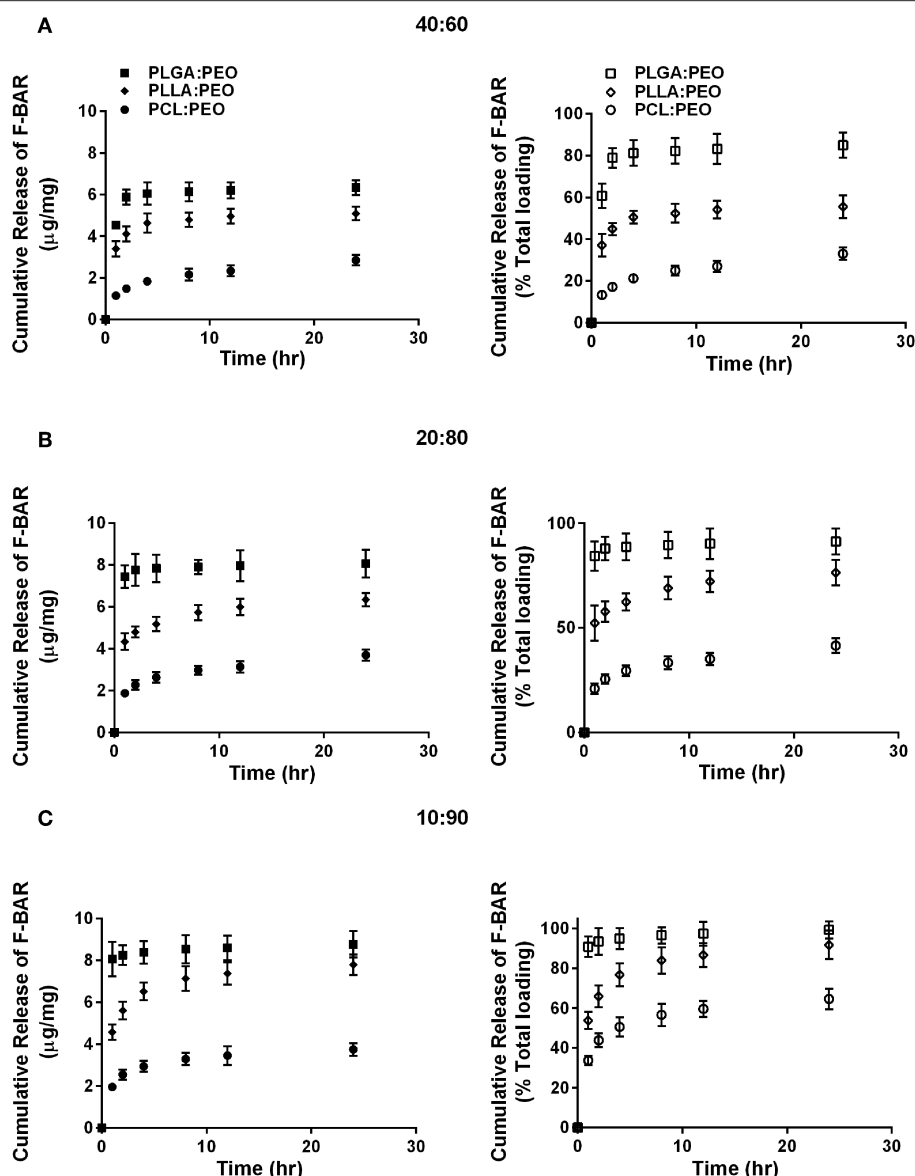


FIGURE 4 | The cumulative release of F-BAR from 1% w/w F-BAR blended PLGA:PEO, PLLA:PEO, and PCL:PEO fibers **(A)** 40:60, **(B)** 20:80, and **(C)** 10:90. The cumulative release is reported as the total quantity of F-BAR released on the left (μg F-BAR per mg of fiber), and as the percent of total loaded F-BAR on the right. Error bars represent the mean \pm the standard deviation ($n = 3$) of three independent experiments.

inhibition observed was similar to the 81% inhibition observed with free BAR ($3\ \mu\text{M}$). BAR-incorporated EFs potently inhibited biofilm formation in a dose-dependent manner ($\text{IC}_{50} = 1.3\ \mu\text{M}$). As expected, no statistical significance ($P > 0.05$) in inhibition was observed between BAR-incorporated EFs and free BAR.

***P. gingivalis*/*S. gordonii* Biofilm Disruption**

The ability of the 10:90 PLGA:PEO BAR-incorporated EFs to disrupt or “treat” pre-existing *P. gingivalis*/*S. gordonii* biofilms was assessed (**Figures 7, 8B**). Dual-species biofilms were formed for 24 h, and were subsequently incubated for 3 h with BAR-incorporated EFs or free BAR. Biofilm formation was disrupted

by 29, 34, or 66% by 0.3, 0.7, and $3.0\ \mu\text{M}$ BAR-EFs. The maximum inhibition observed was similar to the 66% inhibition observed with free BAR ($3\ \mu\text{M}$). Taken together, BAR-EFs exhibited effective biofilm disruption ($\text{IC}_{50} = 2\ \mu\text{M}$) that was similar to free BAR ($P > 0.05$).

Assessment of BAR and BAR-EFs *in vitro* Cytotoxicity

Hemolytic Assay

The cytotoxicity of free BAR and 10:90 PLGA:PEO BAR-EFs was initially assessed by measuring the hemolytic activity against sheep red blood cells (RBCs). As shown in **Figure 9A**, neither

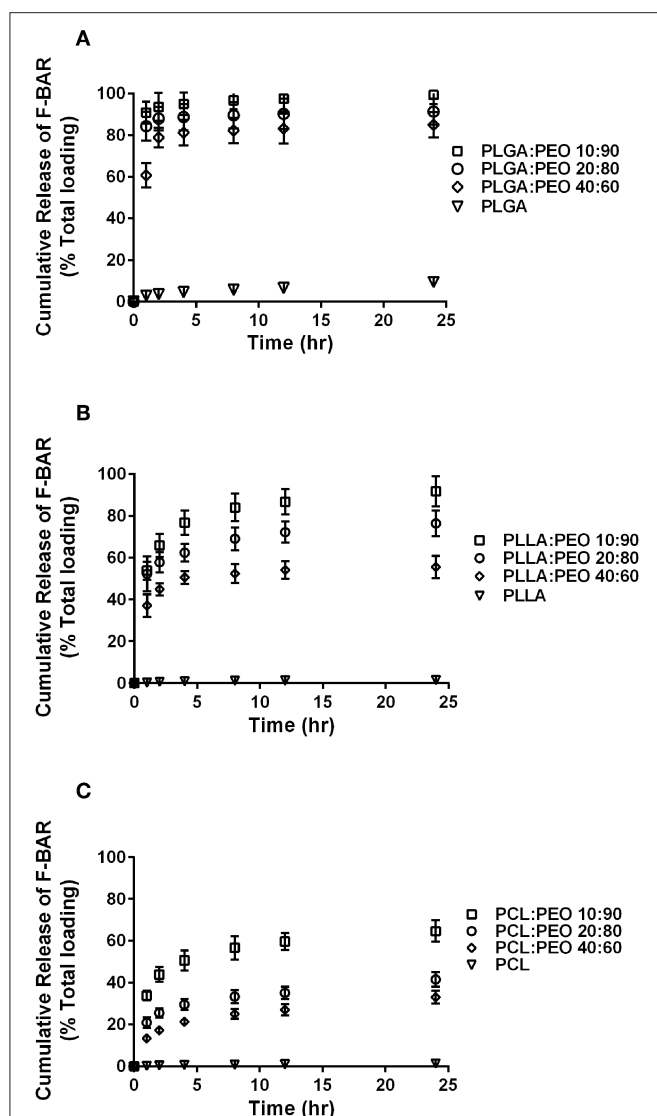


FIGURE 5 | The cumulative release of F-BAR from the non-blended and PEO-blended formulations as a function of hydrophobic polymer type **(A)** PLGA, **(B)** PLLA, or **(C)** PCL and PEO ratio in each blend. The release of encapsulated BAR increases with an increase in PEO fraction. PLGA and PEO blends exhibit the most significant and rapid F-BAR release, relative to PLLA and PCL blends. For all polymer types, the 10:90 blends show the greatest release of BAR as compared to the 20:80 and 40:60 formulations at any given time point. PLGA:PEO (10:90) fibers provide the highest amount of BAR release across formulations. Data represent the mean \pm standard deviation ($n = 3$) of three independent experiments.

free BAR nor BAR-EFs (1.3 or 3.4 μ M BAR) induced hemolysis of RBCs.

MTT Assay

To determine the effect of free BAR or BAR-EFs on TIGK cell viability, cells were treated with free BAR or 10:90 PLGA:PEO BAR-EFs (1.3 or 3.4 μ M) and viability was assessed using the MTT assay. As shown in **Figure 9B**, free BAR (1.3 or 3.4 μ M) treated cells exhibited no loss in viability

($P > 0.05$), while BAR-EF (1.3 or 3.4 μ M) treated cells showed higher viability ($P \leq 0.05$), relative to medium-only treated cells.

ATP Assay

The metabolic activity of TIGK cells was assessed by measuring ATP levels. As shown in **Figure 9C**, cells treated with free BAR (1.3 or 3.4 μ M) or 10:90 PLGA:PEO BAR-EFs (1.3 μ M) showed no decrease in ATP relative to medium-only treated cells, while, cells treated with 10:90 PLGA:PEO BAR-EFs (3.4 μ M) exhibited slightly lower levels of ATP relative to medium-only treated cells (9303.5 ± 1399 and 12094 ± 181 relative light units (RLUs), respectively, $P \leq 0.01$). Staurosporine-treated cells demonstrated significantly lower levels of ATP ($P \leq 0.0001$) than were observed for medium-only, free BAR, and 10:90 PLGA:PEO BAR-EF treated cells.

LDH Assay

Since some peptides are known to damage the cell membrane, LDH released in the cell media was evaluated as a marker for cell membrane integrity after free BAR or 10:90 PLGA:PEO BAR-EF treatment. **Figure 9D** shows that free BAR or BAR-EFs (1.3 or 3.4 μ M) induced no change in levels of LDH released from cells, relative to medium-only treated cells. However, staurosporine induced a significantly higher level of LDH released from TIGK cells relative to cells treated with medium-only, free BAR, and BAR-EFs ($P \leq 0.0001$).

Oxidative DNA Damage

The number of AP sites was determined as an oxidative stress marker for cells treated with free BAR or 10:90 PLGA:PEO BAR-EFs (1.3 or 3.4 μ M). As shown in **Figure 10**, free BAR or BAR-EF treated (1.3 or 3.4 μ M) cells demonstrated no change in the number of AP sites relative to medium-only treated cells, while cells treated with 2 mM H_2O_2 exhibited a significant increase in the number of AP sites relative to free BAR, BAR-EFs (1.3 or 3.4 μ M), and medium-only treated cells ($***P \leq 0.001$). These results suggested that neither free BAR nor BAR-EFs (1.3 or 3.4 μ M) induce oxidative stress in TIGK cells.

DISCUSSION

One of the primary challenges facing the translation of active agents to clinical periodontitis therapy is the delivery and retention of efficacious concentrations of agent within the oral cavity. Local drug delivery vehicles in the form of films (Shifrovitch et al., 2009), strips (Friesen et al., 2002; Leung et al., 2005), and wafers (Bromberg et al., 2000) have been applied to periodontal disease, where the subgingival pockets act as a natural reservoir for these drug-loaded carriers. However, the methods used to fabricate these dosage forms include solvent casting, melt spinning and direct milling methods, which often prove to be labor intensive, time consuming, expensive, and potentially detrimental to the incorporation of more labile biological agents. Delivery platforms such as nanoparticles have also been investigated for both oral delivery and periodontitis applications by our group (Kalia et al., 2017; Mahmoud et al.,

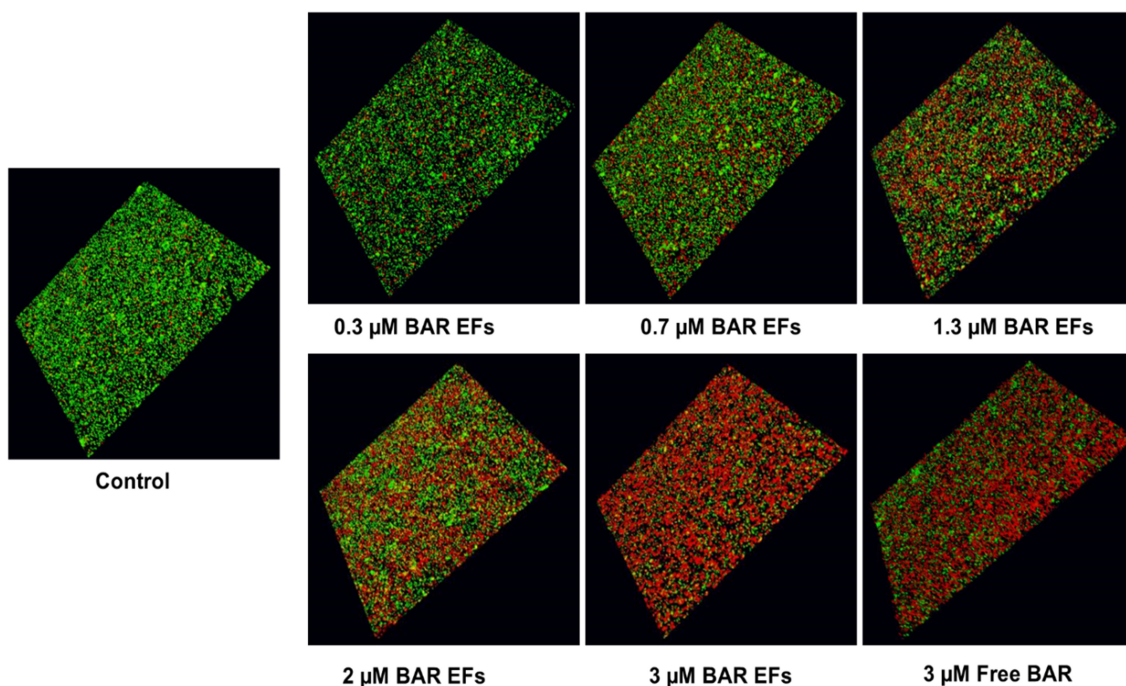


FIGURE 6 | BAR-incorporated PLGA:PEO (10:90) EFs prevent *P. gingivalis* adherence to *S. gordonii*. Biofilms were visualized with confocal microscopy and the ratio of green (*P. gingivalis*) to red (*S. gordonii*) fluorescence in z-stack images was determined using Volocity image analysis software. Each grid represents 21 μm .

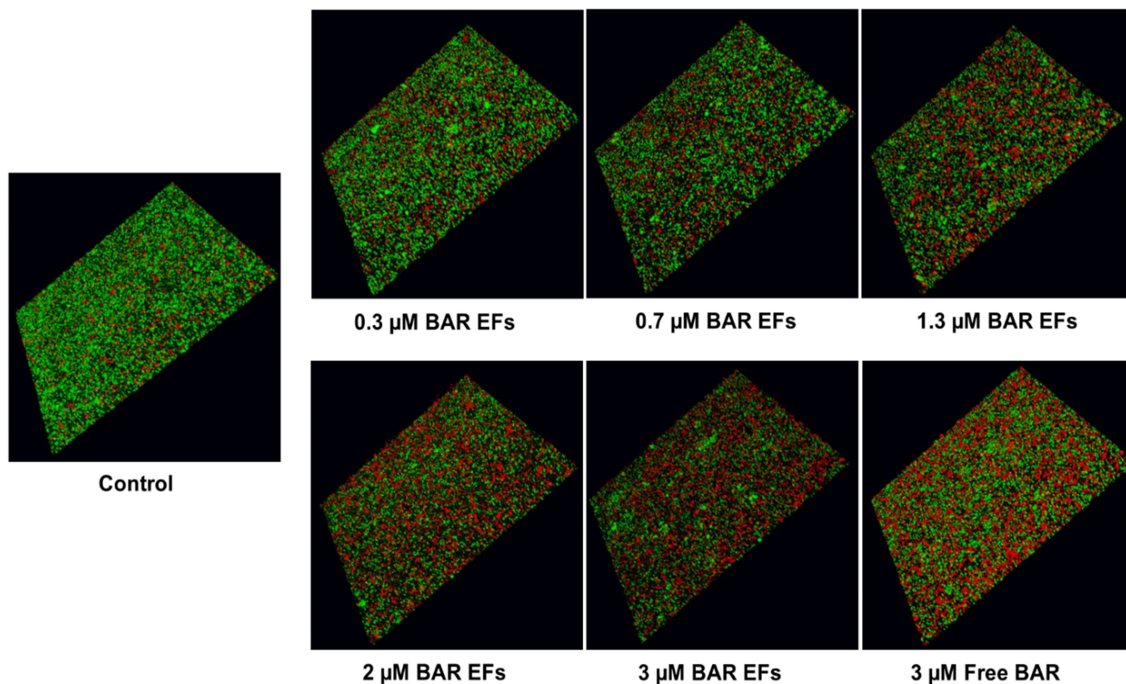


FIGURE 7 | BAR-incorporated PLGA:PEO (10:90) EFs disrupt pre-established *P. gingivalis*-*S. gordonii* biofilms. Biofilms were visualized with confocal microscopy and the ratio of green (*P. gingivalis*) to red (*S. gordonii*) fluorescence in z-stack images was determined using Volocity image analysis software. Each grid represents 21 μm .

2018, 2019) and others (Napimoga et al., 2012; Seneviratne et al., 2014; Yao et al., 2014) to localize active agent delivery to the oral cavity (Napimoga et al., 2012; Seneviratne et al.,

2014; Yao et al., 2014; Abou Neel et al., 2015; Kalia et al., 2017; Mahmoud et al., 2018, 2019). However, encapsulant release is less easily modulated, due to the large surface area and limited

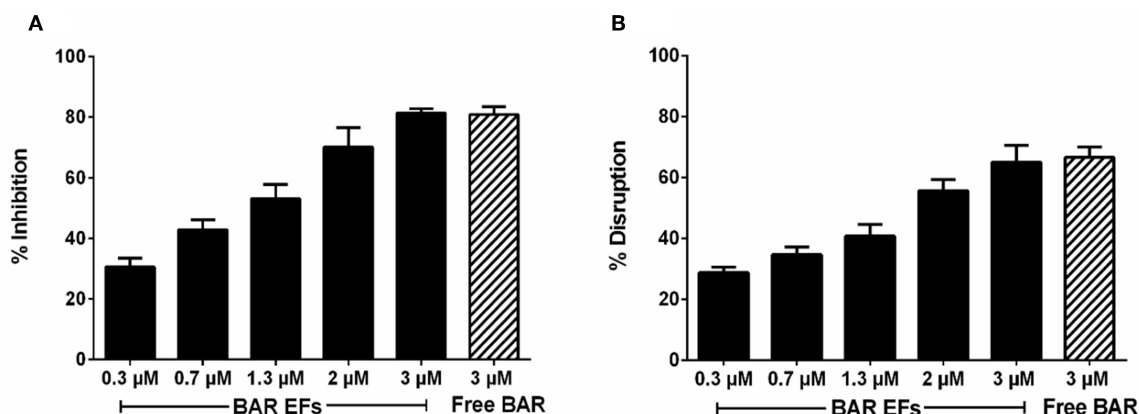


FIGURE 8 | (A) Biofilm inhibition (prevention) and **(B)** disruption (treatment), as a function of different concentrations of BAR-incorporated PLGA:PEO (10:90) EFs and free BAR (3 μ M). Data represent the mean \pm standard deviation ($n = 6$) of six independent experiments.

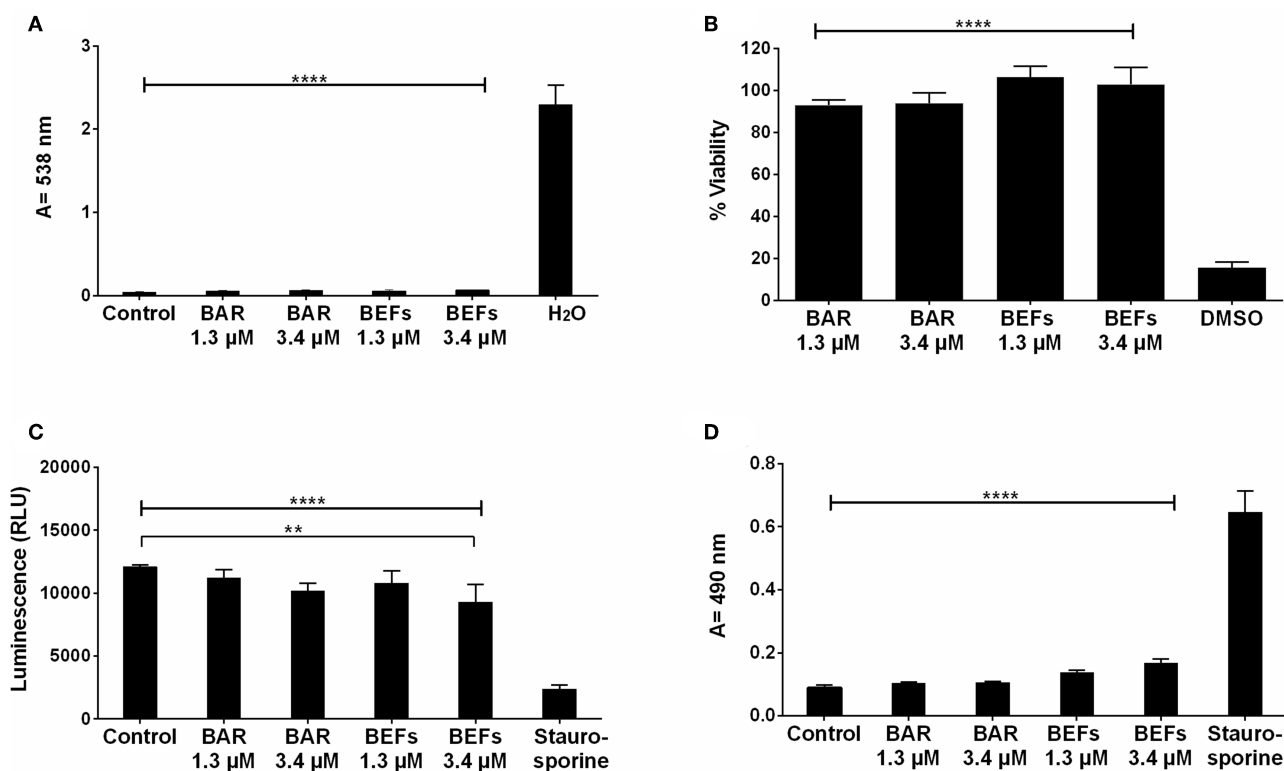
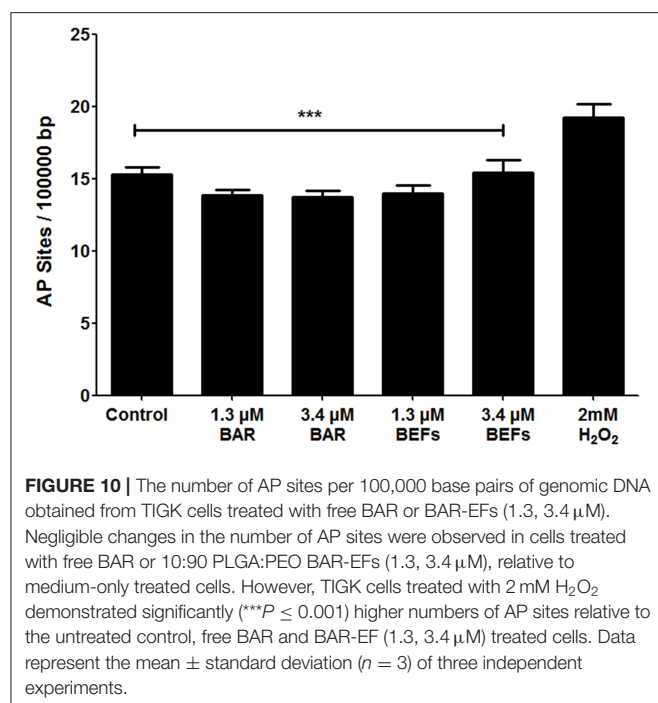


FIGURE 9 | (A) The hemolytic activity of free BAR or 10:90 PLGA:PEO BAR-EFs (1.3, 3.4 μ M) was assessed after administration to sheep erythrocytes for 3 h. Free BAR and BAR-EFs showed negligible hemolysis for sheep erythrocyte relative to release from H₂O-treated cells (**** $P \leq 0.0001$). **(B)** The effect of free BAR and BAR-EFs (1.3, 3.4 μ M) on TIGK cell viability was assessed. Free BAR and BAR-EFs were non-toxic, relative to cells treated with DMSO (**** $P \leq 0.0001$). **(C)** Metabolic activity of cells treated with free BAR or BAR-EFs (1.3, 3.4 μ M) was assessed. BAR-EF (3.4 μ M) treated cells showed decreases in ATP levels relative to medium-only treated cells, while TIGK cells treated with staurosporine demonstrated lower ATP levels than the cells treated with medium-only, free BAR, and BAR-EFs (** $P \leq 0.01$, **** $P \leq 0.0001$). **(D)** TIGK cell membrane integrity was assessed after administration of free BAR or BAR-EFs (1.3, 3.4 μ M) by measuring LDH release levels. None of free BAR or BAR-EF (1.3, 3.4 μ M) treated cells released a significant level of LDH relative to medium-only treated cells. Staurosporine-treated cells demonstrated significantly elevated LDH levels (**** $P \leq 0.0001$). Data represent the mean \pm standard deviation ($n = 5$) of five independent experiments.

encapsulation efficiency (Gref et al., 1994; Kim et al., 2004). Moreover, nanoparticles may be “washed away” with saliva, resulting in lower retention in, and inadequate delivery to the oral cavity, necessitating increased doses to achieve efficacy.

In contrast, EFs, produced using a time and cost-efficient electrospinning process, can offer several advantages relative to other dosage forms. Some of these advantages include, the large surface-to-volume ratio of EFs, which can provide increased



contact between the encapsulated bioactive molecule and the surrounding tissue, promoting release; high encapsulation efficiency, important for more labile biological molecules; mechanical stability and durability within the surrounding environment (Su et al., 2009); and importantly, the ability to tailor drug release, with for example, immediate, smooth, pulsatile, delayed, and biphasic release profiles (Sundararaj et al., 2013; Falde et al., 2015). In addition, fibers have the capacity to serve as a more durable delivery vehicle, providing enhanced retention and ensuring active agent release within the oral cavity, relative to the digestive tract. The durability of EFs may also offer a more convenient administration method, similar to films, but with the capability of providing prolonged release in desired applications. Given these attributes (Morie et al., 2016), we envisioned that designing EFs for administration to the oral cavity may provide a new dosage form in which to administer BAR, relative to the administration of free BAR, and a mechanism to improve therapeutic outcomes by increasing the localized concentration of, and in future work, retention of BAR. While we initially sought to test the capabilities of more rapid-release fibers for twice-daily applications, long-term we envision BAR-EFs may be administered similarly to rapid-release dental strips or as more slowly degradable implants to eliminate the need for surgical removal.

To date, polymeric EFs have been used in several biomedical applications including wound dressing materials (Liu et al., 2017), tissue regeneration (Inanç et al., 2009; Yang et al., 2009), and as drug delivery vehicles for bioactive molecules, antimicrobial agents (Chaturvedi et al., 2013), anti-inflammatory drugs (Batool et al., 2018), and anesthetics (Zafar et al., 2016). For periodontal applications, PLGA fibers have acted as cell scaffolds (Inanç et al., 2009), and have been combined with

other polymers including PCL and PLA to deliver traditional antibiotics such as doxycycline (Chaturvedi et al., 2013) and metronidazole for the localized treatment of periodontitis (Zamani et al., 2010; Reise et al., 2012). However, hydrophobic-only fibers have exhibited delivery limitations such as poor wettability, combined with inadequate flexibility and stiffness properties. Despite this, these and other more biodegradable fiber types such as polydioxanone and PLA:PCL/gelatin fibers incorporating ciproflaxin and tetracycline respectively, have significantly inhibited periodontal pathogens (Bottino et al., 2014; Shahi et al., 2017). However, these fiber types have focused on the delivery of non-specific antibiotics that may have adverse effects on healthy microbiota in the oral cavity.

Given this delivery potential combined with our observed specific targeting with BAR peptide (Kalia et al., 2017; Mahmoud et al., 2018, 2019), we sought to fabricate and compare non-blended (hydrophobic-only polymeric fibers) with blended BAR-incorporated EFs using a uniaxial electrospinning approach. We initially formulated 1% w/w (BAR/polymer) EFs, resulting in a theoretical loading of 10 μ g BAR per mg of polymer, a concentration shown in our previous work to inhibit biofilm formation. All resulting EFs demonstrated high F-BAR loading; however, the release kinetics of the non-blended PLGA, PLLA, and PCL fibers revealed minimal release of F-BAR over 24 h. We attributed the high hydrophobicity of the non-blended PLGA, PLLA, and PCL fibers to minimal eluate penetration past the outermost fiber layer. Moreover, hydrophobic sequences in BAR peptide may promote hydrophobic interactions with the purely hydrophobic non-blended fibers, resulting in lower release.

While hydrophobic polymers have been used in numerous applications outside of the oral cavity, to obtain time frames of release relevant to oral delivery (here, twice-daily), we sought to modulate fiber hydrophobicity with the addition of hydrophilic PEO in ratios (PLGA/PLA/PCL:PEO 40:60, 20:80, and 10:90). In addition, varying of EFs processing variables and type of materials resulted in diameter, porosity, and morphology changes that can regulate the drug profile (Huang et al., 2006). Previous work has shown that blending hydrophobic polymers with more hydrophilic polymers increases the release of biological molecules such as lysozyme, while maintaining protein activity (Li et al., 2008). In addition, many studies have shown that the addition of PEO to protein solutions can improve protein stability (Casper et al., 2005; Li et al., 2006, 2008) and increase mucoadhesivity (Choi et al., 2014), which may help to increase retention in future applications. Moreover, recent work has demonstrated that the incorporation of PEO within hydrophobic fibers increases pore formation and fiber weight loss, prompting more rapid degradation relative to non-blended fibers (Kim et al., 2007; Evrova et al., 2016).

In agreement with other studies (Evrova et al., 2016), increasing the fiber hydrophilicity with the addition of PEO significantly improved BAR release from the blended fibers. Moreover, the incorporation of PEO enabled rapid degradation, eliminating the need for fiber removal after administration. Last, while hydrophilic molecules have been

shown to have more affinity to and miscibility with PEO (enabling release), we postulate that the electrospinning process itself can impact encapsulant location, particularly within hydrophobic:hydrophilic blended fibers, prompting variable release kinetics. That is, electrospinning may promote F-BAR aggregation near the fiber surface, due to charge repulsion (Szentivanyi et al., 2011), contributing to the burst release observed in all blended fibers. Among the hydrophobic polymers, PLGA EFs demonstrated the highest release at early time points, followed by PLLA and PCL formulations. We propose that the increased release of BAR from PLGA EFs is attributed to its amorphous and less hydrophobic properties, relative to the more hydrophobic PLLA and PCL polymers, while PCL:PEO EFs demonstrated the least release due to their crystalline and slightly more hydrophobic characteristics.

Although EFs demonstrated high encapsulation efficiency, potentially inhibited biofilm formation, and disrupted pre-existing biofilms, they demonstrated burst release within 4 h and minimal release thereafter. To achieve the IC₅₀ of BAR (4 µg/mL) over a duration of 12 h, we acknowledge that loading capacity and release must be increased and optimized, respectively. The fibers fabricated in this study were formulated with 1% w/w BAR/polymer, as previous work has shown that fibers fabricated with a theoretical loading higher than 1% w/w, using a uniaxial blended spinning process, may result in significant initial burst release (Kim et al., 2004). In future work, techniques like co-axial or emulsion electrospinning may be adopted to increase loading and optimize release kinetics while maintaining peptide stability (Li et al., 2010; Sebe et al., 2015). Several studies have used co-axial electrospinning to sustain the release and maintain the bioactivity of biological molecules since aqueous solutions and solvents can remain separate during the electrospinning process (Ji et al., 2010). Alternatively, emulsion electrospinning may help to encapsulate hydrophilic agents within the core, thereby providing more sustained and incremental release (Li et al., 2010).

In addition to achieving delivery and retention within the oral cavity, the penetration and disruption of complex biofilms is an obstacle to delivery, which is not fully reflected in *in vitro* models. Achieving high localized concentrations within the oral cavity has traditionally required the administration of elevated doses, which may induce adverse effects (van Winkelhoff et al., 2000). However, a delivery system, such as fibers, that can facilitate ease of administration, while localizing doses applied directly to the subgingival pocket or as topically administered dental strips, may be one option to improve efficacy and overcome toxicity challenges associated with high dose and repeated administrations. To meet these needs, both non-degradable and lesser studied degradable vehicles have been developed for the delivery of antibiotics as primary or adjunct therapies and some are commercially available (Friesen et al., 2002; Kenawy et al., 2002; Ahuja et al., 2003; Aimetti et al., 2004; Kim et al., 2004; Zamani et al., 2010; Batool et al., 2018). However, the utilization of non-biodegradable vehicles requires surgical removal, which can increase the risk of infection

and foreign body response (Vyas et al., 2000). Conversely, a degradable delivery platform, such as those described here, for intra-pocket or topical administration may eliminate the need for removal and avoid the risk of associated infection and immune response.

In addition to minimizing surgery and/or surgical intervention, the specific localization or “targeting” of active agents and delivery vehicles, can enhance their efficacy against periodontal diseases and decrease adverse effects (Maze et al., 1996). Many broadly active mucoadhesive materials such as carboxymethyl cellulose (CMC) (Cai et al., 2017), polyacrylic acid (Carbopol) (Kilicarslan et al., 2014); polyethylene glycol (PEG) (Endo et al., 2013) and polyvinyl alcohol (PVA) (Nafee et al., 2003) have been integrated to improve agent adhesion and retention in the oral cavity; however, these are non-specific approaches that facilitate adhesion to all oral tissue. An alternative approach is to exploit specific protein-protein interactions that drive interspecies coaggregation between oral organisms that promote adhesion and infection within specific niches in the oral cavity. One of these proteins, coaggregation factor A (CafA) (Reardon-Robinson et al., 2014), is known to facilitate *Actinomyces/Streptococcus* coaggregation in the oral cavity (Reardon-Robinson et al., 2014). Thus one strategy to improve BAR-EF delivery and retention in future work is to surface-modify BAR-EFs with CafA for targeting to streptococcal cells. These advancements may be helpful in achieving dual-targeting via BAR and CafA as intra-pocket delivery systems, in which fibers can be immobilized in the subgingival pocket for a longer duration. Thus in ongoing work, we are focused on the development of targeted EFs to enhance retention and adherence to specific bacterial targets in the oral cavity. Ultimately, advanced formulations that extend release and target keystone species via adhesion may be applied once- or twice-daily to localize BAR release and exert enhanced prophylactic effect in the oral cavity without the need to remove the fibers after application.

CONCLUSIONS

Taken together, these results demonstrate the feasibility, versatility, and straightforward approach of electrospinning EFs that release therapeutically-relevant concentrations of BAR, to specifically target periodontal pathogens. In our studies, fibers with increasing PEO content significantly enhanced F-BAR release, while the most promising 10:90 PLGA:PEO formulation provided 95% F-BAR release after 4 h, inhibited biofilm formation in a dose-dependent manner (IC₅₀ = 1.3 µM), and efficiently disrupted dual-species biofilms (IC₅₀ = 2 µM). Our results suggest that BAR-incorporated EFs may provide an alternative and specifically-targeted rapid-release platform to inhibit and disrupt dual-species biofilms, that we envision may be applied twice-daily to exert prophylactic effect in the oral cavity without the need to remove the fibers after application. Future studies will be focused on optimizing the release kinetics of BAR from blended EFs for more sustained durations of 12–24 h, by utilizing

altered fabrication procedures like emulsion and co-axial electrospinning (Li et al., 2010; Sebe et al., 2015).

DATA AVAILABILITY STATEMENT

The datasets generated for this study are available on request to the corresponding author.

AUTHOR CONTRIBUTIONS

MM and SS performed the experiments, statistical analysis, and drafted the manuscript. KC imaged electrospun fibers by using scanning electron microscopy. JS-R conceived of the study, participated in its design and coordination, reviewed experimental data, and drafted the manuscript. DD conceived of the study, participated in its design and coordination, reviewed

experimental data, and drafted the manuscript. All authors read and approved the final manuscript.

FUNDING

This work was supported by grants R01DE023206 and R21DE025345 from the National Institute for Dental and Craniofacial Research and from grant GM125504 and from COBRE grant P20-GM125504 from the National Institute of General Medical Sciences.

ACKNOWLEDGMENTS

An abstract comprised of parts of this study was presented on March 24, 2017 at the International Association of Dental Research Meeting in San Francisco, CA.

REFERENCES

- Abou Neel, E. A., Bozec, L., Perez, R. A., Kim, H. W., and Knowles, J. C. (2015). Nanotechnology in dentistry: prevention, diagnosis, and therapy. *Int. J. Nanomed.* 10, 6371–6394. doi: 10.2147/IJN.S86033
- Ahuja, A., Ali, J., Sarkar, R., Shareef, A., and Khar, R. K. (2003). Targeted retentive device for oro-dental infections: formulation and development. *Int. J. Pharm.* 259, 47–55. doi: 10.1016/s0378-5173(03)00204-7
- Aimetti, M., Romano, F., Torta, I., Cirillo, D., Caposio, P., and Romagnoli, R. (2004). Debridement and local application of tetracycline-loaded fibres in the management of persistent periodontitis: results after 12 months. *J. Clin. Periodontol.* 31, 166–172. doi: 10.1111/j.0303-6979.2004.00457.x
- Allaker, R. P., and Ian Douglas, C. W. (2015). Non-conventional therapeutics for oral infections. *Virulence* 6, 196–207. doi: 10.4161/21505594.2014.983783
- Batool, F., Morand, D. N., Thomas, L., Bugueno, I. M., Aragon, J., Irusta, S., et al. (2018). Synthesis of a novel electrospun polycaprolactone scaffold functionalized with ibuprofen for periodontal regeneration: an *in vitro* and *in vivo* study. *Materials* 11:580. doi: 10.3390/ma11040580
- Bottino, M. C., Arthur, R. A., Waeiss, R. A., Kamocki, K., Gregson, K. S., and Gregory, R. L. (2014). Biodegradable nanofibrous drug delivery systems: effects of metronidazole and ciprofloxacin on periodontopathogens and commensal oral bacteria. *Clin. Oral Investig.* 18, 2151–2158. doi: 10.1007/s00784-014-1201-x
- Bromberg, L. E., Brame, V. M., Rothstein, D. M., Spacciapoli, P., O'Connor, S. M., Nelson, E. J., et al. (2000). Sustained release of silver from periodontal wafers for treatment of periodontitis. *J. Control. Release* 68, 63–72. doi: 10.1016/s0168-3659(00)00233-9
- Brooks, W., Demuth, D. R., Gil, S., and Lamont, R. J. (1997). Identification of a *Streptococcus gordonii* SspB domain that mediates adhesion to *Porphyromonas gingivalis*. *Infect. Immun.* 65, 3753–3758.
- Cai, X., Han, B., Liu, Y., Tian, F., Liang, F., and Wang, X. (2017). Chlorhexidine-loaded amorphous calcium phosphate nanoparticles for inhibiting degradation and inducing mineralization of type I collagen. *ACS Appl. Mater. Interfaces* 9, 12949–12958. doi: 10.1021/acsami.6b14956
- Casper, C. L., Yamaguchi, N., Kiick, K. L., and Rabolt, J. F. (2005). Functionalizing electrospun fibers with biologically relevant macromolecules. *Biomacromolecules* 6, 1998–2007. doi: 10.1021/bm050007e
- Chaturvedi, T. P., Srivastava, R., Srivastava, A. K., Gupta, V., and Verma, P. K. (2013). Doxycycline poly E-caprolactone nanofibers in patients with chronic periodontitis – a clinical evaluation. *J. Clin. Diagn. Res.* 7, 2339–2342. doi: 10.7860/JCDR/2013/5858.3519
- Choi, S. G., Lee, S. E., Kang, B. S., Ng, C. L., Davaa, E., and Park, J. S. (2014). Thermosensitive and mucoadhesive sol-gel composites of paclitaxel/dimethyl-beta-cyclodextrin for buccal delivery. *PLoS ONE* 9:e109090. doi: 10.1371/journal.pone.0109090
- Chou, S. F., and Woodrow, K. A. (2017). Relationships between mechanical properties and drug release from electrospun fibers of PCL and PLGA blends. *J. Mech. Behav. Biomed. Mater.* 65, 724–733. doi: 10.1016/j.jmbbm.2016.09.004
- Daep, C. A., James, D. M., Lamont, R. J., and Demuth, D. R. (2006). Structural characterization of peptide-mediated inhibition of *Porphyromonas gingivalis* biofilm formation. *Infect. Immun.* 74, 5756–5762. doi: 10.1128/IAI.00813-06
- Daep, C. A., Lamont, R. J., and Demuth, D. R. (2008). Interaction of *Porphyromonas gingivalis* with oral streptococci requires a motif that resembles the eukaryotic nuclear receptor box protein-protein interaction domain. *Infect. Immun.* 76, 3273–3280. doi: 10.1128/IAI.00366-08
- Daep, C. A., Novak, E. A., Lamont, R. J., and Demuth, D. R. (2011). Structural dissection and *in vivo* effectiveness of a peptide inhibitor of *Porphyromonas gingivalis* adherence to *Streptococcus gordonii*. *Infect. Immun.* 79, 67–74. doi: 10.1128/IAI.00361-10
- Darveau, R. P., Hajishengallis, G., and Curtis, M. A. (2012). *Porphyromonas gingivalis* as a potential community activist for disease. *J. Dent. Res.* 91, 816–820. doi: 10.1177/0022034512453589
- Drisko, C. H. (1996). Non-surgical pocket therapy: pharmacotherapeutics. *Ann. Periodontol.* 1, 491–566. doi: 10.1902/annals.1996.1.1.491
- Eke, P. I., Dye, B. A., Wei, L., Slade, G. D., Thornton-Evans, G. O., Borgnakke, W. S., et al. (2015). Update on prevalence of periodontitis in adults in the United States: NHANES 2009 to 2012. *J. Periodontol.* 86, 611–622. doi: 10.1902/jop.2015.140520
- Endo, K., Ueno, T., Kondo, S., Wakisaka, N., Muro, S., Ito, M., et al. (2013). Tumor-targeted chemotherapy with the nanopolymer-based drug NC-6004 for oral squamous cell carcinoma. *Cancer Sci.* 104, 369–374. doi: 10.1111/cas.12079
- Evrova, O., Hosseini, V., Milleret, V., Palazzolo, G., Zenobi-Wong, M., Sulser, T., et al. (2016). Hybrid randomly electrospun poly(lactic-co-glycolic acid):poly(ethylene oxide) (PLGA:PEO) fibrous scaffolds enhancing myoblast differentiation and alignment. *ACS Appl. Mater. Interfaces* 8, 31574–31586. doi: 10.1021/acsami.6b11291
- Falde, E. J., Freedman, J. D., Herrera, V. L., Yohe, S. T., Colson, Y. L., and Grinstaff, M. W. (2015). Layered superhydrophobic meshes for controlled drug release. *J. Control. Release* 214, 23–29. doi: 10.1016/j.jconrel.2015.06.042
- Friesen, L. R., Williams, K. B., Krause, L. S., and Killoy, W. J. (2002). Controlled local delivery of tetracycline with polymer strips in the treatment of periodontitis. *J. Periodontol.* 73, 13–19. doi: 10.1902/jop.2002.73.1.13
- Garg, T., Singh, O., Arora, S., and Murthy, R. (2012). Scaffold: a novel carrier for cell and drug delivery. *Crit. Rev. Ther. Drug Carrier Syst.* 29, 1–63. doi: 10.1615/critrevtherdrugcarriersyst.v29.i1.10
- Gref, R., Minamitake, Y., Peracchia, M. T., Trubetskoy, V., Torchilin, V., and Langer, R. (1994). Biodegradable long-circulating polymeric nanospheres. *Science* 263, 1600–1603. doi: 10.1126/science.8128245
- Griffen, A. L., Beall, C. J., Campbell, J. H., Firestone, N. D., Kumar, P. S., Yang, Z. K., et al. (2012). Distinct and complex bacterial profiles in human

- periodontitis and health revealed by 16S pyrosequencing. *ISME J.* 6, 1176–1185. doi: 10.1038/ismej.2011.191
- Herrera, D., Matesanz, P., Bascones-Martínez, A., and Sanz, M. (2012). Local and systemic antimicrobial therapy in periodontics. *J. Evid. Based Dent. Pract.* 12, 50–60. doi: 10.1016/S1532-3382(12)70013-1
- Huang, Z. M., He, C. L., Yang, A., Zhang, Y., Han, X. J., Yin, J., et al. (2006). Encapsulating drugs in biodegradable ultrafine fibers through co-axial electrospinning. *J. Biomed. Mater. Res. A* 77, 169–179. doi: 10.1002/jbm.a.30564
- Inanç, B., Arslan, Y. E., Seker, S., Elcin, A. E., and Elcin, Y. M. (2009). Periodontal ligament cellular structures engineered with electrospun poly(DL-lactide-co-glycolide) nanofibrous membrane scaffolds. *J. Biomed. Mater. Res. A* 90, 186–195. doi: 10.1002/jbm.a.32066
- Ji, W., Yang, F., van den Beucken, J. J., Bian, Z., Fan, M., Chen, Z., et al. (2010). Fibrous scaffolds loaded with protein prepared by blend or coaxial electrospinning. *Acta Biomater.* 6, 4199–4207. doi: 10.1016/j.actbio.2010.05.025
- Jun, Z., Hou, H. Q., Schaper, A. H., Wendorff, J., and Greiner, A. (2003). Poly-L-lactide nanofibers by electrospinning—influence of solution viscosity and electrical conductivity on fiber diameter and fiber morphology. *E-Polymers* 3. doi: 10.1515/epoly.2003.3.1.102
- Kalia, P., Jain, A., Radha Krishnan, R., Demuth, D. R., and Steinbach-Rankins, J. M. (2017). Peptide-modified nanoparticles inhibit formation of *Porphyromonas gingivalis* biofilms with *Streptococcus gordonii*. *Int. J. Nanomed.* 12, 4553–4562. doi: 10.2147/IJN.S139178
- Kassebaum, N. J., Bernabé, E., Dahiya, M., Bhandari, B., Murray, C. J., and Marcenes, W. (2014). Global burden of severe periodontitis in 1990–2010: a systematic review and meta-regression. *J. Dent. Res.* 93, 1045–1053. doi: 10.1177/0022034514552491
- Kenawy el, R., Bowlin, G. L., Mansfield, K., Layman, J., Simpson, D. G., Sanders, E. H., et al. (2002). Release of tetracycline hydrochloride from electrospun poly(ethylene-co-vinylacetate), poly(lactic acid), and a blend. *J. Control. Release* 81, 57–64. doi: 10.1016/S0168-3659(02)00041-X
- Kilicarslan, M., Koerber, M., and Bodmeier, R. (2014). In situ forming implants for the delivery of metronidazole to periodontal pockets: formulation and drug release studies. *Drug Dev. Ind. Pharm.* 40, 619–624. doi: 10.3109/03639045.2013.873449
- Kim, K., Luu, Y. K., Chang, C., Fang, D., Hsiao, B. S., Chu, B., et al. (2004). Incorporation and controlled release of a hydrophilic antibiotic using poly(lactide-co-glycolide)-based electrospun nanofibrous scaffolds. *J. Control. Release* 98, 47–56. doi: 10.1016/j.jconrel.2004.04.009
- Kim, T. G., Lee, D. S., and Park, T. G. (2007). Controlled protein release from electrospun biodegradable fiber mesh composed of poly(epsilon-caprolactone) and poly(ethylene oxide). *Int. J. Pharm.* 338, 276–283. doi: 10.1016/j.ijpharm.2007.01.040
- Leung, W. K., Jin, L., Yau, J. Y., Sun, Q., and Corbet, E. F. (2005). Microflora cultivable from minocycline strips placed in persisting periodontal pockets. *Arch. Oral Biol.* 50, 39–48. doi: 10.1016/j.archoralbio.2004.08.002
- Li, C., Vepari, C., Jin, H. J., Kim, H. J., and Kaplan, D. L. (2006). Electrospun silk-BMP-2 scaffolds for bone tissue engineering. *Biomaterials* 27, 3115–3124. doi: 10.1016/j.biomaterials.2006.01.022
- Li, W. J., Laurencin, C. T., Caterson, E. J., Tuan, R. S., and Ko, F. K. (2002). Electrospun nanofibrous structure: a novel scaffold for tissue engineering. *J. Biomed. Mater. Res.* 60, 613–621. doi: 10.1002/jbm.10167
- Li, X., Su, Y., Liu, S., Tan, L., Mo, X., and Ramakrishna, S. (2010). Encapsulation of proteins in poly(L-lactide-co-caprolactone) fibers by emulsion electrospinning. *Colloids Surf. B Biointerfaces* 75, 418–424. doi: 10.1016/j.colsurf.2009.09.014
- Li, Y., Jiang, H., and Zhu, K. (2008). Encapsulation and controlled release of lysozyme from electrospun poly(epsilon-caprolactone)/poly(ethylene glycol) non-woven membranes by formation of lysozyme-oleate complexes. *J. Mater. Sci. Mater. Med.* 19, 827–832. doi: 10.1007/s10856-007-3175-6
- Liu, M., Duan, X. P., Li, Y. M., Yang, D. P., and Long, Y. Z. (2017). Electrospun nanofibers for wound healing. *Mater. Sci. Eng. C Mater. Biol. Appl.* 76, 1413–1423. doi: 10.1016/j.msec.2017.03.034
- Mahmoud, M. Y., Demuth, D. R., and Steinbach-Rankins, J. M. (2018). BAR-encapsulated nanoparticles for the inhibition and disruption of *Porphyromonas gingivalis-Streptococcus gordonii* biofilms. *J. Nanobiotechnol.* 16:69. doi: 10.1186/s12951-018-0396-4
- Mahmoud, M. Y., Steinbach-Rankins, J. M., and Demuth, D. R. (2019). Functional assessment of peptide-modified PLGA nanoparticles against oral biofilms in a murine model of periodontitis. *J. Control. Release* 297, 3–13. doi: 10.1016/j.jconrel.2019.01.036
- Marsh, P. D. (1994). Microbial ecology of dental plaque and its significance in health and disease. *Adv. Dent. Res.* 8, 263–271. doi: 10.1177/08959374940080022001
- Maze, G. I., Reinhardt, R. A., Payne, J. B., Maze, C., Baker, R. A., Bouwsma, O. J., et al. (1996). Gingival fluid tetracycline release from bioerodible gels. *J. Clin. Periodontol.* 23, 1133–1136. doi: 10.1111/j.1600-051x.1996.tb01815.x
- Morie, A., Garg, T., Goyal, A. K., and Rath, G. (2016). Nanofibers as novel drug carrier—An overview. *Artif. Cells Nanomed. Biotechnol.* 44, 135–143. doi: 10.3109/21691401.2014.927879
- Nafee, N. A., Ismail, F. A., Boraie, N. A., and Mortada, L. M. (2003). Mucoadhesive buccal patches of miconazole nitrate: *in vitro/in vivo* performance and effect of ageing. *Int. J. Pharm.* 264, 1–14. doi: 10.1016/S0378-5173(03)00371-5
- Napimoga, M. H., da Silva, C. A., Carregaro, V., Farnesi-de-Assunção, T. S., Duarte, P. M., de Melo, N. F., et al. (2012). Exogenous administration of 15d-PGJ2-loaded nanocapsules inhibits bone resorption in a mouse periodontitis model. *J. Immunol.* 189, 1043–1052. doi: 10.4049/jimmunol.1200730
- Pihlstrom, B. L., Michalowicz, B. S., and Johnson, N. W. (2005). Periodontal diseases. *Lancet* 366, 1809–1820. doi: 10.1016/S0140-6736(05)67728-8
- Reardon-Robinson, M. E., Wu, C., Mishra, A., Chang, C., Bier, N., Das, A., et al. (2014). Pilus hijacking by a bacterial coaggregation factor critical for oral biofilm development. *Proc. Natl. Acad. Sci. U.S.A.* 111, 3835–3840. doi: 10.1073/pnas.1321417111
- Reise, M., Wyrwa, R., Müller, U., Zylinski, M., Völpe, A., Schnabelrauch, M., et al. (2012). Release of metronidazole from electrospun poly(L-lactide-co-D/L-lactide) fibers for local periodontitis treatment. *Dent. Mater.* 28, 179–188. doi: 10.1016/j.dental.2011.12.006
- Sebe, I., Szabo, P., Kallai-Szabo, B., and Zelko, R. (2015). Incorporating small molecules or biologics into nanofibers for optimized drug release: A review. *Int. J. Pharm.* 494, 516–530. doi: 10.1016/j.ijpharm.2015.08.054
- Seneviratne, C. J., Leung, K. C., Wong, C. H., Lee, S. F., Li, X., Leung, P. C., et al. (2014). Nanoparticle-encapsulated chlorhexidine against oral bacterial biofilms. *PLoS ONE* 9:e103234. doi: 10.1371/journal.pone.0103234
- Shahi, R. G., Albuquerque, M. T. P., Munchow, E. A., Blanchard, S. B., Gregory, R. L., and Bottino, M. C. (2017). Novel bioactive tetracycline-containing electrospun polymer fibers as a potential antibacterial dental implant coating. *Odontology* 105, 354–363. doi: 10.1007/s10266-016-0268-z
- Shifrovitch, Y., Binderman, I., Bahar, H., Berdicevsky, I., and Zilberman, M. (2009). Metronidazole-loaded bioabsorbable films as local antibacterial treatment of infected periodontal pockets. *J. Periodontol.* 80, 330–337. doi: 10.1902/jop.2009.080216
- Socransky, S. S., Haffajee, A. D., Cugini, M. A., Smith, C., and Kent, R. L. Jr. (1998). Microbial complexes in subgingival plaque. *J. Clin. Periodontol.* 25, 134–144. doi: 10.1111/j.1600-051x.1998.tb02419.x
- Son, W. K., Youk, J. H., Lee, T. S., and Park, W. H. (2004). The effects of solution properties and polyelectrolyte on electrospinning of ultrafine poly(ethylene oxide) fibers. *Polymer* 45, 2959–2966. doi: 10.1016/j.polymer.2004.03.006
- Su, Y., Li, X., Tan, L., Chen, H., and Xiumei, M. (2009). Poly(L-lactide-co-epsilon-caprolactone) electrospun nanofibers for encapsulating and sustained releasing proteins. *Polymer* 50, 4212–4219. doi: 10.1016/j.polymer.2009.06.058
- Sundararaj, S. C., Thomas, M. V., Peyyala, R., Dziubla, T. D., and Puleo, D. A. (2013). Design of a multiple drug delivery system directed at periodontitis. *Biomaterials* 34, 8835–8842. doi: 10.1016/j.biomaterials.2013.07.093
- Szentivanyi, A., Chakradeo, T., Zernetsch, H., and Glasmacher, B. (2011). Electrospun cellular microenvironments: understanding controlled release and scaffold structure. *Adv. Drug Deliv. Rev.* 63, 209–220. doi: 10.1016/j.addr.2010.12.002
- Thakur, S., Dhiman, M., and Mantha, A. K. (2018). APE1 modulates cellular responses to organophosphate pesticide-induced oxidative damage in non-small cell lung carcinoma A549 cells. *Mol. Cell. Biochem.* 441, 201–216. doi: 10.1007/s11010-017-3186-7
- Tyo, K. M., Vuong, H. R., Malik, D. A., Sims, L. B., Alattasi, H., Duan, J., et al. (2017). Multipurpose tenofovir disoproxil fumarate electrospun fibers for the prevention of HIV-1 and HSV-2 infections *in vitro*. *Int. J. Pharm.* 531, 118–133. doi: 10.1016/j.ijpharm.2017.08.061

- van Winkelhoff, A. J., Herrera Gonzales, D., Winkel, E. G., Dellemijn-Kippuw, N., Vandenbroucke-Grauls, C. M., and Sanz, M. (2000). Antimicrobial resistance in the subgingival microflora in patients with adult periodontitis. A comparison between The Netherlands and Spain. *J. Clin. Periodontol.* 27, 79–86. doi: 10.1034/j.1600-051x.2000.027002079.x
- Vyas, S. P., Sihorkar, V., and Mishra, V. (2000). Controlled and targeted drug delivery strategies towards intraperiodontal pocket diseases. *J. Clin. Pharm. Ther.* 25, 21–42. doi: 10.1046/j.1365-2710.2000.00261.x
- Walker, C. B. (1996). The acquisition of antibiotic resistance in the periodontal microflora. *Periodontol.* 2000 10, 79–88. doi: 10.1111/j.1600-0757.1996.tb00069.x
- Yang, F., Both, S. K., Yang, X., Walboomers, X. F., and Jansen, J. A. (2009). Development of an electrospun nano-apatite/PCL composite membrane for GTR/GBR application. *Acta Biomater.* 5, 3295–3304. doi: 10.1016/j.actbio.2009.05.023
- Yao, W., Xu, P., Pang, Z., Zhao, J., Chai, Z., Li, X., et al. (2014). Local delivery of minocycline-loaded PEG-PLA nanoparticles for the enhanced treatment of periodontitis in dogs. *Int. J. Nanomed.* 9, 3963–3970. doi: 10.2147/IJN.S67521
- Zafar, M., Najeeb, S., Khurshid, Z., Vazirzadeh, M., Zohaib, S., Najeeb, B., et al. (2016). Potential of electrospun nanofibers for biomedical and dental applications. *Materials* 9:73. doi: 10.3390/ma9020073
- Zamani, M., Morshed, M., Varshosaz, J., and Jannesari, M. (2010). Controlled release of metronidazole benzoate from poly epsilon-caprolactone electrospun nanofibers for periodontal diseases. *Eur. J. Pharm. Biopharm.* 75, 179–185. doi: 10.1016/j.ejpb.2010.02.002

Conflict of Interest: The authors declare that the research was conducted in the absence of any commercial or financial relationships that could be construed as a potential conflict of interest.

Copyright © 2020 Mahmoud, Sapare, Curry, Demuth and Steinbach-Rankins. This is an open-access article distributed under the terms of the Creative Commons Attribution License (CC BY). The use, distribution or reproduction in other forums is permitted, provided the original author(s) and the copyright owner(s) are credited and that the original publication in this journal is cited, in accordance with accepted academic practice. No use, distribution or reproduction is permitted which does not comply with these terms.



Immobilized Acylase PvdQ Reduces *Pseudomonas aeruginosa* Biofilm Formation on PDMS Silicone

Jan Vogel, Marijke Wakker-Havinga, Rita Setroikromo and Wim J. Quax*

Chemical and Pharmaceutical Biology Department, University of Groningen, Groningen, Netherlands

OPEN ACCESS

Edited by:

Manuel Simões,
University of Porto, Portugal

Reviewed by:

Harshad Harshad Lade,
Hallym University, South Korea
Uelinton Manoel Pinto,
University of São Paulo, Brazil

*Correspondence:

Wim J. Quax
w.j.quax@rug.nl

Specialty section:

This article was submitted to
Medicinal and Pharmaceutical
Chemistry,
a section of the journal
Frontiers in Chemistry

Received: 21 August 2019

Accepted: 17 January 2020

Published: 05 February 2020

Citation:

Vogel J, Wakker-Havinga M,
Setroikromo R and Quax WJ (2020)
Immobilized Acylase PvdQ Reduces
Pseudomonas aeruginosa Biofilm
Formation on PDMS Silicone.
Front. Chem. 8:54.
doi: 10.3389/fchem.2020.00054

The bacterial biofilm plays a key role in nosocomial infections, especially those related to medical devices in sustained contact with patients. The active dispersion of bacterial cells out of biofilms acts as a reservoir for infectious diseases. The formation of such biofilms is a highly complex process, which is coordinated by many regulatory mechanisms of the pathogen including quorum sensing (QS). Many bacteria coordinate the expression of key virulence factors dependent on their population density through QS. The inhibition of this system is called quorum quenching (QQ). Thus, preventing the development of biofilms is considered a promising approach to prevent the development of hard to treat infections. Enzymatic QQ is the concept of interfering with the QS system of bacteria outside the cell. PvdQ is an acylase with an N-terminal nucleophile (Ntn-hydrolase) that is a part of the pyoverdine gene cluster (*pvd*). It is able to cleave irreversibly the amide bond of long chain N-acyl homoserine lactones (AHL) rendering them inactive. Long chain AHLs are the main signaling molecule in the QS system of the gram-negative pathogen *Pseudomonas aeruginosa* PA01, which is known for surface-associated biofilms on indwelling catheters and is also the cause of catheter-associated urinary tract infections. Furthermore, PA01 is a well characterized pathogen with respect to QS as well as QQ. In this study, we immobilized the acylase PvdQ on polydimethylsiloxane silicone (PDMS), creating a surface with quorum quenching properties. The goal is to control infections by minimizing the colonization of indwelling medical devices such as urinary catheters or intravascular catheters. The enzyme activity was confirmed by testing the degradation of the main auto-inducer that mediates QS in *P. aeruginosa*. In this article we report for the first time a successful immobilization of the quorum quenching acylase PvdQ on PDMS silicone. We could show that immobilized PvdQ retained its activity after the coating procedure and showed a 6-fold reduction of the auto-inducer 3-oxo-C12 in a biosensor setup. Further we report significant reduction of a *P. aeruginosa* PA01 biofilm on a coated PDMS surface compared to the same untreated material.

Keywords: N-Acylhomoserine lactones, acylases, quorum sensing, quorum quenching, surface coating, biofilm

INTRODUCTION

The bacterial colonization of surfaces is an omnipresent observation in almost every environment. However, in healthcare settings biofilms formed by pathogenic bacteria represent a constant threat to the patient's health (Fux et al., 2005). Hospitals follow strict hygiene protocols to keep the clinical environment free of bacteria, however reports show that pathogens can persist for months on surfaces (Kramer et al., 2006). Especially surgical equipment and surfaces need to be sanitized and sterilized, as for example can be seen from the extremely persistent pathogen *Acinetobacter baumannii*. It could be shown that surface attached *Acinetobacter* could withstand dehydration and surface sanitization by ethanol (Harding et al., 2017). Together with *Pseudomonas aeruginosa* this pathogen is a cause for ventilator associated infections (Sievert et al., 2013).

Biofilms can be found on almost every surface ranging from abiotic surfaces to living tissues, such as skin wounds, the lungs and also the teeth. Especially surfaces of medical implants and indwelling medical devices are of importance. In hospital settings indwelling medical devices such as catheters or infusion catheters provide an entryway to the human body making it vulnerable toward bacterial infections (Jacobsen et al., 2008). Since a long time research is being performed to improve urinary catheters especially in respect to minimizing the infection risk by bacteria leading to a catheter-associated urinary tract infections (Lawrence and Turner, 2005). Recently research efforts are being undertaken to reduce the biofilm associated infections by modifying the silicone surface (Swartjes et al., 2013; Ivanova et al., 2015b).

Bacteria organized in a biofilm have been shown to be more resistant to treatment with antibiotics as well as to the host immune system when compared to planktonic pathogens (Ciofu and Tolker-Nielsen, 2010). This has several reasons with one being the protective effect of extracellular polymeric substances and another being the metabolic state of cells persisting within the biofilm. Those cells resemble more the state of cells in the stationary phase (Spoering and Lewis, 2001). In combination with the fact that horizontal gene transfer is promoted within biofilms this creates favorable conditions for the development of resistance of the bacteria (Flemming et al., 2016).

Facing this rise of multidrug resistant pathogenic (MDR) bacteria alternative treatments to antibiotics can be considered to be an effective strategy (Grandclément et al., 2015; Utari et al., 2018). This is generally the case if the patients have to undertake a long term treatment. Accordingly, limiting the formation of biofilms can be beneficial to actively make pathogens more susceptible to antibiotics and also accessible to the host immune response (Brackman et al., 2011; Christensen et al., 2012).

Bacteria can monitor their population density via quorum sensing. Individual cells excrete signaling molecules, so called auto-inducers (Camilli and Bassler, 2006). These signals can be recognized by specialized response regulators which act as transcription factors and play a role in the regulation of various target genes. The auto-inducers do not resemble a single class of molecules but are a diverse group. They differ from gram positive to gram negative bacteria and also within this major groups

there are distinguishable differences. In the case of gram negative bacteria the auto-inducing molecules belong to the class of *N*-acylhomoserine lactones (AHL). AHLs consist of a homoserine ring and an acyl chain that can vary in length (Bassler and Losick, 2006). For many pathogenic bacteria, it could be shown that the expression of virulence factors is controlled in a population density depended manner via QS systems (Christiaen et al., 2014). Amongst these virulence factors are also regulative steps toward biofilm formation and differentiation of bacterial biofilms (Fux et al., 2005).

Data collected in the United States suggests that 7.5% of all general healthcare associated infections are connected to *P. aeruginosa* (Sievert et al., 2013). *P. aeruginosa* is a gram negative opportunistic pathogen, which is also considered a model organism for bacterial biofilms. The formation of differentiated biofilm is a complex process containing a number of regulatory networks. However, it could be shown that the *lasIR* QS circuit plays a major role in the development of a mature biofilm. The *lasI* synthase produces *N*-3-oxo dodecanoyl-homoserine lactone (3-oxo-C12 HSL) (Hentzer et al., 2002).

PvdQ is a Ntn-hydrolase from *P. aeruginosa* PAO1, which is studied as a QQ enzyme aimed at degrading long chain AHLs of gram negative pathogens. All Ntn-Hydrolases share a similar hydrolysis mechanism. The N-terminal amino acid, which can be a serine, cysteine or a threonine launches a nucleophilic attack on the carbonyl carbon of the substrate. This results in a tetrahedral intermediate which is stabilized by residues in the active center (Figure 1B) (Peräkyl and Rouvinen, 1996). Subsequently, the α -amino group of the nucleophile donates its proton to the nitrogen of the scissile peptide bond. This results in the formation of a covalent bond with a part of the substrate, while the leaving amino product is released. In a following deacetylation step the carbonyl group of the acyl-enzyme complex will be cleaved in the presence of water (Duggleby et al., 1995). In the case of PvdQ it could be shown that the acyl group of the AHL perfectly fits into a hydrophobic pocket at the active centre (Figure 1A), placing the amide bond in proximity to the N-terminal nucleophile (Bokhove et al., 2010). It could be successfully utilized to reduce the virulence of *P. aeruginosa* PAO1 in several infection models such as *Caenorhabditis elegans* and a mouse infection model (Papaioannou et al., 2009; Utari et al., 2018).

In this work we constructed a surface with QQ properties utilizing the quenching potential of the acylase PvdQ. The surface of interest in this study is PDMS, which is extensively used to make urinary catheters. Many groups worldwide are working on surface modifications for this material (Diaz Blanco et al., 2014; Francesko et al., 2016). This is the first time a successful immobilization of the acylase PvdQ derived from *P. aeruginosa* was performed. The chosen immobilization technique is based on electrostatically interactions and thus makes it possible to work under mild conditions for the protein (Figure 2) (Ivanova et al., 2015a). Furthermore we present proof of enzyme attachment to the surface as well as confirm its activity with a biosensor based activity assay. The functionalized surface shows a significantly lower level of colonialization than compared to untreated PDMS. This strategy

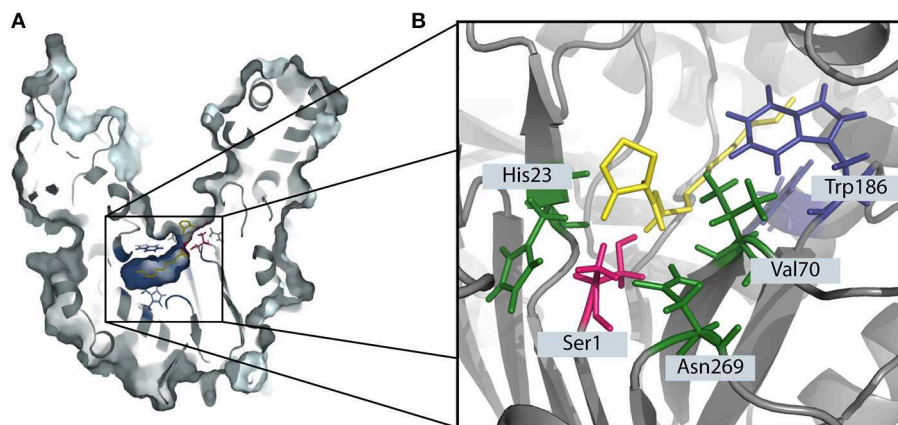


FIGURE 1 | The degradation of 3-oxo-C12 HSL by the Ntn-hydrolase PvdQ. **(A)** The crystal structure of PvdQ (PDB ID: 2WYC) shows the orientation 3-oxo-C12 HSL in the hydrophobic binding pocket (indicated in blue). The N-terminal amino acid serine (highlighted in pink) launches a nucleophilic attack on the amid bond of the auto-inducer. **(B)** The amino acids Val70, His23, and Asn269 in the active center stabilize the transition state, forming the oxyanion hole. Hydrophobic AA such as Trp186 form a hydrophobic pocket.

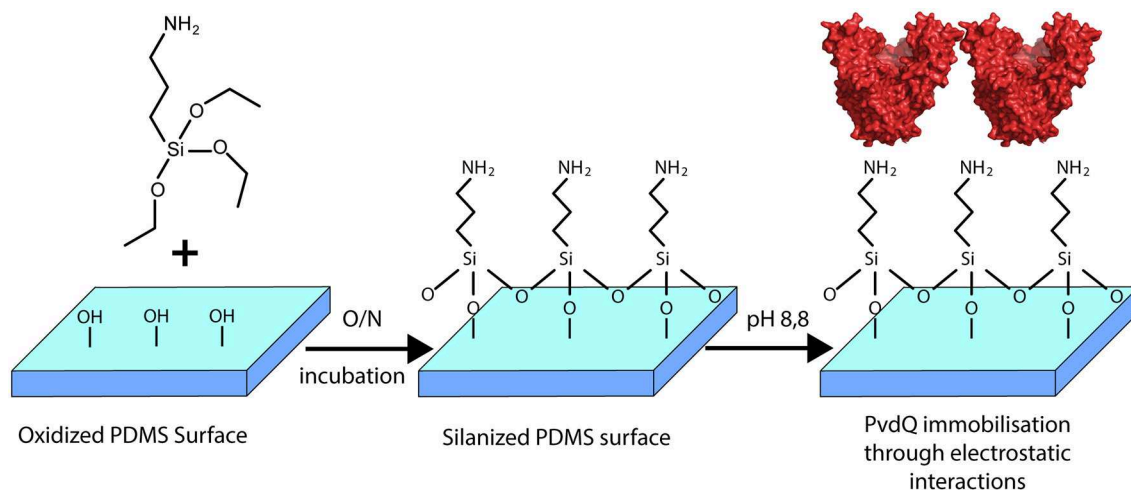


FIGURE 2 | Overview of the surface modification with PvdQ. PDMS silicone surface is treated with (APTES) introducing free amid bonds to the surface. In the chosen pH conditions, due to the negative charge of PvdQ, the protein attaches electrostatically to the surface.

may be used to degrade the QS signaling pathway of gram-negative bacteria to interfere with the biofilm formation on PDMS surfaces.

MATERIALS AND METHODS

Bacterial Strains and Growing Condition

P. aeruginosa PAO1 was obtained from Barbara Iglewski (University of Rochester Medical Center, Rochester, NY) (Sio et al., 2006). The overnight cultures of the biosensors were prepared by inoculating a loop of frozen glycerol stock in Luria Bertani (LB) medium, followed by incubation at 37°C, 200 rpm. *E. coli* JM109 pSB1142 was inoculated in LB and incubated at 37°C, 200 rpm with selective AB supplementation (Winson et al., 1998).

PDMS Silicone

The polydimethylsiloxane was prepared using a Sylgard 184 elastomer kit acquired from Dow Corning, VWR chemicals, Amsterdam, The Netherlands, and the preparation was done according to the supplier's information. PDMS samples were prepared by mixing the silicone elastomer base and silicone curing agent at a weight ratio of 10:1. To prevent bubble formation, the mixture was degassed under vacuum, providing a 1 mm thick PDMS substrate. Molds were placed in an oven and cured at 70°C overnight. The surface roughness of the PDMS was measured using atomic force microscopy (AFM) model Dimension 3100 Nanoscope V system (Veeco, Plainview, NY, USA) in contact mode and with 0.24 N/m tips. All data were processed using Nanoscope Analysis (Veeco, Version 1.70). The surface roughness was calculated

on a $5 \times 5 \mu\text{m}^2$ region. The mean surface roughness (Ra) was 3 nm.

Activity Assay

The enzymatic degradation of long chain AHLs was measured by employing the biosensor strain *E. coli JM109* carrying the reporter plasmid pSB1142 (Winson et al., 1998). The vector is containing a *lux* operon, which is under control of a *lasI* promoter. The corresponding transcription factor is the quorum sensing response regulator LasR. Upon the binding of long chain AHLs ranging from C10 to C14 carbon chains the activated response regulator LasR upregulates the *Lux* operon and thus detects their presence with light emission. The amount of light produced by the biosensor was measured every 5 min during a 15 h time course in a multifunctional microplate reader (FLUOstar Omega, BMG Labtech). Data points obtained immediately prior to maximum light production were used for comparisons.

The activity of the immobilized enzyme PvdQ was assessed with this biological assay. In brief, PDMS slices of 3×15 mm were incubated in 400 μl 50 mM Tris-Cl pH 8.8 containing 0.1 mM 3-oxo-C12 HSL. The PDMS samples were incubated for 24 h at 30°C shaking at 100 rpm. After the incubation 100 μl of the buffer solution was used for the biosensor assay. Measurements were performed three times in individual experiments in quadruplicates.

PvdQ Purification

PvdQ was produced and purified as reported previously (Bokhove et al., 2010). In short: *E. coli DH10B* carrying the plasmid pMCT_PvdQ was grown in 2xTY medium containing 16 g/l Tryptone, 10 g/l Yeast extract, 5 g/l as well as chloramphenicol (50 $\mu\text{g}/\text{mL}$) for 30 h at 30°C, 200 rpm. The cells were harvested and sonicated in a three times volume of lysis buffer (50 mM Tris Cl pH 8.8; 2 mM EDTA). Cell lysate was centrifuged at 17,000 rpm for 1 h. All purification steps were performed with an Äkta Pure system from GE Healthcare Life Sciences. The clear lysate was applied to an anion exchange HiTrap Q-sepharose column, PvdQ can be detected in the flow through. Next purification step is with a hydrophobic interaction phenyl sepharose column, for this the flow through is diluted in buffer with 2.8 M ammonium sulfate concentration to a final concentration of 750 mM. PvdQ could be detected at the end of the ammonium sulfate gradient elution step. Lastly the flow through was applied to a gel filtration superdex75 16/60 column. PvdQ was collected and stored at -80°C until further use. All protein chromatography columns were obtained from GE Healthcare Life Sciences.

Fluorochrome Labeling of PvdQ

To be able to detect PvdQ on the PDMS surface, 200 μl PvdQ was first labeled with 20 μl FITC thiocyanate (0.1 mg/50 μl DMF) overnight at 4°C according to manufacturer's manual. The unbound FITC was removed with a PD10 Desalting column (GE Healthcare). The labeled protein was incubated together with respective PDMS slices of 5×15 mm to confirm the attachment of the protein to the PDMS surface. All experiments were done with the same batch of labeled PvdQ.

Biofilm Assay

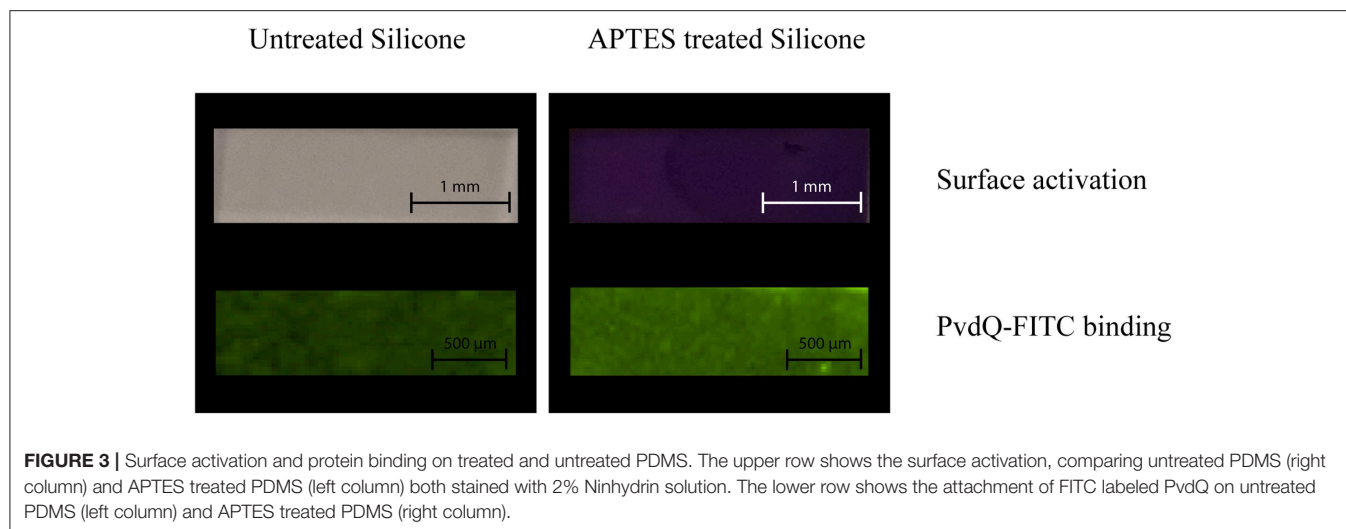
The ability of *P. aeruginosa* strains to attach to surfaces as an initial step of the biofilm formation was tested by using Crystal violet staining. The attached cell mass was determined by a biofilm assay published by O'Tool et al. with modifications (O'Toole, 2010). Briefly, bacterial strains were grown overnight at 37°C and were diluted in LB broth to a concentration of OD 0.8. Aliquots of 100 μl were added to wells of a 96-well plate containing a PDMS piece (3×15 mm) and incubated at 37°C for 3 h to allowing the bacteria to adhere to the surface. The medium and planktonic cells were removed and the PDMS slices were washed three times with 200 μl PBS. The Biofilms were fixed for 60 min at 60°C and stained using 150 μl 0.1% (v/v) crystal violet solution for 15 min. The PDMS slices were washed in distilled water, and the water was removed. The plate containing the PDMS slices was then air-dried and the dye was eluted with 110 μl 33% acetic acid. The signal was measured using a FLUOstar Omega plate reader (BMG Labtech) at a wavelength of 585 nm. Measurements were performed in three biological repetitions consisting of 4 replications each. The reduction of cell mass was assessed by comparing treated and untreated samples. As a negative control to assess the amount of background dye which is staining PDMS an additional staining was performed with wells only containing PDMS and medium without bacterial cells. This was considered the technical negative control.

RESULTS

Attachment of QQ Acylase PvdQ to PDMS Silicone

As a proof of principle to confirm the activation of the PDMS surface as well as the attachment of the acylase PvdQ to this activated surface we performed the following experiment before proceeding to activity assays. The PDMS was washed and the surface activation was confirmed by immersing the PDMS in a 2% Ninhydrin solution. As shown in **Figure 3** an APTES treated PDMS sample incubated in Ninhydrin solution shows a clear deep purple signal confirming the uniform activation of the surface. The comparison to a piece of PDMS which was not pre-treated with APTES acted as a control experiment. **Figure 3** clearly shows no color staining and hence indicates that there is no surface modification. After proofing the success of the surface activation, the conditions were used for all the following coating experiments. The negative net charge of the acylase PvdQ under this conditions was confirmed by a measurement of the zeta potential (**Table S1**). The chosen pH conditions and the resulting negative net charge of PvdQ make it possible to perform a protein immobilization based on electrostatic interactions between surface and enzyme.

Next, we confirmed the binding of FITC labeled PvdQ to the activated PDMS. For this the APTES activated PDMS surface was incubated in a 1.5 mg/ml solution of the acylase PvdQ for 24 h. The chosen buffer conditions were set to a pH of 8.8. To proof a successful attachment of the enzyme, we used FITC labeled PvdQ acylase and incubated it together with pretreated PDMS under storage buffer conditions for 24 h. The immobilized PvdQ acylase



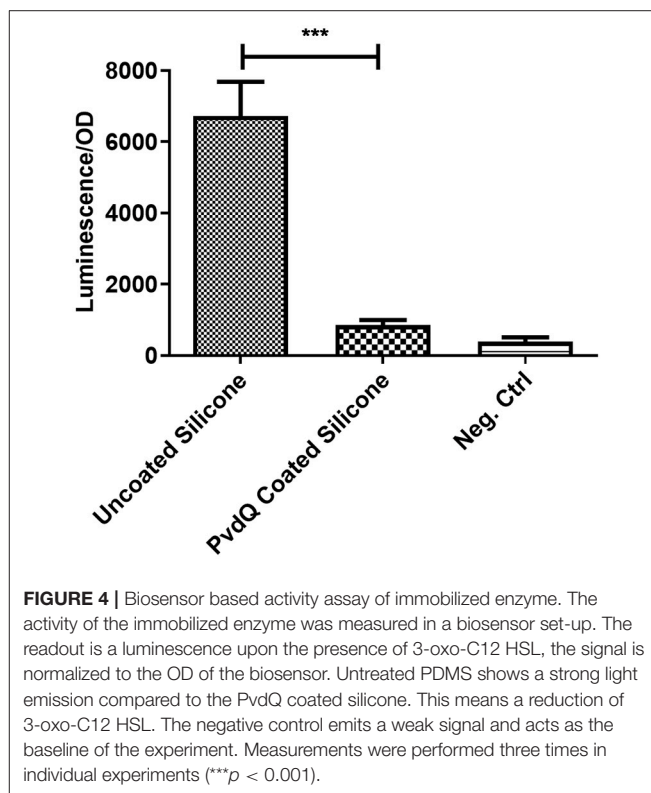
on the surface was visualized under UV light. FITC labeled PvdQ could clearly be recognized on the PDMS surface under UV light (**Figure 3**). The same experiment was performed with non APTES activated PDMS showing a residual luminescence which was significantly less than the PDMS with the APTES activated surface (**Figure 3**). This experiment clearly confirms the attachment of the acylase PvdQ to the surface.

Activity of Immobilized QQ Enzyme PvdQ

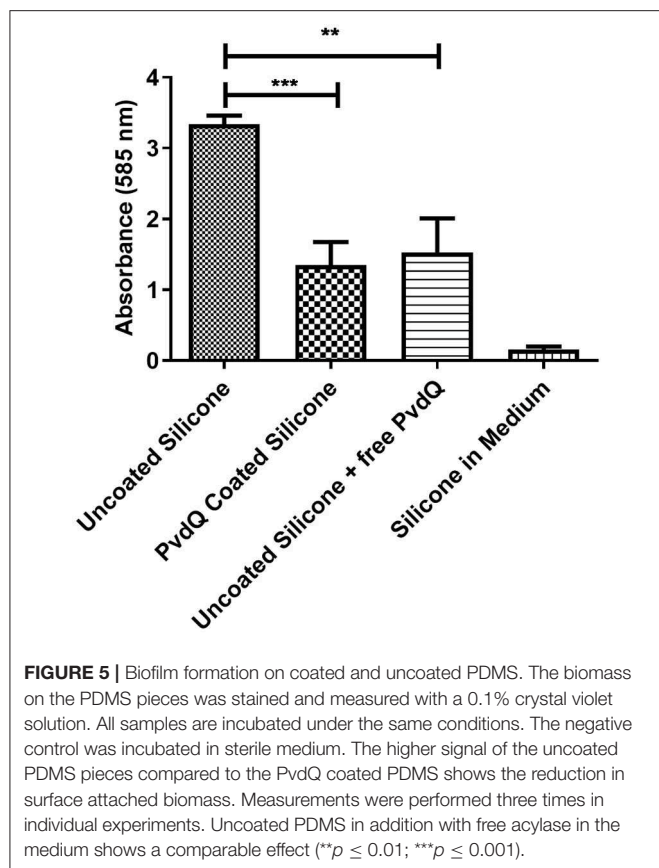
To assess the activity of the immobilized enzyme, the coated PDMS was incubated for 24 h at 30°C in the presence of 3-oxo-C12 HSL. This molecule is the main auto-inducer of the pathogenic bacterium *P. aeruginosa*. Previous studies showed that this signaling molecule is involved in the biofilm formation and hence is the molecule of interest for this study (de Kievit, 2009). In this experiment the presence of AHLs was determined in a biosensor setup. After the incubation time the quenching ability was measured by comparing the AHL levels after incubation in the set-ups with coated and uncoated PDMS slices. In the set-up with the uncoated PDMS (**Figure 4**) a high luminescence signal of the biosensor system can be observed indicating the presence of AHLs. Compared to the same set-up including the PDMS with the immobilized acylase PvdQ a 6-fold reduction in luminescence is visible, showing that the enzyme is able to degrade the signal molecule and thus shows activity. As a positive control free acylase in solution was used to confirm that the assay shows the right sensitivity to measure QQ activity. This experiment confirms a successful functionalization of a PDMS surface with QQ properties.

Inhibition of Biofilm Formation

After confirming that the PDMS silicone surface was functionalized with QQ properties we were investigating if the QQ potency of the treated PDMS surface has an impact on the capability of *P. aeruginosa* PAO1 cells to attach to the surface and form a biofilm. For this purpose we grew a biofilm on PDMS slices by submerging coated and uncoated PDMS slices in complex medium inoculated with *P. aeruginosa* PAO1. The cells



were given time to attach to the surface and the biomass on the PDMS was measured using the crystal violet staining method. Accordingly, the colonization of treated and untreated PDMS was compared to evaluate the reduction in biofilm formation. It could be observed that the initial attachment of bacterial cells was significantly reduced, compared to untreated silicone (**Figure 5**). The absorbance signal resembling the biomass on the PDMS slices shows a reduction of about 50% on the treated surface compared to the untreated surface (**Figure 5**). As a control



experiment untreated PDMS in combination with 500 mg/ml QQ soluble acylase PvdQ was used showing a comparable result. This highlights the similarity between the QQ effect of PvdQ in solution, as well as the quenching effect of the enzyme when immobilized on a surface. To ensure that the biomass staining is not a result of attachment of parts of the complex medium to the PDMS surface, we incubated an uncoated PDMS slide in sterile medium. The measurement confirms that the signal measured represents the attached biomass to the surface and it is not due to unspecific binding of crystal violet to the PDMS surface.

DISCUSSION

Studies have shown that even though the formation of a bacterial biofilm is not solely depending on QS but involves a multitude of different regulatory networks, QS systems play an important role in the formation and differentiation of a mature *P. aeruginosa* biofilm (Stoodley et al., 2002).

In this study we purified the Ntn-hydrolase PvdQ derived from *P. aeruginosa* PAO1 and immobilized it on a silicone surface in a comparable fashion to Ivanova et al. (2015b). One natural function of this enzyme is removing the fatty acid chain from the pyoverdine precursor PVDIq (Nadal-Jimenez et al., 2014). Furthermore, in previous studies we also could show that PvdQ effectively degrades long chain AHLs and has an impact on the virulence of *P. aeruginosa* (Jimenez et al., 2010; Utari et al., 2018).

A first step toward a successful immobilization was to find a surface activation that can be used for the attachment of PvdQ. We performed a surface activation with APTES and we could see a full activation by staining the treated PDMS with a 2% Ninhydrin solution. This confirmed the presence of free amid bonds on the surface. Incubating the treated PDMS in a 1.5 mg/ml solution of FITC labeled PvdQ showed a clear fluorescent signal when viewed under UV light after washing the PDMS slides in distilled water. Based on the UV-Vis measurement of the FITC-conjugated PvdQ we could see that the amount of FITC labeling of the protein was sufficient to observe a clear signal on the PDMS surface. We could see a clear difference between the APTES activated and the untreated PDMS surface as shown in Figure 3. This confirms that PvdQ can be attached via interactions with the APTES activated PDMS surface.

We could show that PvdQ retained its activity when immobilized on the PDMS surface in our experimental conditions. The biosensor set-up showed a 6-fold difference between the sample containing the uncoated PDMS and the sample that harbored the PDMS slice with immobilized PvdQ. The signal reduction represents the quenching of the auto-inducer signal 3-oxo-C12 HSL.

To explore the QQ effect of the PvdQ coated surface we performed a biofilm assay with *P. aeruginosa* PAO1. Most importantly we could show in this biofilm set-up a significant reduction of the attached biofilm on the treated PDMS in comparison to the same material without the immobilized acylase. Comparing the immobilized PvdQ with the soluble PvdQ in combination with untreated PDMS, we could see a similar reduction of attached bacterial cell mass. Both of these set-ups showed a reduced biofilm formation compared to the untreated PDMS without PvdQ. The comparison of the PvdQ treated surface and the untreated surface with added PvdQ leads to the conclusion that the reduction in biomass is indeed due to the quenching ability of PvdQ (Figure S1). Ivanova et al. could show in their research that a surface functionalized with a commercially available acylase preparation from *Aspergillus melleus* can reduce the bacterial biofilm (Ivanova et al., 2015b). In this study we utilized the well-characterized acylase PvdQ, which is here shown to have QQ properties due to activity toward long chain AHLs. It has been shown in our group that this enzyme also has a positive impact on the course of a *P. aeruginosa* induced mouse infection model, which shows the potency of this enzyme as a potential treatment option (Utari et al., 2018).

The reduction of biofilm formation on the PDMS surface shows that the acylase PvdQ can have preventive anti biofilm properties by hindering the initial attachment of *P. aeruginosa* cells, which is mediated by degrading the auto-inducer 3-oxo-C12 HSL. Biofilms are highly organized structures and exhibit a complex architecture. This differentiation requires a high degree of regulation with the involvement of the QS system (Chang, 2018). In *P. aeruginosa* it is known that the las system, which is utilizing 3-oxo-C12 as its cognate signaling molecule, plays a crucial role in the differentiation of the biofilm. A deletion of the las systems leads to a biofilm, which is flat and does not show the same differentiated phenotype as the wild type biofilm (Rasamiravaka et al., 2015). Culturing conditions play an integral

role of the phenotype of the biofilm (Kirisits and Parsek, 2006). In the case of *P. aeruginosa* biofilms it could be shown that under iron limiting conditions, mutations in iron acquisition genes such as *pvdA* have a huge influence on the biofilm morphology (Banin et al., 2005). In this background it is essential for this work to highlight the necessity to explore different growth conditions.

This knowledge can be applied on various medically relevant surfaces especially of indwelling medical devices. PvdQ specifically targets long chain AHLs such as 3-oxo-C12 HSL, which is the main auto-inducer used by *P. aeruginosa* PAO1. Immobilizing this enzyme on a surface provides a surface that shows a significant reduction in the attached cell mass in the initial stage of the biofilm formation, which is the crucial step toward the development of a mature biofilm. This technique has the potential to contribute to novel strategies to prevent nosocomial infections targeting especially pathogens based on their respective QS system.

Furthermore, utilizing QQ strategies as a potential treatment could prove advantageous since it does not apply direct selective pressure on the pathogens. Accordingly, it is hypothesized that the development of resistance strategies is less likely to occur compared to antibiotic treatments.

Treatment options such as QQ are a promising strategy to overcome problems of rising numbers in multi-drug-resistant bacterial infections. On the surface dispersed bacterial cells from biofilms can act as a reservoir for infection. QQ strategies on medical surfaces can reduce the biofilm load which can result in a lower number of biofilm originated pathogens and thereby support the host immune system. In this work we could show that the attachment of *P. aeruginosa* cells to an abiotic PDMS surface could be significantly reduced in laboratory conditions. The potential of PvdQ as a treatment strategy against bacterial infections could be shown in previous studies in our group in which dissolved PvdQ was administered intranasal to the lungs. We could observe a protective effect of PvdQ against a *P. aeruginosa* induced pulmonary infection in a mouse model. Furthermore the same study pointed out that PvdQ does not show any negative effect in the lung environment of the mouse model and can be regarded as safe (Utari et al., 2018). The results presented here show that PvdQ has a positive effect on the biofilm inhibition, however we have to take into account that different environmental factors play a role on the formation of biofilms (Kirisits and Parsek, 2006). Further research has to be conducted to show the potency of PvdQ as possible treatment option under more clinical conditions.

The QQ strategies we present in this work could be tailor made strategies targeting gram negative pathogens such as *P. aeruginosa* and *A. baumannii*, since these organisms communicate with long chain AHLs. Furthermore previous work in our group demonstrated that an engineered PvdQ variant was able to degrade the auto-inducer used by *Burkholderia cenocepacia* and had an positive effect on an performed infection model (Koch et al., 2014). Enzymatic

QQ efforts toward gram positive bacteria are to our knowledge still vastly undiscovered. The only characterized QQ enzyme targeting auto-inducer 2 of gram positive bacteria is the kinase Lsk (Roy et al., 2010). However, its dependency on ATP make this enzyme a difficult candidate as a treatment option.

In conclusion the interference with the QS system with QQ enzymes can be described as a promising strategy to fight infectious diseases. We demonstrate a significant reduction of *P. aeruginosa* cell attachment in the early biofilm state. It is very likely that MDR strains are susceptible toward QS interference and since the treatment does not apply direct evolutionary pressure on the pathogens it is hypothesized that a QQ treatment could be a lasting treatment strategy for longer hospitalized patients. After achieving a successful immobilization of the QQ acylase PvdQ future perspectives are the refinement of the coating technique and a conclusive analysis of its stability as well as studying different environmental conditions for the biofilm formation. The findings presented here open up the way toward investigations applying the immobilized PvdQ in an animal model for catheter applications.

DATA AVAILABILITY STATEMENT

All datasets generated for this study are included in the article/**Supplementary Material**.

AUTHOR CONTRIBUTIONS

WQ was the principal investigator who initiated the project of quorum quenching. JV designed the experiments. MW-H, RS, and JV performed the experiments and analyzed the data. The manuscript was written by JV and was carefully revised by WQ.

FUNDING

The project leading to this application has received funding from the European Union's Horizon 2020 research and innovation program under the Marie Skłodowska-Curie grant agreement no. 713482.

ACKNOWLEDGMENTS

The authors want to thank Dr. Patrick van Rijn for helpful discussions. Putri Dwi Utari for the setup of the QQ assays. Torben van der Boon and Damla Keskin for discussions during the experimental design and Robbert Cool for critically reading the manuscript.

SUPPLEMENTARY MATERIAL

The Supplementary Material for this article can be found online at: <https://www.frontiersin.org/articles/10.3389/fchem.2020.00054/full#supplementary-material>

REFERENCES

- Banin, E., Vasil, M. L., and Greenberg, E. P. (2005). Iron and *Pseudomonas aeruginosa* biofilm formation. *Proc. Natl. Acad. Sci. U.S.A.* 102, 11076–11081. doi: 10.1073/pnas.0504266102
- Bassler, B. L., and Losick, R. (2006). Bacterially speaking. *Cell* 125, 237–246. doi: 10.1016/j.cell.2006.04.001
- Bokhove, M., Nadal Jimenez, P., Quax, W. J., and Dijkstra, B. W. (2010). The quorum-quenching *N*-acyl homoserine lactone acylase PvdQ is an Ntn-hydrolase with an unusual substrate-binding pocket. *Proc. Natl. Acad. Sci. U.S.A.* 107, 686–691. doi: 10.1073/pnas.0911839107
- Brackman, G., Cos, P., Maes, L., Nelis, H. J., and Coenye, T. (2011). Quorum sensing inhibitors increase the susceptibility of bacterial biofilms to antibiotics *in vitro* and *in vivo*. *Antimicrob. Agents Chemother.* 55, 2655–2661. doi: 10.1128/AAC.00045-11
- Camilli, A., and Bassler, B. L. (2006). Bacterial small-molecule signaling pathways. *Science* 311, 1113–1116. doi: 10.1126/science.1121357
- Chang, C.-Y. (2018). Surface sensing for biofilm formation in *Pseudomonas aeruginosa*. *Front. Microbiol.* 8:2671. doi: 10.3389/fmicb.2017.02671
- Christensen, L. D., van Gennip, M., Jakobsen, T. H., Alhede, M., Hougen, H. P., Hoiby, N., et al. (2012). Synergistic antibacterial efficacy of early combination treatment with tobramycin and quorum-sensing inhibitors against *Pseudomonas aeruginosa* in an intraperitoneal foreign-body infection mouse model. *J. Antimicrob. Chemother.* 67, 1198–1206. doi: 10.1093/jac/dks002
- Christiaen, S. E. A., Matthijs, N., Zhang, X.-H., Nelis, H. J., Bossier, P., and Coenye, T. (2014). Bacteria that inhibit quorum sensing decrease biofilm formation and virulence in *Pseudomonas aeruginosa* PAO1. *Pathog. Dis.* 70, 271–279. doi: 10.1111/2049-632X.12124
- Ciofu O., and Tolker-Nielsen T. (2010). “Antibiotic tolerance and resistance in biofilms,” in *Biofilm Infections*, eds T. Bjarnsholt, P. Jensen, C. Moser, and N. Hoiby (New York, NY: Springer), 215–229. doi: 10.1007/978-1-4419-6084-9_13
- de Kievit, T. R. (2009). Quorum sensing in *Pseudomonas aeruginosa* biofilms. *Environ. Microbiol.* 11, 279–288. doi: 10.1111/j.1462-2920.2008.01792.x
- Diaz Blanco, C., Ortner, A., Dimitrov, R., Navarro, A., Mendoza, E., and Tzanov, T. (2014). Building an antifouling zwitterionic coating on urinary catheters using an enzymatically triggered bottom-up approach. *ACS Appl. Mater. Interfaces* 6, 11385–11393. doi: 10.1021/am501961b
- Duggleby, H. J., Tolley, S. P., Hill, C. P., Dodson, E. J., Dodson, G., and Moody, P. C. E. (1995). Penicillin acylase has a single-amino-acid catalytic centre. *Nature* 373, 264–268. doi: 10.1038/373264a0
- Flemming, H.-C., Wingender, J., Szewzyk, U., Steinberg, P., Rice, S. A., and Kjelleberg, S. (2016). Biofilms: an emergent form of bacterial life. *Nat. Rev. Microbiol.* 14, 563–575. doi: 10.1038/nrmicro.2016.94
- Francesko, A., Fernandes, M. M., Ivanova, K., Amorim, S., Reis, R. L., Pashkuleva, I., et al. (2016). Bacteria-responsive multilayer coatings comprising polycationic nanospheres for bacteria biofilm prevention on urinary catheters. *Acta Biomater.* 33, 203–212. doi: 10.1016/j.actbio.2016.01.020
- Fux, C. A., Costerton, J. W., Stewart, P. S., and Stoodley, P. (2005). Survival strategies of infectious biofilms. *Trends Microbiol.* 13, 34–40. doi: 10.1016/j.tim.2004.11.010
- Grandclément, C., Tannières, M., Moréra, S., Dessaux, Y., and Denis, D., Faure (2015). Quorum quenching: role in nature and applied developments. *FEMS Microbiol. Rev.* 40, 86–116. doi: 10.1093/femsre/fuv038
- Harding, C. M., Hennon, S. W., and Feldman, M. F. (2017). Uncovering the mechanisms of *Acinetobacter baumannii* virulence. *Nat. Rev. Microbiol.* 16, 91–102. doi: 10.1038/nrmicro.2017.148
- Hentzer, M., Riedel, K., Rasmussen, T. B., Heydorn, A., Andersen, J. B., Parsek, M. R., et al. (2002). Inhibition of quorum sensing in *Pseudomonas aeruginosa* biofilm bacteria by a halogenated furanone compound. *Microbiology* 148, 87–102. doi: 10.1099/00221287-148-1-87
- Ivanova, K., Fernandes, M. M., Francesko, A., Mendoza, E., Guezguez, J., Burnet, M., et al. (2015a). Quorum-quenching and matrix-degrading enzymes in multilayer coatings synergistically prevent bacterial biofilm formation on urinary catheters. *ACS Appl. Mater. Interfaces* 7, 27066–27077. doi: 10.1021/acsami.5b09489
- Ivanova, K., Fernandes, M. M., Mendoza, E., and Tzanov, T. (2015b). Enzyme multilayer coatings inhibit *Pseudomonas aeruginosa* biofilm formation on urinary catheters. *Appl. Microbiol. Biotechnol.* 99, 4373–4385. doi: 10.1007/s00253-015-6378-7
- Jacobsen, S. M., Stickler, D. J., Mobley, H. L. T., and Shirtliff, M. E. (2008). Complicated catheter-associated urinary tract infections due to *Escherichia coli* and *Proteus mirabilis*. *Clin. Microbiol. Rev.* 21, 26–59. doi: 10.1128/CMR.00019-07
- Jimenez, P. N., Koch, G., Papaioannou, E., Wahjudi, M., Krzeslak, J., Coenye, T., et al. (2010). Role of PvdQ in *Pseudomonas aeruginosa* virulence under iron-limiting conditions. *Microbiology* 156, 49–59. doi: 10.1099/mic.0.030973-0
- Kirisits, M. J., and Parsek, M. R. (2006). Does *Pseudomonas aeruginosa* use intercellular signalling to build biofilm communities? *Cell. Microbiol.* 8, 1841–1849. doi: 10.1111/j.1462-5822.2006.00817.x
- Koch, G., Nadal-Jimenez, P., Reis, C. R., Muntendam, R., Bokhove, M., Melillo, E., et al. (2014). Reducing virulence of the human pathogen *Burkholderia* by altering the substrate specificity of the quorum-quenching acylase PvdQ. *Proc. Natl. Acad. Sci. U.S.A.* 111, 1568–1573. doi: 10.1073/pnas.1311263111
- Kramer, A., Schwabke, I., and Kampf, G. (2006). How long do nosocomial pathogens persist on inanimate surfaces? A systematic review. *BMC Infect. Dis.* 6, 130. doi: 10.1186/1471-2334-6-130
- Lawrence, E. L., and Turner, I. G. (2005). Materials for urinary catheters: a review of their history and development in the UK. *Med. Eng. Phys.* 27, 443–453. doi: 10.1016/j.medengphy.2004.12.013
- Nadal-Jimenez, P., Koch, G., Reis, C. R., Muntendam, R., Raj, H., Jeronimus-Stratingh, C. M., et al. (2014). PvdP Is a tyrosinase that drives maturation of the pyoverdine chromophore in *Pseudomonas aeruginosa*. *J. Bacteriol.* 196, 2681–2690. doi: 10.1128/JB.01376-13
- O'Toole, G. A. (2010). Microtiter dish biofilm formation assay. *J. Vis. Exp.* e2437. doi: 10.3791/2437
- Papaioannou, E., Wahjudi, M., Nadal-Jimenez, P., Koch, G., Setroikromo, R., and Quax, W. J. (2009). Quorum-quenching acylase reduces the virulence of *Pseudomonas aeruginosa* in a *Caenorhabditis elegans* infection model. *Antimicrob. Agents Chemother.* 53, 4891–4897. doi: 10.1128/AAC.00380-09
- Peräkylä, M., and Rouvinen, J. (1996). Ab initio quantum mechanical model calculations on the catalytic mechanism of Aspartylglucosaminidase (AGA): a serine protease-like mechanism with an N-terminal threonine and substrate-assisted catalysis. *Chem. A Eur. J.* 2, 1548–1551. doi: 10.1002/chem.19960021212
- Rasamiravaka, T., Labtani, Q., Duez, P., and El Jaziri, M. (2015). The formation of biofilms by *Pseudomonas aeruginosa*: a review of the natural and synthetic compounds interfering with control mechanisms. *Biomed Res. Int.* 2015, 1–17. doi: 10.1155/2015/759348
- Roy, V., Fernandes, R., Tsao, C.-Y., and Bentley, W. E. (2010). Cross species quorum quenching using a native AI-2 processing enzyme. *ACS Chem. Biol.* 5, 223–232. doi: 10.1021/cb9002738
- Sievert, D. M., Ricks, P., Edwards, J. R., Schneider, A., Patel, J., Srinivasan, A., et al. (2013). Antimicrobial-resistant pathogens associated with healthcare-associated infections summary of data reported to the national healthcare safety network at the centers for disease control and prevention, 2009–2010. *Infect. Control Hosp. Epidemiol.* 34, 1–14. doi: 10.1086/668770
- Sio, C. F., Otten, L. G., Cool, R. H., Diggle, S. P., Braun, P. G., Bos, R., et al. (2006). Quorum quenching by an *N*-acyl-homoserine lactone acylase from *Pseudomonas aeruginosa* PAO1. *Infect. Immun.* 74, 1673–1682.
- Spoering, A. L., and Lewis, K. (2001). Biofilms and planktonic cells of *Pseudomonas aeruginosa* have similar resistance to killing by antimicrobials. *J. Bacteriol.* 183, 6746–6751. doi: 10.1128/JB.183.23.6746-6751.2001
- Stoodley, P., Sauer, K., Davies, D. G., and Costerton, J. W. (2002). Biofilms as complex differentiated communities. *Annu. Rev. Microbiol.* 56, 187–209. doi: 10.1146/annurev.micro.56.012302.160705
- Swartjes, J. J. T. M., Das, T., Sharifi, S., Subbiahdoss, G., Sharma, P. K., Krom, B. P., et al. (2013). A functional DNase I coating to prevent adhesion of

- bacteria and the formation of biofilm. *Adv. Funct. Mater.* 23, 2843–2849. doi: 10.1002/adfm.201202927
- Utari, P. D., Setroikromo, R., Melgert, B. N., and Quax, W. J. (2018). PvdQ quorum quenching acylase attenuates *Pseudomonas aeruginosa* virulence in a mouse model of pulmonary infection. *Front. Cell. Infect. Microbiol.* 8:119. doi: 10.3389/fcimb.2018.00119
- Winston, M. K., Swift, S., Fish, L., Throup, J. P., Jørgensen, F., Chhabra, S. R., et al. (1998). Construction and analysis of *luxCDABE*-based plasmid sensors for investigating *N*-acyl homoserine lactone-mediated quorum sensing. *FEMS Microbiol. Lett.* 163, 185–192. doi: 10.1111/j.1574-6968.1998.tb13044.x

Conflict of Interest: The authors declare that the research was conducted in the absence of any commercial or financial relationships that could be construed as a potential conflict of interest.

Copyright © 2020 Vogel, Wakker-Havinga, Setroikromo and Quax. This is an open-access article distributed under the terms of the Creative Commons Attribution License (CC BY). The use, distribution or reproduction in other forums is permitted, provided the original author(s) and the copyright owner(s) are credited and that the original publication in this journal is cited, in accordance with accepted academic practice. No use, distribution or reproduction is permitted which does not comply with these terms.



Screening for Diguanylate Cyclase (DGC) Inhibitors Mitigating Bacterial Biofilm Formation

Kyu Hong Cho^{1*}, R. Grant Tryon^{1†} and Jeong-Ho Kim²

¹ Department of Biology, Indiana State University, Terre Haute, IN, United States, ² Department of Biology and Chemistry, Liberty University, Lynchburg, VA, United States

OPEN ACCESS

Edited by:

Manuel Simões,
University of Porto, Portugal

Reviewed by:

Andrei I. Khlebnikov,
Tomsk Polytechnic University, Russia
Rajeev K. Singla,
Sichuan University, China

*Correspondence:

Kyu Hong Cho
kyuhong.cho@indstate.edu

†Present address:

R. Grant Tryon,
Ivy Tech Community College, Terre
Haute, IN, United States

Specialty section:

This article was submitted to
Medicinal and Pharmaceutical
Chemistry,
a section of the journal
Frontiers in Chemistry

Received: 28 September 2019

Accepted: 18 March 2020

Published: 21 April 2020

Citation:

Cho KH, Tryon RG and Kim J-H
(2020) Screening for Diguanylate
Cyclase (DGC) Inhibitors Mitigating
Bacterial Biofilm Formation.
Front. Chem. 8:264.
doi: 10.3389/fchem.2020.00264

The majority of bacteria in the natural environment organize themselves into communal biofilms. Biofilm formation benefits bacteria conferring resistance to harmful molecules (e.g., antibiotics, disinfectants, and host immune factors) and coordinating their gene expression through quorum sensing (QS). A primary signaling molecule promoting bacterial biofilm formation is the universal second messenger cyclic di-GMP. This dinucleotide predominantly controls the gene expression of motility, adhesins, and capsule production to coordinate biofilm formation. Cyclic di-GMP is synthesized by diguanylate cyclases (DGCs) that have a GGDEF domain and is degraded by phosphodiesterases (PDEs) containing either an EAL or an HD-GYP domain. Since high cellular c-di-GMP concentrations are correlated with promoting the ability of bacteria to form biofilms, numerous research endeavors to identify chemicals capable of inhibiting the c-di-GMP synthesis activity of DGCs have been performed in order to inhibit bacterial biofilm formation. This review describes currently identified chemical inhibitors that disturb the activity of DGCs and the methods of screening and assay for their discovery.

Keywords: biofilm, diguanylate cyclases, DGC inhibitors, high throughput screening, DGC activity assay

INTRODUCTION

Bacterial Biofilms and Human Health

Biofilms are sessile multicellular bacterial communities encased in a three-dimensional meshwork formed by extracellular polymeric substances (EPSs) (Roy et al., 2018). EPSs consisting of polysaccharides, proteinaceous filaments, and/or nucleic acids can compose as much as 90% of biofilm's biomass (Limoli et al., 2015). EPSs can provide protection against mechanical stress by the formation of a protective physical barrier and control the diffusion of signaling molecules, nutrients, and toxic compounds (Morgan et al., 2014). Extensive intercellular communication and interactions have been observed within biofilms through quorum sensing (QS), which uses diffusible molecules known as autoinducers to regulate population behaviors (Li and Tian, 2012). QS appears to participate in the development of biofilm formation (Lin Chua et al., 2017; Kim et al., 2018). For example, N-acyl homoserine lactone (AHL) QS systems observed in *P. aeruginosa* biofilms were identified as mechanisms by which extracellular DNA (eDNA) was released while *P. aeruginosa* produced EPSs.

Chronic infections such as contamination of artificial medical implants, otitis media, chronic healing wounds, and lung pneumonia of cystic fibrosis patients are mostly associated with bacterial biofilm formation (Bjarnsholt, 2013). It is estimated that nineteen million annual infections are due to biofilm-based infections in the United States (Wolcott et al., 2010). Biofilm formation promotes

increased antibiotic tolerance up to ~1,000 times greater than that observed in planktonic bacteria (Ito et al., 2009). Besides, biofilms resist host immune defense strategies, such as mechanical clearance, complement-mediated killing, antibody recognition, and phagocytosis (Domenech et al., 2013). Often, biofilm-based infections cannot be comprehensively treated due to ineffective antibiotic therapy (Sambanthamoorthy et al., 2012).

c-di-GMP Signaling Systems Control Bacterial Biofilm Formation

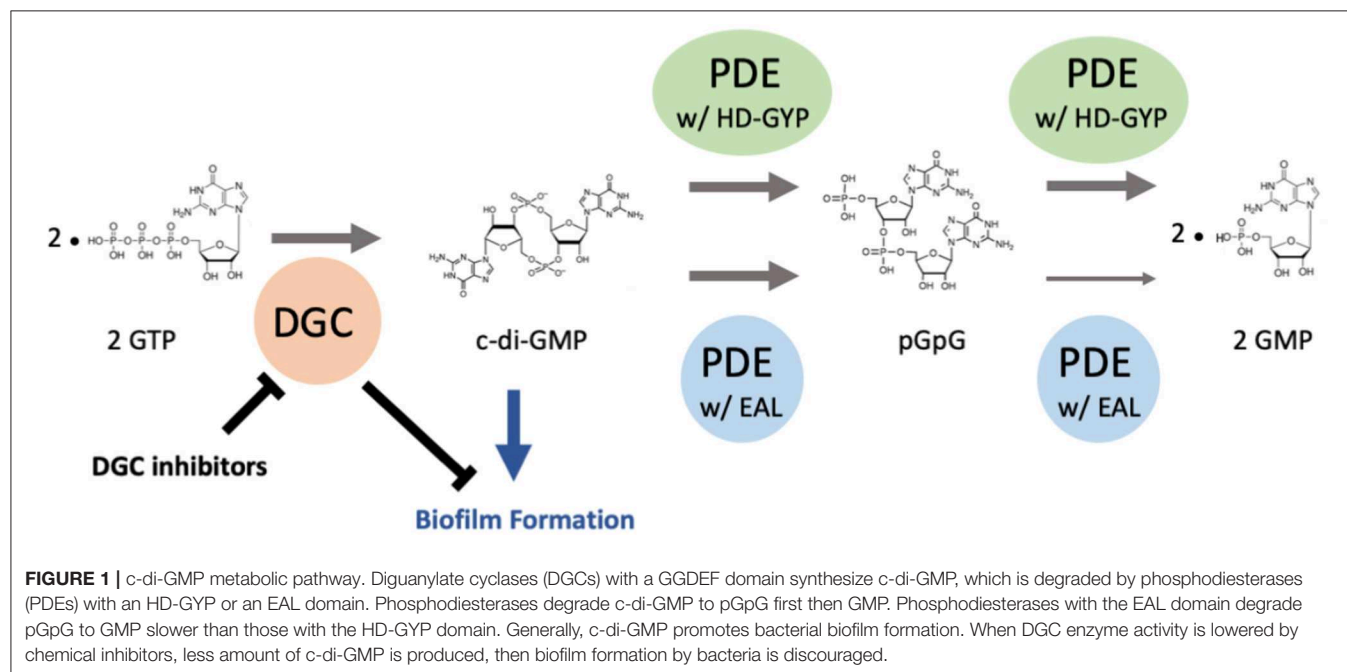
c-di-GMP (bis-(3'-5')-cyclic dimeric guanosine monophosphate or cyclic diguanylate monophosphate) is one of dinucleotide second messengers in bacteria. It was discovered in 1987 while researchers were studying cellulose synthesis in *Gluconoacetobacter xylinus* (Ross et al., 1987). Further studies revealed that it controls various cellular functions including EPS synthesis and secretion, flagellar motility, adhesion, cell cycle initiation and regulation, and virulence factor synthesis in bacteria (Caly et al., 2015; Kim et al., 2018). The main common role of c-di-GMP signaling in diverse bacteria is to regulate bacterial lifestyle by controlling the transition of bacteria between a planktonic lifestyle and a biofilm lifestyle (Chua et al., 2014). Generally, high c-di-GMP content in bacterial cells reduces their motility by inhibiting flagella assembly and increases the synthesis of the EPS matrix, resulting in biofilm formation. Low intracellular c-di-GMP concentration increases bacterial motility and disperse biofilms (Hengge, 2009; Lee et al., 2010; Chua et al., 2015; Gao et al., 2017). Since c-di-GMP signaling systems are highly conserved in bacteria but not in eukaryotic organisms, and c-di-GMP promotes biofilm formation, enzymes associated with its metabolism are attractive targets for the interference with bacterial biofilm formation. Many important human pathogens whose biofilm formation

ability plays a pivotal role in their virulence possess numerous c-di-GMP metabolizing enzymes, including *P. aeruginosa*, *Clostridium difficile*, *Salmonella typhimurium*, and *Vibrio cholerae* (Navarro et al., 2009; Solano et al., 2009; Antoniani et al., 2010; Bordeleau et al., 2011; Ha and O'Toole, 2015; Conner et al., 2017).

Enzymes Involved in c-di-GMP Synthesis and Degradation

The intracellular levels of c-di-GMP at a given time are determined by the combination of activities of diguanylate cyclases (DGCs) and phosphodiesterases (PDEs) (Figure 1) (Christen et al., 2006). Both classes of enzymes possess several N-terminal sensory domains allowing a prompt response to various environmental stimuli, including the presence of oxygen, light, nitric oxide, and other specific compounds (Gomelsky and Klug, 2002; Tuckerman et al., 2009; Plate and Marletta, 2012). DGCs and PDEs are often physically linked together even though they perform opposing reactions, but the catalytic function of one of them has usually lost and instead has gained a function to control the protein activity. Up to now, only a few proteins have been found to possess both c-di-GMP synthesizing and degradative activities (Wirebrand et al., 2018).

Two molecules of guanosine triphosphate (GTP) are synthesized into c-di-GMP via the activity of a GGDEF domain located in DGCs (Christen et al., 2006). The GGDEF signature domain forms part of the active site "A-site" where GTP is bound (one molecule of GTP substrate per monomer) (Chan et al., 2004). Structural analysis of a GGDEF domain protein PleD (a DGC of *Caulobacter crescentus*) showed that it binds dimeric c-di-GMP at an allosteric site "I-site" that is characterized by the RxxD motif (Chan et al., 2004). Subsequent structural determination of PleD and WspR (a DGC in *P. aeruginosa*)



bound to c-di-GMP confirmed that the activity of the GGDEF domain is regulated by feedback inhibition, in which the binding of c-di-GMP to the I-site prevents the formation of an enzymatically active DGC dimer (Wassmann et al., 2007; De N et al., 2008). Thus, the binding of c-di-GMP at the I-site accounts for a strong non-competitive product inhibition, which establishes a limit on the cellular c-di-GMP concentration.

PDEs possessing either an EAL or an HD-GYP domain are responsible for degrading c-di-GMP (Caly et al., 2015). Generally, PDEs with the EAL domain degrade c-di-GMP into linear pGpG, and the ones with the HD-GYP domain degrade into two molecules of GMP (Povolotsky and Hengge, 2012; Sundriyal et al., 2014). The PDEs with the EAL domain predominantly produce pGpG from c-di-GMP first then GMP from pGpG very slowly, suggesting that the pGpG-degrading activity is irrelevant *in vivo* (Shanahan et al., 2013). The PDEs with the HD-GYP domain that contains a HHExxDGxxGYP motif are a subgroup of the HD superfamily of metal-dependent phosphohydrolases and convert c-di-GMP to GMP via the linear nucleotide pGpG (Dow et al., 2006; Stelitano et al., 2013a).

It is estimated that ~80% of human infections are caused by microbial biofilms (Hall-Stoodley et al., 2004), so there have been many elaborate scientific studies in order to inhibit the biofilm formation or destroy established biofilms. One of the promising ways is to develop inhibitory chemicals against di-guanylate cyclases (DGCs) that produce c-di-GMP that promotes biofilm formation in diverse bacteria. This paper reviews what DGC inhibitors have been found so far, what are their strength and weakness as biofilm inhibitors, and what screening methods have been used to find the inhibitors.

DGC INHIBITORS

Since high cellular c-di-GMP concentrations promote biofilm formation and maintenance, the main target enzyme in the c-di-GMP metabolism for the development of biofilm inhibitors has been DGCs. Thus, there have been many studies to find effective inhibitors against DGCs. In this section, DGC inhibitors that have been discovered so far, and their screening and assay methods are described, which is summarized in **Table 1**.

Natural Molecules

Glycosylated Triterpenoid Saponin (GTS)

A unique triterpenoid saponin extracted from the pea plant (*Pisum sativum*) was identified as a potent inhibitor of a DGC in *Gluconoacetobacter xylinus* (formerly *Acetobacter xylinum*) (Ohana et al., 1998). Spectral analyses identified this compound as 3-o- α -L-rhamnopyranosyl-(12)- β -D-galactopyranosyl-(12)- β -D-gluconopyranosyl soyasapogenol B 22-o- α -D-gluconopyranoside (**Figure 2A**). This family of compounds is widely distributed in higher plants, but its role in plants has not been elucidated yet. A compound with an identical or at least very similar structure is also produced by the cellulose synthesizing bacterium *G. xylinus*. This study suggests this type of saponin might be involved in cellulose synthesis in

plants and the bacterium *G. xylinus*. The IC₅₀ (50% inhibitory concentration) is about 5 μ M *in vitro*. The GTS, however, does not inhibit DGC activity *in vivo*, probably due to non-permeable nature to the outer membrane.

c-di-GMP Analogs

2'-F-c-di-GMP

Zhou et al. developed a potent DGC inhibitor by substituting 2'-OH of c-di-GMP to fluoride (Zhou et al., 2013). The chemical 2'-F-c-di-GMP (**Figure 2B**) binds to the I-site, and IC₅₀ was 11 μ M when it was tested with WspR, a DGC of *P. aeruginosa*. Interestingly, this chemical also inhibits PDEs, and the inhibitory activity against PDEs is stronger than that against the DGC, which could increase the cellular concentration of c-di-GMP. Unfortunately, this chemical is also not membrane-permeable like most other c-di-GMP and GTP analogs, so cell membrane-permeable derivatives are required to perturb cellular c-di-GMP signaling *in vivo*.

c-di-Inosinylic Acid

c-di-inosinylic acid (**Figure 2C**) was identified as an effective inhibitor against a DGC, Slr1143 of *Synechocystis* sp. after testing five structural analogs of c-di-GMP (Ching et al., 2010). c-di-inosinylic acid has a hypoxanthine base instead of the guanine base. For the analysis, each inhibitor was mixed with purified Slr1143, and its inhibitory effect on the c-di-GMP production by Slr1143 was determined by a high-performance liquid chromatograph (HPLC) assay. Since c-di-inosinylic acid is structurally similar to c-di-GMP, this analog is predicted to bind to the I-site of the DGC, Slr1143. c-di-Inosinylic acid has a stronger inhibitory activity than c-di-GMP with ~100 μ M of IC₅₀. This study, however, did not determine whether or not c-di-inosinylic acid inhibited the biofilm formation of *Synechocystis* sp.

Triazole-Linked Analogs

A target in the c-di-GMP structure for developing DGC inhibitors is the phosphodiester moiety. One of the benefits of the modification of the phosphodiester moiety is that it can confer the resistance to the hydrolysis by PDEs. Fericola et al. designed new molecules in which the phosphodiester moiety was replaced with isosteric non-hydrolyzable 1,2,3-triazole moiety. At the same time, the length between two guanine bases was varied by adding different triazole connectors (Fericola et al., 2015). These molecules were synthesized as linear forms instead of cyclic forms because linear forms are easier to be synthesized chemically than cyclic forms. These synthesized molecules were tested for their ability to inhibit both PleD, a DGC of *C. crescentus* and RocR, a PDE of *P. aeruginosa*. From an *in vitro* analysis using purified enzymes, two molecules inhibiting the DGC were identified. However, among these two, only DCI058 did not significantly inhibit the PDE, RocR. DCI058 (**Figure 2D**) binds to the I-site of the DGC, and its inhibitory activity against DGC is comparable to 2'-F-c-di-GMP. The PleD activity with 100 μ M of DCI058 and 100 μ M of GTP is ~32% of that without

TABLE 1 | Identified chemical inhibitors against Diguanylate Cyclases (DGCs).

Name of chemical	Mode of action	Screening and DGC activity assay methods	Chemical library used for screening	References
Natural molecules				
Glycosylated Triterpenoid Saponin	Non-competitive inhibition	<i>In vitro</i> enzyme activity assay analyzed by TLC (thin layer chromatograph) followed by autoradiography	Plant extract	Ohana et al., 1998
c-di-GMP analogs				
2'-F-c-di-GMP	Non-competitive inhibition binding to the DGC I-site	<i>In vitro</i> enzyme activity assay analyzed by TLC followed by autoradiography	Three c-di-GMP analogs chemically synthesized	Zhou et al., 2013
c-di-Inosinylic Acid	Non-competitive inhibition binding to the DGC I-site	<i>In vitro</i> enzyme activity assay analyzed by HPLC (high performance liquid chromatography)	Five c-di-GMP analogs chemically synthesized	Ching et al., 2010
Triazole-Linked Analog DC1058	Non-competitive inhibition binding to the DGC I-site	<i>In vitro</i> enzyme activity assay analyzed by circular dichroism (CD) spectroscopy	16 c-di-GMP analogs chemically synthesized	Fernicola et al., 2015
GTP analogs				
MANT-GTP and MANT-GTP γ S	Unknown, probably competitive inhibition	<i>In vitro</i> enzyme activity assay analyzed by HPLC-MS/MS	8 NTP derivatives	Spangler et al., 2011
TNP-GTP	Unknown, probably competitive inhibition	<i>In vitro</i> enzyme activity assay analyzed by HPLC-MS/MS	8 NTP derivatives	Spangler et al., 2011
Small synthetic molecules				
Ebselen	Cysteine residue modification near the I-site	DRaCALA (Differential Radial Capillary Action of Ligand Assay)	NIH clinical collection 1 (NCC1) library	Lieberman et al., 2014
Catechol-containing Sulfonohydrazide compounds	Competitive inhibition of active site	<i>In silico</i> (3-D Pharmacophore) prediction followed by <i>in vitro</i> enzyme activity assay	The purchasable subset of the ZINC database ($\sim 2.3 \times 10^7$ compounds)	Fernicola et al., 2016
Sulfasalazine	Competitive inhibition of active site	<i>In silico</i> prediction with OpenEye Scientific Software followed by <i>in vitro</i> enzyme activity assay	1,500 FDA-approved drugs in the DrugBank database	Wiggers et al., 2018
Eprosartan	Competitive inhibition of active site	<i>In silico</i> prediction with OpenEye Scientific Software followed by <i>in vitro</i> enzyme activity assay	1,500 FDA-approved drugs in the DrugBank database	Wiggers et al., 2018
N-(4-anilinophenyl)benzamide (aka. DI-3)	Unknown	Screening with an <i>in vivo</i> luciferase reporter assay followed by an <i>in vitro</i> enzyme activity assay	66,000 compounds/natural product extracts at the Center for Chemical Genomics at the University of Michigan	Sambanthamoorthy et al., 2012
[2-oxo-2-(2-oxopyrrolidin-1-yl)ethyl] 1,3-benzothiazole-6-carboxylate	Non-competitive inhibition binding to the DGC I-site	FRET (Foster resonance energy transfer)-based <i>in vitro</i> enzyme activity assay	27,502 commercially available small molecules	Christen et al., 2019
4-(2,5-dimethylphenoxy)-N-(4-morpholin-4-ylphenyl)butanamide	Non-competitive inhibition binding to the DGC I-site	FRET (Foster resonance energy transfer)-based <i>in vitro</i> enzyme activity assay	27,502 commercially available small molecules derived from chemical libraries at the Institute of Chemical Biology at Harvard University	Christen et al., 2019
N'-((1E)-{4-ethoxy-3-[(8-oxo-1,5,6,8-tetrahydro-2H-1,5-methanopyrido[1,2-a][1,5]diazocin-3(4H)-yl)methyl]phenyl)methylene)-3,4,5-trihydroxybenzohydrazide (aka. LP-3134)	Competitive inhibition of active site	<i>In silico</i> (3-D Pharmacophore) prediction followed by <i>in vitro</i> enzyme activity assay	A database of commercially available compounds	Sambanthamoorthy et al., 2014

DC1058. Even though DC1058 has promising characteristics as a drug for the inhibition of biofilm formation through the inhibitory effect against bacterial DGCs, it did not inhibit bacterial biofilm formation probably due to low membrane

permeability. Thus, it needs to be chemically modified to improve membrane permeability.

To measure the inhibitory activity of the compounds toward DGCs or PDEs in this study, circular dichroism (CD)

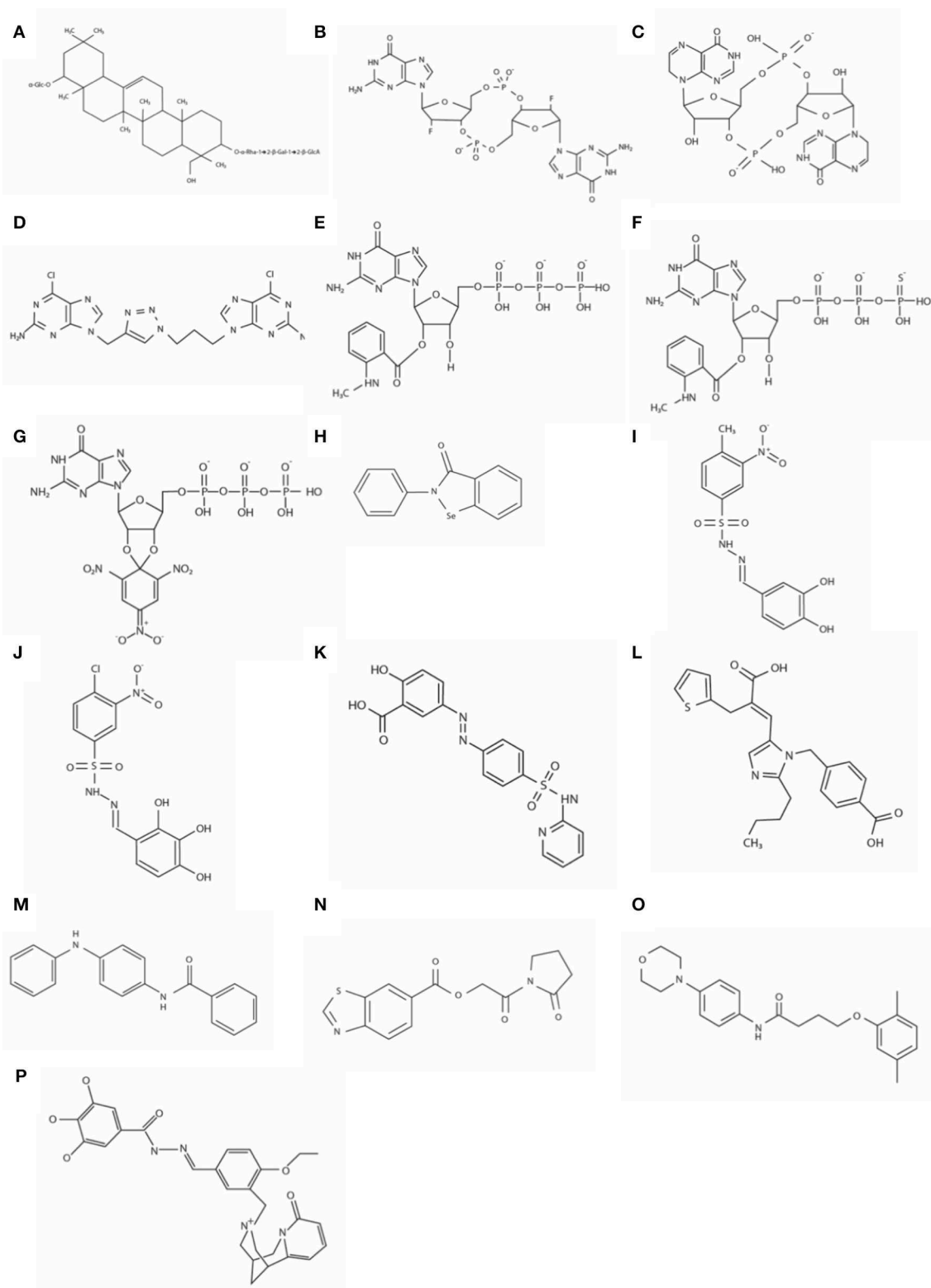


FIGURE 2 | The structures of DGC inhibitors. **(A)** 3- α -L-rhamnopyranosyl-(12)- β -D-galactopyranosyl-(12)- β -D-gluconopyranosyl soyasapogenol B 22- α -D-glucopyranoside; **(B)** 2'-F-c-di-GMP; **(C)** c-di-inosinic acid; **(D)** DC1058; **(E)** MANT-GTP; **(F)** MANT-GTP γ S; **(G)** TNP-GTP; **(H)** Ebselen; **(I)** Amb2250087; **(J)** Amb379455; **(K)** Sulfasalazine; **(L)** Eprosartan; **(M)** N-(4-anilinophenyl)benzamide; **(N)** [2-oxo-2-(2-oxopyrrolidin-1-yl)ethyl] 1,3-benzothiazole-6-carboxylate; **(O)** 4-(2,5-dimethoxyphenoxy)-N-(4-morpholin-4-ylphenyl)butanamide; and **(P)** N'-[(1E)-{4-ethoxy-3-[(8-oxo-1,5,6,8-tetrahydro-2H-1,5-methanopyrido[1,2-a][1,5]diazocin-3(4H)-yl)methylphenyl)methylene]-3,4,5-trihydroxybenzohydrazide, aka LP3134.

spectroscopy was used (Stelitano et al., 2013b). In the presence of manganese, c-di-GMP forms a dimer by intercalating each other. In this structure, four guanines are aligned, and this alignment increases dichroic signal that can be detected by CD spectroscopy. However, this dichroic signal increase does not occur along with the dimer formation of c-di-AMP, another common bacterial second signaling molecule.

GTP Analogs

MANT-GTP, MANT-GTP γ S, and TNP-GTP

Since 2',3'-O-(2,4,6-trinitrophenyl) (TNP)- and 2' (3')-O-(N-methylantraniloyl) (MANT)- substituted nucleotides are potent inhibitors of guanylyl and adenylyl cyclases, and the catalytic domain of DGCs is similar to the catalytic domain of mammalian adenylyl cyclases, Spangler et al. tested various MANT- and TNP- substituted nucleotides to identify if they were inhibitors against DGCs (Spangler et al., 2011). Among those nucleotide analogs, MANT-GTP (**Figure 2E**), MANT-GTP γ S (**Figure 2F**), and TNP-GTP (**Figure 2G**) acted as potent inhibitors against an *E. coli* DGC, YdeH in *in vitro* enzyme activity assay, in which the enzymatic product c-di-GMP was quantified by HPLC-MS/MS (high-performance liquid chromatography-tandem mass spectroscopy) analysis. The IC₅₀ values of these chemicals were below 1 μ M. In a fluorometric analysis observing fluorescence resonance energy transfer (FRET) between tyrosine and tryptophan residues of YdeH and the MANT group, MANT-GTP closely interacted with YdeH. Even though the exact interaction mechanism has not been identified, the fluorometric analysis indicates that probably MANT-GTP interacts with the YdeH active site instead of GTP. If so, MANT-GTP not only interferes with c-di-GMP signaling, but it may also interfere with other pathways where GTP is involved *in vivo*. Membrane permeability of the MANT- or TNP- substituted GTP has not been tested, but they are probably not membrane-permeable when their chemical structures are considered.

Small Synthetic Molecules

Ebselen

Ebselen (**Figure 2H**) was identified by a rapid and quantitative high-throughput screen based on the differential radial capillary action of ligand assay (DRaCALA) as an inhibitor of a DGC/c-di-GMP interaction (Lieberman et al., 2014). In this study, the NIH clinical collection 1 (NCC1) library was used to screen for inhibitors of c-di-GMP-binding to the I-site of DGCs, PelD, and WspR. The NCC1 library is comprised of molecules that have a history of use in human clinical trials (Austin et al., 2004). Ebselen reduces DGC activity by covalently modifying cysteine residues near the c-di-GMP binding pocket, and consequently inhibits c-di-GMP regulation of flagella-mediated motility and biofilm formation in *P. aeruginosa*. Favorably, ebselen does not bind to PDE or PilZ proteins from *P. aeruginosa*. The IC₅₀ values of ebselen for PelD and WspR are about 5.0 and 13.6 μ M, respectively. Ebselen has favorable drug-like properties and has been used in phase III clinical trials (Ogawa et al., 1999).

DRaCALA is based on the differential mobility of protein-bound and -free radiolabeled ligands on a nitrocellulose membrane (Roelofs et al., 2011). In this assay, each purified

protein is mixed with ³²P radiolabeled c-di-GMP, and spotted on a nitrocellulose membrane. Then the distribution of the radioactivity is imaged directly by a phosphorimager (autoradiography). If radiolabeled c-di-GMP binds to the protein, a clear spot appears because of the low mobility of the protein. Otherwise, c-di-AMP disperses, resulting in no clear spot but a gray background. One of the advantages of this assay compared to spectroscopic methods is that the interference caused by spectroscopic properties of molecules is eliminated by direct measurement of radioactivity.

Catechol-Containing Sulfonohydrazide Compounds

Fernicola et al. used a three-dimensional pharmacophore model to identify small-molecule inhibitors of the well-characterized DGC enzyme PleD of *C. crescentus* (Fernicola et al., 2016). In this study, the Ligandscout algorithm (Wolber and Langer, 2005) and the purchasable subset of the ZINC database (Irwin and Shoichet, 2005) were used for screening inhibitors. The crystal structure of PleD bound by the non-cleavable substrate analog GTP- α -S and a pharmacophore-based approach revealed that the key amino acids in PleD interacting with the substrate are F330, F331, D344, R366, and K442. Also, a magnesium ion interacts with the β -, γ -bisphosphate moiety in the binding pocket. The chemical structures from the ZINC data base compounds were examined to test whether or not the structures interact with the amino acids and the magnesium ion in the binding pocket of PleD using Molegro Visual Docker software (CLCbio). Seven molecules which were selected by this *in silico* analysis were tested *in vitro* for their ability to inhibit the activity of the purified DGC. In the assay using circular dichroism spectroscopy, two catechol-containing sulfonohydrazide compounds, Amb2250087 (**Figure 2I**) and Amb379455 (**Figure 2J**) were identified to inhibit PleD competitively. These compounds were predicted to interact with the amino acid residues, N335, D344, and R366 and the magnesium ion in the binding pocket. The IC₅₀ values of these compounds are both \sim 11 μ M. These two inhibitors are found to bind to the catalytic site, not the I-site of the DGC. Previously, c-di-GMP analogs had been synthesized and tested for their ability to bind to the I site and inhibit DGC enzymes, and these compounds are likely ineffective against those DGCs without an I-site. However, since the catechol-containing sulfonohydrazide compounds directly inhibit the catalytic site, it might be effective to most DGCs. Unfortunately, these compounds do not reduce the intracellular level of c-di-GMP in bacteria probably due to a membrane permeability issue, so further chemical modifications are necessary to improve the delivery of these compounds inside cells.

Sulfasalazine and Eprosartan

Recently, Wiggers et al. screened 1500 FDA-approved drugs in the DrugBank database through a virtual screening method to find competitive inhibitors binding to the A-site of the DGC, *C. crescentus* PleD (Wiggers et al., 2018). The authors used the combination of the molecular docking strategy and ligand-based methods. In the molecular docking strategy, among the nine amino acid residues involved in the recognition of the GTP substrate in the structure of DGCs, two highly conserved

residues playing an important role in the specificity to GTP over other nucleotides, N³³⁵ and D³⁴⁴ were set as constraints. In the ligand-based methods which search for the compounds similar to GTP, the distribution of shape and electrostatics similarity of compounds were analyzed. Among the top 200 candidates from the analysis, 10 compounds were selected based on the properties of the compounds such as A-site occupancy, constraint matching, hydrogen bonding network, and molecular diversity.

After the screening, the authors tested the top 10 candidates with *in vitro* enzyme assay using purified DGCs, WspR from *P. aeruginosa* and YdeH from *E. coli*, and discovered four chemicals inhibiting the activity of the DGCs. Further binding study with a mass spectrometry analysis revealed that the inhibition occurred through interacting with the active site in the GGDEF domain. Among those four, two had favorable biological properties as DGC inhibitors such as no inhibition of bacterial growth and no signs of interference with other metabolic pathways. Those two inhibitors are the anti-inflammatory sulfasalazine (**Figure 2K**) and the anti-hypersensitive eprosartan (**Figure 2L**). They inhibit the DGC activity in the micromolar range. The IC₅₀ values of sulfasalazine are 200 μ M for YdeH and 360 μ M for WspR, and those of eprosartan are 888 μ M for YdeH and 170 μ M for WspR, respectively. The big difference between the IC₅₀ values of eprosartan for the different DGCs indicates that not only the key conserved residues interacting with the substrate GTP in DGCs but also different A-site peripheral residues should be considered for designing a virtual inhibitor screening to discover inhibitors with a broad DGC spectrum. Both compounds reduce aggregation of *E. coli* in the culture broth, suggesting that these two chemicals have anti-biofilm property *in vivo* (Wiggers et al., 2018).

N-(4-anilinophenyl)benzamide

A high throughput screen using a bacterial reporter assay identified seven DGC inhibitors (Sambanthamoorthy et al., 2012). The *V. cholerae* reporter system used in the study is consisted of two plasmids, one of which contains luciferase reporter genes (*lux* genes) and the other a DGC enzyme gene, respectively. A luciferase gene is transcriptionally fused with the promoter of the VC1673 gene of *V. cholerae* whose transcription is induced by c-di-GMP. The second plasmid encodes a DGC enzyme gene to increase the intracellular c-di-GMP level. Out of 66,000 compounds/natural product extracts at the Center for Chemical Genomics at the University of Michigan, the authors identified 7 small molecule compounds that inhibited at least two DGC enzymes, VC2370 from *V. cholerae* and WspR from *P. aeruginosa* after determining IC₅₀, toxicity to eukaryotic cells, inhibition of bacterial growth, etc. In addition, some inhibitors inhibited the formation of *V. cholerae* biofilm and/or *P. aeruginosa* biofilm. Especially, N-(4-anilinophenyl)benzamide (**Figure 2M**) is effective against both biofilms and decreases *in vivo* c-di-GMP concentration, which makes this compound one of the most promising antibiofilm drugs among the seven inhibitors. However, it does not disperse a preformed biofilm. The IC₅₀ values of the compound is 1 μ M for VC2370 and 17.83 μ M for WspR.

[2-oxo-2-(2-oxopyrrolidin-1-yl)ethyl] 1,3-benzothiazole-6-carboxylate and 4-(2,5-dimethylphenoxy)-N-(4-morpholin-4-ylphenyl)butanamide

Recently, a FRET (Foster resonance energy transfer)-based assay that can measure a cellular c-di-GMP concentration was developed (Christen et al., 2010). For the construction of this FRET-based activity assay system, mYPet and cCYPet fluorescence proteins were attached at the N- and C-terminus of the c-di-GMP binding domain of the PilZ protein, YcgR. When the YcgR domain binds c-di-GMP, the angle of the two fluorescent proteins each other changes due to the conformational change of the YcgR domain, then the fluorescence property reflecting c-di-GMP levels (535/470 nm) changes. Using this assay, Christen et al. screened a compound library containing 27,502 commercially available small chemicals to discover inhibitors of a DGC, *C. crescentus* DgcA (Christen et al., 2019). The authors first identified 49 compounds as potent inhibitors. After secondary assay considering IC₅₀, cytotoxicity, and easiness of chemical synthesis and modification, two compounds were selected as promising DGC inhibitors, which were [2-oxo-2-(2-oxopyrrolidin-1-yl)ethyl] 1,3-benzothiazole-6-carboxylate (**Figure 2N**) and 4-(2,5-dimethylphenoxy)-N-(4-morpholin-4-ylphenyl)butanamide (**Figure 2O**). Their IC₅₀ values are 4.0 and 6.4 μ M for the *C. crescentus* DGC enzyme DgcA, respectively. When the scaffolds of the two compounds were chemically modified to produce 44 derivatives, more than half of them acted as allosteric inhibitors.

N'-((1E)-{4-ethoxy-3-[(8-oxo-1,5,6,8-tetrahydro-2H-1,5-methanopyrido[1,2-a][1,5]diazocin-3(4H)-yl)methyl]phenyl}Methylene)-3,4,5-Trihydroxybenzohydrazide

Another *in silico* virtual screening performed by the group discovered N-(4-anilinophenyl)benzamide led the discovery of several potent DGC inhibitors (Sambanthamoorthy et al., 2014). For this virtual screening, two pharmacophore data were used: one generated based on the interaction between the amino acid residues of the *C. crescentus* DGC PleD and a guanine base and the other based on the oroidin template containing some of the features of the guanine base. By using these two pharmacophores, a chemical library from a database of commercially available compounds was generated, and 250 compounds in the library were experimentally analyzed. For DGC inhibition assay, the conversion of GTP to c-di-GMP by DGCs, *Thermotoga maritima* tDGC and *P. aeruginosa* WspR, was monitored by measuring the amount of pyrophosphate produced during the c-di-GMP synthesis reaction. Out of 250 compounds they tested, 4 compounds showed significant inhibitory activity. Among those 4 compounds, LP3134, N'-((1E)-{4-ethoxy-3-[(8-oxo-1,5,6,8-tetrahydro-2H-1,5-methanopyrido[1,2-a][1,5]diazocin-3(4H)-yl)methyl]phenyl}methylene)-3,4,5-trihydroxybenzohydrazide (**Figure 2P**) was the most promising biofilm inhibitor because it inhibited the biofilm development of both *P. aeruginosa* and *Acetobacter baumannii* under both static and flow conditions. In addition, it showed the lowest

cytotoxicity to human keratinocytes; it did not show any cytotoxicity below 300 μM , which is much higher than the IC_{50} value for WspR, 45 μM .

DISCUSSION

Diverse approaches have been used to discover DGC inhibitors so far. Those approaches are: (1) Chemical modification of the substrate GTP. This method screens competitive inhibitors of DGCs that bind to the active site A-site. Since the inhibitors can be structurally similar to the substrate GTP, a caveat of this approach is that they might interfere with other GTP-involved metabolic pathways in bacteria or host cells. Thus, this aspect should be tested when they are considered as antibiofilm drugs. (2) Chemical modification of the DGC product, c-di-GMP. Many DGCs have the I-site that provides a feedback inhibition by binding the enzyme's product c-di-GMP. Most c-di-GMP analog inhibitors bind the allosteric inhibitory site I-site, and act as non-competitive inhibitors. Generally, the inhibitors binding to the I-site are not effective to DGCs with no I-site. (3) Chemical modification of backbone molecules similar to the structure of c-di-GMP. c-di-GMP analogs can be degraded by PDEs. To avoid this problem, scientists designed non-cyclic (for easy chemical synthesis) backbone molecules similar to c-di-GMP, and tested their chemical derivatives for inhibitory activity against DGCs. This type of chemical generally acts as non-competitive inhibitors by binding to the I-site. (4) High throughput screening of chemical libraries through *in vitro* assays. Chemical libraries provided for research by NIH, FDA, university centers, etc. have been tested for inhibitory activity against DGCs. For *in vitro* high throughput screening, scientists developed *in vitro* assay methods that can measure the binding of c-di-GMP to purified DGCs by FRET (Foster Resonance Energy Transfer) (Christen et al., 2019) or DRaCALA (Differential Radial Capillary Action of Ligand Assay) (Lieberman et al., 2014). (5) High throughput screening of chemical libraries using *in vivo* assays. An ideal high throughput screening for chemical inhibitors of DGCs would incorporate a system that monitors the changes of cellular c-di-GMP concentration *in situ*. This kind of assay methods determines its efficacy on whole bacteria, including membrane permeability. One example is to develop a luciferase reporter system responding to a cellular c-di-AMP concentration *in situ* (Sambanthamoorthy et al., 2012). However, this method does not always find inhibitors of DGCs. When a chemical lowers cellular c-di-AMP concentration, this can be caused by an inhibitory effect of the chemical on DGC activity directly or inhibitory effect on other metabolic pathways influencing cellular c-di-AMP concentrations, including pathways affecting GTP synthesis. This aspect should be tested after screening. (6) High throughput screening of chemical libraries through *in silico* methods followed by *in vitro* assays. This method uses computer algorithms to screen small molecule databases. For this method, the structure of DGCs bound by GTP (targeting the A site) or c-di-GMP (targeting the I-site) must be determined by X-ray crystallography or NMR. Based on the binding patterns of

the ligands to DGCs, it is determined if a chemical has the potential to bind to DGCs. Since there are several computer algorithms developed already, this method can be an approach for initial screening of various chemicals if crystal structures of ligand-bound target proteins are available. Some computer algorithms for this type of screening are collected in websites, such as click2drug.org.

The genomes of most gram-negative bacteria encode multiples of GGDEF domain-containing proteins. For example, total 34 GGDEF domain proteins (18 GGDEF domain proteins and 16 GGDEF-EAL domain proteins) are encoded on the chromosome of *P. aeruginosa* (Valentini and Filloux, 2016) and 12 GGDEF domain proteins on the chromosome of *Salmonella enterica* serovar Typhimurium (Romling et al., 2005). It was shown that multiple DGCs affect biofilm formation, so an inhibitor inhibiting only one DGC might not affect biofilm formation (Kulasakara et al., 2006). The inhibitory activity of the discovered DGC inhibitors has been tested using only one or two DGCs. Thus, further studies are necessary to figure out whether or not these inhibitors show a broad-spectrum inhibitory activity toward diverse DGCs before being developed as antibiofilm drugs.

Each microorganism has a unique cell wall structure, which might confer different penetrability to each chemical. Currently, however, there are very little data on what microorganisms are affected by the discovered DGC inhibitors in terms of biofilm formation, which should be tested in the future.

Although several types of DGC inhibitors are identified, precise molecular actions of most inhibitors are not well-determined. Further studies such as determining the structures of inhibitor-bound DGCs will facilitate to design derivatives with better inhibitory ability.

CONCLUSION

c-di-GMP plays an essential role in biofilm formation in diverse bacteria, so targeting c-di-GMP signaling appears to be a promising approach to control bacterial biofilm formation. The discovery of novel DGC inhibitors has been greatly assisted by the development of assays suitable for high-throughput screening (HTS) of chemical compounds. HTS should be based on reliable assays and, whenever possible, performed using living cells along with purified enzymes to select membrane-permeable compounds. The high throughput methods used to identify DGC inhibitors can also be used to discover diadenylate cyclase (DAC) inhibitors. Many gram-positive bacteria including firmicutes and some gram-negative bacteria produce cyclic diadenylate monophosphate (c-di-AMP) instead of or accompanying with c-di-GMP. c-di-AMP is also essential for biofilm formation by some pathogenic bacteria (Corrigan et al., 2011; Du et al., 2014; Cheng et al., 2016; Peng et al., 2016; Fahmi et al., 2019). It is expected that more potent DGC inhibitors with better druggable chemicals will be identified or designed in the near future.

AUTHOR CONTRIBUTIONS

KC designed and wrote the manuscript, made the figures and added information to the table. RT wrote the manuscript and made the table. J-HK added information to the manuscript.

REFERENCES

- Antoniani, D., Bocci, P., Maciag, A., Raffaelli, N., and Landini, P. (2010). Monitoring of diguanylate cyclase activity and of cyclic-di-GMP biosynthesis by whole-cell assays suitable for high-throughput screening of biofilm inhibitors. *Appl. Microbiol. Biotechnol.* 85, 1095–104. doi: 10.1007/s00253-009-2199-x
- Austin, C. P., Brady, L. S., Insel, T. R., and Collins, F. S. (2004). NIH molecular libraries initiative. *Science* 306, 1138–1139. doi: 10.1126/science.1105511
- Bjarnsholt, T. (2013). The role of bacterial biofilms in chronic infections. *APMIS* 121, 1–58. doi: 10.1111/apm.12099
- Bordeleau, E., Fortier, L. C., Malouin, F., and Burrus, V. (2011). c-di-GMP turn-over in *Clostridium difficile* is controlled by a plethora of diguanylate cyclases and phosphodiesterases. *PLoS Genet.* 7:e1002039. doi: 10.1371/journal.pgen.1002039
- Caly, D. L., Bellini, D., Walsh, D. A., Dow, J. M., and Ryan, R. P. (2015). Targeting cyclic di-GMP signalling: a strategy to control biofilm formation? *Curr. Pharm. Des.* 21, 12–24. doi: 10.2174/1381612820666140905124701
- Chan, C., Paul, R., Samoray, D., Amiot, N. C., Giese, B., Jenal, U., et al. (2004). Structural basis of activity and allosteric control of diguanylate cyclase. *Proc. Natl. Acad. Sci. U.S.A.* 101, 17084–17089. doi: 10.1073/pnas.0406134101
- Cheng, X., Zheng, X., Zhou, X., Zeng, J., Ren, Z., Xu X., et al. (2016). Regulation of oxidative response and extracellular polysaccharide synthesis by a diadenylate cyclase in *Streptococcus mutans*. *Environ. Microbiol.* 18, 904–922. doi: 10.1111/1462-2920.13123
- Ching, S. M., Tan, W. J., Chua, K. L., and Lam, Y. (2010). Synthesis of cyclic dinucleotidic acids as potential inhibitors targeting diguanylate cyclase. *Bioorg. Med. Chem.* 18, 6657–6665. doi: 10.1016/j.bmc.2010.07.068
- Christen, B., Christen, M., Paul, R., Schmid, F., Folcher, M., Jenoe, P., et al. (2006). Allosteric control of cyclic di-GMP signaling. *J. Biol. Chem.* 281, 32015–32024. doi: 10.1074/jbc.M603589200
- Christen, M., Kamischke, C., Kulasekara, H. D., Olivas, K. C., Kulasekara, B. R., Christen, B., et al. (2019). Identification of small-molecule modulators of diguanylate cyclase by, FRET-based high-throughput screening. *Chembiochem* 20, 394–407. doi: 10.1002/cbic.201800593
- Christen, M., Kulasekara, H. D., Christen, B., Kulasekara, B. R., Hoffman, L. R., and Miller, S. I. (2010). Asymmetrical distribution of the second messenger c-di-GMP upon bacterial cell division. *Science* 328, 1295–1297. doi: 10.1126/science.1188658
- Chua, S. L., Liu, Y., Yam, J. K., Chen, Y., Vejborg, R. M., Tan, B. G., et al. (2014). Dispersed cells represent a distinct stage in the transition from bacterial biofilm to planktonic lifestyles. *Nat. Commun.* 5:4462. doi: 10.1038/ncomms5462
- Chua, S. L., Sivakumar, K., Rybtke, M., Yuan, M., Andersen, J. B., Nielsen, T. E., et al. (2015). C-di-GMP regulates *Pseudomonas aeruginosa* stress response to tellurite during both planktonic and biofilm modes of growth. *Sci. Rep.* 5:10052. doi: 10.1038/srep10052
- Conner, J. G., Zamorano-Sanchez, D., Park, J. H., Sondermann, H., and Yildiz, F. H. (2017). The ins and outs of cyclic di-GMP signaling in *Vibrio cholerae*. *Curr. Opin. Microbiol.* 36:20–29. doi: 10.1016/j.mib.2017.01.002
- Corrigan, R. M., Abbott, J. C., Burhenne, H., Kaever, V., and Grundling, A. (2011). c-di-AMP is a new second messenger in *Staphylococcus aureus* with a role in controlling cell size and envelope stress. *PLoS Pathog.* 7:e1002217. doi: 10.1371/journal.ppat.1002217
- De N, Pirruccello, M., Krasteva, P. V., Bae, N., Raghavan, R. V., and Sondermann, H. (2008). Phosphorylation-independent regulation of the diguanylate cyclase Wsp R. *PLoS Biol.* 6:e67. doi: 10.1371/journal.pbio.0060067
- Domenech, M., Ramos-Sevillano, E., Garcia, E., Moscoso, M., and Yuste, J. (2013). Biofilm formation avoids complement immunity and phagocytosis of *Streptococcus pneumoniae*. *Infect. Immun.* 81, 2606–2615. doi: 10.1128/IAI.00491-13
- Dow, J. M., Fouhy, Y., Lucey, J. F., Ryan, R. P. (2006). The HD-GYP domain, cyclic di-GMP signaling, and bacterial virulence to plants. *Mol. Plant Microbe Interact.* 19, 1378–1384. doi: 10.1094/MPMI-19-1378
- Du, B., Ji, W., An, H., Shi, Y., Huang, Q., Cheng, Y., et al. (2014). Functional analysis of c-di-AMP phosphodiesterase, Gdp P in *Streptococcus suis* serotype 2. *Microbiol Res.* 169, 749–758. doi: 10.1016/j.micres.2014.01.002
- Fahmi, T., Faozia, S., Port, G. C., and Cho, K. H. (2019). The Second Messenger c-di-AMP regulates diverse cellular pathways involved in stress response biofilm formation cell wall homeostasis, Spe B expression, and virulence in *Streptococcus pyogenes*. *Infect. Immun.* 87:e00147–19. doi: 10.1128/IAI.00147-19
- Fernicola, S., Paiardini, A., Giardina, G., Rampioni, G., Leoni, L., Cutruzzola, F., et al. (2016). *In silico*, discovery and *in vitro* validation of catechol-containing sulfonohydrazide compounds as potent inhibitors of the diguanylate cyclase PleD. *J. Bacteriol.* 198, 147–156. doi: 10.1128/JB.00742-15
- Fernicola, S., Torquati, L., Paiardini, A., Giardina, G., Rampioni, G., Messina, M., et al. (2015). Synthesis of triazole-linked analogues of c-di-GMP and their interactions with diguanylate cyclase. *J. Med. Chem.* 58, 8269–8284. doi: 10.1021/acs.jmedchem.5b01184
- Gao, T., Meng, Q., and Gao, H. (2017). Thioesterase YbgC affects motility by modulating c-di-GMP levels in *Shewanella oneidensis*. *Sci. Rep.* 7:3932. doi: 10.1038/s41598-017-04285-5
- Gomelsky, M., and Klug, G. (2002). BLUF: a novel FAD-binding domain involved in sensory transduction in microorganisms. *Trends Biochem. Sci.* 27, 497–500. doi: 10.1016/S0968-0004(02)02181-3
- Ha, D. G., and O'Toole, G. A. (2015). c-di-GMP and its effects on biofilm formation and dispersion: a *Pseudomonas aeruginosa*. *Rev. Microbiol. Spectr.* 3:MB-0003-2014. doi: 10.1128/microbiolspec.MB-0003-2014
- Hall-Stoodley, L., Costerton, J. W., and Stoodley, P. (2004). Bacterial biofilms: from the natural environment to infectious diseases. *Nat. Rev. Microbiol.* 2, 95–108. doi: 10.1038/nrmicro821
- Hengge, R. (2009). Principles of c-di-GMP signalling in bacteria. *Nat. Rev. Microbiol.* 7, 263–273. doi: 10.1038/nrmicro2109
- Irwin, J. J., and Shoichet, B. K. (2005). ZINC a free database of commercially available compounds for virtual screening. *J. Chem. Inf. Model.* 45, 177–182. doi: 10.1021/ci049714+
- Ito, A., Taniuchi, A., May, T., Kawata, K., and Okabe, S. (2009). Increased antibiotic resistance of *Escherichia coli* in mature biofilms. *Appl. Environ. Microbiol.* 75, 4093–4100. doi: 10.1128/AEM.02949-08
- Kim, B., Park, J. S., Choi, H. Y., Yoon, S. S., and Kim, W. G. (2018). Terrein is an inhibitor of quorum sensing and c-di-GMP in *Pseudomonas aeruginosa*: a connection between quorum sensing and c-di-GMP. *Sci. Rep.* 8:8617. doi: 10.1038/s41598-018-26974-5
- Kulasakara, H., Lee, V., Brencic, A., Liberati, N., Urbach, J., Miyata, S., et al. (2006). Analysis of *Pseudomonas aeruginosa* diguanylate cyclases and phosphodiesterases reveals a role for bis-(3'-5')-cyclic-GMP in virulence. *Proc. Natl. Acad. Sci. U.S.A.* 103, 2839–2844. doi: 10.1073/pnas.0511090103
- Lee, H. S., Gu, F., Ching, S. M., Lam, Y., and Chua, K. L. (2010). CdpA is a *Burkholderia pseudomallei* cyclic di-GMP phosphodiesterase involved in autoaggregation, flagellum synthesis, motility, biofilm formation, cell invasion, and cytotoxicity. *Infect. Immun.* 78, 1832–1840. doi: 10.1128/IAI.00446-09
- Li, Y. H., and Tian, X. (2012). Quorum sensing and bacterial social interactions in biofilms. *Sensors* 12, 2519–2538. doi: 10.3390/s120302519
- Lieberman, O. J., Orr, M. W., Wang, Y., and Lee, V. T. (2014). High-throughput screening using the differential radial capillary action of ligand assay identifies

ACKNOWLEDGMENTS

We thank spencer Weathers in Academic Media Services/Office of Information Technology at Indiana State University for drawing the structures of DGC inhibitors.

- ebesen as an inhibitor of diguanylate cyclases. *ACS Chem. Biol.* 9, 183–192. doi: 10.1021/cb400485k
- Limoli, D. H., Jones, C. J., and Wozniak, D. J. (2015). Bacterial extracellular polysaccharides in biofilm formation and function. *Microbiol. Spectr.* 3. doi: 10.1128/microbiolspec.MB-0011-2014
- Lin Chua, S., Liu, Y., Li, Y., Jun Ting, H., Kohli, G. S., Cai, Z., et al. (2017). Reduced intracellular c-di-GMP content increases expression of quorum sensing-regulated genes in *Pseudomonas aeruginosa*. *Front. Cell Infect. Microbiol.* 7:451. doi: 10.3389/fcimb.2017.00451
- Morgan, J. L., McNamara, J. T., and Zimmer, J. (2014). Mechanism of activation of bacterial cellulose synthase by cyclic di-GMP. *Nat. Struct. Mol. Biol.* 21, 489–496. doi: 10.1038/nsmb.2803
- Navarro, M. V., De, N., Bae, N., Wang, Q., and Sondermann, H. (2009). Structural analysis of the GGDEF-EAL domain-containing c-di-GMP receptor FimX. *Structure* 17, 1104–1116. doi: 10.1016/j.str.2009.06.010
- Ogawa, A., Yoshimoto, T., Kikuchi, H., Sano, K., Saito, I., Yamaguchi, T., et al. (1999). Ebselen in acute middle cerebral artery occlusion: a placebo-controlled, double-blind clinical trial. *Cerebrovasc. Dis.* 9, 112–118. doi: 10.1159/000015908
- Ohana, P., Delmer, D. P., Carlson, R. W., Glushka, J., Azadi, P., Bacic, T., et al. (1998). Identification of a novel triterpenoid saponin from *Pisum sativum* as a specific inhibitor of the diguanylate cyclase of *Acetobacter xylinum*. *Plant Cell Physiol.* 39, 144–152. doi: 10.1093/oxfordjournals.pcp.a029351
- Peng, X., Zhang, Y., Bai, G. C., Zhou, X. D., and Wu, H. (2016). Cyclic di-AMP mediates biofilm formation. *Mol. Microbiol.* 99, 945–959. doi: 10.1111/mmi.13277
- Plate, L., and Marletta, M. A. (2012). Nitric oxide modulates bacterial biofilm formation through a multicomponent cyclic-di-GMP signaling network. *Mol. Cell.* 46, 449–460. doi: 10.1016/j.molcel.2012.03.023
- Povolotsky, T. L., and Hengge, R. (2012). 'Life-style' control networks in *Escherichia coli*: signaling by the second messenger c-di-GMP. *J. Biotechnol.* 160, 10–6. doi: 10.1016/j.jbiotec.2011.12.024
- Roelofs, K. G., Wang, J., Sintim, H. O., and Lee, V. T. (2011). Differential radial capillary action of ligand assay for high-throughput detection of protein-metabolite interactions. *Proc. Natl. Acad. Sci. U.S.A.* 108, 15528–15533. doi: 10.1073/pnas.1018949108
- Romling, U., Gomelsky, M., and Galperin, M. Y. (2005). C-di-GMP: the dawning of a novel bacterial signalling system. *Mol. Microbiol.* 57, 629–639. doi: 10.1111/j.1365-2958.2005.04697.x
- Ross, P., Weinhouse, H., Aloni, Y., Michaeli, D., Weinberger-Ohana, P., Mayer, R., et al. (1987). Regulation of cellulose synthesis in *Acetobacter xylinum* by cyclic diguanylic acid. *Nature* 325, 279–281. doi: 10.1038/325279a0
- Roy, R., Tiwari, M., Donelli, G., and Tiwari, V. (2018). Strategies for combating bacterial biofilms: a focus on anti-biofilm agents and their mechanisms of action. *Virulence* 9, 522–554. doi: 10.1080/21505594.2017.1313372
- Sambanthamoorthy, K., Luo, C., Pattabiraman, N., Feng, X., Koestler, B., Waters, C. M., et al. (2014). Identification of small molecules inhibiting diguanylate cyclases to control bacterial biofilm development. *Biofouling* 30, 17–28. doi: 10.1080/08927014.2013.832224
- Sambanthamoorthy, K., Sloup, R. E., Parashar, V., Smith, J. M., Kim, E. E., Semmelhack, M. F., et al. (2012). Identification of small molecules that antagonize diguanylate cyclase enzymes to inhibit biofilm formation. *Antimicrob. Agents Chemother.* 56, 5202–5211. doi: 10.1128/AAC.01396-12
- Shanahan, C. A., Gaffney, B. L., Jones, R. A., and Strobel, S. A. (2013). Identification of c-di-GMP derivatives resistant to an EAL domain phosphodiesterase. *Biochemistry* 52, 365–377. doi: 10.1021/bi301510v
- Solano, C., Garcia, B., Latasa, C., Toledo-Arana, A., Zorraquino, V., Valle, J., et al. (2009). Genetic reductionist approach for dissecting individual roles of GGDEF proteins within the c-di-GMP signaling network in *Salmonella*. *Proc. Natl. Acad. Sci. U.S.A.* 106, 7997–8002. doi: 10.1073/pnas.0812573106
- Spangler, C., Kaever, V., and Seifert, R. (2011). Interaction of the diguanylate cyclase YdeH of *Escherichia coli* with 2', (3')-substituted purine and pyrimidine nucleotides. *J. Pharmacol. Exp. Ther.* 336, 234–241. doi: 10.1124/jpet.110.170993
- Stelitano, V., Brandt, A., Fericola, S., Franceschini, S., Giardina, G., Pica, A., et al. (2013a). Probing the activity of diguanylate cyclases and c-di-GMP phosphodiesterases in real-time by CD spectroscopy. *Nucleic Acids Res.* 41:e79. doi: 10.1093/nar/gkt028
- Stelitano, V., Giardina, G., Paiardini, A., Castiglione, N., Cutruzzola, F., and Rinaldo, S. (2013b). C-di-GMP hydrolysis by *Pseudomonas aeruginosa* HD-GYP phosphodiesterases: analysis of the reaction mechanism and novel roles for pGpG. *PLoS ONE* 8:e74920. doi: 10.1371/journal.pone.0074920
- Sundriyal, A., Massa, C., Samoray, D., Zehender, F., Sharpe, T., Jenal, U., et al. (2014). Inherent regulation of EAL domain-catalyzed hydrolysis of second messenger cyclic di-GMP. *J. Biol. Chem.* 289, 6978–6990. doi: 10.1074/jbc.M113.516195
- Tuckerman, J. R., Gonzalez, G., Sousa, E. H., Wan, X., Saito, J. A., Alam, M., et al. (2009). An oxygen-sensing diguanylate cyclase and phosphodiesterase couple for c-di-GMP control. *Biochemistry* 48, 9764–9774. doi: 10.1021/bi901409g
- Valentini, M., and Filloux, A. (2016). Biofilms and cyclic di-GMP (c-di-GMP) signaling: lessons from *Pseudomonas aeruginosa* and other bacteria. *J. Biol. Chem.* 291, 12547–12555. doi: 10.1074/jbc.R115.711507
- Wassmann, P., Chan, C., Paul, R., Beck, A., Heerklotz, H., Jenal, U., et al. (2007). Structure of BeF₃-modified response regulator PleD: implications for diguanylate cyclase activation, catalysis, and feedback inhibition. *Structure* 15, 915–927. doi: 10.1016/j.str.2007.06.016
- Wiggers, H., Crusca, E., Silva, E., Cheleski, J., Torres, N., and Navarro, M. (2018). Identification of anti-inflammatory and anti-hypertensive drugs as inhibitors of bacterial diguanylate cyclases. *J. Brazil. Chem. Soc.* (2017) 29, 297–309. doi: 10.21577/0103-5053.20170141
- Wirebrand, L., Osterberg, S., Lopez-Sanchez, A., Govantes, F., and Shingler, V. (2018). PP4397/FlgZ provides the link between PP2258 c-di-GMP signalling and altered motility in *Pseudomonas putida*. *Sci. Rep.* 8:12205. doi: 10.1038/s41598-018-29785-w
- Wolber, G., and Langer, T. (2005). LigandScout: 3-D pharmacophores derived from protein-bound ligands and their use as virtual screening filters. *J. Chem. Inf. Model.* 45, 160–169. doi: 10.1021/ci049885e
- Wolcott, R. D., Rhoads, D. D., Bennett, M. E., Wolcott, B. M., Gogokhia, L., Costerton, J. W., et al. (2010). Chronic wounds and the medical biofilm paradigm. *J. Wound Care* 19, 2–3. doi: 10.12968/jowc.2010.19.2.46966
- Zhou, J., Watt, S., Wang, J., Nakayama, S., Sayre, D. A., Lam, Y. F., et al. (2013). Potent suppression of c-di-GMP synthesis via I-site allosteric inhibition of diguanylate cyclases with 2'-F-c-di-GMP. *Bioorg. Med. Chem.* 21, 4396–404. doi: 10.1016/j.bmc.2013.04.050

Conflict of Interest: The authors declare that the research was conducted in the absence of any commercial or financial relationships that could be construed as a potential conflict of interest.

Copyright © 2020 Cho, Tryon and Kim. This is an open-access article distributed under the terms of the Creative Commons Attribution License (CC BY). The use, distribution or reproduction in other forums is permitted, provided the original author(s) and the copyright owner(s) are credited and that the original publication in this journal is cited, in accordance with accepted academic practice. No use, distribution or reproduction is permitted which does not comply with these terms.



Hit Identification of New Potent PqsR Antagonists as Inhibitors of Quorum Sensing in Planktonic and Biofilm Grown *Pseudomonas aeruginosa*

OPEN ACCESS

Edited by:

Manuel Simões,
University of Porto, Portugal

Reviewed by:

Gabriella Guerrini,
University of Florence, Italy
Letizia Crocetti,
University of Florence, Italy

*Correspondence:

Miguel Cámara
miguel.camara@nottingham.ac.uk
Michael J. Stocks
michael.stocks@nottingham.ac.uk

† These authors have contributed
equally to this work as joint first
authors

Specialty section:

This article was submitted to
Medicinal and Pharmaceutical
Chemistry,
a section of the journal
Frontiers in Chemistry

Received: 20 December 2019

Accepted: 04 March 2020

Published: 04 May 2020

Citation:

Soukariéh F, Liu R, Romero M,
Roberston SN, Richardson W,
Lucanto S, Oton EV, Qudus NR,
Mashabi A, Grossman S, Ali S, Sou T,
Kukavica-Ibrulj I, Levesque RC,
Bergström CAS, Halliday N,
Mistry SN, Emsley J, Heeb S,
Williams P, Cámara M and Stocks MJ
(2020) Hit Identification of New Potent
PqsR Antagonists as Inhibitors of
Quorum Sensing in Planktonic and
Biofilm Grown *Pseudomonas*
aeruginosa. Front. Chem. 8:204.
doi: 10.3389/fchem.2020.00204

Fadi Soukariéh^{1,2†}, Ruiling Liu^{3†}, Manuel Romero^{1,2}, Shaun N. Roberston^{1,2}, William Richardson³, Simone Lucanto^{1,2}, Eduard Vico Oton¹, Naim Ruhul Qudus¹, Alaa Mashabi³, Scott Grossman³, Sadiqur Ali¹, Tomás Sou^{4,5}, Irena Kukavica-Ibrulj⁶, Roger C. Levesque⁶, Christel A. S. Bergström^{4,7}, Nigel Halliday¹, Shailesh N. Mistry³, Jonas Emsley^{2,3}, Stephan Heeb¹, Paul Williams^{1,2}, Miguel Cámara^{1,2*} and Michael J. Stocks^{2,3*}

¹ School of Life Sciences, University of Nottingham Biodiscovery Institute, University of Nottingham, Nottingham, United Kingdom, ² The National Biofilms Innovation Centre, University of Nottingham, Nottingham, United Kingdom, ³ School of Pharmacy, University of Nottingham Biodiscovery Institute, University of Nottingham, Nottingham, United Kingdom, ⁴ Drug Delivery Group, Department of Pharmacy, Uppsala University, Uppsala, Sweden, ⁵ Pharmacometrics Group, Department of Pharmaceutical Biosciences, Uppsala University, Uppsala, Sweden, ⁶ Institut de Biologie Intégrative et des Systèmes, Université Laval, Quebec City, QC, Canada, ⁷ The Swedish Drug Delivery Center, Department of Pharmacy, Uppsala University, Uppsala, Sweden

Current treatments for *Pseudomonas aeruginosa* infections are becoming less effective because of the increasing rates of multi-antibiotic resistance. Pharmacological targeting of virulence through inhibition of quorum sensing (QS) dependent virulence gene regulation has considerable therapeutic potential. In *P. aeruginosa*, the *pqs* QS system regulates the production of multiple virulence factors as well as biofilm maturation and is a promising approach for developing antimicrobial adjuvants for combatting drug resistance. In this work, we report the hit optimisation for a series of potent novel inhibitors of PqsR, a key regulator of the *pqs* system, bearing a 2-((5-methyl-5H-[1,2,4]triazino[5,6-*b*]indol-3-yl)thio) acetamide scaffold. The initial hit compound **7** (PAO1-L IC₅₀ 0.98 ± 0.02 μM, PA14 inactive at 10 μM) was obtained through a virtual screening campaign performed on the PqsR ligand binding domain using the University of Nottingham Managed Chemical Compound Collection. Hit optimisation gave compounds with enhanced potency against strains PAO1-L and PA14, evaluated using *P. aeruginosa* *pqs*-based QS bioreporter assays. Compound **40** (PAO1-L IC₅₀ 0.25 ± 0.12 μM, PA14 IC₅₀ 0.34 ± 0.03 μM) is one of the most potent PqsR antagonists reported showing significant inhibition of *P. aeruginosa* pyocyanin production and *pqs* system signaling in both planktonic cultures and biofilms. The co-crystal structure of **40** with the PqsR ligand binding domain revealed the specific binding interactions occurring between inhibitor and this key regulatory protein.

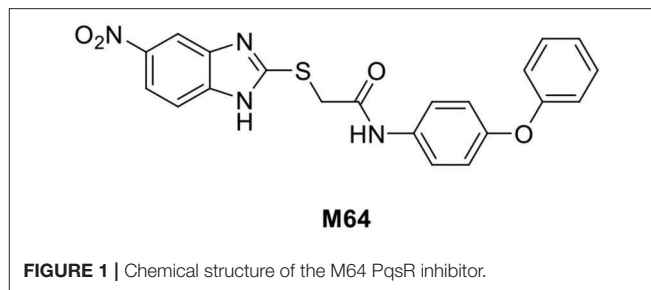
Keywords: *Pseudomonas aeruginosa*, PqsR, MvfR, *Pseudomonas* quinolone signal (PQS), alkylquinolone, biofilms, quorum sensing inhibition, quorum quenching

INTRODUCTION

Pseudomonas aeruginosa is a Gram-negative pathogen able to infect a range of human body sites causing serious tissue damage, blood stream invasion, and systemic dissemination (Strateva and Yordanov, 2009). This opportunistic pathogen is particularly devastating for immuno-compromised patients and a leading cause of death for those with cystic fibrosis (Winstanley et al., 2016). Current treatments for *P. aeruginosa* infections rely mainly on antibiotics inhibiting essential bacterial targets required for survival. These therapies, whilst effective in some cases, impose selective pressures leading to the rapid emergence of resistance, particularly in biofilms (Blair et al., 2015). There are ~50,000 cases of *P. aeruginosa* infections in the USA every year and around 13% are due to multidrug-resistant strains (Ventola, 2015). *Pseudomonas aeruginosa* has developed resistance to most antibiotic classes including aminoglycosides, cephalosporins, fluoroquinolones and even carbapenems (Potron et al., 2015). Therefore, there is an urgent need to develop alternative strategies for effectively treating infections caused by this organism. The pathogenicity of *P. aeruginosa* stems from a wide range of secreted and cell-associated virulence factors (Gellatly and Hancock, 2013). Anti-virulence strategies, through the attenuation of virulence without interfering with bacterial growth, are viewed as a promising alternative approach to combat drug resistance since they exert less selective pressures on the pathogen (Muhlen and Dersch, 2016; Fleitas Martinez et al., 2019).

QS is a bacterial cell-to-cell communication mechanism that allows bacteria to coordinate gene expression in response to population density reflecting the local concentration of extracellular signaling molecules termed autoinducers (AIs). *P. aeruginosa* employs a quorum sensing (QS) network to regulate the production of a wide range of virulence traits including but not limited to, exoproducts such as pyocyanin, HCN, elastase, lectinA, pyoverdine, drug efflux pumps, and factors required for immune evasion (Williams and Camara, 2009). QS also plays a key role in controlling biofilm development and biofilm mediated resistance to antibiotics (Bjarnsholt et al., 2005; Thomann et al., 2016; Maura and Rahme, 2017; Soukarieh et al., 2018a). *Pseudomonas aeruginosa* has three highly interconnected QS systems: two *N*-acylhomoserine lactone (AHL)-dependent QS systems (the *las* and *rhl* systems) and the *Pseudomonas* Quinolone Signal (*pqs*) system which relies on alkylquinolone (AQ)-derived autoinducers (Lee and Zhang, 2015; Whiteley et al., 2017).

The *P. aeruginosa pqs* system uses the LysR-type transcriptional regulator PqsR (also known as MvFR), to control the expression of the *pqsABCDE* operon that encodes the enzymes required for the biosynthesis of 4-hydroxy-2-heptylquinoline (HHQ) which, upon the action of the mono-oxygenase PqsH, is converted to 2-heptyl-3-hydroxy-4-quinolone (PQS). PQS and HHQ interact with the C-terminal ligand binding domain of PqsR, resulting in a conformational change that leads to the activation of the *pqs* operon likely through the interaction of the helix-turn-helix DNA binding domain of this protein with the *pqsA* promoter.



This triggers the production virulence factors and secondary metabolites through a range of PqsR-dependent and PqsR-independent mechanisms, some of which involve PqsE (Diggle et al., 2007; Ben Haj Khalifa et al., 2011; Rampioni et al., 2016).

The *pqs* system is crucial for *P. aeruginosa* pathogenicity and has been regarded as a promising therapeutic target to alleviate antibiotic-resistant infections (Fleitas Martinez et al., 2018). Several attempts to target the *pqs* system with various PqsR inhibitors have previously been reported (Soukarieh et al., 2018a,b). Of these inhibitors, **M64** (Figure 1) was the first PqsR inhibitor to show *in vivo* activity in a mouse lung infection model (Starkey et al., 2014). Due to the lipophilic nature of the PqsR ligand binding site, finding a new series of *pqs* inhibitors, with improved drug-likeness remains a challenge (Ilangoan et al., 2013). In this work, we report the synthesis and biological evaluation of a new series of high potency PqsR inhibitors and demonstrate their ability to inhibit QS in both planktonic and biofilms cultures.

MATERIALS AND METHODS

Data Management and Analysis

Instant JChem was used for Structure Database Management, Search and Prediction, Instant JChem 16.2.15.0 2016, ChemAxon (<http://www.chemaxon.com>). Sigmoidal dose-response curves and the representation of all data were prepared using GraphPad Prism.

General Chemistry

Reagents and anhydrous solvents were purchased from Sigma Aldrich, Alfa Aesar and Fisher Scientific, and were used without further purification. Nuclear magnetic resonance: ^1H -NMR and ^{13}C -NMR, were obtained at room temperature using a Bruker AV400 spectrometer operating at 400 MHz. The samples were prepared in deuterated solvent: DMSO- d_6 and CDCl_3 . Chemical shifts (δ) were recorded in ppm and coupling constants (J) were recorded in Hz. The spectra were analyzed using MestReNova 12.0.1 software. Mass spectrometry: Analytical HPLC were performed on a Shimadzu UFLCXR system coupled to an Applied Biosystems API2000. Three columns thermostated at 40°C were used. Column one: Phenomenex Gemini-NX 3 μm C18, 50 \times 2 mm Column two: Phenomenex Luna 3 μm (PFP2) 110A, 50 \times 2 mm. Column three: Waters X terra MS C8 2.5 μm , 4.6 \times 30 mm. Flow rate 0.5 mL/min. UV detection at 220 (channel

2) and 254 nm (channel 1). Short gradient: Pre-equilibration run for one min at 5% B; then method run: 5–98% solvent B in 2 min, 98% B for 2 min, 98–5% B in 0.5 min then 5% for 1 min. Long gradient: Pre-equilibration run for one min at 5% B; then method run: 5% B for 0.5 min, 10–98% solvent B in 8 min, 98% B for 2 min, 98–5% B in 0.5 min then 5% B for 1 min. Solvent A: 0.1% Formic acid in water; solvent B: 0.1% Formic acid in MeCN. Chromatography: Thin-layer chromatography (TLC) was performed, UV light and standard TLC stains were used to visualize the Merck Silica gel 60 Å F₂₅₄ plates. Compounds were purified via column chromatography using either a Thompson pump or normal phase Interchim Puriflash pre-packed cartridges consisting of 50 µM silica, or a glass column using Merck Geduran silica gel 60 Å (230–240 µm) Column size selected was generally 40–60 times the loading amount.

General Procedure A: Alkylation of Thiols With *tert*-butyl 2-Bromoacetate (3–4)

tert-Butyl 2-bromoacetate (1 mmol) was added dropwise to a suspension of 5-methyl-5*H*-[1,2,4]triazino[5,6-*b*]indole-3-thiols (1–2) (Sharma et al., 2014) (1 mmol) and triethylamine (1 mmol) in anhydrous toluene (10 mL) at 0°C under N₂. The reaction mixture was allowed to slowly warm up to room temperature and stirred for 3 h and was quenched with water (5 mL) and stirred at room temperature for further 5 min. The mixture was then diluted with water (30 mL) and then extracted with EtOAc (20 mL × 3). The organic layers were combined and washed with brine and dried over Na₂SO₄. The crude compound was purified by column chromatography.

***tert*-Butyl 2-((5-methyl-5*H*-[1,2,4]triazino[5,6-*b*]indol-3-yl)thio)acetate (3).** The title compound was prepared from 5-methyl-5*H*-[1,2,4]triazino[5,6-*b*]indole-3-thiol (1) (0.40 g, 1.83 mmol), *tert*-butyl 2-bromoacetate (0.280 g, 1.83 mmol) and triethylamine (0.185 g, 1.83 mmol) according to general procedure A. The crude product was purified by column chromatography (petroleum ether/EtOAc 4:1) to give a white solid (0.37 g, 62%). ¹H NMR (400 MHz, DMSO-*d*₆) δ 8.36 (d, *J* = 7.6 Hz, 1H), 7.79 (d, *J* = 4.1 Hz, 2H), 7.51 (dq, *J* = 8.0, 4.3 Hz, 1H), 4.10 (s, 2H), 3.83 (s, 3H), 1.42 (s, 9H). ¹³C NMR (101 MHz, CDCl₃) δ 168.04, 166.84, 146.28, 141.42, 141.14, 130.74, 122.90, 122.12, 118.01, 109.84, 82.07, 34.54, 28.03, 27.22. LCMS *m/z* calc for C₁₆H₁₈N₄O₂S [M+H]⁺: 330.2, found 330.4 with *t*_R 2.91 min, purity 95%.

***tert*-Butyl 2-((8-bromo-5-methyl-5*H*-[1,2,4]triazino[5,6-*b*]indol-3-yl)thio)acetate (4).** The title compound was prepared from 8-bromo-5-methyl-5*H*-[1,2,4]triazino[5,6-*b*]indole-3-thiol (2) (0.15 g, 0.53 mmol), *tert*-butyl 2-bromoacetate (0.081 g, 0.53 mmol) and triethylamine (0.53 g, 0.53 mmol) according to general procedure A. The crude product was purified by column chromatography (petroleum ether/EtOAc 4:1) to give a yellow solid (0.20 g, 88%). ¹H NMR (400 MHz, DMSO-*d*₆) δ 8.52 (d, *J* = 2.0 Hz, 1H), 7.94 (dd, *J* = 8.7, 2.0 Hz, 1H), 7.78 (d, *J* = 8.7 Hz, 1H), 4.11 (s, 2H), 3.81 (s, 3H), 1.42 (s, 9H). ¹³C NMR (101 MHz, CDCl₃) δ 167.92, 167.77, 146.62, 140.30, 140.13, 133.28, 125.09, 119.92, 116.10, 111.39, 82.22, 34.61, 28.02, 27.41. LCMS

m/z calc for C₁₆H₁₇BrN₄O₂S [M+H]⁺: 408.0, found 408.3 with *t*_R 3.05 min, purity 95%.

General Procedure B: *tert*-butyl Ester Deprotection (5–6)

Intermediates (3–4) were dissolved in DCM (3 mL/mmole), 4M HCl in 1,4-dioxane (excess, 2 mL/mmole) was added to the suspension. The mixture was then allowed to stir at room temperature overnight. The solvent was removed under vacuum to yield a light yellow solid. The crude product was washed with diethyl ether and DCM and was used directly for next steps without further purification.

2-((5-Methyl-5*H*-[1,2,4]triazino[5,6-*b*]indol-3-yl)thio)acetic acid (5). The title compound was prepared from *tert*-butyl 2-((5-methyl-5*H*-[1,2,4]triazino[5,6-*b*]indol-3-yl)thio)acetate (3) (0.40 g, 1.21 mmol) according to general procedure B. The product was obtained as a yellow solid (280 mg, 84.34%). ¹H NMR (400 MHz, DMSO-*d*₆) δ 8.34 (d, *J* = 7.7 Hz, 1H), 7.79 (d, *J* = 4.0 Hz, 2H), 7.51 (dq, *J* = 8.1, 4.5 Hz, 1H), 4.10 (s, 2H), 3.83 (s, 3H). ¹³C NMR (101 MHz, DMSO-*d*₆) δ 170.50, 166.81, 146.54, 142.14, 131.47, 123.40, 121.92, 117.75, 111.70, 79.46, 33.58, 27.81. LCMS *m/z* calc. for C₁₂H₁₀N₄O₂S [M+H]⁺: 274.4, found 274.3 with *t*_R 2.40 min, purity 95%.

2-((8-Bromo-5-methyl-5*H*-[1,2,4]triazino[5,6-*b*]indol-3-yl)thio)acetic acid (6). The title compound was prepared from *tert*-butyl 2-((8-bromo-5-methyl-5*H*-[1,2,4]triazino[5,6-*b*]indol-3-yl)thio)acetate (4) (0.19 g, 0.46 mmol) according to general procedure B. The product was obtained as a yellow solid (0.13 g, 81.7%). ¹H NMR (400 MHz, DMSO-*d*₆) δ 8.50 (d, *J* = 2.0 Hz, 1H), 7.94 (dd, *J* = 8.7, 2.0 Hz, 1H), 7.78 (d, *J* = 8.7 Hz, 1H), 4.14 (s, 2H), 3.81 (s, 3H). ¹³C NMR (101 MHz, DMSO-*d*₆) δ 168.10, 146.66, 140.93, 133.76, 124.20, 119.65, 115.51, 115.49, 113.88, 81.73, 34.30, 28.15. LCMS *m/z* calc for C₁₂H₉BrN₄O₂S [M+H]⁺: 353.2, found 353.2 with *t*_R 2.63 min, purity 95%.

General Procedure C: HATU-Mediated Amide Bond Formation (7–28)

Carboxylic acids (5–6) (1.0 eq), HATU (1.5 equiv.), DMAP (0.10 equiv.) and various anilines (1.0 equiv.) were dissolved in anhydrous NMP (0.1 mmol/ 3 mL) and stirred at room temperature for 5 min before addition of DIPEA (6 equiv.). The reaction mixture was allowed to stir at room temperature for overnight. The reaction was monitored by TLC and quenched by addition of water (20 mL). The mixture was diluted with water (10 mL) and extracted with EtOAc (15 mL × 3) and the combined organic layers were washed with Sat. NaHCO₃ (20 mL × 3) and brine (20 mL) and dried over Na₂SO₄. Solvent was removed under vacuum and the crude product was purified by column chromatography to afford the target compounds.

***N*-(4-Chlorophenyl)-2-((5-methyl-5*H*-[1,2,4]triazino[5,6-*b*]indol-3-yl)thio)acetamide (7).** The title compound was prepared from 2-((5-methyl-5*H*-[1,2,4]triazino[5,6-*b*]indol-3-yl)thio)acetic acid (5) (0.050 g, 0.18 mmol) and 4-chloroaniline (0.023 g, 0.18 mmol) according to general procedure C. The crude product was purified by column chromatography (petroleum ether/EtOAc 2:1) to give a white solid (0.022 g, 31%).

^1H NMR (400 MHz, DMSO- d_6) δ 10.56 (s, 1H), 8.32 (d, J = 7.9 Hz, 1H), 7.81–7.72 (m, 2H), 7.71–7.63 (m, 2H), 7.48 (td, J = 6.9, 5.9, 2.2 Hz, 1H), 7.42–7.33 (m, 2H), 4.28 (s, 2H), 3.77 (s, 3H). ^{13}C NMR (101 MHz, DMSO- d_6) δ 167.07, 166.92, 146.51, 142.05, 141.40, 138.50, 131.38, 129.19, 127.37, 123.32, 121.86, 121.11, 117.71, 111.62, 35.99, 27.72. LCMS m/z calc. for $\text{C}_{18}\text{H}_{14}\text{ClN}_5\text{OS}$ $[\text{M}+\text{H}]^+$: 383.3, found 383.9 with t_R 2.84 min, purity 95%.

2-((8-Bromo-5-methyl-5H-[1,2,4]triazino[5,6-*b*]indol-3-yl)thio)-*N*-(4-chlorophenyl)acetamide (8). The title compound was prepared from 2-((8-bromo-5-methyl-5H-[1,2,4]triazino[5,6-*b*]indol-3-yl)thio)acetic acid (**6**) (0.050 g, 0.1415 mmol) and 4-chloroaniline (0.020 g, 0.1562 mmol) according to general procedure C. The crude product was purified by column chromatography (petroleum ether/EtOAc 2:1) to give a white solid (0.010 g, 15%). ^1H NMR (400 MHz, DMSO- d_6) δ 10.57 (s, 1H), 8.50 (d, J = 2.0 Hz, 1H), 7.93 (dd, J = 8.7, 2.0 Hz, 1H), 7.76 (d, J = 8.7 Hz, 1H), 7.72–7.60 (m, 2H), 7.42–7.34 (m, 2H), 4.28 (s, 1H), 3.77 (s, 1H). ^{13}C NMR (101 MHz, DMSO- d_6) δ 167.86, 166.82, 146.71, 140.96, 140.55, 138.49, 133.71, 129.20, 127.38, 124.18, 121.11, 119.71, 115.45, 113.86, 36.01, 27.90. LCMS m/z calc. for $\text{C}_{18}\text{H}_{14}\text{BrClN}_5\text{OS}$ $[\text{M}+\text{H}]^+$: 462.3, found 462.7 with t_R 2.91 min, purity 95%.

2-((5-Methyl-5H-[1,2,4]triazino[5,6-*b*]indol-3-yl)thio)-*N*-phenylacetamide (9). The title compound was prepared from 2-((5-methyl-5H-[1,2,4]triazino[5,6-*b*]indol-3-yl)thio)acetic acid (**5**) (0.050 g, 0.18 mmol) and aniline (0.017 g, 0.18 mmol) according to general procedure C. The crude product was purified by column chromatography (petroleum ether/EtOAc 2:1) to give a white solid (0.013 g, 20%). ^1H NMR (400 MHz, DMSO- d_6) δ 10.42 (s, 1H), 8.33 (d, J = 7.8 Hz, 1H), 7.81–7.72 (m, 2H), 7.66–7.58 (m, 2H), 7.49 (ddd, J = 8.1, 5.2, 3.0 Hz, 1H), 7.32 (t, J = 7.9 Hz, 2H), 7.11–7.02 (m, 1H), 4.28 (s, 2H), 3.79 (s, 3H). ^{13}C NMR (101 MHz, DMSO- d_6) δ 167.17, 166.70, 146.54, 142.07, 141.40, 139.56, 131.39, 129.27, 123.83, 123.34, 121.88, 119.57, 117.74, 111.65, 36.01, 27.75. LCMS m/z calc. for $\text{C}_{18}\text{H}_{15}\text{N}_5\text{OS}$ $[\text{M}+\text{H}]^+$: 349.4, found 349.4 with t_R 2.72 min, purity 95%.

2-((8-Bromo-5-methyl-5H-[1,2,4]triazino[5,6-*b*]indol-3-yl)thio)-*N*-phenylacetamide (10). The title compound was prepared from 2-((8-bromo-5-methyl-5H-[1,2,4]triazino[5,6-*b*]indol-3-yl)thio)acetic acid (**6**) (0.050 g, 0.14 mmol) and aniline (0.013 g, 0.14 mmol) according to general procedure C. The crude product was purified by column chromatography (petroleum ether/EtOAc 2:1) to give a white solid (0.015 g, 25%). ^1H NMR (400 MHz, DMSO- d_6) δ 10.42 (s, 1H), 8.49 (d, J = 1.9 Hz, 1H), 7.93 (dd, J = 8.7, 2.0 Hz, 1H), 7.76 (d, J = 8.7 Hz, 1H), 7.62 (d, J = 7.9 Hz, 2H), 7.32 (t, J = 7.9 Hz, 2H), 7.06 (t, J = 7.4 Hz, 1H), 4.29 (s, 2H), 3.78 (s, 3H). ^{13}C NMR (101 MHz, DMSO- d_6) δ 167.96, 166.60, 146.71, 140.94, 140.52, 139.54, 133.69, 132.07, 129.27, 129.14, 124.16, 123.84, 119.71, 119.57, 115.44, 113.85, 36.03, 27.91. LCMS m/z calc. for $\text{C}_{18}\text{H}_{14}\text{BrN}_5\text{OS}$ $[\text{M}+\text{H}]^+$: 429.2, found 428.3 with t_R 2.87 min, purity 95%.

***N*-(3-Chlorophenyl)-2-((5-methyl-5H-[1,2,4]triazino[5,6-*b*]indol-3-yl)thio)acetamide (11).** The title compound was prepared from 2-((5-methyl-5H-[1,2,4]triazino[5,6-*b*]indol-3-yl)thio)acetic acid (**5**) (0.040 g, 0.15 mmol) and 3-chloroaniline (0.019 g, 0.15 mmol) according to general procedure C. The

crude product was purified by column chromatography (petroleum ether/EtOAc 2:1) to give white solid (0.013 g, 23%). ^1H NMR (400 MHz, DMSO- d_6) δ 10.62 (s, 1H), 8.34 (d, J = 7.8 Hz, 1H), 7.84 (t, J = 2.0 Hz, 1H), 7.78 (d, J = 3.9 Hz, 2H), 7.54–7.28 (m, 2H), 7.36 (t, J = 8.1 Hz, 1H), 7.18–7.05 (m, 1H), 4.29 (s, 2H), 3.78 (s, 3H). ^{13}C NMR (101 MHz, DMSO- d_6) δ 167.19, 167.01, 146.55, 142.11, 141.46, 140.98, 133.60, 131.42, 131.02, 123.56, 123.35, 121.91, 119.00, 117.94, 117.74, 111.67, 36.01, 27.74. LCMS m/z calc. for $\text{C}_{15}\text{H}_{14}\text{ClN}_5\text{OS}$ $[\text{M}+\text{H}]^+$: 383.8, found 383.9 with t_R 2.87 min, purity 95%.

2-((8-Bromo-5-methyl-5H-[1,2,4]triazino[5,6-*b*]indol-3-yl)thio)-*N*-(3-chlorophenyl)acetamide (12). The title compound was prepared from 2-((8-bromo-5-methyl-5H-[1,2,4]triazino[5,6-*b*]indol-3-yl)thio)acetic acid (**6**) (0.050 g, 0.14 mmol) and 3-chloroaniline (0.018 g, 0.14 mmol) according to general procedure C. The crude product was purified by column chromatography (petroleum ether/EtOAc 2:1) to give a white solid (0.010 g, 15.4%). ^1H NMR (400 MHz, DMSO- d_6) δ 10.63 (s, 1H), 8.50 (d, J = 1.9 Hz, 1H), 7.93 (dd, J = 8.7, 2.0 Hz, 1H), 7.84 (t, J = 2.1 Hz, 1H), 7.76 (d, J = 8.6 Hz, 1H), 7.52–7.45 (m, 1H), 7.35 (d, J = 8.1 Hz, 1H), 7.16–7.07 (m, 1H), 4.29 (s, 2H), 3.77 (s, 3H). ^{13}C NMR (101 MHz, DMSO- d_6) δ 167.79, 167.09, 146.71, 140.96, 140.58, 133.71, 133.60, 131.02, 124.17, 123.57, 119.69, 119.00, 117.94, 115.45, 113.86, 36.03, 27.90. LCMS m/z calc. for $\text{C}_{18}\text{H}_{14}\text{BrClN}_5\text{OS}$ $[\text{M}+\text{H}]^+$: 464.2, found 464.3 with t_R 2.98 min, purity 95%.

***N*-(3,4-Dichlorophenyl)-2-((5-methyl-5H-[1,2,4]triazino[5,6-*b*]indol-3-yl)thio)acetamide (13).** The title compound was prepared from 2-((5-methyl-5H-[1,2,4]triazino[5,6-*b*]indol-3-yl)thio)acetic acid (**5**) (0.070 g, 0.25 mmol) and 3,4-dichloroaniline (0.041 g, 0.25 mmol) according to general procedure C. The crude product was purified by column chromatography (petroleum ether/EtOAc 2:1) to give a white solid (0.005 g, 5%). ^1H NMR (400 MHz, DMSO- d_6) δ 10.73 (s, 1H), 8.33 (d, J = 7.8 Hz, 1H), 8.02 (d, J = 2.4 Hz, 1H), 7.84–7.74 (m, 2H), 7.60 (d, J = 8.8 Hz, 1H), 7.56–7.28 (m, 2H), 4.29 (s, 2H), 3.78 (s, 3H). ^{13}C NMR (101 MHz, DMSO- d_6) δ 167.37, 166.94, 146.55, 142.12, 141.48, 139.62, 131.53, 131.44, 131.28, 125.26, 123.37, 121.91, 120.72, 119.61, 117.74, 111.69, 36.00, 27.75. LCMS m/z calc. for $\text{C}_{18}\text{H}_{13}\text{Cl}_2\text{N}_5\text{OS}$ $[\text{M}+\text{H}]^+$: 418.3, found 418.2 with t_R 2.95 min, purity 95%.

2-((8-Bromo-5-methyl-5H-[1,2,4]triazino[5,6-*b*]indol-3-yl)thio)-*N*-(3,4-dichlorophenyl)acetamide (14). The title compound was prepared from 2-((8-bromo-5-methyl-5H-[1,2,4]triazino[5,6-*b*]indol-3-yl)thio)acetic acid (**6**) (0.070 g, 0.20 mmol) and 3,4-dichloroaniline (0.035 g, 0.21 mmol) according to general procedure C. The crude product was purified by column chromatography (petroleum ether/EtOAc 2:1) to give white solid (0.005 g, 5%). ^1H NMR (400 MHz, DMSO- d_6) δ 10.73 (d, J = 7.6 Hz, 1H), 8.50 (d, J = 1.9 Hz, 1H), 8.02 (d, J = 2.3 Hz, 1H), 7.94 (dd, J = 8.7, 1.9 Hz, 1H), 7.76 (d, J = 8.7 Hz, 1H), 7.60 (d, J = 8.8 Hz, 1H), 7.53 (dd, J = 8.9, 2.4 Hz, 1H), 4.29 (s, 2H), 3.76 (s, 3H). ^{13}C NMR (101 MHz, DMSO- d_6) δ 167.37, 166.94, 146.55, 142.12, 141.48, 139.62, 131.53, 131.44, 131.28, 125.26, 123.37, 121.91, 120.72, 119.61, 117.74, 111.69, 36.00, 27.75. LCMS m/z calc. for $\text{C}_{18}\text{H}_{12}\text{BrCl}_2\text{N}_5\text{OS}$ $[\text{M}+\text{H}]^+$: 497.2, found 497.19 with t_R 3.06 min, purity 95%.

***N*-(4-Fluorophenyl)-2-((5-methyl-5*H*-[1,2,4]triazino[5,6-*b*]indol-3-yl)thio)acetamide (15).** The title compound was prepared from 2-((5-methyl-5*H*-[1,2,4]triazino[5,6-*b*]indol-3-yl)thio)acetic acid (5) (0.070 g, 0.26 mmol) and 4-fluoroaniline (0.028 g, 0.26 mmol) according to general procedure C. The crude product was purified by column chromatography (petroleum ether/EtOAc 2:1) to give a white solid (0.030 g, 32%). ¹H NMR (400 MHz, DMSO-*d*₆) δ 10.48 (s, 1H), 8.33 (d, *J* = 7.8 Hz, 1H), 7.86–7.71 (m, 2H), 7.69–7.59 (m, 2H), 7.49 (ddd, *J* = 8.0, 5.3, 2.9 Hz, 1H), 7.16 (t, *J* = 8.9 Hz, 2H), 4.27 (s, 2H), 3.78 (s, 3H). ¹³C NMR (101 MHz, DMSO-*d*₆) δ 167.12, 166.64, 146.54, 142.08, 141.41, 135.96, 131.40, 123.34, 121.88, 121.38, 121.30, 117.74, 115.96, 115.74, 111.65, 35.91, 27.74. LCMS *m/z* calc. for C₁₈H₁₄FN₅OS [M+H]⁺: 367.1, found 367.4 with *t*_R 2.75 min, purity 95%.

2-((8-Bromo-5-methyl-5*H*-[1,2,4]triazino[5,6-*b*]indol-3-yl)thio)-*N*-(4-fluorophenyl)acetamide (16). The title compound was prepared from 2-((8-bromo-5-methyl-5*H*-[1,2,4]triazino[5,6-*b*]indol-3-yl)thio)acetic acid (6) (0.070 g, 0.20 mmol) and 4-fluoroaniline (0.022 g, 0.20 mmol) according to general procedure C. The crude product was purified by column chromatography (petroleum ether/EtOAc 2:1) to give a white solid (0.027 g, 30%): ¹H NMR (400 MHz, DMSO-*d*₆) δ 10.48 (s, 1H), 8.49 (d, *J* = 2.0 Hz, 1H), 7.92 (dd, *J* = 8.7, 2.0 Hz, 1H), 7.75 (d, *J* = 8.7 Hz, 1H), 7.68–7.57 (m, 2H), 7.16 (t, *J* = 8.9 Hz, 2H), 4.27 (s, 2H), 3.77 (s, 3H). ¹³C NMR (101 MHz, DMSO-*d*₆) δ 167.91, 166.55, 146.71, 140.95, 140.54, 135.92, 133.70, 124.17, 121.38, 121.30, 119.70, 115.96, 115.74, 115.45, 113.85, 35.93, 27.90. LCMS *m/z* calc. for C₁₈H₁₃BrFN₅OS [M+H]⁺: 446.3, found 446.3 with *t*_R 2.88 min, purity 95%.

2-((5-Methyl-5*H*-[1,2,4]triazino[5,6-*b*]indol-3-yl)thio)-*N*-(*p*-tolyl)acetamide (17). The title compound was prepared from 2-((5-methyl-5*H*-[1,2,4]triazino[5,6-*b*]indol-3-yl)thio)acetic acid (5) (0.070 g, 0.26 mmol) and 4-methylaniline (0.027 g, 0.26 mmol) according to general procedure C. The crude product was purified by column chromatography (petroleum ether/EtOAc 2:1) to give a white solid (0.032 g, 35%). ¹H NMR (400 MHz, DMSO-*d*₆) δ 10.33 (s, 1H), 8.29 (d, *J* = 7.8 Hz, 1H), 7.74 (d, *J* = 6.8 Hz, 2H), 7.49 (dd, *J* = 17.2, 7.7 Hz, 3H), 7.12 (d, *J* = 8.0 Hz, 2H), 4.26 (s, 2H), 3.76 (s, 3H), 2.25 (s, 3H). ¹³C NMR (101 MHz, DMSO-*d*₆) δ 167.19, 166.28, 146.48, 142.00, 141.33, 137.06, 132.74, 131.33, 129.63, 123.29, 121.82, 119.58, 117.70, 111.57, 35.98, 27.72, 20.91. LCMS *m/z* calc. for C₁₉H₁₇N₅OS [M+H]⁺: 363.4, found 363.4 with *t*_R 2.78 min, purity 95%.

2-((8-Bromo-5-methyl-5*H*-[1,2,4]triazino[5,6-*b*]indol-3-yl)thio)-*N*-(*p*-tolyl)acetamide (18). The title compound was prepared from 2-((8-bromo-5-methyl-5*H*-[1,2,4]triazino[5,6-*b*]indol-3-yl)thio)acetic acid (6) (0.070 g, 0.20 mmol) and 4-methylaniline (0.030 g, 0.20 mmol) according to general procedure C. The crude product was purified by column chromatography (petroleum ether/EtOAc 2:1) to give a white solid (0.015 g, 12 %). ¹H NMR (400 MHz, DMSO-*d*₆) δ 10.34 (s, 1H), 8.47 (d, *J* = 2.0 Hz, 1H), 7.91 (dd, *J* = 8.7, 2.0 Hz, 1H), 7.74 (d, *J* = 8.7 Hz, 1H), 7.51 (d, *J* = 8.4 Hz, 2H), 7.12 (d, *J* = 8.1 Hz, 2H), 4.27 (s, 2H), 3.77 (s, 3H), 2.25 (s, 3H). ¹³C NMR (101 MHz, DMSO-*d*₆) δ 168.00, 166.33, 146.69, 140.91, 140.49, 137.05, 133.67, 132.74, 129.63, 124.14, 119.70, 119.58, 115.44,

113.84, 36.00, 27.91, 20.92. LCMS *m/z* calc. for C₁₉H₁₆BrN₅OS [M+H]⁺: 442.3, found 442.1 with *t*_R 2.95 min, purity 95%.

***N*-(4-Methoxyphenyl)-2-((5-methyl-5*H*-[1,2,4]triazino[5,6-*b*]indol-3-yl)thio)acetamide (19).** The title compound was prepared from 2-((5-methyl-5*H*-[1,2,4]triazino[5,6-*b*]indol-3-yl)thio)acetic acid (5) (0.070 g, 0.26 mmol) and 4-methoxy aniline (0.031 g, 0.26 mmol) according to general procedure C. The product was obtained as a yellow solid (0.095 g, 98%). ¹H NMR (400 MHz, DMSO-*d*₆) δ 10.27 (s, 1H, H-7), 8.32 (d, *J* = 7.7 Hz, 1H), 7.88–7.70 (m, 2H), 7.56–7.51 (m, 2H), 7.48 (ddd, *J* = 2.6, 5.6, 8.1 Hz, 1H), 6.96–6.71 (m, 2H), 4.25 (s, 2H, H-6), 3.79 (s, 3H), 3.72 (s, 3H). ¹³C NMR (101 MHz, DMSO-*d*₆) δ 167.20, 166.15, 155.75, 146.45, 142.06, 141.37, 132.70, 131.38, 123.33, 121.86, 121.13, 117.75, 114.37, 111.64, 38.71, 35.88, 27.74. LCMS *m/z* calc for C₁₉H₁₇N₅O₂S+ [M+H]⁺: 380.4, found 379.4 with *t*_R 2.70 min, purity 95%.

2-((8-Bromo-5-methyl-5*H*-[1,2,4]triazino[5,6-*b*]indol-3-yl)thio)-*N*-(4-methoxyphenyl)acetamide (20). The title compound was prepared from 2-((8-bromo-5-methyl-5*H*-[1,2,4]triazino[5,6-*b*]indol-3-yl)thio)acetic acid (6) (0.070 g, 0.20 mmol) and 4-methoxyaniline (0.023 g, 0.20 mmol) according to general procedure C. The crude product was purified by column chromatography (petroleum ether/EtOAc 2:1) to give a light yellow solid (0.017 g, 18%). ¹H NMR (400 MHz, DMSO-*d*₆) δ 10.28 (s, 1H), 8.49 (d, *J* = 2.0 Hz, 1H), 7.93 (dd, *J* = 8.7, 2.0 Hz, 1H), 7.76 (d, *J* = 8.7 Hz, 1H), 7.56–7.49 (m, 2H), 6.93–6.85 (m, 2H), 4.25 (s, 2H, H5), 3.78 (s, 3H), 3.72 (s, 3H). ¹³C NMR (101 MHz, DMSO-*d*₆) δ 168.03, 166.05, 155.76, 146.72, 140.94, 140.50, 133.68, 132.69, 124.15, 121.13, 119.72, 115.44, 114.38, 113.85, 38.72, 35.90, 27.92. LCMS *m/z* calc. for C₁₉H₁₇BrN₅O₂S [M+H]⁺: 458.3, found 458.3 with *t*_R 2.87 min, purity 95%.

2-((5-Methyl-5*H*-[1,2,4]triazino[5,6-*b*]indol-3-yl)thio)-*N*-(4(trifluoromethoxy)phenyl)acetamide (21). The title compound was prepared from 2-((5-methyl-5*H*-[1,2,4]triazino[5,6-*b*]indol-3-yl)thio)acetic acid (5) (0.050 g, 0.18 mmol) and 4-trifluoromethoxyaniline (0.032 g, 0.18 mmol) according to general procedure C. The crude product was purified by column chromatography (petroleum ether/EtOAc 2:1) to give a white solid (0.005 g, 6%). ¹H NMR (400 MHz, DMSO-*d*₆) δ 10.63 (s, 1H), 8.33 (d, *J* = 7.9 Hz, 1H), 7.84–7.62 (m, 4H), 7.49 (ddd, *J* = 8.1, 5.3, 2.8 Hz, 1H), 7.34 (d, *J* = 8.6 Hz, 2H), 4.29 (s, 2H), 3.78 (d, *J* = 1.7 Hz, 3H). ¹³C NMR (101 MHz, DMSO-*d*₆) δ 178.30, 167.05, 167.00, 146.55, 142.10, 141.44, 138.74, 131.41, 123.35, 122.18, 121.90, 120.92, 117.74, 111.66, 35.95, 27.75. LCMS *m/z* calc. for C₁₉H₁₄F₃N₅O₂S [M+H]⁺: 283.4, found 283.4 with *t*_R 2.91 min, purity 95%.

2-((8-Bromo-5-methyl-5*H*-[1,2,4]triazino[5,6-*b*]indol-3-yl)thio)-*N*-(4-(trifluoromethoxy)phenyl)acetamide (22). The title compound was prepared from 2-((8-bromo-5-methyl-5*H*-[1,2,4]triazino[5,6-*b*]indol-3-yl)thio)acetic acid (6) (0.050 g, 0.14 mmol) and 4-trifluoromethoxyaniline (0.021 mL, 0.16 mmol) according to general procedure C. The crude product was purified by column chromatography (petroleum ether/EtOAc 2:1) to give a white solid (0.007 g, 9%). ¹H NMR (400 MHz, DMSO-*d*₆) δ 10.63 (s, 1H), 8.48 (d, *J* = 2.0 Hz, 1H), 7.92 (dd, *J* = 8.7, 2.0 Hz, 1H), 7.83–7.64 (m, 3H), 7.34 (d, *J* = 8.6 Hz, 2H), 4.29 (s, 2H), 3.77 (d, *J* = 5.3 Hz, 3H). ¹³C NMR (101 MHz, DMSO-*d*₆)

δ 167.83, 167.00, 166.91, 146.70, 142.09, 140.95, 140.56, 138.73, 133.70, 124.16, 122.18, 120.93, 119.69, 119.33, 115.45, 113.85, 111.66, 35.97, 27.74. LCMS m/z calc. for $C_{19}H_{13}BrF_3N_5O_2S$ $[M+H]^+$: 512.1, found 512.3 with t_R 3.05 min, purity 95%.

***N*-(4-(Cyanomethyl)phenyl)-2-((5-methyl-5*H*-[1,2,4]triazino[5,6-*b*]indol-3-yl)thio)acetamide (23).** The title compound was prepared from 2-((5-methyl-5*H*-[1,2,4]triazino[5,6-*b*]indol-3-yl)thio)acetic acid (**5**) (0.080 g, 0.029 mmol) and 2-(4-aminophenyl)acetonitrile (0.028 g, 0.32 mmol) according to general procedure C. The crude product was purified by column chromatography (petroleum ether/EtOAc 2:1) to give a white solid (58.9 mg, 52%). 1H NMR (400 MHz, DMSO- d_6) δ 10.52 (d, J = 10.1 Hz, 1H), 8.29 (d, J = 7.7 Hz, 1H), 7.95 (s, 1H), 7.78–7.68 (m, 2H), 7.67–7.60 (m, 1H), 7.46 (ddd, J = 1.8, 6.5, 8.0 Hz, 1H), 7.30 (d, J = 8.3 Hz, 2H), 4.27 (s, 2H), 3.97 (s, 2H), 3.76 (s, 3H). ^{13}C NMR (101 MHz, DMSO- d_6) δ 167.12, 166.85, 146.49, 142.01, 141.34, 138.94, 131.39, 129.04, 126.39, 123.33, 121.84, 120.00, 119.81, 117.67, 111.58, 35.96, 27.70, 22.30. LCMS m/z calc. for $C_{20}H_{17}N_6OS$ $[M+H]^+$: 389.4, found 389.3 with t_R 2.66 min, purity > 95%.

2-((5-Methyl-5*H*-[1,2,4]triazino[5,6-*b*]indol-3-yl)thio)-*N*-(4-phenoxyphenyl)acetamide (24). The title compound was prepared from 2-((5-methyl-5*H*-[1,2,4]triazino[5,6-*b*]indol-3-yl)thio)acetic acid (**5**) (0.10 g, 0.36 mmol) and 4-phenoxyaniline (0.067 g, 0.36 mmol) according to general procedure C. The crude product was purified by column chromatography (petroleum ether/EtOAc 2:1) to give a white solid (0.094 g, 58%). 1H NMR (400 MHz, DMSO- d_6) δ 10.45 (s, 1H), 8.35–8.27 (m, 1H), 7.82–7.71 (m, 2H), 7.70–7.60 (m, 2H), 7.48 (ddd, J = 8.1, 5.6, 2.6 Hz, 1H), 7.40–7.31 (m, 2H), 7.13–7.05 (m, 1H), 7.04–6.92 (m, 4H), 4.28 (s, 2H), 3.79 (s, 3H). ^{13}C NMR (101 MHz, DMSO- d_6) δ 174.23, 166.53, 142.06, 141.39, 135.47, 131.38, 130.28, 123.46, 123.32, 121.86, 121.29, 119.98, 118.34, 117.74, 111.63, 35.93, 27.75. LCMS m/z calc. for $C_{24}H_{19}N_5O_2S$ $[M+H]^+$: 441.5, found 441.5 with t_R 2.95 min, purity 95%.

2-((8-Bromo-5-methyl-5*H*-[1,2,4]triazino[5,6-*b*]indol-3-yl)thio)-*N*-(4-phenoxyphenyl)acetamide (25). The title compound was prepared from 2-((8-bromo-5-methyl-5*H*-[1,2,4]triazino[5,6-*b*]indol-3-yl)thio)acetic acid (**6**) (0.10 g, 0.28 mmol) and 4-phenoxy aniline (0.052 g, 0.28 mmol) according to general procedure C. The crude product was purified by column chromatography (petroleum ether/EtOAc 2:1) to give a white solid (0.027 g, 18%). 1H NMR (400 MHz, DMSO- d_6) δ 10.46 (s, 1H), 8.47 (d, J = 2.0 Hz, 1H), 7.91 (dd, J = 8.7, 2.0 Hz, 1H), 7.74 (d, J = 8.7 Hz, 1H), 7.68–7.58 (m, 2H), 7.42–7.29 (m, 2H), 7.13–7.07 (m, 1H), 7.05–6.90 (m, 4H), 4.28 (s, 2H), 3.78 (s, 3H). ^{13}C NMR (101 MHz, DMSO- d_6) δ 166.28, 157.78, 152.30, 146.68, 140.92, 140.51, 135.45, 133.67, 130.28, 124.13, 123.47, 121.29, 119.97, 119.68, 118.35, 115.44, 113.83, 35.96, 27.92. LCMS m/z calc. for $C_{24}H_{18}BrN_5O_2S$ $[M+H]^+$: 520.4, found 520.4 with t_R 3.06 min, purity 95%.

***N*-(4-Bromophenyl)-2-((5-methyl-5*H*-[1,2,4]triazino[5,6-*b*]indol-3-yl)thio)acetamide (26).** The title compound was prepared from 2-((5-methyl-5*H*-[1,2,4]triazino[5,6-*b*]indol-3-yl)thio)acetic acid (**5**) (0.070 g, 0.26 mmol) and 4-bromoaniline (0.044 g, 0.26 mmol) according to general procedure C. The crude product was purified by column chromatography

(petroleum ether/EtOAc 2:1) to give a white solid (0.030 g, 27%). 1H NMR (400 MHz, DMSO- d_6) δ 10.56 (s, 1H), 8.33 (d, J = 7.7 Hz, 1H), 7.89–7.72 (m, 2H), 7.69–7.57 (m, 2H), 7.55–7.28 (m, 3H), 4.28 (s, 2H), 3.77 (s, 3H). ^{13}C NMR (101 MHz, DMSO- d_6) δ 167.08, 166.94, 146.55, 142.10, 141.28, 138.92, 132.11, 131.42, 123.36, 121.90, 121.50, 117.75, 115.40, 111.68, 36.01, 27.75. LCMS m/z calc. for $C_{18}H_{14}BrN_5OS$ $[M+H]^+$: 428.3, found 428.3 with t_R 2.87 min, purity 95%.

2-((8-Bromo-5-methyl-5*H*-[1,2,4]triazino[5,6-*b*]indol-3-yl)thio)-*N*-(4-bromophenyl)acetamide (27). The title compound was prepared from 2-((8-bromo-5-methyl-5*H*-[1,2,4]triazino[5,6-*b*]indol-3-yl)thio)acetic acid (**6**) (0.070 g, 0.20 mmol) and 4-bromoaniline (0.034 g, 0.20 mmol) according to general procedure C. The crude product was purified by column chromatography (petroleum ether/EtOAc 2:1) to give a yellow solid (0.007 g, 7%). 1H NMR (400 MHz, DMSO- d_6) δ 10.57 (s, 1H), 8.49 (d, J = 2.0 Hz, 1H), 7.93 (dd, J = 8.7, 2.1 Hz, 1H), 7.76 (d, J = 8.7 Hz, 1H), 7.64–7.56 (m, 2H), 7.55–7.44 (m, 2H), 4.28 (s, 2H), 3.76 (s, 3H). ^{13}C NMR (101 MHz, DMSO- d_6) δ 167.08, 166.95, 146.55, 142.10, 141.44, 138.92, 132.11, 131.42, 123.36, 121.91, 121.50, 117.75, 115.39, 111.68, 36.01, 27.75. LCMS m/z calc. for $C_{18}H_{13}Br_2N_5OS$ $[M+H]^+$: 507.2, found 507.2 with t_R 2.87 min, purity 95%.

2-((5-Methyl-5*H*-[1,2,4]triazino[5,6-*b*]indol-3-yl)thio)-*N*-(4-(pyrimidin-2-yloxy)phenyl)acetamide (28). 4-(pyrimidin-2-yloxy)aniline (0.065 g, 0.238 mmol), 2-((5-methyl-5*H*-[1,2,4]triazino[5,6-*b*]indol-3-yl)thio)acetic acid (**5**) (0.064 g, 0.238 mmol), HATU (0.135 g, 0.357 mmol), DIPEA (0.165 mL, 0.952 mmol), and DMAP (0.030 g, 0.0238 mmol) were dissolved in NMP (2 mL). The reaction mixture was allowed to stir at room temperature overnight and monitored by TLC. The crude product was purified by column chromatography (petroleum ether/EtOAc 1:1) to give a white solid (31 mg, 29%). 1H NMR (400 MHz, DMSO- d_6) δ 10.50 (s, 1H), 8.63 (d, J = 4.8 Hz, 2H), 8.31 (d, J = 7.8 Hz, 1H), 7.75 (d, J = 5.2 Hz, 2H), 7.67 (d, J = 8.5 Hz, 2H), 7.47 (ddd, J = 2.6, 5.8, 8.2 Hz, 1H), 7.25 (t, J = 4.8 Hz, 1H), 7.16 (d, J = 8.4 Hz, 2H), 4.30 (s, 2H), 3.79 (s, 3H). ^{13}C NMR (101 MHz, DMSO- d_6) δ 167.13, 166.67, 165.37, 160.47, 148.77, 146.53, 142.06, 141.40, 136.67, 131.38, 123.32, 122.46, 121.88, 120.83, 117.73, 117.30, 111.61, 35.96, 27.76. LCMS m/z calc. for $C_{22}H_{18}N_7O_2S^+$ $[M+H]^+$: 444.5, found 444.3 with t_R 2.62 min, purity >95%.

General Procedure D: Acylation of Anilines to Form Bromoacetatamides (32–37)

Aniline, 4-chloroaniline or 4-chloro-*N*-methylaniline and Et_3N (2 equiv.) were dissolved in anhydrous DCM at 0°C under N_2 protection followed by addition of various bromoacetyl chlorides (**29–31**) (1.0 equiv.). The reaction mixture was allowed to slowly warm up to room temperature and stirred for 4 h with monitored by TLC. Once the reaction was complete, solvent was removed under vacuum and crude product was used directly for next step without further purification (Deora et al., 2019).

2-Bromo-*N*-(4-(pyridin-2-yloxy)phenyl)acetamide (33). The title compound was prepared according to general procedures B from 4-(Pyridin-2-yloxy) aniline (100 mg, 32.57

mmol), Et₃N (3 equiv.) and 2-bromoacetyl chloride (**29**) (1.1 equiv.). The crude product was purified by column chromatography (petroleum ether/EtOAc 5:1) to give a solid (71 mg, 47%). ¹H NMR (400 MHz, CDCl₃) δ 8.19 (dd, *J* = 2.0, 5.1 Hz, 1H), 7.64 (ddd, *J* = 2.0, 7.1, 8.2 Hz, 1H), 6.99–6.90 (m, 3H), 6.83 (dd, *J* = 1.0, 8.3 Hz, 1H), 6.76–6.67 (m, 2H), 3.65 (s, 2H). ¹³C NMR (101 MHz, CDCl₃) δ 164.54, 147.74, 146.04, 143.50, 139.19, 122.29, 117.88, 116.14, 110.78, 45.81. LCMS *m/z* calc. for C₁₃H₁₁BrN₂O₂ [M+H]⁺: 307.1, found 307.0 with *t*_R 2.59 min, purity > 95%.

2-Bromo-*N*-(4-chlorophenyl)acetamide (37). The title compound was prepared from 2-bromopropanoyl chloride (**30**) (0.10 g, 0.71 mmol) and 4-chloro-*N*-methylaniline (0.12 g, 0.71 mmol) according to general procedure D. The crude product was purified by column chromatography (petroleum ether/EtOAc 6:1) to give a white solid (149 mg, 76%). ¹H NMR (400 MHz, CDCl₃) δ 7.44 (d, *J* = 8.3 Hz, 2H), 7.26 (d, *J* = 8.2 Hz, 2H), 4.24 (q, *J* = 6.6 Hz, 1H), 3.28 (s, 3H), 1.74 (d, *J* = 6.7 Hz, 3H). ¹³C NMR (101 MHz, CDCl₃) δ 169.47, 141.35, 134.42, 130.22, 128.64, 38.78, 38.13, 21.74. LCMS *m/z* calc. for C₈H₈BrClNO [M+H]⁺: 249.5, found 250.0 with *t*_R 2.63 min, purity > 95%.

General Procedure E: Alkylation of Thiols (1–2) With Bromoacetamides (32–37) to Give Thioethers (38–44)

The substituted 5-methyl-5*H*-[1,2,4]triazino[5,6-*b*]indole-3-thiol intermediates **1–2** (1 equiv.) and Et₃N (2 equiv.) were dissolved in anhydrous DCM (0.1 mmol/5 mL) followed by addition of bromoacetamides (**32–37**) (1.0 equiv.) at 0°C under N₂. The reaction mixture was allowed slowly warm up to room temperature and stir for 4 h. The reaction was monitored by TLC. Once the reaction finished, solvent was removed under vacuum. The crude product was purified by column chromatography.

***N*-(2-Chlorophenyl)-2-((5-methyl-5*H*-[1,2,4]triazino[5,6-*b*]indol-3-yl)thio)acetamide (38).** The title compound was prepared from 2-bromo-*N*-(2-chlorophenyl)acetamide (**32**) (Sun et al., 2014) (0.1 g, 0.41 mmol) and 5-methyl-5*H*-[1,2,4]triazino[5,6-*b*]indole-3-thiol (**1**) (0.088 g, 0.41 mmol) according to general procedure E. The crude product was purified by column chromatography (petroleum ether/EtOAc 2:1) to give a white solid (0.029 g, 18%). ¹H NMR (400 MHz, DMSO-*d*₆) δ 9.93 (s, 1H), 8.34 (d, *J* = 7.7 Hz, 1H), 7.87–7.73 (m, 3H), 7.50 (ddd, *J* = 7.7, 5.1, 2.4 Hz, 2H), 7.40–7.25 (m, 1H), 7.18 (td, *J* = 7.7, 1.6 Hz), 4.35 (s, 2H), 3.81 (s, 3H). ¹³C NMR (101 MHz, DMSO-*d*₆) δ 167.33, 166.90, 146.55, 142.14, 141.50, 135.29, 131.47, 129.94, 127.99, 126.66, 125.83, 123.39, 121.93, 117.74, 111.68, 35.28, 27.85. LCMS *m/z* calc. for C₁₈H₁₅ClN₅OS [M+H]⁺: 384.2, found 383.8 with *t*_R 2.82 min, purity 95%.

2-((8-Bromo-5-methyl-5*H*-[1,2,4]triazino[5,6-*b*]indol-3-yl)thio)-*N*-(2-chlorophenyl)acetamide (39). The title compound was prepared from 2-bromo-*N*-(2-chlorophenyl)acetamide (**32**) (0.1 g, 0.3387 mmol) and 8-bromo-5-methyl-5*H*-[1,2,4]triazino[5,6-*b*]indole-3-thiol (**2**) (0.083 g, 0.3387 mmol) according to general procedure E. The crude product was purified by column chromatography (petroleum ether/EtOAc 2:1) to give a white solid (0.053 g, 35%).

¹H NMR (400 MHz, DMSO-*d*₆) δ 9.94 (s, 1H), 8.50 (t, *J* = 2.8 Hz, 1H), 7.93 (dt, *J* = 9.3, 2.7 Hz, 1H), 7.88–7.64 (m, 2H), 7.50 (dd, *J* = 7.9, 1.6 Hz, 1H), 7.28–7.25 (m, 1H), 7.23–7.08 (m, 1H), 4.36 (d, *J* = 3.3 Hz, 2H), 3.80 (s, 3H). ¹³C NMR (101 MHz, DMSO-*d*₆) δ 167.71, 167.22, 146.72, 140.99, 140.61, 135.28, 133.76, 129.96, 127.98, 126.70, 126.29, 125.94, 124.20, 119.69, 115.50, 113.88, 35.45, 28.00. LCMS *m/z* calc. for C₁₈H₁₃BrClN₅OS [M+H]⁺: 462.7, found 462.7 with *t*_R 3.01 min, purity 95%.

2-((5-Methyl-5*H*-[1,2,4]triazino[5,6-*b*]indol-3-yl)thio)-*N*-(4-(pyridin-2-yloxy)phenyl)acetamide (40). The title compound was prepared from 5-Methyl-5*H*-[1,2,4]triazino[5,6-*b*]indole-3-thiol (**1**) (0.030 g, 0.14 mmol), Et₃N (1.5 equiv.) and 2-bromo-*N*-(4-(pyridin-2-yloxy)phenyl)acetamide (**33**) (0.051 g, 0.17 mmol) according to general procedure E. The reaction mixture was allowed slowly warm up to room temperature and stirred overnight and monitored by TLC. The crude product was purified by column chromatography (petroleum ether/EtOAc 1:1) to give a white solid (39 mg, 64%). ¹H NMR (400 MHz, CDCl₃) δ 9.87 (s, 1H), 8.46 (dt, *J* = 1.1, 7.8 Hz, 1H), 8.16 (ddd, *J* = 0.8, 2.1, 5.0 Hz, 1H), 7.77 (ddd, *J* = 1.2, 7.4, 8.5 Hz, 1H), 7.68–7.56 (m, 3H), 7.55–7.47 (m, 2H), 7.14–7.04 (m, 2H), 6.96 (ddd, *J* = 1.0, 5.0, 7.2 Hz, 1H), 6.86 (dt, *J* = 0.9, 8.3 Hz, 1H), 4.13 (d, *J* = 1.5 Hz, 2H), 3.87 (s, 3H). ¹³C NMR (101 MHz, CDCl₃) δ 167.21, 167.08, 150.16, 147.70, 146.55, 142.15, 139.35, 134.91, 131.51, 123.44, 122.66, 121.76, 121.07, 118.33, 117.96, 111.22, 110.16, 35.75, 27.53. LCMS *m/z* calc. for C₂₃H₁₉N₆O₂S [M+H]⁺: 443.5, found 443.2 with *t*_R 2.78 min, purity > 95%.

***N*-(4-Chlorophenyl)-2-((5-methyl-5*H*-[1,2,4]triazino[5,6-*b*]indol-3-yl)thio)propanamide (41).** The title compound (**41**) was prepared from (**34**) (Deora et al., 2019) (0.20 g, 0.93 mmol) and (**1**) (0.24 g, 0.93 mmol) according to the general procedure E. The crude product was purified by column chromatography (petroleum ether/EtOAc 2:1) to give a white solid (0.083 g, 22%). ¹H NMR (400 MHz, DMSO-*d*₆) δ 10.61 (s, 1H), 8.30 (d, *J* = 7.7 Hz, 1H), 7.75 (d, *J* = 5.9 Hz, 2H), 7.68 (d, *J* = 8.6 Hz, 2H), 7.47 (ddd, *J* = 8.0, 6.0, 2.3 Hz, 1H), 7.38 (d, *J* = 8.8 Hz, 2H), 4.85 (q, *J* = 7.0 Hz, 1H), 3.77 (s, 3H), 1.68 (d, *J* = 7.1 Hz, 3H). ¹³C NMR (101 MHz, DMSO-*d*₆) δ 170.55, 166.85, 146.49, 142.08, 141.47, 138.40, 131.42, 129.19, 127.53, 123.33, 121.88, 121.25, 117.71, 111.61, 45.12, 27.76, 18.65. LCMS *m/z* calc. for C₁₉H₁₇ClN₅OS⁺ [M]⁺: 398.8, found 397.8 with *t*_R 3.03 min, purity 95%.

***N*-(4-Chlorophenyl)-*N*-methyl-2-((5-methyl-5*H*-[1,2,4]triazino[5,6-*b*]indol-3-yl)thio)acetamide (43).** The title compound was prepared from 2-bromo-*N*-(4-chlorophenyl)-*N*-methylacetamide (**36**) (0.050 g, 0.19 mmol) and 5-methyl-5*H*-[1,2,4]triazino[5,6-*b*]indole-3-thiol (**1**) (0.041 g, 0.19 mmol) according to general procedure E. The crude product was purified by column chromatography (petroleum ether/EtOAc 1:1) to give a white solid (32.5 mg, 28%): ¹H NMR (400 MHz, DMSO-*d*₆) δ 8.32 (d, *J* = 7.8 Hz, 1H), 7.78 (d, *J* = 4.1 Hz, 2H), 7.65–7.35 (m, 5H), 4.05 (d, *J* = 22.3 Hz, 2H), 3.76 (s, 3H), 3.23 (s, 3H). ¹³C NMR (101 MHz, DMSO-*d*₆) δ 170.55, 166.85, 146.49, 142.08, 141.47, 138.40, 131.42, 129.19, 127.53, 123.33, 121.88, 121.25, 117.71, 111.61, 45.12, 27.76, 18.65. LCMS *m/z* calc. for C₁₉H₁₇ClN₅OS [M+H]⁺: 398.2, found 397.8 with *t*_R 3.03 min, purity 95%.

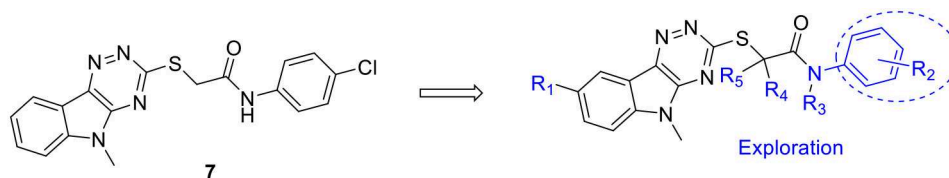


FIGURE 2 | Chemical structure of hit compound **7** and plans for chemical optimisation.

***N*-(4-Chlorophenyl)-*N*-methyl-2-((5-methyl-5*H*-[1,2,4]triazino[5,6-*b*]indol-3-yl)thio)propanamide (**44**).**

The title compound was prepared from 5-methyl-5*H*-[1,2,4]triazino[5,6-*b*]indole-3-thiol (**1**) (0.050 g, 0.23 mmol) and 2-bromo-*N*-(4-chlorophenyl)acetamide (**37**) (0.064 g, 0.23 mmol) according to general procedure E. The crude product was purified by column chromatography (petroleum ether/EtOAc 1:1) to give a gray solid (59 mg, 76%). ¹H NMR (400 MHz, DMSO-*d*₆) δ 8.33 (d, *J* = 7.7 Hz, 1H), 7.79 (d, *J* = 3.8 Hz, 2H), 7.69–7.40 (m, 3H), 7.36 (d, *J* = 8.0 Hz, 2H), 4.80 (q, *J* = 6.9 Hz, 1H), 3.70 (s, 3H), 3.20 (s, 3H), 1.51 (d, *J* = 6.9 Hz, 3H). ¹³C NMR (101 MHz, DMSO-*d*₆) δ 171.18, 170.94, 166.01, 146.30, 142.40, 142.15, 141.44, 132.85, 131.49, 130.07, 129.96, 123.38, 121.91, 117.69, 111.61, 55.39, 44.54, 37.69, 27.62, 24.57, 22.19, 19.31. LCMS *m/z* calc. for C₂₀H₂₀ClN₅OS [M+H]⁺: 412.9, found 412.2 with *t*_R 2.90 min, purity > 95%.

***N*-(4-Chlorophenyl)-2-methyl-2-((5-methyl-5*H*-[1,2,4]triazino[5,6-*b*]indol-3-yl)thio)propanamide (**42**).** 5-Methyl-5*H*-[1,2,4]triazino[5,6-*b*]indole-3-thiol (**1**) (0.100 g, 0.46 mmol) was dissolved in anhydrous DMF (15 mL) under N₂ protection in an ice bath, followed by addition of NaH 60% dispersion in mineral oil (0.020 g, 0.51 mmol) in one portion. The mixture was stirred for 45 min with ice bath cooling followed by addition of 2-bromo-*N*-(4-chlorophenyl)-2-methylpropanamide (**35**) (0.128 g, 0.46 mmol). The mixture was then slowly warmed up to room temperature and stirred overnight. Once the reaction was finished, the mixture was poured onto sat. NH₄Cl (100 mL) and stirred vigorously for 10 min. The resulting suspension was extracted with EtOAc (30 mL × 3). The combined organic layers were washed with brine, dried over Na₂SO₄, and concentrated. The crude product was purified by column chromatography (petroleum ether/EtOAc 3:1) to give a yellow solid (0.140 g, 74%). ¹H NMR (400 MHz, DMSO-*d*₆) δ 9.98 (s, 1H), 8.29 (dt, *J* = 7.8, 1.0 Hz, 1H), 7.85–7.62 (m, 4H), 7.45 (ddd, *J* = 8.0, 6.7, 1.5 Hz, 1H), 7.38–7.17 (m, 2H), 3.73 (s, 3H), 1.81 (s, 6H). ¹³C NMR (101 MHz, DMSO-*d*₆) δ 172.39, 166.56, 146.24, 141.98, 141.26, 138.68, 131.44, 128.76, 127.36, 123.33, 122.25, 121.90, 117.71, 111.60, 52.77, 27.78, 26.61. LCMS *m/z* calc. for C₁₉H₁₆ClN₅OS [M+H]⁺: 411.9, found 411.9 with *t*_R 2.99 min, purity 95%.

RESULTS

Virtual Screening and Hit Identification of PqsR Inhibitors

In silico virtual screening was performed on the PqsR ligand binding domain (LBD) crystal structure [PDB: 4JVI; (Ilangoan

et al., 2013)] using the University of Nottingham Managed Chemical Compound Collection (MCCC) containing 85,061 compounds. Molecular docking was performed using both the OpenEye docking (OpenEye Scientific Software Inc. (Hawkins et al., 2007) and Schrödinger Suite for molecular modeling (Friesner et al., 2004; Halgren et al., 2004). A cut off value of the docking score function was set to -9.0 and the resulting high scoring compounds were further examined (Friesner et al., 2004; Halgren et al., 2004). This gave a library of around 500 diverse molecules that were evaluated using *in vitro* screening in a *P. aeruginosa* PAO1-L mCTX::P_{pqsA}-*lux* reporter assay (Diggle et al., 2011).

Compound **7** (Figure 2) with a PAO1-L IC₅₀ of 0.98 μM, was chosen for further optimisation. Disappointingly, this compound proved inactive when screened against the *P. aeruginosa* strain PA14, harboring the mCTX::P_{pqsA}-*lux* reporter. However, the hit compound **7** provided a good chemical starting point to undertake rapid optimisation.

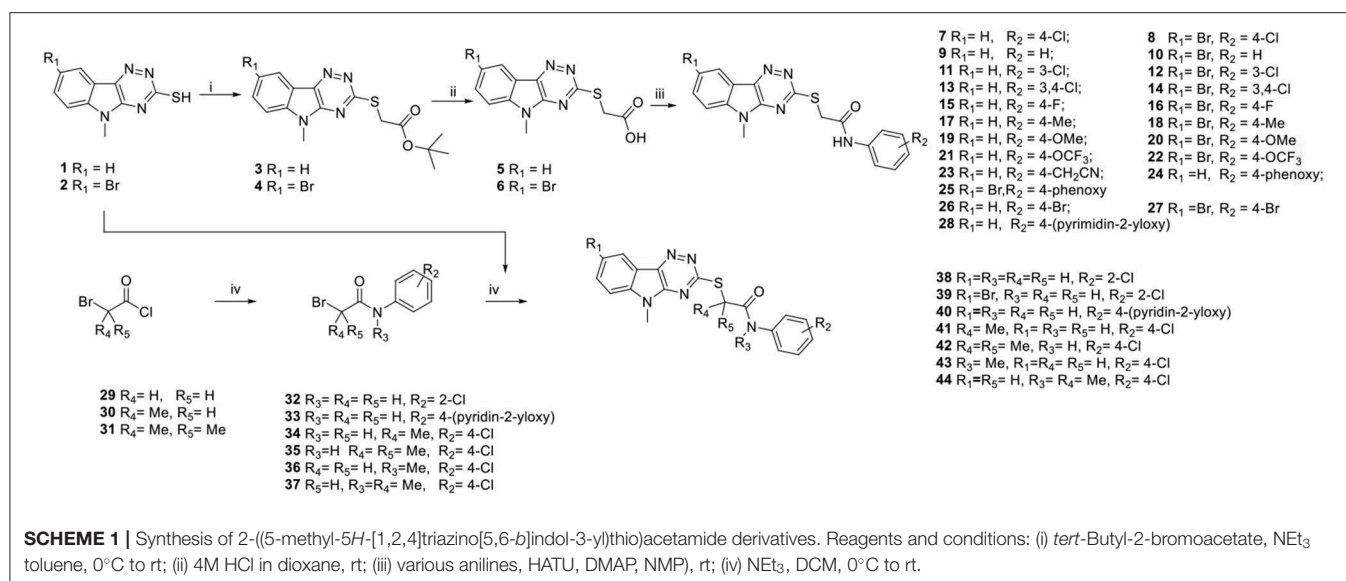
Optimisation of the PqsR Inhibitor Hit

The chemical exploration of **7** initially focused on modifying the 4-chloroanilide, investigating the effect of substitution on the 8-position of the tricyclic ring and exploration of the effect of the core linking group substituents (groups R_{3–5}). The compounds were readily synthesized according to the methods outlined below (Scheme 1).

The 1,2,4-triazino[5,6-*b*]indole-3-thiol derivatives (**1&2**) (Sharma et al., 2014) were functionalised in two steps through the alkylation using *tert*-butyl-2-bromoacetate and then deprotection to give the carboxylic acids (**5–6**). These key intermediates were either reacted with a wide range of anilines using HATU as the amide coupling agent to afford compounds (**7–28**) in high yield. In a complementary method, intermediates (**1&2**) were directly alkylated with 2-bromoacetamide intermediates (**32–37**) (Deora et al., 2019) to give compounds (**38–44**) in high over all yield (Scheme 1).

Pharmacological Evaluation and Structure-Activity Relationship Studies

As shown in Table 1, introduction of a bromine atom to the 8-position of the 5-methyl-5*H*-[1,2,4]triazino[5,6-*b*]indole ring **8** maintained biological activity against PAO1-L and showed comparable activity against PA14. Limited SAR exploration of the core linking group showed that substitution led to a loss of biological activity (**41–44**). SAR exploration of the terminal aryl group proved more interesting and demonstrated differences



in biological activity between the unsubstituted and 8-bromo-substituted 5-methyl-5H-[1,2,4]triazino[5,6-b]indole analogs. Removing the chlorine atom abolished biological activity (**9** and **10**), however substitution of the 4-chlorine atom with a bromine atom **26** maintained biological activity against PAO1-L and PA14. Disappointingly, removing the bromine atom ($R_1 = H$) **27** led to a reduction in biological activity against PAO1-L and inactivity against PA14 (compare **26** and **27**). Moving the chlorine atom from the *para*- (**7** and **8**) to the *meta*-position (**11** and **12**) resulted in some level of biological activity against the PAO1-L strain however, **11** and **12** proved inactive against PA14. The *ortho*-chloro substituted analogs (**38** and **39**) were inactive against both strains and the 3, 4-dichloro analogs only showed activity in the 8-bromo substituted series (compare **14** vs. **13**) demonstrating divergence of SAR between the 2 series ($R^1 = H$ vs. Br). This surprising SAR was also demonstrated with the 4-fluoro analogs (**15** and **16**), where only **16** showed biological activity against the PAO1-L strain, and the 4-methyl analog **17** which was active against the PAO1-L strain (compare **17** vs. **18**). The 4-methoxy (**19** and **20**) and 4-trifluoromethoxy analogs (**21** and **22**) lost activity against both strains. Interestingly, the addition of a 4-cyanomethyl group **23** gave a compound with activity against both strains. Introduction of a phenoxy group **24** provided the activity in both strains with almost 2.5-fold higher in PAO1-L compared to **7**, although activity was again lost in the 8-bromo-5-methyl-5H-[1,2,4]triazino[5,6-b]indole series **25**. Introduction of a pyridine-2-yloxy group produced the most active compound **40** against both PAO1-L and PA14. Interestingly, increasing the number of heteroatoms on R_2 **28** led to decreased PqsR inhibition. On the basis that the phenoxy group of **M64** formed a π - π stacking interaction with the side chain of Tyr²⁵⁸ (Kitao et al., 2018) and combined with docking studies, it is suggested that introducing a 6-membered heterocycle would lead to enhanced π - π stacking with Tyr²⁵⁸ in the PqsR LBD. The resulting pyridine-2-yloxy analog **40** displayed similar activity compared to **M64** at PAO1-L and an

enhanced inhibition in PA14 with IC₅₀ values of 0.25 ± 0.12 and $0.34 \pm 0.03 \mu M$, respectively. The proposed π - π stacking interaction between **40** and Tyr²⁵⁸ was observed by obtaining the co-crystal structure of **40** in the PqsR LBD (**Figure 3**).

Crystal Structure of PqsR LBD in Complex With 40

In order to determine the mode of binding of **40** to PqsR, the co-crystal structure with the PqsR LBD was obtained at resolution of 3.2 Å (**Figure 3A**). The ligand-bound complex reveals that the tricyclic head group inserts deeply into the hydrophobic pocket, whilst the thioacetamide linker was positioned in the outer narrow U-shaped channel. In a similar fashion to **M64**, the sulfur atom on the linker allowed **40** to adopt the required conformation to fit into the binding pocket. The aromatic tail group points outside this pocket and shows a π - π stacking interaction with Tyr²⁵⁸ with a distance of 4.55 Å. Interestingly, compared to the reported crystal structure of **M64**, compound **40** did not establish a hydrogen bond with Gln¹⁹⁴ but instead formed a hydrogen bond with Leu²⁰⁷. In addition, the pyridinyl side chain of compound **40** had an enhanced overlap with Tyr²⁵⁸ compared to the phenyl side chain of **M64** (**Figure 3B**), which suggests that **40** could have an enhanced π - π stacking interaction with Tyr²⁵⁸ (see **Supplementary Figure 1** and **Supplementary Table 1** for further poses and table of crystallographic properties and refinement).

Impact of PqsR Inhibitors on Pyocyanin Production

Pyocyanin is an important virulence factor for *P. aeruginosa* infections and in particular respiratory and urinary tract infections. Pyocyanin is a redox-active phenazine the production of which is regulated via PqsR and PqsE (Hall et al., 2016; Rampioni et al., 2016; Higgins et al., 2018). Therefore, pyocyanin production serves as an indirect readout of the activity of the *pqs* QS system. In this study, we measured pyocyanin expression in

TABLE 1 | *Pseudomonas aeruginosa* P_{pqsA}-lux bioreporter assays of the compounds synthesized.



Example	R ¹	R ²	R ³	R ⁴	R ⁵	IC ₅₀ (μM) or Remaining Activity % (RA%) at 10 μM (bold)	
						PAO1-L	PA14
7	H	4-Cl	H	H	H	0.98 ± 0.02	NA
8	Br	4-Cl	H	H	H	1.99 ± 0.23	1.60 ± 0.16
9	H	H	H	H	H	NA	NA
10	Br	H	H	H	H	NA	NA
11	H	3-Cl	H	H	H	RA% 34 ± 7.3	NA
12	Br	3-Cl	H	H	H	RA% 43 ± 20.2	NA
13	H	3,4-dichloro	H	H	H	NA	NA
14	Br	3,4-dichloro	H	H	H	3.1 ± 0.52	7.58 ± 0.82
15	H	4-F	H	H	H	NA	NA
16	Br	4-F	H	H	H	1.36 ± 0.21	NA
17	H	4-Me	H	H	H	1.86 ± 0.01	NA
18	Br	4-Me	H	H	H	RA% 32 ± 6.2	NA
19	H	4-OMe	H	H	H	NA	NA
20	Br	4-OMe	H	H	H	NA	NA
21	H	4-OCF ₃	H	H	H	RA% 29 ± 6	NA
22	Br	4-OCF ₃	H	H	H	RA% 23 ± 9	NA
23	H	4-(cyanomethyl)	H	H	H	0.62 ± 0.10	2 ± 0.17
24	H	4-phenoxy	H	H	H	0.38 ± 0.06	0.35 ± 0.06
25	Br	4-phenoxy	H	H	H	4.36 ± 0.42	NA
26	H	4-Br	H	H	H	1.71 ± 0.26	1.35 ± 0.19
27	Br	4-Br	H	H	H	23 ± 9	NA
28	H	4-(pyrimidin-2-ylloxy)	H	H	H	1.04 ± 0.12	1.33 ± 0.33
38	H	2-Cl	H	H	H	NA	NA
39	Br	2-Cl	H	H	H	NA	NA
40	H	4-(pyridin-2-ylloxy)	H	H	H	0.25 ± 0.12	0.34 ± 0.03
41	H	4-Cl	Me	H	H	NA	NA
42	H	4-Cl	H	Me	Me	NA	NA
43	H	4-Cl	H	Me	H	NA	NA
44	H	4-Cl	Me	H	Me	NA	NA
M64						0.32 ± 0.14	1.22 ± 0.34

Data shown are based on n = 9. NA, not active at 10 M concentration. Bold values represent percentage of remaining activities at 10 μM concentration.

the presence of the most active *pqs* inhibitors in this series. The inhibitors showed a trend consistent with their corresponding IC₅₀ values in the bioreporter assays. All the compounds showed inhibition of pyocyanin production of at least 50% compared with the control when used at a concentration three times higher

than their IC₅₀ (Figure 4). Compound 23 represented the most potent inhibitor in reducing pyocyanin production particularly in PA14. Compound 40 reduced pyocyanin production by over 80% in both strains in agreement with bioreporter assay results.

Impact of 40 on AQ Production in Planktonic and Biofilm Cultures

Since PqsR controls expression of the *pqsABCDE* operon encoding the enzymes required for different stages of AQ biosynthesis, quantification of HHQ, and PQS provides a direct measurement for inhibition of the biosynthetic pathway. Compound 40 was evaluated for its effect on AQ biosynthesis at a concentration three times the corresponding IC₅₀ values for PAO1-L and PA14. Inhibitor 40 was found to substantially reduce the production of HHQ and PQS in planktonic cultures of both *P. aeruginosa* strains (Figure 5).

Biofilms are a major challenge in the treatment of chronic *P. aeruginosa* infections because of their resilience and protection of bacteria from environmental stresses such as those posed by the host immune system and antimicrobial agents (Flemming et al., 2007; Rybtke et al., 2015). Many genes that are involved in biofilm formation are directly linked to *pqs* QS signaling (Rampioni et al., 2016; Lin et al., 2018). To evaluate the effect of 40 on AQ signaling in biofilm cultures, PAO1-L was grown in M9 minimal medium and challenged with either DMSO control or of 40 (10 μM). Following incubation and cell removal, supernatants were subjected to LC/MS-MS analysis. Figure 5 shows that compound 40 was able to effectively inhibit the biosynthesis of AQ signals in biofilm cultures (Figure 6).

Effect of 40 on Biofilm Viability

Biofilms are highly recalcitrant to the action of antimicrobials. Compound M64 has been shown to sensitize biofilms to antibiotics. To study whether 40 could also impact on biofilm formation this PqsR inhibitor was administered to pre-established PAO1-L biofilms (48 h) and their viability investigated using the LIVE/DEAD® BacLight™ bacterial viability kit and confocal laser scanning microscopy (CLSM). Moreover, to assess whether 40 can act as a non-growth inhibitory adjuvant to the broad spectrum antibiotic ciprofloxacin (CIP), combination therapy against mature PAO1-L biofilms was also tested. PAO1-L biofilms were established for 2 days before challenging with these treatments for 6 and 24 h followed by Live/Dead staining. Results showed that untreated biofilms presented only live bacteria but when the biofilms were exposed to 40 the growth of the community increased with respect to untreated controls after both 6 and 24 h (Figure 6). When the biofilms were exposed to CIP, some evidence of dead bacteria was obtained due to areas of red staining within the biofilm and, contrary to our hypothesis, treatment with the quorum sensing inhibitor 40 combined with CIP did not result in an enhanced biofilm killing (Figure 7) (see Supplementary Figures 2, 3).

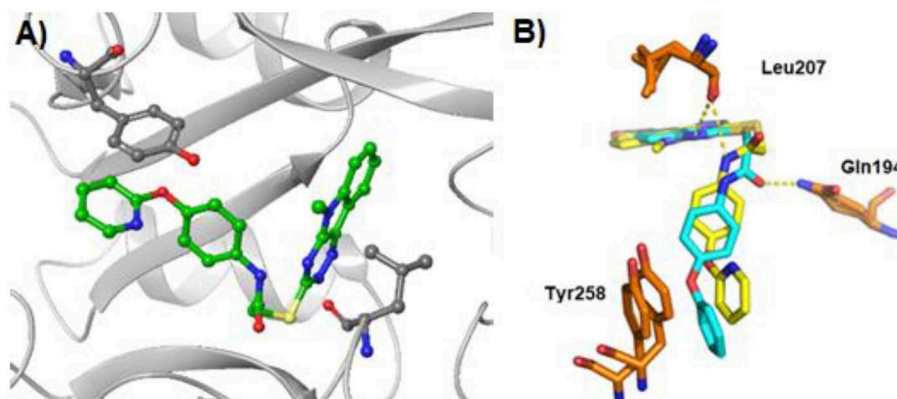


FIGURE 3 | X-ray crystal structure of PqsR in complex with compound **40** and **M64** (PDB:6B8A) (Kitao et al., 2018) **(A)** X-ray co-crystal structure of **40** bound to PqsR LBD. The protein structure is presented in gray and residues Tyr²⁵⁸ and Leu²⁰⁷ are labeled in black. **(B)** Overlapping crystal structures of **40** and **M64** in complex with PqsR ligand binding domain. Compound **40** is represented in yellow and **M64** in light blue.

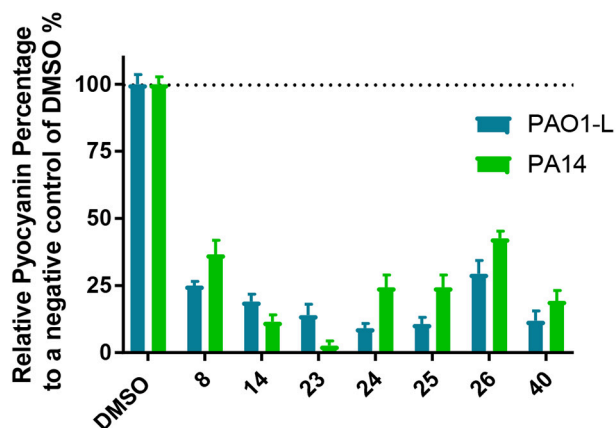


FIGURE 4 | Pyocyanin production by *Pseudomonas aeruginosa* after treatment with pqs inhibitors **8**, **14**, **23**, **34**, **25**, **26**, and **40**. Quantification of pyocyanin production after inhibitor treatment at $3 \times \text{IC}_{50}$ for both PAO1-L and PA14. The graph represents the average of three independent experiments carried out in triplicate ($n = 9$).

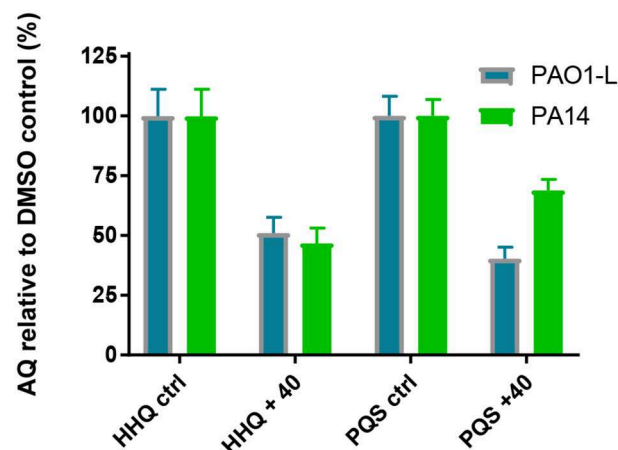


FIGURE 5 | Effect of compound **40** on AQ production: Quantification of AQ concentrations after treatment with the PqsR inhibitor **40** at $3 \times \text{IC}_{50}$ value for PAO1-L and PA14 each strain. The graph represents the average of three independent experiments carried out in triplicate ($n = 9$) for both strains.

DISCUSSION

Here, we presented the results of a hit to lead optimisation process on compound **7** (PAO1-L IC_{50} $0.98 \pm 0.02 \mu\text{M}$, PA14 inactive at $10 \mu\text{M}$) which was discovered in an initial screening for PqsR antagonists using a bacterial cell-based reporter assay. A secondary aim of this work was to improve the potency against different *P. aeruginosa* strains. This aspect is of vital importance in antimicrobial drug discovery as the potency of inhibitors can vary widely in a strain dependent manner which has a detrimental downstream effects on their prospective success as antimicrobial agents (Jackson et al., 2018). In fact, the majority of published work in relation to PqsR inhibition has only been validated in a single strain. For this purpose, both PAO1-L and PA14 were chosen as two of the most studied laboratory strains

belonging to the two major *P. aeruginosa* genomic clusters to account for any strain differences (Freschi et al., 2015).

To inform the structural variation of **7**, crystal structures with the endogenous ligand [4-hydroxy-2-heptylquinoline (NHQ)] and the inhibitor **M64** were used (Ilango et al., 2013; Kitao et al., 2018). The PqsR LBD is dominated by lipophilic interactions, therefore the current SAR exploration mainly focused on varying the aromatic tail substituents and examining the effect of 8-position substitution. The rationale for these modifications was primarily based on molecular docking studies that provided insights into the mode of binding of **7** and approaches intended to improve potency. The substituent at the *para*- position of the aromatic ring appeared to be crucial for biological activity due to the vital π - π stacking interaction of this group with Tyr²⁵⁸. Compound **40** demonstrated almost

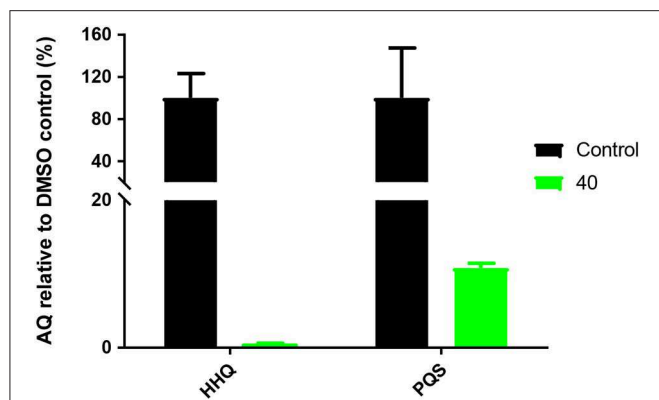


FIGURE 6 | Quantification of AQ concentrations in PAO1-L biofilm cultures treated with **40** (10 μ M). The y axis shows the % of Aqs production in relation to a non-treated DMSO control. Biofilms were grown in M9 minimal medium for 18 h in 24-well glass bottom plates and supernatants extracted for AQ analysis.

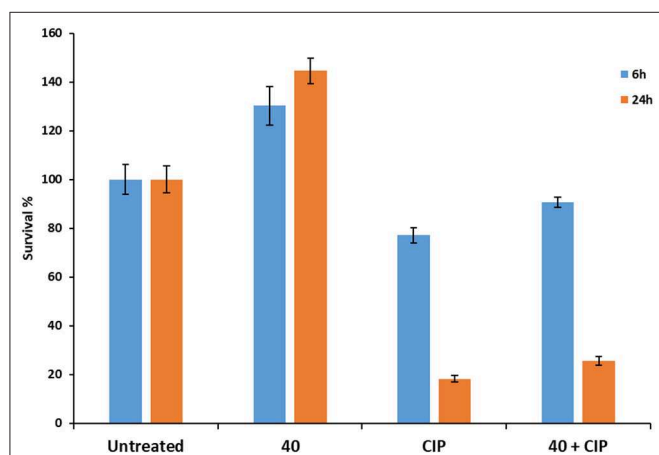


FIGURE 7 | Bar chart showing PAO1-L biofilm viability quantified after treatment with different conditions for 6 or 24 h. The concentrations of the drugs used were ciprofloxacin 60 μ g/mL (CIP), **40** 10 μ M.

equal sub-micromolar potency in both bioreporter strains in which a chromosomal transcriptional fusion of P_{pqsA} -lux was introduced to report on PqsR activation by HHQ and PQS. These strains emit light upon activation of PqsR by the endogenous production of these signal molecules. However, upon interaction with antagonists PqsR is unable to activate the P_{pqsA} promoter and hence a reduction in bioluminescence is observed (Ilangoan et al., 2013; Soukarieh et al., 2018a). The results of the SAR in this assay highlight the importance of testing any prospective anti-virulence strategy on multiple genetically distinct *P. aeruginosa* strains as a means to reduce the chance of failure at both pre-clinical and clinical stages (Freschi et al., 2015).

However, compounds active in the P_{pqsA} -lux reporter assay may either be inhibitors of PqsR or of the AQ biosynthetic enzymes. To confirm PqsR as the potential target for this series, the co-crystal structure of **40** with PqsR ligand binding domain was obtained. The crystal structure revealed the binding is dominated by the π - π stacking interaction with Tyr²⁵⁸ and the

hydrogen bonding interaction between the amide linker of **40** and the side chain of Leu²⁰⁷, similar to that previously reported (Kitao et al., 2018).

To further confirm the inhibition of *pqs* system, the end products of this biosynthetic pathway were quantified and the inhibitory effect of **40** was clearly apparent in the phenotypic assays. The *pqs* inhibitor **40** reduced the expression of pyocyanin substantially at sub-micromolar concentrations and interfered with the biosynthesis of AQ signals leading to a significant decrease in their production in both *P. aeruginosa* genotypes corroborating the results of the bioreporter assay. Collectively, these results, along with the co-crystal structure, provide strong evidence for PqsR as the *pqs* pathway target of **40** (Zender et al., 2013; Lu et al., 2014a,b; Starkey et al., 2014). Interestingly, the inhibitory effect of **40** on AQ production extended beyond the planktonic growth of *P. aeruginosa* and was also significant in biofilm cultures where **40** drastically reduced the AQ levels. AQ signals and particularly PQS is involved in wide spectrum of functions including iron acquisition, cytotoxicity, and host immune response modulation, therefore it is of therapeutic benefit to reduce or deplete the concentration of these molecule in *P. aeruginosa* communities (Hooi et al., 2004; Diggle et al., 2007; Kim et al., 2010; Lin et al., 2018). Nevertheless, biofilm treated with **40** showed a slight increase in viability and hence growth compared to the untreated control contradicting our hypothesis. The reasons behind this observation were not investigated but may be due to multiple factors including biofilm permeability, the presence of efflux pumps or off target effects (Masi et al., 2017). Compounds with similar scaffolds were reported previously to act on PqsBC, a β -keto acyl synthase III enzyme responsible for the condensation of 2-ABA (Maura et al., 2017). Inhibition of PqsBC leads to the accumulation of 2-aminoanthranilic acid (2-AA) and 2,4-dihydroxyquinoline DHQ metabolites that increase *P. aeruginosa* persistence and promote chronic infections (Kesarwani et al., 2011; Gruber et al., 2016). Further investigation is required to ascertain the reasons behind the inability of **40** to potentiate killing by ciprofloxacin whilst being a robust inhibitor of PqsR, the production of alkylquinolones and pyocyanin.

DATA AVAILABILITY STATEMENT

The datasets generated for this study can be found in the <https://www.rcsb.org/> PDB: 6TPR.

AUTHOR CONTRIBUTIONS

FS performed *in silico* and *in vitro* screening and directed the microbiology experiments. RL designed and performed syntheses, microbiology experiments, and contributed to writing and X-ray crystallography. FS, MS, PW, and MC designed, supervised the study and lead the writing of the manuscript. EO, MR, SR, SL, NQ, SA, SG, AM, and NH performed the experimental microbiology. WR and JE performed and designed crystallography experiments. SM, SH, TS, CB, IK-I, and RCL contributed to experimental design.

FUNDING

This work was supported by the Engineering and Physical Sciences Research Council [grant numbers EP/N006615/1 and EP/K005138/1, EP/N03371X/1] and JPI-AMR and MRC for funding SENBIOTAR program (Ref. MR/N501852/1). FS, MR, SR, PW, MS, JE, and MC are funded by the National Biofilms Innovation Centre (NBIC) which is an Innovation and Knowledge Centre funded by the Biotechnology and Biological Sciences Research Council, Innovate UK and Hartree Centre

REFERENCES

- Ben Haj Khalifa, A., Moissenet, D., Vu Thien, H., and Khedher, M. (2011). Virulence factors in *Pseudomonas aeruginosa*: mechanisms and modes of regulation. *Ann. Biol. Clin.* 69, 393–403. doi: 10.1684/abc.2011.0589
- Bjarnsholt, T., Jensen, P. O., Burmolle, M., Hentzer, M., Haagensen, J. A., Hougen, H. P., et al. (2005). *Pseudomonas aeruginosa* tolerance to tobramycin, hydrogen peroxide and polymorphonuclear leukocytes is quorum-sensing dependent. *Microbiology* 151, 373–383. doi: 10.1099/mic.0.27463-0
- Blair, J. M., Webber, M. A., Baylay, A. J., Ogbolu, D. O., and Piddock, L. J. (2015). Molecular mechanisms of antibiotic resistance. *Nat. Rev. Microbiol.* 13, 42–51. doi: 10.1038/nrmicro3380
- Deora, G. S., Qin, C. X., Vecchio, E. A., Debono, A. J., Priebbenow, D. L., Brady, R. M., et al. (2019). Substituted Pyridazin-3(2H)-ones as highly potent and biased formyl peptide receptor agonists. *J. Med. Chem.* 62, 5242–5248. doi: 10.1021/acs.jmedchem.8b01912
- Diggle, S. P., Fletcher, M. P., Camara, M., and Williams, P. (2011). Detection of 2-alkyl-4-quinolones using biosensors. *Methods Mol. Biol.* 692, 21–30. doi: 10.1007/978-1-60761-971-0_2
- Diggle, S. P., Matthijs, S., Wright, V. J., Fletcher, M. P., Chhabra, S. R., Lamont, I. L., et al. (2007). The *Pseudomonas aeruginosa* 4-quinolone signal molecules HHQ and PQS play multifunctional roles in quorum sensing and iron entrapment. *Chem. Biol.* 14, 87–96. doi: 10.1016/j.chembiol.2006.11.014
- Fleitas Martinez, O., Cardoso, M. H., Ribeiro, S. M., and Franco, O. L. (2019). Recent advances in anti-virulence therapeutic strategies with a focus on dismantling bacterial membrane microdomains, toxin neutralization, quorum-sensing interference and biofilm inhibition. *Front. Cell. Infect. Microbiol.* 9:74. doi: 10.3389/fcimb.2019.00074
- Fleitas Martinez, O., Rigueiras, P. O., Pires, A. D. S., Porto, W. F., Silva, O. N., de la Fuente-Nunez, C., et al. (2018). Interference with quorum-sensing signal biosynthesis as a promising therapeutic strategy against multidrug-resistant pathogens. *Front. Cell. Infect. Microbiol.* 8:444. doi: 10.3389/fcimb.2018.00444
- Flemming, H. C., Neu, T. R., and Wozniak, D. J. (2007). The EPS matrix: the “house of biofilm cells”. *J. Bacteriol.* 189, 7945–7947. doi: 10.1128/JB.00858-07
- Freschi, L., Jeukens, J., Kukavica-Ibrulj, I., Boyle, B., Dupont, M. J., Laroche, J., et al. (2015). Clinical utilization of genomics data produced by the international *Pseudomonas aeruginosa* consortium. *Front. Microbiol.* 6:1036. doi: 10.3389/fmicb.2015.01036
- Friesner, R. A., Banks, J. L., Murphy, R. B., Halgren, T. A., Klicic, J. J., Mainz, D. T., et al. (2004). Glide: a new approach for rapid, accurate docking and scoring. 1. Method and assessment of docking accuracy. *J. Med. Chem.* 47, 1739–1749. doi: 10.1021/jm0306430
- Gellatly, S. L., and Hancock, R. E. (2013). *Pseudomonas aeruginosa*: new insights into pathogenesis and host defenses. *Pathog. Dis.* 67, 159–173. doi: 10.1111/2049-632X.12033
- Gruber, J. D., Chen, W., Parnham, S., Beauchesne, K., Moeller, P., Flume, P. A., et al. (2016). The role of 2,4-dihydroxyquinoline (DHQ) in *Pseudomonas aeruginosa* pathogenicity. *PeerJ*. 4:e1495. doi: 10.7717/peerj.1495
- Halgren, T. A., Murphy, R. B., Friesner, R. A., Beard, H. S., Frye, L. L., Pollard, W. T., et al. (2004). Glide: a new approach for rapid, accurate docking and scoring. [Award Number BB/R012415/1. SL was funded by the Cystic Fibrosis Trust, UK VIA Award No: 062. SG and WR are funded via the Wellcome Trust doctoral training programme in antimicrobials and antimicrobial resistance (ref: 108876/B/15/Z).

SUPPLEMENTARY MATERIAL

The Supplementary Material for this article can be found online at: <https://www.frontiersin.org/articles/10.3389/fchem.2020.00204/full#supplementary-material>

2. Enrichment factors in database screening. *J. Med. Chem.* 47, 1750–1759. doi: 10.1021/jm030644s

Hall, S., McDermott, C., Anoopkumar-Dukie, S., McFarland, A. J., Forbes, A., Perkins, A. V., et al. (2016). Cellular effects of pyocyanin, a secreted virulence factor of *Pseudomonas aeruginosa*. *Toxins* 8:236. doi: 10.3390/toxins8080236

Hawkins, P. C., Skillman, A. G., and Nicholls, A. (2007). Comparison of shape-matching and docking as virtual screening tools. *J. Med. Chem.* 50, 74–82. doi: 10.1021/jm0603365

Higgins, S., Heeb, S., Rampioni, G., Fletcher, M. P., Williams, P., and Camara, M. (2018). Differential regulation of the phenazine biosynthetic operons by quorum sensing in *Pseudomonas aeruginosa* PAO1-N. *Front. Cell. Infect. Microbiol.* 8:252. doi: 10.3389/fcimb.2018.00252

Hooi, D. S. W., Bycroft, B. W., Chhabra, S. R., Williams, P., and Pritchard, D. I. (2004). Differential immune modulatory activity of *Pseudomonas aeruginosa* quorum-sensing signal molecules. *Infect. Immun.* 72, 6463–6470. doi: 10.1128/IAI.72.11.6463-6470.2004

Ilangovan, A., Fletcher, M., Rampioni, G., Pustelny, C., Rumbaugh, K., Heeb, S., et al. (2013). Structural basis for native agonist and synthetic inhibitor recognition by the *Pseudomonas aeruginosa* quorum sensing regulator PqsR (MvfR). *PLoS Pathog.* 9:e1003508. doi: 10.1371/journal.ppat.1003508

Jackson, N., Czaplewski, L., and Piddock, L. J. V. (2018). Discovery and development of new antibacterial drugs: learning from experience? *J. Antimicrob. Chemother.* 73, 1452–1459. doi: 10.1093/jac/dky019

Kesarwani, M., Hazan, R., He, J., Que, Y. A., Apidianakis, Y., Lesic, B., et al. (2011). A quorum sensing regulated small volatile molecule reduces acute virulence and promotes chronic infection phenotypes. *PLoS Pathog.* 7:e1002192. doi: 10.1371/journal.ppat.1002192

Kim, K., Kim, Y. U., Koh, B. H., Hwang, S. S., Kim, S. H., Lepine, F., et al. (2010). HHQ and PQS, two *Pseudomonas aeruginosa* quorum-sensing molecules, down-regulate the innate immune responses through the nuclear factor- κ B pathway. *Immunology* 129, 578–588. doi: 10.1111/j.1365-2567.2009.03160.x

Kitao, T., Lepine, F., Bablouti, S., Walte, F., Steinbacher, S., Maskos, K., et al. (2018). Molecular insights into function and competitive inhibition of *Pseudomonas aeruginosa* multiple virulence factor regulator. *MBio* 9:e02158–17. doi: 10.1128/mBio.02158-17

Lee, J., and Zhang, L. (2015). The hierarchy quorum sensing network in *Pseudomonas aeruginosa*. *Protein Cell* 6, 26–41. doi: 10.1007/s13238-014-0100-x

Lin, J., Cheng, J., Wang, Y., and Shen, X. (2018). The *Pseudomonas* quinolone signal (PQS): not just for quorum sensing anymore. *Front. Cell. Infect. Microbiol.* 8:230. doi: 10.3389/fcimb.2018.00230

Lu, C., Kirsch, B., Maurer, C. K., de Jong, J. C., Braunshausen, A., Steinbach, A., et al. (2014a). Optimization of anti-virulence PqsR antagonists regarding aqueous solubility and biological properties resulting in new insights in structure-activity relationships. *Eur. J. Med. Chem.* 79, 173–183. doi: 10.1016/j.ejmech.2014.04.016

Lu, C., Maurer, C. K., Kirsch, B., Steinbach, A., and Hartmann, R. W. (2014b). Overcoming the unexpected functional inversion of a PqsR antagonist in *Pseudomonas aeruginosa*: an *in vivo* potent antivirulence agent

- targeting pqs quorum sensing. *Angew. Chem. Int. Ed Engl.* 53, 1109–1112. doi: 10.1002/anie.201307547
- Masi, M., Refregiers, M., Pos, K. M., and Pages, J. M. (2017). Mechanisms of envelope permeability and antibiotic influx and efflux in Gram-negative bacteria. *Nat. Microbiol.* 2:17001. doi: 10.1038/nmicrobio.12017.1
- Maura, D., Drees, S. L., Bandyopadhyaya, A., Kitao, T., Negri, M., Starkey, M., et al. (2017). Polypharmacology approaches against the *Pseudomonas aeruginosa* MvfR regulon and their application in blocking virulence and antibiotic tolerance. *ACS Chem. Biol.* 12, 1435–1443. doi: 10.1021/acscchembio.6b01139
- Maura, D., and Rahme, L. G. (2017). Pharmacological inhibition of the *Pseudomonas aeruginosa* MvfR quorum-sensing system interferes with biofilm formation and potentiates antibiotic-mediated biofilm disruption. *Antimicrob. Agents Chemother.* 61:e01362–17. doi: 10.1128/AAC.01362-17
- Muhlen, S., and Dersch, P. (2016). Anti-virulence strategies to target bacterial infections. *Curr. Top. Microbiol. Immunol.* 398, 147–183. doi: 10.1007/82_2015_490
- Potron, A., Poirel, L., and Nordmann, P. (2015). Emerging broad-spectrum resistance in *Pseudomonas aeruginosa* and *Acinetobacter baumannii*: mechanisms and epidemiology. *Int. J. Antimicrob. Agents* 45, 568–585. doi: 10.1016/j.ijantimicag.2015.03.001
- Rampioni, G., Falcone, M., Heeb, S., Frangipani, E., Fletcher, M. P., Dubern, J. F., et al. (2016). Unravelling the genome-wide contributions of specific 2-Alkyl-4-quinolones and PqsE to quorum sensing in *Pseudomonas aeruginosa*. *PLoS Pathog.* 12:e1006029. doi: 10.1371/journal.ppat.1006029
- Rybtke, M., Hultqvist, L. D., Givskov, M., and Tolker-Nielsen, T. (2015). *Pseudomonas aeruginosa* biofilm infections: community structure, antimicrobial tolerance and immune Response. *J. Mol. Biol.* 427, 3628–3645. doi: 10.1016/j.jmb.2015.08.016
- Sharma, R., Pandey, A. K., Shivahare, R., Srivastava, K., Gupta, S., and Chauhan, P. M. (2014). Triazino indole-quinoline hybrid: a novel approach to antileishmanial agents. *Bioorg. Med. Chem. Lett.* 24, 298–301. doi: 10.1016/j.bmcl.2013.11.018
- Soukarieh, F., Vico Oton, E., Dubern, J. F., Gomes, J., Halliday, N., de Pilar Crespo, M., et al. (2018a). *In silico* and *in vitro*-guided identification of inhibitors of alkylquinolone-dependent quorum sensing in *Pseudomonas aeruginosa*. *Molecules* 23:257. doi: 10.3390/molecules23020257
- Soukarieh, F., Williams, P., Stocks, M. J., and Camara, M. (2018b). *Pseudomonas aeruginosa* quorum sensing systems as drug discovery targets: current position and future perspectives. *J. Med. Chem.* 61, 10385–10402. doi: 10.1021/acs.jmedchem.8b00540
- Starkey, M., Lepine, F., Maura, D., Bandyopadhyaya, A., Lesic, B., He, J., et al. (2014). Identification of anti-virulence compounds that disrupt quorum-sensing regulated acute and persistent pathogenicity. *PLoS Pathog.* 10:e1004321. doi: 10.1371/journal.ppat.1004321
- Strateva, T., and Yordanov, D. (2009). *Pseudomonas aeruginosa* - a phenomenon of bacterial resistance. *J. Med. Microbiol.* 58, 1133–1148. doi: 10.1099/jmm.0.009142-010.1099/jmm.0.009142-0
- Sun, Z., Khan, J., Makowska-Grzyska, M., Zhang, M., Cho, J. H., Suebsuwong, C., et al. (2014). Synthesis, *in vitro* evaluation and cocrystal structure of 4-oxo-[1]benzopyrano[4,3-c]pyrazole *Cryptosporidium parvum* inosine 5'-monophosphate dehydrogenase (CpIMPDH) inhibitors. *J. Med. Chem.* 57, 10544–10550. doi: 10.1021/jm501527z
- Thomann, A., de Mello Martins, A. G., Brengel, C., Empting, M., and Hartmann, R. W. (2016). Application of dual inhibition concept within looped autoregulatory systems toward antivirulence agents against *Pseudomonas aeruginosa* infections. *ACS Chem. Biol.* 11, 1279–1286. doi: 10.1021/acscchembio.6b00117
- Ventola, C. L. (2015). The antibiotic resistance crisis: part 1: causes and threats. *P T* 40, 277–283.
- Whiteley, M., Diggle, S. P., and Greenberg, E. P. (2017). Progress in and promise of bacterial quorum sensing research. *Nature* 551, 313–320. doi: 10.1038/nature24624
- Williams, P., and Camara, M. (2009). Quorum sensing and environmental adaptation in *Pseudomonas aeruginosa*: a tale of regulatory networks and multifunctional signal molecules. *Curr. Opin. Microbiol.* 12, 182–191. doi: 10.1016/j.mib.2009.01.005
- Winstanley, C., O'Brien, S., and Brockhurst, M. A. (2016). *Pseudomonas aeruginosa* evolutionary adaptation and diversification in cystic fibrosis chronic lung infections. *Trends Microbiol.* 24, 327–337. doi: 10.1016/j.tim.2016.01.008
- Zender, M., Klein, T., Henn, C., Kirsch, B., Maurer, C. K., Kail, D., et al. (2013). Discovery and biophysical characterization of 2-amino-oxadiazoles as novel antagonists of PqsR, an important regulator of *Pseudomonas aeruginosa* virulence. *J. Med. Chem.* 56, 6761–6774. doi: 10.1021/jm400830r

Conflict of Interest: The authors declare that the research was conducted in the absence of any commercial or financial relationships that could be construed as a potential conflict of interest.

Copyright © 2020 Soukarieh, Liu, Romero, Roberston, Richardson, Lucanto, Oton, Qudus, Mashabi, Grossman, Ali, Sou, Kukavica-Ibrulj, Levesque, Bergström, Halliday, Mistry, Emsley, Heeb, Williams, Cámara and Stocks. This is an open-access article distributed under the terms of the Creative Commons Attribution License (CC BY). The use, distribution or reproduction in other forums is permitted, provided the original author(s) and the copyright owner(s) are credited and that the original publication in this journal is cited, in accordance with accepted academic practice. No use, distribution or reproduction is permitted which does not comply with these terms.

Advantages of publishing in Frontiers



OPEN ACCESS

Articles are free to read
for greatest visibility
and readership



FAST PUBLICATION

Around 90 days
from submission
to decision



HIGH QUALITY PEER-REVIEW

Rigorous, collaborative,
and constructive
peer-review



TRANSPARENT PEER-REVIEW

Editors and reviewers
acknowledged by name
on published articles

Frontiers

Avenue du Tribunal-Fédéral 34
1005 Lausanne | Switzerland

Visit us: www.frontiersin.org

Contact us: info@frontiersin.org | +41 21 510 17 00



REPRODUCIBILITY OF RESEARCH

Support open data
and methods to enhance
research reproducibility



DIGITAL PUBLISHING

Articles designed
for optimal readership
across devices



FOLLOW US

[@frontiersin](https://twitter.com/frontiersin)



IMPACT METRICS

Advanced article metrics
track visibility across
digital media



EXTENSIVE PROMOTION

Marketing
and promotion
of impactful research



LOOP RESEARCH NETWORK

Our network
increases your
article's readership